The Star-formation History and Accretion Disk Fraction of the Scorpius-Centaurus OB Association

by

Mark J. Pecaut

Submitted in Partial Fulfillment
of the Requirements for the Degree

Doctor of Philosophy

Supervised by
Professor Eric E. Mamajek

Department of Physics and Astronomy
Arts, Sciences and Engineering
School of Arts and Sciences

University of Rochester
Rochester, New York

2013

Biographical Sketch

Mark Pecaut was born in Missouri in April of 1975. He attended Truman State University from 1993 to 1998, and graduated summa cum laude with a Bachelor of Science in Physics and Mathematics. He was awarded the President's Recognition Award, General Honors in Arts and Sciences, Honors in Mathematics, Honors in Physics, Outstanding Student in Mathematics, and Outstanding Student in Physics.

He began graduate work at the University of Rochester in 2008, earning a Master of Arts in Physics in 2010. While at the University of Rochester, Mark worked with Eric Mamajek in observational astronomy, studying the nearest site of recent massive star formation and the properties of its members. He was awarded the American Association of Physics Teachers (AAPT) Teaching Prize in 2009 and the University of Rochester Edward Peck Curtis Awards for Excellence in Teaching by a Graduate Student in 2013.

Publications

- "A Spitzer MIPS Study of 2.5-2.0 M_{sun} Stars in Scorpius-Centaurus", Christine H. Chen, Mark Pecaut, Eric E. Mamajek, Kate Y. L. Su, Martin Bitner 2012, ApJ, 756, 133

- "A Revised Age for Upper Scorpius and The Star-Formation History Among the F-Type Members of the Scorpius-Centaurus OB Association", Mark J. Pecaut, Eric E. Mamajek, Eric J. Bubar 2012, ApJ, 746, 154

- "Planetary Construction Zones in Occultation: Discovery of an Extrasolar Ring System Transiting a Young Sun-like Star and Future Prospects for Detecting Eclipses by Circumsecondary and Circumplanetary Disks" Eric E. Mamajek, Alice C. Quillen, Mark J. Pecaut, Fred Moolekamp, Erin L. Scott, Matthew A. Kenworthy, Andrew Collier Cameron, Neil R. Parley 2012, AJ, 143, 72

- "A Magellan MIKE and Spitzer MIPS Study of 1.5-1.0 M_{sun} Stars in Scorpius-Centaurus" Christine H. Chen, Eric E. Mamajek, Martin A. Bitner, Mark Pecaut, Kate Y. L. Su, Alycia J. Weinberger, 2011, ApJ, 738, 122

- "HD 101088, An Accreting 14 AU Binary in Lower Centaurus Crux with Very Little Circumstellar Dust" Martin A. Bitner, Christine H. Chen, James Muzerolle, Alycia J. Weinberger, Mark Pecaut, Eric E. Mamajek, Melissa K. Mclure, ApJL, 714, 1542

Acknowledgments

Special thanks to my advisor and mentor Professor Eric Mamajek. His enthusiasm for research, his advice on the nuances of navigating an academic career, and his generosity with his data and time is greatly appreciated. More than anything, Eric taught me how to think like a scientist, which is what I came to Rochester for in the first place. I'd also like to thank Dan M. Watson for giving me the chance to teach during the Summer of 2011, his mentorship, and especially for nominating me for the Curtis Teaching Award. In addition I thank my family, Amy, Athena, Ambrose and Odessa for their patience with me during my too-frequent trips to telescopes and conferences.

This research has made use of NASA's Astrophysics Data System Abstract Service, data from the Two Micron All Sky Survey (2MASS), data from the Wide-field Infrared Survey Explorer (WISE), the SIMBAD database, the AAVSO Photometric All-Sky Survey (APASS) and especially the VizieR catalogue access tool. This work was funded by NSF grant AST-1008908.

Abstract

We present a study of the star-formation history and accretion disk fraction of ∼0.6-1.8 $M_{\odot}$ stars in the nearest OB Association, Scorpius-Centaurus (Sco-Cen; 10-20 Myr; 100-200 pc). We have performed a low-resolution spectroscopic survey for new, low-mass K- and M-type members of all three subgroups – Upper Scorpius (US), Upper Centaurus-Lupus (UCL) and Lower Centaurus-Crux (LCC). We find that young, pre-main sequence stars have different intrinsic colors for a given spectral type than their main-sequence (MS) counterparts and therefore MS colors and temperatures are unsuitable for de-reddening the low-mass members of Sco-Cen and placing them on an H-R diagram. Using nearby, pre-MS, unreddened moving groups, we derive a spectral type–intrinsic color sequence appropriate for 5-30 Myr old pre-MS stars, and use synthetic spectral energy distribution fits to infer the proper temperature and bolometric correction scale for these young stars. We use this new pre-MS intrinsic color and temperature calibration to place our ∼150 newly identified members of Sco-Cen on an H-R diagram. We derive isochronal ages for the B-type MS turn-off and the pre-MS F-type, G-Type members and the K- and M-type members of Sco-Cen. We find a $T_{\rm eff}$-dependent age trend in the K/M-type stars, similar to previous studies of other nearby star-forming regions. Our F- and G-type isochronal ages for Upper Centaurus-Lupus (UCL; 16±2 Myr; $< d >$=142 pc) and Lower Centaurus-Crux (LCC; 16±3 Myr; $< d >$=118 pc) are consistent with previous results. However, our

results for Upper Scorpius (US; 10±3 Myr; $< d >$=145 pc) indicate it is a factor of two older than previously thought. Using ∼650 of the pre-MS members of Sco-Cen, we construct an age map, which reveals regions which are systematically younger or older than the mean Sco-Cen age, suggesting that the star-formation history of the three subgroups is more complex than the simple division into three subgroups would imply. Finally, we find a primordial disk fraction for US, UCL and LCC of 9^{+4}_{-2}%, 5^{+2}_{-1}% and 3^{+3}_{-1}%, respectively, for K-type stars decreasing to <19% (95% CL), 2^{+5}_{-1}%, and 2^{+4}_{-1}%, respectively, for F-type stars at ∼10 Myr, ∼16 Myr, and ∼16 Myr, respectively.

Contributors and Funding Sources

This work was supervised by a dissertation committee consisting of Professors Eric E. Mamajek (advisor), Dan M. Watson, and Alice C. Quillen of the Department of Physics and Astronomy and Professor Cynthia J. Ebinger of the Department of Earth & Environmental Sciences. The spectra from the Siding Springs 2.3m telescope in Chapter 4 were provided by Professor Mamajek. Appendix C and Table C.1 were compiled by Professor Mamajek, with the exception of the WISE colors, which were compiled by the student. All other work conducted for the dissertation was completed by the student independently. Graduate study was supported by NSF grant AST-1008908 and funds from the School of Arts and Sciences at the University of Rochester Sciences through Eric Mamajek.

Table of Contents

List of Tables

List of Figures

1 Introduction

1.1 Star Formation

The Shu et al. (1987) picture of isolated star formation begins with the gravitational collapse of molecular gas. With the formation of the protostellar core, the newly formed protostar begins to accrete material from its infalling envelope. Once the envelope has been accreted or removed by another mechanism (e.g., an outflow), the star enters the pre-main sequence phase of its evolution. During this phase, the star contracts towards the main sequence, powered by gravitational contraction. During the early pre-main sequence phase, the star will continue to accrete gas and dust from its circumstellar disk. Planet formation occurs in the gas and dust disk during this phase. In principle the age of the star may be determined through comparing the effective temperature ($T_{\rm eff}$) and luminosity (or equivalently, the radius) with theoretical stellar evolutionary models.

This idealized model for isolated star formation is fairly well-understood (Shu et al., 1987). However, most stars in the Galaxy form in large clusters (Lada & Lada, 2003) which complicates the picture considerably and leaves many open questions. Do all the stars form approximately simultaneously or does star formation persist in a molecular cloud over >10 megayears (Myr)? What triggers the star formation

process? Any theory of star formation in clusters must be consistent with the mean ages, the predicted age spreads and age gradients, the spatial scales and the internal velocity dispersions. Briceño et al. (2007) summarized two different pictures of star formation, the "KLL" model (after Kroupa et al. 2001; Lada & Lada 2003) and "BBC" model (after Bonnell, Bate and Clark; Clark et al. 2005). In the KLL picture, star formation proceeds in a dense, bound, virialized giant molecular cloud but because of the low star formation efficiency, the resulting star cluster is globally unbound (though a bound cluster core may remain; e.g., Kroupa et al. 2001). In the BBC model, star formation proceeds in a giant molecular cloud, not necessarily bound nor virialized, in locally compressed sheets due to converging flows. This can happen rapidly in less than a crossing time without external triggering. Constraining observed mean ages, age spreads and velocity dispersions in nearby sites of recent star-formation are key observational tests of these models.

A complicating ingredient in star formation is the notion of triggered star formation (Elmegreen & Lada, 1977; Elmegreen, 1998; Preibisch et al., 2002; Preibisch & Zinnecker, 2007). Several specific mechanisms for triggering star formation in molecular clouds have been proposed. Two models which consider the effects of massive stars are the collect-and-collapse model (Elmegreen & Lada, 1977; Dale et al., 2007) and the radiation driven implosion model (RDI; e.g., Kessel-Deynet & Burkert, 2003). In the collect-and-collapse model, the ionizing radiation from a newly formed massive star can sweep up nearby material (the "collect" phase) until the swept-up shell becomes self-gravitating and begins to fragment and collapse. In the RDI model, the ionizing radiation photoevaporates the outer layers of a nearby molecular cloud. This induces a shock which induces collapse in existing cores in the molecular cloud. Observations have attempted to discern which of these mechanisms may be at play in particular star-forming regions (e.g., Getman et al., 2007; Dirienzo et al., 2012),

but it is not known if either of these are the dominant triggering mechanism in the Galaxy.

The collect-and-collapse model predicts that the triggering and triggered stars will have two distinct ages, not a continuum of ages (Elmegreen, 1998). In contrast, the RDI model predicts that the massive OB stars form first, then trigger the formation of lower mass stars nearby. Thus there will be an age gradient with the stars nearest the OB stars being the oldest and progressively younger stars farther away (Preibisch & Zinnecker, 2007). For all triggering mechanisms, clear causality must be established - the difference in ages between the triggering and triggered stars must be consistent with the velocity of the triggering mechanism (e.g., supernova shock) and the distance between the triggering and triggered stars (Elmegreen, 2011).

1.2 Disk Dispersal Timescales

The Shu et al. (1987) model of isolated star formation includes a disk in the birth process. This picture is corroborated by observations of protostars in molecular clouds. The presence of circumstellar disks around very young stars is supported by observational evidence in the form of accretion diagnostics, such as $H\alpha$ emission above some threshold, or near-IR or IR emission consistent with gas-rich disk models. The fraction of stars born with gas-rich circumstellar disks is thought to be 100% but these primordial disks are absent around $\sim$Gyr-old main-sequence stars. A variety of disk dissipation mechanisms have been proposed, such as dynamical clearing due to giant planet formation (e.g., Artymowicz & Lubow, 1994), photoevaporation by radiation from the central star (e.g., Alexander et al., 2006) and/or grain growth (e.g., Muzerolle et al., 2006). Since the circumstellar gas in the disk provides the material to build gas giant planets, a fundamental constraint to planet formation theory is the

lifetime of circumstellar disks. In a recent review, Mamajek (2009) collected observed disk fractions in ∼20 stellar samples with well-defined ages and fit an exponential to the data to obtain an e-folding timescale of 2.5 Myr. Constraints on disk lifetimes have, in turn, been used by Jeffries et al. (2011) to place limits on age spreads in the Orion Nebula Cluster.

Aside from placing limits on the planet formation timescale, circumstellar disk lifetimes are an essential ingredient in stellar angular momentum evolution models (e.g., Bouvier et al., 1997). Disk locking, a magnetic connection between the disk and the star which produces a torque on the star and transfers angular momentum to the disk, is thought to be an important effect for T Tauri stars with magnetic fields of a kilogauss or more (Koenigl, 1991). Observational support for disk locking is inconsistent, with some studies showing clear evidence (Dahm et al., 2012; Rebull et al., 2006), while others have found no clear signature (Nguyen et al., 2009; Rebull, 2001). Stellar angular momentum evolution models which attempt to account for disk-locking require a clear understanding of the disk lifetime and its dependence on stellar mass (e.g., Herbst et al., 2002) or stellar environment (e.g., Littlefair et al., 2010).

1.3 Stellar Ages

Determining the timescales for planet formation, the duration of star formation in a molecular cloud, and evaluating the timing for triggered star formation scenarios involves obtaining reliable ages for individual stars. There are several different chronometers for age-dating stars (e.g., lithium depletion, activity-rotation, spectroscopic surface gravity indicators; Hillenbrand 2009; see also Soderblom 2010) but our primary tool is comparing the Hertzsprung-Russell diagram positions of individual

stars with theoretical stellar evolutionary models and isochrones. Newly formed stars have radii which are several times larger than stars on the main-sequence, and are therefore much more luminous. High-mass stars ($\gtrsim$5 $M_\odot$) contract to the main-sequence in $\sim 10^5$ yr (Iben, 1965) and therefore essentially emerge from their natal envelopes on the main sequence. However, solar-mass stars take $\sim$40 Myr to contract to the main sequence, so we can estimate meaningful ages for pre-main sequence (pre-MS) 1 $M_\odot$ stars even with sizable observational uncertainties.

While it seems a straightforward task simply to place a pre-main sequence star on a color-magnitude diagram and compare the position with the predictions from evolutionary models, there are many sources of systematic uncertainty which must be considered in order to obtain accurate ages. Most pre-main sequence stars are subject to interstellar reddening and extinction, and the observed photometry must be corrected accordingly. Another aspect which is often ignored is that stellar evolutionary models calculate the stellar effective temperature ($T_{\rm eff}$) and luminosity ($\log(L/L_\odot)$) and often convert these quantities into observational variables like color or absolute magnitude. These conversions are typically based on either synthetic colors or empirically-derived calibrations, both of which may not be appropriate for pre-main sequence stars. There have been studies which have found that pre-main sequence stars have different intrinsic colors than their main-sequence counterparts (e.g., Luhman, 1999; Luhman et al., 2010b). In addition, the $T_{\rm eff}$ scale which relates either color or spectral type to $T_{\rm eff}$ for pre-main sequence stars is not certain. Luhman (1999) has developed a $T_{\rm eff}$ scale for pre-MS M-type stars which is intermediate between the $T_{\rm eff}$ scale of dwarfs and giants and is calibrated to make the four components of GG Tau appear coeval when compared to the evolutionary models of Baraffe et al. (1998). Though there is evidence that binaries are closer to coeval than random pairings of stars in the same star-forming region (e.g., Taurus; Kraus & Hillenbrand,

2009), calibrating a temperature scale in this way is not ideal because evolutionary models for cool ($\lesssim$4000 K) stars are much more poorly matched to observations than solar-type stars (e.g., Hillenbrand & White, 2004; Torres & Ribas, 2002). A temperature scale which is biased to match evolutionary models is not a useful tool for testing the predictive power of those same models.

1.4 The Nearest OB Association

Most star formation in our Galaxy occurs in massive clusters, the majority of which do not survive as bound structures for more than ∼100 Myr (Lada & Lada, 2003). Most of these massive clusters shed their molecular clouds and transition into the field population, forming OB associations during their transition. OB associations are gravitationally unbound stellar groups of stars, identified by their hot and massive O- and B-type stars. The stellar members of an OB association exhibit similar ages and kinematics and likely share a common origin. However, due to their low stellar density ($\leq 0.1\ M_{\odot}\ pc^{-3}$) they only remain coherent structures for ∼50 Myr and then disperse into the field population due to galactic tidal forces.

The nearest OB association, Scorpius-Centaurus (Sco-Cen), was first identified by Kapteyn (1914) as an overdensity of bright, blue B-type stars on the sky. Though there was some debate whether the stars were related, it was later convincingly argued by Blaauw (1946) that they shared a common origin, based on their common space motions and small velocity dispersions. Blaauw (1964a) divided Sco-Cen into the subregions Upper Scorpius (US), Upper Centaurus-Lupus (UCL) and Lower Centaurus-Crux (LCC). The nearest site of recent massive star formation, Sco-Cen presents a convenient astrophysical laboratory to test star formation theories, and constrain the star formation and planet formation timescales. Sco-Cen is discussed in detail in a

comprehensive review in Preibisch & Mamajek (2008). However, we briefly highlight some of the recent studies of Sco-Cen to provide context for this thesis.

Blaauw (1964a) had estimated kinematic expansion ages of ∼20 Myr for Sco-Cen. However, one of the most recent modern age estimates for the subgroups of Sco-Cen is from de Geus et al. (1989). Using Walraven photometry with reddening-free indices sensitive to surface gravity and temperature, de Geus et al. (1989) estimated the main-sequence turn-off ages for the three subgroups of 5-6 Myr, 14-15 Myr, and 11-12 Myr for US, UCL and LCC, respectively. The first significant population of low-mass stars in Upper Sco was uncovered by Walter et al. (1994), using the EINSTEIN X-ray observatory (Harnden et al., 1984) to find 28 G/K/M-type low-mass members. This was before *Hipparcos* data were available, and the mean distances to the subgroups was still quite uncertain. Similarly, Preibisch et al. (1998) found 39 G/K/M-type members of Upper Sco using an X-ray selected sample. These studies all demonstrated small age spreads, which is inconsistent with "bimodal" star formation, (e.g., Larson, 1986), and demonstrated that OB associations contained significant numbers of low-mass stars.

Aside from these two studies, the low-mass population remained largely hidden until the study by de Zeeuw et al. (1999) used *Hipparcos* astrometry to perform a kinematic membership selection and analysis of the nearest OB associations, including Sco-Cen. This revealed the intermediate-mass members and established trigonometric distances for the three subgroups of ∼145 pc, ∼142 pc and ∼118 pc for US, UCL and LCC, respectively (Figure 1.1). The studies by Preibisch & Zinnecker (1999) and Mamajek et al. (2002) built on the early successes of X-ray selected samples and revealed many more low-mass G/K/M members of Sco-Cen using X-ray selected samples. The Mamajek et al. (2002) study changed our picture of the older subgroups of Sco-Cen, with the finding that the two older subgroups, UCL and LCC, were

approximately coeval, with LCC slightly older than UCL, and revised the mean ages of UCL and LCC subgroups to ∼16 Myr. Their revised ages were based on isochronal age estimates for the G-type members and updated main sequence turn-off isochronal ages for the massive stars. They detected 1σ age spreads of ±3 Myr and ±2 Myr for UCL and LCC, respectively. Preibisch et al. (2002) then extended the census for low-mass members in US down to spectral type ∼M6 with a photometric selection. Using this sample together with the de Zeeuw et al. (1999) *Hipparcos* sample and the G/K/M samples from previous studies in Upper Sco, Preibisch et al. (2002) constructed an H-R diagram for the full stellar population of US from $\sim$0.1 $M_\odot$ to $\sim$20 $M_\odot$ and, comparing it to pre-MS and post-MS isochrones, used it to infer a 5 Myr age for the association, with an age spread of <2 Myr. They argued that the narrow age spread of Upper Sco was consistent with triggering by a supernova in UCL. Preibisch et al. (2002) also used the completeness of their samples to infer an IMF for US which was consistent with the field mass function.

Sco-Cen has also been used to study the evolution of circumstellar disks and search for planetary-mass companions. Mamajek et al. (2002) used Hα and K-band data to constrain the disk fraction around their sample of 110 G- and K-type stars in UCL and LCC. They found $0.9^{+2.1}_{-0.8}$% of pre-MS solar-type ($\sim$1.1-1.5 $M_\odot$) stars harbored an accretion disk at ∼16 Myr. Carpenter et al. (2006) used the *Spitzer* Space Telescope (Werner et al., 2004) to perform a census of circumstellar disks in around 204 members of Upper Sco. They found that 19% of the K0 through M5 stars (0.1-1.0 $M_\odot$) stars had primordial disks, but ≤1% of the more massive stars possessed such a disk. This provided strong evidence that the evolution timescale for circumstellar disks was mass-dependent. This was further corroborated by Luhman & Mamajek (2012) using a sample of 863 members of Sco-Cen, from B-type stars to L-dwarfs, using *Spitzer* and WISE photometry. Several directly-imaged substellar

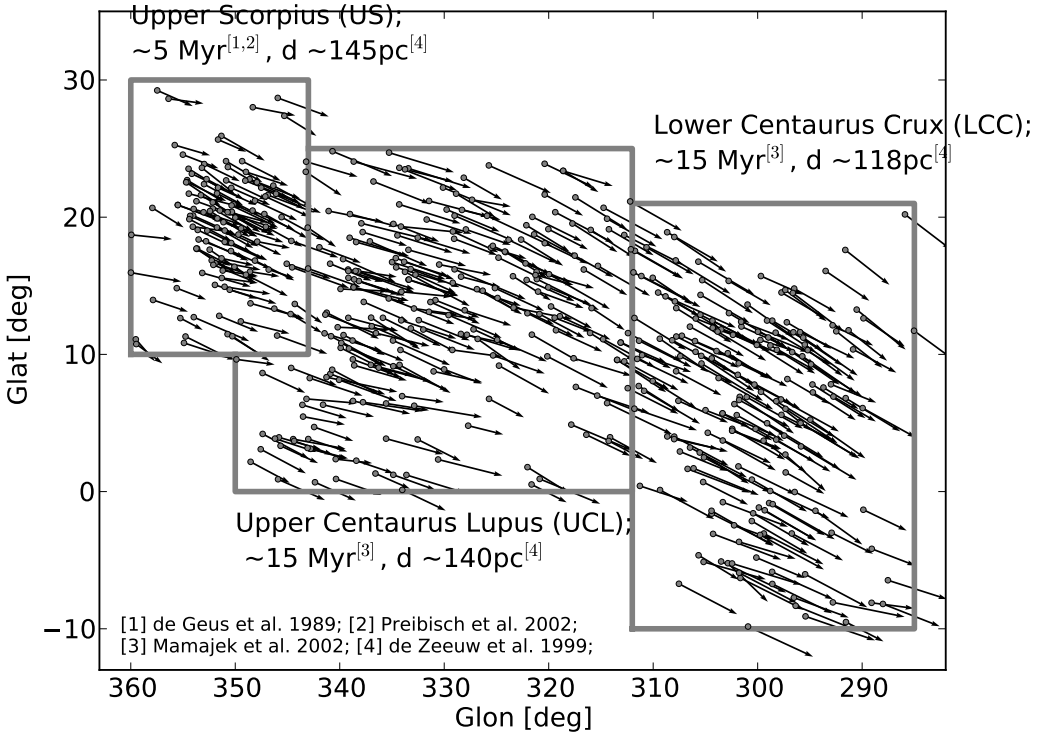

Figure 1.1 The positions and proper motions of the de Zeeuw et al. (1999) *Hipparcos* Sco-Cen members in galactic coordinates, with the mean ages summarized from the literature before the commencement of this thesis work.

companions have been discovered in Upper Sco (Lafrenière et al., 2008, 2011; Ireland et al., 2011) and Lower-Centaurus Crux (Quanz et al., 2013).

The interpretation of the results for the evolution of circumstellar disks and substellar companions are sensitive to the mean ages of the subgroups of Sco-Cen. Constraints on the primordial disk lifetimes are obviously sensitive to the adopted age of the samples. But more subtlely, studies typically map the observed spectral types to masses using an adopted age. This is necessary to compare results from samples of different ages, e.g., G5 stars at 5 Myr will become F-type stars on the main sequence. Similarly, in order to infer masses for directly-imaged substellar companions, an age is

adopted. For a substellar object of a given luminosity, a younger age implies a much lower mass (e.g.,Oph 1622-2405; Luhman et al., 2007). Therefore, it is important to continue to evaluate the established ages and age scales with more accurate data and improved methods of estimating the ages.

1.5 Objectives

In this thesis, we aim to provide observational constraints which inform star and planet formation theories, using the nearest site of recent massive star formation. To that end, the goals of this thesis are:

1. To use members of Sco-Cen to estimate the mean subgroup ages and age spreads, using stars in different mass ranges.

2. To reduce the systematic uncertainties placing young, solar-type and cooler stars on the theoretical H-R diagram ($T_{\rm eff}$, $\log(L/L_{\odot})$).

3. To constrain the primordial disk lifetime around intermediate-mass ($\sim$1.2-1.7 $M_{\odot}$) and solar-mass ($\sim$0.6-1.2 $M_{\odot}$) stars, using one of the largest $\sim$10-20 Myr samples.

4. To identify previously unknown, young, solar analog members of Sco-Cen spectroscopically.

5. To investigate possible substructure in Sco-Cen by evaluating the spatial distribution of ages and the implications for the formation of Sco-Cen.

Do the observed mean ages and age spreads in Sco-Cen indicate star formation is a "slow" process over many Myr or did it take place in less than a crossing time?

What constraints can we place on the planet formation timescale from the census of circumstellar disks in Sco-Cen?

2 A Revised Age for Upper Scorpius and The Star-Formation History Among the F-Type Members of the Scorpius-Centaurus OB Association[1]

2.1 Introduction and Background

Embedded clusters hosting massive stars dominate the star formation of the galaxy (Lada & Lada, 2003), and OB associations appear to be the unbound "fossils" of dissolved embedded clusters. Subgroups within OB associations are thought to be an approximately "coeval" stellar population (e.g., Briceño et al., 2007), sharing a common age, chemical abundance and velocity. Ages of stellar populations are a critical key to determining the evolutionary timescales of various stages of circumstellar

[1]This chapter has been published previously as Pecaut, Mamamjek & Bubar 2012, ApJ, 746, 154

disk evolution and, together with the accretion disk fraction, constrain planet formation timescales (e.g., Chen et al., 2011; Mamajek, 2009). In addition, the estimated masses for very low-mass companions to members of the stellar population depend critically on the assumed age (e.g., Lafrenière et al., 2008; Ireland et al., 2011). It is therefore important to estimate a consistent age for the stellar population so it can be used with confidence for such calculations, and to periodically test this derived age with constantly improving observational data against modern theoretical evolutionary models.

In this chapter, we explore the F-type ($\sim$1.2–1.7 $M_{\odot}$ for ages $\sim$10-15 Myr) stars of Scorpius-Centaurus (Sco-Cen), the nearest OB association (Preibisch & Mamajek, 2008). Sco-Cen consists of three subgroups: Upper Scorpius (US), Upper Centaurus-Lupus (UCL), and Lower Centaurus-Crux (LCC), with mean distances of 145pc, 140pc and 118pc, respectively (de Zeeuw et al., 1999). As the nearest site of recent massive star formation, the stellar membership of Sco-Cen offers important samples of young stars for understanding circumstellar disk evolution across the mass spectrum.

Ages for the Sco-Cen subgroups have been determined primarily from the main sequence turn-off and the low-mass pre-main sequence population combining H-R diagram positions with theoretical evolutionary tracks. For the high-mass stars, this has been performed most recently for UCL and LCC by Mamajek et al. (2002), obtaining ages $\sim$17 Myr and $\sim$16 Myr, respectively. The most recent published age-dating of the massive stars of US was performed by de Geus et al. (1989), obtaining an age of $\sim$5 Myr using the evolutionary tracks of Maeder (1981) and corroborated by Preibisch et al. (2002).

Our goal in this chapter is to explore the star-formation history and accretion disk fraction of the F-type members of three subgroups of Scorpius-Centaurus: Upper Scorpius (US), Upper Centaurus-Lupus (UCL) and Lower Centaurus-Crux (LCC). Specif-

ically, we have employed the kinematically-selected *Hipparcos* sample from de Zeeuw et al. (1999) and have 1) placed them on a theoretical H-R diagram, 2) used published evolutionary tracks to obtain ages and masses, 3) compared the star-formation history of the F-type stars with previous results (Mamajek et al., 2002; Preibisch et al., 2002), and 4) estimated the spectroscopic accretion disk fraction to constrain the disk dispersal timescale for intermediate mass stars.

2.2 Sample Selection

Our sample of Sco-Cen F-stars was taken from the kinematic analysis by de Zeeuw et al. (1999) which used both a refurbished convergent point method (de Bruijne, 1999a) and the "spaghetti method" (Hoogerwerf & Aguilar, 1999) to identify members based on *Hipparcos* positions, parallax and proper motions. The kinematic selection methods are described in detail in de Zeeuw et al. (1999), but briefly, the selection applied the convergent point method and spaghetti method independently to early-type stars to create a list of "secure" members of the OB association. A kinematic solution is obtained using both methods and the results of this are applied to a broader collection of stars in the *Hipparcos* catalog, with appropriate position, proper motion and distance limits for the particular OB association. Stars selected by both methods are included in their membership lists, and they also provide an estimate of the overall number of interlopers present in the membership list for each subgroup. For our sample (F-type candidate members only) the number of expected interlopers is $\sim$5 in US, $\sim$15 in UCL and $\sim$9 in LCC. Further critical examination of the F-type samples was conducted by Chen et al. (2011).

2.3 Observations and Data

Low-resolution blue (∼3700Å–5200Å) and red (∼5600Å–6900Å) optical spectra were obtained from the SMARTS 1.5m telescope at Cerro Tololo Inter-American Observatory (CTIO). Observations were made in queue mode with the RC spectrograph between February 2009 and December 2009. The blue spectra were obtained with a 600 grooves mm^{-1} grating (designated 26/Ia) blazed at 4450Å and no filter, while the red spectra were taken with a 831 grooves mm^{-1} grating (47/Ib) blazed at 7100Å and GG495 filter. Both setups use a slit width of 110.5μm. One comparison lamp of HeAr and Neon for blue and red, respectively, was taken immediately before three consecutive exposures of each target. The blue spectra have a resolution of 4.3 Å or R ∼1100 at Hβ and the red spectra have a resolution of 3.1 Å or R ∼2100 at Hα.

The data were reduced using Fred Walter's SMARTS RC Spectrograph IDL pipeline[2]. The three object images are median combined, bias-trimmed, overscan- and bias-subtracted, then flat-fielded and wavelength-calibrated. Finally, we normalize the spectra to the continuum with a 6th order spline in preparation for spectral classification.

We have adopted V magnitudes and B-V and V-I_C colors from the *Hipparcos* (Perryman & ESA, 1997) catalog and JHK_S photometry from *2MASS* (Skrutskie et al., 2006). We have taken proper motion data, used to calculate a kinematically improved parallax (more on this in section 2.4.3) from both the revised *Hipparcos* data (van Leeuwen, 2007) and the Tycho-2 (Høg et al., 2000) catalogs. We used revised *Hipparcos* data if the fit obtained is that for a single star (i.e., a five-parameter solution with no peculiarities). Otherwise we use the long-baseline proper motions from the Tycho-2 catalog. The motivation behind this choice is to use the most

[2]http://www.astro.sunysb.edu/fwalter/SMARTS/smarts_15msched.html#RCpipeline

precise and accurate proper motion data to calculate the most accurate kinematic parallax possible. The presence of a companion or other peculiarities present in the astrometric solution could significantly influence the detected proper motions if a three-year baseline is used, as with the *Hipparcos* data, whereas the longer baseline proper motions from the Tycho-2 catalog should be less affected. Our input data are listed in Table 2.1.

Table 2.1. Input Observables For Sco-Cen Candidate Members

HIP	Group	2MASS	$\mu_{\alpha*}$ (mas yr^{-1})	μ_{δ} (mas yr^{-1})	V (mag)	B-V (mag)	J (mag)	H (mag)	K_S (mag)	PM Ref.
55334	LCC	11195276-7037065	-43.28±0.66	4.41±0.58	8.14	0.413±0.004	7.319±0.024	7.153±0.027	7.084±0.021	H
56227	LCC	11313495-6743545	-41.49±0.61	-3.09±0.51	8.34	0.316±0.017	7.779±0.027	7.683±0.036	7.612±0.021	H
56673	LCC	11371464-6940272	-42.40±1.30	-5.20±1.30	6.62	0.518±0.006	5.688±0.024	5.459±0.024	5.326±0.023	T
57595	LCC	11482700-5409185	-27.60±2.00	-4.50±1.90	9.45	0.475±0.024	8.512±0.027	8.285±0.047	8.215±0.024	T
57950	LCC	11530799-5643381	-38.41±0.71	-10.37±0.58	8.26	0.401±0.016	7.467±0.024	7.312±0.027	7.276±0.027	H
58075	LCC	11543559-5443572	-29.38±0.83	-7.05±0.82	9.02	0.418±0.019	8.228±0.056	7.997±0.047	7.925±0.027	H
58146	LCC	11552884-6211471	-34.95±0.46	-4.51±0.39	7.86	0.391±0.012	7.051±0.020	6.914±0.024	6.833±0.027	H
58167	LCC	11554354-5410506	-36.17±0.73	-8.56±0.62	8.30	0.404±0.013	7.473±0.024	7.361±0.051	7.284±0.020	H
58220	LCC	11562655-5849168	-37.38±0.74	-8.22±0.58	8.48	0.443±0.013	7.672±0.021	7.490±0.034	7.390±0.023	H
58528	LCC	12000940-5707021	-38.71±0.74	-9.28±0.62	8.54	0.484±0.018	7.707±0.029	7.480±0.047	7.423±0.029	H
58899	LCC	12044446-5221156	-36.98±0.74	-11.46±0.70	8.41	0.416±0.012	7.597±0.018	7.421±0.034	7.346±0.033	H
59084	LCC	12070066-5941408	-29.18±0.77	-13.38±0.67	8.64	0.230±0.015	7.932±0.023	7.775±0.026	7.710±0.021	H
59481	LCC	12115882-5046124	-33.35±0.71	-11.01±0.70	8.48	0.426±0.011	7.704±0.030	7.564±0.047	7.508±0.021	H
59603	LCC	12132235-5653356	-33.18±0.90	-7.01±0.77	8.56	0.425±0.014	7.699±0.019	7.520±0.033	7.433±0.031	H
59693	LCC	12142864-4736461	-27.43±0.98	-7.27±0.75	9.70	0.542±0.030	8.632±0.024	8.360±0.034	8.300±0.023	H
59716	LCC	12145071-5547235	-37.40±1.80	-10.70±1.80	8.45	0.480±0.014	7.516±0.019	7.357±0.034	7.280±0.024	T
59764	LCC	12151855-6325301	-36.66±0.79	-10.32±0.66	8.43	0.605±0.016	7.246±0.026	6.960±0.027	6.850±0.021	H
59781	LCC	12152822-6232207	-20.00±1.90	0.40±1.60	8.84	0.573±0.015	7.821±0.030	7.538±0.033	7.504±0.027	T
59960	LCC	12175319-5558319	-38.79±0.58	-12.21±0.56	7.80	0.458±0.003	6.946±0.030	6.759±0.038	6.683±0.026	H
60205	LCC	12204420-5215249	-25.33±1.37	-8.38±1.30	10.06	0.521±0.042	9.120±0.023	8.868±0.025	8.827±0.022	H

Table 2.1 (cont'd)

HIP	Group	2MASS	$\mu_{\alpha*}$ (mas yr^{-1})	μ_{δ} (mas yr^{-1})	V (mag)	B-V (mag)	J (mag)	H (mag)	K_S (mag)	PM Ref.
60245	LCC	12211172-4803192	-27.94±0.69	-8.54±0.56	8.90	0.387±0.014	8.165±0.023	8.015±0.038	8.003±0.038	H
60348	LCC	12222484-5101343	-35.30±1.20	-11.70±1.10	8.80	0.490±0.014	7.950±0.023	7.759±0.038	7.671±0.021	T
60513	LCC	12241829-5858352	-28.77±0.70	-12.50±0.59	8.52	0.414±0.014	7.687±0.023	7.498±0.047	7.457±0.026	H
60567	LCC	12245491-5200157	-28.72±1.43	-8.87±1.06	9.77	0.541±0.028	8.698±0.029	8.469±0.044	8.386±0.033	H
61049	LCC	12304626-5811168	-38.21±0.78	-12.72±0.72	8.59	0.518±0.013	7.465±0.021	7.189±0.024	7.072±0.024	H
61086	LCC	12311262-5141497	-24.20±2.40	2.60±2.30	10.57	0.441±0.069	9.836±0.023	9.729±0.025	9.653±0.019	T
61087	LCC	12311264-6154315	-35.53±0.66	-12.45±0.54	8.00	0.504±0.010	7.012±0.021	6.819±0.027	6.740±0.024	H
62032	LCC	12425487-5049000	-26.30±0.94	-8.01±0.87	8.74	0.345±0.016	8.054±0.019	7.925±0.051	7.896±0.024	H
62056	LCC	12430803-5028125	-29.40±1.88	-7.43±1.39	10.48	0.523±0.067	9.453±0.023	9.205±0.022	9.138±0.019	H
62134	LCC	12440192-5330205	-30.30±0.93	-9.96±0.81	8.62	0.408±0.015	7.879±0.020	7.730±0.027	7.708±0.026	H
62171	LCC	12442659-5420480	-34.18±0.97	-12.97±0.83	8.90	0.445±0.018	8.048±0.027	7.828±0.053	7.748±0.024	H
62427	LCC	12473870-5824567	-29.97±0.94	-8.15±0.70	9.28	0.454±0.023	8.363±0.026	8.172±0.036	8.122±0.029	H
62428	LCC	12473920-5817511	-33.25±0.42	-14.18±0.33	6.95	0.261±0.005	6.418±0.021	6.376±0.031	6.294±0.020	H
62431	LCC	12474180-5825558	-30.20±1.80	-4.30±1.40	8.02	0.379±0.009	7.250±0.021	7.084±0.038	6.987±0.029	T
62657	LCC	12501971-4951488	-36.61±0.86	-16.47±0.59	8.91	0.502±0.014	8.002±0.023	7.830±0.057	7.717±0.024	H
62674	LCC	12503322-4730552	-26.31±1.30	-11.52±0.95	10.27	0.420±0.020	9.460±0.024	9.321±0.023	9.294±0.023	H
62677	LCC	12503583-6805288	-29.70±1.90	-15.20±1.90	9.36	0.535±0.030	8.314±0.019	8.155±0.033	8.109±0.025	T
63022	LCC	12545378-5102499	-29.78±0.93	-10.69±0.88	9.77	0.402±0.029	9.050±0.021	8.902±0.022	8.852±0.019	H
63041	LCC	12550391-6338267	-39.46±0.60	-11.97±0.57	8.05	0.383±0.004	7.339±0.032	7.210±0.031	7.137±0.031	H
63272	LCC	12575777-5236546	-34.24±0.63	-13.67±0.50	8.40	0.351±0.011	7.684±0.024	7.557±0.049	7.456±0.016	H

Table 2.1 (cont'd)

HIP	Group	2MASS	$\mu_{\alpha*}$ (mas yr^{-1})	μ_{δ} (mas yr^{-1})	V (mag)	B-V (mag)	J (mag)	H (mag)	K_S (mag)	PM Ref.
63435	LCC	12595641-5054350	-30.13±0.88	-9.20±0.74	9.21	0.489±0.018	8.239±0.023	8.001±0.031	7.988±0.033	H
63439	LCC	12595987-5023224	-28.60±1.12	-12.37±0.55	9.14	0.413±0.018	8.278±0.023	8.145±0.051	8.039±0.021	H
63527	LCC	13010436-5308084	-30.64±0.51	-16.81±0.41	7.79	0.358±0.015	7.055±0.018	6.938±0.038	6.860±0.017	H
63836	LCC	13045944-4723485	-31.16±0.92	-17.66±0.64	9.00	0.447±0.023	8.090±0.026	7.892±0.036	7.868±0.029	H
63886	LCC	13053261-5832078	-38.09±0.76	-16.39±0.63	8.15	0.404±0.001	7.387±0.023	7.297±0.040	7.223±0.027	H
63975	LCC	13063577-4602018	-33.50±2.00	-18.30±1.90	7.48	0.405±0.021	6.725±0.026	6.594±0.027	6.489±0.024	T
64044	LCC	13073350-5254198	-32.43±0.96	-19.08±0.69	8.83	0.540±0.014	7.823±0.029	7.614±0.038	7.513±0.021	H
64184	LCC	13091620-6018300	-40.04±0.56	-19.31±0.50	8.20	0.445±0.015	7.403±0.019	7.226±0.023	7.163±0.031	H
64316	LCC	13105627-5147063	-26.41±1.32	-11.09±1.39	10.19	0.493±0.055	9.297±0.027	9.072±0.023	9.012±0.021	H
64322	LCC	13105901-6205157	-26.86±0.67	-12.75±0.61	8.23	0.436±0.015	7.419±0.026	7.250±0.049	7.194±0.031	H
64877	LCC	13175541-6100388	-38.32±0.69	-16.45±0.69	8.47	0.456±0.015	7.622±0.032	7.411±0.036	7.408±0.031	H
64995	LCC	13191952-5928202	-33.53±0.62	-17.81±0.56	8.23	0.398±0.015	7.504±0.023	7.385±0.036	7.337±0.023	H
65136	LCC	13205161-4843196	-26.57±0.78	-16.23±0.68	9.23	0.391±0.020	8.519±0.030	8.421±0.069	8.326±0.024	H
65617	LCC	13271219-5938142	-27.73±1.19	-13.03±0.91	9.60	0.549±0.019	8.642±0.021	8.398±0.026	8.360±0.023	H
65875	LCC	13300897-5829043	-31.32±0.80	-18.64±0.63	8.08	0.498±0.015	7.166±0.023	6.973±0.040	6.897±0.029	H
66285	LCC	13350807-5821593	-33.80±1.70	-13.40±1.30	8.34	0.533±0.003	7.316±0.021	7.068±0.036	7.036±0.024	T
67068	LCC	13444395-4917577	-28.64±0.83	-21.77±0.65	8.45	0.401±0.015	7.686±0.029	7.520±0.029	7.475±0.029	H
67230	LCC	13463539-6204096	-29.97±0.60	-20.59±0.66	8.03	0.474±0.007	7.136±0.027	6.931±0.027	6.888±0.021	H
67428	LCC	13490922-5413422	-22.29±1.06	-17.72±0.91	8.91	0.520±0.018	7.938±0.024	7.713±0.042	7.631±0.023	H
67497	UCL	13495450-5014238	-29.34±0.59	-20.63±0.50	8.40	0.377±0.012	7.708±0.026	7.568±0.049	7.516±0.024	H

Table 2.1 (cont'd)

HIP	Group	2MASS	$\mu_{\alpha*}$ (mas yr^{-1})	μ_{δ} (mas yr^{-1})	V (mag)	B-V (mag)	J (mag)	H (mag)	K_S (mag)	PM Ref.
67957	UCL	13550129-5045020	-24.64±1.11	-16.06±0.82	9.23	0.592±0.024	8.050±0.020	7.763±0.036	7.658±0.033	H
67970	UCL	13550999-5044429	-27.18±0.87	-19.51±0.65	8.70	0.427±0.018	7.874±0.024	7.695±0.046	7.676±0.020	H
68335	UCL	13591805-5153342	-27.67±0.60	-22.13±0.51	8.43	0.489±0.013	7.528±0.029	7.325±0.049	7.215±0.026	H
68534	LCC	14014704-6118459	-12.20±1.70	-20.00±1.70	9.32	0.400±0.495	8.421±0.020	8.225±0.024	8.168±0.020	T
69291	UCL	14105961-3616016	-24.71±0.87	-20.29±0.77	8.61	0.411±0.015	7.849±0.026	7.729±0.044	7.666±0.018	H
69327	UCL	14111998-5437560	-33.70±0.79	-26.23±0.61	8.54	0.348±0.014	7.868±0.021	7.746±0.031	7.705±0.020	H
69720	UCL	14161698-5349021	-27.15±0.81	-17.69±0.79	8.81	0.391±0.017	8.048±0.021	7.905±0.034	7.856±0.020	H
70350	UCL	14233787-4357426	-29.41±0.75	-29.20±0.72	8.13	0.569±0.015	7.006±0.023	6.723±0.031	6.680±0.021	H
70376	UCL	14235639-5029585	-28.10±2.00	-18.10±1.80	9.20	0.662±0.031	8.041±0.020	7.718±0.026	7.661±0.021	T
70558	UCL	14255851-4449232	-21.35±1.10	-17.16±0.89	9.06	0.394±0.029	8.334±0.029	8.155±0.029	8.128±0.027	H
70689	UCL	14273044-5231304	-30.80±0.72	-24.32±0.88	8.53	0.373±0.015	7.802±0.024	7.622±0.059	7.510±0.023	H
70833	UCL	14290715-4321427	-28.98±0.94	-20.16±1.04	8.82	0.423±0.017	8.020±0.023	7.841±0.040	7.787±0.020	H
71023	UCL	14313339-4445019	-22.50±1.19	-17.76±0.80	8.94	0.394±0.019	8.185±0.027	8.085±0.046	7.974±0.024	H
71767	UCL	14404593-4247063	-16.74±1.08	-20.68±1.32	9.02	0.496±0.023	8.096±0.023	7.834±0.049	7.770±0.023	H
72033	UCL	14440435-4059223	-20.25±1.35	-21.30±1.34	9.17	0.635±0.035	8.024±0.035	7.743±0.036	7.578±0.017	H
72099	UCL	14445687-3422537	-16.38±1.97	-20.16±1.68	9.66	0.540±0.040	8.651±0.018	8.426±0.024	8.397±0.025	H
72164	UCL	14453753-4001493	-18.10±1.70	-13.40±1.60	8.86	0.433±0.107	8.222±0.021	8.105±0.059	7.986±0.031	T
73666	UCL	15033194-3122343	-27.23±0.80	-27.60±0.63	7.94	0.534±0.015	6.900±0.021	6.724±0.029	6.641±0.029	H
73667	UCL	15033198-4035230	-20.80±1.40	-12.60±1.20	8.82	0.471±0.018	7.919±0.029	7.698±0.034	7.673±0.027	T
73742	UCL	15042588-4758374	-20.57±0.79	-26.96±0.78	8.61	0.589±0.018	7.517±0.020	7.263±0.021	7.216±0.017	H

Table 2.1 (cont'd)

HIP	Group	2MASS	$\mu_{\alpha*}$ (mas yr^{-1})	μ_{δ} (mas yr^{-1})	V (mag)	B-V (mag)	J (mag)	H (mag)	K_S (mag)	PM Ref.
73913	UCL	15061795-3524222	-19.63±0.88	-19.83±0.67	8.71	0.340±0.015	8.003±0.023	7.838±0.040	7.826±0.036	H
74499	UCL	15132796-3308502	-25.94±1.06	-27.75±0.87	8.77	0.461±0.024	7.878±0.023	7.732±0.051	7.651±0.024	H
74772	UCL	15165338-4934175	-13.70±1.70	-18.91±1.57	9.82	0.435±0.048	8.894±0.026	8.772±0.024	8.687±0.020	H
74865	UCL	15175611-3028414	-22.19±1.34	-28.20±0.98	8.89	0.511±0.047	8.064±0.020	7.901±0.044	7.808±0.021	H
74959	UCL	15190542-3621440	-24.59±1.29	-25.59±1.24	9.37	0.469±0.026	8.393±0.018	8.223±0.033	8.154±0.029	H
75367	UCL	15240425-4109416	-21.28±1.50	-18.57±1.18	10.26	0.427±0.067	9.118±0.021	8.888±0.025	8.825±0.019	H
75459	UCL	15245612-3730055	-15.10±1.30	-35.20±1.30	8.51	0.500±0.495	7.692±0.019	7.489±0.033	7.450±0.024	T
75480	UCL	15250939-2634310	-21.79±0.99	-31.31±0.80	8.33	0.404±0.018	7.566±0.024	7.433±0.042	7.376±0.026	H
75491	UCL	15251605-3809286	-20.12±0.96	-23.34±0.83	8.45	0.416±0.017	7.622±0.021	7.473±0.057	7.431±0.026	H
75683	UCL	15274232-3614131	-21.56±2.34	-25.34±1.91	9.47	0.473±0.015	8.608±0.030	8.414±0.036	8.374±0.024	H
75824	UCL	15292309-4009499	-19.37±1.17	-17.33±1.05	8.81	0.465±0.017	7.958±0.023	7.763±0.033	7.770±0.027	H
75891	UCL	15300427-4107101	-19.78±1.03	-25.70±0.97	8.62	0.437±0.016	7.793±0.024	7.608±0.024	7.566±0.021	H
75933	UCL	15303404-3829463	-22.77±0.94	-19.28±0.92	8.91	0.481±0.015	7.959±0.024	7.771±0.047	7.719±0.027	H
76084	UCL	15322013-3108337	-18.87±0.98	-21.85±0.89	8.62	0.446±0.001	7.764±0.026	7.562±0.031	7.507±0.027	H
76457	UCL	15365348-3810511	-25.70±1.20	-33.90±1.30	8.18	0.396±0.015	7.454±0.024	7.299±0.023	7.234±0.017	T
76501	UCL	15372791-3229060	-22.85±1.27	-28.98±1.10	8.62	0.501±0.019	7.722±0.024	7.570±0.059	7.516±0.023	H
76875	UCL	15415321-3453199	-21.26±1.25	-27.76±1.05	8.37	0.397±0.006	7.606±0.019	7.471±0.038	7.410±0.023	H
77038	UCL	15434763-3528298	-17.23±1.60	-22.63±1.27	9.15	0.478±0.023	8.223±0.024	8.028±0.031	7.918±0.029	H
77432	UCL	15482478-4237049	-16.36±1.19	-30.31±1.02	8.96	0.434±0.020	8.112±0.019	7.939±0.051	7.872±0.027	H
77502	UCL	15493198-3115396	-14.33±1.09	-21.90±0.94	8.89	0.444±0.021	8.088±0.029	7.927±0.031	7.874±0.029	H

Table 2.1 (cont'd)

HIP	Group	2MASS	$\mu_{\alpha*}$ (mas yr^{-1})	μ_{δ} (mas yr^{-1})	V (mag)	B-V (mag)	J (mag)	H (mag)	K_S (mag)	PM Ref.
77520	UCL	15493963-3846391	-16.02±1.75	-25.33±1.29	9.25	0.440±0.015	8.324±0.027	8.131±0.034	7.996±0.026	H
77713	UCL	15515975-3449414	-20.73±1.32	-19.13±1.38	9.15	0.450±0.024	8.322±0.024	8.160±0.033	8.113±0.021	H
77780	UCL	15525514-4548032	-27.80±1.55	-29.64±1.14	9.13	0.590±0.020	8.176±0.019	7.969±0.024	7.914±0.024	H
77813	US	15532089-1923535	-10.88±1.56	-27.39±1.22	9.25	0.739±0.020	7.782±0.026	7.418±0.049	7.302±0.024	H
78043	UCL	15560561-3653345	-18.60±1.66	-24.26±1.50	8.97	0.474±0.020	8.153±0.021	7.974±0.042	7.940±0.020	H
78233	US	15582930-2124039	-7.89±1.51	-20.75±1.17	9.06	0.513±0.020	7.994±0.021	7.811±0.046	7.690±0.033	H
78555	UCL	16021853-3516117	-15.50±1.26	-30.86±0.97	8.64	0.387±0.018	7.926±0.023	7.816±0.047	7.734±0.027	H
78663	US	16033342-3008133	-14.49±1.18	-23.37±1.05	8.91	0.496±0.020	7.973±0.026	7.784±0.047	7.702±0.024	H
78881	UCL	16060937-3802180	-14.90±1.30	-26.30±1.70	8.03	0.523±0.015	7.083±0.019	6.881±0.034	6.790±0.018	T
78977	US	16071778-2203364	-10.59±1.34	-25.74±1.00	8.70	0.654±0.022	7.543±0.027	7.146±0.047	7.047±0.031	H
79054	US	16081050-2351024	-12.67±0.96	-19.71±0.83	9.16	0.501±0.026	8.149±0.024	7.909±0.040	7.828±0.024	H
79083	US	16083514-2045296	-9.28±1.61	-24.61±1.04	8.41	0.605±0.020	7.094±0.030	6.773±0.042	6.677±0.026	H
79097	US	16084366-2522367	-13.28±1.01	-22.78±0.77	8.76	0.520±0.019	7.601±0.027	7.328±0.042	7.254±0.026	H
79258	US	16103595-3245427	-6.00±1.20	-18.97±1.02	9.32	0.475±0.028	8.433±0.026	8.228±0.034	8.206±0.034	H
79288	US	16105511-2531214	-11.44±0.99	-25.71±0.77	8.97	0.463±0.020	8.081±0.023	7.949±0.031	7.882±0.020	H
79369	US	16115551-2106179	-7.38±1.73	-22.49±1.29	8.97	0.489±0.020	7.855±0.021	7.652±0.038	7.562±0.026	H
79516	UCL	16133433-4549035	-20.06±1.18	-28.84±1.18	8.91	0.458±0.019	8.021±0.029	7.851±0.046	7.792±0.024	H
79606	US	16144016-2014030	-17.28±1.49	-28.79±1.12	9.14	0.755±0.020	7.526±0.029	7.235±0.051	7.072±0.023	H
79643	US	16150927-2345348	-8.27±2.06	-23.27±1.19	9.53	0.568±0.015	8.363±0.029	8.146±0.049	8.028±0.018	H
79644	US	16151045-2207099	-9.57±1.96	-21.07±1.44	10.20	0.742±0.058	8.897±0.021	8.658±0.049	8.539±0.025	H

Table 2.1 (cont'd)

HIP	Group	2MASS	$\mu_{\alpha*}$ (mas yr^{-1})	μ_{δ} (mas yr^{-1})	V (mag)	B-V (mag)	J (mag)	H (mag)	K_S (mag)	PM Ref.
79673	UCL	16153714-4138585	-20.46±1.15	-28.03±1.12	8.84	0.410±0.015	8.047±0.024	7.904±0.024	7.839±0.033	H
79710	UCL	16160384-4904293	-19.85±1.16	-30.60±0.83	8.42	0.358±0.017	7.774±0.021	7.648±0.029	7.605±0.026	H
79742	UCL	16162838-3844123	-17.12±1.73	-30.21±1.52	9.16	0.492±0.028	8.275±0.018	8.061±0.038	8.065±0.016	H
79908	UCL	16183856-3839117	-25.21±1.61	-34.60±1.29	9.05	0.601±0.021	8.010±0.020	7.769±0.047	7.689±0.024	H
79910	US	16183914-2135341	-10.91±1.46	-25.94±1.30	9.00	0.569±0.020	7.838±0.021	7.612±0.031	7.542±0.023	H
79977	US	16192923-2124132	-10.93±1.09	-26.24±0.98	9.09	0.492±0.020	8.062±0.019	7.854±0.031	7.800±0.024	H
80586	US	16271252-2711219	-14.00±1.50	-22.80±1.40	8.20	0.473±0.001	7.419±0.019	7.270±0.046	7.193±0.026	T
80663	UCL	16280830-4654043	-9.49±2.57	-20.12±2.20	10.20	0.519±0.043	9.028±0.021	8.813±0.023	8.742±0.021	H
80896	US	16311105-2959523	-15.26±1.49	-25.40±0.92	8.53	0.433±0.015	7.693±0.019	7.548±0.063	7.452±0.021	H
80921	UCL	16312848-4455439	-11.12±2.15	-20.32±1.88	10.31	0.475±0.062	9.039±0.021	8.819±0.024	8.761±0.025	H
81455	US	16381081-2940401	-7.04±1.62	-25.64±1.15	9.15	0.465±0.020	8.256±0.021	8.046±0.034	8.036±0.018	H
81851	US	16430538-2627307	-12.88±1.34	-33.34±0.95	8.44	0.406±0.015	7.693±0.027	7.566±0.044	7.508±0.021	H
82218	US	16474733-1952319	-15.01±1.26	-26.27±0.87	9.05	0.485±0.020	8.057±0.027	7.887±0.036	7.800±0.029	H
82319	US	16491221-2242416	-6.40±1.40	-22.60±1.40	8.89	0.427±0.028	8.050±0.024	7.900±0.031	7.883±0.036	T
82534	US	16521331-2655108	-13.09±1.02	-29.15±0.73	8.30	0.386±0.018	7.600±0.026	7.430±0.040	7.370±0.033	H
82569	UCL	16524171-3845372	-8.30±1.06	-23.00±0.82	8.85	0.461±0.015	7.913±0.029	7.727±0.047	7.558±0.023	H
82747	UCL	16544485-3653185	-8.91±2.11	-29.61±1.51	9.21	0.746±0.040	7.676±0.026	7.059±0.033	6.503±0.020	H
83159	UCL	16594248-3726168	-8.31±1.40	-29.11±1.01	9.02	0.395±0.032	8.148±0.026	7.961±0.031	7.916±0.017	H

Note. — Proper motion references: (H) – van Leeuwen (2007), (T) – Høg et al. (2000)

2.4 Analysis

2.4.1 Spectral Classification

The optical spectra were visually classified using the primary temperature classification spectral features for F-type stars: the strength and profile of the Balmer lines, followed by several metal lines including the G-band at ∼4310Å (Gray & Corbally, 2009). Pre-main sequence stars may exhibit enhanced chromospheric activity, which will weaken the strength of the Balmer absorption lines or they may be seen in emission. In this case a correct classification can still be obtained using the wings of the hydrogen line profiles (Gray, private communication 2010). In addition to the hydrogen lines and the strength and shape of the G-band, we used the strength of the temperature-sensitive Ca I λ4226 and Fe I λ4383 lines to confirm the classifications, although in this temperature region we found them less useful than the G-band.

Stellar spectral classification is greatly facilitated by the ability visually to overlay the object on spectral standards obtained with the same spectral resolution. To that end, we developed a visual classification tool (*sptool*) which presents the object spectrum against two standard star spectra and allows the user to change the comparison standards with a single key stroke. The tool allows the classifier to easily move in temperature and luminosity subtype space by using the arrow keys on the keyboard. The tool, written in Python, is freely available online[3] and only requires a dense grid of spectral standard stars.

To obtain accurate spectral classifications for our program stars, we obtained a grid of optical spectra of F-type MK spectral standard stars with the same telescope and setup as our program stars. Our choices for standards are listed in Table 2.2. Although there are many choices for spectral standards, ours were chosen based on

[3]http://www.pas.rochester.edu/~mpecaut/sptool/

Table 2.2. Spectral Standard Stars Used for Classification

Standard	Spectral Type	B-V (mag)	Instrument/Source	References
HD 158352	A8 V	0.237	SMARTS 1.5m/Rochester	1, A
HD 73450	A9 V	0.251	SMARTS 1.5m/Rochester	2, B
HD 23585	F0 V	0.291	SMARTS 1.5m/NStars	3, C
HD 27397	F0 IV	0.283	SMARTS 1.5m/Stony Brook	3, A
HD 89025	F0 IIIa	0.307	SMARTS 1.5m/Rochester	3, A
HD 167858	F1 V	0.312	SMARTS 1.5m/Rochester	4, A
HD 113139	F2 V	0.368	DSO/NStars	3, A
HD 40535	F2 III-IV	0.333	SMARTS 1.5m/Stony Brook	4, A
HD 26015	F3 V	0.397	SMARTS 1.5m/Stony Brook	3, A
HD 27561	F4 V	0.412	SMARTS 1.5m/Rochester	5, A
HD 27524	F5 V	0.434	SMARTS 1.5m/Rochester	3, A
HD 17918	F5 III	0.457	SMARTS 1.5m/Stony Brook	7, A
HD 30652	F6 IV-V	0.484	SMARTS 1.5m/Stony Brook	3, A
HD 160365	F6 III-IV	0.567	SMARTS 1.5m/Nstars	3, A
HD 222368	F7 V	0.507	SMARTS 1.5m/Stony Brook	3, A
HD 27808	F8 V	0.518	SMARTS 1.5m/Stony Brook	3, A
HD 220657	F8 III	0.617	SMARTS 1.5m/Stony Brook	3, A
HD 10647	F9 V	0.551	SMARTS 1.5m/Stony Brook	6, A
HD 109358	G0 V	0.588	DSO/Nstars	3, A
HD 6903	G0 IIIa	0.697	SMARTS 1.5m/Stony Brook	3, A

Note. — Notes: Spectral Type sources: (1) Cowley et al. (1969); (2) Gray & Corbally (2002); (3) Gray et al. (2001b); (4) Gray & Garrison (1989); (5) Morgan & Hiltner (1965); (6) Gray et al. (2006); (7) Gray (1989); B-V color sources: (A) van Leeuwen (2007); (B) Neckel & Klare (1980); (C) Mermilliod (2006);

a careful consideration of the consistency of previous classifications and accessibility from the SMARTS 1.5m telescope at CTIO.

Unfortunately, A8V and F4V spectral standards do not appear in the literature (e.g. Morgan & Keenan (1973); Gray & Corbally (2009)), and the only A9V standard that we could find in the literature (44 Cet = HR 401; Gray & Garrison (1989)) had several discrepant published spectral types. For subtypes A8V and A9V we adopted a star that had been assigned that spectral class by at least one expert classifier and had colors representative of other stars of the same classification. We adopted the Hyades member HD 27561 as a F4V standard. The star was originally classified as F4V by Morgan & Hiltner (1965), and its Hipparcos B-V color (0.41) is intermediate in color between the F3V and F5V standards classified by Morgan (and retained

as standards by Morgan & Abt (1973), Morgan et al. (1978), and Gray (1989)) – HD 26015 (F3V standard, B-V=0.40) and HD 27524 (F5V standard, B-V=0.434) – both of which are also Hyades. We have confirmed that its spectrum is intermediate between the F3V and F5V standards. For the A8V standard, we adopt the star HD 158352 (HR 6507), which was classified as A8V by Cowley et al. (1969), Abt & Morrell (1995), and as A8Vp by Mora et al. (2001). For the A9V standard, we adopted the Praesepe member HD 73450 (BS Cnc), based on its A9V classifications by Bidelman (1956), Abt (1986), and Gray & Corbally (2002). We verified that the adopted A8V and A9V "standards" had optical spectra that were morphologically intermediate between the A7V and F0V MK standards.

With our visual classification tool and a complete grid of dwarfs, we iteratively classified the 138 program stars at least four times before settling on a final spectral type. We conservatively estimate our classifications to be correct to within one subtype.

Spectral types for many of our candidate members are available through the Michigan Spectral Survey (Houk & Smith-Moore, 1988; Houk, 1982, 1978; Houk & Cowley, 1975) which allows us to compare directly our newly obtained spectral types with past results from plate surveys. As Figure 2.1 shows, the newly obtained spectral types agree quite well with those obtained in the Michigan Spectral Survey. The average difference is small: 0.5 ± 1.1 (1σ). The Houk classifications are based on comparison to the "MK" standards from Johnson & Morgan (1953), whereas we have relied heavily on the "revised MK" F-type standards from Morgan et al. (1978, "MK78") (these later types have been adopted by Gray, Garrison, Corbally and collaborators in their surveys). Any systematic differences in the classifications likely come from differences in the choice of standard star, which differ between us and Houk mostly among the earliest and latest F stars.

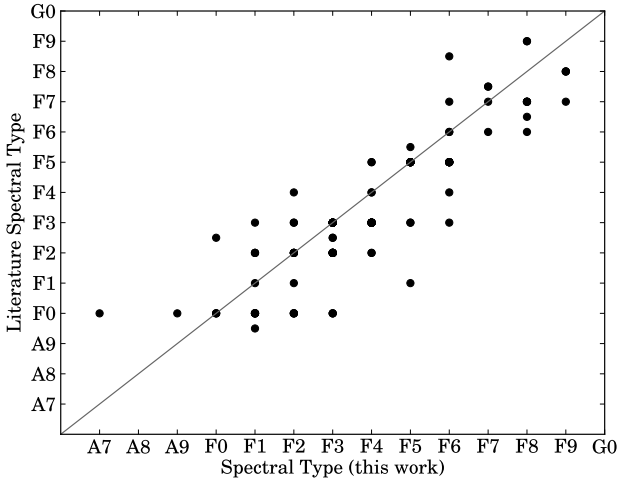

Figure 2.1 Comparison of our newly obtained spectral types with those available in the literature: Houk & Smith-Moore (1988); Houk (1982); Houk & Cowley (1975); Houk (1978). A line with unit slope is plotted to guide the eye.

2.4.2 Extinction

To calculate individual extinctions in the Johnson-Cousins and 2MASS bands, we constructed a modern spectral type-intrinsic color calibration with B-V, V-I_c, V-K_S, J-H, and H-K_S colors using samples of nearby dwarf stars from the Hipparcos catalog (Perryman & ESA, 1997), normal cool dwarfs from Neill Reid's compiled photometric catalog for stars in the 3rd Catalog of Nearby Stars[4], and a cross-matched catalog combining the new Gliese-2MASS catalog (Stauffer et al., 2010) and the catalog of average Johnson UBV photometry from Mermilliod (2006). For the Hipparcos sample, only dwarfs with luminosity class "V" and M_V within 1 mag of the Wright (2005) main sequence were selected, and only stars with parallaxes greater than 13.33 mas and relative parallax error less than 12.5% were included (d < 75 pc), to select those stars ostensibly within the "Local Bubble" which has negligible reddening. An intrinsic

[4]http://www.stsci.edu/~inr/cmd.html

Table 2.3. Intrinsic Colors of Dwarfs and Adopted T_{eff}, BC Values

Spectral Type	U-B (mag)	B-V (mag)	V-I_C (mag)	V-J (mag)	V-H (mag)	V-K_S (mag)	BC_V (mag)	T_{eff} (K)
A0V	-0.014	0.000	0.004	0.046	0.014	0.042	-0.17	9550
A1V	0.033	0.043	0.044	0.094	0.070	0.101	-0.11	9200
A2V	0.063	0.074	0.092	0.167	0.158	0.192	-0.05	8760
A3V	0.077	0.090	0.110	0.197	0.196	0.231	-0.02	8550
A4V	0.097	0.140	0.165	0.296	0.318	0.355	0.00	8270
A5V	0.100	0.160	0.187	0.334	0.366	0.404	0.01	8080
A6V	0.098	0.170	0.198	0.355	0.391	0.429	0.02	8000
A7V	0.091	0.210	0.242	0.433	0.488	0.528	0.04	7800
A8V	0.082	0.253	0.291	0.512	0.589	0.632	0.04	7500
A9V	0.080	0.255	0.294	0.517	0.595	0.638	0.04	7440
F0V	0.053	0.294	0.339	0.589	0.687	0.732	0.03	7200
F1V	0.013	0.343	0.396	0.678	0.802	0.850	0.03	7030
F2V	-0.008	0.374	0.432	0.735	0.875	0.925	0.01	6810
F3V	-0.016	0.389	0.449	0.763	0.910	0.961	0.01	6720
F4V	-0.026	0.412	0.476	0.806	0.965	1.017	0.00	6640
F5V	-0.029	0.438	0.506	0.852	1.025	1.079	0.00	6510
F6V	-0.021	0.484	0.553	0.929	1.128	1.185	-0.01	6340
F7V	-0.012	0.510	0.579	0.971	1.184	1.244	-0.02	6240
F8V	0.000	0.530	0.599	1.004	1.229	1.290	-0.03	6150
F9V	0.014	0.552	0.620	1.040	1.277	1.340	-0.04	6040
G0V	0.049	0.588	0.656	1.097	1.355	1.421	-0.05	5940
G1V	0.067	0.604	0.672	1.123	1.390	1.458	-0.06	5880
G2V	0.120	0.642	0.706	1.185	1.473	1.545	-0.07	5780
G3V	0.152	0.661	0.722	1.217	1.516	1.590	-0.08	5700
G4V	0.175	0.674	0.733	1.239	1.546	1.621	-0.10	5640
G5V	0.185	0.680	0.738	1.249	1.559	1.635	-0.10	5620
G6V	0.229	0.704	0.759	1.290	1.614	1.693	-0.11	5580
G7V	0.243	0.713	0.766	1.303	1.632	1.712	-0.12	5520
G8V	0.284	0.737	0.786	1.344	1.686	1.768	-0.13	5490
G9V	0.358	0.777	0.820	1.409	1.774	1.861	-0.17	5340

color sequence was constructed for B through M-type stars, and the adopted intrinsic colors for a given dwarf spectral subtype were adopted based on a best B-V color[5]. The stellar intrinsic colors we adopt are in Table 2.3.

Many of the stars in our sample had very low extinction, and where we obtained a non-physical negative extinction we set the extinction to zero. We used a total-to-selective extinction of R_V=3.1 and calculated A_V using the color excesses E(B-V), E(V-I_c), E(V-J), E(V-H) and E(V-K_S) with the extinction ratios A_{I_c}/A_V=0.58, A_J/A_V=0.27, A_H/A_V=0.17, A_{K_S}/A_V=0.11 (Fiorucci & Munari, 2003) to estimate

[5]Detailed notes for each subtype are available in the files listed at http://www.pas.rochester.edu/~emamajek/spt/ or http://www.ctio.noao.edu/~emamajek/spt/

extinctions for each star. We adopted the median A_V with the standard deviation as a conservative estimate of the uncertainty. These are listed in Table 2.4 with our other derived stellar parameters.

Table 2.4. Stellar Parameters for F-type Sco-Cen Members

HIP	Group	Spectral Type	π_{kin} (mas)	EW(Hα) (Å)	A_V (mag)	log(T_{eff}) (dex)	log($L/L_\odot$) (dex)	Mass D08 ($M_\odot$)	Age D08 (Myr)	Mass YY04 ($M_\odot$)	Age YY04 (Myr)	Mass S00 ($M_\odot$)	Age S00 (Myr)	Mass DM97 ($M_\odot$)	Age DM97 (Myr)	Median Mass ($M_\odot$)
55334	LCC	F2V	12.63±0.90	4.7	0.12±0.01	3.833±0.006	0.49±0.06	1.5*	>19	1.5*	>22	1.6*	...	1.5*	>25	1.5
56673	LCC	F5IVe	11.95±0.90	-1.9	0.20±0.05	3.814±0.011	1.18±0.07	2.0	5	2.0	5	2.0	7	2.0	5	2.0
57950	LCC	F3V	10.79±0.73	4.9	0.04±0.01	3.827±0.005	0.55±0.06	1.4	23	1.4	27	1.6*	>20	1.5*	>14	1.5
58075	LCC	F2V	8.13±0.57	5.1	0.14±0.04	3.833±0.006	0.53±0.06	1.5*	>14	1.5*	>15	1.6*	>30	1.5*	>17	1.5
58146	LCC	F3V	9.67±0.65	5.1	0.04±0.02	3.827±0.005	0.80±0.06	1.5	13	1.6	13	1.6	13	1.6	10	1.6
58167	LCC	F2V	9.96±0.67	5.2	0.09±0.02	3.833±0.006	0.62±0.06	1.5	19	1.5	21	1.6*	>16	1.5	22	1.5
58220	LCC	F4V	10.39±0.71	4.3	0.08±0.04	3.822±0.009	0.51±0.06	1.4	23	1.4	28	1.5*	>22	1.5*	>15	1.5
58528	LCC	F5V	10.68±0.72	4.3	0.04±0.06	3.814±0.011	0.44±0.06	1.4	21	1.4	26	1.5*	>23	1.4*	>15	1.4
58899	LCC	F3V	10.12±0.66	5.1	0.08±0.02	3.827±0.005	0.56±0.06	1.4	21	1.4	24	1.6*	>19	1.5*	>13	1.5
59084	LCC	F1V	8.38±0.58	5.4	0.04±0.20	3.845±0.012	0.61±0.10	1.6*	>12	1.6*	>14	1.6*	>14	1.6*	>12	1.6
59481	LCC	F3V	8.99±0.58	4.9	0.02±0.05	3.827±0.005	0.61±0.06	1.5	15	1.5	18	1.5	40	1.5	18	1.5
59603	LCC	F4V	8.86±0.60	3.9	0.08±0.03	3.822±0.009	0.61±0.06	1.4	16	1.5	17	1.5	24	1.5	16	1.5
59693	LCC	F7IV	7.07±0.49	3.9	0.13±0.04	3.795±0.007	0.38±0.06	1.2	20	1.3	19	1.3	40	1.3	18	1.3
59716	LCC	F5V	10.11±0.79	4.5	0.11±0.02	3.814±0.011	0.55±0.07	1.3	17	1.4	18	1.4	27	1.4	16	1.4
59764	LCC	F8V	10.11±0.68	3.0	0.25±0.05	3.788±0.007	0.63±0.06	1.4	12	1.5	11	1.4	15	1.4	12	1.4
59960	LCC	F5V	10.52±0.67	4.4	0.04±0.02	3.814±0.011	0.75±0.06	1.5	13	1.6	12	1.5	14	1.5	12	1.5
60205	LCC	F7V	6.76±0.54	3.9	0.01±0.03	3.795±0.007	0.23±0.07	1.2	32	1.2	83	1.4*	>62	1.3*	>19	1.3
60245	LCC	F1V	7.23±0.46	5.2	0.10±0.03	3.845±0.012	0.66±0.06	1.5	23	1.5	29	1.6*	>18	1.6*	>13	1.5
60348	LCC	F5V	9.34±0.64	4.3	0.06±0.06	3.814±0.011	0.46±0.07	1.4	18	1.4	22	1.5*	>20	1.4*	>15	1.4

Table 2.4 (cont'd)

HIP	Group	Spectral Type	π_{kin} (mas)	EW(Hα) (Å)	A_V (mag)	log($T_{\rm eff}$) (dex)	log($L/L_\odot$) (dex)	Mass D08 ($M_\odot$)	Age D08 (Myr)	Mass YY04 ($M_\odot$)	Age YY04 (Myr)	Mass S00 ($M_\odot$)	Age S00 (Myr)	Mass DM97 ($M_\odot$)	Age DM97 (Myr)	Median Mass ($M_\odot$)
60513	LCC	F4V	8.05±0.53	5.0	0.04±0.02	3.822±0.009	0.70±0.06	1.4	15	1.6	14	1.5	15	1.5	13	1.5
60567	LCC	F8V	7.54±0.58	3.5	0.09±0.03	3.788±0.007	0.28±0.07	1.2	23	1.2	22	1.4*	>22	1.2	22	1.2
61049	LCC	F8V	10.28±0.66	3.6	0.17±0.12	3.788±0.007	0.52±0.07	1.3	15	1.4	15	1.4	18	1.3	15	1.3
61087	LCC	F6V	9.72±0.63	4.1	0.06±0.01	3.802±0.007	0.75±0.06	1.5	11	1.6	11	1.5	14	1.6	9	1.5
62032	LCC	A9V	6.62±0.45	6.7	0.25±0.02	3.872±0.017	0.85±0.06	1.6	15	1.7	16	1.7	20	1.6	13	1.6
62134	LCC	F2V	7.79±0.51	6.0	0.02±0.05	3.833±0.006	0.68±0.06	1.5	14	1.6	15	1.5	23	1.5	14	1.5
62171	LCC	F3V	8.99±0.58	5.1	0.17±0.03	3.827±0.005	0.50±0.06	1.4	30	1.5*	>15	1.6*	>30	1.5*	>17	1.5
62427	LCC	F5V	7.70±0.52	4.8	0.09±0.03	3.814±0.011	0.45±0.06	1.4	18	1.4	25	1.5*	>23	1.4*	>15	1.4
62431	LCC	F1V	7.42±0.64	6.1	0.13±0.04	3.845±0.012	1.00±0.08	1.6	10	1.7	9	1.7	10	1.7	9	1.7
62657	LCC	F5V	9.59±0.59	4.3	0.13±0.05	3.814±0.011	0.42±0.06	1.3	26	1.3	33	1.5*	>30	1.4*	>16	1.4
62677	LCC	F5IV-V	8.39±0.72	4.3	0.25±0.04	3.814±0.011	0.41±0.08	1.3	29	1.3	43	1.5*	>25	1.4*	>15	1.4
63041	LCC	F1V	10.38±0.65	5.8	0.07±0.04	3.845±0.012	0.67±0.06	1.5	21	1.5	24	1.6*	>16	1.5	23	1.5
63272	LCC	F1V	8.80±0.53	5.6	0.05±0.03	3.845±0.012	0.67±0.05	1.5	21	1.5	25	1.6*	>17	1.5	25	1.5
63435	LCC	F6V	7.35±0.47	4.5	0.04±0.03	3.802±0.007	0.50±0.06	1.3	18	1.4	17	1.4	19	1.3	16	1.3
63439	LCC	F4V	7.35±0.49	4.9	0.04±0.04	3.822±0.009	0.53±0.06	1.4	20	1.4	23	1.5*	>19	1.5*	>14	1.5
63527	LCC	F1V	8.34±0.49	5.4	0.06±0.02	3.845±0.012	0.96±0.05	1.6	10	1.7	10	1.7	11	1.7	9	1.7
63836	LCC	F6V	8.30±0.50	4.4	0.00±0.03	3.802±0.007	0.47±0.05	1.3	19	1.4	18	1.4	28	1.3	17	1.3
63886	LCC	F3V	10.09±0.62	5.1	0.00±0.05	3.827±0.005	0.63±0.06	1.5	15	1.5	15	1.5	25	1.5	17	1.5
63975	LCC	F2V	8.77±0.67	5.1	0.07±0.03	3.833±0.006	1.05±0.07	1.7	8	1.8	8	1.7	9	1.8	8	1.8

Table 2.4 (cont'd)

HIP	Group	Spectral Type	π_{kin} (mas)	EW(Hα) (Å)	A_V (mag)	log($T_{\rm eff}$) (dex)	log($L/L_\odot$) (dex)	Mass D08 ($M_\odot$)	Age D08 (Myr)	Mass YY04 ($M_\odot$)	Age YY04 (Myr)	Mass S00 ($M_\odot$)	Age S00 (Myr)	Mass DM97 ($M_\odot$)	Age DM97 (Myr)	Median Mass ($M_\odot$)
64044	LCC	F6IV	8.89±0.55	3.1	0.14±0.03	3.802±0.007	0.53±0.06	1.3	17	1.4	17	1.4	18	1.4	16	1.4
64184	LCC	F4V	10.84±0.65	5.0	0.02±0.04	3.822±0.009	0.56±0.06	1.4	16	1.4	19	1.5*	>16	1.4	27	1.4
64322	LCC	F2V	7.29±0.46	4.7	0.13±0.03	3.833±0.006	0.93±0.06	1.6	10	1.7	10	1.7	11	1.7	9	1.7
64877	LCC	F4V	10.10±0.61	4.8	0.11±0.04	3.822±0.009	0.55±0.06	1.4	17	1.4	20	1.5*	>17	1.5*	>13	1.5
64995	LCC	F3V	9.11±0.55	5.5	0.00±0.05	3.827±0.005	0.69±0.06	1.5	14	1.6	14	1.5	17	1.5	13	1.5
65136	LCC	F0V	7.12±0.43	6.2	0.19±0.06	3.855±0.010	0.57±0.06	1.6*	>24	1.6*	...	1.7*	...	1.6*	...	1.6
65617	LCC	F6V	7.29±0.50	3.6	0.09±0.06	3.802±0.007	0.37±0.07	1.3	22	1.3	21	1.5*	>19	1.3	27	1.3
65875	LCC	F6V	8.60±0.52	4.1	0.00±0.03	3.802±0.007	0.80±0.05	1.6	10	1.6	10	1.5	12	1.6	9	1.6
67068	LCC	F3V	8.03±0.46	4.7	0.02±0.02	3.827±0.005	0.72±0.05	1.4	14	1.6	14	1.6	15	1.5	13	1.5
67230	LCC	F5V	8.55±0.51	4.4	0.09±0.02	3.814±0.011	0.86±0.05	1.6	11	1.6	11	1.6	12	1.6	9	1.6
67428	LCC	F6IV	6.44±0.42	4.1	0.09±0.02	3.802±0.007	0.76±0.06	1.5	11	1.6	11	1.5	13	1.6	9	1.5
67497	UCL	F2V	9.28±0.65	5.3	0.00±0.03	3.833±0.006	0.61±0.06	1.5	20	1.5	23	1.6*	>16	1.4	37	1.5
67957	UCL	F9V	7.57±0.58	3.6	0.19±0.06	3.781±0.007	0.54±0.07	1.4	13	1.5	12	1.4	17	1.4	13	1.4
67970	UCL	F3V	8.62±0.62	4.2	0.10±0.02	3.827±0.005	0.59±0.06	1.5	16	1.5	19	1.6*	>15	1.4	24	1.5
68335	UCL	F5V	9.13±0.64	3.1	0.13±0.03	3.814±0.011	0.66±0.06	1.4	15	1.5	13	1.5	15	1.5	13	1.5
68534	LCC	F2V	4.89±0.52	5.0	0.23±0.37	3.833±0.006	0.88±0.17	1.6	11	1.6	11	1.6	12	1.6	9	1.6
69291	UCL	F3V	7.58±0.51	5.7	0.00±0.05	3.827±0.005	0.70±0.06	1.5	14	1.6	14	1.6	16	1.5	13	1.5
69720	UCL	F3V	8.27±0.59	5.0	0.00±0.01	3.827±0.005	0.54±0.06	1.4	24	1.4	28	1.6*	>20	1.5*	>14	1.5
70350	UCL	F8V	10.02±0.66	3.2	0.16±0.04	3.788±0.007	0.72±0.06	1.6	10	1.6	10	1.5	13	1.6	9	1.6

Table 2.4 (cont'd)

HIP	Group	Spectral Type	π_{kin} (mas)	EW(Hα) (Å)	A_V (mag)	log(T_{eff}) (dex)	log(L/ $L_\odot$) (dex)	Mass D08 ($M_\odot$)	Age D08 (Myr)	Mass YY04 ($M_\odot$)	Age YY04 (Myr)	Mass S00 ($M_\odot$)	Age S00 (Myr)	Mass DM97 ($M_\odot$)	Age DM97 (Myr)	Median Mass ($M_\odot$)
70376	UCL	F9V	8.28±0.73	3.1	0.24±0.06	3.781±0.007	0.50±0.08	1.3	14	1.4	14	1.3	18	1.3	14	1.3
70558	UCL	F1V	6.63±0.49	5.9	0.12±0.04	3.845±0.012	0.68±0.07	1.5	20	1.5	22	1.6*	>14	1.5	21	1.5
70689	UCL	F2V	9.85±0.68	5.2	0.02±0.04	3.833±0.006	0.51±0.06	1.5*	>17	1.5*	>18	1.6*	...	1.5*	>18	1.5
71023	UCL	F2V	6.90±0.51	5.5	0.05±0.03	3.833±0.006	0.67±0.07	1.5	14	1.6	15	1.5	25	1.5	17	1.5
71767	UCL	F4V	6.28±0.49	4.5	0.26±0.04	3.822±0.009	0.80±0.07	1.5	12	1.6	12	1.6	13	1.6	10	1.6
72033	UCL	F7V	6.92±0.53	2.7	0.29±0.06	3.795±0.007	0.68±0.07	1.5	12	1.5	11	1.5	14	1.4	12	1.5
72099	UCL	F6V	5.98±0.55	4.0	0.13±0.03	3.802±0.007	0.54±0.08	1.3	17	1.4	17	1.4	18	1.4	15	1.4
72164	UCL	F2IV	5.22±0.51	5.5	0.00±0.12	3.833±0.006	0.92±0.10	1.6	11	1.6	10	1.7	11	1.7	9	1.7
73666	UCL	F3IV	8.84±0.56	5.5	0.38±0.03	3.827±0.005	0.98±0.06	1.7	9	1.7	9	1.7	10	1.7	8	1.7
73667	UCL	F4V	5.43±0.47	4.8	0.15±0.02	3.822±0.009	0.96±0.08	1.7	9	1.7	9	1.7	10	1.7	8	1.7
73742	UCL	F9V	8.04±0.54	3.5	0.08±0.02	3.781±0.007	0.70±0.06	1.6	9	1.6	10	1.5	13	1.6	9	1.6
73913	UCL	F1V	6.40±0.43	5.8	0.04±0.03	3.845±0.012	0.82±0.06	1.6	12	1.6	14	1.6	14	1.6	12	1.6
74499	UCL	F4V	8.66±0.57	4.5	0.12±0.02	3.822±0.009	0.56±0.06	1.4	16	1.5	19	1.5*	>16	1.4	25	1.4
74772	UCL	F3V	5.53±0.52	4.6	0.17±0.04	3.827±0.005	0.55±0.08	1.4	22	1.4	25	1.6*	>15	1.5*	>13	1.5
74865	UCL	F4V	8.16±0.55	4.4	0.07±0.12	3.822±0.009	0.55±0.08	1.4	17	1.4	20	1.5*	>15	1.4	39	1.4
74959	UCL	F6V	8.11±0.57	3.9	0.02±0.04	3.802±0.007	0.35±0.06	1.3	23	1.3	24	1.5*	>26	1.3	39	1.3
75367	UCL	F9V	6.44±0.51	3.5	0.11±0.23	3.781±0.007	0.24±0.12	1.1	24	1.2	23	1.4*	>19	1.2	22	1.2
75459	UCL	F3V	8.43±0.60	4.8	0.11±0.11	3.827±0.005	0.69±0.08	1.5	14	1.6	14	1.5	17	1.5	13	1.5
75480	UCL	F2V	8.65±0.55	5.4	0.04±0.03	3.833±0.006	0.71±0.06	1.5	14	1.6	14	1.6	18	1.5	13	1.5

Table 2.4 (cont'd)

HIP	Group	Spectral Type	π_{kin} (mas)	EW(Hα) (Å)	A_V (mag)	log(T_{eff}) (dex)	log(L/ $L_\odot$) (dex)	Mass D08 ($M_\odot$)	Age D08 (Myr)	Mass YY04 ($M_\odot$)	Age YY04 (Myr)	Mass S00 ($M_\odot$)	Age S00 (Myr)	Mass DM97 ($M_\odot$)	Age DM97 (Myr)	Median Mass ($M_\odot$)
75491	UCL	F2V	7.07±0.47	4.3	0.12±0.01	3.833±0.006	0.87±0.06	1.5	12	1.6	12	1.6	12	1.6	9	1.6
75683	UCL	F6V	7.60±0.66	4.5	0.00±0.03	3.802±0.007	0.35±0.08	1.3	23	1.3	23	1.5*	>19	1.3	35	1.3
75891	UCL	F3V	7.47±0.51	5.4	0.12±0.02	3.827±0.005	0.75±0.06	1.5	13	1.6	13	1.6	14	1.5	12	1.5
75933	UCL	F3V	6.71±0.46	4.7	0.26±0.02	3.827±0.005	0.79±0.06	1.5	13	1.6	13	1.6	13	1.5	12	1.5
76084	UCL	F1V	6.56±0.45	5.4	0.30±0.03	3.845±0.012	0.93±0.06	1.6	11	1.7	11	1.7	11	1.7	9	1.7
76457	UCL	F3V	9.73±0.65	5.3	0.00±0.03	3.827±0.005	0.65±0.06	1.5	15	1.5	15	1.5	22	1.5	14	1.5
76501	UCL	F3V	8.39±0.57	5.0	0.19±0.08	3.827±0.005	0.68±0.07	1.5	14	1.6	14	1.5	18	1.5	13	1.5
76875	UCL	F2V	7.96±0.54	5.1	0.04±0.02	3.833±0.006	0.77±0.06	1.5	13	1.6	14	1.6	14	1.5	13	1.6
77038	UCL	F5V	6.48±0.50	4.7	0.12±0.03	3.814±0.011	0.66±0.07	1.4	15	1.5	13	1.5	15	1.5	13	1.5
77432	UCL	F5V	7.84±0.54	4.7	0.00±0.01	3.814±0.011	0.53±0.06	1.3	17	1.4	19	1.4	37	1.4	16	1.4
77502	UCL	F4V	5.94±0.42	4.7	0.00±0.05	3.822±0.009	0.80±0.06	1.5	13	1.6	12	1.6	13	1.6	10	1.6
77520	UCL	F4V	6.83±0.53	4.8	0.16±0.07	3.822±0.009	0.60±0.07	1.4	16	1.5	17	1.5	28	1.5	16	1.5
77713	UCL	F4V	6.28±0.49	5.2	0.03±0.04	3.822±0.009	0.66±0.07	1.4	15	1.5	14	1.5	17	1.5	13	1.5
77780	UCL	F7V	9.33±0.65	3.9	0.00±0.12	3.795±0.007	0.32±0.08	1.2	22	1.3	23	1.4*	>20	1.3	23	1.3
77813	US	F9V	7.97±0.70	3.1	0.59±0.10	3.781±0.007	0.65±0.09	1.5	10	1.5	10	1.4	14	1.5	11	1.5
78043	UCL	F4V	6.95±0.55	5.1	0.04±0.08	3.822±0.009	0.64±0.08	1.4	15	1.5	14	1.5	20	1.5	14	1.5
78233	US	F0IV	5.96±0.56	6.2	0.67±0.04	3.855±0.010	0.99±0.08	1.6	10	1.7	10	1.8	10	1.7	9	1.7
78555	UCL	F1V	7.78±0.52	5.3	0.06±0.04	3.845±0.012	0.68±0.06	1.5	20	1.5	22	1.6*	>14	1.5	20	1.5
78663	US	F6V	7.11±0.59	4.6	0.03±0.02	3.802±0.007	0.65±0.07	1.4	14	1.5	12	1.5	15	1.4	14	1.4

Table 2.4 (cont'd)

HIP	Group	Spectral Type	π_{kin} (mas)	EW(Hα) (Å)	A_V (mag)	log(T_{eff}) (dex)	log(L/ $L_\odot$) (dex)	Mass D08 ($M_\odot$)	Age D08 (Myr)	Mass YY04 ($M_\odot$)	Age YY04 (Myr)	Mass S00 ($M_\odot$)	Age S00 (Myr)	Mass DM97 ($M_\odot$)	Age DM97 (Myr)	Median Mass ($M_\odot$)
78881	UCL	F4V	6.86±0.55	3.9	0.25±0.05	3.822±0.009	1.12±0.07	1.9	7	1.9	7	1.8	8	1.9	7	1.9
78977	US	F8V	7.53±0.64	3.1	0.38±0.08	3.788±0.007	0.83±0.08	1.7	8	1.7	8	1.6	11	1.6	8	1.7
79054	US	F3V	6.24±0.53	5.4	0.35±0.05	3.827±0.005	0.78±0.08	1.5	13	1.6	13	1.6	13	1.5	12	1.5
79083	US	F3V	7.16±0.63	4.2	0.76±0.13	3.827±0.005	1.13±0.09	1.9	7	1.9	7	1.9	8	1.9	7	1.9
79097	US	F4V	6.99±0.57	4.4	0.48±0.12	3.822±0.009	0.90±0.09	1.6	11	1.6	10	1.6	11	1.7	9	1.6
79288	US	F2V	7.50±0.60	5.1	0.21±0.04	3.833±0.006	0.65±0.07	1.5	15	1.5	16	1.5	36	1.5	18	1.5
79369	US	F1V	6.42±0.62	6.2	0.60±0.10	3.845±0.012	0.93±0.09	1.6	11	1.7	11	1.7	11	1.7	9	1.7
79516	UCL	F5V	8.07±0.56	4.0	0.05±0.01	3.814±0.011	0.54±0.06	1.3	17	1.4	18	1.4	29	1.4	16	1.4
79606	US	F8V	9.19±0.79	3.8	0.81±0.14	3.788±0.007	0.65±0.09	1.5	11	1.5	11	1.4	15	1.4	12	1.5
79643	US	F3V	6.63±0.62	4.8	0.56±0.05	3.827±0.005	0.67±0.08	1.5	14	1.5	14	1.5	20	1.5	14	1.5
79644	US	F6V	6.30±0.64	4.1	0.53±0.11	3.802±0.007	0.44±0.10	1.3	20	1.3	19	1.3	39	1.3	18	1.3
79673	UCL	F4V	7.90±0.54	4.3	0.00±0.02	3.822±0.009	0.57±0.06	1.4	16	1.5	19	1.5*	>15	1.4	23	1.4
79710	UCL	F1V	8.45±0.56	5.8	0.00±0.05	3.845±0.012	0.67±0.06	1.5	21	1.5	24	1.6*	>15	1.5	23	1.5
79742	UCL	F6V	7.89±0.59	4.5	0.00±0.05	3.802±0.007	0.45±0.07	1.3	19	1.3	19	1.3	36	1.3	18	1.3
79908	UCL	F8V	9.71±0.67	3.0	0.08±0.07	3.788±0.007	0.35±0.07	1.2	21	1.2	20	1.3	30	1.2	19	1.2
79910	US	F4V	7.70±0.69	4.2	0.49±0.04	3.822±0.009	0.72±0.08	1.4	14	1.6	13	1.6	14	1.5	13	1.5
79977	US	F3V	7.79±0.66	4.6	0.36±0.05	3.827±0.005	0.63±0.08	1.5	15	1.5	15	1.5	27	1.5	17	1.5
80586	US	F5IV-V	7.02±0.65	4.7	0.00±0.10	3.814±0.011	0.93±0.09	1.6	9	1.7	9	1.6	11	1.7	8	1.7
80663	UCL	F1V	5.09±0.61	5.4	0.68±0.09	3.845±0.012	0.67±0.11	1.5	21	1.5	24	1.6*	>11	1.5	23	1.5

Table 2.4 (cont'd)

HIP	Group	Spectral Type	π_{kin} (mas)	EW(Hα) (Å)	A_V (mag)	log(T_{eff}) (dex)	log(L/ $L_\odot$) (dex)	Mass D08 ($M_\odot$)	Age D08 (Myr)	Mass YY04 ($M_\odot$)	Age YY04 (Myr)	Mass S00 ($M_\odot$)	Age S00 (Myr)	Mass DM97 ($M_\odot$)	Age DM97 (Myr)	Median Mass ($M_\odot$)
80896	US	F3V	7.67±0.64	5.3	0.12±0.02	3.827±0.005	0.77±0.07	1.5	13	1.6	13	1.6	13	1.5	12	1.5
80921	UCL	F2IV	5.30±0.55	5.1	0.70±0.21	3.833±0.006	0.61±0.12	1.5	20	1.5	23	1.6*	>12	1.4	30	1.5
81455	US	F5IV-V	7.01±0.61	4.0	0.08±0.02	3.814±0.011	0.58±0.08	1.3	17	1.4	17	1.5	21	1.4	15	1.4
81851	US	F3V	9.61±0.78	5.2	0.00±0.04	3.827±0.005	0.56±0.07	1.4	21	1.4	24	1.7†	>16	1.6†	>13	1.5
82218	US	F3V	8.39±0.72	4.8	0.30±0.02	3.827±0.005	0.55±0.08	1.4	22	1.4	25	1.7†	>16	1.6†	>13	1.5
82319	US	F3V	4.67±0.96	5.5	0.10±0.02	3.827±0.005	1.05±0.18	1.7	8	1.8	8	1.7	9	1.8	8	1.7
82534	US	F3V	8.55±0.68	5.6	0.00±0.03	3.827±0.005	0.72±0.07	1.4	14	1.6	14	1.6	15	1.5	13	1.5
82569	UCL	F4V	5.52±0.38	4.0	0.18±0.06	3.822±0.009	0.95±0.07	1.6	10	1.7	9	1.7	11	1.7	8	1.7
82747	UCL	F5Ve	6.94±0.55	-0.7	0.96±0.40	3.814±0.011	0.92±0.18	1.6	10	1.7	9	1.6	11	1.7	9	1.6
83159	UCL	F6V	6.79±0.47	4.4	0.00±0.08	3.802±0.007	0.63±0.07	1.4	14	1.5	12	1.4	16	1.4	14	1.4

Note. — Spectral Types are from this work (Section 2.4.1). Uncertainties in Log(T_{eff}) are calculated with a spectral type uncertainty of 1 subtype. In cases where the H-R diagram position was too close to the main sequence to yield a unique age, we provide upper limits (denoted by <) based on the 2σ upper limit on the luminosity. We have provided the median mass of all evolutionary tracks as the preferred mass for each member. Given the sizes of the observational uncertainties, it is preferable to adopt the median subgroup ages rather than these individual isochronal ages.
$*$ – mass was derived assuming a 15 Myr age.. † – mass was derived assuming a 10 Myr age.

2.4.3 Distances

While the stars in our sample have been selected from the *Hipparcos* catalog and therefore have trigonometric parallaxes, we can refine the distance determination by employing moving cluster, or "convergent point", parallaxes. This works by leveraging the longer-baseline astrometric measurements employed to determine proper motions and taking advantage of the common space motion for the group. Kinematically improved parallaxes have been shown to reduce scatter in the H-R diagram (see the Hyades in de Bruijne et al. (2001) for a good example) and a comparison with trigonometric parallaxes can further help identify interlopers. One caveat is that kinematic parallaxes are meaningless for stars which are not true members.

For our kinematic parallax calculations we followed Mamajek (2005) and used updated space motions for US, UCL and LCC tabulated in Chen et al. (2011)[6]. As described previously, we use proper motion data from the revised *Hipparcos* reduction (van Leeuwen, 2007) for stars with single star (five-parameter) solutions and data from Tycho-2 (Høg et al., 2000) otherwise. Our kinematic parallaxes compare very well with the *Hipparcos* trigonometric parallax data (Figure 2.2).

2.4.4 Field Star Contamination

While the techniques used to define the sample in de Zeeuw et al. (1999) ensure that the candidate members are physically coincident with Sco-Cen and moving with similar space motion, the selection is purely based on astrometric information. Here we attempt to use our spectroscopic observations in conjunction with an additional kinematic criterion to identify interlopers.

While the strength of Li can be used as a youth indicator in G- and K-type stars,

[6]These updated space motions should yield the best available predicted radial velocities and kinematic parallaxes.

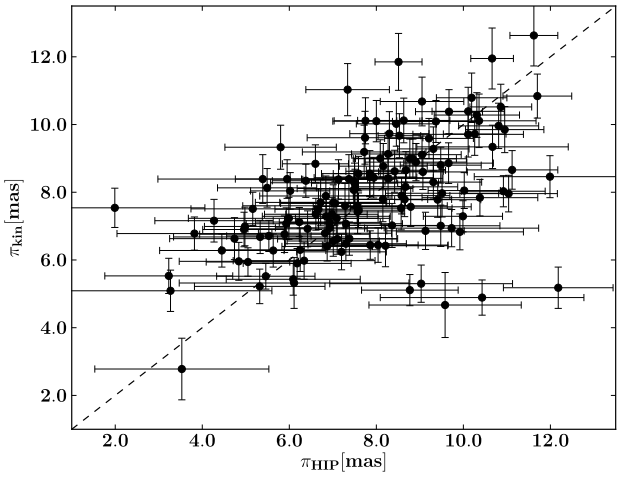

Figure 2.2 Comparison between *Hipparcos* trigonometric parallaxes and our kinematic parallaxes. A line with unit slope is plotted for comparison.

older F-type stars will show less Li depletion and thus we cannot rely on this spectral feature alone as a youth indicator in our sample (Balachandran, 1991, however see Chen et al., 2011). We can, however, use Li to determine membership for any G/K stars which are companions to F-type stars, excluding or confirming the *pair* as members. Since our sample should consist of stars with predominantly dwarf and subgiant like gravities, we can also identify and exclude any giants found in our sample.

For members, the kinematic parallaxes should be in agreement with the trigonometric parallaxes. As a conservative criterion, we reject any star as a member if the difference between trigonometric parallax and kinematic parallax exceeds three times the uncertainty in those quantities added in quadrature. The motivation is that if the disagreement between the trigonometric and kinematic parallaxes is significant at the 3σ level, the object clearly has a different space motion than the group and can be safely rejected.

US Interlopers

Using our conservative kinematic rejection criteria, we rule out HIP 79258 as a member. A kinematic parallax of 5.11±0.46 mas disagreed with the trigonometric parallax of 8.77±1.11 mas at a confidence level $> 3\sigma$. This is the only interloper we were able to identify in Upper Sco. We then expect that the US sample of 21 still contains ∼4 interlopers, ∼19%.

UCL Interlopers

Chen et al. (2011) reject HIP 70833 as a member of UCL since the cooler K3IV companion has an EW(Li $\lambda 6707\mathring{A}$) of only 0.01 Å. Chen et al. (2011) also reject HIP 75824 based on its low Li, with EW(Li $\lambda 6707\mathring{A}$)<8 Å. Finally, HIP 69327 lies far below the zero-age main sequence, an un-physical portion of the H-R diagram, when the kinematic distance is used. As this is inconsistent with group membership, we identify it as an interloper.

With these non-members identified in UCL, there still remain ∼12 interlopers in our UCL sample of 53, or ∼23%.

LCC Interlopers

We reject one giant as a LCC member (HIP 62428, A7III; also rejected by Chen et al. 2011). It was also classified as a giant by Houk & Cowley (1975). Chen et al. (2011) also exclude HIP 66285 as a member, based on the lack of Li in its cooler co-moving companion. HIP 59781 has a kinematic parallax of 5.18±0.61 mas and a trigonometric parallax of 12.58±1.26 mas, disagreeing above our 3σ threshold so we reject it. HIP 56227 has a kinematic parallax of 11.85±0.84 mas and a trigonometric parallax of 8.51±0.54 mas, also disagreeing above our 3σ threshold so we reject it.

Table 2.5. Stars Rejected as Sco-Cen Members

Name	Spectral Type	Rejection Criteria	Ref.
HIP 56227	F0IV	Kinematic Parallax	1
HIP 57595	F6V	Trigonometric Parallax	1
HIP 59781	F8V	Kinematic Parallax	1
HIP 61086	F1V	HRD Position	1
HIP 62056	F6V	HRD Position	1
HIP 62428	A7III	Giant	1
HIP 62674	F3V	HRD Position	1
HIP 63022	F0V	HRD Position	1
HIP 64316	F3V	HRD Position	1
HIP 66285	F7V	Companion Li-poor	1
HIP 69327	F1V	Kinematic Parallax	1
HIP 70833	F3V	Companion Li-poor	1
HIP 75824	F3V	Li-poor	1
HIP 77457	A7IV	Kinematic Parallax	2
HIP 79258	F4V	Kinematic Parallax	1
HIP 81392	G2/3 V	Li-poor	2
HIP 83542	G8/K0 III	Giant	3

Note. — Spectral Type References: (1) this work, (2) Houk (1982) (3) Houk & Smith-Moore (1988)

HIP 57595 has a trigonometric parallax of 3.53±2.00 mas, which places it 165 pc from the mean distance of LCC. The Tycho-2 proper motion for this star supports it being an unrelated background star – the kinematic parallax assuming it were a member of LCC places even further from LCC (π_{kin}=2.78±0.91 mas), so we reject it. Finally, HIP 63022, HIP 61086, HIP 64316, HIP 62674, and HIP 62056 occupy an un-physical portion of the H-R diagram (below the zero-age main sequence) when the kinematic distances are used. As this is inconsistent with group membership, we identify these objects as interlopers.

With these interlopers identified in LCC, we believe that few, if any, of the remaining F-type stars are interlopers. Stars rejected as Sco-Cen members are listed in Table 2.5.

2.4.5 Accretion Disk Fraction

We can examine our red optical spectra for evidence of accretion with the Hα feature. Accreting stars are thought to produce Hα emission due to hot infalling gas. For our accretion criterion we use the Hα full width at 10% peak (W_{10}(Hα)). White & Basri (2003) find that independent of spectral type, a full width at 10% peak > 270 km s^{-1} is a good indicator of accretion. We do not estimate the mass accretion rates as that is is beyond the scope of this study.

Using this criterion, we find only two stars in our sample with Hα emission consistent with accretion, both of which are binaries: the near-equal mass system AK Sco (HIP 82747; Andersen et al., 1989; Alencar et al., 2003) and the recently studied HD 101088 (HIP 56673; Bitner et al., 2010) with 10% peaks widths of 710 km s^{-1} and 400 km s^{-1}, respectively. The spectral resolution of our red optical spectra at Hα is $\sim$140 km s^{-1}. The Hα profiles of these accretors are shown in Figure 2.3 along with the Hα profile of a non-accreting star in our sample (HIP 67230, F5V) with the same spectral type as HD 101088 and AK Sco.

Using the classical T Tauri star color-color locus as determined by Meyer et al. (1997) and the intrinsic color locus of main-sequence stars we look for near-IR photometric signatures of accretion among our Sco-Cen members using *2MASS* near-IR photometry. The plot in Figure 2.4 shows our Sco-Cen members (without reddening corrections applied) clustered around the locus with spread consistent with the uncertainties in the colors. The one obvious outlier with H-$K_S > 0.4$ is the known near-equal mass binary AK Sco referred to above. AK Sco is the star to the right of the locus, and its position is similar to that of the Herbig Ae/Be stars in Hernández et al. (2005).

Here we estimate the optical spectroscopic accretion disk fraction for F stars in

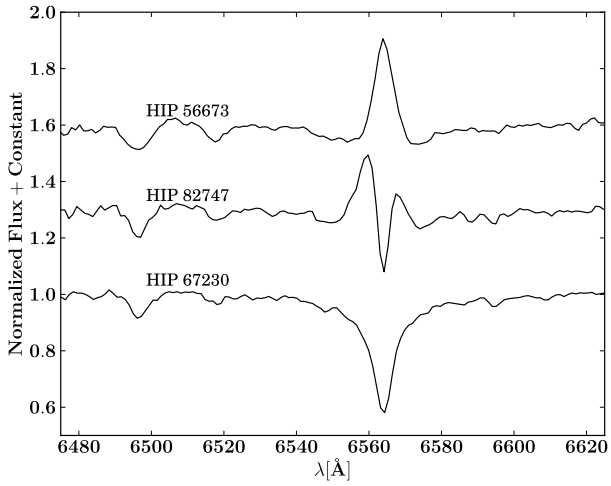

Figure 2.3 Hα region showing the two accretors in our sample, HD 101088 (HIP 56673, F5IVe) and AK Sco (HIP 82747, F5Ve), along with a non-accreting star (HIP 67230, F5V) of the same spectral type.

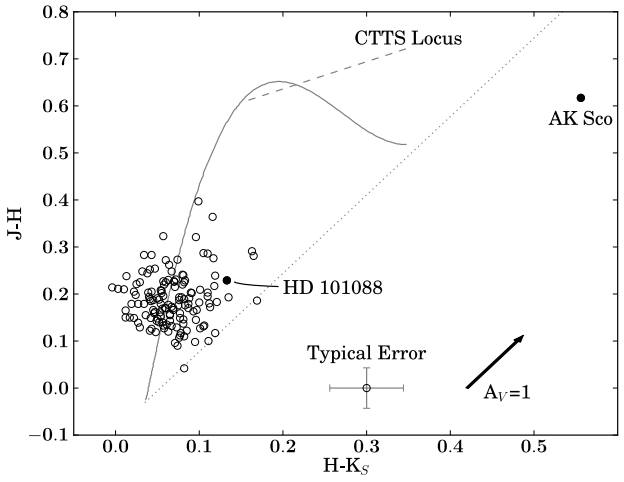

Figure 2.4 H-K$_S$ vs. J-H for the program stars (not de-reddened; excluding interlopers). The solid line is the dwarf color locus and the dashed line is the classical T Tauri locus of Meyer et al. (1997), shown for reference. The dotted line is the reddening line of a standard A0 star. The solid circle outlier to the right is the eclipsing binary AK Sco, indicating that AK Sco's NIR color excess cannot be due to reddening.

our sample as 0/17 (<19%; 95% C.L.) for US, while UCL has 1/41 (2^{+5}_{-1}%; 68% C.L.) accretors and LCC has 1/50 (2^{+4}_{-1}%; 68% C.L.) F-type accretors. This compares well with the Carpenter et al. (2006) *Spitzer* results in which 0/30 (<11%; 95% C.L.) F- and G-type stars were found to have IR excesses. The F-type results in UCL and LCC are consistent with the lower-mass G- and K-type stars studied by Mamajek et al. (2002), in which 1/110 ($0.9^{+2.0}_{-0.3}$%; 68% C.L.) members exhibited spectroscopic evidence of accretion.

As mentioned previously, pre-main sequence stars may exhibit enhanced chromospheric activity, which will manifest itself through partially filled Hα absorption lines. To examine this effect we measured the strength of the Hα lines with IRAF[7] for all our program stars as well as our spectral standards and plot the EW(Hα) against $T_{\rm eff}$ (Figure 2.5). The members plotted here indicate slightly enhanced chromospheric activity, although most are still within the 2σ spread of the spectral standards.

2.4.6 H-R Diagram

In order to compare Sco-Cen members with theoretical models and explore the star formation history of the F-type members, we construct a theoretical H-R diagram. The adopted effective temperature scale and bolometric correction scale was taken from an extensive set of notes for spectral subtypes by EM[6]. This new $T_{\rm eff}$ scale comes from careful review and inter-comparison of spectroscopic and photometric temperature estimates for high quality MK standards as well as large samples of field dwarfs with MK classifications. The bolometric corrections are consensus estimates for the adopted temperatures, which rely heavily on the BCs for hot dwarf stars from Bessell et al. (1998) and for cool dwarf stars on the series of papers by Casagrande et al. (2006,

[7]IRAF is distributed by the National Optical Astronomy Observatory, which is operated by the Association of Universities for Research in Astronomy (AURA) under cooperative agreement with the National Science Foundation.

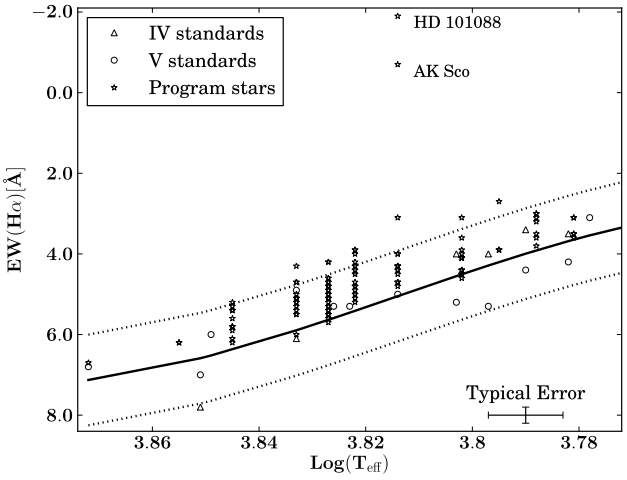

Figure 2.5 Hα EWs for the member stars compared with inactive field dwarfs and subgiants. The solid line is a third order polynomial fit to the field stars and the dotted lines represent the 2σ scatter in the fit to the field stars. While the Sco-Cen program stars (interlopers not shown) are heavily represented above the trend line, most of them still lie within of the 2σ spread of the field stars.

2008, 2010). However, BCs were also calculated interpolating the scales of Code et al. (1976), Balona (1994), Flower (1996), and Bertone et al. (2004) for comparison. The adopted temperatures and bolometric corrections are listed in Table 2.3.

We combine our extinction estimates with our kinematic parallaxes and V-band photometry (Perryman & ESA, 1997) to estimate bolometric luminosity and place the members on a theoretical H-R diagram. We compare our data to the Dartmouth PMS models (Dotter et al., 2008) in Figure 2.6.

2.5 Discussion

Immediately noticeable in the H-R diagram (Figure 2.6) is that the Upper Sco F-stars are not clustered around the 5 Myr isochrone, the age often quoted for US (de Geus et al., 1989; Preibisch et al., 2002). In fact if a "moving median" empirical isochrone

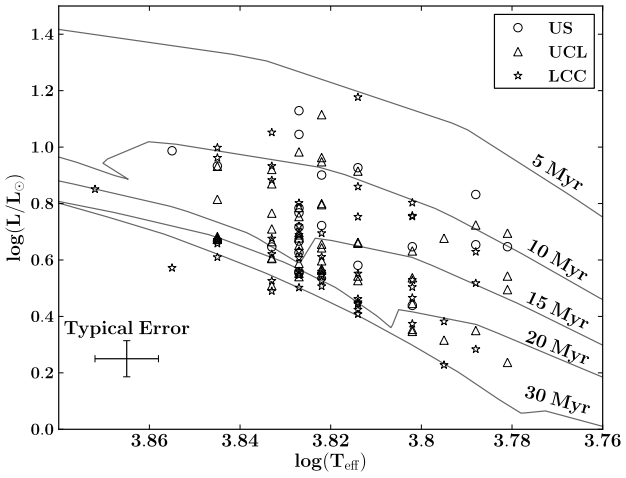

Figure 2.6 H-R diagram for all stars except identified interlopers. Circles, triangles and star symbols are US, UCL and LCC candidate members, respectively. Plotted for comparison are 5, 10, 15, 20 and 30 Myr isochrones from the Dotter et al. (2008) models.

is plotted (Figure 2.7), it is ∼0.4 dex below the 5 Myr theoretical isochrone from the Dotter et al. (2008) models. While a choice of different theoretical tracks vary this disagreement slightly (e.g., D'Antona & Mazzitelli (1997), Siess et al. (2000), Demarque et al. (2004)) the disparity is at least ∼0.4 dex at spectral type F3, which corresponds to a factor of $\gtrsim$ 2.5 in luminosity, or about 1 mag. This is such a large effect that it clearly cannot be attributed to the uncertainty in the photometry or the errors in spectral types.

Although there is some scatter, the positions of the empirical isochrones in Figure 2.7 are consistent with the age rank from previous results (Mamajek et al., 2002); from oldest to youngest: LCC, UCL, US. A close examination of the empirical isochrones reveals that UCL appears to be reaching the main sequence at $\log(T_{\rm eff})$ $\simeq$3.84 or spectral type ∼F2, while LCC appears to be reaching the main sequence at $\log(T_{\rm eff})$ $\simeq$3.82 or spectral type ∼F4. The F-type members of US appear to be

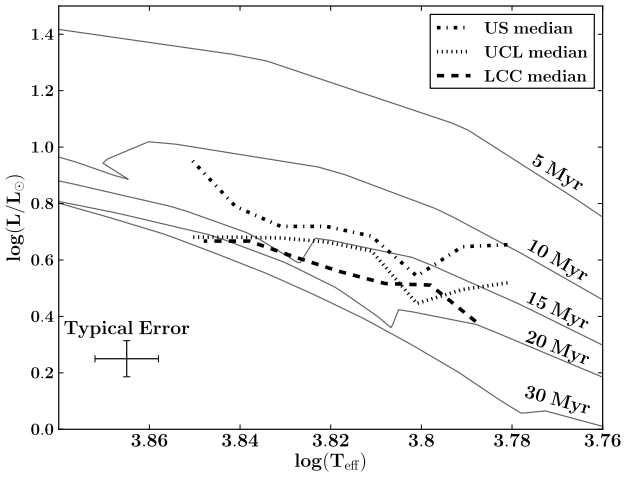

Figure 2.7 H-R diagram with empirical isochrones for US (dot-dashed), UCL (dotted) and LCC (solid), constructed by taking the median luminosity over a 0.01 dex T_{eff} step size with a 0.025 dex $\log(T_{eff})$ window. Plotted for comparison are the Dotter et al. (2008) models.

all pre-main sequence, and thus we do not see a main sequence turn-on point for US among F-type stars.

2.5.1 Ages

For stars in UCL and LCC earlier than ∼F5, the H-R diagram positions of the stars are very near the main sequence and thus we can not reliably determine ages from pre-main sequence evolutionary tracks. Therefore, we only use F5 and cooler stars to estimate the median age of UCL and LCC. For all stars in US and those later than F5 in UCL and LCC we calculate ages and masses by linearly interpolating between isochrones from Dotter et al. (2008), Demarque et al. (2004), Siess et al. (2000), and D'Antona & Mazzitelli (1997). Figure 2.8 shows the distribution of ages for the three subgroups. Individual results for our ages and masses are listed in Table 2.4. For stars which are too close to the main sequence to infer a reliable age, we determine

Table 2.6. Median Age Estimates of the PMS F-Type members of US, UCL and LCC

Evolutionary Tracks	US (Myr)	UCL (Myr)	LCC (Myr)
Dartmouth	13±4	16±5	18±7
Yonsei-Yale	13±4	15±5	18±9
SDF00	14±5	16±9	15±6
DM97	12±3	15±6	15±5
Median	13	16	17
Statistical Unc.	±1	±1	±1
Systematic Unc.	±1	±1	±2

Note. — Uncertainties represent the 1σ dispersion in the Chauvenet's-criterion clipped ages (Bevington & Robinson, 2003) for the members for which we were able to determine an age. The overall uncertainty is the 68% C.L. of the median (Gott et al., 2001) (statistical) and the dispersion in ages (systematic). Median ages for UCL and LCC are only defined by members F5 or cooler, as earlier members are too close to the main sequence to yield reliable ages.

a lower limit on the age using the 2σ upper limit on the luminosity and estimate a mass by assuming an age of 15 Myr (10 Myr for US). Our median age estimates for each subgroup are listed in Table 2.6.

Interestingly, we obtain a significantly older median age for Upper Sco than other studies of the low-mass members (5 Myr, Preibisch et al. 2002; 6-8 Myr, de Zeeuw & Brand 1985; 10 Myr, Glaspey 1971). As seen in Figure 2.8, we obtain a median age of 13 Myr for Upper Sco using the evolutionary tracks of Dotter et al. (2008) and an overall median age from all tracks of 13±1 Myr (68% C.L.). This is disconcerting, especially considering the median F-star ages we obtain for LCC and UCL are consistent with the main sequence turn-off ages and the pre-main sequence G- and K-type stars examined in Mamajek et al. (2002). Motivated to resolve this large discrepancy, we revisit the Upper Sco main sequence turn-off ages, the age of the M supergiant

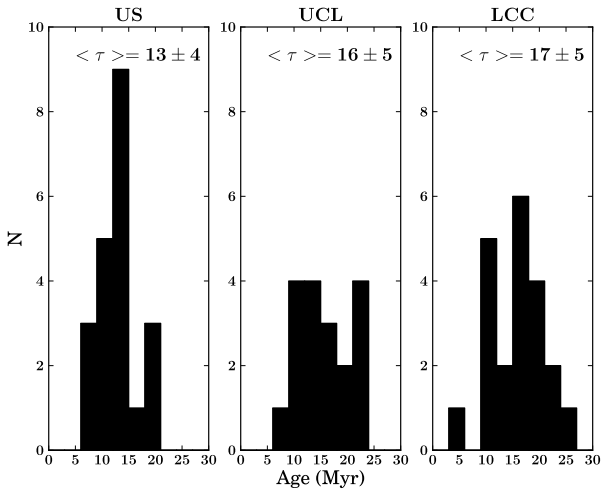

Figure 2.8 Distribution of ages obtained with the Dotter et al. (2008) evolutionary models. For UCL and LCC, only stars cooler than F5 were considered.

Antares, examine the ages of the A-type stars and the ages for the pre-main sequence G-type stars. We also examine a kinematic expansion age for Upper Sco.

Intrinsic Age Spreads

In order to constrain how much of the observed spread in ages is due to observational uncertainty and estimate the intrinsic age spread, we performed a simple Monte Carlo simulation. First we calculated the observed 1σ dispersion in ages for each subgroup by simply taking the standard deviation of the ages (F5 and later stars for UCL and LCC), with deviant outliers clipped using Chauvenet's criterion (Bevington & Robinson, 2003). These observed spreads are shown in Table 2.6.

For each subgroup, we generated a synthetic population of 10^4 H-R diagram positions using the median H-R diagram position and median uncertainties for our member stars (F5 or later only for UCL and LCC), assuming a Gaussian distribution of errors. We then obtained ages and calculated the 1σ spread in ages for these three

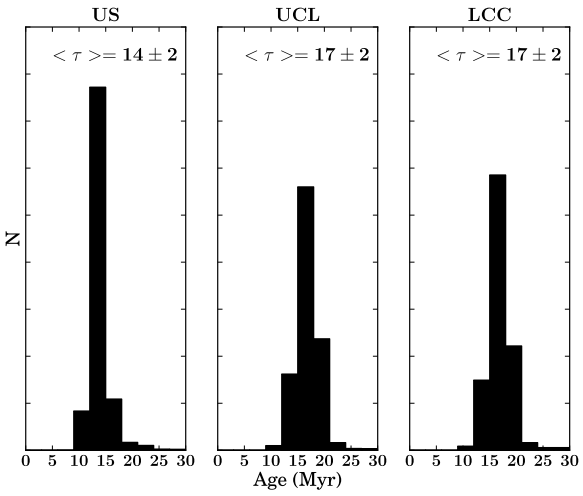

Figure 2.9 Distribution of ages obtained from a simulated population of 10^4 stars with median H-R diagram position and uncertainty with a Gaussian distribution (for UCL and LCC only members F5 or later were used). Ages (in Myr) were obtained using the Dotter et al. (2008) models.

synthetic populations, again clipping deviant outliers with Chauvenet's criterion since the same criterion was applied to our real data to obtain the 1σ dispersion in ages. The distribution of ages for these simulated populations with the Dotter et al. (2008) evolutionary tracks are shown in Figure 2.9.

Our estimates here assume that the observed dispersion in ages is the result of the true dispersion in ages and the dispersion in ages as a result of the observational uncertainties, i.e. $\sigma^2_{observed} = \sigma^2_{intrinsic} + \sigma^2_{uncertainties}$. Using the Dotter et al. (2008) models, we then estimate the intrinsic dispersion in ages using the dispersions from our real and simulated populations. Rather than give preference to one set of evolutionary models, we repeat this calculation for each of our evolutionary models. This way we obtain a range of intrinsic age dispersions.

For US the observed 1σ dispersion in ages ranges from ± 3 Myr with the D'Antona & Mazzitelli (1997) models to ± 5 Myr with the Siess et al. (2000) models. When

we account for the age dispersion from the observational uncertainties, we find the intrinsic 1σ age dispersion ranges from ±1 Myr to ±3 Myr, again depending on the models. For UCL and LCC, which have an observed age dispersion of ±5–9 Myr and ±5–9 Myr (depending on models), we find intrinsic age dispersions of ±4–7 Myr and ±0–8 Myr, respectively. This indicates that 68% of the star formation in Sco-Cen occurred over a time span of 2–6 Myr (US), 8–14 Myr (UCL) and $<$16 Myr (LCC). These are upper limits as we have not accounted for stellar binarity. Our findings show a much smaller age dispersion for US than the other two subgroups, consistent with the smaller age spreads found by Preibisch et al. (2002) and Slesnick et al. (2008), who also found a very small intrinsic dispersion in age. For UCL and LCC our age spreads are larger than that found in Mamajek et al. (2002), who found that 68% of the star formation had occurred within 4–6 Myr for UCL and LCC.

2.5.2 Upper Sco Main Sequence Turn-Off Revisited

The most recent age determination for the turn-off was performed by de Geus et al. (1989) using Walraven photometry in which they estimated a turn-off age of 5 Myr using Maeder (1981) evolutionary tracks with overshooting but no mass loss or rotation. Preibisch et al. (2002) examined the H-R diagram again and argued that the data were consistent with an age of 5 Myr with very little spread in ages. We now have updated stellar evolutionary models and *Hipparcos* astrometry which we employ to revisit the turn-off age. We use the early-type members from de Zeeuw et al. (1999) with the addition of δ Sco, a long-period binary that is certainly a member of US but was not a de Zeeuw et al. (1999) member of US due to its perturbed motion. To construct the H-R diagram, we take Strömgren photometry from Hauck & Mermilliod (1998) and de-reddened it according to the prescription of Shobbrook (1983). We then

use the $T_{\rm eff}$ and BC_V calibration of Balona (1994) with the de-reddened Strömgren photometry. Since we are using the spread in isochrones near where the stars evolve off the main sequence, we restrict ourselves to stars hotter than $\log(T_{\rm eff}) > 4.40$ dex or more luminous than $\log(L/L_\odot) > 4.00$ dex. For stars cooler or less luminous than this the derived ages are very sensitive to the observational uncertainties and we are unable to estimate meaningful ages. Our derived temperatures and luminosities are given in Table 2.7. A plot of the data, with and without corrections for binarity (see below), are shown in Figure 2.10 with the evolutionary tracks of Bertelli et al. (1994).

Table 2.7. Stellar Parameters for US Turnoff Stars

Name	$\log(T_{\rm eff})$ (dex)	$\log(L/L_\odot)$ (dex)	$v\sin i$ (km s^{-1})	B94 Age (Myr)	B94 Mass ($M_\odot$)	E11 Age (no rot.) (Myr)	E11 Mass (no rot.) ($M_\odot$)	E11 Age (rot.) (Myr)	E11 Mass (rot.) ($M_\odot$)
ω Sco	4.424 ± 0.019	3.96 ± 0.05	100±6	2	11.4	5	11.2	5	11.4
β^1 Sco	4.419 ± 0.010	4.29 ± 0.05	91±8	9	12.2	11	12.1	11	12.2
π Sco	4.402 ± 0.007	4.34 ± 0.10	100±15	12	12.4	12	12.9	14	12.6
τ Sco	4.475 ± 0.073	4.31 ± 0.16	10±2	2	14.7	5	14.5	5	14.7
δ Sco	4.438 ± 0.033	4.58 ± 0.14	148±8	9	14.4	9	14.9	10	14.6
σ Sco	4.443 ± 0.015	4.98 ± 0.12	56±15	8	17.7	8	18.0	10	17.2

Note. — References: (B94) Bertelli et al. (1994), (E11) Ekström et al. (2012). $v\sin i$ values adopted from Brown & Verschueren (1997)

We have not used the runaway star ζ Oph in our analysis, for several reasons. First, while Hoogerwerf et al. (2000) used Hipparcos astrometry to conclude that ζ Oph most likely originated from Upper Sco $\sim$1 Myr ago, they note that it could have also originated from UCL $\sim$3 Myr ago. Unfortunately, the radial velocity of this star is poorly constrained[8] and thus the UVW space motion is not sufficiently constrained to associate it with Upper Sco with great confidence. More importantly, however, close examination of the abundance patterns in ζ Oph indicate that it has an anomalously high helium abundance (Herrero et al., 1992) and thus likely participated in a mass transfer event, perhaps from a close former binary companion. For this reason it is not reliable to use it to determine the turn-off age since it may have received extra nuclear fuel unaccounted for by the evolutionary models.

With only six B-type stars determining the turn-off age, it is important to assess the binarity of these stars since it may significantly alter the H-R diagram positions and, therefore, the derived ages. Only two stars, ω Sco and τ Sco, do not have a detected companion. β^1 Sco is a binary with ΔV=1.26$\pm$0.17 (Elliot et al., 1976). This magnitude shift, when accounted for, moves the primary down on the H-R diagram $\sim$0.1 dex in luminosity and gives an age for the primary of 9 Myr. π Sco is a binary with ΔV $\sim$3.7 (Stickland et al., 1996), which moves the primary down on the H-R diagram $\sim$0.01 dex in luminosity, having virtually no effect on the derived age for π Sco. δ Sco is a binary with ΔV=1.5-1.9 (Tango et al., 2009), shifting the primary down $\sim$0.07-0.1 dex in luminosity. However, because of its position it effectively moves parallel to the 9 Myr isochrone and thus does not affect the derived age for the primary. σ Sco is a quadruple system discussed extensively by North et al. (2007). They report the system as a spectroscopic pair (which includes the primary),

[8] +15 km s^{-1}, Reid et al. (1993); +6 km s^{-1}, Garmany et al. (1980); -12.6 km s^{-1}, Conti et al. (1977); -15 km s^{-1}, Valdes et al. (2004)

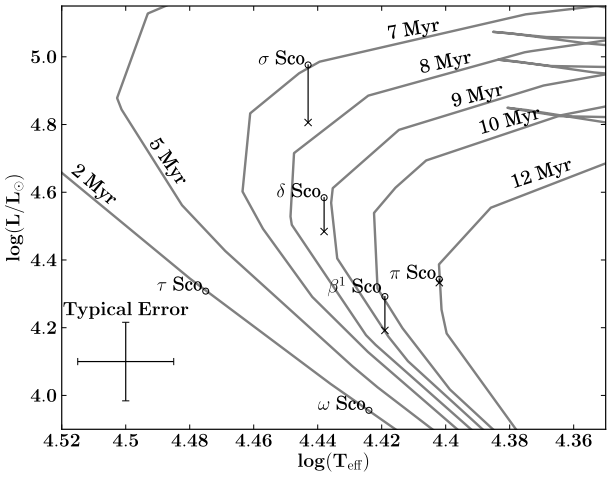

Figure 2.10 Upper Sco main sequence turn-off plotted with the Bertelli et al. (1994) evolutionary tracks. The crosses represent the H-R diagram position corrected for known binarity (see text for a discussion of each binary). The circles are the H-R diagram positions uncorrected for companions. ω Sco and τ Sco do not have known companions.

a tertiary B7 component and a B9.5V common proper motion companion separated by 20". They deconstructed the spectroscopic pair into a B1III primary with a B1V secondary with $\Delta V \simeq 0.80$, and a system age of $\sim$10 Myr using the Claret (2004) evolutionary models. Correcting our derived H-R diagram position for the magnitude of the secondary, we find that the primary moves down $\sim$0.2 dex, which changes our derived age to 8 Myr for the primary.

Unfortunately, the massive stars in Upper Scorpius do not trace a well-defined turn-off, even with corrections for known companions. Including the shifted H-R diagram positions when accounting for the binarity, we estimate the turnoff age from the following stars: ω Sco (2 Myr), τ Sco (2 Myr), β^1 Sco (9 Myr), δ Sco (9 Myr), π Sco (12 Myr), and σ Sco (8 Myr). The median age for these stars is 9$\pm$3 Myr (68% C.L.) with 1σ dispersion 4 Myr, midway between the previous age estimates of

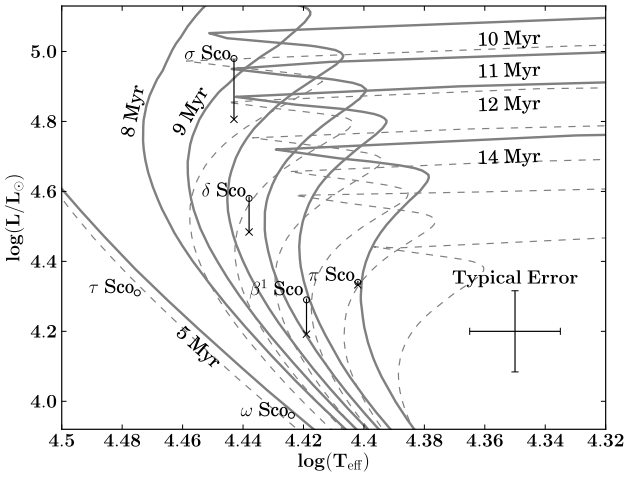

Figure 2.11 Upper Sco main sequence turn-off plotted with the Ekström et al. (2012) evolutionary tracks without rotation (dashed lines) and with $v=0.4v_{breakup}$ (solid lines). The crosses and circles represent the H-R diagram positions corrected and uncorrected for known binarity, respectively.

∼5 Myr and our value of ∼13 Myr from the F-type members.

While most current stellar evolutionary models have ignored rotation, theoretical studies have shown that a moderate rotational velocity of v_{eq} ∼200 km s^{-1} will increase inferred main sequence lifetimes about 20–30%. (Meynet & Maeder, 2000; Maeder & Meynet, 2000; Talon et al., 1997). This represents a significant difference in ages obtained with evolutionary tracks ignoring rotation vs. those which include a treatment of rotation. For this reason, we also considered the evolutionary tracks of Ekström et al. (2012) which include tracks for stars with and without rotation. It should be noted that neither the Bertelli et al. (1994) models nor the Ekström et al. (2012) models considered here include pre-main sequence evolution, but since the pre-main sequence evolution for a ∼9 $M_\odot$ star is ∼10^5 yr (Iben, 1965) the pre-main sequence time can be safely neglected. Plotted in Figure 2.11 is the H-R diagram positions of the US main sequence turnoff stars along with isochrones generated from the

evolutionary tracks of Ekström et al. (2012) with no rotation (dashed lines) and those with a rotational velocity equal to 40% of the breakup velocity. The median age with rotation at 40% of breakup is 10±2 Myr (68% C.L.) while the median age without is 9±2 Myr (68% C.L.). Since the US turnoff stars are rotating with a median projected rotational velocity of $<v\sin i>$=96 km s^{-1} (see Table 2.7) and $< v_{eq} >=\frac{4}{\pi}<v\sin i>$, then the turnoff stars have $< v_{eq} >\simeq$120 km s^{-1}. Using mass estimates from the Bertelli et al. (1994) tracks, we estimate the median break-up velocity of the US turnoff stars as ∼450 km s^{-1} and thus the median observed rotational velocity is ∼25% of breakup. This is a significant median rotational velocity and indicates that rotation should be considered. Therefore we adopt the median age obtained with the rotating evolutionary tracks of 10±2 Myr (68% C.L.).

Our Upper Sco turn-off age is much older than the age derived by the de Geus et al. (1989) study. We believe the major source of discrepancy between the de Geus et al. (1989) US turn-off ages and our US turn-off ages are the updated evolutionary tracks. If we use the de Geus et al. (1989) H-R diagram positions with the Bertelli et al. (1994) evolutionary tracks, we obtain a median age of 9 Myr, the same age we obtain with our modern data (though our individual H-R diagram positions are not the same as those in the de Geus et al. 1989 study). We also note that the use of evolutionary tracks which account for rotation tends to increase the derived ages by ∼25% in general (Meynet & Maeder, 2000). For example, the using the Ekström et al. (2012) rotating evolutionary tracks for a typical upper main sequence star in LCC and UCL gives an age ∼30% older than ages derived with the Bertelli et al. (1994) evolutionary tracks.

2.5.3 Antares

Antares (α Sco) is a rare M1.5Iab-Ib supergiant (Keenan & McNeil, 1989) in Upper Scorpius. As the most massive secure member of US, it places tight constraints on the age of the group. To estimate the H-R diagram of Antares we use the updated temperature scale of Levesque et al. (2005) for red supergiants, together with the revised *Hipparcos* parallax (van Leeuwen, 2007) of π=5.89±1.00 mas and the angular diameter measurement of 41.3±1.0 mas (Richichi & Lisi, 1990). We obtain $\log(T_{\rm eff})$=3.569±0.009 dex (assuming spectral type uncertainty of 1 subtype), $\log(L/L_{\odot})$=4.99±0.15 dex. This H-R diagram position is plotted in Figure 2.12. With this H-R diagram position we obtain an initial mass of 16.6 $M_{\odot}$ and an age of 11^{+3}_{-1} Myr with the evolutionary tracks of Bertelli et al. (1994). However, just as with the main sequence turn-off stars, the main sequence lifetime of Antares was likely significantly altered by rotation and therefore we again consider the rotating evolutionary tracks of Ekström et al. (2012), shown in Figure 2.13. From these rotating evolutionary tracks we obtain an initial mass of 17.2 $M_{\odot}$ and an age of 12^{+3}_{-1} Myr, which we adopt as our final age for Antares.

However, independent of this H-R diagram position we can still place constraints on the age of Antares using only the $T_{\rm eff}$ derived from the spectral type. Using the previously mentioned $T_{\rm eff}$ calibration for supergiants, a $T_{\rm eff}$ of 3710 K ($\log(T_{\rm eff})$=3.569) means that the age must be 9 Myr or more, since younger isochrones are not predicted to reach temperatures that low. This is illustrated in Figure 2.12 with the placement of the 5 Myr isochrone to the left.

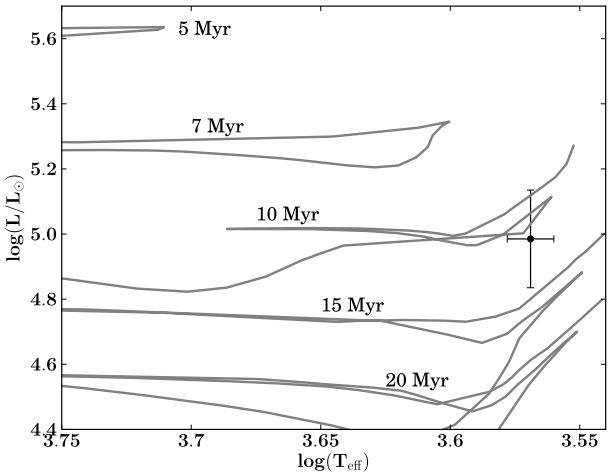

Figure 2.12 The H-R diagram for M1.5Iab-Ib supergiant Antares (α Sco). The theoretical isochrones overlap in this region, but the best fit is 11^{+3}_{-1} Myr using Bertelli et al. (1994) evolutionary tracks.

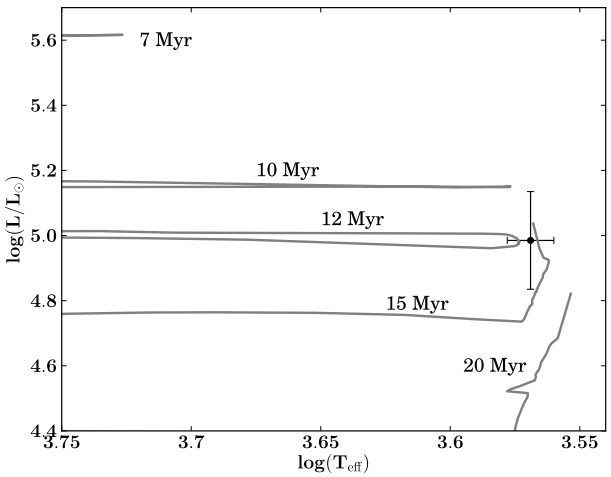

Figure 2.13 The H-R diagram for Antares with the rotating evolutionary tracks of Ekström et al. (2012). We adopt a final age of Antares of 12^{+3}_{-1} Myr.

2.5.4 Ages of Upper Sco A-Type Stars

We place the A-type stars of US on the H-R diagram as another independent age indicator. The F-type stars do not appear to have reached the main sequence and thus we expect that some A-type stars will be pre-main sequence and therefore useful as an age indicator.

We use the A-type US members kinematically-selected by de Zeeuw et al. (1999) and perform essentially the same analysis as used on the F-type stars. We estimate individual reddenings using the procedure described in Section 2.4.2. We calculate a kinematic parallax, again using the revised *Hipparcos* astrometry if the solution is that of a single star and use the Tycho-2 proper motions otherwise. We reject one star, HIP 77457, since its trigonometric parallax of 8.58±0.86 mas disagrees with the kinematic parallax of 5.10±0.42 mas by more than 3σ. Our individual H-R diagram position data for the US A-type stars is listed in Table 2.8 and plotted in Figure 2.14. As with the F-type stars, we do not see the A-type stars clustered around the 5 Myr isochrone, but rather mostly between the 5 Myr and 12 Myr isochrones.

Table 2.8. Stellar Parameters For A-type Upper Sco Members

HIP	Spectral Type	A_V (mag)	π_{kin} (mas)	$\log(T_{\rm eff})$ (dex)	$\log(L/L_\odot)$ (dex)	Ref.
76310	A0V	0.14 ± 0.03	8.22 ± 0.62	3.980 ± 0.031	1.271 ± 0.070	1
77545	A2/3V	1.25 ± 0.04	6.83 ± 0.62	3.937 ± 0.014	1.053 ± 0.081	2
77815	A5V	0.85 ± 0.07	6.89 ± 0.58	3.907 ± 0.007	1.195 ± 0.077	2
77960	A4IV/V	0.75 ± 0.02	8.56 ± 0.71	3.918 ± 0.012	0.973 ± 0.093	2
78099	A0V	0.59 ± 0.03	7.42 ± 0.59	3.980 ± 0.031	1.367 ± 0.073	2
78196	A0V	0.00 ± 0.04	8.45 ± 0.63	3.980 ± 0.031	1.302 ± 0.070	3
78494	A2mA7-F2	0.75 ± 0.06	7.26 ± 0.57	3.943 ± 0.016	1.395 ± 0.077	2
78809	A1Vnn	0.21 ± 0.05	7.29 ± 0.57	3.964 ± 0.019	1.244 ± 0.071	1
78847	A0V	0.63 ± 0.06	6.76 ± 0.55	3.980 ± 0.031	1.445 ± 0.078	1
78963	A9V	0.64 ± 0.06	5.11 ± 0.46	3.872 ± 0.010	1.314 ± 0.084	3
78996	A9V	0.47 ± 0.03	7.25 ± 0.57	3.872 ± 0.010	1.019 ± 0.069	2
79124	A0V	0.78 ± 0.05	6.51 ± 0.53	3.980 ± 0.031	1.550 ± 0.078	2
79156	A0V	0.60 ± 0.07	6.43 ± 0.54	3.980 ± 0.031	1.366 ± 0.081	1
79250	A3III/IV	0.33 ± 0.05	9.60 ± 0.75	3.932 ± 0.012	0.963 ± 0.072	2
79366	A3V	0.80 ± 0.02	7.35 ± 0.60	3.932 ± 0.012	1.202 ± 0.071	2
79392	A2IV	0.71 ± 0.04	5.81 ± 0.49	3.943 ± 0.016	1.300 ± 0.076	2
79476	A8IVe	1.02 ± 0.40	7.56 ± 0.61	3.875 ± 0.010	1.006 ± 0.175	4
79733	A1mA9-F2	1.25 ± 0.04	4.51 ± 0.43	3.964 ± 0.019	1.480 ± 0.092	3
79860	A0V	0.38 ± 0.03	4.91 ± 0.40	3.980 ± 0.031	1.432 ± 0.075	3
79878	A0V	0.00 ± 0.02	7.35 ± 0.55	3.980 ± 0.031	1.407 ± 0.070	5
79987	A7V	1.69 ± 0.18	3.84 ± 0.40	3.892 ± 0.014	1.308 ± 0.116	6
80019	A0V	1.03 ± 0.07	7.81 ± 0.68	3.980 ± 0.031	1.374 ± 0.084	1
80059	A7III/IV	0.56 ± 0.07	7.74 ± 0.64	3.892 ± 0.014	0.907 ± 0.075	2
80088	A9V	0.61 ± 0.03	6.11 ± 0.66	3.872 ± 0.010	0.960 ± 0.095	2
80130	A9V	0.66 ± 0.02	6.41 ± 0.57	3.872 ± 0.010	1.089 ± 0.077	2
80196	A1Vn	2.36 ± 0.18	5.94 ± 0.56	3.964 ± 0.019	1.602 ± 0.102	6
80238	A2.5V	0.74 ± 0.09	8.00 ± 0.68	3.937 ± 0.014	1.389 ± 0.081	7
80311	A1V	0.93 ± 0.05	5.51 ± 0.49	3.964 ± 0.019	1.266 ± 0.080	6
80425	A1V	1.52 ± 0.17	7.25 ± 0.64	3.964 ± 0.019	1.392 ± 0.096	6
80799	A3V	0.25 ± 0.04	7.97 ± 0.62	3.932 ± 0.012	1.078 ± 0.068	6
81624	"A3*"	2.56 ± 0.78	5.08 ± 0.48	3.932 ± 0.012	2.003 ± 0.316	8

Table 2.8 (cont'd)

HIP	Spectral Type	A_V (mag)	π_{kin} (mas)	log(T_{eff}) (dex)	log($L/L_\odot$) (dex)	Ref.
82397	A3V	0.00 ± 0.03	7.85 ± 0.62	3.932 ± 0.012	1.118 ± 0.072	3

Note. — Uncertainties in log(T_{eff}) are determined assuming a spectral type uncertainty of 1 subtype.
Spectral Type References: (1) Paunzen et al. (2001), (2) Houk & Smith-Moore (1988), (3) Houk (1982), (4) Vieira et al. (2003), (5) Glaspey (1972), (6) Garrison (1967), (7) Abt (1981), (8) Gray & Corbally (1998)
* We list the hydrogen type in the table, the full type from Gray & Corbally (1998) is "kA1 hA3 mA3 Vaer Bd1 ≤ Nem1"

While the A-type stars in US have individual H-R diagram positions that are too close to the main sequence to yield reliable ages, we can examine the trend of the empirical isochrone and determine what ages are consistent with the ensemble. Shown in Figure 2.14 is the empirical isochrone, which we use to estimate the main sequence turn-on for Upper Sco at spectral type ∼A3 or log(T_{eff})≃3.93 dex. We compare our empirical isochrones with the Dotter et al. (2008) evolutionary models, noting that an age of 8 Myr is too young to be consistent with the clump of stars at spectral type A3, and an age of 12 Myr is too old to be consistent with the clump of stars at spectral type A8-A9. Using these constraints, we estimate an age of 10±2 Myr with the Dotter et al. (2008) evolutionary tracks. We obtain similar age estimates with other evolutionary models, summarized in Table 2.9. For the A-type stars we adopt the median age among all four evolutionary models considered of 10±1±1 Myr (statistical, systematic).

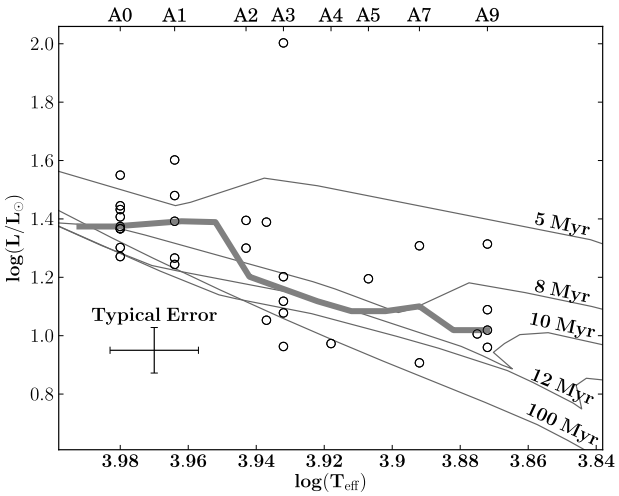

Figure 2.14 H-R diagram for Upper Sco A-type stars taken from de Zeeuw et al. (1999). Plotted for comparison are 5, 8, 10, 12 and 100 Myr isochrones (solid lines) from the Dotter et al. (2008) models. The star well above the 5 Myr isochrone is HD 150193 (HIP 81624), a known Herbig Ae/Be star (Hernández et al., 2005). While situated in de Zeeuw et al's Upper Sco "box", it appears to be associated with the Oph filamentary clouds L1729 and 1712, far from most of the other Upper Sco members. The thick solid line is an empirical isochrone constructed by taking the median luminosity over a 0.01 dex T_{eff} step size with a 0.035 dex window. Uncertainties in $\log(T_{eff})$ are determined assuming a spectral type uncertainty of 1 subtype.

Table 2.9. Age Constraints for Upper Sco from the A-type Main Sequence Turn-on

Evolutionary Tracks	Age (Myr)
Dartmouth	10±2
Yonsei-Yale	10±2
SDF00	12±3
DM97	9±2
Median	10
Statistical Unc.	±1
Systematic Unc.	±1

Note. — The overall uncertainty is the 68% C.L. of the median (Gott et al., 2001) (statistical) and the dispersion in ages (systematic).

2.5.5 Ages of Upper Sco Pre-Main Sequence G-type Stars Revisited

Since our F-type median ages for LCC and UCL agree very well with previous results obtained with the G-type pre-main sequence stars (Mamajek et al., 2002), we wish to directly compare our new results for Upper Scorpius with a similar sample of G-type stars in an attempt to resolve this discrepancy in ages. We use the X-ray selected G-type stars from Preibisch & Zinnecker (1999) and the kinematically selected G-type stars from de Zeeuw et al. (1999). Ages for the X-ray selected objects from the Preibisch & Zinnecker (1999) study had been estimated previously using UKST Schmidt plate photometry. However, more precise Tycho-2 and 2MASS photometry are now available and thus we may be able to obtain a more reliable age estimate. Ages for the US G-type stars in the de Zeeuw et al. (1999) sample have not been previously examined.

For the X-ray-selected sample we cross-reference the Preibisch & Zinnecker (1999) sample with the Tycho-2 catalog (Høg et al., 2000) and select objects which have proper motions within the de Zeeuw et al. (1999) proper motion boundaries for Upper Sco (i.e., $0 < \mu < 37$ mas yr^{-1}). This leaves us with ten X-ray selected G-type US members. We correct for extinction using (B-V), (V-J), (V-H), and (V-K) colors from Tycho-2 and 2MASS photometry, with the Tycho-2 photometry converted to Johnson using the conversions found in Mamajek et al. (2002, 2006). To estimate bolometric luminosity we use the converted V-band photometry, kinematic distances using the Tycho-2 proper motions and temperatures and bolometric corrections listed in Table 2.3. For the kinematically-selected sample, we first identify two interlopers, HIP 83542 and HIP 81392. Houk & Smith-Moore (1988) classified HIP 83542 as G8/K0 III, a giant, and the H-R diagram position is well above the 1 Myr isochrones,

consistent with this assessment. HIP 81392 and HIP 83542 both exhibit weak lithium absorption features, significantly lower than the other six kinematically-selected US candidates from de Zeeuw et al. (1999) and inconsistent with the youth of Upper Sco (E. Mamajek, private communication 2011). With these interlopers removed, we are then left with six G-type US members from de Zeeuw et al. (1999). For the de Zeeuw et al. (1999) G-type US candidate members we estimate extinction, T_{eff} , distance, and bolometric luminosity using the same method as for the F-type stars as previously discussed. Our newly-derived extinctions, distances, and H-R data is listed in Table 2.10, with the H-R diagram for this analysis shown in Figure 2.15.

Table 2.10. Stellar Parameters for G-Type Upper Sco Members

Object	TYC	SpT	π_{kin} (mas)	A_V (mag)	log(T_{eff}) (dex)	log($L/L_\odot$) (dex)	D08 (Myr)	YY04 (Myr)	S00 (Myr)	DM97 (Myr)	Ref.
[PZ99] J155548.7-251223	6783-2045-1	G3	6.56 ± 0.85	0.70 ± 0.17	3.756	0.38 ± 0.13	11	12	18	12	(1)
[PZ99] J161618.0-233947	6793-1406-1	G7	7.17 ± 0.81	0.73 ± 0.06	3.742	0.34 ± 0.10	9	10	16	9	(1)
[PZ99] J160843.4-260216	6784-39-1	G7	7.39 ± 0.66	0.65 ± 0.09	3.742	0.36 ± 0.09	9	10	15	9	(1)
[PZ99] J161459.2-275023	6801-186-1	G5	7.66 ± 0.92	0.73 ± 0.31	3.750	0.08 ± 0.16	23	23	30	21	(1)
[PZ99] J160040.6-220032	6212-1183-1	G9	6.36 ± 1.06	0.65 ± 0.17	3.728	0.27 ± 0.16	8	9	15	7	(1)
[PZ99] J160000.7-250941	6783-1747-1	G0	6.86 ± 0.65	0.36 ± 0.19	3.774	0.19 ± 0.11	24	24	...	22	(1)
[PZ99] J160158.2-200811	6208-1543-1	G5	6.31 ± 0.77	1.22 ± 0.25	3.750	0.65 ± 0.15	5	6	10	5	(1)
[PZ99] J155812.7-232835	6779-780-1	G2	6.60 ± 0.77	0.86 ± 0.18	3.762	0.49 ± 0.12	10	10	16	10	(1)
[PZ99] J161731.4-230334	6793-501-1	G0	5.37 ± 0.78	0.72 ± 0.15	3.774	0.71 ± 0.14	8	8	12	8	(1)
[PZ99] J161318.6-221248	6213-306-1	G9	6.90 ± 0.75	1.16 ± 0.16	3.728	0.60 ± 0.12	4	4	7	4	(1)
HIP 78483	6787-1367-1	G2IV	6.46 ± 0.61	0.22 ± 0.12	3.762	0.64 ± 0.10	7	8	12	7	(2)
HIP 78581	7329-1646-1	G1V	9.26 ± 0.75	0.04 ± 0.06	3.769	0.38 ± 0.08	15	15	20	15	(3)
HIP 79252	6213-75-1	G7IV(e)	8.94 ± 0.86	0.64 ± 0.23	3.742	0.45 ± 0.12	7	8	13	7	(2)
HIP 79462	6793-1271-1	G2V	7.03 ± 0.61	0.45 ± 0.15	3.762	0.70 ± 0.10	6	7	10	7	(4)
HIP 80320	6806-833-1	G3IV	7.97 ± 0.63	0.00 ± 0.04	3.756	0.42 ± 0.07	10	11	17	11	(2)
HIP 80535	6802-183-1	G0V	7.59 ± 0.64	0.00 ± 0.02	3.774	0.71 ± 0.07	8	8	12	8	(3)

Note. — Spectral Type References – (1) Preibisch & Zinnecker (1999), (2) Torres et al. (2006), (3) Houk (1982), (4) Houk & Smith-Moore (1988)

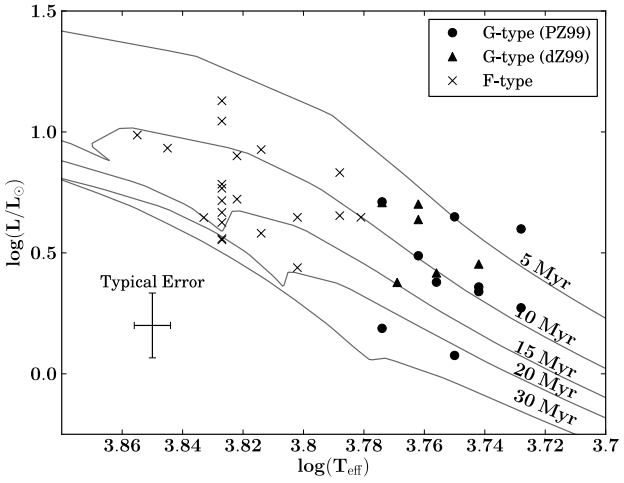

Figure 2.15 H-R diagram for Upper Sco G-type stars taken from Preibisch & Zinnecker (1999) (solid triangles) and de Zeeuw et al. (1999) (solid circles) with Tycho-2 proper motions within the de Zeeuw et al. (1999) boundaries. F-type members (this work) are shown for continuity (crosses). Plotted for comparison are 5, 10, 15, 20 and 30 Myr isochrones from the Dotter et al. (2008) models.

For the 16 G-type members of Upper Sco described above, we find median ages of 8-14 Myr using the evolutionary tracks of Dotter et al. (2008), Demarque et al. (2004), Siess et al. (2000), and D'Antona & Mazzitelli (1997). Our derived ages for these G-type stars of Upper Sco are summarized in Table 2.11, with an overall median age among all tracks of 9±2±3 Myr (statistical, systematic). The kinematically-selected members are slightly more biased towards younger-ages than the X-ray selected members. However, this slight difference may be attributed to the brightness limits of the *Hipparcos* catalog. The difference may not be significant, though, with such small numbers of members.

Table 2.11. Median Ages of the G-Type Upper Sco Members

Evolutionary Tracks	Age (Myr)
Dartmouth	8±4
Yonsei-Yale	9±3
SDF00	14±4
DM97	8±4
Median	9
Statistical Unc.	±2
Systematic Unc.	±3

Note. — Uncertainties represent the 1σ dispersion in the Chauvenet's-criterion clipped ages (Bevington & Robinson, 2003). The uncertainty in the median is the 68% confidence limit as described in Gott et al. (2001) (statistical) and the dispersion in ages (systematic).

2.5.6 Upper Sco Expansion Age

One of the earlier published ages for US is an expansion age of ∼5 Myr derived by Blaauw (1978). Deriving ages using kinematic data holds obvious appeal since it does not depend on stellar evolution models. However, Brown et al. (1997), performing simulations of expanding OB associations and analyzing the resulting simulated proper motion data, found major problems with kinematic expansion ages which only rely on proper motion data. They found that expansion ages determined by tracing the proper motion of the stars back to their smallest configuration, as was performed in Blaauw (1978) to obtain the often quoted age of 5 Myr for US, always leads to underestimated ages and that all age estimates converge to ∼4 Myr. Furthermore, they found that the initial size of the OB association provided by this method is always overestimated. The Brown et al. (1997) study found that kinematic expansion ages

determined using proper motion data alone are essentially meaningless.

Radial velocities must be considered in order to derive a meaningful expansion age. Given the availability of good quality trigonometric parallax and radial velocity data and the findings of Brown et al. (1997), we revisit the expansion age for US here. Following Mamajek (2005), we adopt a Blaauw expansion model (Blaauw, 1956, 1964b) which gives the observed radial velocity for parallel motion as

$$v_{obs} = vcos\lambda + \kappa r + K,$$

where v is the centroid speed of the group, λ is the angular distance to the convergent point, $vcos\lambda = v_{\rm pred}$ is the predicted radial velocity with no expansion, κ is the expansion term in units of km s^{-1} pc^{-1}, r is the distance to the star in pc, and K is an offset term which may include intrinsic effects (e.g., convective blueshift or gravitational redshift). We then write the difference between the predicted and observed radial velocity as

$$v_{obs} - v_{pred} = \Delta V_R = \kappa r + K,$$

so that κ is the slope in the plot of ΔV_R versus r:

$$\kappa = \frac{d(\Delta V_R)}{dr}.$$

The expansion age in Myr is then

$$\tau = \gamma^{-1}\kappa^{-1},$$

where γ=1.0227 pc s Myr^{-1} km^{-1}, a conversion factor.

To determine the expansion age we have started with the entire de Zeeuw et al. (1999) sample for which radial velocity measurements were available in the literature (listed in Table 2.12), since these all have individual trigonometric parallaxes. We have used radial velocities from Dahm et al. (2012), Chen et al. (2011), Gontcharov (2006), and Duflot et al. (1995). We limited the sample to those de Zeeuw et al. (1999) candidate members which have revised *Hipparcos* distances (van Leeuwen, 2007)[9] within 50 pc of the mean US distance (145 pc, de Zeeuw et al. 1999). We also excluded candidate members with radial velocities more than 20 km s^{-1} discrepant from the predicted radial velocities, as these are almost certainly non-members or unresolved binaries. Our $v_{\rm pred}$ is calculated using the new best estimate of the mean UVW motion of Upper Sco, detailed in Chen et al. (2011). The 1-D velocity dispersion in US is 1.3 km s^{-1} (de Bruijne, 1999b). In order to determine if there is evidence of expansion, we plot the distance r versus ΔV_R in Figure 2.16. Expansion would be exhibited by a positive correlation between the distance and ΔV_R, characterized by the slope (κ) of a line fit to the data. To take into account the observational errors in distance and radial velocity in fitting a line to the data, we performed a Monte Carlo simulation in which we added random Gaussian errors commensurate with each observational uncertainty to the observed data point, and then we fit a line using an unweighted total least squares algorithm. We performed 50,000 trials and then used the median and 1σ spread to quantify the effect of the uncertainties in the observational data on the slope. This yielded a Pearson–r of -0.03 ± 0.11 and a best-fit line with a slope of $\kappa = -0.01 \pm 0.04$ km s^{-1} pc^{-1}. If we consider only models of expansion (i.e., $\kappa > 0$), then the 99% confidence lower limit on the expansion age is 10.5 Myr. However, the *results are statistically consistent with no expansion.* For an expansion age of 5 ± 2 Myr we would expect $\kappa = 0.20^{+0.13}_{-0.06}$ km s^{-1} pc^{-1}, and

[9]Distances are simply the inverse of the trigonometric parallax.

Table 2.12. Properties of Upper Sco Members Used For Expansion Age

HIP	d (pc)	v_{rad}(pred.) (km s^{-1}	v_{rad}(obs.) (km s^{-1}	Ref.
76071	175 ± 20	-5.3	-6.1 ± 2.3	1
76310	151 ± 13	-4.4	-2.5 ± 0.6	1
76503	190 ± 13	-4.4	3.7 ± 20.0	2
76633	145 ± 18	-6.2	-2.8 ± 2.2	3
77635	152 ± 6	-5.0	-3.0 ± 4.7	3
77813	105 ± 14	-6.8	-5.4 ± 0.4	4
77840	154 ± 12	-5.2	-9.3 ± 1.6	3
77858	129 ± 9	-5.4	-6.3 ± 20.0	2
77859	131 ± 6	-5.6	-9.2 ± 3.1	3
77900	158 ± 12	-4.6	-1.3 ± 2.6	3
77909	158 ± 11	-5.2	-8.7 ± 4.3	3
77911	148 ± 12	-5.9	-2.9 ± 2.6	1
78099	141 ± 15	-5.9	-6.5 ± 2.9	3
78104	145 ± 4	-4.2	3.3 ± 20.0	2
78207	143 ± 5	-8.3	1.5 ± 2.2	1
78246	170 ± 7	-5.5	-12.1 ± 3.4	3
78265	180 ± 21	-5.1	-11.7 ± 10.0	2
78530	157 ± 13	-6.4	-9.0 ± 4.4	3
78549	146 ± 12	-6.2	-5.0 ± 5.0	3
78663	144 ± 24	-4.1	-11.3 ± 0.3	4
78809	144 ± 12	-6.0	-5.5 ± 3.2	1
78820	124 ± 12	-7.1	-1.0 ± 2.0	3
78847	162 ± 21	-6.5	-23.0 ± 3.0	1
78877	161 ± 17	-6.0	-6.6 ± 4.3	3
78933	145 ± 5	-6.9	-4.4 ± 3.0	3
78996	108 ± 10	-6.0	-7.9 ± 2.0	1
79031	119 ± 6	-5.9	-4.9 ± 2.8	3
79054	139 ± 20	-6.0	-4.1 ± 0.7	4
79098	136 ± 6	-6.1	-16.0 ± 5.4	5
79124	123 ± 10	-7.4	-18.1 ± 1.9	1

an expansion age of 10±2 Myr would have $\kappa = 0.10 \pm 0.02$ km s^{-1} pc^{-1}. Given that we are only able to obtain a lower limit on the expansion age for US and our expansion data are statistically consistent with no expansion, we do not consider our 99% confidence lower limit in the final age determination for US.

Table 2.12 (cont'd)

HIP	d (pc)	v_{rad}(pred.) (km s^{-1}	v_{rad}(obs.) (km s^{-1}	Ref.
79156	170 ± 26	-7.3	-3.7 ± 1.9	1
79252	126 ± 35	-6.6	-3.8 ± 0.3	4
79258	114 ± 14	-3.6	-18.0 ± 0.3	4
79288	150 ± 22	-5.7	-2.9 ± 0.3	4
79369	122 ± 21	-6.9	-6.7 ± 0.3	4
79374	145 ± 16	-7.4	-14.2 ± 1.6	5
79404	147 ± 3	-5.0	-3.8 ± 10.0	2
79410	140 ± 22	-7.3	-6.2 ± 2.6	1
79439	132 ± 19	-7.4	-5.6 ± 0.2	1
79530	144 ± 13	-6.0	3.4 ± 2.5	3
79596	175 ± 11	-3.6	-22.6 ± 0.4	3
79599	109 ± 7	-7.0	-7.8 ± 1.7	3
79622	149 ± 9	-5.8	-8.4 ± 2.7	3
79785	101 ± 6	-7.0	-6.4 ± 0.2	1
79878	129 ± 8	-5.1	-3.4 ± 0.6	1
79910	149 ± 33	-7.0	-6.6 ± 0.7	4
79977	123 ± 16	-7.1	-2.8 ± 0.3	4
80019	173 ± 33	-7.4	-15.0 ± 3.9	5
80024	163 ± 21	-7.4	-4.0 ± 1.4	1
80088	139 ± 34	-6.8	-7.5 ± 2.2	1
80126	151 ± 13	-6.5	-3.0 ± 6.5	5
80320	142 ± 23	-4.8	1.7 ± 0.3	4
80324	110 ± 12	-3.8	-2.1 ± 1.5	3
80461	125 ± 12	-6.6	-6.8 ± 2.9	5
80473	111 ± 11	-6.6	-11.4 ± 3.0	3
80474	135 ± 11	-6.7	-11.0 ± 2.4	5
80493	135 ± 16	-5.8	-7.4 ± 1.9	1
80535	120 ± 17	-5.5	-4.0 ± 0.3	4
80569	161 ± 6	-8.1	-19.0 ± 2.1	3
80763	170 ± 29	-5.9	-3.5 ± 0.8	3

Table 2.12 (cont'd)

HIP	d (pc)	v_{rad}(pred.) (km s^{-1}	v_{rad}(obs.) (km s^{-1}	Ref.
80896	142 ± 25	-4.9	3.3 ± 2.7	1
81266	145 ± 11	-5.5	1.7 ± 0.9	3
81455	105 ± 15	-5.2	-3.2 ± 0.5	4
82218	136 ± 20	-8.2	-6.7 ± 0.3	4
82319	104 ± 19	-7.4	-18.3 ± 1.3	1

Note. — Distances are derived using trigonometric parallaxes from van Leeuwen (2007). References: (1) Dahm et al. (2012); (2) Duflot et al. (1995); (3) Gontcharov (2006); (4) Chen et al. (2011); (5) Barbier-Brossat & Figon (2000);

2.5.7 What is the best median age for Upper Sco?

Every age indicator we have examined thus far has yielded an age of Upper Sco of 9-13 Myr, summarized in Table 2.13. The youngest median age comes from the G-type stars at ∼9 Myr, and the oldest from the F-type stars at ∼13 Myr, so we can conclude with confidence that US must be between 9 and 13 Myr old. Regarding each segment of the H-R diagram as independent, we simply take the mean age of our values – ∼10 Myr for the main sequence turn-off, ∼12 Myr for Antares, ∼10 Myr for the A-type stars, ∼13 Myr for the F-type members and ∼9 Myr for the G-type members. This gives a final adopted age of 11±1 Myr (s.e.m., statistical) for Upper Sco, which is more than twice the currently accepted age (Preibisch et al., 2002). As each segment of the H-R diagram provides an independent age, we estimate our systematic uncertainty as the 1σ dispersion of these independent ages, which yields a systematic uncertainty of ±2 Myr.

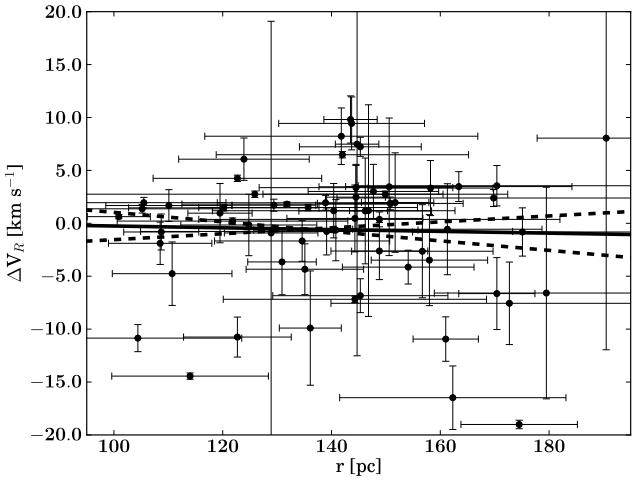

Figure 2.16 Distance (r) vs. the difference between the observed and predicted radial velocity (V_R). The sample includes US candidate members from de Zeeuw et al. (1999) within 50 pc of the mean US distance and with measured radial velocities within 20 km s^{-1} of the predicted value. If US is expanding, the closest members should be more blueshifted and the further members should be more redshifted. A series of Monte Carlo simulations gives a best-fit slope of $\kappa = -0.01 \pm 0.04$ km s^{-1} pc^{-1}, which places a 99% confidence lower limit on the expansion age of 10.5 Myr.

Table 2.13. Upper Sco Age Estimates

Sample	Age (Myr)
F-Type PMS	13±1
Main-sequence Turn-off	10±2
Antares	12±2
A-Type Turn-on	10±3
G-Type PMS	9±2
Adopted Age	11
Statistical Unc.	±1
Systematic Unc.	±2

2.5.8 Implications of an Older Upper Sco

Upper Sco has been a benchmark stellar population in studies of circumstellar disk lifetimes (e.g., Carpenter et al., 2006), but has a lower primordial disk fraction when compared to other stellar populations at 5 Myr (e.g., λ Ori; Barrado y Navascués et al. 2007). Considered in the context of 11 Myr age, the observed primordial disk fraction is consistent with those of similarly-aged stellar populations (e.g., NGC 7160, Sicilia-Aguilar et al. 2006). Our detailed analysis of the isochronal ages for massive and intermediate-mass Upper Sco stars may indicate that the ages of similarly aged groups may also be due for further investigation and significant revision. Naylor (2009) have also found evidence that the nuclear ages for massive stars in <10 Myr-old groups are typically 1.5–2$\times$ the pre-MS contraction ages. In particular, Naylor (2009) finds that two of Upper Sco's ∼5-Myr-old siblings (NGC 2362 and Cep OB3b, each with pre-MS ages of 4.5 Myr) have best fit isochronal ages for the massive stars of 9.1 Myr and 10 Myr, respectively. In this regard the doubling of Upper Sco's age does not seem surprising. Naylor (2009) have proposed that the nuclear ages may be the more correct ones, and that protoplanetary disks may correspondingly have nearly twice as long to form gas giant planets as previously believed.

In addition to circumstellar disk studies, Upper Sco has been the subject of many surveys for low-mass companions (e.g., Lafrenière et al., 2008; Ireland et al., 2011). A low-mass companion to [PZ99] J160930.3-210459[10] was discovered at a very large

[10]Although the star is commonly called 1RXS J160929.1-210524 or 1RXS 1609, this is technically not an appropriate name. 1RXS is one of the acronyms used for ROSAT X-ray sources, however it refers to the X-ray source itself rather than any optical counterpart, as sometimes there may be multiple plausible optical counterparts (hence why one does not normally encounter stars called by 1RXS names in the literature, but by "RX J" names or others). The likely optical counterpart (star) was first identified as a pre-MS Upper Sco member in Preibisch et al. (1998) (listed as GSC 6213-1358), and later was referred to as "Upper Sco 160930.3-210459" in Preibisch & Zinnecker (1999). SIMBAD standardized the "Upper Sco" names to "[PZ99] J" to comply with IAU guidelines for position-based names, and the [PZ99] J-names are now in common use.

separation by Lafrenière et al. (2008). The mass[11] of this companion was determined to be 8 M_{Jup} using the assumed age of 5 Myr. However, we use our revised age for Upper Sco of 11 Myr and the object's reported T_{eff} of 1800±200 K (Lafrenière et al., 2010) to obtain a mass of 13^{+2}_{-3} M_{Jup} using the DUSTY models (Chabrier et al., 2000; Baraffe et al., 2002). Alternatively, using the object's bolometric luminosity of $\log(L/L_{\odot})$=-3.55±0.2 (Lafrenière et al., 2010) and the 11 Myr age we estimate a mass of 14^{+2}_{-3} M_{Jup}, consistent with the estimates from T_{eff} . Here we follow Lafrenière et al. (2010) and adopt the estimates from the luminosity, listed in Table 2.14. Similarly, a companion to GSC 06214-00210 was discovered by Ireland et al. (2011) and thought to have a mass of ∼14 M_{Jup} at an age of 5 Myr. However, at an age of 11 Myr the mass is slightly higher at 17±3 M_{Jup}, using the DUSTY models and the estimated absolute magnitudes M_J ∼10.5, M_H ∼9.6, M_K ∼ 9.1 (Ireland et al., 2011). The substellar companion to HIP 78530 (Lafrenière et al., 2011) was estimated to have a mass of ∼21–26 M_{Jup} with an assumed age of 5±1 Myr. We use the bolometric luminosity of $\log(L/L_{\odot})$ = -2.55±0.13 (Lafrenière et al., 2011) and our revised age of 11 Myr to obtain a mass for HIP 78530B of 30^{+17}_{-8} M_{Jup}. The substellar companion to the young brown dwarf UScoCTIO 108 has a mass of 14^{+2}_{-8} M_{Jup} with an assumed age of 5–6 Myr (Béjar et al., 2008). Using the reported luminosity of $\log(L/L_{\odot})$=-3.14±0.20 (Béjar et al., 2008) and our revised age of 11 Myr, we estimate a mass

[11]This companion was considered the first directly imaged exoplanet orbiting a Sun-like star. The discoverers considered the companion a "planet" (Lafrenière et al., 2010) based on their calculated mass and demonstration of common motion, following the IAU Working Group on Extrasolar Planets (WGESP) definition, which defined a planet as "objects with true masses below the limiting mass for thermonuclear fusion of deuterium (currently calculated to be 13 Jupiter masses for objects of solar metallicity) that orbit stars or stellar remnants"; see http://www.dtm.ciw.edu/boss/definition.html and Boss et al. 2007. Recent work by Spiegel et al. (2011) shows that objects with protosolar composition and masses of >11.9 M_{Jup} can burn at least 10% of their initial deuterium over 10 Gyr. Hence, following the definition of "planet" and "brown dwarf" adopted by the IAU and the discoverers, the companion should probably best be considered a "brown dwarf". Given that the GSC or [PZ99] designation should be preferred over the 1RXS name, and brown dwarf companion should probably be called "GSC 06213-01358 B" or "[PZ99] J160930.3-210459 B".

Table 2.14. Revised Mass Estimates for Substellar Objects in Upper Sco

Object	Mass at 11 Myr (M_{jup})
[PZ99] J160930.3-210459B	14^{+2}_{-3}
GSC 06214-00210B	17±3
HIP 78530B	30^{+17}_{-8}
UScoCTIO 108B	16^{+3}_{-2}
Oph 1622-2405A	53^{+9}_{-7}
Oph 1622-2405B	21±3

Note. — Masses estimated using the DUSTY models of Chabrier et al. (2000); Baraffe et al. (2002) and an age for Upper Sco of 11±2 Myr.

of 16±2 M_{Jup} for UScoCTIO 108b. The substellar binary Oph J1622-2405 initially had component mass estimates of ∼14 M_{Jup} and ∼7 M_{Jup} based on an assumed age of 1 Myr (Jayawardhana & Ivanov, 2006). However, followup spectroscopic studies (Allers et al., 2007; Close et al., 2007; Luhman et al., 2007) found higher masses. Here we estimate the masses using the effective temperatures from Luhman et al. (2007) with our revised age of 11 Myr and find masses of 53^{+9}_{-7} M_{Jup} and 21±3 M_{Jup} for Oph J1622-2405A and Oph J1622-2405B, respectively, with the DUSTY models. This is in agreement with the results from Luhman et al. (2007), who used H-R diagram positions with the DUSTY models for their mass estimates. The revised mass estimates discussed above are summarized in Table 2.14. Hence, we believe that none of the substellar companions directly imaged in Upper Sco have inferred masses below the deuterium-burning limit.

Sco-Cen has been used as an example of triggered star formation, with supernova in UCL/LCC triggering star formation in US and supernova in US triggering star formation in ρ Oph (de Geus, 1992; Preibisch & Zinnecker, 1999). The UCL shell has an expansion velocity of 10±2 km s^{-1} and radius 110±10 pc, suggesting it originated in UCL ∼11 Myr ago and passed through US about 4 Myr ago (de Geus, 1992).

However, given the revised age estimates for US, it does not seem likely that the passage of this superbubble would have triggered star formation in US since it would have arrived too late. This does not mean that star formation in US was not triggered by UCL, it simply means that the timescales and ages are not consistent with the arrival of the UCL shell in US as the triggering event. Similarly, the shell around US has an expansion velocity of 10±2 km s^{-1} and a radius of 40±4 pc, consistent with an age for the shell of ∼4 Myr. At 10 km s^{-1} it would have traveled the ∼15 pc from US to ρ Oph in about 1.5 Myr. With the revised 11 Myr age for US and ρ Oph ages of ∼2-3 Myr (Erickson et al., 2011), there is sufficient time for star formation in ρ Oph to have been triggered by the US shell.

Another important implication of our result is to drive down the inferred progenitor mass for the runaway young neutron star RX J1856.5-3754. Tetzlaff et al. (2011) claim that RX J1856 formed in Upper Sco and was ejected 0.5 Myr ago. Assuming a progenitor mass of 5 Myr, Tetzlaff et al. (2011) predicted that the progenitor would have had a mass of ∼37-45 $M_\odot$ and main sequence spectral type of O5-O7. Smartt (2009) reviewed the observational and theoretical constraints on the supernovae and their progenitors, and suggests that progenitors with masses of >30 $M_\odot$ almost certainly form black holes, not neutron stars. However, if the progenitor of J1856 was a 10.5 Myr-old star when it exploded 0.5 Myr ago, then the progenitor was most likely a ∼18–20 $M_\odot$ O9-type star (using the Ekström et al. 2012 tracks), with the remnant being either a neutron star or black hole (likely depending on the rotation or whether it was in an interacting binary; Smartt 2009). Indeed, if the empirically constrained set of supernova outcomes outlined by Smartt (2009) are correct, and if one adopts the previous age of 5 Myr, then the deceased high mass stars in Upper Sco should have *all* turned into black holes. This would leave the "young" neutron star RX J1856 with a well constrained distance and proper motion but without a plausible birth site.

We conclude that the RX J1856 runaway scenario is more plausible if Upper Sco is 11 Myr, and the progenitor would have been a much easier to form ∼18–20 $M_\odot$ star rather than a rarer ∼37–45 $M_\odot$ star.

2.6 Conclusions

We can summarize our conclusions as follows:

1. The pre-main sequence "turn-on" for UCL and LCC occur near spectral type ∼F2 and ∼F4, respectively. The F-type members of US appear to be all pre-main sequence. Examining the A-type members of US allows us to estimate the pre-main sequence turn-on for US to be near spectral type ∼A3.

2. The good agreement between the isochronal ages of F-type stars studied here and the G- and K-type stars studied in Mamajek et al. (2002) provides greater confidence in those ages, and more firmly establishes that UCL is slightly younger than, or roughly coeval with, LCC. In order of youngest to oldest: Upper Scorpius (US), Upper Centaurus-Lupus (UCL), Lower Centaurus-Crux (LCC).

3. The median ages obtained with the pre-main sequence F-type members (those later than F5) for UCL and LCC agree with previous results for early B-type stars and pre-main sequence G-type stars. (Mamajek et al., 2002), with median ages of 16±1 Myr and 17±1 Myr, respectively.

4. The F-type members have a median isochronal age of 13±1 Myr (68% C.L.) for US, which is much older than previous results. Using the approximate pre-main sequence turn-on point with the A-type stars allows us to estimate an age

of 10±3 Myr. Re-examining the early B-type stars and the G-type pre-main sequence stars in US yields median ages of 10±2 Myr and 9±2 Myr, respectively. Age estimates for the M1.5Iab-Ib supergiant US member Antares give 12^{+3}_{-1} Myr. Considering these to be independent estimates, we obtain an overall mean age for Upper Sco of 11±1±2 Myr (statistical, systematic) with the uncertainty in the mean age dominated by systematic differences between the isochronal ages inferred from different mass ranges.

5. We find a 99% confidence lower limit on the kinematic expansion age for Upper Sco of 10.5 Myr using trigonometric parallax and radial velocity data. However, the astrometry and radial velocities are statistically consistent with no expansion.

6. Based on Hα emission accretion diagnostics, we estimate a spectroscopic accretion disk fraction of 0/17 (<19%; 95% C.L.) in US, consistent with the *Spitzer* results by Carpenter et al. (2006) of 0/30 (<11%; 95% C.L.) for F- and G-type stars. In UCL we find 1/41 (2^{+5}_{-1}%; 68% C.L.) accretors and in LCC we find 1/50 (2^{+4}_{-1}%; 68% C.L.) accretors, which are both consistent with the spectroscopic accretion disk fraction for the G- and K-type members of UCL and LCC from Mamajek et al. (2002) for G- and K-type stars.

7. The revised age of 11 Myr for Upper Sco may explain the lower than expected disk fraction compared to 5 Myr groups (e.g., λ Ori; Barrado y Navascués et al. 2007). We reevaluate the masses of the known substellar companions in Upper Sco using available published data and our revised age of 11 Myr, and find that inferred masses are typically ∼20–70% more massive than previously estimated. All of the imaged companions thus far appear to be more massive than the deuterium-burning limit and so none of the companions are in the

planetary-mass regime. In addition to larger substellar masses, the older age for Upper Sco implies a more realistic, lower progenitor mass of $\sim$18–20 $M_{\odot}$ for the young neutron star RX J1856.5-3754.

3 Intrinsic Colors and Temperatures of Pre-main Sequence Stars

3.1 Introduction and Background

Knowledge of the stellar intrinsic color locus is an essential ingredient in studying young stellar populations. Recently-formed stars are typically either distant, and thus outside of the "Local Bubble", or they are still embedded in their natal molecular cloud. Hence, we cannot assume negligible reddening and extinction for most pre-main sequence (pre-MS) stars. Interstellar reddening is conventionally estimated using tabulated intrinsic colors of dwarf field stars on the main sequence (e.g., Kenyon & Hartmann, 1995). However, this likely introduces systematic errors in the analysis since the pre-MS stars are in a different evolutionary stage than the main sequence calibrators and may not exhibit "standard" dwarf colors. Accurate H-R diagram placement depends on accurate extinction and effective temperature (T_{eff}) estimates. If the extinction or T_{eff} is systematically in error because of systematics in the intrinsic color and T_{eff} tabulations as a function of spectral type, this will obviously introduce systematic errors in the H-R diagram placement. For pre-MS objects, this may result

in erroneous age estimates, which may result in systematic errors in estimates of e.g., protoplanetary disk dissipation timescales (e.g., Mamajek, 2009) and thus the planet formation timescale. The H-R diagram presents an opportunity for stellar theoretical evolutionary models to make contact with observations, but if our H-R diagram placement is plagued with systematic errors, this makes testing evolutionary models impossible. Thus it is imperative that the intrinsic color and $T_{\rm eff}$ scale be accurately known and as free of systematic errors as possible.

Previous studies have noted that the intrinsic colors of young stars differ from that of main sequence stars (e.g., Gullbring et al., 1998; Luhman, 1999). Stauffer et al. (2003) investigated Pleiades (age ∼125 Myr; Stauffer et al. 1998) zero-age main sequence K-stars exhibiting bluer B–V colors as a function of spectral type than their counterparts in Praesepe (age ∼750 Myr; Gáspár et al. 2009), and concluded that the effect was age-dependent. Their study identified starspots and plages as the most likely cause of the bluer B–V colors and concluded that all young K dwarfs will exhibit this effect. Da Rio et al. (2010) constructed a young star intrinsic color sequence in their study of the star-formation history of Orion Nebula Cluster by merging synthetic colors interpolated to a 2 Myr isochronal surface gravity with empirical colors from Kenyon & Hartmann (1995). However, this implicitly charges the color discrepancy solely to lower surface gravity. Furthermore, synthetic near-infrared colors such as J–H and H–K_S do not follow observed intrinsic color sequences for M-dwarfs redder than V–$K_S \gtrsim 4.0$ (see e.g., Casagrande et al., 2008), so we do not expect synthetic colors will accurately predict the sequences of young stars (though, see also Scandariato et al., 2012). Luhman et al. (2010b,a) compiled a list of the near-IR and IR photospheric colors for young K4 through L0-type objects by fitting the blue envelope of the spectral type-color sequence of young, nearby stars from Taurus, Chamaeleon I, the η Cha cluster, the ϵ Cha cluster and the TW Hydra Association

(TWA). The Luhman et al. (2010b) tabulation is empirically derived and thus does not depend on synthetic colors.

Here we offer an alternative and expanded pre-MS intrinsic color tabulation by including optical BVI_C colors, including earlier spectral types, and using the young stars' spectral energy distributions to estimate effective temperatures and construct a temperature and bolometric correction scale. In this work we examine spectral types F0 through M9.5, but our temperature scale only extends to types as late as M5. In Section 3.2 we demonstrate some problems associated with estimating extinction of young stars using dwarf intrinsic colors. In Section 3.3 we describe our sample, and in Section 3.4 we describe the spectroscopy and photometry data used for our analysis. In Section 3.5 we describe our spectroscopy, the derivation of our pre-MS intrinsic colors, and the derivation of our effective temperature and bolometric correction scale for pre-MS stars. Finally, in Section 3.6 we compare our temperature scale and angular diameter estimates to previous results in the literature.

3.2 Problems Estimating Extinction Using Dwarf Colors

An illustration of the problem dereddening pre-MS stars with dwarf intrinsic colors is the discrepancy in the differential extinction distributions of the high-mass stars and the low-mass stars in the Upper Centaurus-Lupus (UCL) and Lower Centaurus-Crux (LCC) subgroups of the Scorpius-Centaurus OB Association. For the high-mass stars, de Geus et al. (1989) employed Walraven $VBLUW$ photometry to derive reddening-free parameters which they used to estimate the effective temperature ($T_{\rm eff}$), $\log(g)$, and then estimate the reddening using tables of intrinsic colors as a function of $T_{\rm eff}$.

Their results do not depend on the measured spectral types of the stars. de Geus et al. (1989) obtained a mean extinction in UCL and LCC of $<A_V>$=0.07 mag with rms $\sigma_{<A_V>}$=0.09 mag. Extinction estimates using the V–K_S intrinsic color tabulation for dwarfs listed in appendix C with the estimated spectral types for UCL and LCC F-type members from Pecaut et al. (2012) give $<A_V>$=0.12 mag with rms $\sigma_{<A_V>}$=0.12 mag, consistent with the de Geus et al. (1989) results for the B/A stars obtained with a completely different method. In contrast, extinction estimates for UCL and LCC G- and K-type members from Mamajek et al. (2002), using the same dwarf V–K_S color tabulation, give $<A_V>$=0.44 mag and rms of $\sigma_{<A_V>}$=0.21 mag. When we compare the extinction distributions, shown in Figure 3.1, it is immediately apparent that though the high-mass, intermediate-mass and low-mass stars have similar spatial distributions, the estimated extinction distributions for the G/K stars are very different from the B/A/F stars. Since there is no plausible physical mechanism to explain why the G/K stars should be subject to a >0.3 mag larger extinction on average than the B/A/F stars, we question the appropriateness of expecting pre-MS stars to have main sequence colors. A 0.3 mag systematic shift in H-R diagram placement would cause a 15 Myr old K-type star to erroneously appear 10 Myr old. In addition, when we have attempted to estimate extinctions for several hundred G/K/M type members of Sco-Cen (Pecaut & Mamajek, in preparation) we find that the A_V estimated from V–K_S colors are systematically larger than when the same is estimated from V–J colors. This is the same color-dependent systematic effect noticed and discussed by Gullbring et al. (1998). They considered several sources of the color anomalies and reasoned that one likely source of the effect was starspots, though they concluded that systematic errors were minimized by dereddening using optical spectral types with optical V–R colors and did not attempt to quantify the effect.

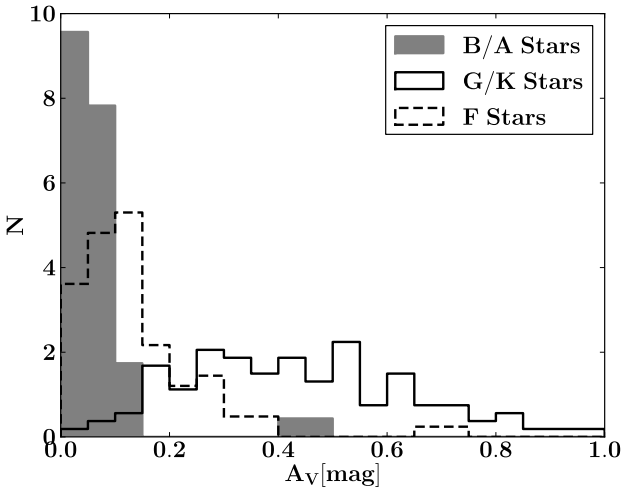

Figure 3.1 Comparison of visual extinction (A_V) distributions from de Geus et al. (1989) for the high mass B/A type stars, the F type stars from Pecaut et al. (2012) and the low mass G/K type stars from Mamajek et al. (2002), all from the UCL and LCC subgroups of the Scorpius-Centaurus OB Association. Though all samples are part of the same stellar population and have similar spatial distributions, the mean extinction obtained from the G/K type stars is >0.3 mag larger than that of the B/A/F stars.

3.3 Sample Selection

Our sample consists of members of young ($\lesssim$30 Myr), nearby moving groups including the β Pic moving group, TW Hydra Association (TWA), Tucana-Horologium moving group (Tuc-Hor) and the η Cha cluster. The members of these groups are all predominantly pre-main sequence (with the exception of a handful of intermediate-mass A-type stars, which we omit) and thus will allow us to study the observed color differences between main sequence stars and pre-main sequence stars. β Pic, TWA and Tuc-Hor members are less than 75 pc distant and thus lie within the Local Bubble, within which objects are subject to negligible reddening (E(B–V)$<$ 0.002, using $N_H \lesssim 10^{19}$ cm^{-2} inside the local bubble from Cox & Reynolds 1987 and N(H I)/E(B–V) = 4.8$\times$10^{21} cm^{-2} mag^{-1} from Savage & Mathis 1979). η Cha is slightly more distant ($\sim$95 pc) but also has $A_V \simeq 0$ (Mamajek et al., 1999; Luhman & Steeghs, 2004). This lack of interstellar reddening allows us to use their intrinsic colors to tabulate an intrinsic color-spectral type relation for young stars in the widely used Johnson-Cousins BVI_C, Two Micron All Sky Survey (2MASS Skrutskie et al., 2006) JHK_S photometric bands and the Wide-Field Infrared Survey Explorer (WISE; Wright et al., 2010) $W1$, $W2$, $W3$ and $W4$ infrared bands at 3.4 μm, 4.6 μm, 12 μm, and 22 μm, respectively.

Our sample was assembled from members of these four groups from Mamajek et al. (1999), Luhman & Steeghs (2004), Lyo et al. (2004), Song et al. (2004), Zuckerman & Song (2004), Scholz et al. (2005), Torres et al. (2006), Lépine & Simon (2009), Kiss et al. (2011), Schlieder et al. (2010), Rice et al. (2010b), Zuckerman et al. (2011), Shkolnik et al. (2011), Rodriguez et al. (2011), Schlieder et al. (2012b) and Schneider et al. (2012b). Following the Weinberger et al. (2012) and Mamajek (2005) studies, we reject TWA 22 as a member of TWA based on its discrepant space motion. However,

we retain it as a member of β Pic following Teixeira et al. (2009). In addition, based on the study by Mamajek (2005) and parallax data from Weinberger et al. (2012), objects TWA 14, TWA 15A, TWA 15B, TWA 17, TWA 18, TWA 19A, TWA 19B, and TWA 24 are likely members of the Lower Centaurus-Crux subgroup of the Scorpius-Centaurus OB association and thus may be subject to non-negligible reddening, so we exclude them from our sample. We include TWA 9 as a member of TWA, though Weinberger et al. (2012) reject it. We discuss our justification for including it in Appendix A. Our sample includes 54 members of β Pic with spectral types F0-M8, 34 members of TWA with spectral types K3-M9.5, 45 members of Tuc-Hor with spectral types F2-M2, and 15 members of η Cha with spectral types K5-M5.75.

3.4 Data

3.4.1 Spectroscopy

Though the objects in our sample have published spectral types, they are from a variety of sources and resolutions. In order to check the consistency of spectral types in the literature, we obtain new spectral types using a grid of standards from Keenan & Yorka (1988); Keenan & McNeil (1989), Kirkpatrick et al. (1991) and Henry et al. (2002). We acquired low-resolution blue ($\sim$3700Å-5200Å) and red ($\sim$5600Å-6900Å) optical spectra from the SMARTS 1.5m telescope in Cerro Tololo, Chile for 52 members of β Pic, TWA and η Cha. The objects chosen for spectroscopy were selected based on (1) target brightness and (2) optimizing telescope time to avoid interfering with higher priority programs. The faintest targets would require prohibitively large exposure times with the RC spectrograph on the SMARTS 1.5m telescope to obtain useful S/N for spectral classification. This spectroscopic sample includes objects down

to m_V ∼14 mag, with spectral types F3-M4. Observations were made in queue mode with the RC spectrograph between February 2011 and July 2011. The blue spectra were taken with the "26/Ia" setup which consists of a grating with groove density of 600 grooves mm^{-1}, blaze wavelength 4450Å and no filter. The red spectra were taken with the "47/Ib" setup which consists of a grating with groove density of 831 grooves mm^{-1}, blaze wavelength 7100Å, and a GG495 filter. Both used a slit with of 110.5μm. The resolution for the blue and red spectra are ∼4.3 Å and ∼3.1 Å, respectively. One comparison lamp exposure, HeAr for blue spectra and Neon for red, was taken immediately before three consecutive exposures of each target. The data were reduced using the SMARTS RC Spectrograph IDL pipeline of Fred Walter (Walter et al., 2004)[1]. The three object images are median combined, bias-trimmed, overscan- and bias-subtracted and flat-fielded. The spectrum is wavelength-calibrated and, as a final step, we normalize the spectra to the continuum with a low order spline in preparation for spectral classification.

3.4.2 Photometry

After compiling the list of nearby ≲30 Myr old stars, we assembled the most precise available photometry from the literature, listed in Table 3.1. All stars in our list have counterparts in the 2MASS Point Source Catalog. A few objects are known binaries but are unresolved in the 2MASS catalog. In these cases, we retain the primary in our lists but do not include the secondary since it would be of limited use without distinct near-infrared photometry. Tuc-Hor member TYC 7065-0879-1 (K0V; Torres et al. 2006) is a 1.8″ binary, resolved in Tycho-2 (Høg et al., 2000) but unresolved in 2MASS. The 2MASS PSF photometry differs significantly from the 2MASS aperture photometry (e.g., $H_{\rm PSF} - H_{\rm AP} = 0.356$ mag), presumably due to a poorly fit PSF to

[1]http://www.astro.sunysb.edu/fwalter/SMARTS/smarts_15msched.html#RCpipeline

the unresolved binary. Thus for TYC 7065-0879-1 we adopt unresolved BVI_C optical photometry and the unresolved 2MASS aperture photometry. All other objects in our sample have 2MASS PSF photometry which agrees well with the aperture photometry (when available) and therefore we simply adopt the PSF photometry. We adopt *WISE* bands $W1$, $W2$, $W3$, and $W4$ photometry from the *WISE* All-Sky Point Source Catalog, centered at 3.4, 4.6, 12, and 22 μm, respectively (Wright et al., 2010). Objects saturated in $W2$ ($\lesssim$ 6.3 mag) exhibit a flux over-estimation bias[2], so to avoid these biases we exclude $W2$ photometry with $W2 < 6.0$ mag. For stars with *Hipparcos* catalog entries, we adopt V and B–V photometry from that catalog ESA (1997). We then fill missing B–V photometry using Tycho-2 photometry (B_T, V_T) converted to Johnson B–V with the conversions of Mamajek et al. (2002, 2006), resorting to the conversions in Høg et al. (2000) when $B_T - V_T > 2.0$. We adopted AAVSO Photometric All-Sky Survey (APASS) Data Release 6 (Henden et al., 2012) BV and SACY (Torres et al., 2006) BVI_C photometry where available. Conservative estimates for SACY BVI_C photometric uncertainties obtained with the FOTRAP instrument are 0.01 mag for objects brighter than $V \sim 12$ mag (C.A.O. Torres, 2012 private communication). We only adopted B–V colors when $\sigma_{B-V} < 0.08$ mag. We adopted V–I_C photometry from Torres et al. (2006), Lawson et al. (2001) and the *Hipparcos* catalog, when it was directly observed (value "A" in field H42), since a significant portion of the tabulated V–I_C photometry in the *Hipparcos* catalog is inferred from photometry in other bands or from the spectral type of the star. Though it was available for many of our objects, we did not adopt DEep Near-Infrared Survey of the Southern Sky (DENIS) i band photometry since it saturates at ∼10.3 mag (Epchtein et al., 1997) and therefore most of our objects are too bright to have reliable DENIS i photometry.

[2]http://wise2.ipac.caltech.edu/docs/release/allsky/expsup/sec6_3c.html

Table 3.1. Spectral Types and Optical/Near-IR Photometry for Young, Nearby, Moving Group Members.

Star	Grp	SpT	Ref.	V (mag)	$B-V$ (mag)	$V-I_C$ (mag)	Ref.	J^a (mag)	H^a (mag)	K_S^a (mag)	$W1^b$ (mag)	$W2^b$ (mag)	$W3^b$ (mag)	$W4^b$ (mag)
HIP 490	TH	G0V	1	7.510±0.010	0.595±0.008		2,2	6.464±0.020	6.189±0.023	6.117±0.020	6.043±0.053	6.053±0.023	6.105±0.015	5.975±0.041
HR 9	BP	F3V	3	6.190±0.010	0.386±0.007		2,2	5.451±0.024	5.331±0.047	5.240±0.024	5.245±0.072		5.234±0.014	4.514±0.023
HIP 1113	TH	G6V	4	8.760±0.010	0.752±0.021	0.820±0.010	2,5,6	7.406±0.021	7.087±0.029	6.962±0.023	6.888±0.035	6.932±0.020	6.907±0.015	6.954±0.066
HIP 1481	TH	F8/G0V	4	7.460±0.010	0.537±0.008		2,2	6.462±0.018	6.248±0.036	6.149±0.017	6.141±0.048	6.102±0.023	6.138±0.015	5.746±0.031
TYC 1186-706-1	BP	K7V(e)	3	10.842±0.095			5	8.138±0.020	7.498±0.018	7.337±0.021	7.181±0.028	7.200±0.021	7.130±0.016	6.976±0.082
HIP 1910	TH	M0Ve	6	11.330±0.015	1.390±0.015	1.840±0.020	2,2,2	8.385±0.026	7.708±0.034	7.494±0.021	7.354±0.026	7.306±0.019	7.226±0.016	7.110±0.087
HIP 1993	TH	M0Ve	6	11.260±0.020	1.350±0.020		2,2	8.615±0.027	7.943±0.040	7.749±0.026	7.606±0.025	7.594±0.020	7.515±0.016	7.505±0.111
HIP 2729	TH	K5V	4	9.560±0.010	1.050±0.020	1.380±0.010	2,2,6	7.337±0.018	6.721±0.034	6.533±0.018	6.427±0.044	6.443±0.019	6.405±0.015	6.279±0.048
HIP 3556	TH	M1.5	7	11.910±0.015	1.480±0.015	2.180±0.020	2,2,2	8.481±0.020	7.867±0.024	7.623±0.027	7.509±0.026	7.428±0.021	7.329±0.016	7.320±0.107
TYC 5853-1318-1	BP	M1	8	11.457±0.071			9	8.149±0.020	7.473±0.024	7.252±0.033	7.150±0.030	7.118±0.019	7.047±0.015	7.003±0.077
CPD-64 120	TH	K1Ve	6	10.290±0.010	0.870±0.010	1.010±0.010	6,6,6	8.615±0.021	8.123±0.023	8.011±0.021	7.849±0.024	7.888±0.021	7.822±0.017	7.710±0.124
HD 8558	TH	G6V	4	8.530±0.010	0.705±0.015	0.770±0.010	2,2,6	7.241±0.021	6.946±0.034	6.847±0.029	6.753±0.037	6.809±0.021	6.792±0.015	6.745±0.058
HD 9054	TH	K2+ V k	10	9.350±0.010	0.951±0.030	1.010±0.010	2,2,6	7.405±0.019	6.944±0.026	6.834±0.023	6.765±0.036	6.813±0.020	6.764±0.015	6.660±0.058
TYC 1208-468-1	BP	K3Ve	11	9.891±0.020	1.171±0.067		9,9	7.479±0.019	6.861±0.018	6.716±0.018	6.575±0.041	6.584±0.020		6.444±0.050
HIP 9141	TH	G4V	6	8.070±0.010	0.651±0.012	0.720±0.010	2,2,6	6.856±0.023	6.555±0.038	6.472±0.026	6.391±0.045	6.440±0.019	6.436±0.015	6.159±0.041
HD 12894	TH	F2V	4	6.450±0.010	0.386±0.005	0.430±0.010	2,2,6	5.696±0.044	5.489±0.027	5.448±0.018	5.393±0.069		5.442±0.016	5.353±0.033
HD 13183	TH	G5V	4	8.640±0.010	0.701±0.017	0.760±0.010	2,2,6	7.347±0.024	6.986±0.042	6.894±0.023	6.865±0.034	6.908±0.019	6.861±0.015	6.733±0.069
HD 13246	TH	F8V	4	7.500±0.010	0.544±0.012	0.590±0.010	2,2,6	6.534±0.020	6.304±0.033	6.204±0.020			6.111±0.015	5.469±0.030
CD-60 416	TH	K5Ve	6	10.680±0.010	1.160±0.010	1.420±0.010	6,6,6	8.328±0.026	7.709±0.042	7.537±0.018			7.281±0.016	7.215±0.077
HIP 10679	BP	G3V	3	7.750±0.010	0.622±0.008		2,2	6.570±0.021	6.355±0.026	6.262±0.017				5.667±0.032
HIP 10680	BP	F7V	3	6.990±0.021	0.515±0.016		2,5	6.050±0.026	5.840±0.033	5.787±0.027				5.316±0.030
HIP 11152	BP	M1V	12	11.090±0.010	1.444±0.035		2,9	8.182±0.018	7.561±0.021	7.346±0.018			7.181±0.016	7.272±0.095
BD+30 397B	BP	M0	13	12.440±0.020	1.400±0.015		14,14	8.817±0.043	8.141±0.027	7.921±0.031			7.555±0.017	7.573±0.129
AG Tri	BP	K8V	15	10.120±0.010	1.205±0.015		2,2	7.870±0.034	7.235±0.018	7.080±0.026			6.976±0.015	6.466±0.060
TYC 7558-655-1	BP	K5V(e)	6	10.309±0.039	1.071±0.060		9,9	8.018±0.027	7.430±0.034	7.231±0.027	7.171±0.029	7.224±0.020	7.143±0.015	7.035±0.061
GSC 8056-0482	TH	M2Ve	6	12.110±0.010	1.480±0.010	2.330±0.010	6,6,6	8.420±0.023	7.755±0.023	7.501±0.027	7.415±0.027	7.312±0.022	7.211±0.016	7.106±0.073
HIP 12545	BP	K5IVe	3	10.570±0.023	1.250±0.017	1.470±0.013	16,16,16	7.904±0.027	7.234±0.031	7.069±0.031	6.946±0.034	6.943±0.020	6.879±0.016	6.801±0.070
CD-53 544	TH	K6Ve	6	10.220±0.010	1.260±0.010	1.600±0.010	6,6,6	7.582±0.023	6.934±0.034	6.763±0.026			6.599±0.016	6.485±0.047
GSC 8491-1194	TH	M2Ve	6	12.210±0.010	1.490±0.010	2.420±0.010	6,6,6	8.481±0.027	7.851±0.034	7.641±0.027				7.092±0.068

Table 3.1 (cont'd)

Star	Grp	SpT	Ref.	V (mag)	$B-V$ (mag)	$V-I_C$ (mag)	Ref.	J^a (mag)	H^a (mag)	K_S^a (mag)	$W1^b$ (mag)	$W2^b$ (mag)	$W3^b$ (mag)	$W4^b$ (mag)
GSC 8497-0995	TH	K5Ve	6	10.980±0.010	1.230±0.010	1.470±0.010	6,6,6	8.564±0.024	7.965±0.036	7.784±0.024	7.719±0.025	7.743±0.020	7.651±0.017	7.689±0.103
HIP 12925	TH	F7V	3	7.880±0.010	0.551±0.015		2,2	6.859±0.035	6.632±0.051	6.517±0.036	6.445±0.043	6.466±0.020	6.493±0.015	6.392±0.058
HIP 15247	TH	F6V	17	7.480±0.015	0.534±0.015		2,2	6.457±0.021	6.209±0.026	6.099±0.021	6.031±0.050		6.061±0.015	6.029±0.048
HIP 16853	TH	G2V	1	7.620±0.010	0.592±0.009		2,2	6.492±0.027	6.264±0.038	6.137±0.020			6.066±0.014	5.995±0.033
HIP 17782	TH	G8V	18	8.750±0.010	0.774±0.005		2,2	7.222±0.021	6.859±0.031	6.747±0.015	6.707±0.038	6.715±0.021	6.687±0.016	6.596±0.066
HD 25402	TH	G3V	1	8.360±0.010	0.611±0.014		2,2	7.203±0.019	6.939±0.017	6.875±0.027			6.839±0.013	6.743±0.052
51 Eri	BP	F0IV	19	5.220±0.010	0.283±0.006	0.330±0.020	2,2,2			4.537±0.024			4.538±0.014	4.387±0.021
GJ 3305	BP	M0Ve	3	10.534±0.010	1.409±0.009		9,9	7.299±0.019	6.639±0.049	6.413±0.018				6.002±0.041
HIP 21632	TH	G3V	6	8.470±0.010	0.611±0.012		2,2	7.273±0.023	6.970±0.033	6.866±0.016		6.899±0.022	6.896±0.016	6.837±0.070
HIP 21965	TH	F2/3 IV/V	20	7.120±0.010	0.411±0.008		2,2	6.288±0.020	6.068±0.034	6.023±0.023	5.931±0.058		6.019±0.015	5.957±0.042
V962 Per	BP	M2V	12	13.318±0.091			9	9.711±0.022	9.030±0.021	8.801±0.018	8.655±0.023	8.555±0.018	8.346±0.023	7.551±0.158
HIP 22295	TH	F7V	4	8.140±0.010	0.538±0.015	0.558±0.017	2,2,2	7.170±0.021	6.991±0.026	6.868±0.029	6.788±0.038	6.821±0.019	6.825±0.015	6.575±0.044
V1005 Ori	BP	K8IVe	3	10.050±0.020	1.394±0.020	1.840±0.010	2,2,2	7.117±0.020	6.450±0.031	6.261±0.017	6.173±0.046	6.079±0.023	6.054±0.016	6.002±0.047
HIP 23309	BP	K8Ve	3	10.020±0.010	1.260±0.063	1.790±0.010	2,5,6	7.095±0.021	6.429±0.029	6.244±0.024	6.129±0.050	6.093±0.022	6.061±0.014	5.934±0.031
HIP 23418	BP	M4IVe	3	11.450±0.015	1.540±0.015		2,2	7.212±0.023	6.657±0.029	6.370±0.021	6.180±0.048		5.970±0.015	5.796±0.040
HIP 24947	TH	F6V	6	7.390±0.010	0.510±0.003		2,2	6.416±0.023	6.218±0.034	6.144±0.024	6.109±0.053	6.057±0.024	6.101±0.014	5.865±0.033
HIP 25486	BP	F7V	3	6.300±0.010	0.553±0.007		2,2	5.268±0.027	5.087±0.026	4.926±0.021	4.924±0.070		4.910±0.016	4.808±0.028
TYC 7600-0516-1	TH	K1V(e)	6	9.520±0.010	0.800±0.010	0.970±0.010	6,6,6	7.905±0.021	7.462±0.036	7.303±0.021	7.231±0.030	7.243±0.022	7.194±0.016	7.155±0.073
TYC 7065-0879-1	TH	K0V	6	10.563±0.015	0.833±0.033	0.930±0.010	9,9,6	9.233±0.033	8.994±0.046	8.696±0.033	8.437±0.023	8.479±0.021	8.432±0.019	8.441±0.255
HIP 28036	TH	F7V	6	7.460±0.010	0.492±0.009		2,2	6.494±0.020	6.308±0.049	6.206±0.023	6.175±0.048	6.153±0.022	6.190±0.016	6.134±0.043
2MASS J06085283-2753583	BP	M8.5γ	21					13.595±0.028	12.897±0.026	12.371±0.026	11.976±0.024	11.623±0.021	11.314±0.113	
HIP 29964	BP	K3.5V	3	9.950±0.010	1.075±0.054		2,5	7.530±0.019	6.984±0.034	6.814±0.029	6.679±0.040	6.692±0.020	6.635±0.015	6.588±0.036
HIP 30030	TH	G0V	17	7.950±0.010	0.587±0.014		2,2	6.848±0.021	6.591±0.020	6.552±0.020	6.408±0.041	6.485±0.021	6.484±0.016	6.319±0.055
HIP 30034	TH	K2V	4	9.130±0.010	0.883±0.026		2,5	7.576±0.024	7.088±0.021	6.981±0.024	6.888±0.035	6.906±0.020	6.862±0.015	6.869±0.055
HIP 32235	TH	G6V	4	8.940±0.010	0.699±0.019		2,2	7.693±0.029	7.380±0.033	7.278±0.042	7.276±0.030	7.319±0.020	7.280±0.015	7.191±0.061
HIP 32435	TH	F5V	4	7.460±0.010	0.460±0.001		2,2	6.553±0.029	6.396±0.031	6.299±0.021	6.312±0.046		6.278±0.015	5.760±0.029
HIP 33737	TH	K3V	4	10.110±0.010	0.996±0.053		2,5	8.265±0.023	7.831±0.057	7.652±0.026	7.620±0.024	7.656±0.020		
RECX 18	EC	M5.5	22	17.660±0.020		3.760±0.028	23,23	11.849±0.024	11.277±0.026	10.945±0.021	10.687±0.022	10.438±0.020	10.329±0.040	
RECX 1	EC	K5IVe	3	10.610±0.020		1.420±0.028	24,24	8.155±0.019	7.498±0.049	7.338±0.021	7.137±0.031		7.064±0.015	6.978±0.056

Table 3.1 (cont'd)

Star	Grp	SpT	Ref.	V (mag)	$B-V$ (mag)	$V-I_C$ (mag)	Ref.	J^a (mag)	H^a (mag)	K_S^a (mag)	$W1^b$ (mag)	$W2^b$ (mag)	$W3^b$ (mag)	$W4^b$ (mag)
RECX 17	EC	M5.25	22	16.820±0.020		3.540±0.028	23,23	11.275±0.023	10.721±0.022	10.428±0.023		9.957±0.019	9.788±0.029	9.748±0.535
RECX 14	EC	M4.75	22	17.070±0.020		3.250±0.028	25,25	11.809±0.027	11.241±0.027	10.983±0.023	10.713±0.022	10.354±0.021	8.982±0.021	7.335±0.069
RECX 3	EC	M3.5IV-Ve	3	14.370±0.020		2.580±0.028	24,24	10.349±0.023	9.647±0.022	9.415±0.019			9.088±0.021	8.831±0.221
RECX 4	EC	M0IVe	3	12.730±0.020		1.920±0.028	24,24	9.535±0.024	8.779±0.061	8.615±0.019			8.308±0.016	7.755±0.098
RECX 5	EC	M4	22	15.200±0.020		2.810±0.028	24,24	10.777±0.023	10.099±0.021	9.855±0.021			7.859±0.016	5.192±0.027
RECX 6	EC	M3	22	14.080±0.020		2.400±0.028	24,24	10.232±0.027	9.584±0.023	9.290±0.021	9.238±0.024	9.105±0.020	8.953±0.020	8.772±0.222
RECX 7	EC	K5IV(e)	3	10.840±0.020		1.400±0.028	24,24	8.420±0.024	7.758±0.034	7.635±0.033				7.193±0.061
RECX 15	EC	M3.25	22	13.970±0.020		2.200±0.028	25,25	10.505±0.026	9.834±0.021	9.431±0.023				3.400±0.016
RECX 16	EC	M5.75	22					12.505±0.024	11.976±0.022	11.618±0.024	11.193±0.024	10.680±0.021	9.088±0.025	7.249±0.069
RECX 9	EC	M4.5	22	15.000±0.020		2.990±0.028	24,24	10.260±0.026	9.668±0.026	9.335±0.024		8.750±0.020	7.241±0.016	5.485±0.027
RECX 10	EC	K9IV-Ve	3	12.530±0.020		1.780±0.028	24,24	9.653±0.023	8.919±0.063	8.732±0.021	8.596±0.023	8.581±0.020	8.460±0.019	8.321±0.174
RECX 11	EC	K5IVe	3	11.130±0.020		1.370±0.028	24,24	8.729±0.020	8.025±0.055	7.655±0.038	7.231±0.031	6.899±0.019	5.385±0.015	3.716±0.019
RECX 12	EC	M3.25	22	13.170±0.020		2.370±0.028	24,24	9.323±0.024	8.683±0.082	8.410±0.031	8.292±0.023	8.151±0.020	8.012±0.017	7.938±0.107
HIP 47133	BP	K5V	26	11.090±0.010	1.440±0.015		2,14	8.085±0.018	7.429±0.026	7.235±0.018	7.153±0.030	7.168±0.020	7.087±0.016	6.957±0.079
TWA 21	TWA	K3IV(e)	3	9.831±0.059	0.973±0.049		5,5	7.870±0.023	7.353±0.034	7.194±0.021	7.133±0.029	7.170±0.021		7.134±0.112
DK Leo	BP	K7	27	10.042±0.012	1.409±0.008	1.802±0.009	28,28,28	7.074±0.023	6.448±0.020	6.261±0.023	6.140±0.048	6.069±0.022	6.054±0.015	5.971±0.041
TWA 22	BP	M5	13	13.960±0.014	1.726±0.032		9,9	8.554±0.021	8.085±0.046	7.689±0.021	7.495±0.023			6.809±0.056
TWA 6	TWA	M0Ve	6	11.620±0.010	1.310±0.010	1.680±0.010	6,6,6	8.869±0.034	8.180±0.036	8.042±0.021			7.717±0.019	7.784±0.152
2MASS J10252092-4241539	TWA	M1	29	12.729±0.042	1.425±0.060		9,9	9.500±0.030	8.812±0.023	8.588±0.019	8.517±0.024	8.453±0.020	8.332±0.020	8.086±0.183
2MASS J10260210-4105537	TWA	M1	29	12.553±0.057	1.416±0.078		9,9	9.176±0.020	8.494±0.047	8.272±0.027	8.150±0.023	8.064±0.019	7.938±0.019	8.068±0.194
TWA 34	TWA	M4.9	30					10.953±0.027	10.410±0.026	10.026±0.024	9.592±0.023	9.116±0.020	8.243±0.020	6.845±0.075
TWA 7	TWA	M3IVe	3	11.650±0.010	1.460±0.010	2.440±0.010	6,6,6	7.792±0.021	7.125±0.029	6.899±0.027			6.595±0.015	6.005±0.039
TWA 1	TWA	K8IVe	3	10.920±0.010		1.690±0.010	2,6	8.217±0.024	7.558±0.042	7.297±0.024	7.101±0.033	6.947±0.020	4.534±0.014	1.516±0.016
TWA 28	TWA	M8.5e	31	21.460±0.040		3.560±0.050	32,32	13.034±0.024	12.356±0.022	11.887±0.024	11.435±0.024	10.793±0.021	9.385±0.033	8.021±0.186
TWA 2	TWA	M1.5IVe	3	11.070±0.010	1.480±0.010	2.240±0.010	6,6,6	7.629±0.030	6.927±0.040	6.710±0.026	6.637±0.038	6.537±0.021	6.468±0.016	6.335±0.052
TWA 3	TWA	M4IVe	3	12.053±0.013	1.474±0.020	2.850±0.010	9,9,6	7.651±0.019	7.041±0.027	6.774±0.020	6.601±0.038	6.341±0.021	3.876±0.016	1.734±0.014
TWA 12	TWA	M2IVe	3	12.850±0.010	1.530±0.010	2.360±0.010	6,6,6	8.999±0.034	8.334±0.033	8.053±0.029	8.046±0.023	7.950±0.020	7.814±0.017	8.010±0.183
TWA 13A	TWA	M1Ve	6	11.460±0.010	1.420±0.010	1.890±0.010	6,6,6	8.431±0.043	7.727±0.067	7.491±0.038			7.425±0.027	6.998±0.141
TWA 13B	TWA	M1Ve	6	11.960±0.010	1.470±0.010	2.080±0.010	6,6,6	8.429±0.037	7.684±0.055	7.460±0.027			7.378±0.026	7.518±0.222

Table 3.1 (cont'd)

Star	Grp	SpT	Ref.	V (mag)	$B-V$ (mag)	$V-I_C$ (mag)	Ref.	J^a (mag)	H^a (mag)	K_S^a (mag)	$W1^b$ (mag)	$W2^b$ (mag)	$W3^b$ (mag)	$W4^b$ (mag)
TWA 4	TWA	K6IV(e)	3	8.890±0.010	1.192±0.032	1.390±0.010	2,5,6	6.397±0.020	5.759±0.027	5.587±0.021	5.487±0.062		3.109±0.012	0.194±0.010
2MASS J11254754-4410267	TWA	M1	29	14.634±0.017	1.620±0.031		9,9	10.341±0.026	9.753±0.023	9.476±0.023	9.331±0.023	9.144±0.020	8.996±0.022	8.808±0.249
TWA 5A	TWA	M2IVe	3	11.390±0.039	1.478±0.055	2.360±0.010	9,9,6	7.669±0.026	6.987±0.034	6.745±0.023	6.654±0.038	6.507±0.020	6.407±0.016	6.315±0.050
TWA 30B	TWA	M4V	33					15.350±0.047	14.531±0.050	13.721±0.040	12.302±0.023	10.621±0.021	7.345±0.017	5.070±0.027
TWA 30A	TWA	M5V	33					9.641±0.024	9.030±0.023	8.765±0.021	8.796±0.022	8.436±0.021	7.071±0.016	5.156±0.028
TWA 8B	TWA	M5.5	34					9.837±0.024	9.276±0.022	9.012±0.025			8.434±0.044	8.633±0.366
TWA 8A	TWA	M3IVe	3	12.230±0.010	1.460±0.010	2.410±0.010	6,6,6	8.337±0.024	7.663±0.042	7.430±0.017			7.130±0.013	7.037±0.092
TWA 33	TWA	M4.7	30	15.065±0.010	1.644±0.020		9,9	9.985±0.021	9.414±0.023	9.118±0.023	8.765±0.022	8.404±0.019	7.135±0.017	5.518±0.038
TWA 26	TWA	M8IVe	35					12.686±0.026	11.996±0.022	11.503±0.023	11.155±0.023	10.793±0.020	10.626±0.075	
TWA 9B	TWA	M3.5	34	14.000±0.010	1.430±0.010		6,6	9.981±0.027	9.381±0.023	9.151±0.024			8.810±0.044	
TWA 9A	TWA	K7IVe	3	11.130±0.010	1.281±0.011	1.620±0.010	2,9,6	8.684±0.034	8.034±0.040	7.848±0.036			7.571±0.019	7.410±0.122
TWA 31	TWA	M4.2	36					13.048±0.022	12.490±0.024	12.115±0.021	11.752±0.023	11.271±0.021	9.948±0.041	7.836±0.134
TWA 23	TWA	M1	13	12.638±0.035	1.519±0.059		9,9	8.618±0.029	8.025±0.044	7.751±0.031	7.642±0.026	7.506±0.022	7.407±0.017	7.229±0.085
TWA 27	TWA	M8IVe	35					12.995±0.026	12.388±0.027	11.945±0.026	11.556±0.023	11.009±0.020	9.456±0.027	8.029±0.133
TWA 25	TWA	K9IV-Ve	3	11.440±0.010	1.410±0.010	1.940±0.010	6,6,6	8.166±0.034	7.504±0.042	7.306±0.020	7.264±0.029	7.208±0.020	7.128±0.016	7.079±0.075
2MASS J12265135-3316124	TWA	M6.3	36					10.691±0.024	10.122±0.028	9.783±0.025	9.556±0.024	9.207±0.021	7.787±0.017	5.787±0.037
TWA 20	TWA	M3IVe	3	13.171±0.034	1.514±0.061		9,9	9.331±0.030	8.693±0.063	8.412±0.029	8.329±0.025	8.208±0.021	8.063±0.024	7.775±0.149
TWA 16	TWA	M2IVe	3	12.580±0.017	1.468±0.021		9,9	8.994±0.026	8.332±0.038	8.090±0.023	7.942±0.023	7.856±0.020	7.741±0.017	7.544±0.103
TWA 10	TWA	M2Ve	6	12.960±0.010	1.430±0.010	2.470±0.010	6,6,6	9.122±0.024	8.477±0.044	8.186±0.029	8.086±0.023	7.964±0.020	7.866±0.018	7.748±0.107
TWA 11C	TWA	M4.5	37	14.427±0.042			9	9.790±0.026	9.223±0.022	8.943±0.024	8.796±0.022	8.593±0.020	8.350±0.019	7.813±0.114
TWA 29	TWA	M9.5e	38					14.518±0.032	13.800±0.033	13.369±0.036				
HD 139084B	BP	M5Ve	6					10.050±0.046	9.449±0.057	9.188±0.038				8.183±0.228
HD 139084	BP	G8V	3	8.153±0.014	0.817±0.007	0.900±0.010	5,2,6	6.382±0.024	5.994±0.031	5.852±0.031			5.816±0.015	5.795±0.046
2MASS J16430128-1754274	BP	M0.5	8					9.443±0.025	8.759±0.046	8.549±0.025	8.440±0.022	8.411±0.020	8.367±0.026	
HD 155555	BP	G5V+K1V	3	6.870±0.010	0.798±0.007		2,2	5.288±0.032		4.702±0.016			4.600±0.013	4.520±0.027
HIP 84642	TH	G8/K0V	4	9.510±0.010	0.754±0.027	0.850±0.010	2,2,6	8.008±0.018	7.671±0.021	7.527±0.023	7.449±0.026	7.464±0.020	7.445±0.016	7.647±0.146
CD-54 7336	BP	K1V	6	9.550±0.010	0.850±0.010	0.950±0.010	6,6,6	7.941±0.030	7.462±0.029	7.364±0.026	7.336±0.027	7.358±0.019	7.279±0.017	6.901±0.069
HD 160305	BP	F8/G0V	1	8.330±0.010	0.574±0.023		2,2	7.345±0.021	7.092±0.047	6.992±0.020	6.937±0.033	6.980±0.019	6.954±0.016	6.676±0.071
HD 161460	BP	G9V	3	8.986±0.019	0.856±0.025	0.910±0.010	5,5,6	7.316±0.023	6.925±0.040	6.776±0.023				6.697±0.068

Table 3.1 (cont'd)

Star	Grp	SpT	Ref.	V (mag)	$B-V$ (mag)	$V-I_C$ (mag)	Ref.	J^a (mag)	H^a (mag)	K_S^a (mag)	$W1^b$ (mag)	$W2^b$ (mag)	$W3^b$ (mag)	$W4^b$ (mag)
HIP 88399	BP	F4.5V	3	7.010±0.010	0.458±0.015		2,2	6.159±0.019	6.022±0.031	5.913±0.020			5.960±0.013	4.982±0.030
HD 164249B	BP	M2Ve	6					8.910±0.071	8.522±0.036	8.273±0.027			8.225±0.058	8.345±0.495
V4046 Sgr	BP	K4IVe	3	10.680±0.090			5	8.071±0.023	7.435±0.051	7.249±0.020	7.123±0.027	7.094±0.019	4.960±0.015	1.928±0.016
GSC 7396-0759	BP	M1IVe	3	12.780±0.010	1.360±0.010	2.140±0.010	6,6,6	9.443±0.023	8.766±0.038	8.539±0.023	8.457±0.022	8.382±0.019	8.320±0.023	8.024±0.191
HD 168210	BP	G3IV	3	8.797±0.020	0.639±0.025	0.780±0.010	5,5,6	7.526±0.023	7.198±0.018	7.053±0.033	6.917±0.034	6.961±0.018	7.000±0.015	6.884±0.107
CD-64 1208	BP	K4V(e)	3	9.433±0.052			9	6.906±0.021	6.318±0.042	6.096±0.027				
TYC 9073-0762-1	BP	M1Ve	3	12.080±0.010	1.460±0.010	2.090±0.010	6,6,6	8.746±0.019	8.047±0.040	7.854±0.024	7.748±0.024	7.705±0.022	7.634±0.017	7.662±0.136
TYC 7408-0054-1	BP	K8IVe	3	11.200±0.010	1.350±0.010	1.760±0.010	6,6,6	8.314±0.021	7.667±0.047	7.462±0.027	7.402±0.026	7.368±0.019	7.321±0.017	7.386±0.137
PZ Tel	BP	G9IV	6	8.430±0.010	0.784±0.021	0.850±0.010	2,2,6	6.856±0.021	6.486±0.049	6.366±0.024	6.257±0.049	6.285±0.022	6.274±0.014	6.260±0.047
TYC 6872-1011-1	BP	K8IVe	3	11.780±0.010	1.300±0.010	1.800±0.010	6,6,6	8.863±0.021	8.162±0.029	8.018±0.021				7.689±0.180
CD-26 13904	BP	K3.5IV(e)	3	10.270±0.010	1.050±0.010	1.180±0.010	6,6,6	8.081±0.020	7.556±0.024	7.366±0.018	7.281±0.026	7.312±0.018	7.323±0.021	7.558±0.238
HIP 95270	BP	F6V	3	7.040±0.010	0.480±0.004		2,2	6.200±0.024	5.980±0.044	5.910±0.029	5.877±0.053		5.893±0.015	3.956±0.023
2MASS J19560294-3207186	BP	M4	8					8.959±0.027	8.344±0.038	8.114±0.027			7.655±0.017	7.628±0.149
TYC 7443-1102-1	BP	K9IVe	3	11.589±0.023	1.420±0.033		9,9	8.710±0.029	8.027±0.040	7.846±0.021			7.632±0.017	7.323±0.109
2MASS J20013718-3313139	BP	M1	8	12.374±0.030	1.472±0.042		9,9	9.155±0.024	8.461±0.055	8.244±0.024	8.139±0.024	8.096±0.019	8.032±0.021	7.868±0.189
AT Mic	BP	M4IVe	3	10.270±0.020	1.550±0.020	2.900±0.020	2,2,2	5.807±0.026	5.201±0.046	4.944±0.042	4.680±0.089		4.461±0.016	4.330±0.024
AU Mic	BP	M0Ve	3	8.757±0.020	1.452±0.038	2.100±0.000	5,5,2	5.436±0.017	4.831±0.016		4.499±0.086		4.312±0.014	4.137±0.025
HD 199143	BP	F7V	1	7.270±0.015	0.544±0.015		2,2	6.207±0.019	5.945±0.038	5.811±0.020	5.718±0.056		5.763±0.014	5.650±0.039
AZ Cap	BP	K5IVe	3	10.620±0.010	1.220±0.010	1.490±0.010	6,6,6	7.849±0.021	7.249±0.031	7.039±0.020	6.837±0.034	6.846±0.021	6.830±0.015	6.855±0.077
HIP 105388	TH	G5V	4	8.650±0.010	0.690±0.015	0.800±0.010	2,2,6	7.386±0.021	7.026±0.038	6.908±0.023	6.815±0.035	6.872±0.020	6.849±0.016	6.552±0.055
HIP 105404	TH	G9V	6	8.890±0.010	0.854±0.022	1.040±0.010	2,2,6	7.184±0.026	6.699±0.031	6.574±0.024	6.536±0.041	6.520±0.021	6.507±0.015	6.383±0.047
HIP 107345	TH	M0Ve	6	11.720±0.015	1.400±0.015	1.840±0.020	2,2,2	8.751±0.026	8.087±0.023	7.874±0.026	7.781±0.024	7.755±0.020	7.672±0.018	7.632±0.120
HIP 107947	TH	F6V	4	7.220±0.010	0.510±0.001		2,2	6.358±0.027	6.149±0.031	6.027±0.021	6.013±0.052		6.041±0.015	5.862±0.036
HIP 108195	TH	F3V	4	5.920±0.010	0.393±0.003		2,2			4.909±0.017	4.903±0.074		4.935±0.014	4.864±0.026
HIP 108422	TH	G8V	4	8.900±0.010	0.767±0.017	0.900±0.010	2,2,6	7.310±0.026	6.858±0.040	6.745±0.017	6.672±0.043	6.670±0.023	6.632±0.017	6.571±0.056
TYC 2211-1309-1	BP	K8IVe	3	11.366±0.041	1.296±0.057		9,9	8.556±0.034	7.949±0.024	7.724±0.016	7.602±0.025	7.602±0.020	7.536±0.023	7.279±0.111
CPD-72 2713	BP	K7IVe	3	10.600±0.010	1.350±0.010	1.730±0.010	6,6,6	7.791±0.021	7.123±0.047	6.894±0.018	6.758±0.037	6.772±0.018	6.712±0.015	6.623±0.054
HIP 112312	BP	M4IVe	6	12.160±0.030	1.500±0.020	2.780±0.020	39,39,39	7.786±0.019	7.154±0.031	6.932±0.029			6.514±0.015	6.378±0.055
TX PsA	BP	M5IVe	6	13.420±0.020	1.580±0.020	3.040±0.010	39,39,39	8.681±0.020	8.057±0.034	7.793±0.026			7.311±0.016	7.203±0.105

Table 3.1 (cont'd)

Star	Grp	SpT	Ref.	V (mag)	$B-V$ (mag)	$V-I_C$ (mag)	Ref.	J^a (mag)	H^a (mag)	K_S^a (mag)	$W1^b$ (mag)	$W2^b$ (mag)	$W3^b$ (mag)	$W4^b$ (mag)
BD-13 6424	BP	M0V-IVe	3	10.540±0.010	1.430±0.010	1.980±0.010	6,6,6	7.450±0.021	6.769±0.040	6.569±0.018	6.489±0.040	6.426±0.019	6.387±0.016	6.246±0.050
HD 222259B	TH	K3Ve	6	9.840±0.010	1.000±0.010	1.160±0.010	6,6,6	7.630±0.058	7.193±0.034	7.032±0.063				6.958±0.119
HD 222259	TH	G6V	6	8.469±0.013	0.693±0.017	0.770±0.010	5,5,6	7.122±0.024	6.759±0.023	6.676±0.034			6.777±0.023	6.668±0.094

Note. — Groups: (BP) – β Pic Moving Group; (EC) – η Cha Cluster; (TWA) – TW Hydra Association; (TH) – Tucana–Horologium Association; References for Spectral Type and optical BVI_C photometry: (1) Houk (1978); (2) Perryman & ESA (1997); (3) This Work (4) Houk & Cowley (1975); (5) Converted from Tycho-2 using Mamajek et al. (2002, 2006); (6) Torres et al. (2006); (7) Hawley et al. (1996); (8) Riaz et al. (2006); (9) Gray et al. (2006); (10) Jeffries (1995); (11) Henden et al. (2012); (12) Zuckerman & Song (2004); (13) Weis (1993); (14) Vyssotsky (1956); (15) Robertson & Hamilton (1987); (16) Houk & Swift (1999); (17) Stephenson & Sanwal (1969); (18) Gray & Garrison (1989); (19) Houk & Smith-Moore (1988); (20) Schlieder et al. (2012a); (21) Rice et al. (2010b); (22) Luhman & Steeghs (2004); (23) Lyo et al. (2004); (24) Lawson et al. (2001); (25) Lawson et al. (2002); (26) Stephenson (1986); (27) Reid et al. (1995); (28) Koen et al. (2010); (29) Rodriguez et al. (2011); (30) Schneider et al. (2012b); (31) Scholz et al. (2005); (32) Teixeira et al. (2008); (33) Looper et al. (2010b); (34) White & Hillenbrand (2004); (35) Barrado Y Navascués (2006); (36) Shkolnik et al. (2011); (37) Kastner et al. (2008); (38) Looper et al. (2007); (39) Song et al. (2002);
(^{a}) JHK_S photometry from the 2MASS All-Sky Point Source Catalog (Cutri et al., 2003);
(^{b}) $W1\,W2\,W3\,W4$ photometry from *WISE* All Sky Data Release (Cutri & et al., 2012);

3.5 Analysis

3.5.1 Spectral Classification

The optical spectra were visually classified by directly comparing them with spectral standards using a custom spectral software tool, *sptool*[3], described in Pecaut et al. (2012). F- and G-type standards are taken from Table 2 of Pecaut et al. 2012; K- and M-type standards are listed in Table 3.2. For the blue spectra, the F-type stars were classified using the strength and profile of the Balmer lines, with particular attention to the wings of the lines in case the line depths were filled in by chromospheric emission. In addition, we use the G-band at ∼4310Å as it is a very useful temperature indicator for solar metallicity F-type stars (Gray & Corbally, 2009). For G-type stars we use the G-band, Fe I lines at 4046Å, 4325Å, and 4383Å, the Ca I line at 4227Å, and the Mg Ib triplet at ∼5170Å. Spectral classification using the features described here is discussed in greater detail in Gray & Corbally (2009).

For objects with red spectra (∼5600Å-6900Å) only, we first determine if it is a K- or M-type star based on the overall appearance of the spectrum. For K-type stars we obtain accurate spectral classifications using the Ca I lines at 6102Å, 6122Å, 6162Å, and 6169Å, the Fe I lines at 6137Å, the relative strength of the V I and Fe I blend at 6252Å to Ti I at 6258Å, and the relative strength of the V, Ti, and Fe blend at 6297Å to the Fe I blend at 6302Å[4]. We also made use of Ca I lines at $\lambda\lambda$ 6438 and 6449, the Ca I/Fe I blend at 6462Å, the Fe I, Ti I and Cr I blend at 6362Å, the Ba II, Fe I and Ca I blend at 6497Å, and for the latest K-types, the TiO bands from ∼6651Å-6852Å. For M-type stars we use the Ca I lines at 6122Å and 6162Å, but predominantly rely on TiO bands from ∼5847Å-6858Å, ∼6080Å-6390Å, and ∼6651Å-6852Å. Following

[3]http://www.pas.rochester.edu/˜mpecaut/sptool

[4]Many of these lines were identified using the VALD service (Kupka et al., 1999). http://vald.astro.univie.ac.at/

Table 3.2. Spectral standard stars used for classification.

Standard	Spectral Type	Telescope/Source	References
HD 8512	K0IIIb	SMARTS 1.5m/Stony Brook	1
HD 3651	K0V	SMARTS 1.5m/Stony Brook	2
HD 10476	K1V	SMARTS 1.5m/Stony Brook	1
HD 153210	K2III	SMARTS 1.5m/Stony Brook	1
HD 22049	K2V	SMARTS 1.5m/Stony Brook	1
HD 16160	K3V	SMARTS 1.5m/Stony Brook	1
α Sct	K3III	SMARTS 1.5m/Rochester	1
TW PsA	K4Ve	SMARTS 1.5m/Rochester	1
β Cnc	K4III Ba0.5	SMARTS 1.5m/Rochester	1
HD 82668	K5III	SMARTS 1.5m/Rochester	1
HD 36003	K5V	SMARTS 1.5m/Stony Brook	1
GJ 529	K6Va	SMARTS 1.5m/Rochester	1
GJ 673	K7V	SMARTS 1.5m/Rochester	2
HIP 111288	K8V k	SMARTS 1.5m/Rochester	3
HD 142574	K8IIIb	SMARTS 1.5m/Rochester	1
HIP 3261	K9V	SMARTS 1.5m/Stony Brook	3
GJ 701	M0.0V	SMARTS 1.5m/Rochester	4
υ Gem	M0III	SMARTS 1.5m/Rochester	1
GJ 229A	M1.0V	SMARTS 1.5m/Rochester	4
ν Vir	M1III	SMARTS 1.5m/Rochester	1
GJ 411	M2+V	SMARTS 1.5m/Rochester	1
GJ 752A	M3-V	SMARTS 1.5m/Rochester	1
GJ 402	M4.0V	SMARTS 1.5m/Rochester	4
Gl 9066	M5-V	SMARTS 1.5m/Stony Brook	1
HD 151061	M5-M5.5IIIb	SMARTS 1.5m/Rochester	1
GJ 406	M6.0V	SMARTS 1.5m/Rochester	4
HD 118767	M6III	SMARTS 1.5m/Rochester	1

Note. — References: (1) Keenan & McNeil (1989); (2) Gray et al. (2003); (3) Gray et al. (2006); (4) Henry et al. (2002)
Spectral standards for F- and G-type stars were taken from Table 2 of Pecaut et al. (2012).

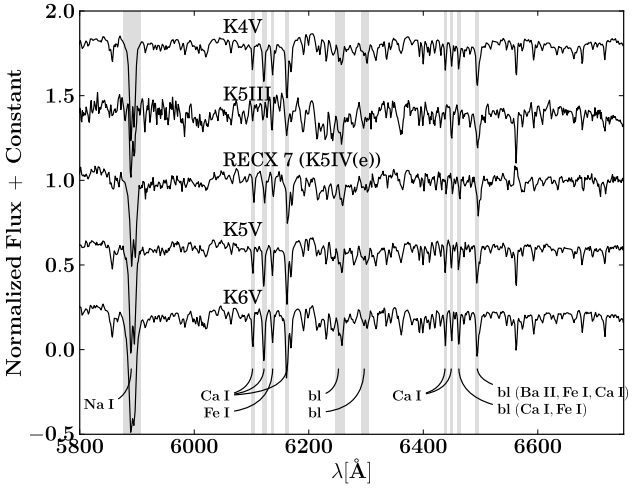

Figure 3.2 A spectrum of η Cha member RECX 7 (K5IV(e)) with spectral standards K4Ve (TW PsA), K5III (HD 82668), K5V (HD 36003), and K6Va (GJ 529). The primary regions used for spectral classification of K-type stars are highlighted in grey.

Gray et al. (2003, 2006), we assign spectral types K8 and K9, where appropriate. This is discussed in more detail in Appendix B. Example spectra with the lines used are shown in Figure 3.2.

While obtaining temperature types for our sample we ignored the Na I doublet at $\sim 5889/5896$Å because it is sensitive both to temperature and to surface gravity and is thus useful in discriminating between stars with dwarf-like, subgiant-like or giant-like gravity. The young stars in our sample are pre-main sequence and thus may have a Na I doublet line similar to subgiants. Once a temperature type had been established, we compared the Na I doublet to that of a dwarf and a giant of the same temperature subclass, assigning the luminosity class "IV" if the strength was intermediate between the dwarf and giant, "IV-V" if the strength was very similar to that of a dwarf but only slightly weaker, and "V" if the Na doublet was indistinguishable from a dwarf. The results of our spectral classification are listed in Table 3.3.

Table 3.3. Observations and New Spectral Types

Object	Spectral Type (This Work)	Spectral Coverage	Spectral Type (Literature)	Ref.
HR 9	F3V	Blue	F3Vn	1
TYC 1186-706-1	K7V(e)	Blue	K5	2
HIP 10679	G3V	Blue	G2V	3
HIP 10680	F7V	Blue	F7V	3
HIP 12545	K5IVe	Blue/Red	K6Ve	4
HIP 12925	F7V	Blue	F8	5
GJ 3305	M0Ve	Blue/Red	M1.1	6
V1005 Ori	K8IVe	Blue/Red	M0Ve	4
HIP 23309[b]	K8Ve	Blue/Red	K8V kee	1
HIP 23418	M4IVe	Red	M4	2
HIP 25486	F7V	Blue	F8V(n)k	1
HIP 29964	K3.5V	Blue	K3.5V ke	1
RECX 1	K5IVe	Red	K6	7
RECX 3	M3.5IV-Ve	Red	M3.25	7
RECX 4	M0IVe	Red	M1.75	7
RECX 7	K5IV(e)	Red	K6	7
RECX 10	K9IV-Ve	Red	M1	7
RECX 11	K5IVe	Red	K5.5	7
TWA 21	K3IV(e)	Red	K3Ve	4
TWA 7	M3IVe	Red	M2Ve	4
TWA 1	K8IVe	Red	K6Ve	4
TWA 2	M1.5IVe	Red	M2Ve	4
TWA 3	M4IVe	Red	M4Ve	4
TWA 12	M2IVe	Red	M2	8
TWA 4	K6IV(e)	Red	K5V	4
TWA 5A	M2IVe	Red	M2Ve	4
TWA 8A	M3IVe	Red	M3	9
TWA 9A	K7IVe	Red	K7	9
TWA 25	K9IV-Ve	Red	M1Ve	4
TWA 20	M3IVe	Red	M2	10
TWA 16	M2IVe	Red	M1.5e	11

Table 3.3 (cont'd)

Object	Spectral Type (This Work)	Spectral Coverage	Spectral Type (Literature)	Ref.
HD 139084	G8V	Blue	K0V k	1
HD 155555AB[a]	G5V, K1V	Blue/Red	G5IV+K0IV-V	12
HD 161460	G9V	Blue	K0IV	4
HIP 88399	F4.5V	Blue/Red	F6V	4
V4046 Sgr	K4IVe	Blue	K1e	13
GSC 7396-0759	M1IVe	Red	M1Ve	4
HD 168210	G3IV	Blue	G5V	4
CD-64 1208	K4V(e)	Blue	K5Ve	4
TYC 9073-0762-1	M1Ve	Red	M1Ve	4
TYC 7408-0054-1	K8IVe	Red	K8Ve	4
TYC 6872-1011-1	K8IVe	Red	M0Ve	4
CD-26 13904	K3.5IV(e)	Red	K4V(e)	4
HIP 95270	F6V	Blue	F6V	4
TYC 7443-1102-1	K9IVe	Red	M0.0Ve	14
AT Mic A	M4IVe	Red	M4Ve	4
AT Mic B	M4IVe	Red	M4Ve	4
AU Mic	M0Ve	Red	M1Ve Ba1	15
AZ Cap	K5IVe	Red	K6Ve	4
TYC 2211-1309-1[c]	K8IVe	Red	M0.0Ve	14
CPD-72 2713	K7IVe	Red	K7Ve	4
BD-13 6424	M0V-IVe	Red	M0Ve	4

Note. — References: (1) Gray et al. (2006); (2) Stephenson (1986); (3) Harlan (1969); (4) Torres et al. (2006); (5) Cannon & Pickering (1918); (6) Shkolnik et al. (2009); (7) Luhman & Steeghs (2004); (8) Sterzik et al. (1999); (9) White & Hillenbrand (2004); (10) Reid (2003);
(11) Zuckerman et al. (2001); (12) Strassmeier & Rice (2000); (13) Stephenson & Sanduleak (1977); (14) Lépine & Simon (2009); (15) Keenan & McNeil (1989);
[a] Our blue spectrum of this object was classified as G5V while our red spectrum was classified as a K1V. Therefore we adopted an overall spectral type of G5V,K1V.
[b] Our spectrum of this object did not cover the Na doublet feature;
[c] McCarthy & White (2012) were unable to detect Li in a high-resolution spectrum of this object, casting doubt on its membership in β Pic; however, we retain it as a member for the purposes of this study.

3.5.2 Synthetic Colors

In order to compare observed colors to model atmosphere predictions for the color locus and the predicted effects of surface gravity, we compare our observed colors with synthetic colors calculated from the "BT-Settl" models from the Phoenix/NextGen group (Hauschildt et al., 1999; Allard et al., 2012) and the "ATLAS9" models from Castelli & Kurucz (2004). The BT-Settl models offer synthetic spectra with 400 K <$\mathrm{T_{eff}}$< 70000 K, $-0.5 < \log(g) < 5.5$ and $-4.0 < [M/H] < +0.5$, with α-element enhance-

ment between +0.0 and +0.6 dex. The ATLAS9 models offer synthetic spectra with 3500 K <T_{eff}< 50000 K, $0.0 < \log(g) < 5.0$, $-5.5 < [M/H] < +0.5$ with α-element enhancement between +0.0 and +0.4 dex. However, since our objects are young and are in the solar neighborhood, we assume solar metallicity with no α-element enhancement. This is consistent with the findings of Viana Almeida et al. (2009), who have spectroscopically analyzed a small sample of these young stars, obtaining <[Fe/H]>=-0.06±0.09 dex for a sample of nine Tuc-Hor stars and [Fe/H]=-0.13±0.08 dex for β Pic member HD 322990. We computed synthetic colors, listed in Table 3.4, for solar metallicity models with with $3.0 < \log(g) < 5.0$, 1400 K <T_{eff}< 50000 K for the BT-Settl models and 3500 K <T_{eff}< 50000 K for the ATLAS9 models, with no α-element enhancement. Pre-MS stars have lower surface gravities than main sequence stars at the same T_{eff} but both should have $3.0 < \log(g) < 5.0$. We wish to evaluate model predictions of color trends as a function of surface gravity, so we plot $\log(g) = 3.0$ synthetic colors and $\log(g) = 5.0$ synthetic colors. A coeval population will have a surface gravity which varies as a function of mass, so we also plot a sequence with surface gravities given by a 20 Myr isochrone from the Baraffe et al. (1998) models. We plot commonly used colors against V–K_S. We chose V–K_S because it is available for nearly all our objects, and it offers a very large baseline compared to other colors so it is useful as a proxy for T_{eff}. To compute the synthetic photometry for the models, we use the updated BVI_C normalized photonic bandpasses and zero points from Bessell & Murphy (2012), including the additional zeropoints listed in their Table 5. To compute the 2MASS JHK_S synthetic photometry, we use the relative system response (RSR) curves available on the IPAC website[5] with the zero magnitude flux given in Rieke et al. (2008). Similarly, for the WISE bands we use RSR curves available on

[5]http://www.ipac.caltech.edu/2mass/releases/allsky/doc/sec6_4a.html

the IPAC website[6] with the zero magnitude flux given in Jarrett et al. (2011). The ATLAS9 models are sparsely sampled past $\sim$10μm, with only 9 points from 10μm to 160μm, so we multiply by λ^4, linearly interpolate between points and then divide the result by λ^4. This is not necessary for the BT-Settl models because they are sampled at 0.2Å spectral resolution for $\lambda > 5.2\mu$m. The BT-Settl models shown use the Asplund et al. (2009) solar abundances and the ATLAS9 models shown use the Grevesse & Sauval (1998) solar abundances. The computed synthetic colors are listed in Table 3.4.

[6]http://wise2.ipac.caltech.edu/docs/release/prelim/expsup/sec4_3g.html

Table 3.4. Synthetic Color Indices From BT-Settl and ATLAS9 models

$T_{\rm eff}$ (K)	log(g) (dex)	U–B (mag)	B–V (mag)	V–I_C (mag)	R_C–I_C (mag)	J–H (mag)	H–K_S (mag)	V–K_S (mag)	K–$W1$ (mag)	K–$W2$ (mag)	K–$W3$ (mag)	K–$W4$ (mag)	V–V_T (mag)	B_T–V_T (mag)	V–$H_{\rm p}$ (mag)	Model
1400	3.5	3.475	3.191	5.213	2.454	1.916	1.344	13.151	1.379	1.967	2.652	2.921	-0.405	3.747	0.979	BT-Settl
1400	4.0	4.909	0.795	7.250	2.854	1.149	0.635	13.788	0.983	1.083	2.226	2.292	0.091	1.668	2.550	BT-Settl
1400	4.5	4.959	-0.165	7.918	3.184	0.919	0.306	13.929	0.923	1.148	2.326	2.426	0.561	1.123	2.903	BT-Settl
1400	5.0	4.957	-0.945	8.421	3.433	0.893	0.098	14.184	0.873	1.363	2.474	2.631	1.085	0.836	3.189	BT-Settl
1500	3.5	3.642	3.306	5.223	2.433	1.467	1.048	12.157	1.088	1.594	2.323	2.577	-0.412	3.929	1.006	BT-Settl

Note. — All synthetic colors are computed using solar metallicity models. The BT-Settl model colors presented here adopt the Asplund et al. (2009) solar composition, whereas the ATLAS9 model colors presented here adopt the Grevesse & Sauval (1998) solar composition. Table 3.4 is published in its entirety in the electronic edition of ApJS. A portion is shown here for guidance regarding its form and content.

3.5.3 Empirical Colors of Dwarfs Versus Pre-MS Stars

To compare dwarfs colors with pre-MS colors, we plot color-color diagrams (Figure 3.3) for the young stars listed in Table 3.1. Figures 3.3 and 3.4 show V–K_S versus B–V, V–I_C, J–H, H–K_S, K_S–$W1$, K_S–$W2$, K_S–$W3$ and K_S–$W4$ for the young stars along with the dwarf sequence described in Appendix C (listed in Table C.1) and the empirical giant sequence for B–V from Alonso et al. (1999) and for V–I_C, J–H, and H–K_S from Bessell & Brett (1988) converted to the 2MASS photometric system with the conversions of Carpenter (2001). For reference we include the BVI_C solar colors estimated by Ramírez et al. (2012) and 2MASS JHK_S and WISE $W1\,W2\,W3\,W4$ solar colors estimated by Casagrande et al. (2012).

Color-color plots V–K_S versus B–V and V–K_S versus J–H show the largest color difference between our young stars and the dwarf locus. Redward of V–$K_S \sim 2.0$ mag, young stars are bluer in B–V than the dwarf locus, and for V–$K_S \geq 4.0$ they are well-matched by the 20 Myr isochronal colors. Models predict the B–V colors are bluer at lower surface gravity at a given V–K_S, consistent with our observations, though the agreement is not perfect. Models predict little sensitivity to surface gravity for V–K_S versus V–I_C, consistent with the location of the dwarf and giant locus as well as the placement of the young stars. For V–K_S versus J–H locus, a bifurcation between the dwarf and giant empirical locus occurs at V–K_S ∼3 mag, which corresponds to a spectral type of ∼K5. This split is explained by the models as an effect of surface gravity, due to the CO and H_2O bands and H^- opacity (Jorgensen, 1996). The young stars in our sample have surface gravities intermediate between that of the giants and dwarfs, and as a result they populate the region between the dwarf and giant loci. For V–$K_S \leq 3.5$, the young stars lie above the dwarf locus for colors H–K_S and K_S–$W1$, indicating that these two colors are redder for young stars

at a given V–K_S. We exclude photometry for objects which have previously identified infrared excesses in that respective infrared band, likely due to a dusty circumstellar disk. Objects RECX 11 and RECX 15 are known class II sources so we exclude their WISE and 2MASS K_S band photometry (Sicilia-Aguilar et al., 2009). Objects RECX 5, RECX 9, RECX 14, RECX 16, and TWA 27 have identified *Spitzer* IRAC 3.6μm and 4.5μm excesses (Megeath et al., 2005; Riaz et al., 2006), so we exclude all of their WISE photometry. We exclude $W3$ and $W4$ band photometry for TWA 1, TWA 28, TWA 31, TWA 33, TWA 34, 2MASS J12265135-3316124 and V4046 Sgr because of the identified excesses in those bands (Schneider et al., 2012a,b; Hutchinson et al., 1990). Finally, we exclude $W4$ band photometry for objects HR 9, HIP 10679, HIP 88399, HIP 95270, RECX 2, RECX 3, RECX 4, HIP 1113, HIP 1481, CPD-64 120, HD 8558, HIP 9141, HD 13246, HIP 16853, HIP 22295, HIP 24947, TYC 7600-0516-1, HIP 30030, HIP 30034, HIP 32235, HIP 32435, HIP 84642, HIP 105388, HIP 105404, HIP 108422, TWA 3, TWA 4, and TWA 7 due to their identified *Spitzer* MIPS 24μm or WISE $W4$ excesses (Rebull et al., 2008; Gautier et al., 2008; Zuckerman et al., 2011; Schneider et al., 2012a). The binary pair HIP 10679 and HIP 10680 were studied in Rebull et al. (2008), with only HIP 10679 identified as having a 24 μm excess. However, they are separated by $\sim$14$''$ and thus it is likely that the HIP 10680 $W4$ photometry is contaminated by the HIP 10679 $W4$ excess, so we exclude the HIP 10680 $W4$ photometry as well.

3.5.4 Spectral Type-Color Sequence

To define the intrinsic color sequence empirically, with the constraint of satisfying the color-color plots, we first fit a spline to spectral type versus V–K_S and spectral type versus V–I_C. We then verify that these relations provide a good fit to the V–K_S versus

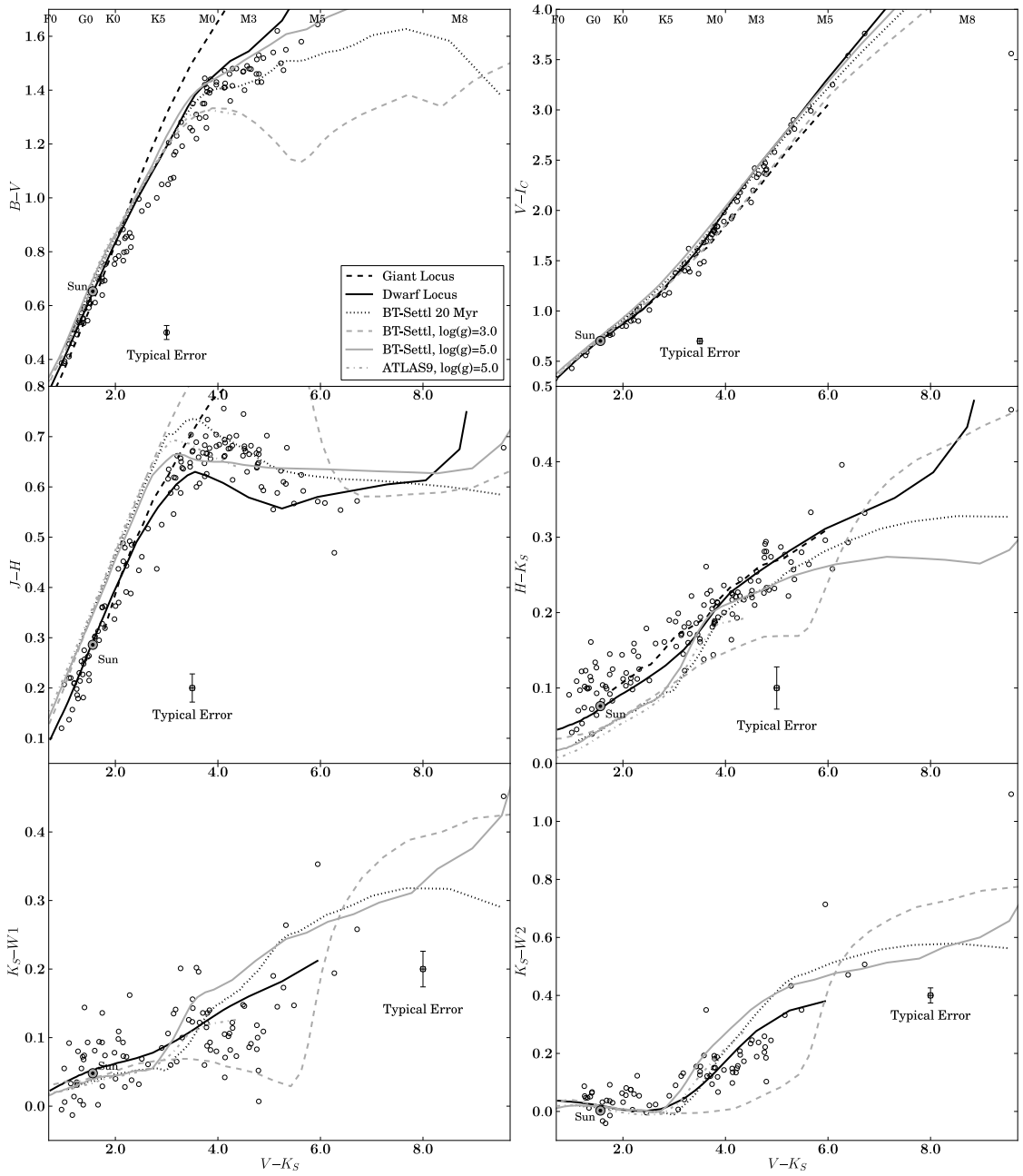

Figure 3.3 Comparison of B–V, V–I_C, J–H, H–K_S, K_S–$W1$, and K_S–$W2$ versus V–K_S of young stars from β Pic, η Cha, TWA and Tuc-Hor moving groups (circles) with the dwarf color locus described in Appendix C and the giant color locus from Bessell & Brett (1988), except the B–V giant locus, which is from Alonso et al. (1999). Spectral types corresponding to the V–K_S colors of dwarfs are plotted along the top. Objects with a known near-IR or IR excess have been excluded (see text for details).

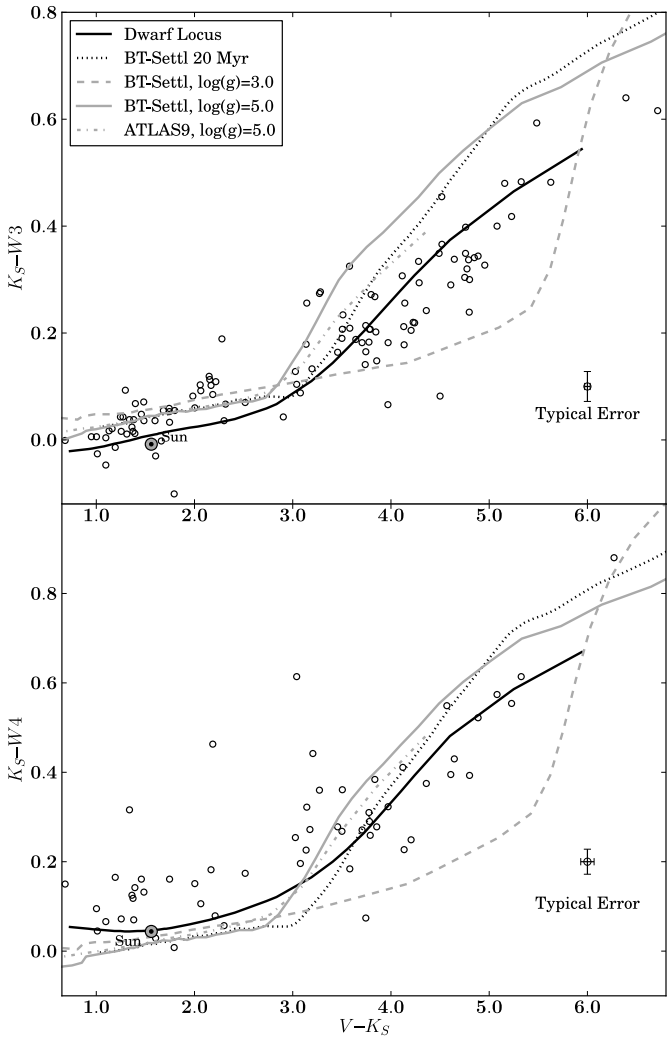

Figure 3.4 Same as Figure 3.3, except V–K_S versus K_S–$W3$ and K_S–$W4$.

V–I_C color-color relation as well. We then fit splines to V–K_S versus J–H and V–K_S versus H–K_S and use our spectral type-V–K_S relation to anchor J–H and H–K_S to spectral type. Finally, we fit splines to spectral type versus color for the colors B–V, K_S–$W1$, K_S–$W2$, K_S–$W3$ and K_S–$W4$. V–I_C data is sparse for types earlier than G5, but appears consistent with the dwarf sequence, so we simply adopt the dwarf V–I_C sequence for spectral types F0 through G5. In Figure 3.5 we see that pre-MS stars later than K3 become *bluer* in B–V than their main sequence counterparts, while those hotter than K2 are nearly indistinguishable from main sequence stars. Figure 3.5 also shows that young stars G5 and later have redder V–K_S and J–H colors than field dwarfs, while those earlier than G5 have V–K_S and J–H colors indistinguishable from field dwarfs. Young stars have H–K_S colors redder than field dwarfs between spectral types F0 and M2, shown in Figure 3.5. The spectral type sequence for K_S–$W1$, K_S–$W2$, K_S–$W3$ and K_S–$W4$ (Figures 3.5 and 3.6) show larger scatter than for the previously discussed colors, and greater care must be taken to exclude those stars with a color excess due to the presence of a circumstellar disk. We have excluded photometry for objects with infrared excesses as listed in Section 3.5.3. AG Tri was discussed in Rebull et al. (2008) as having a possible MIPS 24μm excess. We find that it has a K_S–$W4$ color excess 4.5σ above the young color sequence. We also identify HD 160305 and CD-54 7336 as having a K_S–$W4$ color excess at 2.9σ and 5.4σ above the young color sequence, so we also exclude them from the K_S–$W4$ fit. Our pre-MS intrinsic color sequence is listed in Table 3.5.

Table 3.5. Intrinsic colors of 5-30 Myr old Stars and Adopted T_{eff} values

Spectral Type	T_{eff} (K)	B–V (mag)	V–I_C (mag)	V–K_S (mag)	J–H (mag)	H–K_S (mag)	K_S–$W1$ (mag)	K_S–$W2$ (mag)	K_S–$W3$ (mag)	K_S–$W4$ (mag)	BC_V (mag)	BC_J (mag)
F0	7280	0.28	0.34	0.73	0.11	0.06	0.04	0.03	0.00	0.08	0.01	0.57
F1	6990	0.34	0.39	0.89	0.14	0.07	0.04	0.04	0.00	0.09	0.00	0.68
F2	6710	0.38	0.43	0.99	0.15	0.08	0.04	0.05	0.00	0.09	-0.01	0.75
F3	6660	0.41	0.45	1.01	0.16	0.08	0.04	0.05	0.01	0.09	-0.01	0.76
F4	6590	0.43	0.48	1.05	0.17	0.08	0.04	0.06	0.01	0.09	-0.01	0.79
F5	6420	0.47	0.51	1.14	0.19	0.08	0.04	0.03	0.01	0.10	-0.02	0.85
F6	6250	0.50	0.55	1.25	0.21	0.09	0.04	0.04	0.02	0.10	-0.04	0.91
F7	6140	0.53	0.58	1.31	0.22	0.09	0.05	0.04	0.02	0.10	-0.05	0.95
F8	6100	0.55	0.60	1.34	0.23	0.09	0.05	0.04	0.03	0.10	-0.06	0.96
F9	6090	0.56	0.62	1.35	0.23	0.09	0.05	0.04	0.03	0.10	-0.06	0.97
G0	6050	0.57	0.66	1.37	0.24	0.09	0.06	0.04	0.03	0.11	-0.06	0.98
G1	5970	0.59	0.67	1.42	0.25	0.10	0.06	0.03	0.04	0.11	-0.07	1.00
G2	5870	0.60	0.71	1.49	0.27	0.10	0.07	0.03	0.04	0.11	-0.09	1.03
G3	5740	0.63	0.72	1.58	0.29	0.10	0.07	0.03	0.05	0.12	-0.11	1.08
G4	5620	0.66	0.73	1.68	0.31	0.11	0.07	0.03	0.05	0.12	-0.14	1.12
G5	5500	0.70	0.76	1.77	0.33	0.11	0.08	0.03	0.06	0.13	-0.17	1.16
G6	5390	0.74	0.79	1.86	0.35	0.12	0.08	0.03	0.06	0.13	-0.20	1.19
G7	5290	0.77	0.83	1.95	0.37	0.12	0.09	0.04	0.07	0.14	-0.23	1.23
G8	5210	0.79	0.87	2.02	0.39	0.12	0.09	0.04	0.08	0.14	-0.26	1.25
G9	5120	0.80	0.91	2.10	0.41	0.13	0.09	0.05	0.08	0.15	-0.29	1.27

Table 3.5 (cont'd)

Spectral Type	T_{eff} (K)	B–V (mag)	V–I_C (mag)	V–K_S (mag)	J–H (mag)	H–K_S (mag)	K_S–$W1$ (mag)	K_S–$W2$ (mag)	K_S–$W3$ (mag)	K_S–$W4$ (mag)	BC_V (mag)	BC_J (mag)
K0	5030	0.82	0.93	2.19	0.43	0.13	0.09	0.06	0.09	0.16	-0.33	1.30
K1	4920	0.86	0.96	2.32	0.46	0.14	0.09	0.06	0.10	0.18	-0.38	1.34
K2	4760	0.93	1.01	2.49	0.49	0.14	0.09	0.07	0.12	0.19	-0.46	1.40
K3	4550	1.02	1.12	2.75	0.55	0.16	0.09	0.08	0.13	0.21	-0.60	1.44
K4	4330	1.11	1.27	3.06	0.60	0.17	0.09	0.09	0.14	0.22	-0.77	1.52
K5	4140	1.18	1.44	3.35	0.64	0.18	0.09	0.10	0.16	0.24	-0.95	1.58
K6	4020	1.24	1.57	3.54	0.66	0.19	0.10	0.10	0.17	0.27	-1.08	1.61
K7	3970	1.28	1.66	3.62	0.66	0.19	0.10	0.12	0.19	0.29	-1.14	1.63
K8	3940	1.32	1.74	3.67	0.67	0.20	0.10	0.13	0.21	0.32	-1.17	1.63
K9	3880	1.37	1.83	3.77	0.67	0.20	0.11	0.15	0.23	0.35	-1.24	1.66
M0	3770	1.41	1.95	3.96	0.68	0.21	0.11	0.17	0.25	0.38	-1.38	1.69
M1	3630	1.45	2.11	4.22	0.68	0.22	0.12	0.20	0.27	0.42	-1.58	1.74
M2	3490	1.46	2.28	4.50	0.67	0.23	0.14	0.23	0.31	0.47	-1.80	1.80
M3	3360	1.47	2.48	4.78	0.66	0.25	0.16	0.28	0.36	0.51	-2.03	1.84
M4	3160	1.53	2.78	5.23	0.62	0.27	0.19	0.35	0.43	0.56	-2.43	1.91
M5	2880	1.65	3.31	6.08	0.55	0.31	0.22	0.43	0.52	0.62	-3.21	2.01
M6	...	...	...	7.38	0.54	0.36	0.27	0.54	0.63	...	...	...
M7	...	...	...	8.47	0.58	0.41	0.33	0.67	0.77	...	...	...
M8	...	...	...	9.28	0.65	0.45	0.40	0.84	0.93	...	...	...
M9	...	...	...	9.80	0.70	0.47	0.49	1.05	1.13	...	...	...

Table 3.5 (cont'd)

Spectral Type	T_{eff} (K)	B–V (mag)	V–I_C (mag)	V–K_S (mag)	J–H (mag)	H–K_S (mag)	K_S–$W1$ (mag)	K_S–$W2$ (mag)	K_S–$W3$ (mag)	K_S–$W4$ (mag)	BC_V (mag)	BC_J (mag)

For some spectral type and color combinations, extinction estimates using these intrinsic colors will give different results than those which adopt dwarf colors. For example, a typical unreddened pre-MS K0 star has a V–K_S color 0.24 mag redder than a main-sequence K0. This object would appear to have A_V=1.12$E(V-K_S)$ $\simeq$0.27 mag of artificial extinction, based on the apparent V–K_S color difference between pre-MS and a main-sequence K0 stars (assuming a standard R_V=3.1 reddening law). This is consistent with the systematically higher extinction observed in the solar-type pre-MS stars in Sco-Cen discussed previously.

3.5.5 Temperature Scale

Technique

The effective temperature (T_{eff}) scale for giants (e.g., van Belle et al., 1999) as a function of spectral type is ∼700-400 K cooler than dwarfs for spectral types G8 through K5, whereas giants are ∼100-400 K hotter than dwarfs for spectral types M0-M9. Since pre-MS stars have surface gravities intermediate between dwarfs and giants, we expect that a pre-MS T_{eff} scale will be intermediate between dwarfs and giants (e.g., Luhman et al., 2003).

All T_{eff} scales depend on models (e.g., atmospheric models, limb-darkening models) to some degree. Arguably, the least model-dependent methods are those *direct* methods based on the angular diameter of the star, measured interferometrically or by lunar occultation methods. While some of the objects in our sample are candidates for angular diameter measurements (see McCarthy & White, 2012), only two have actual measurements in the literature (HR 9 and 51 Eri; Simon & Schaefer 2011; see Section 3.6 for details). There are also *indirect* methods, such as the infrared flux method (IRFM), performed by Alonso et al. (1999), and more recently for M-dwarfs

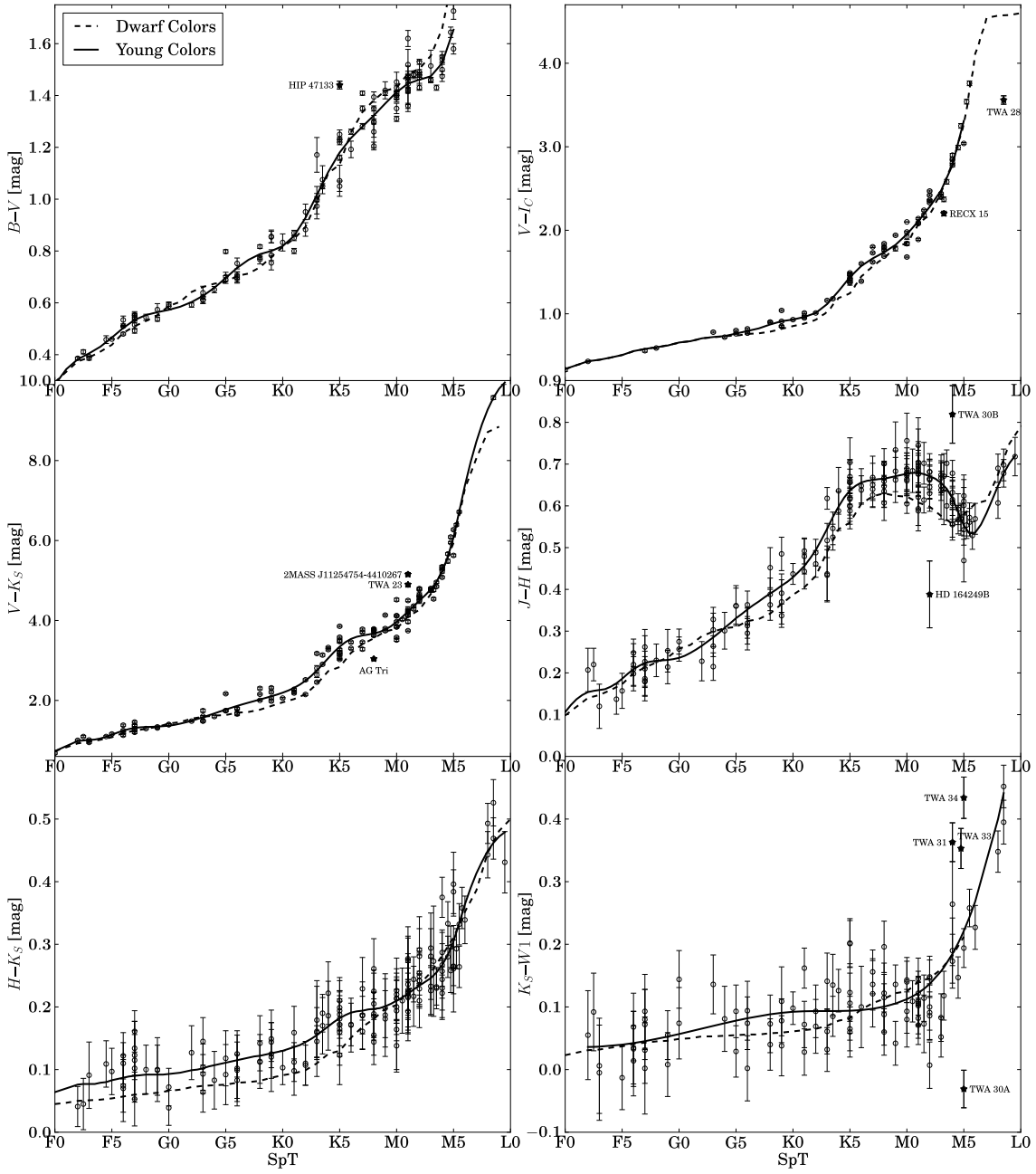

Figure 3.5 Comparison of B–V, V–I_C, V–K_S, J–H, H–K_S, and K_S–$W1$ of young stars from β Pic, η Cha, TWA and Tuc-Hor moving groups (circles) with the dwarf color sequence described in this work (dashed line). The outliers (filled stars) HIP 47133, RECX 15, TWA 28, 2MASS J11254754-4410267, TWA 23, AG Tri, HD 164249B, TWA 30B, TWA 30A, TWA 31, TWA 33 and TWA 34 were excluded from the fit.

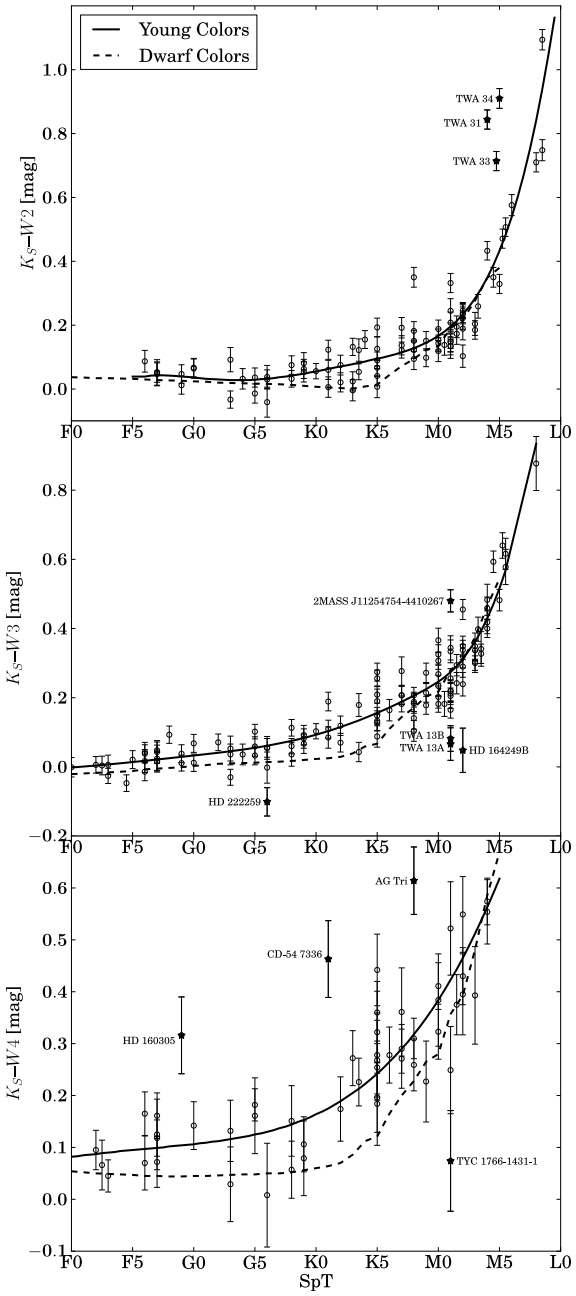

Figure 3.6 Same as in Figure 3.5, except showing colors K_S–$W2$, K_S–$W3$, and K_S–$W4$. The outliers (filled stars) TWA 31, TWA 33, TWA 34, HD 222259, TWA 13A, TWA 13B, 2MASS J11254754-4410267, HD 164249B, TYC 1766-1431-1 were excluded from the fit. Objects with known infrared excesses have also been excluded from the plot (see text for details). HD 160305, CD-54 7336, AG Tri have $W4$ band excesses (identified in this work) and have also been excluded.

by Casagrande et al. (2008), or directly fitting spectral energy distributions to synthetic model photometry, as described by Masana et al. (2006).

Based on spectroscopy, young stars have been shown to exhibit more than one photospheric T_{eff}(Gullbring et al., 1998; Stauffer et al., 2003), so fitting synthetic spectra to observed spectra will yield a different T_{eff} depending on the spectral region selected for fitting. An example of this is TW Hydra, which has been consistently typed as a late K star based on optical spectra (K7e, de la Reza et al. 1989; K6e, Hoff et al. 1998; K6Ve, Torres et al. 2006; K8IVe, this work) but near-IR spectroscopy indicate a spectral type of M2.5V (Vacca & Sandell, 2011). We need a method to infer temperatures that will simultaneously take into account the observed optical-IR photometry. Therefore we attempt to infer the effective temperatures by simultaneously fitting the observed photometry to synthetic models (the "Spectral Energy Distribution Fitting" (SEDF) method, see Masana et al. 2006). The downside of this method is that we are using models which do not completely correctly predict the colors of young stars. However, since the T_{eff} is *defined* by the integrated spectral energy distribution (SED) and the stellar radius, the observed photometry is the most direct link to the effective temperature of objects in our sample. We closely follow the formalism and methods of Masana et al. (2006) and fit the observed photometry to models by minimizing χ^2, defined as

$$
\begin{aligned}
\chi^2 &= \left(\frac{B - B_{\rm syn} - \mathcal{A}}{\sigma_B}\right)^2 \\
&+ \left(\frac{V - V_{\rm syn} - \mathcal{A}}{\sigma_V}\right)^2 \\
&+ \left(\frac{I_C - I_{C\rm syn} - \mathcal{A}}{\sigma_{I_C}}\right)^2 \\
&+ \left(\frac{J - J_{\rm syn} - \mathcal{A}}{\sigma_J}\right)^2 \\
&+ \left(\frac{H - H_{\rm syn} - \mathcal{A}}{\sigma_H}\right)^2 \\
&+ \left(\frac{K_S - K_{S\rm syn} - \mathcal{A}}{\sigma_{K_S}}\right)^2 \\
&+ \left(\frac{W1 - W1_{\rm syn} - \mathcal{A}}{\sigma_{W1}}\right)^2 \\
&+ \left(\frac{W2 - W2_{\rm syn} - \mathcal{A}}{\sigma_{W2}}\right)^2 \\
&+ \left(\frac{W3 - W3_{\rm syn} - \mathcal{A}}{\sigma_{W3}}\right)^2 \\
&+ \left(\frac{W4 - W4_{\rm syn} - \mathcal{A}}{\sigma_{W4}}\right)^2
\end{aligned}
$$

With B, V, I_C, J, H, K_S, $W1$, $W2$, $W3$, and $W4$ being the observed photometry, $B_{\rm syn}$, $V_{\rm syn}$, $I_{C\rm syn}$, $J_{\rm syn}$, $H_{\rm syn}$, $K_{S\rm syn}$, $W1_{\rm syn}$, $W2_{\rm syn}$, $W3_{\rm syn}$, and $W4_{\rm syn}$ are the apparent magnitudes at the stellar surface, and $\mathcal{A}$ is the magnitude difference between the flux observed on Earth (obs) and the theoretical flux at the surface of the star (surface)[7]:

$$\mathcal{A} = -2.5\log(F_{surface}/F_{obs})$$

[7]This flux is the unresolved flux integrated over the disk of the star and does not represent the resolved flux one would observe if placed on the stellar surface. The flux we are referring to is the counterpart to the apparent magnitude at the stellar surface (e.g., $B_{\rm syn}$).

related to the angular semi-diameter:

$$\theta \;=\; \frac{R}{d} = 10^{-0.2\mathcal{A}}$$

We fit the observed photometry to synthetic photometry from two different libraries of synthetic spectra: the BT-Settl models[8] of Allard et al. (2012) with the Asplund et al. (2009) solar composition and the ATLAS9 models[9] of Castelli & Kurucz (2004) with the Grevesse & Sauval (1998) solar composition. The differences in the solar composition are particularly important for low-mass stars and brown dwarfs, due to the importance of TiO and VO compounds in their spectra. The solar oxygen abundance has been revised downward by 38% by Asplund et al. (2009) when compared to the Grevesse & Sauval (1998) oxygen abundances. Spectra using the newer Asplund et al. (2009) abundances exhibit improved agreement with the spectral energy distribution of low-mass stars over models using the Grevesse & Noels (1993) solar abundances (Allard et al., 2011). Another major difference between the ATLAS9 models and the BT-Settl models is the treatment of line opacities. The ATLAS9 models include opacity distribution functions (ODFs) to account for line blanketing, whereas the BT-Settl models are generated by the PHOENIX code in which the individual contribution of atoms and molecules is directly sampled over all computed points in the spectrum (Hauschildt et al., 1997). Given that the BT-Settl models offer continuity in our ability to model SEDs of F-type down to M-type stars, and the recent successes the BT-Settl models have had fitting NIR colors of low-mass stars down to ∼3000 K (Allard et al., 2012), we adopt the temperatures derived from the BT-Settl models with the Asplund et al. (2009) abundances, but include the re-

[8]http://phoenix.ens-lyon.fr/Grids/BT-Settl/AGSS2009/
[9]http://wwwuser.oat.ts.astro.it/castelli/grids.html

sults from the ATLAS9 models to demonstrate the size of the systematic differences resulting from the assumed solar composition or model implementation.

Testing Technique on Objects with Measured Angular Diameters

As a reliability check for the usefulness of our method, we use the estimated solar BVI_C colors from Ramírez et al. (2012) together with the solar 2MASS JHK and WISE $W1$, $W2$, $W3$ and $W4$ colors from Casagrande et al. (2012) to estimate the $T_{\rm eff}$ of the Sun, assuming $\log(g) = 4.44$ and adopting the apparent V band magnitude of -26.74±0.02 mag (Mamajek, 2012). With these ten bands, the BT-Settl models SEDF method gives $T_{\rm eff\odot}$=5776±22 K (remarkably within 4 K of the modern solar $T_{\rm eff}$ of 5771.8±0.7 K; Mamajek 2012), and an angular diameter of 1949″±7″. The ATLAS9 models give $T_{\rm eff\odot}$=5737±21 K, 35 K too low but still within 2σ, and an angular diameter of 1953″±7″. Both angular diameter measurements are systematically higher than the 1918.3″±0.3″ angular diameter implied by the solar radius estimate of Haberreiter et al. (2008), which strongly suggests that our adopted $V_\odot$ is too high. If we instead adopt $V_\odot$ ≡26.71±0.02 mag, we obtain angular diameters with the SEDF method of 1922″±7″ and 1926″±7″ with the BT-Settl and ATLAS9 models, respectively, consistent with the modern solar angular diameter estimates. Thus for consistency with the solar values, we adopt $V_\odot$=-26.71±0.02 mag,[10].

We also check the technique on nearby K- and M-type field dwarfs with directly measured angular diameters from the recent work of Boyajian et al. (2012b). We use photometry from Table 7 of Boyajian et al. (2012b), converting Johnson I to the Cousins system using the conversions in Bessell (1979) and converting Johnson

[10] $V_\odot$=-26.71±0.02 mag implies that $M_{V,\odot}$=4.862±0.020 mag. Based on the IAU scale the luminosity estimate of Mamajek (2012) leads to $M_{bol,\odot}$=4.7554±0.0004 mag, $BC_{V,\odot}$=-0.107±0.02 mag. A summary of solar V magnitude estimates is available at https://sites.google.com/site/mamajeksstarnotes/basic-astronomical-data-for-the-sun

JHK to the 2MASS system using the conversions of Carpenter (2001). We adopt WISE $W1$, $W3$ and $W4$ photometry with contamination and confusion flags '0' from the WISE All Sky Point Source Catalog. Following Boyajian et al. (2012b), we adopted $\log(g) = 4.5$ and the metallicity appropriate for each system. We assume uncertainties of $\sigma_{\log(g)}$=0.2 dex and $\sigma_{[m/H]}$=0.1 dex. Our SEDF-derived $T_{\rm eff}$ for these objects are listed in Table 3.6, and plotted with the Boyajian et al. (2012b) $T_{\rm eff}$ values in Figure 3.11. The mean difference between our SEDF-derived $T_{\rm eff}$ values and those based on angular diameter measurements from Boyajian et al. (2012b) is 13 K with a 1σ dispersion of 108 K. The consistency of the SEDF models with the temperature estimates for the Sun as well as cooler K and M-type objects gives us confidence that this method will accurately predict the effective temperatures of our pre-MS stars.

Results

For many objects in our sample, one or more bands of photometry are not available. In those cases we simply omit the term containing the missing band data. We do not fit bands with poor quality photometry (in 2MASS, anything other than quality flag 'A'; for WISE bands, anything other than contamination and confusion flag '0'). We have again excluded photometry for objects with infrared excesses, listed in Section 3.5.3. RECX 11 and RECX 15 have K_S-band excesses, so we exclude them from SED fitting entirely. We also exclude TWA 30A due to its time variable extinction (Looper et al., 2010b) and TWA 30B due to the time variable near-infrared excess (Looper et al., 2010a). TWA 31, TWA 33 and TWA 34 have $W1$ and $W2$-band excesses (Figures 3.5 and 3.6) so we exclude their WISE $W1$, $W2$, $W3$, and $W4$ band photometry. This leaves TWA 31 and TWA 34 with only JHK_S photometry, so we exclude them entirely. TWA 29 had only 2MASS JHK_S photometry, and objects HD 139084B and HD 164249B had 2MASS photometry and only two bands

Table 3.6. T_{eff} Comparison: SEDF versus Diameter-Derived T_{eff}

Object	Spectral Type	Ref.	T_{eff}[a] (K)	T_{eff}[b] (K)	m^{c}_{bol} (mag)
GJ 15A	M1.5V	1	3535±14	3567±11	6.560±0.014
GJ 33	K2.5V	2	5047±19	4950±14	5.459±0.017
GJ 53A	K1V Fe-2	3	5362±22	5348±26	4.981±0.016
GJ 75	G9V	3	5395±20	5398±75	5.452±0.018
GJ 105	K3V	2	4827±18	4662±17	5.406±0.015
GJ 144	K2V (k)	2	5097±19	5077±35	3.457±0.016
GJ 166A	K0.5V	2	5162±21	5147±14	4.169±0.016
GJ 205	M1.5V	1	3703±36	3801±9	6.443±0.016
GJ 338A	M0.0V	1	3896±24	3907±35	6.471±0.017
GJ 338B	K7.0V	1	3887±25	3867±37	6.479±0.017
GJ 380	K8V	3	4039±23	4085±14	5.544±0.016
GJ 411	M2.0V	1	3481±14	3464±15	5.873±0.015
GJ 412A	M1.0V	1	3584±13	3497±39	7.308±0.014
GJ 436	M3.0V	1	3419±17	3416±53	8.778±0.011
GJ 526	M1.5V	1	3642±15	3618±31	7.028±0.013
GJ 551	M5.5V	1	2739±12	3054±79	7.280±0.010
GJ 570A	K4V	2	4627±16	4507±58	5.245±0.013
GJ 581	M2.5V	1	3304±13	3442±54	8.560±0.010
GJ 631	K0V (k)	2	5272±19	5337±41	5.527±0.017
GJ 687	M3.0V	1	3377±13	3413±28	7.231±0.010
GJ 699	M4.0V	1	3089±11	3222±10	7.173±0.012
GJ 725A	M3.0V	1	3316±12	3407±15	7.007±0.014
GJ 725B	M3.5V	1	3218±12	3104±28	7.587±0.013
GJ 764	G9V	3	5364±21	5246±26	4.498±0.018
GJ 809	M0.0V	1	3715±14	3692±22	7.205±0.011
GJ 820A	K5V	3	4498±14	4361±17	4.599±0.014
GJ 820B	K7V	3	4117±23	3932±25	5.082±0.019
GJ 845	K4V (k)	2	4713±16	4555±24	4.217±0.014
GJ 880	M1.5V	1	3656±16	3713±11	7.178±0.020
GJ 887	M2V	4	3617±19	3676±35	5.871±0.015
GJ 892	K3V	3	4878±18	4699±16	5.191±0.016

Note. — [a]: T_{eff} from this work using the SEDF method. See Section 3.5.5 for details. [b]: T_{eff} from Boyajian et al. (2012b) computed using direct angular diameter measurements. [c]: apparent bolometric magnitude estimated from our SED fit.

Spectral Type References: (1) Henry et al. (2002); (2) Gray et al. (2006); (3) Gray et al. (2003); (4) Torres et al. (2006);

Table 3.7. Objects Rejected From SED-$T_{\rm eff}$ fitting

Object	Rejection Reason
HD 139084B	Uncertain photometry resulting in poorly constrained $T_{\rm eff}$
HD 164249B	Uncertain photometry resulting in poorly constrained $T_{\rm eff}$
RECX 11	K_S band excess
RECX 15	K_S band excess
RECX 16	*IRAC* 3.6μm and 4.5μm excess
TWA 27	*IRAC* 3.6μm and 4.5μm excess
TWA 29	Only three good bands of photometry (JHK_S)
TWA 30A	time-variable extinction
TWA 30B	time-variable NIR excess
TWA 31	Only three good bands of photometry (JHK_S)
TWA 34	Only three good bands of photometry (JHK_S)

of WISE photometry with large uncertainties (> 0.1 mag), which resulted in poorly constrained temperatures (e.g., $\sigma_{T_{\rm eff}} > 300$ K) so we excluded them from SED fitting as well. Objects excluded from SED fitting are listed in Table 3.7. The behavior of χ^2 as a function of $T_{\rm eff}$ is consistent with Gaussian errors and χ^2 has a quadratic dependence on $T_{\rm eff}$ near the best-fit value. A representative SED from our sample with the observed and best-fit model are shown in Figure 3.7.

In general the synthetic photometry is a function of $\log(g)$, $T_{\rm eff}$, and metallicity ([m/H]). As discussed previously, we use solar metallicity synthetic models. We have also fixed the $\log(g)$ values at $\log(g) = 4.3$ dex. Pre-main sequence evolutionary tracks from Baraffe et al. (1998) between 8-30 Myr predict that $\log(g)$ varies between 4.1 dex and 4.5 dex so we simply adopt 4.3$\pm$0.2 dex. Though it is possible to fit both $T_{\rm eff}$ and $\log(g)$ simultaneously, this often gives spuriously large or small $\log(g)$ values, and even when the values of $\log(g)$ obtained from the fit are within an expected range, they are not well-constrained (e.g., formal errors on $\log(g) \sim 1.0$ dex). This is because most of the synthetic colors do not depend sensitively on the adopted $\log(g)$, and furthermore, we found that the best-fit $T_{\rm eff}$ did not vary significantly between $\log(g) = 4.1$ and $\log(g) = 4.5$. The mean difference in $T_{\rm eff}$ between $\log(g) = 4.1$

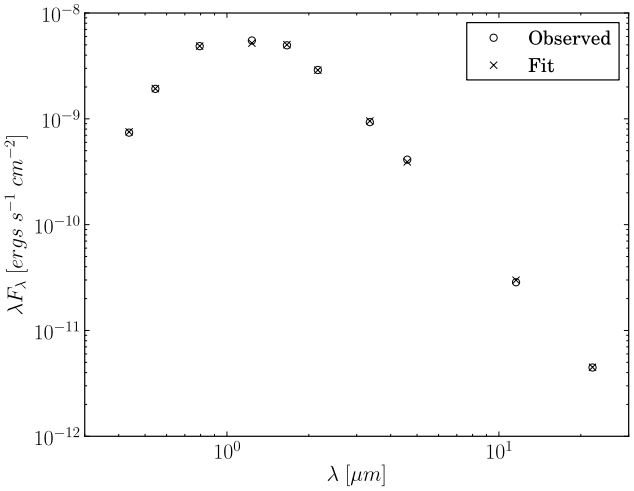

Figure 3.7 Representative observed SED (circles) with the best fit BT-Settl SED (crosses) of T_{eff}=3866±18 K for β Pic member V1005 Ori (K8IVe). Uncertainties are smaller than the symbol markers.

and 4.5 is 4 K with a dispersion of 31 K. Therefore, in our fitting procedure we set T_{eff} as the only free parameter. During the fitting procedure, we first determine $\mathcal{A}$ as the inverse-variance weighted mean difference between the observed and synthetic photometry at the stellar surface. However, rather than numerically minimizing χ^2 (as done in Masana et al. 2006) we simply find the minimum value over our grid, interpolated to T_{eff} increments of 20 K from 1400 K to 9800 K for the BT-Settl models and from 3500 K to 9750 K for the ATLAS9 models. We then fit a parabola in the region surrounding the minimum.

The effective temperatures we obtained are listed in Table 3.8, and plotted in Figure 3.8. We estimate our uncertainties by performing a Monte Carlo simulation. For each object, we select trial photometry values from a distribution with mean and standard deviation equal to the observed photometry value and uncertainty, and use the trial photometry values to obtain the best-fit T_{eff} and angular diameter estimate. We perform 300 trials for each object and use the standard deviation of the resulting

T_{eff} and angular diameter distribution as our statistical uncertainties. However this does not account for systematics caused by uncertainties in our assumed surface gravity and metallicity. To account for these systematics, we repeat our fitting procedure for each object, varying $\log(g)$ from 4.1 dex to 4.5 dex and [m/H] from +0.2 dex to -0.2 dex. We adopt the dispersion in T_{eff} and angular diameter obtained for the systematic uncertainty, *typically* $\sim$11 K in T_{eff} and $\sim$1 μas in angular diameter. The uncertainties quoted in Table 3.8 are the statistical and (internal) systematic uncertainties added in quadrature. This does not account for any systematic uncertainties from the underlying Phoenix/NextGen models or the assumed solar abundances.

Table 3.8. T_{eff}, Bolometric Magnitudes, Bolometric Corrections and Angular Diameter Estimates From SED Fitting

Object	2MASS	BT-Settl						Kurucz					
		T_{eff} (K)	θ (μas)	BC_V (mag)	BC_J (mag)	m_{bol} (mag)	$\log(L/L_\odot)$ (dex)	T_{eff} (K)	θ (μas)	BC_V (mag)	BC_J (mag)	m_{bol} (mag)	$\log(L/L_\odot)$ (dex)
HIP 490	00055255-4145109	5990±16	250±1	-0.06±0.02	0.98±0.02	7.45±0.02	0.114±0.048	5968±15	250±1	-0.05±0.02	1.00±0.02	7.46±0.02	0.108±0.047
HR 9	00065008-2306271	6796±25	346±1	0.00±0.02	0.74±0.03	6.19±0.02	0.617±0.033	6773±21	348±1	0.01±0.02	0.75±0.03	6.20±0.02	0.614±0.032
HIP 1113	00135300-7441178	5434±15	180±1	-0.17±0.02	1.18±0.03	8.59±0.02	-0.238±0.074	5401±16	180±1	-0.15±0.02	1.21±0.03	8.61±0.02	-0.247±0.074
HIP 1481	00182612-6328389	6150±18	242±1	-0.06±0.02	0.94±0.02	7.41±0.02	0.177±0.045	6123±17	242±1	-0.04±0.02	0.96±0.02	7.42±0.02	0.171±0.045
TYC 1186-706-1	00233468+2014282	4055±15	189±1	-1.09±0.10	1.61±0.03	9.75±0.03	...	3888±42	197±1	-1.00±0.11	1.70±0.05	9.84±0.05	...
HIP 1910	00240899-6211042	3823±18	188±2	-1.31±0.02	1.64±0.03	10.02±0.03	-0.659±0.288	3805±24	189±2	-1.31±0.02	1.64±0.03	10.03±0.02	-0.660±0.288
HIP 1993	00251465-6130483	4015±14	159±1	-1.09±0.03	1.56±0.03	10.17±0.03	-0.845±0.222	3975±17	161±1	-1.07±0.03	1.57±0.03	10.19±0.03	-0.850±0.222
HIP 2729	00345120-6154583	4376±10	252±1	-0.76±0.02	1.46±0.02	8.80±0.02	-0.330±0.087	4318±9	256±1	-0.74±0.01	1.48±0.02	8.82±0.02	-0.339±0.087
HIP 3556	00452814-5137339	3576±23	190±2	-1.63±0.02	1.80±0.02	10.28±0.03	-0.998±0.214	3590±32	190±3	-1.64±0.02	1.79±0.02	10.27±0.02	-0.993±0.214
TYC 5853-1318-1	01071194-1935359	3782±33	208±1	-1.61±0.08	1.70±0.04	9.85±0.05	...	3686±29	214±2	-1.56±0.08	1.74±0.04	9.89±0.04	...
CPD-64 120	01131535-6411351	4909±12	120±1	-0.39±0.01	1.29±0.02	9.90±0.02	...	4868±11	121±1	-0.36±0.01	1.31±0.02	9.93±0.02	...
HD 8558	01232126-5728507	5571±17	187±1	-0.14±0.02	1.15±0.03	8.39±0.02	-0.064±0.083	5543±15	187±1	-0.12±0.02	1.17±0.03	8.41±0.02	-0.072±0.083
HD 9054	01280868-5238191	4726±10	206±1	-0.46±0.02	1.49±0.02	8.89±0.02	-0.542±0.072	4673±10	208±1	-0.43±0.02	1.52±0.02	8.92±0.02	-0.553±0.073
TYC 1208-468-1	01373940+1835332	4245±14	241±1	-0.87±0.03	1.55±0.03	9.03±0.03	...	4201±16	242±1	-0.83±0.03	1.58±0.03	9.06±0.03	...
HIP 9141	01574896-2154052	5709±17	218±1	-0.12±0.02	1.10±0.03	7.95±0.02	-0.056±0.056	5682±16	218±1	-0.10±0.02	1.12±0.03	7.97±0.02	-0.064±0.056
HD 12894	02043513-5452540	6713±20	316±1	-0.01±0.02	0.75±0.05	6.44±0.02	0.682±0.045	6688±21	317±1	0.00±0.02	0.76±0.05	6.45±0.02	0.680±0.045
HD 13183	02071805-5311565	5525±16	181±1	-0.15±0.02	1.15±0.03	8.49±0.02	-0.081±0.066	5496±15	182±1	-0.13±0.02	1.17±0.03	8.51±0.02	-0.089±0.066
HD 13246	02072611-5940459	6126±20	238±1	-0.05±0.02	0.92±0.03	7.45±0.02	0.211±0.042	6100±19	239±1	-0.03±0.02	0.94±0.03	7.47±0.02	0.205±0.042
CD-60 416	02073220-5940210	4280±11	163±1	-0.85±0.01	1.50±0.03	9.83±0.02	...	4223±10	166±1	-0.83±0.01	1.52±0.03	9.85±0.02	...
HIP 10679	02172472+2844305	5867±19	237±1	-0.10±0.02	1.08±0.03	7.65±0.02	-0.285±0.319	5836±19	237±1	-0.07±0.02	1.11±0.03	7.68±0.02	-0.295±0.319
HIP 10680	02172527+2844423	6299±35	283±2	-0.03±0.03	0.91±0.04	6.96±0.04	0.196±0.200	6269±36	284±2	-0.02±0.03	0.92±0.04	6.97±0.04	0.190±0.200
HIP 11152	02232663+2244069	3906±20	192±2	-1.22±0.01	1.69±0.02	9.87±0.01	-1.132±0.163	3898±24	192±2	-1.20±0.01	1.71±0.02	9.89±0.01	-1.138±0.163
BD+30 397B	02272804+3058405	3470±21	173±2	-1.83±0.02	1.80±0.05	10.62±0.03	...	...	...	...	...	...	...
AG Tri	02272924+3058246	4359±12	195±1	-0.75±0.01	1.50±0.04	9.37±0.02	-0.641±0.180	4308±10	197±1	-0.72±0.01	1.53±0.04	9.40±0.02	-0.655±0.180
TYC 7558-655-1	02303239-4342232	4360±25	181±1	-0.78±0.05	1.51±0.04	9.53±0.05	...	4312±22	183±1	-0.76±0.05	1.53±0.04	9.55±0.05	...
GSC 8056-0482	02365171-5203036	3436±20	209±2	-1.86±0.01	1.83±0.03	10.25±0.02	...	...	...	...	...	...	...
HIP 12545	02412589+0559181	4044±14	212±1	-1.06±0.03	1.61±0.03	9.51±0.04	-0.656±0.127	4004±16	215±1	-1.05±0.03	1.62±0.03	9.52±0.04	-0.660±0.127
CD-53 544	02414683-5259523	4096±14	239±1	-1.02±0.01	1.62±0.03	9.20±0.02	...	4049±14	244±1	-1.02±0.01	1.62±0.03	9.20±0.02	...

Table 3.8 (cont'd)

Object	2MASS	BT-Settl						Kurucz					
		$T_{\rm eff}$ (K)	θ (μas)	BC_V (mag)	BC_J (mag)	m_{bol} (mag)	$\log(L/L_\odot)$ (dex)	$T_{\rm eff}$ (K)	θ (μas)	BC_V (mag)	BC_J (mag)	m_{bol} (mag)	$\log(L/L_\odot)$ (dex)
GSC 8491-1194	02414730-5259306	3380±20	215±2	-1.95±0.02	1.78±0.03	10.26±0.02	...	...	...	...	...	...	...
GSC 8497-0995	02423301-5739367	4262±11	144±1	-0.86±0.01	1.56±0.03	10.12±0.02	...	4202±10	147±1	-0.84±0.01	1.58±0.03	10.14±0.02	...
HIP 12925	02461462+0535333	6033±16	207±1	-0.05±0.01	0.97±0.04	7.83±0.01	...	6013±17	207±1	-0.04±0.01	0.98±0.04	7.84±0.01	...
HIP 15247	03164066-0331489	6049±23	250±1	-0.07±0.02	0.95±0.03	7.41±0.03	0.323±0.060	6029±21	250±1	-0.06±0.02	0.97±0.03	7.42±0.03	0.318±0.060
HIP 16853	03365341-4957288	5880±15	252±1	-0.11±0.02	1.02±0.03	7.51±0.02	0.170±0.064	5850±16	251±1	-0.08±0.02	1.05±0.03	7.54±0.02	0.160±0.064
HIP 17782	03482301+5202163	5234±14	203±1	-0.26±0.02	1.27±0.02	8.49±0.02	-0.067±0.168	5211±12	203±1	-0.24±0.02	1.29±0.02	8.51±0.02	-0.075±0.168
HD 25402	04003198-4144544	5872±16	179±1	-0.10±0.02	1.06±0.02	8.26±0.02	-0.031±0.070	5841±17	179±1	-0.07±0.02	1.09±0.02	8.29±0.02	-0.042±0.070
51 Eri	04373613-0228248	7275±24	471±2	0.01±0.02	0.48±0.04	5.23±0.02	0.749±0.023	7251±25	472±1	0.02±0.02	0.50±0.04	5.24±0.02	0.744±0.024
GJ 3305	04373746-0229282	3648±29	331±5	-1.54±0.01	1.70±0.02	8.99±0.01	...	3696±38	317±7	-1.50±0.01	1.73±0.02	9.03±0.01	...
HIP 21632	04384393-2702018	5774±18	178±1	-0.12±0.02	1.07±0.03	8.35±0.02	0.063±0.101	5743±16	178±1	-0.10±0.02	1.10±0.03	8.37±0.02	0.052±0.101
HIP 21965	04431720-2337419	6544±19	247±1	-0.03±0.02	0.80±0.02	7.09±0.02	0.673±0.125	6520±22	247±1	-0.02±0.02	0.81±0.03	7.10±0.02	0.668±0.125
V962 Per	04435686+3723033	3468±28	117±1	-1.85±0.10	1.75±0.04	11.46±0.05	...	...	...	...	...	...	...
HIP 22295	04480518-8046452	6181±19	174±1	-0.04±0.02	0.93±0.03	8.10±0.02	0.233±0.063	6155±19	174±1	-0.02±0.02	0.95±0.03	8.12±0.02	0.227±0.063
V1005 Ori	04593483+0147007	3866±18	324±3	-1.27±0.03	1.67±0.03	8.78±0.03	-0.785±0.132	3843±23	327±3	-1.26±0.02	1.68±0.02	8.79±0.03	-0.790±0.132
HIP 23309	05004714-5715255	3884±17	322±2	-1.24±0.02	1.68±0.02	8.78±0.02	-0.753±0.061	3867±22	326±3	-1.25±0.02	1.68±0.02	8.77±0.02	-0.752±0.061
HIP 23418	05015881+0958587	3211±15	392±3	-2.27±0.02	1.97±0.03	9.18±0.02	-0.727±0.635	...	...	...	...	...	...
HIP 24947	05203803-3945179	6232±17	243±1	-0.05±0.02	0.92±0.03	7.34±0.02	0.336±0.041	6205±17	243±1	-0.04±0.02	0.94±0.03	7.35±0.02	0.329±0.041
HIP 25486	05270477-1154033	6062±18	427±1	-0.07±0.02	0.97±0.03	6.23±0.02	0.273±0.028	6042±18	427±1	-0.05±0.02	0.98±0.03	6.25±0.02	0.267±0.028
TYC 7600-0516-1	05370530-3932265	5020±14	160±1	-0.34±0.02	1.27±0.02	9.18±0.02	...	4984±12	161±1	-0.32±0.02	1.29±0.02	9.20±0.02	...
TYC 7065-0879-1	05423423-3415422	5180±16	89±1	-0.25±0.02	1.09±0.04	10.32±0.03	...	5143±17	89±1	-0.22±0.02	1.11±0.04	10.34±0.03	...
HIP 28036	05554314-3806162	6246±17	234±1	-0.05±0.02	0.91±0.02	7.41±0.02	0.411±0.049	6220±18	235±1	-0.04±0.02	0.93±0.03	7.42±0.02	0.405±0.049
2MASS J06085283-2753583	06085283-2753583	2118±20	46±1		2.04±0.05	15.64±0.06	...	...	...	...	...	...	...
HIP 29964	06182824-7202416	4260±9	232±1	-0.86±0.02	1.56±0.02	9.09±0.02	-0.561±0.070	4204±11	235±1	-0.83±0.02	1.59±0.02	9.12±0.02	-0.572±0.070
HIP 30030	06190805-0326203	5951±16	208±1	-0.08±0.02	1.03±0.03	7.87±0.02	0.138±0.080	5926±17	208±1	-0.06±0.02	1.04±0.03	7.89±0.02	0.131±0.081
HIP 30034	06191291-5803156	5024±13	189±1	-0.31±0.02	1.25±0.03	8.82±0.02	-0.300±0.064	4982±12	189±1	-0.28±0.02	1.28±0.03	8.85±0.02	-0.312±0.064
HIP 32235	06434625-7158356	5661±17	149±1	-0.12±0.02	1.13±0.03	8.82±0.02	-0.096±0.085	5631±16	149±1	-0.10±0.02	1.15±0.03	8.84±0.02	-0.105±0.085
HIP 32435	06461348-8359294	6427±17	219±1	-0.04±0.02	0.87±0.03	7.43±0.02	0.429±0.042	6399±19	220±1	-0.02±0.02	0.89±0.03	7.44±0.02	0.424±0.042
HIP 33737	07003046-7941459	4781±12	141±1	-0.43±0.02	1.41±0.03	9.68±0.02	-0.429±0.105	4725±13	142±1	-0.41±0.02	1.44±0.03	9.70±0.02	-0.440±0.105

Table 3.8 (cont'd)

Object	2MASS	BT-Settl						Kurucz					
		T_{eff} (K)	θ (μas)	BC_V (mag)	BC_J (mag)	m_{bol} (mag)	$\log(L/L_\odot)$ (dex)	T_{eff} (K)	θ (μas)	BC_V (mag)	BC_J (mag)	m_{bol} (mag)	$\log(L/L_\odot)$ (dex)
RECX 18	08361072-7908183	2764±8	61±1	-3.79±0.02	2.02±0.03	13.87±0.03	-1.704±0.011	...	...	...	...	...	
RECX 1	08365623-7856454	4125±20	189±1	-0.93±0.03	1.52±0.03	9.68±0.03	-0.028±0.013	4094±17	190±1	-0.92±0.03	1.54±0.02	9.69±0.03	-0.034±0.012
RECX 17	08385150-7916136	2829±8	75±1	-3.51±0.02	2.04±0.03	13.31±0.03	-1.482±0.012	...	...	...	...	...	
RECX 14	08413030-7853064	2880±10	58±1	-3.27±0.03	1.99±0.03	13.80±0.03	-1.678±0.012	...	...	...	...	...	
RECX 3	08413703-7903304	3286±23	94±1	-2.18±0.03	1.84±0.03	12.19±0.03	-1.032±0.012	...	...	...	...	...	
RECX 4	08422372-7904030	3670±25	117±1	-1.50±0.03	1.69±0.03	11.23±0.03	-0.649±0.012	3687±32	116±2	-1.51±0.02	1.68±0.03	11.22±0.03	-0.644±0.012
RECX 5	08422710-7857479	3090±16	87±1	-2.58±0.03	1.85±0.03	12.62±0.03	-1.206±0.012	...	...	...	...	...	
RECX 6	08423879-7854427	3370±23	94±1	-2.01±0.03	1.84±0.03	12.07±0.03	-0.985±0.012	...	...	...	...	...	
RECX 7	08430723-7904524	4215±20	159±1	-0.88±0.03	1.54±0.03	9.96±0.04	-0.141±0.013	4174±20	160±1	-0.85±0.03	1.57±0.03	9.99±0.04	-0.153±0.013
RECX 9	08441637-7859080	3006±13	114±1	-2.85±0.03	1.90±0.03	12.16±0.03	-1.019±0.012	...	...	...	...	...	
RECX 10	08443188-7846311	3846±21	105±1	-1.27±0.03	1.60±0.03	11.26±0.03	-0.659±0.012	3836±26	106±1	-1.27±0.03	1.60±0.03	11.26±0.03	-0.659±0.012
RECX 12	08475676-7854532	3361±22	144±1	-2.01±0.03	1.84±0.03	11.16±0.03	-0.621±0.012	...	...	...	...	...	
HIP 47133	09361593+3731456	3843±19	205±2	-1.29±0.01	1.72±0.02	9.81±0.02	...	3829±24	206±2	-1.28±0.01	1.73±0.02	9.81±0.02	...
TWA 21	10131476-5230540	4673±34	177±1	-0.55±0.07	1.41±0.04	9.28±0.05	-0.332±0.061[a]	4627±32	178±1	-0.53±0.07	1.43±0.04	9.30±0.05	-0.342±0.061[a]
DK Leo	10141918+2104297	3861±17	325±2	-1.26±0.02	1.71±0.03	8.79±0.02	...	3837±23	328±3	-1.25±0.02	1.72±0.03	8.79±0.02	...
TWA 22	10172689-5354265	2843±8	264±2	-3.39±0.02	2.01±0.02	10.57±0.02	-1.837±0.025[c]	...	...	...	...	...	
TWA 6	10182870-3150029	3982±15	140±1	-1.14±0.02	1.61±0.04	10.48±0.02	...	3946±19	142±1	-1.13±0.01	1.62±0.04	10.49±0.02	...
2MASS J10252092-4241539	10252092-4241539	3696±22	116±1	-1.52±0.05	1.71±0.04	11.21±0.05	...	3673±27	117±1	-1.51±0.05	1.72±0.04	11.22±0.05	...
2MASS J10260210-4105537	10260210-4105537	3603±27	141±1	-1.65±0.06	1.73±0.04	10.90±0.04	...	3585±29	142±2	-1.65±0.06	1.73±0.03	10.90±0.04	...
TWA 7	10423011-3340162	3370±19	284±2	-1.99±0.01	1.87±0.02	9.66±0.02	...	...	...	...	...	...	
TWA 1	11015191-3442170	3912±22	204±2	-1.18±0.02	1.52±0.03	9.74±0.02	-0.532±0.230	3903±24	205±2	-1.18±0.02	1.53±0.03	9.74±0.02	-0.534±0.230
TWA 28	11020983-3430355	2178±160	59±6	-6.47±0.20	1.96±0.20	14.99±0.20	-2.610±0.190[b]	...	...	...	...	...	
TWA 2	11091380-3001398	3556±22	288±3	-1.67±0.01	1.78±0.03	9.41±0.02	-0.524±0.121[a]	3572±31	288±4	-1.68±0.01	1.76±0.03	9.39±0.02	-0.516±0.121[a]
TWA 3	11102788-3731520	3112±13	355±3	-2.53±0.02	1.88±0.02	9.53±0.02	...	...	...	...	...	...	
TWA 12	11210549-3845163	3379±18	159±1	-1.94±0.01	1.91±0.04	10.91±0.02	-0.848±0.090[a]	...	...	...	...	...	
TWA 13A	11211723-3446454	3812±21	179±2	-1.32±0.02	1.71±0.05	10.14±0.02	-0.664±0.081[a]	3793±26	181±2	-1.33±0.02	1.70±0.04	10.14±0.02	-0.661±0.081[a]
TWA 13B	11211745-3446497	3549±24	191±2	-1.66±0.02	1.87±0.04	10.30±0.02	-0.667±0.089[a]	3582±34	188±3	-1.66±0.01	1.88±0.04	10.31±0.02	-0.668±0.089[a]
TWA 4	11220530-2446393	4223±15	389±3	-0.88±0.02	1.61±0.02	8.01±0.02	0.004±0.208	4166±15	395±2	-0.86±0.02	1.63±0.02	8.03±0.02	-0.005±0.208

Table 3.8 (cont'd)

Object	2MASS	BT-Settl						Kurucz					
		$T_{\rm eff}$ (K)	θ (μas)	BC_V (mag)	BC_J (mag)	m_{bol} (mag)	$\log(L/L_\odot)$ (dex)	$T_{\rm eff}$ (K)	θ (μas)	BC_V (mag)	BC_J (mag)	m_{bol} (mag)	$\log(L/L_\odot)$ (dex)
2MASS J11254754-4410267	11254754-4410267	3169±16	97±1	-2.36±0.02	1.93±0.03	12.28±0.03	...	...	...	...	...	...	
TWA 5A	11315526-3436272	3435±22	299±3	-1.91±0.04	1.81±0.03	9.48±0.04	-0.489±0.072[a]	...	...	...	...	...	
TWA 8B	11324116-2652090	3191±63	122±1		1.90±0.09	11.73±0.09	...	...	...	...	...	...	
TWA 8A	11324124-2651559	3358±18	221±2	-2.00±0.01	1.89±0.03	10.23±0.02	...	...	...	...	...	...	
TWA 33	11393382-3040002	2915±9	133±1	-3.12±0.01	1.96±0.02	11.94±0.02	...	...	...	...	...	...	
TWA 26	11395113-3159214	2176±17	66±1		2.06±0.04	14.74±0.05	-2.748±0.219[a]	...	...	...	...	...	
TWA 9B	11482373-3728485	3288±20	109±1	-2.14±0.02	1.88±0.03	11.86±0.02	-1.151±0.111	...	...	...	...	...	
TWA 9A	11482422-3728491	4144±16	150±1	-0.97±0.02	1.48±0.04	10.16±0.02	-0.472±0.111	4089±15	153±1	-0.96±0.02	1.48±0.04	10.17±0.02	-0.472±0.111
TWA 23	12072738-3247002	3329±21	195±2	-2.10±0.04	1.92±0.04	10.54±0.05	-0.851±0.054[a]	...	...	...	...	...	
TWA 25	12153072-3948426	3704±20	203±2	-1.46±0.01	1.82±0.04	9.99±0.02	-0.625±0.134[a]	3702±28	205±2	-1.47±0.01	1.81±0.04	9.97±0.02	-0.620±0.134[a]
2MASS J12265135-3316124	12265135-3316124	2760±11685	105±1		2.00±18.39	12.69±18.39	...	...	...	...	...	...	
TWA 20	12313807-4558593	3377±23	141±1	-1.99±0.04	1.85±0.04	11.18±0.05	-0.793±0.096[a]	...	...	...	...	...	
TWA 16	12345629-4538075	3475±21	160±2	-1.80±0.02	1.79±0.03	10.78±0.03	-0.623±0.079[a]	...	...	...	...	...	
TWA 10	12350424-4136385	3367±18	157±1	-2.00±0.01	1.84±0.03	10.96±0.02	...	...	...	...	...	...	
TWA 11C	12354893-3950245	3075±18	130±1	-2.67±0.05	1.97±0.03	11.76±0.04	-1.124±0.073[a]	...	...	...	...	...	
HD 139084	15385757-5742273	4986±15	307±1	-0.36±0.02	1.41±0.03	7.80±0.02	-0.044±0.088	4954±15	308±1	-0.34±0.02	1.44±0.03	7.82±0.02	-0.053±0.089
2MASS J16430128-1754274	16430128-1754274	3741±24	116±1		1.71±0.03	11.15±0.04	...	3754±65	116±1		1.70±0.07	11.14±0.07	...
HD 155555	17172550-6657039	5053±13	537±2	-0.34±0.01	1.24±0.03	6.53±0.02	0.286±0.032	5025±12	536±1	-0.32±0.02	1.27±0.03	6.55±0.02	0.276±0.033
HIP 84642	17181464-6027275	5214±14	142±1	-0.23±0.02	1.27±0.02	9.28±0.02	-0.268±0.158	5178±14	142±1	-0.21±0.02	1.29±0.02	9.30±0.02	-0.278±0.158
CD-54 7336	17295506-5415487	5033±13	156±1	-0.32±0.02	1.29±0.03	9.23±0.02	...	4998±12	156±1	-0.30±0.02	1.31±0.03	9.25±0.02	...
HD 160305	17414903-5043279	6065±21	166±1	-0.05±0.02	0.94±0.03	8.28±0.02	0.311±0.127	6041±20	166±1	-0.04±0.02	0.95±0.03	8.30±0.02	0.304±0.127
HD 161460	17483374-5306433	5013±22	203±1	-0.31±0.03	1.36±0.03	8.67±0.03	...	4975±21	204±1	-0.29±0.03	1.38±0.03	8.69±0.03	...
HIP 88399	18030341-5138564	6560±11	256±1	-0.01±0.01	0.84±0.02	7.00±0.02	0.466±0.054	6539±17	256±1	0.00±0.02	0.85±0.02	7.01±0.02	0.463±0.055
V4046 Sgr	18141047-3247344	4006±45	201±1	-1.01±0.10	1.60±0.06	9.67±0.06	...	3932±54	204±2	-0.97±0.11	1.64±0.06	9.72±0.06	...
GSC 7396-0759	18142207-3246100	3629±23	121±1	-1.59±0.01	1.75±0.03	11.19±0.02	...	3637±31	121±2	-1.60±0.01	1.74±0.03	11.18±0.02	...
HD 168210	18195221-2916327	5524±26	170±1	-0.16±0.03	1.11±0.03	8.63±0.04	0.171±0.149	5499±23	170±1	-0.15±0.03	1.13±0.03	8.65±0.03	0.163±0.149
CD-64 1208	18453704-6451460	4211±21	317±2	-0.97±0.06	1.55±0.03	8.46±0.04	...	4147±39	321±3	-0.93±0.07	1.60±0.05	8.50±0.05	...
TYC 9073-0762-1	18465255-6210366	3623±23	166±2	-1.56±0.01	1.77±0.02	10.52±0.02	...	3635±31	166±2	-1.57±0.01	1.76±0.02	10.51±0.02	...

Table 3.8 (cont'd)

Object	2MASS	BT-Settl						Kurucz					
		$T_{\rm eff}$ (K)	θ (μas)	BC_V (mag)	BC_J (mag)	m_{bol} (mag)	$\log(L/L_\odot)$ (dex)	$T_{\rm eff}$ (K)	θ (μas)	BC_V (mag)	BC_J (mag)	m_{bol} (mag)	$\log(L/L_\odot)$ (dex)
TYC 7408-0054-1	18504448-3147472	3927±15	179±1	-1.20±0.01	1.69±0.02	10.00±0.02	...	3892±19	183±1	-1.20±0.01	1.69±0.02	10.00±0.02	...
PZ Tel	18530587-5010499	5116±15	247±1	-0.27±0.02	1.31±0.03	8.16±0.02	0.061±0.101	5077±12	248±1	-0.24±0.02	1.33±0.02	8.19±0.02	0.051±0.101
TYC 6872-1011-1	18580415-2953045	3893±23	144±2	-1.26±0.02	1.66±0.03	10.52±0.02	...	3875±26	144±2	-1.24±0.02	1.68±0.02	10.54±0.02	...
CD-26 13904	19114467-2604085	4491±9	165±1	-0.67±0.01	1.52±0.02	9.61±0.02	...	4430±9	167±1	-0.64±0.01	1.55±0.02	9.63±0.02	...
HIP 95270	19225894-5432170	6446±20	262±1	-0.02±0.02	0.82±0.03	7.02±0.02	0.522±0.068	6419±17	263±1	0.00±0.02	0.84±0.03	7.04±0.02	0.517±0.068
2MASS J19560294-3207186	19560294-3207186	3462±48	164±1		1.79±0.06	10.75±0.07	...	...	...	...	...	...	
TYC 7443-1102-1	19560438-3207376	3895±19	154±1	-1.23±0.03	1.65±0.03	10.36±0.04	...	3869±24	155±1	-1.21±0.03	1.67±0.03	10.38±0.04	...
2MASS J20013718-3313139	20013718-3313139	3687±22	136±1	-1.50±0.04	1.72±0.03	10.88±0.04	...	3682±29	137±2	-1.50±0.03	1.72±0.03	10.87±0.04	...
AT Mic	20415111-3226073	3123±12	790±4	-2.49±0.02	1.97±0.03	7.78±0.03	-1.151±0.079	...	...	...	...	...	
AU Mic	20450949-3120266	3642±22	757±7	-1.56±0.02	1.77±0.02	7.20±0.03	-0.987±0.024	3652±31	753±10	-1.56±0.02	1.76±0.02	7.20±0.03	-0.986±0.023
HD 199143	20554767-1706509	5931±19	290±1	-0.10±0.02	0.96±0.02	7.17±0.03	0.353±0.071	5906±20	290±1	-0.08±0.02	0.98±0.03	7.19±0.03	0.346±0.072
AZ Cap	20560274-1710538	4018±13	215±1	-1.11±0.01	1.66±0.02	9.51±0.02	-0.584±0.071	3979±15	218±1	-1.10±0.01	1.67±0.02	9.52±0.02	-0.587±0.071
HIP 105388	21204994-5302030	5518±17	182±1	-0.16±0.02	1.11±0.03	8.49±0.02	-0.228±0.085	5491±15	182±1	-0.14±0.02	1.12±0.03	8.51±0.02	-0.236±0.085
HIP 105404	21205980-5228400	4912±13	228±1	-0.38±0.02	1.33±0.03	8.51±0.02	-0.194±0.127	4867±11	229±1	-0.35±0.02	1.36±0.03	8.54±0.02	-0.204±0.127
HIP 107345	21443012-6058389	3843±18	154±1	-1.29±0.02	1.68±0.03	10.43±0.03	-0.991±0.225	3823±24	155±2	-1.28±0.02	1.69±0.03	10.44±0.02	-0.994±0.225
HIP 107947	21520973-6203085	6347±18	250±1	-0.02±0.02	0.84±0.03	7.20±0.02	0.337±0.061	6319±17	250±1	-0.01±0.02	0.85±0.03	7.21±0.02	0.330±0.061
HIP 108195	21551140-6153119	6708±19	405±1	-0.01±0.02	0.67±0.04	5.91±0.02	0.874±0.040	6685±19	406±1	0.00±0.02	0.67±0.04	5.92±0.02	0.870±0.040
HIP 108422	21575146-6812501	5055±14	207±1	-0.31±0.02	1.28±0.03	8.59±0.02	-0.008±0.123	5016±12	208±1	-0.28±0.02	1.31±0.03	8.62±0.02	-0.017±0.123
TYC 2211-1309-1	22004158+2715135	3961±22	160±1	-1.16±0.05	1.65±0.04	10.21±0.05	...	3917±27	162±2	-1.13±0.05	1.68±0.04	10.24±0.05	...
CPD-72 2713	22424896-7142211	3932±14	235±1	-1.19±0.01	1.62±0.02	9.41±0.02	...	3900±19	238±2	-1.19±0.01	1.62±0.02	9.42±0.02	...
HIP 112312	22445794-3315015	3179±14	308±2	-2.41±0.03	1.96±0.02	9.75±0.03	-1.261±0.169	...	...	...	...	...	
TX PsA	22450004-3315258	3031±10	223±1	-2.77±0.02	1.97±0.02	10.65±0.03	-1.585±0.170	...	...	...	...	...	
BD-13 6424	23323085-1215513	3764±20	288±3	-1.38±0.01	1.71±0.02	9.16±0.02	...	3755±26	290±3	-1.39±0.01	1.71±0.02	9.16±0.02	...
HD 222259B	23393929-6911396	4653±18	176±1	-0.54±0.02	1.67±0.06	9.30±0.02	-0.499±0.078	4585±18	180±1	-0.53±0.02	1.69±0.06	9.32±0.02	-0.504±0.078
HD 222259	23393949-6911448	5542±21	196±1	-0.15±0.02	1.20±0.03	8.32±0.03	-0.105±0.078	5522±20	195±1	-0.13±0.02	1.21±0.03	8.34±0.02	-0.113±0.078

Note. — $T_{\rm eff}$ values were fit at $\log(g) = 4.3$.
a Indicates $\log(L/L_\odot)$ estimates use parallaxes from Weinberger et al. (2012).
b Indicates $\log(L/L_\odot)$ estimate uses parallax from Teixeira et al. (2008).
c Indicates $\log(L/L_\odot)$ estimate uses parallax from Teixeira et al. (2009).
In addition, we have used a weighted mean distance of 94.3±1.2 pc for η Cha cluster members. For objects HD 139084B, HD 164249B, AZ Cap, and HD 222259B we have adopted parallaxes from their brighter companions.

For comparison, in Figure 3.8 we have also plotted the giant temperature scale of van Belle et al. (1999), the "literature consensus" dwarf T_{eff} scale described in Appendix C, and the young star scale of Luhman et al. (2003) using the spectral type-color sequence described in this work for young stars. As a function of V–K_S, our derived temperature scale for young stars is intermediate between giants and dwarfs, and is also intermediate between dwarfs and the temperature scale of Luhman et al. (2003). This is consistent with our expectations, given that the Luhman et al. (2003) T_{eff} scale was calibrated to make the four components of GG Tau coeval when compared to Baraffe et al. (1998) evolutionary models and our young stars are much older than GG Tau (∼1 Myr), but much younger than field dwarfs. Similar to many other authors, we find that V–K_S provides the closest correlation to temperature with relatively little scatter. To take advantage of the utility of V–K_S as a proxy for T_{eff}, we estimate the spectral type-temperature calibration by fitting a polynomial to T_{eff} as a function of V–K_S. The coefficients for this polynomial are listed in Table 3.9. We then apply this polynomial to our spectral type-intrinsic color sequence. Unfortunately only one object in our sample later than spectral type M5.5 has V band photometry, so we do not provide effective temperature estimates for spectral types M6-M9, though we do provide intrinsic colors for those spectral types. Our spectral type, intrinsic color and T_{eff} sequence for young stars is listed in Table 3.5.

Table 3.9. T_{eff}, Bolometric Correction, and Bolometric Magnitude Polynomial Coefficients for 5-30 Myr Old Stars

Y	X	Range	a_0	a_1	a_2	a_3	a_4	a_5	a_6	a_7
T_{eff}	$V-K_S$	$1.0 < V-K_S < 6.7$	9.323430×10^{3}	-3.516011×10^{3}	1.046787×10^{3}	-1.863349×10^{2}	1.641182×10^{1}	-5.188853×10^{-1}	...	
T_{eff}	$V-J$	$0.8 < V-J < 5.8$	9.593475×10^{3}	-5.095204×10^{3}	2.053259×10^{3}	-4.813940×10^{2}	5.816754×10^{1}	-2.779565×10^{0}	...	
BC_V	$V-K_S$	$1.0 < V-K_S < 6.7$	-7.443324×10^{-2}	2.471780×10^{-1}	-1.923234×10^{-1}	1.318867×10^{-2}	-3.630511×10^{-4}	...	...	
BC_V	T_{eff}	$2750 < T_{eff} < 7350$	-2.855844×10^{2}	3.832453×10^{-1}	-2.225832×10^{-4}	7.150667×10^{-8}	-1.364193×10^{-11}	1.542389×10^{-15}	-9.566224×10^{-20}	2.511807×10^{-24}
BC_J	$V-K_S$	$1.0 < V-K_S < 6.7$	-4.805196×10^{-1}	1.842350×10^{0}	-7.837156×10^{-1}	1.859281×10^{-1}	-2.153500×10^{-2}	9.489583×10^{-4}		
BC_J	$V-J$	$0.8 < V-J < 5.8$	-4.557821×10^{-1}	2.299875×10^{0}	-1.191653×10^{0}	3.442879×10^{-1}	-4.932544×10^{-2}	2.724400×10^{-3}		
BC_J	T_{eff}	$2750 < T_{eff} < 6750$	2.920272×10^{0}	-3.220428×10^{-4}	...	...	...	...		
m_{bol}	J	K4 through M8	1.224151×10^{0}	1.061610×10^{0}	...	...	...	...		
m_{bol}	H	K4 through M8	1.926191×10^{0}	1.059132×10^{0}	...	...	...	...		
m_{bol}	K_S	K4 through M8	1.787487×10^{0}	1.107039×10^{0}	...	...	...	...		

Note. — $Y = a_0 + a_1X + a_2X^2 + a_3X^3 + a_4X^4 + a_4X^4 + a_5X^5 + a_6X^6 + a_7X^7$

3.5.6 Bolometric Corrections

As a byproduct of estimating the effective temperature of stars in our sample using the method of SED fitting, we automatically obtain an estimate of each object's angular diameter. This can then be used to estimate the apparent bolometric luminosity (m_{bol}) and, more usefully, the bolometric correction in any band (BC_x). The basic equation that relates stellar bolometric magnitude to luminosity is

$$\begin{aligned} M_{\rm bol} &= -2.5\log\left(\frac{L}{L_\odot}\right) + M_{\rm bol,\odot} \\ &= -2.5\log\left(\frac{\sigma T_{\rm eff}^4 4\pi R^2}{\sigma T_{\rm eff,\odot}^4 4\pi R_\odot^2}\right) + M_{\rm bol,\odot} \\ &= -10\log\left(\frac{T_{\rm eff}}{T_\odot}\right) - 5\log\left(\frac{R}{R_\odot}\right) + M_{\rm bol,\odot}. \end{aligned}$$

We can also write this in terms of apparent magnitude m_x in band x with the distance d and bolometric correction BC_x:

$$M_{\rm bol} = m_x - 5\log\left(\frac{d}{10pc}\right) + BC_x.$$

Equating these two, using the angular semi-diameter $\theta = \frac{R}{d} = 10^{-0.2\mathcal{A}}$, and solving for BC_x we find

$$\begin{aligned} BC_x &= \mathcal{A} + 5\log\left(\frac{R_\odot}{10pc}\right) + M_{\rm bol,\odot} \\ &\quad -10\log\left(\frac{T_{\rm eff}}{T_{\rm eff,\odot}}\right) - m_x. \end{aligned}$$

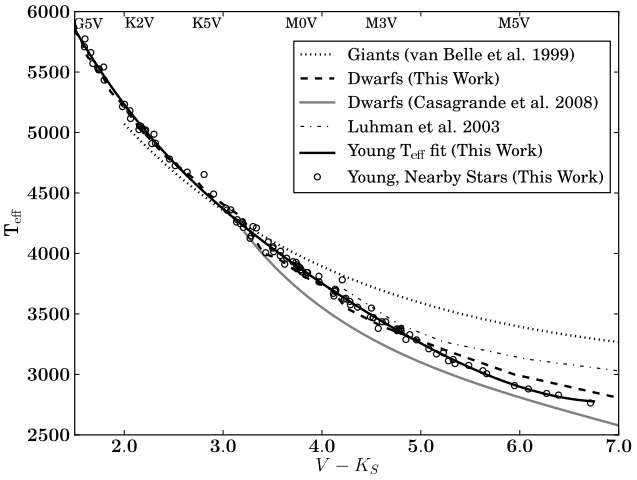

Figure 3.8 V–K_S versus $T_{\rm eff}$ for the young stars studied in this work (circles) and the Dwarf (dashed line) and young star (solid line) effective temperature scales derived in this work plotted against the giant temperature scale of van Belle et al. (1999) (dotted line). As a function of V–K_S, our young stellar temperature scale is intermediate between the temperature scale of Luhman et al. (2003) (appropriate for ∼1 Myr old stars) and the dwarf temperature scale, though ours is much closer to the dwarf $T_{\rm eff}$ scale.

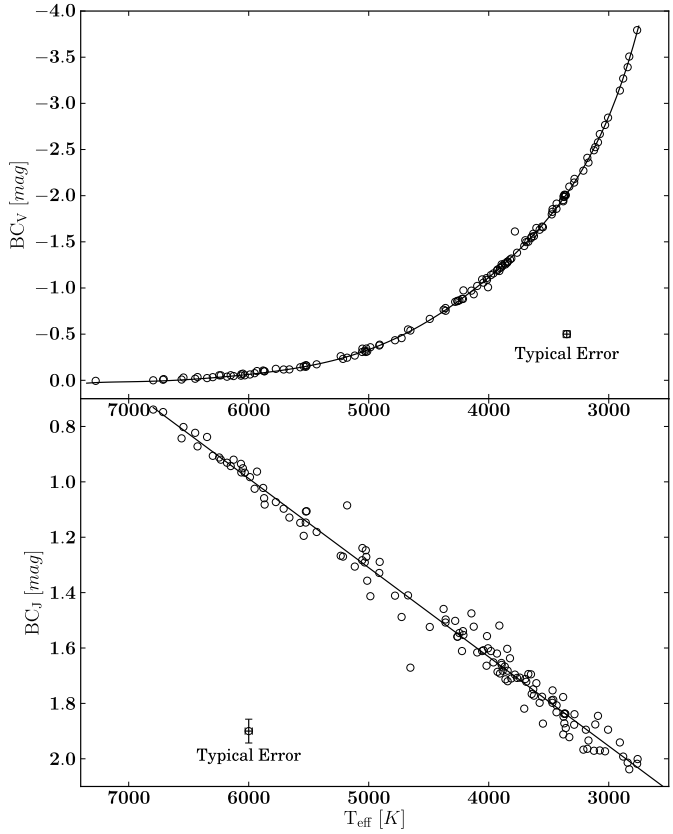

Figure 3.9 Bolometric corrections for V and J band magnitudes as a function of effective temperature. Note that for $T_{\rm eff} \lesssim 5000$ K, BC_V becomes a sensitive function of $T_{\rm eff}$ and therefore it is preferable to use $M_{bol} = M_J + BC_J$ for cooler stars. Coefficients for polynomial fit are listed in Table 3.9.

We use mutually consistent solar values of $T_{\rm eff,\odot} = 5772\ K$, $R_\odot = 695660$ km, $m_{V,\odot} = -26.70$ mag, and $M_{\rm bol,\odot} = 4.755$ mag as adopted by Mamajek (2012)[11]. The uncertainties in BC_x are

$$(\sigma_{BC_x})^2 \;=\; \left(\frac{10\sigma_{T_{\rm eff}}}{T_{\rm eff}\ln 10}\right)^2 + (\sigma_{\mathcal{A}})^2 + (\sigma_{m_x})^2\,.$$

[11]See also "Basic Astronomical Data for the Sun", https://sites.google.com/site/mamajeksstarnotes/basic-astronomical-data-for-the-sun more complete discussion on solar data, including motivation for the values adopted here.

Though the zero point of the bolometric correction scale is arbitrary, the combination of bolometric corrections and solar absolute bolometric magnitude are not (see Torres 2010 and Appendix D of Bessell et al. 1998). In Table 3.8 we give the calculated individual bolometric corrections in both Johnson V band and 2MASS J band. We also provide $\log(L/L_{\odot})$ for objects with measured trigonometric parallaxes. For F- and G-type stars ($T_{\rm eff} \gtrsim 5000$ K) it is preferred to estimate bolometric magnitudes using $M_{bol} = M_V + BC_V$ since the V band correction is not a sensitive function of $T_{\rm eff}$ for 5000 K $< T_{\rm eff} <$ 7000 K. However, for K- and M-type stars ($T_{\rm eff} \lesssim 5000$ K) BC_V becomes a steep function of $T_{\rm eff}$ and therefore it is better to use $M_{bol} = M_J + BC_J$. Plots of BC_V and BC_J versus $T_{\rm eff}$ are shown in Figure 3.9. Polynomial fits to BC_V and BC_J as a function of $T_{\rm eff}$ and $V - K_S$ are given in Table 3.9.

3.6 Discussion

Consistent with previous studies (e.g., Da Rio et al., 2010; Luhman et al., 2010b), we have found that pre-MS stars do not have the same intrinsic colors as field dwarfs for certain spectral types and colors. There are two likely main reasons for the differences in colors. The first and most important cause is the different surface gravities of young stars when compared to main sequence dwarfs. The striking bifurcation in the V–K_S versus J–H color-color diagram between dwarfs and giants has been explained as an effect of CO and H_2O bands and H^- opacity (Jorgensen, 1996). The B–V colors for young objects with V–$K_S > 3.0$ are systematically bluer than main sequence stars. At lower surface gravities, the synthetic BT-Settl B–V colors are predicted to be bluer at a given V–K_S than higher-surface gravity objects. Our new spectral type-color relations take these important surface-gravity effects for young stars into account. However, this does not explain the origin of redder colors, particularly H–K_S, for F-

and G-type stars, which have surface gravities very close to main sequence dwarfs.

The second possible explanation for color differences between young stars and older main sequence stars suggested by Gullbring et al. (1998) and Stauffer et al. (2003) is the greater abundance of stellar spots on young stars. Young stars show evidence of stronger magnetic activity than that of older main sequence stars, which is exhibited by hotter plage and cooler spot regions on the surface. In particular, these plage regions have been suggested as contributing to the systematically bluer B–V colors observed in the Pleiades open cluster (Stauffer et al., 2003). Gullbring et al. (1998) estimated a $\sim$50% spot coverage to account for the mean V–J color anomaly in weak-lined T Tauri stars. However, the Stauffer et al. (2003) study is the most comprehensive attempt to date to investigate the contribution of cool spots to stellar colors. Stauffer et al. (2003) found that Pleiades K star red spectra (5700-8400Å) had systematically later spectral types than the blue (3300-5300Å) spectra, whereas the older Praesepe K stars did not suffer from this effect[12]. Stauffer et al. (2003) additionally modeled the $BVRIJHK$ SEDs of several Pleiades, combining observed SEDs of an earlier field dwarf and a later field dwarf to obtain a fit. The best-fit models obtained in the Stauffer et al. (2003) study indicated that the K-type Pleiades were covered in $\gtrsim$50% "cool spots", consistent with the Gullbring et al. (1998) results. They use $BVRIJHK$ photometry to fit observed Pleiad SEDs. On the basis of their spectroscopy and SED fitting, Stauffer et al. (2003) concluded that the Pleiades K stars had more than one photospheric temperature, and that spottedness was well-correlated with the B–V color anomaly. While these results point convincingly to stellar spots as a significant contributing factor, especially to bluer B–V colors, we do not attempt to quantify the relative contribution of spots or surface gravity effects

[12]This effect is also seen in G and K stars from the younger Scorpius-Centaurus OB association, where blue spectra ($\sim$3800–5400Å) give systematically earlier spectral types than the red spectra ($\sim$6200–7100Å) by about one spectral subtype (E.E. Mamajek, private communication 2012)

to the intrinsic colors of pre-MS stars. Disentangling the effects of surface gravity and spots would require time-series multi-band photometry for most of the objects in our sample. Quantifying the specific contribution of the spots and plages to the stellar colors is beyond the scope of this study.

McCarthy & White (2012) published predicted angular diameters for many of the β Pic moving group members in our sample using estimated H-R diagram positions and revised *Hipparcos* parallaxes (van Leeuwen, 2007). In addition, Lafrasse et al. (2010) have estimated the angular diameters of thousands of dwarfs and giants with V and V–K surface brightness relations (e.g., Barnes & Evans, 1976). We compare our results to the McCarthy & White (2012) and Lafrasse et al. (2010) results in Figure 3.10. Our angular diameter estimates follow the Lafrasse et al. (2010) estimates very closely, though ours are systematically smaller by 4%. We have attempted to understand the origin of this systematic difference. There is a trend with $T_{\rm eff}$, with hotter objects tend to be more discrepant than cooler objects. However, the origin of this discrepancy is unclear. Our angular diameter estimates also compare well with the results of McCarthy & White (2012), with our estimates being 6% larger on average, but with much larger scatter, this difference is not statistically significant. The larger scatter between our angular diameter estimates and those from McCarthy & White (2012) are likely due to the different methods used to infer the objects $T_{\rm eff}$. For example, we predict TYC 1208-468-1 to have a diameter of 241$\pm$1 μas, but McCarthy & White (2012) predict 120 μas. This object has $BVJHK$ colors consistent with a spectral type of $\sim$K6, but has a reported spectral type of K3Ve (Jeffries, 1995). The $\sim$600 K difference in the assumed $T_{\rm eff}$ translates to a large difference in the predicted angular diameter.

There is considerable overlap between our sample and the sample of Mentuch et al. (2008), who examined Li depletion in several nearby young associations. The Men-

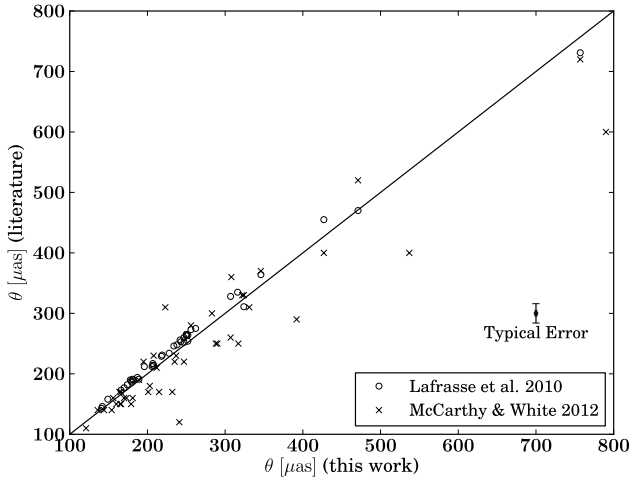

Figure 3.10 The individual angular diameter estimates from this work compared with estimates from McCarthy & White (2012) and Lafrasse et al. (2010).

tuch et al. (2008) study estimated T_{eff} for each object in their sample by least-squares fitting spectral regions $\lambda\lambda$5850-5930, 7900-7980, 8150-8230, 8400-8480, and 8485-8565 to synthetic spectra generated with NextGen model atmospheres. In Figure 3.11 we compare our T_{eff} values obtained by fitting multi-band photometry to the BT-Settl NextGen model colors with the T_{eff} values obtained by Mentuch et al. (2008). Overall there is a systematic difference – the values obtained by Mentuch et al. (2008) are systematically ∼150 K hotter than the values we obtain, with a larger difference (∼230K) above 4500 K and a smaller difference (∼120 K) below 4500 K. This discrepancy could be due to the slightly different synthetic models used – the latest BT-Settl models use the revised solar abundances from Asplund et al. (2009) and include more complete molecular opacity lists, though these updated opacities would mostly affect the lower-mass stars and could not account for the differences above ∼5000 K.

In addition we have compared our estimated T_{eff} values with those derived in the Casagrande et al. (2008) and Casagrande et al. (2011) studies, where possible

(Figure 3.11). Both these studies used theoretical atmospheric models with an implementation of the Infrared flux method (IRFM) or a closely related method (MOITE) to estimate the stellar effective temperature for a large number of objects. The IRFM (Blackwell & Shallis, 1977) compares the ratio of the observed bolometric flux to the observed monochromatic flux density at the Earth ("R_{obs}") to the ratio of theoretical bolometric flux to monochromatic flux density at the surface of the star ("R_{theo}"). R_{theo} is a function of the T_{eff}, and is compared to the R_{obs} ratio to obtain the T_{eff} of the object. Typically for hotter stars the dependence in the IR bands on the model is very minimal and thus this is only used with the ratio of IR flux density (IRFM) to determine the T_{eff}. For cooler stars, Casagrande et al. (2008) have adapted this method to use optical and infrared bands (called "MOITE"). Casagrande et al. (2008) have assumed $log(g)$=5.0 dex throughout with the 'Cond' variant of NextGen models (we have used the 'BT-Settl' variant here with revised solar abundances from Asplund et al. 2009), whereas the Casagrande et al. (2011) study used the Castelli & Kurucz (2004) models which used the Grevesse & Sauval (1998) solar abundances. TX PsA (M5IVe) and HIP 107345 (M0Ve) both have T_{eff} estimates which agree within 2σ of the Casagrande et al. (2008) study. For objects in common, our T_{eff} estimates are typically $\sim$40 K lower than the values from the Casagrande et al. (2011) study (plotted in Figure 3.11).

For the few objects with spectral types M8 or later we obtain cooler temperatures than expected from the temperature scale of Luhman et al. (2003) or the dwarf temperature scale. The Rice et al. (2010a) study fit PHOENIX dusty synthetic spectra to high-resolution spectra in order to find the best-fit T_{eff} and $\log(g)$ of sample of young late M-type objects. Two objects in our sample with SEDF-determined T_{eff}, 2MASS J06085283-2753583 (2M0608-27; M8.5γ; Rice et al. 2010b) and TWA 26 (M8IVe; Barrado Y Navascués 2006), are included in the Rice et al. (2010a) study. For

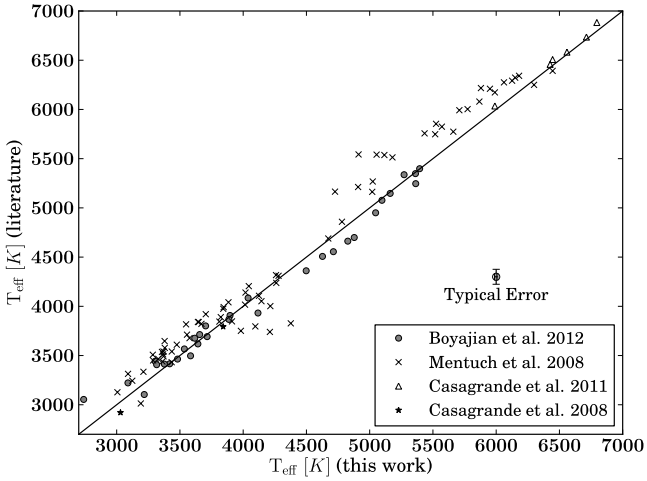

Figure 3.11 The individual T_{eff} values from this work compared with values obtained by least-squares fitting to synthetic NextGen spectra from Mentuch et al. (2008) (crosses) and those in the study of Casagrande et al. (2011) (triangles) and Casagrande et al. (2008) (stars). We also compare a sample of K- and M-type dwarfs which have angular diameter-based T_{eff} estimates from Boyajian et al. (2012b) with estimates using our SEDF implementation (circles). The values in Mentuch et al. (2008) are systematically higher than those estimated in this work, with the difference ∼230 K above 4500 K, reducing to ∼120 K below 4500 K. Those from the Casagrande et al. (2011) study are typically ∼40 K higher than the values from this work.

2M0608-27, assuming $\log(g)$=4.3 dex, we find T_{eff}=2118±20 K, whereas Rice et al. (2010a) adopt $\log(g)$=3.98 and T_{eff}=2529 K, much hotter than our results and consistent with the temperature scale of Luhman et al. (2003). We find T_{eff}=2176±17 K for TWA 26 but Rice et al. (2010a) find $\log(g)$=3.98 and T_{eff}=2609 K, again much hotter than our results and consistent with the T_{eff} scale of Luhman et al. (2003). These four objects lack BVI_C photometry and thus do not have any SED fitting constraints blueward of their SED peak; this could be a contributing factor in their discrepantly cool T_{eff} fit. Because of these discrepancies, we do not include T_{eff} for objects M6-M9 in our pre-MS temperature scale (Table 3.5).

Only two objects in our sample, HR 9 and 51 Eri, have direct angular diameter

measurements available from the literature. Simon & Schaefer (2011) measured angular diameters of 492±32 μas and 518±9 μas for HR 9 and 51 Eri, respectively. Our angular diameter estimates of 346±1 μas for HR 9 and 471±2 μas for 51 Eri are much lower than the interferometric measurements. While we have no reason to suspect the direct measurements are unreliable *a priori*, the angular diameter of 492 μas for HR 9 (F3Vn; Gray et al. 2006) warrants some discussion. If we adopt the estimated bolometric flux at Earth from Casagrande et al. (2011) of 8.6609×10^{-8} mW m^{-2}, and again use the measured angular diameter of 492 μas, we obtain a $T_{\rm eff}$ of 5724 K, similar to a G3V! This is ∼1000 K lower than the 6883±91 K that Casagrande et al. (2011) obtains and our value of 6761±28 K, both of which are consistent with the F3Vn spectral type. The Simon & Schaefer (2011) results indicate a larger angular diameter at H band than K band, which points to unusual calibration errors (M. Simon, private communication 2012). Until updated measurements are published we recommend our predicted angular diameter.

3.7 Conclusions

We can summarize our conclusions as follows:

1. 5-30 Myr old pre-main sequence stars follow slightly different spectral type-intrinsic color sequences than those of main sequence stars. Pre-MS colors follow the dwarf sequence for some colors and spectral types, but for other color and spectral types deviations can exceed 0.3 mag. In Table 3.5 we give a tabulation of the intrinsic colors of young stars for spectral types F0 through M9, including B-V, V–I_C, V–K_S, J–H, H–K_S, K_S–$W1$, K_S–$W2$, K_S–$W3$, and K_S–$W4$.

2. We identify two previously unidentified 22μm excesses for HD 160305 and CD-54 7336 at 2.9σ and 5.4σ significance, respectively. We confirm AG Tri as possessing a 22μm excess at 4.5σ significance, confirming the suggestion of Rebull et al. (2008).

3. Consistent with the findings of previous studies (e.g., Luhman, 1999; Da Rio et al., 2010), color differences between K- and M-type pre-MS stars and dwarfs are predominantly due to the young stars' lower surface gravities. This is demonstrated by theoretical models predicting redder J–H colors and bluer B–V colors for lower surface gravity objects, consistent with observations. However, we cannot exclude hotter plage and cooler spot regions on the stellar surface as contributing factors.

4. A pre-MS $T_{\rm eff}$ scale derived from fitting SEDs to synthetic spectral models is within $\sim$100 K of main sequence stars as a function of V–K_S. As a function of spectral type, the effective temperatures of F0-G4 and K7-M5 pre-MS stars are within $\sim$100 K of their main sequence counterparts, whereas G5-K6 pre-MS stars are $\sim$250 K cooler at a given spectral type. We provide new spectral type-$T_{\rm eff}$ relations and color-$T_{\rm eff}$ relations appropriate for 5-30 Myr old pre-MS stars. We also provide bolometric corrections appropriate for PMS stars as polynomial functions of $T_{\rm eff}$ and V–K_S in Table 3.9 and as part of our spectral type-intrinsic color sequence in Table 3.5.

4 The Star Formation History and Accretion Disk Fraction Among the K-type Members of the Scorpius-Centaurus OB Association

4.1 Introduction and Background

Because of their utility for studying star and planet formation and evolution, a great deal of effort has been directed towards identifying and characterizing samples of nearby young stars. These samples have been indispensable for direct imaging of brown dwarf and planetary-mass companions (e.g., Kraus & Ireland, 2012), exploring the star-disk interaction in young stars (e.g., Nguyen et al., 2009), and studying the evolution of gas-rich and dusty debris disks as a function of age (e.g., Mamajek, 2009; Chen et al., 2011).

The nearest of these samples are small, diffuse, nearby associations of kinematically related stars, (e.g., the β Pictoris moving group, TW Hya Association; Zucker-

man & Song 2004; Torres et al. 2008). They typically have tens of known members, with masses ∼0.02-2 $M_\odot$. While these are extremely useful due to their proximity, studies based on these samples may be subject to small number statistics. Fortunately, there exist large collections of young stars, only slightly more distant, in nearby OB associations. OB associations contain members across the mass spectrum, typically from ∼10 $M_\odot$ through the substellar regime. Though the lower-mass (< 1.5 $M_\odot$) stars blend in with the Galactic field population and are therefore much more difficult to identify than the OB stars, they comprise the dominant stellar component of OB associations, typically present in the thousands (Briceño et al., 2007).

Scorpius-Centaurus (Sco-Cen), the nearest OB association, has been the subject of several efforts to identify its lower-mass population (e.g., de Zeeuw et al., 1999; Preibisch & Zinnecker, 1999; Mamajek et al., 2002; Rizzuto et al., 2011). Sco-Cen harbors a barely explored population of thousands of low-mass K and M-type stars (Preibisch & Mamajek, 2008). The association consists of three subregions: Upper Scorpius (US), Upper Centaurus-Lupus (UCL), and Lower Centaurus-Crux (LCC), with mean distances of 145 pc, 140 pc, and 118 pc, respectively (de Zeeuw et al., 1999). Though many K/M type members of US have been identified in surveys by Walter et al. (1994); Preibisch et al. (1998); Preibisch & Zinnecker (1999); Preibisch et al. (2001, 2002), UCL and LCC have received much less attention, with only ∼90 K/M stars identified in both subgroups, mostly in Mamajek et al. (2002), Preibisch & Mamajek (2008) and Song et al. (2012), though there have been some recent successes finding M-type members using the Galaxy Evolution Explorer (GALEX) data, with 17 new members discovered in Rodriguez et al. (2011).

In this study, we identify and characterize a new sample of K/M-type (∼0.6-1.2 $M_\odot$) members of Sco-Cen selected through their X-ray emission and proper motions. We describe the results of a low-resolution spectroscopic survey to identify

new low-mass K- and M-type members of Sco-Cen. We use these newly identified members, together with known members from existing surveys, to estimate the accretion disk fraction, and probe the star-formation history of each subgroup. Finally, we place these results in context with the results from other stellar populations.

4.2 Sample Selection

We aim to find new K- and M- type members of all three subgroups. Low-mass pre-main sequence stars are X-ray luminous, with $\log(L_x/L_{bol}) \gtrsim -4$, due to their strong magnetic dynamos and coronal emission (Feigelson & Montmerle, 1999). To build our candidate star list, we cross-referenced the PPMX proper-motion catalog (Röser et al., 2008) with X-ray sources within $40''$ in the ROSAT Bright Source (Voges et al., 1999) and Faint Source (Voges et al., 2000) catalogs. We restrict our search to the de Zeeuw et al. (1999) boundaries for Sco-Cen and adopt their proper motion limits with an extra 10 mas yr^{-1} to allow for larger proper motion uncertainties and possible kinematic sub-structure (at $\sim$140 pc, this translates to $\simeq 7\ km\ s^{-1}$). For US, UCL, and LCC this gives limits of $\mu < 47$ mas yr^{-1}, 12 mas yr^{-1}$< \mu <$ 55 mas yr^{-1}, and 15 mas yr^{-1}$< \mu <$ 55 mas yr^{-1}, respectively, with $\mu_\alpha <$ 10 mas yr^{-1} and $\mu_\delta <$ 30 mas yr^{-1} for all three subgroups. We also require that our proper motions have $\mu/\sigma_\mu > 2$ to avoid candidates with poorly constrained proper motions. The intrinsic J-K_S color of an unreddened K0V is 0.50 mag, and we aim to find low-mass K- or M-type members of Sco-Cen so we further make color-magnitude cuts, requiring our candidates to have color J-$K_S > 0.5$ and magnitude $7.0 <$ J $<$ 11.0 from the 2MASS Point Source Catalog (Skrutskie et al., 2006). We removed candidates located in UCL just below US, in $343 < l < 350$ and $0 < b < 10$ in galactic coordinates. This region overlaps with "Lower Sco", and will be discussed in

forthcoming papers (Mamajek et al., in prep.; Nguyen et al., in prep). This leaves us with 677 candidates (Table 4.4). Before assembling a list of targets for observation, we searched the literature to record those stars which had been studied in previous surveys from which spectral type, Li or Hα measurements were available in sufficient detail to make a membership determination. We then omitted stars which were studied in Mamajek et al. (2002), Preibisch et al. (1998), Preibisch et al. (2001), Preibisch et al. (2002), Ardila et al. (2000), Köhler et al. (2000), Slesnick et al. (2006), Krautter et al. (1997), Wichmann et al. (1997), Riaz et al. (2006), and Torres et al. (2006). This left us with 368 candidates in our spectroscopic target list. Objects PPMX J121431.8-511015, PPMX J134751.4-490148, PPMX J143751.3-545649, and PPMX J154348.8-392737 were not observed because they were within 60″ of known Sco-Cen members. However, they may constitute distant companions to previously known Sco-Cen members MML 9, MML 38, MML 47, and HD 140197, respectively.

4.3 Observations and Data

4.3.1 Spectra

Low-resolution red (∼5600Å–6900Å) optical spectra were obtained from the SMARTS 1.5m telescope at Cerro Tololo Inter-American Observatory(CTIO), Chile. Observations were made in queue mode with the RC spectrograph between July 2009 and October 2010, and in classical mode during the nights of UT 7-17 April 2010. The spectra were taken with the "47/Ib" setup, which consists of a grating with groove density of 831 grooves mm^{-1}, blaze wavelength 7100Å, a GG495 filter and a slit width of 110.5μm, giving a spectral resolution of ∼3.1 Å in the red optical. One comparison arc of Ne was taken immediately before three consecutive exposures of each target.

The data were reduced using the SMARTS RC Spectrograph IDL pipeline written by Fred Walter[1]. The three object images are median filtered, bias-trimmed, overscan- and bias-subtracted, and flat-fielded. The spectrum is wavelength-calibrated using the Neon comparison frames. Finally, we normalize the spectra to the continuum with a low order spline in preparation for spectral classification.

In addition, we reanalyzed the low resolution spectra from the Mamajek et al. (2002) study, provided to us by EEM. These blue and red spectra were taken at Sliding Springs Observatory in UT 20-24 April 2000. The blue spectra have spectral resolution of ∼2.8Å with spectral coverage of ∼3850-5400Å. The red spectra have spectral resolution of ∼1.3Å with spectral coverage of ∼6200-7150Å. Further details regarding these spectra are described in Mamajek et al. (2002).

4.3.2 Photometry

Our compiled photometry is listed in Table 4.4. Six of our candidates have BV photometry available from the *Hipparcos* catalog, and we adopted it where possible; for ∼130 candidates, we adopted BV photometry from the Tycho-2 Catalog (Høg et al., 2000), converted to the Johnson system using the conversions in Mamajek et al. (2002, 2006); for ∼350 candidates, we adopted BV photometry from the AAVSO Photometric All-Sky Survey[2] (APASS) Data Release 6 and Data Release 7 (Henden et al., 2012). and the Search for Associations Containing Young stars catalog (SACY; Torres et al., 2006) for ∼100 candidates. For stars with V$\lesssim$12 mag, conservative estimates for SACY photometric uncertainties are 0.01 mag (C.A.O. Torres, 2012 private communication). We adopt JHK$_S$ photometry from the Two Micron All-Sky Survey Point Source Catalog (2MASS; Skrutskie et al., 2006). We adopt 2MASS

[1]http://www.astro.sunysb.edu/fwalter/SMARTS/smarts_15msched.html#RCpipeline
[2]http://www.aavso.org/apass

aperture photometry when the PSF is poorly fit as indicated by the quality flags (qflg other than 'A').

For candidate members, we use mid-IR photometry from the Wide-field Infrared Survey Explorer (*WISE*; Wright et al., 2010). We visually examined all images of members which exhibit infrared excesses (identified in Section 4.4.9) in one or more WISE bands. We flagged photometry which could be affected by blends with adjacent objects, unresolved binaries, or extended emission from nearby bright stars. We exclude photometry with unreliable detections or uncertainties exceeding 0.25 mag. We followed the scheme for evaluating the photometry in Luhman & Mamajek (2012). Our mid-IR WISE photometry is listed in Table 4.8.

A few stars in our sample had WISE photometry contaminated by nearby objects. PDS 415 and CD-23 12840 is a $\sim$4″binary, with but only CD-23 12840 is in the PPMX catalog and thus only CD-23 12840 is in our sample. Both components of the pair are listed in the WISE All-Sky catalog but CD-23 12840 has $K_S - W1 < 0.0$. Examination of the WISE images shows the two are blended. PDS 415 is detected as an infrared source in the AKARI catalog (Ishihara et al., 2010) but CD-23 12840 is not detected. Thus we conclude that PDS 415 is the source of the infrared excess and the CD-23 12840 K_S band excess may be spurious. We exclude the CD-23 12840 WISE photometry. HD 326277 is a blended with a nearby object in $W1$ and $W2$ and had no reliable detection in $W3$ and $W4$. HD 326277 has *Spitzer* 3.6μm and 4.5μm IRAC photometry from the *GLIMPSE* survey ([3.6]=8.165$\pm$0.040 mag, [4.5]=8.178$\pm$0.044 mag; Churchwell et al. 2009) which differs from the WISE $W1$ and $W2$ by $\sim$0.5 mag. This suggests that the WISE photometry for this star is contaminated by blends and therefore we exclude the WISE photometry for HD 326277.

4.3.3 Astrometry

Although our original selection scheme utilized proper motion from the PPMX catalog, we adopt proper motions for our analysis from several catalogs, including the *Hipparcos* catalog (van Leeuwen, 2007), the Tycho-2 catalog (Høg et al., 2000), the PPMX catalog (Röser et al., 2008) and the UCAC4 catalog (Zacharias et al., 2013). We select the source catalog on a case-by-case basis, adopting the proper motions which have the smallest uncertainties, though the majority are from the UCAC4 catalog. Our adopted proper-motions are listed in Table 4.4.

4.4 Analysis

4.4.1 Spectral Classification

The optical spectra were visually classified against a grid of carefully chosen spectral standards[3] with spectral coverage from ∼5600Å–∼6900Å. We use the same spectral standards and classification criteria as described in Pecaut & Mamajek (2013). The G/K stars are on the classification system of Keenan & McNeil (1989) and the M-type stars are on the classification system of Kirkpatrick et al. (1991).

While estimating temperature types for our sample we ignored the Na I doublet at ∼5889/5896Å because it increases in strength with surface gravity and is thus useful in discriminating between dwarfs and giants. For those pre-main sequence (pre-MS) members of Sco–Cen, we expect these to have a Na I doublet line similar to but weaker than dwarfs (Spinrad, 1962; Schlieder et al., 2012a). Once a temperature type had been established, we compared the Na I doublet to that of a dwarf and a giant of the same temperature subclass, assigning an appropriate luminosity class. In a few cases

[3]see http://www.pas.rochester.edu/~emamajek/spt/

the star had a Na I doublet feature which closely resembled a giant (luminosity class III) but the relative strength of the Ca I at λ 6102, λ6122 and λ6162 lines relative to the Fe I line at λ6137 resembled that of a dwarf (luminosity class V). In these cases we assigned the intermediate luminosity class of a subgiant (luminosity class IV).

We also revised the spectral classifications for Sco-Cen members studied in Mamajek et al. (2002). We use the same spectral standards and classification criteria as described in Pecaut & Mamajek (2013). For the blue spectra, we use the depth of the Sr II λ4077 line as compared to neighboring Fe lines as the primary surface gravity indicator (e.g., Mamajek et al., 2002).

4.4.2 Distance Calculation

Very few of our candidate members have measured trigonometric parallaxes, so we estimate distances to each candidate by calculating a "kinematic" or "cluster" parallax (e.g., de Bruijne, 1999a). This method uses the centroid space motion of the group with the proper motion of the candidate member and the angular separation to the convergent point of the group. This method uses the proper motion of the candidate member and the space velocity of the group to estimate the distance to the individual member, with the assumption that they are co-moving. We emphasize that kinematic parallaxes are only meaningful for true members and meaningless for non-members. Kinematic parallaxes have been shown to reduce the scatter in the H-R diagram for cluster members over trigonometric parallaxes (de Bruijne, 1999b). We adopt the formalism and methods of Mamajek (2005) and adopt the updated Sco-Cen subgroup space motions listed in Chen et al. (2011). In addition to providing improved distance estimates over simply adopting the mean subgroup distances, the kinematic parallaxes allow us identify non-members and assess the likelihood that

the candidate member is a bona-fide member.

4.4.3 Membership Criteria

In order to identify likely members from our sample, we demand that all available data paint a consistent picture of association membership, and therefore consider several indicators to discriminate against interlopers. Based on previous surveys (see Preibisch & Mamajek, 2008, and references therein), we expect the K and M-type stars to be pre-MS, and therefore have Li absorption above that of a ∼30-50 Myr population, and have surface gravities intermediate between dwarfs and giants. We identify those stars which have

1. Appropriate levels of Li absorption in their spectra, using the Li 6708Å line
2. Dwarf or subgiant surface gravities, using the Na I doublet at 5889/5896Å
3. Kinematic distances consistent with Sco–Cen
4. "Reasonable" H-R diagram positions ("reasonable" to be defined below)

Obviously we do not want to inadvertently bias our membership selection, so we discuss these criteria in turn.

Lithium

Stars that develop convective envelopes on the main sequence mix Li from the stellar photosphere throughout the convection zone down to interior regions of the star where it is destroyed at ∼2.5 MK. Thus, for these stars, a large photospheric Li abundance is only present when the star is very young. Based on the published nuclear and pre-main sequence ages (de Geus et al., 1989; Preibisch & Zinnecker, 1999; Mamajek

et al., 2002; Pecaut et al., 2012), we expect members of Sco-Cen to exhibit stronger Li absorption lines at a given T_{eff}, within some acceptable scatter, than a ∼30-50 Myr sample.

We measured the equivalent width of the λ6708Å Li feature for all stars in our spectroscopic sample. The λ6708 feature is a blend with a nearby Fe I line at λ6707.44Å, unresolved at our resolution, and thus our EW(Li) values are probably overestimated by ∼0.02Å. However, this is smaller than our uncertainties, so we do not attempt to correct for this blend. The values were measured with IRAF[4] with Vogt profiles after the spectrum was normalized to the continuum. Given our spectral resolution and the repeatability of our measurements, we estimate that our reported EW(Li) values are accurate to ∼0.05Å. Many stars in our parent sample were not observed because they had EW(Li) values available in the literature; for these stars we simply adopted the previously published values.

We compare our EW(Li) measurements at a given T_{eff} to those in nearby open clusters. Figure 4.1 we plot T_{eff} versus EW(Li) for our sample along with data for the young open clusters IC 2602 (Randich et al., 1997) and the Pleiades (Soderblom et al., 1993; Jones et al., 1996). Most stars in our sample exhibit much larger EW(Li) at a given T_{eff} than either IC 2602 (∼45 Myr; Dobbie et al. 2010) or the Pleiades (∼125 Myr; Stauffer et al. 1998). We fit low-order polynomials to the IC 2602 and Pleiades T_{eff} versus EW(Li) data. For our Li-based membership criterion, if the EW(Li) was above the polynomial fit to IC 2602 we marked that star as 'Y' in Table 4.5; if EW(Li) was below the IC 2602 polynomial fit but above the Pleiades polynomial fit, we marked it as 'Y?', and if the EW(Li) is below the Pleiades polynomial fit we marked it as 'N'. Stars studied in Preibisch & Zinnecker (1999), Köhler et al.

[4]IRAF is distributed by the National Optical Astronomy Observatory, which is operated by the Association of Universities for Research in Astronomy (AURA) under cooperative agreement with the National Science Foundation.

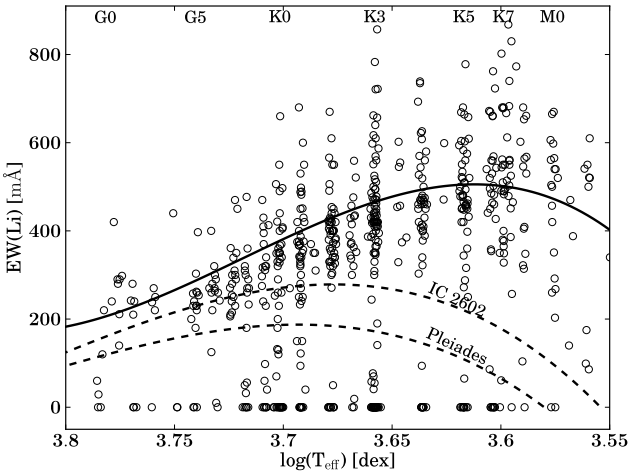

Figure 4.1 Measured EW(Li) from the 6708Å line plotted against $\log(T_{\rm eff})$ for our X-ray sample. Plotted are polynomial fits to data from surveys in IC 2602 (Randich et al., 1997) and the Pleiades (Soderblom et al., 1993; Jones et al., 1996). The location of the EW(Li) for our Sco-Cen candidate members is used to determine the membership indicator in Table 4.5. Those above the IC 2602 curve are marked "Y", those above the Pleiades curve are marked "Y?", while candidates below the Pleiades are marked "N". The solid curve is a polynomial fit to the Sco-Cen candidates marked "Y".

(2000) and Krautter et al. (1997) were confirmed as Li-rich but the measurements were not reported. We marked these candidates as 'Y' in Table 4.5.

Surface Gravity

Based on previous nuclear and pre-MS age determinations of the subgroups of Sco–Cen (Mamajek et al., 2002; Pecaut et al., 2012), the low-mass stars in Sco-Cen are expected to be pre-main sequence and therefore should have surface gravities intermediate between dwarfs and giants. For candidates in our spectroscopic sample we can examine spectral features sensitive to surface gravity, primarily the Na I doublet at 5889Å/5896Å. Details on using Na I as a surface gravity indicator for identifying young stars is discussed in detail in Schlieder et al. (2012a). The Na I doublet

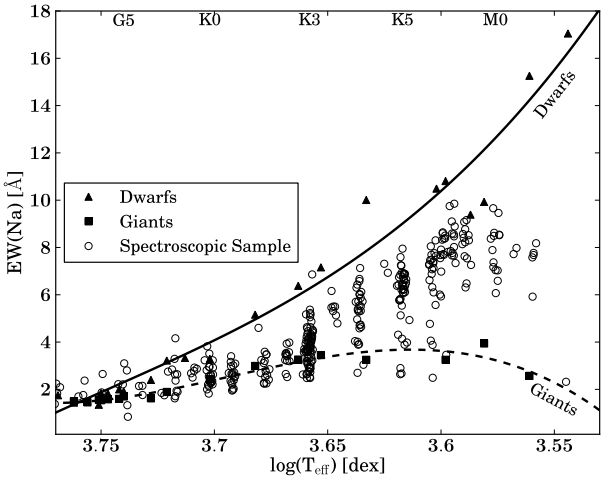

Figure 4.2 Measured EW(Na) from the 6708Å line plotted against $\log(T_{eff})$for our spectroscopic sample. Plotted are polynomial fits to dwarf and giant spectral standard stars used for classification.

decreases in strength at a given T_{eff} as surface gravity decreases. However, the observed strength of the Na I doublet in subgiants among G-type stars is difficult to distinguish from dwarfs. The differences in the Na I doublet strength between dwarfs and subgiants becomes more useful in mid-K-type spectra, as shown in Figure 4.2. For this reason we are fairly conservative in our surface gravity membership criterion, marking G-type stars with luminosity classes of 'IV' with 'Y', 'V' with 'Y?' and 'III' with 'N'. Note that we only use this criterion for stars which we have observed spectroscopically; luminosity classifications from other authors for stars in our parent sample are not used for this criterion.

Distances

As mentioned previously, the majority of our sample lacks trigonometric distance estimates. However, if we calculate a kinematic parallax estimate using the best available proper motion, we can then estimate distances for each star in our sample and verify

that this lies within the range of expected distances for the association and identify stars with discrepant kinematic distances as non-members. We use the results of the recent membership study of Rizzuto et al. (2011), which makes use of the revised *Hipparcos* trigonometric parallaxes (van Leeuwen, 2007), to establish our distance criteria. Rizzuto et al. (2011) concluded that there is no non-arbitrary boundary separating the subgroups, based on the spatial distribution of their candidate members, therefore we do not use distinct kinematic distance criteria for each subgroup. We fit a plane to the B-type members with membership probabilities >50% from the Rizzuto et al. (2011) study, obtaining:

$$\begin{aligned} \pi &= (-0.02081 \pm 0.0061) \times (l - < l >) \\ &\quad +(-0.02993 \pm 0.015845) \times (b - < b >) \\ &\quad +(7.77608 \pm 0.09689), \end{aligned}$$

with $< l >= 328.579030$, $< b >= 13.261621$, The 1σ dispersion in the fit is $\sigma_\pi \simeq 1.25\ mas$. Therefore we model the shape of Sco-Cen with a continuous plane and depth characterized by 1σ dispersion of $\sim$1.25 mas. For our kinematic distance criteria, we mark stars with 'Y' in Table 4.5 if their kinematic parallaxes are within the 2σ (95% C.L.) dispersion from the plane described above, and 'Y?' if they are between 2σ and 3σ. We mark stars with 'N' if they are beyond 3σ of the dispersion from the plane. This criteria effectively provides different distance limits as a function of galactic longitude and latitude, giving typical 2σ distance limits of 141^{+77}_{-37} pc, 130^{+62}_{-32} pc, and 117^{+49}_{-27} pc for US, UCL and LCC, respectively.

HRD position

As a final membership check, we place these stars on the H-R diagram using their kinematic distances, which, for this purpose, *assumes* they are co-moving with other members in the association. Objects that have H-R diagram positions inconsistent with membership, e.g., below the main sequence, are rejected. Below we discuss the few stars which were Li-rich and fell inside our kinematic distance criteria but were rejected because they had discrepant H-R diagram positions. Further analysis can be found in Section 4.4.5.

US Interlopers

HD 144610 is a Li-rich K1IV-III that has a kinematic parallax of $\pi_{\rm kin}$=3.41±0.69 mas which is consistent with a H-R diagram position of log($T_{\rm eff}$)=3.70±0.01, log($L/L_{\odot}$)=1.42±0.18, well above the 1 Myr isochrone, so we reject it.

UCL Interlopers

2MASS J14301461-4520277 is a Li-rich K3IV(e) which, using the kinematic parallax of $\pi_{\rm kin} = 10.92 \pm 0.92$ mas, has an H-R diagram position well below the main sequence (log($T_{\rm eff}$)=3.66±0.02, log($L/L_{\odot}$)=-0.91±0.08), so we reject it. 2MASS J16100321-5026121 is a Li-rich K0III (Torres et al., 2006) which lies well above the 1 Myr isochrone (log($T_{\rm eff}$)=3.70±0.01, log($L/L_{\odot}$)=1.16±0.08), calculated using the kinematic parallax of $\pi_{\rm kin} = 4.19 \pm 0.38$ mas, so we reject it.

LCC Interlopers

2MASS J10111521-6620282, lies well below the main sequence, with log($T_{\rm eff}$)=3.70±0.01, log($L/L_{\odot}$)=-0.86±0.09, calculated using the predicted kinematic parallax of

$\pi_{\rm kin}$=9.63±0.94 mas. This is puzzling because it is a Li-rich K0IV, with a proper motion in excellent agreement with membership in LCC. However, it is ∼0.4 dex underluminious for the main sequence, so we reject it.

Final Membership Assessment

Though we require the Li, surface gravity indicators, kinematic distance criterion, and H-R diagram criterion to indicate membership, the Li and kinematic distance criteria are the most restrictive and are responsible for identifying most non-members. Though we have made every effort to remove interlopers, our list of candidate members may still contain a few non-members, though it will be dominated by true members. From our current sample, we identify 493 stars as likely members, listed in Table 4.6. The 180 stars rejected as Sco-Cen members are listed in Table 4.7. 158 are newly identified young stars.

4.4.4 Extinction

We estimate the reddening and extinction for Sco-Cen members using the spectral type-intrinsic color sequence for pre-MS stars described in Pecaut & Mamajek (2013). These intrinsic colors are calibrated using low-mass members of nearby moving groups which have negligible extinction, and bracket the age range of the Sco-Cen subgroups (5-30 Myr). Many of the stars in our sample had very low extinction, and where we obtained a non-physical negative extinction we set the extinction to zero. We used a total-to-selective extinction of R_V=3.1 and calculated E(B-V), E(V-J), E(V-H), and E(V-K_S) with A_J/A_V=0.27, A_H/A_V=0.17, A_{K_S}/A_V=0.11 (Fiorucci & Munari, 2003) which allowed us to estimate extinctions to each star individually using as many as four different colors. We adopted the median A_V with the standard deviation as our

uncertainty. For the stars which lack reliable V band photometry, we estimate their extinctions using E(J-K_S). Our extinction estimates are listed in Table 4.6.

4.4.5 H-R Diagram for Sco-Cen Members

We place our Sco-Cen members on a theoretical H-R diagram in order to compare with theoretical models and obtain individual isochronal age estimates. We adopt the effective temperature scale ($T_{\rm eff}$) and bolometric correction (BC_V) scale from the Pecaut & Mamajek (2013) study, which was constructed for specifically for 5-30 Myr old pre-MS stars. This $T_{\rm eff}$ and BC_V scale was derived by fitting the spectral energy distributions of members of young, nearby moving groups to the BT-Settl theoretical atmospheric models (Allard et al., 2012). Though this $T_{\rm eff}$ and BC scale is dependent on model atmospheres, the method used to develop the resultant $T_{\rm eff}$ scale is in good agreement with $T_{\rm eff}$ values derived from angular diameter measurements (e.g., Boyajian et al., 2012b). We combine our individual extinction estimates together with our kinematic parallaxes and 2MASS J-band magnitudes to estimate the bolometric luminosities of our stars and place them on a theoretical H-R diagram. We compare our data to the pre-MS models of Dotter et al. (2008) in Figure 4.3.

There is considerable scatter in the H-R diagram so we construct empirical isochrones by plotting the median luminosity along the H-R diagram. Though there is some scatter, the relative age rank of the three groups is consistent with that found in Mamajek et al. (2002), Preibisch & Mamajek (2008), Pecaut et al. (2012); from oldest to youngest: LCC, UCL and US, with UCL and LCC approximately coeval. The other striking feature of the empirical isochrones is the mass-dependent age trend. The lower mass stars appear younger against the theoretical isochrones than the higher mass stars. This is the same mass-dependent age trend seen in other studies

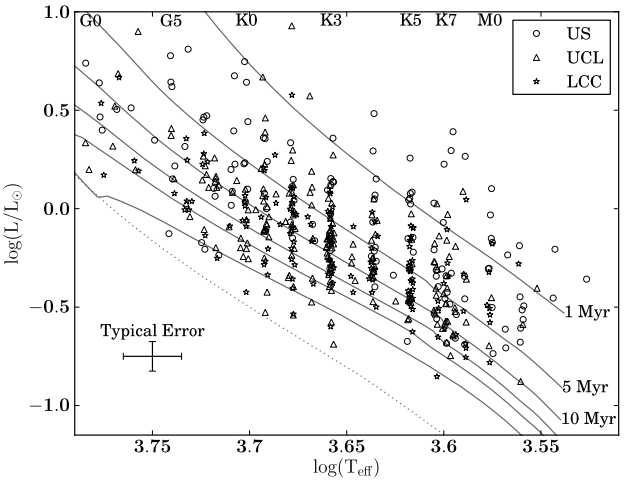

Figure 4.3 H-R diagram for X-ray selected Sco-Cen members with J–$K_S > 0.50$ as described in the text. Circles, triangles and star symbols are US, UCL and LCC candidate members, respectively. Plotted for comparison are 5, 10, 15, 20 and 30 Myr isochrones from Dotter et al. (2008). Artificial scatter of $\delta T_{\rm eff}$=±0.001 dex has been introduced for plotting purposes.

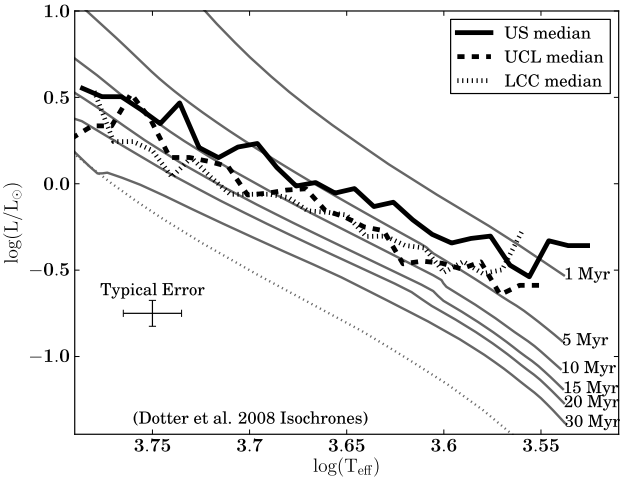

Figure 4.4 H-R diagram with empirical isochrones for US (solid), UCL (dashed) and LCC (dotted). All three subgroups exhibit a mass-dependent age trend.

(e.g., Hillenbrand et al., 2008). At an age of 10 Myr and 15 Myr, our observational uncertainties yield individual age uncertainties of ±3 Myr and ±4 Myr, respectively.

4.4.6 Ages

Pre-MS Ages

We estimate individual ages for our Sco-Cen members by linearly interpolating between isochrones for the theoretical models of Tognelli et al. (2011), Dotter et al. (2008), Siess et al. (2000), and Baraffe et al. (1998). The Pisa evolutionary models (Tognelli et al., 2011) adopt the Asplund et al. (2005) solar composition with a He fraction of Y=0.2533, while the Dartmouth evolutionary models (Dotter et al., 2008) adopt the Grevesse & Sauval (1998) solar composition with a He fraction of Y=0.2740. The Grenoble models (Siess et al., 2000) and the Lyon models (Baraffe et al., 1998) both adopt the Grevesse & Noels (1993) solar abundances, but use different He fractions of Y=0.277 and Y=0.282, respectively. The distributions of ages we obtain with the Dotter et al. (2008) evolutionary models is shown in Figure 4.5. We obtain median ages of 5±2 Myr, 9±1 Myr and 8±1 Myr (standard error of the mean) for US, UCL and LCC, respectively. Surprisingly, these ages are half the mean ages obtained from the F-type members of Sco-Cen (Pecaut et al., 2012). Given the large T_{eff}-dependent trend with age (Figure 4.4), we avoid adopting mean subgroup ages based on the K- and M-type members of Sco-Cen.

In order to extract useful age estimates for the subgroups, we re-examine the G-type pre-MS ages as well as the main-sequence turn-off ages. We do this for two reasons, other than the obvious desire to quote reliable mean ages. The first reason is that estimating realistic intrinsic age spreads requires a reliable age as free of systematic uncertainties as possible. We use Monte Carlo simulations to constrain our

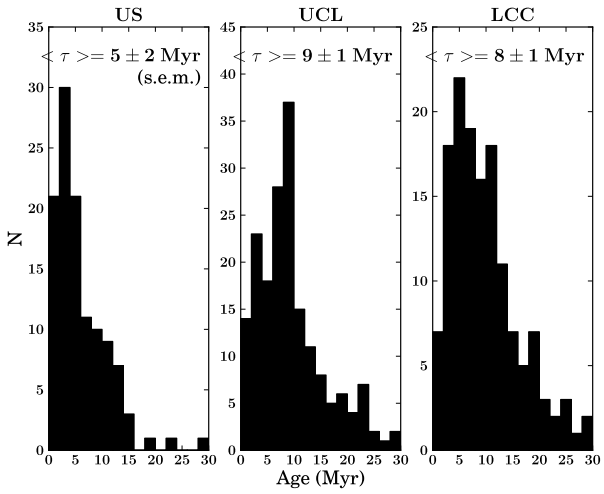

Figure 4.5 Distribution of ages obtained for the Sco-Cen members of our sample using the Dotter et al. (2008) evolutionary models.

intrinsic age spreads, taking into account realistic binarity statistics and observational uncertainties, the details of which are described in Section 4.4.7. Because isochrones evenly spaced in age will not generally be evenly spaced in luminosity, a large intrinsic spread in luminosity at a young age could still be consistent with a small age spread, whereas the same intrinsic spread in luminosity at an older age would imply a larger intrinsic age spread. The second reason we reevaluate the G-type ages and nuclear ages is that updated T_{eff} and bolometric corrections (BCs) have been made available since the ages were last estimated in Mamajek et al. (2002). Nieva (2013) used modern non-local thermodynamic equilibrium (NLTE) spectral synthesis models to re-evaluate the T_{eff} and BC scale for the massive OB stars (34,000 K > T_{eff}> 15,800 K). Their results for dwarfs and subgiants are 1500-6000 K hotter than the scale of Napiwotzki et al. (1993). As previously mentioned, Pecaut & Mamajek (2013) have constructed an updated T_{eff} and BC scale applicable to the Sco-Cen G-type stars. Both of these studies should allow us to place Sco-Cen members on the

H-R diagram with reduced systematic uncertainties.

G-type Ages

To estimate the ages of the G-type pre-MS stars, we collect the G-type members from this study together with those in Walter et al. (1994), Preibisch & Zinnecker (1999), Mamajek et al. (2002), and Preibisch & Mamajek (2008). We supplement this with G-type stars studied in Torres et al. (2006) in the Sco-Cen field which are Li-rich and have proper motions consistent with membership. The stellar properties for these stars are listed in Table 4.6 and Table 4.10, together with the median mass and age obtained through a comparison of their H-R diagram positions with the evolutionary models of Tognelli et al. (2011), Dotter et al. (2008), Siess et al. (2000), and Baraffe et al. (1998).

Turn-off Ages

To estimate nuclear ages, we collect membership lists for the most massive stars from de Zeeuw et al. (1999), Mamajek et al. (2002), Rizzuto et al. (2011) and Pecaut et al. (2012). We collect Strömgren $ubvy\beta$ and Johnson UBV photometry from Hauck & Mermilliod (1998) and Mermilliod & Mermilliod (1994). We estimate the extinction towards each early B-type member with both the Q-method (Johnson & Morgan 1953; updated in Pecaut & Mamajek 2013) using Johnson UBV photometry, and the prescription of Shobbrook (1983), using Strömgren $ubvy\beta$ photometry. For all the massive stars these two methods give similar A_V within the uncertainties, so we adopt the mean value. We calculate the $T_{\rm eff}$ and BC_V for each star using the calibrations with Q, $[u-b]$, $[c1]$ and β in Nieva (2013); we adopt the median $T_{\rm eff}$ when available. We note that the calibrations derived by Nieva (2013) give systematically hotter $T_{\rm eff}$ than the calibrations of Napiwotzki et al. (1993) and Balona (1994), which were used

in Mamajek et al. (2002) and Pecaut et al. (2012), respectively, in the most recent estimation of Sco-Cen nuclear ages. Because of this we expect to obtain slightly younger ages than previously estimated.

Our stellar parameters for the main-sequence turn-off in Sco-Cen are listed in Table 4.9, along with an individual age estimate of each object from a comparison the rotating tracks of Ekström et al. (2012), rotating at $v_{eq} = 0.4v_{crit}$, with the H-R diagram position of the stars. A plot of the main-sequence turnoff for all three subgroups is shown in Figure 4.6. To estimate the turnoff age of Upper Sco we use τ Sco, ω Sco, σ Sco, β^1 Sco, π Sco, and δ Sco. We obtain a median turn-off age for US of $\sim$7 Myr. For Upper Centaurus-Lupus, we use μ Cen, δ Lup, α Lup, μ^1 Sco, μ^2 Sco, β Lup, γ Lup, ν Cen, η Cen, η Lup, ϕ Cen, ϵ Lup, κ Cen, and HR 6143. We obtain a median age for UCL of $\sim$19 Myr. For Lower Centaurus-Crux, we use α^1 Cru, β Cru, β Cen, δ Cru and α Mus. We obtain a median age of $\sim$11 Myr. Note that these are all in the southern part of LCC, for which Preibisch & Mamajek (2008) estimated $\sim$12 Myr. There are no turnoff stars in the northern part of LCC. Our nuclear median subgroup ages are summarized in Table 4.1.

We summarize our derived nuclear, F-type pre-MS and G-type pre-MS ages in Table 4.1 with our adopted values for each subregion.

4.4.7 Intrinsic Age Spreads

When placing members of Sco-Cen on an H-R diagram, there is a large degree of scatter in the H-R diagram positions and therefore an apparent scatter in the ages inferred. Some of this scatter is due to observational uncertainties, but some scatter may be due to true age spreads within the subgroups. Previous studies have found very small intrinsic age spreads in US, but larger age spreads in UCL and

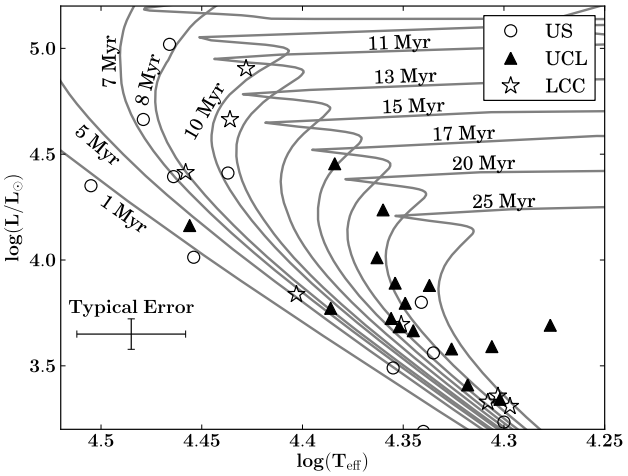

Figure 4.6 Theoretical H-R diagram for the upper main sequence members of Sco-Cen with isochrones from the rotating evolutionary models of Ekström et al. (2012) with solar metallicity.

Table 4.1. Adopted Subgroup Ages

Method	US	UCL	LCC
MS Turnoff	7±2	19±2	11±2
G-Type Pre-MS	10±1	14±1	16±1
F-Type Pre-MS	14±1	16±1	18±2
Adopted	10±3	16±2	16±3

Note. — Uncertainties reported above are the standard error of the mean which represents the uncertainty in how well the mean value is characterized; these numbers do not represent the spread in ages. Median ages are derived considering the B-type main-sequence turn-off, the F-type pre-MS turn-on and the pre-MS G-type stars in each subgroup.

LCC (Preibisch et al., 2002; Slesnick et al., 2006; Mamajek et al., 2002; Preibisch & Mamajek, 2008; Pecaut & Mamajek, 2013). We perform Monte Carlo simulations in order to model the scatter caused by the observational uncertainties, the effects of unresolved binarity, and an intrinsic age spread. We create population of 10^4 simulated members with a distribution of ages, assuming a Kroupa (2001) initial mass function (IMF), a multiplicity fraction of 0.44 and companion mass ratio distribution given by a flat power law distribution with γ=0.3 (using multiplicity properties for $0.7\,M_{\odot} \lesssim M_{*} \lesssim 1.3\,M_{\odot}$ population I main sequence stars as summarized in Duchêne & Kraus 2013 and Raghavan et al. 2010). We then introduce dispersion in their H-R diagram positions with the median observational uncertainties from our sample. This is designed to simulate a population with a given mean age, an intrinsic age spread, and the effects of unresolved binarity and observational uncertainties. Following Hillenbrand et al. (2008), we compare the the observed luminosity spreads around the empirical isochrones in Sco-Cen members to the simulated luminosity spreads. We emphasize that in this comparison, we only compare the distributions of luminosities around the median. We do not compare the median ages obtained since we observe a mass-dependent age trend. However, unlike Hillenbrand et al. (2008), we only model star formation with a given mean age and intrinsic (Gaussian) spread, rather than consider accelerating star formation or other distributions of ages. We perform a two-sample Kolmogorov-Smirnov test against all of our simulations, and adopt the age spread which best matches the simulated luminosity spreads for each Sco-Cen subgroup. We adopted the median subgroup ages listed in Table 4.1 as the mean age of our simulated populations to compare the luminosity spreads in our simulations to those from our observations. We adopt 1 σ Gaussian age spreads of $\pm$6 Myr, $\pm$5 Myr and $\pm$6 Myr for US, UCL and LCC, respectively. A plot showing the best matches to the observed luminosity spreads is shown in Figure 4.7. Our results are summarized

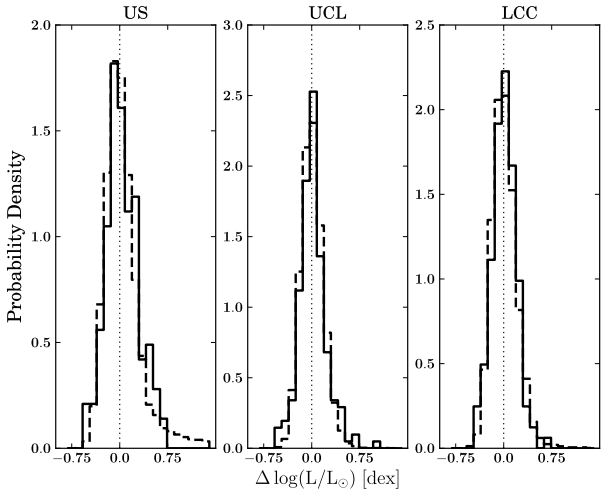

Figure 4.7 Observed luminosity spreads around the empirical isochrone (solid line) compared with the same for a simulated population (dashed line). The simulations used mean ages of 10 Myr, 16 Myr and 16 Myr for US, UCL, and LCC, respectively. We obtained best-fit intrinsic age spreads of ±6 Myr, ±5 Myr, ±6 Myr for US, UCL and LCC, shown above with simulations made with the Baraffe et al. (1998) evolutionary models.

in Table 4.2.

4.4.8 Spatial Variation of Ages

Blaauw (1964a) divided Sco-Cen into the subgroups Upper Scorpius, Upper Centaurus-Lupus and Lower Centaurus Crux. US has consistently been shown to be younger than the other two subgroups, and UCL and LCC have typically been assigned similar ages (Preibisch & Mamajek, 2008; Mamajek et al., 2002; Pecaut et al., 2012). Given the large spatial extent of UCL and LCC, however, it may be too simplistic to place them into two groups, each characterized by a single mean age. Here we attempt to examine the age structure of the entire association to discern if we see evidence for spatial substructure based on systematic differences in age as a function of position on the sky.

Table 4.2. Subregion Intrinsic Age Spreads

Evolutionary Models	US (10 Myr)	UCL (16 Myr)	LCC (16 Myr)
Pisa (Tognelli et al., 2011)	±7	±5	±5
Dartmouth (Dotter et al., 2008)	±6	±6	±6
Grenoble (Siess et al., 2000)	±7	±1	±1
Lyon (Baraffe et al., 1998)	±6	±5	±6
Adopted Intrinsic Age Spreads	±6	±5	±6

Note. — Adopted median ages listed in Table 4.1. Age spreads were estimated comparing observed luminosity spreads to simulated populations with a given intrinsic age spread, taking into account multiplicity and observational uncertainties.

One possible method to investigate spatial variations of ages would be to simply evaluate the age of each member against pre-MS evolutionary tracks and spatially average their ages to create an age map. However, given the strong mass-dependent age trend we find with all the evolutionary tracks, this would tend to show regions with large numbers of low-mass stars as younger regions, when in fact this may be a systematic effect due to the evolutionary tracks. As a result of this bias, we do not use this method. To probe for statistically significant spatial variations of ages, *independent* of any evolutionary tracks, we use all the pre-MS members of all three subgroups which have been studied spectroscopically. We place all stars from all subgroups together on the H-R diagram and construct an empirical isochrone, by evaluating the median luminosity as a function of $T_{\rm eff}$. This is plotted in Figure 4.8. We then spatially average their *offset* above or below the median luminosity, as a function $T_{\rm eff}$, in galactic coordinates shown in Figure 4.9. Regions which are systematically younger than the average of the association will lie systematically above the empirical isochrone and will appear on the age map as more luminous regions. Likewise, older regions will tend to be less luminous on average than the average of the association.

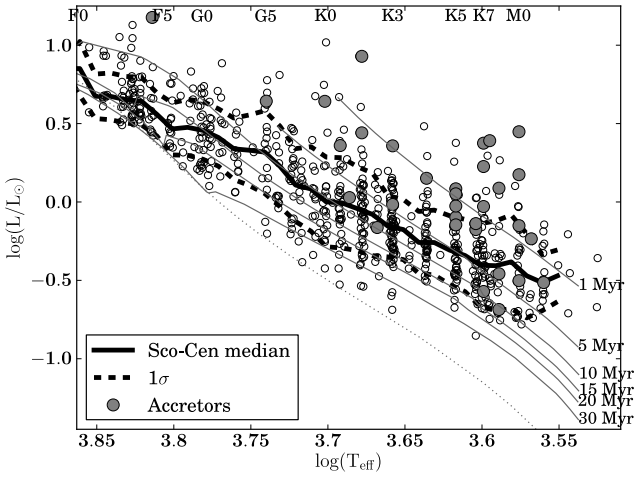

Figure 4.8 Empirical isochrone for 663 F/G/K-type members of all subgroups of Sco-Cen. The empirical isochrone is calculated by evaluating the median luminosity in a $\Delta\log(T_{eff})$=0.025 dex window spaced every 0.010 dex in $\log(T_{eff})$. We use individual stars' offsets from this empirical isochrone to create a relative age map, shown in Figure 4.9.

This method avoids biases due to any mass-dependent age trends. In Figure 4.9, we plot spatial contours of the median offset from empirical isochrone in units of σ. In order to anchor the regions shown on the map to ages, we use the F5 through G0 stars to map the contours to age. So the age map makes use of 662 F-M pre-MS stars to establish relative ages from the mean Sco-Cen empirical isochrone, but the ages are adopted from the F5-G0 stars. We discuss our motivations for adopting the F- and G- type ages in Section 4.5.1.

4.4.9 Circumstellar Disks

Spectroscopic Accretion Disk Fraction

Giant planet formation is fundamentally limited by the lifetimes of gas-rich protoplanetary disks surrounding the host star. The gas disk dissipation timescale therefore

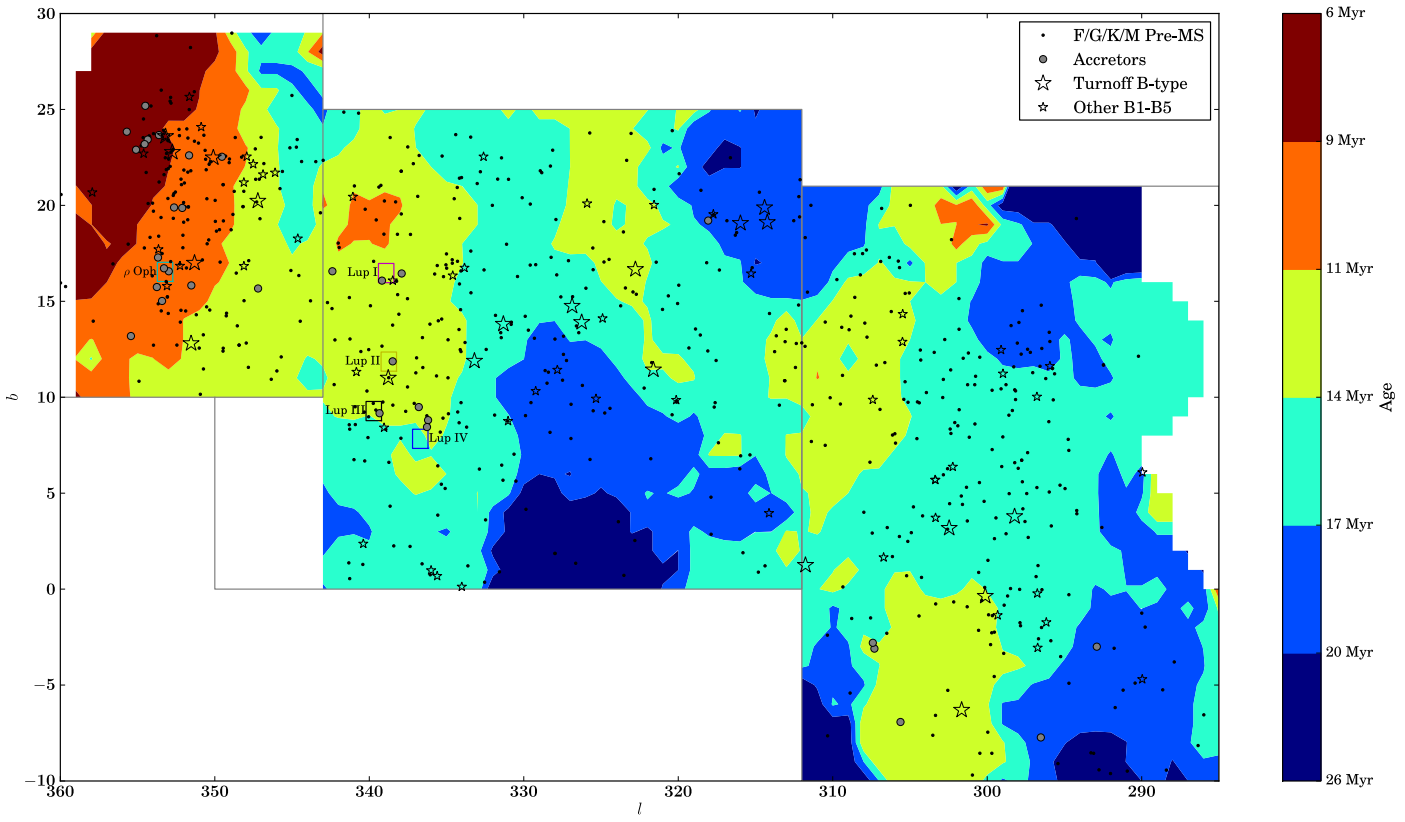

Figure 4.9 Spatial distribution of 662 F/G/K/M-type pre-MS members (solid dots) with spatial age contours. The contours are created by evaluating the median luminosity offset relative to the luminosity uncertainties ($<\log(L/L_{\odot})> - \log(L/L_{\odot}))/\sigma_{\log(L/L_{\odot})}$ of stars in a 5° radius each (l, b). These contour bins are then mapped to ages using the F5 through G9 stars that fall in those bins.

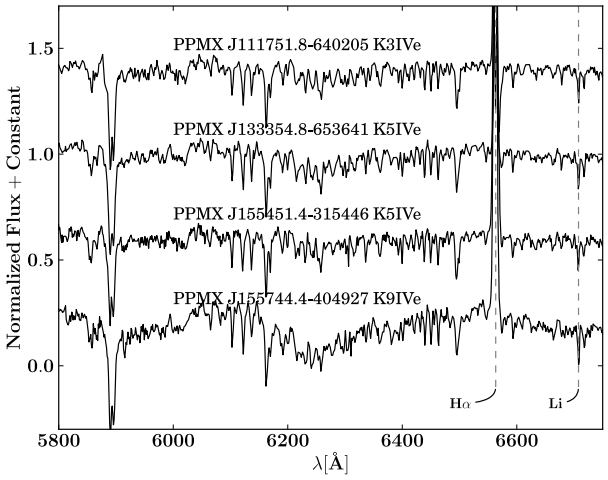

Figure 4.10 Representative spectra of Sco-Cen members with large Hα in emission consistent with accretion.

provides an upper limit to the giant planet formation timescale. Differences in disk dissipation timescales for stars in different mass bins can provides critical data for inferring how the planet formation process differs around stars of various masses. Additionally, a census for gas-rich circumstellar disks allows for follow–up studies of the gas disk itself (e.g., Zhang et al., 2013) or the star–disk interaction (e.g., Bouvier et al., 2007; Nguyen et al., 2009).

Here we use perform a census of accretion disks for our sample using Hα emission as an accretion diagnostic. Various criterion have been proposed using Hα as an accretion indicator, and we adopt the spectral type dependent empirical criterion of Barrado y Navascués & Martín (2003). If our measured or adopted EW(Hα) (see Table 4.6) exceeds the Barrado y Navascués & Martín (2003) criterion, we count the object as an accretor. Our accretion disk fraction excludes the 28 Sco-Cen members in our sample which lack Hα measurements. Sample spectra for Sco-Cen members with Hα in emission consistent with accretion are shown in Figure 4.10.

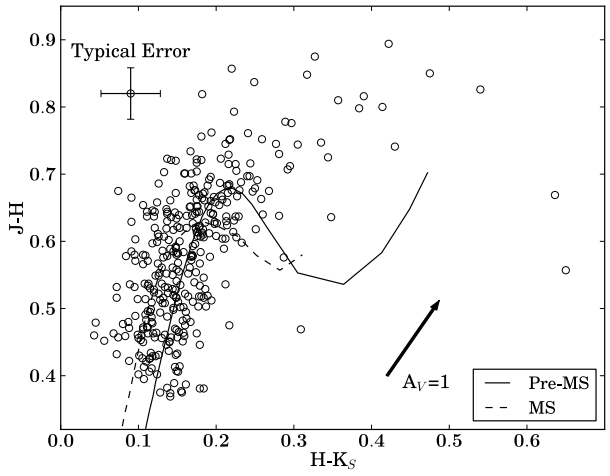

Figure 4.11 H–K_S versus J–H for final candidate members of Sco-Cen. The dwarf and pre-MS stellar locus from Pecaut & Mamajek (2013) are included shown as the dashed and solid lines, respectively.

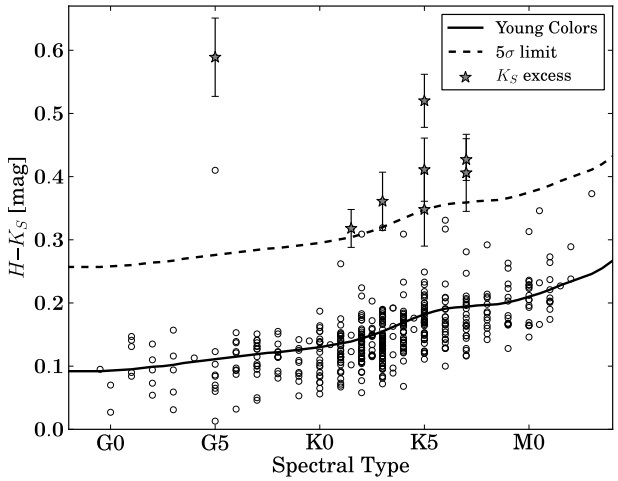

Figure 4.12 Spectral type versus dereddened H–K_S color for Sco-Cen members. The solid line is the pre-MS photospheric colors from Pecaut & Mamajek (2013). The dashed line is the 5σ dispersion in the photospheric colors. Members with color excesses above the 5σ dispersion in the photospheric colors in this and all bands at longer wavelength are identified as having a K_S band excess (gray stars).

Using the Barrado y Navascués & Martín (2003) criteria, we identified 10/108 accretors in US, or a spectroscopic accretion disk fraction of $9.3^{+3.6}_{-2.1}$%. In UCL and LCC we have 5/154 and 4/127 accretors, or spectroscopic accretion disk fractions of $3.2^{+2.1}_{-0.9}$% and $3.1^{+2.4}_{-0.9}$%, respectively. These disk fractions include all K and M-type members in our sample with EW(Hα) measurements; for statistics on the K-type members *only*, refer to Table 4.3.

2MASS and WISE Infrared Excesses

Infrared photometry can be used to identify the presence of circumstellar matter with different wavelengths used to probe matter at different temperatures. To probe cooler, dusty debris around young stars, 20μm and longer wavelengths are useful. We examine Sco-Cen members for excesses in H–K_S, K_S–$W1$, K_S–$W2$, K_S–$W3$, and K_S–$W4$ colors, shown in Figures 4.12 and 4.14, in order to identify Sco-Cen members exhibiting IR excesses which may indicate the presence of a disk and allow us to infer it's evolutionary state. These stars are also plotted against Hα equivalent width (EW(Hα)) in Figure 4.13, demonstrating that accreting stars identified with the Barrado y Navascués & Martín (2003) EW(Hα) criteria also typically exhibit a $W1$ band excess due to the presence of a warm circumstellar gas disk. We identify stars above the 5σ dispersion in the young stellar locus, as defined in Pecaut & Mamajek (2013), as having an excess in that band. To avoid reporting false excesses due to scatter in the photometry, we only report an infrared excess if that object is also above the 5σ dispersion in the young stellar locus for that band *and* all bands at longer wavelengths.

Disks in young populations such as Sco-Cen may be found in a variety of stages of evolution. Here we attempt to classify the disks into the disk classification scheme described by Espaillat et al. (2012), using the observational criteria described by

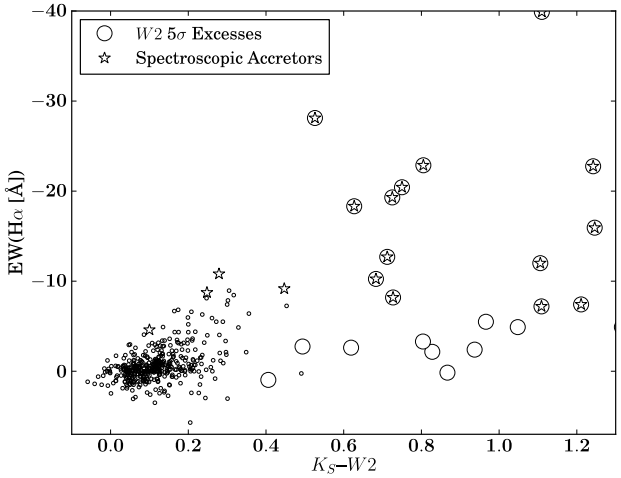

Figure 4.13 K_S–$W2$ versus EW(Hα) for Sco-Cen members. Members spectroscopically identified as accretors with the Barrado y Navascués & Martín (2003) criteria are shown as stars. Members exhibiting a K_S–$W2$ color excess are shown as large circle.

Luhman & Mamajek (2012). Based on the boundary between the full disks and transitional, evolved and debris disks for the stars classified in Luhman & Mamajek (2012), we identify "full disks" as those with E(K_S–$W3$) > 1.5 and E(K_S–$W4$) > 3.2, "transitional disks" as those with E(K_S–$W4$) > 3.2 but have E(K_S–$W3$) < 1.5. We then identify "evolved disks" as those with E(K_S–$W4$) > 3.2 and E(K_S–$W3$) > 0.5 and "debris disks" as those with E(K_S–$W4$) < 3.2 and E(K_S–$W3$) < 0.5. Color excesses and classifications are shown in Figure 4.15. Four stars had excesses in $W1$, $W2$ or $W3$ but no reliable $W4$. We classify them as evolved or debris disks based on their lack of spectroscopic signatures of accretion and their E(K_S–$W2$) and E(K_S–$W3$).

Disks classified using this method are listed in Table 4.8. Our sample contains a small number of G- and M-type members of Sco-Cen. Therefore we only report infrared excess fractions for K-type ($\sim$0.7-1.2 $M_\odot$) Sco-Cen members in the 2MASS

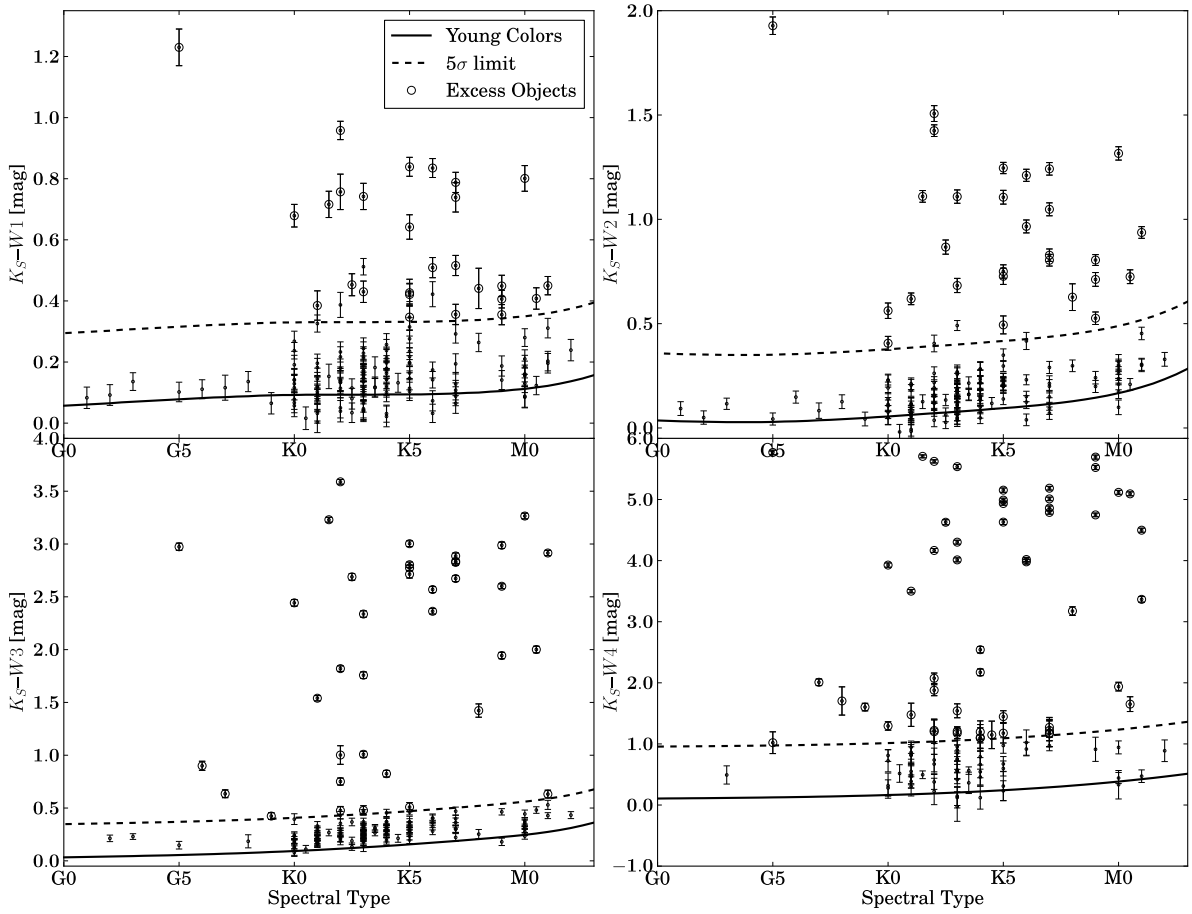

Figure 4.14 Spectral type versus infrared colors K_S–$W1$, K_S–$W2$, K_S–$W3$, and K_S–$W4$ for Sco-Cen members. The solid lines are the pre-MS photospheric colors from Pecaut & Mamajek (2013). Members with color excesses above the 5σ dispersion of photospheric colors in that band and all bands at longer wavelength are identified as having excess emission from circumstellar disks. Objects with color uncertainties greater than 0.25 mag are not shown.

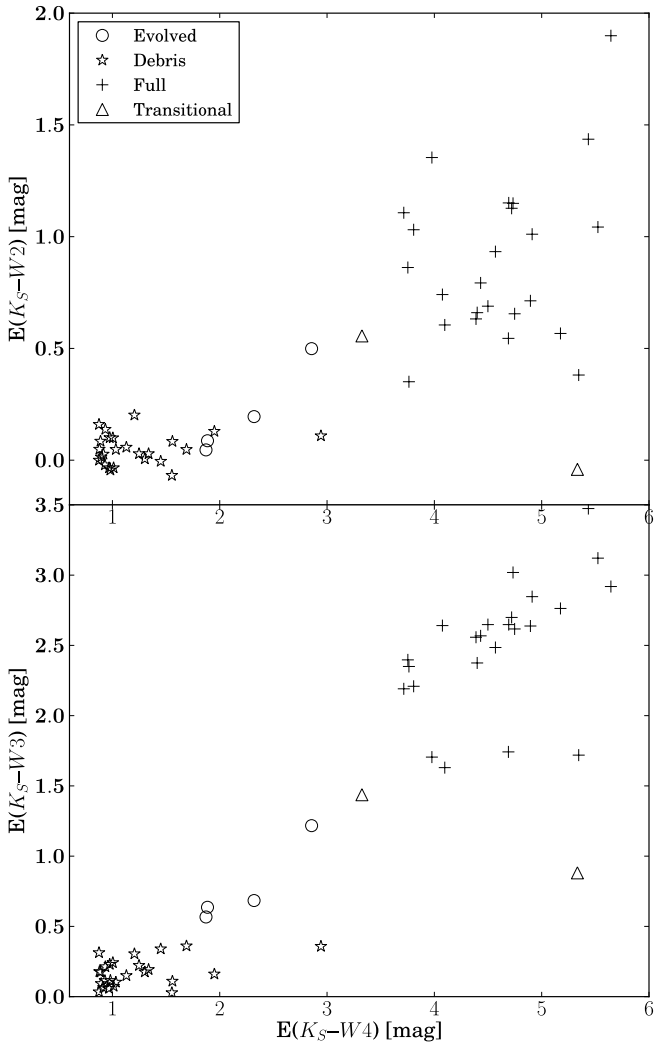

Figure 4.15 Color excesses above the photosphere for stars in Sco-Cen exhibiting an infrared excess.

Table 4.3. Infrared Excess and Spectroscopic Accretion Disk Fractions for K-Type Members in Sco-Cen

Band/Criteria/Disk Type	US	UCL	LCC
EW(Hα)	6/84 ($7.1^{+3.9}_{-1.9}$%)	5/145 ($3.4^{+2.2}_{-1.0}$%)	4/119 ($3.4^{+2.5}_{-1.0}$%)
K_S	3/89 ($3.4^{+3.1}_{-1.0}$%)	2/158 ($1.3^{+1.6}_{-0.4}$%)	2/119 ($1.7^{+2.1}_{-0.5}$%)
$W1$	10/89 ($11.2^{+4.2}_{-2.5}$%)	8/157 ($5.1^{+2.4}_{-1.2}$%)	4/119 ($3.4^{+2.5}_{-1.0}$%)
$W2$	11/89 ($12.4^{+4.3}_{-2.7}$%)	8/157 ($5.1^{+2.4}_{-1.2}$%)	4/119 ($3.4^{+2.5}_{-1.0}$%)
$W3$	15/89 ($16.9^{+4.7}_{-3.2}$%)	10/157 ($6.4^{+2.5}_{-1.4}$%)	4/118 ($3.4^{+2.5}_{-1.0}$%)
$W4$	17/36 ($47.2^{+8.2}_{-7.9}$%)	20/72 ($27.8^{+5.8}_{-4.6}$%)	7/86 ($8.1^{+4.0}_{-2.0}$%)
Full	8/89 ($9.0^{+4.0}_{-2.2}$%)	8/157 ($5.1^{+2.4}_{-1.2}$%)	4/118 ($3.4^{+2.5}_{-1.0}$%)
Transitional	2/89 ($2.2^{+2.8}_{-0.7}$%)	0/157 (<2.3%; 95% C.L.)	0/118 (<3.0%; 95% C.L.)
Evolved	4/89 ($4.5^{+3.3}_{-1.3}$%)	1/157 ($0.6^{+1.4}_{-0.2}$%)	0/118 (<3.0%; 95% C.L.)

Note. — Spectroscopic Accretion and IR Excess fractions shown above for K-type members of Sco-Cen only.

K_S band and the four WISE bands in Table 4.3.

4.5 Discussion

4.5.1 Which Ages are Reliable?

Depending on which isochronal ages we examine, we obtain different mean subgroup ages. However, given the $T_{\rm eff}$-dependent age trend present in Figure 4.4, we see several reasons to distrust ages from M-type stars. The most obvious reason is that evolutionary models have difficulty predicting the radii of main-sequence M-type stars, systematically underestimating their radii by ∼5-20% (Torres & Ribas 2002; Boyajian et al. 2012b; see also Kraus et al. 2011). Hillenbrand & White (2004) have compared dynamically constrained masses with predictions from pre-MS evolutionary models and found that the models systematically underpredict the masses of stars 5%-20% for masses under 0.5 $M_\odot$. On the other hand, they found that for masses above 1.2 $M_\odot$, dynamical masses and predicted masses from all models are consistent. As

stated in Hillenbrand et al. (2008), the likely source for the poor performance of models in the low-mass regime is incomplete knowledge of opacity sources and the difficulty in modeling convection. One of the large sources of uncertainty particularly applicable to modeling low-mass stars is the role magnetic fields play in convection. The results of Torres & Ribas (2002) suggest that isochronal ages for low-mass stars may systematically underpredict ages by a significant margin. Therefore, given that there are higher-mass F- and G-type isochronal ages available, it is preferable to avoid the adopting ages from the M-type members.

What about kinematic ages? Kinematic "expansion" or "traceback" ages are not dependent on stellar interiors models and therefore offer a the prospect of nearly model-free ages. Song et al. (2012) argues that is that kinematic expansion ages can function as model-independent age benchmarks which can be then used to establish a model-independent age scale. Age indicators such as Li can then be used to establish relative ages among different stellar populations. This is an interesting idea in principle, however the major problem is that kinematic ages are problematic. A recent example is that in the TW Hydra Association (TWA). A commonly quoted age for TWA is 8 Myr based on the kinematic traceback of de la Reza et al. (2006). However, their kinematic traceback was based on a sample of only four stars, which was contaminated by TWA 19, a member of LCC (Mamajek et al., 2002). Mamajek (2005) calculated a kinematic expansion age for TWA using kinematic parallaxes and a vetted list of members and obtained a lower limit of $\sim$10 Myr on the expansion age at 95% confidence, though the data were only weakly consistent with expansion. More recently, Weinberger et al. (2012) performed a kinematic traceback of TWA using a vetted list of members and trigonometric parallaxes. The Weinberger et al. (2012) traceback result indicated the members were never in a significantly more compact configuration. Similarly, an often-quoted age for Upper Sco is the 5 Myr expansion

age derived from proper motion data by Blaauw (1978). However, it was demonstrated by Brown et al. (1997), using simulations of expanding OB associations, that expansion ages inferred from proper motions alone all converged to ∼4 Myr, no matter the actual kinematic age. A recent examination of the expansion age in Upper Sco by Pecaut et al. (2012), using radial velocity data, gave a lower limit of ∼10 Myr at 95% confidence, though the data were consistent with no expansion. Finally, we mention that the adopted kinematic expansion age of 12 Myr, estimated by Song et al. (2003), has been re-evaluated by Mamajek (in prep.). Mamajek was unable to reproduce the expansion age for β Pic, using updated membership lists and the revised *Hipparcos* parallaxes (van Leeuwen, 2007). We conclude that the there is no established kinematic traceback age for either Sco-Cen or the groups used to bracket its age (e.g., TWA, β Pic) that has withstood the scrutiny of improved data, and that they simply do not yield useful age constraints given the current precision of the available data.

Another relevant chronometric technique is the use of the lithium depletion boundary (LDB) to determine the age of a stellar population. By detecting the stellar $T_{\rm eff}$ above which all the stars have exhibit Li depletion and comparing this with evolutionary model predictions, one can obtain an age which is independent of distance. LDB ages have been calculated for several of the nearby, young moving groups (Mentuch et al., 2008) but the subgroups of Sco-Cen do not yet have a reliable LDB age. The results of Cargile et al. (2010) suggests that lithium depletion boundary ages and modern nuclear main sequence turn-off ages are in agreement when convective core overshooting is included in the models of high-mass stars (e.g., Ekström et al., 2012). However, LDB ages are typically much older than pre-MS contraction ages, and it has been suggested that this problem is related to the radii discrepancy in M-type stars (Yee & Jensen, 2010). Macdonald & Mullan (2010) have attempted to resolve

this age discrepancy in β Pic by accounting for the effects of magnetic fields in their models. By adjusting the level of convective inhibition caused by magnetic fields in their models, they obtained an internally consistent age for the β Pic moving group of $\sim$40 Myr. This is more than than twice as old as previous pre-MS contraction ages for β Pic, and it suggests that the absence of magnetic fields from most pre-MS models is a major source of systematic error when deriving ages for low-mass K- and M-type stars, where a correct treatment of convection is particularly important.

Macdonald & Mullan (2010) present isochrones from their evolutionary models available with a variety of magnetic inhibition parameters. The magnetic inhibition parameter is defined in Macdonald & Mullan (2010) as:

$$\delta = \frac{B_v^2}{B_v^2 + 4\pi\gamma P_{gas}},$$

where B_v is the vertical magnetic field. They replace the adiabatic gradient Δ_{ad} with

$$\Delta = \frac{\delta}{\theta_e} min(1, \frac{2\pi\gamma\kappa}{\eta\alpha^2}),$$

where θ_e is the thermal expansion coefficient, κ is the thermal conductivity, η is the magnetic diffusivity, and α is the mixing length to pressure scale height ratio (see Macdonald & Mullan 2010 and references therein for more detail). Their isochrones[5] feature δ ranging from δ=0.0 (no magnetic inhibition) to δ=0.04. To explore whether models with the effects of magnetic fields would by qualitatively consistent with our observational isochrones and remove any T_{eff}-age bias, we plotted isochrones from Macdonald & Mullan (2010) with our Upper Sco sample for a variety of δ. We found that a δ=0.02 produced isochrones which ran roughly parallel to our observational

[5]Downloaded from http://www.physics.udel.edu/~jim/

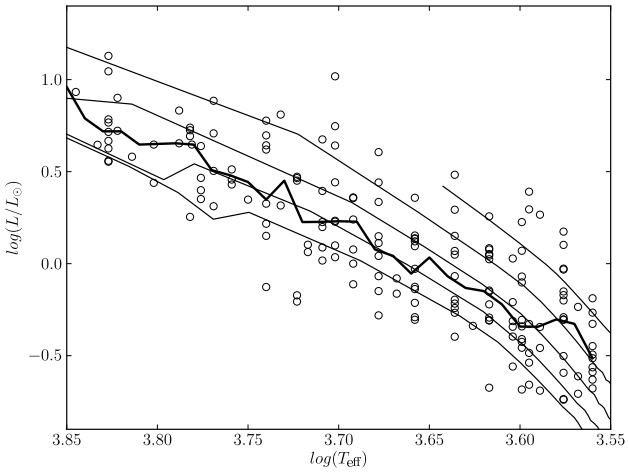

Figure 4.16 H-R diagram for Upper Sco F/G/K/M stars with 5 Myr, 10 Myr, 16 Myr, 24 Myr and 32 Myr isochrones from Macdonald & Mullan (2010), with magnetic inhibition parameter δ=0.02. The inclusion of the effects of magnetic fields removes the $T_{\rm eff}$-age bias.

isochrone for US, shown in Figure 4.16. This strongly suggests that accurate ages for K/M type pre-main sequence stars require evolutionary models which include the effects of magnetic fields.

We avoid using these magnetic models now to obtain age estimates since the models are not yet well-tested with observational data (though the model is calibrated to fit 2M0535-05; MacDonald & Mullan 2009). We are optimistic that the next generation of evolutionary models can include realistic treatments of magnetic fields (e.g., Feiden & Chaboyer, 2012). However, we note that there has been no examination of the LDB ages in any of the subgroups, though the technique could currently be applied to Upper Sco. Given the available data, and the systematic uncertainties, we simply adopt the median of the nuclear ages, the F-type pre-MS ages and the G-type pre-MS ages. This yields mean ages of 10±3 Myr for US, 16±2 Myr for UCL and 16±3 for LCC. The uncertainties quoted are the uncertainty of the median (Gott

et al., 2001), and are dominated by systematic differences in the age estimates from different mass ranges.

4.5.2 Do the Data Support Three "Coeval" Subgroups?

Previous studies of Sco-Cen have attempted to quantify the observed age spread in the subgroups. In Upper Sco, Preibisch et al. (2002), adopting an age of 5 Myr, concluded that the age spread was $\lesssim$1-2 Myr. Their results account for the effects of binarity, a distance spread, and observational uncertainties. This is consistent with the results of Slesnick et al. (2006), who similarly constrained the age spread in the northern part of Upper Sco to be less than $\pm$3 Myr (uniform distribution) using similar assumptions. In their study of UCL and LCC, Mamajek et al. (2002) have examined age spreads in the older subgroups and have constrained the star formation to have occurred over a time period of $\pm$3 Myr and $\pm$2 Myr (1σ) for UCL and LCC, respectively.

Our age spreads are a bit larger than those previously reported, with 1σ age spreads of $\pm$6 Myr, $\pm$5 Myr, and $\pm$6 Myr for US, UCL and LCC, respectively. Our age spread of $\pm$6 Myr for Upper Sco is much larger than the age spreads detected by Preibisch et al. (2002) and Slesnick et al. (2008). However, the age map in Figure 4.9 indicates that there is an age gradient from the southeastern part of US to the northwest, with the northwestern part being younger. The Slesnick et al. (2008) and Preibisch et al. (2002) low-mass samples were drawn from smaller regions ($\sim$150 deg^2 and $\sim$160 deg^2, respectively) than our sample in Upper Sco (drawn from the entire $\sim$320 deg^2), which could be responsible for the smaller detected age spreads. However, the likely reason our inferred age spreads in US are larger than previous results is that we adopt a mean age of 10 Myr, twice as old as the Slesnick et al. (2008)

or Preibisch et al. (2002) studies. A given luminosity spread at a younger age corresponds to a smaller inferred dispersion in ages than the same luminosity spread at an older age, simply because the younger isochrones are spaced farther apart in luminosity than those at older ages.

Slesnick et al. (2008) suggests that spreads in H-R diagram positions may not be an accurate proxy for spreads in age. They demonstrate this by comparing two nearly identical spectra for members in US, with spectroscopic surface gravity indicators which are indicative of nearly identical surface gravity. However, their H-R diagram positions suggests their ages differ by more than 10 Myr! Jeffries et al. (2011) use constraints on the disk lifetime to show that the age spread in the Orion Nebula Cluster must be less than 0.14 dex in log(Age), though the age spreads inferred from the H-R diagram show a 0.4 dex dispersion in log(Age). These results suggest that scatter in the H-R diagram may not be a reliable indicator of age spreads.

Following Jeffries et al. (2011), we investigate our inferred age spreads in Upper Sco further and separate our sample into members which are more luminous (and thus younger, according to the H-R diagram) than the median at given spectral type, and those that are less luminous. According to the test proposed by Jeffries et al. (2011), if there is an age spread greater than the disk lifetime, then the higher luminosity sample will have a higher disk fraction than the lower luminosity sample. For K-type stars, we find 2 accretors out of 40 in the less-luminous group and 4 accretors out of 40 in the more-luminous group. These accretion-disk fractions of $5.0^{+5.9}_{-1.6}$% and $10.0^{+6.8}_{-2.9}$% differ by a factor of two, but agree within the errors. A K-S test comparing their Hα distributions gives a 23% chance that the less-luminous and more-luminous samples were drawn from the same population (with K-S statistic D=0.22). This is not definitive, so we conclude that though our H-R diagram data indicates an age spread of $\pm$6 Myr, the Hα data provide only weak support for an age spread greater

than the >3 Myr disk dispersal timescale (Mamajek, 2009) in Upper Sco.

As stated previously, our age map does indicate there is a clear age gradient in US as it merges into UCL. The southern part of LCC is also noticeably younger than other parts of LCC, confirming the suggestion first raised in Preibisch & Mamajek (2008). We note that there are no main-sequence turnoff stars in northern LCC, which, considering the younger age of southern LCC, accounts for the turn-off age of LCC being much younger than UCL. We avoid speculating on triggered star formation scenarios at this time but note that the star formation history of Sco-Cen, as inferred from the H-R diagram positions, appears to be more complex than previously treated. The spatial distribution of ages is suggestive that the current division of three distinct, coeval subgroups is overly simplistic and a separation into smaller units may be warranted.

4.5.3 Circumstellar Disk Census

Observations of young clusters and associations of ages from ∼1 to >100 Myr have given strong indication that the protoplanetary disk dispersal timescale is very short, with an e-folding time of 2.5 Myr (Mamajek, 2009). This is qualitatively consistent with what we seen in Sco-Cen: 9% of Upper Sco K-type stars host an optically thick protoplanetary disk ("Full Disk" in the Espaillat et al. 2012 nomenclature) at an age of ∼10 Myr, whereas ≃4% of the K-type stars in the older subgroups UCL and LCC host a full disk (Table 4.3). However, the e-folding time of 2.5 Myr was estimated using an age for Upper Sco of 5 Myr, along with many other young clusters. Naylor (2009) has argued that pre-MS ages systematically underestimate cluster ages, and that ages based on high-mass stars, typically double ages estimated from the low-mass stars, are more likely to be correct. Using the ages we adopt for the Sco-Cen

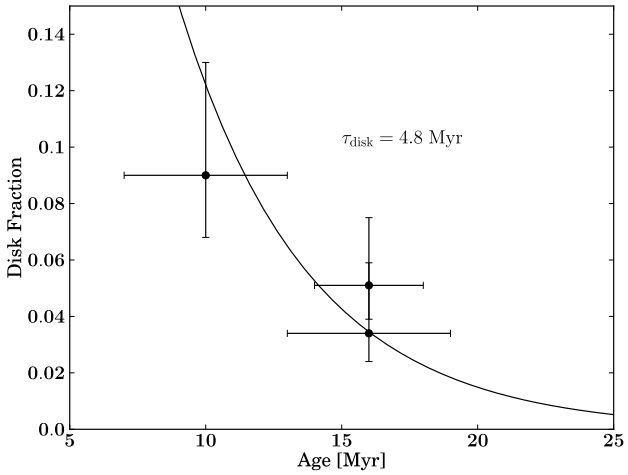

Figure 4.17 Mean subgroup age versus disk fraction ("Full Disk"; see Table 4.3) for K-type stars from the three subgroups of Sco-Cen. The best-fit exponential decay curve $f_{disk} = e^{-t/\tau_{disk}}$ has τ_{disk}=4.8 Myr.

subgroups, what disk dispersal timescale does this imply? We plot the primordial disk fractions ("Full Disk" from Table 4.3) as a function of age in Figure 4.17 and, following Mamajek (2009), fit an exponential decay curve to the data ($f_{disk} = e^{-t/\tau_{disk}}$). We obtain a mean e-folding for K-type stars ($\sim$0.7-1.2 $M_\odot$) timescale of 4.8 Myr. This is $\sim$2 Myr longer than the timescale estimated in Mamajek (2009), and would imply a longer timescale available for planet formation.

Finally, we note that our K-type disk fraction is larger than what is observed for the higher mass-stars in the same subgroups (Mamajek et al., 2002; Pecaut et al., 2012). This is consistent with the mass-dependent trend first identified by Carpenter et al. (2006) and further confirmed by Luhman & Mamajek (2012) in Upper Sco. However, we still have very poor statistics for M-type stars in the older subgroups, which highlights the need for future surveys to push the membership census to cooler spectral types in UCL and LCC (e.g., Rodriguez et al., 2011).

4.6 Conclusions

We can summarize our conclusions as follows:

1. We have performed a survey for new, low-mass K- and M-type members of all three subgroups of Sco-Cen. Using Li and proper motions, we identify 158 previously unknown members of Sco-Cen.

2. Using our newly identified members together with previously known members of Sco-Cen, we utilize Hα as an accretion diagnostic and identify stars with Hα emission levels consistent with accretion. We estimate a spectroscopic accretion disk fraction of $7.1^{+3.9}_{-1.9}$%, $3.4^{+2.2}_{-1.0}$% and $3.4^{+2.5}_{-1.0}$% for K-type stars ($\sim$0.7-1.2 $M_{\odot}$) in US, UCL and LCC, respectively.

3. Similar to previous results in other star-forming regions (e.g., Hillenbrand, 1997; Hillenbrand et al., 2008), we observe a T_{eff}-dependent age trend in all three subgroups of Sco-Cen, for all sets of evolutionary tracks. We find that the T_{eff}-age trend is absent when we compare our empirical isochrones with the Macdonald & Mullan (2010) evolutionary models, which model the effects of magnetic fields with a convective inhibition parameter. This suggests that ages for pre-main sequence K/M type stars may be systematically underestimated with evolutionary models which do not take into account the effects of magnetic fields.

4. Using the newest T_{eff} and BC scales from Nieva (2013), we re-evaluate the nuclear ages for the three subgroups, obtaining median ages of 7 Myr, 19 Myr and 11 Myr for US, UCL and LCC, respectively.

5. We adopt median ages of 10$\pm$3 Myr, 16$\pm$2 Myr and 16$\pm$3 Myr for US, UCL

and LCC, respectively, when considering the revised nuclear ages as well as the pre-MS contraction ages from the F- and G-type stars.

6. We obtain estimates for the intrinsic age spread in each subgroup through a grid of Monte Carlo simulations which take into account binarity and observational uncertainties. Assuming the median ages obtained above, and modeling the age distribution as a Gaussian, we find that 68% of the star formation in US, UCL, and LCC occurred over timescales of $\pm$6 Myr, $\pm$5 Myr, and $\pm$6 Myr, respectively. Thus when adopting an age of $\sim$10 Myr for Upper Sco, we detect an intrinsic age spread of $\pm$6 Myr (1σ).

7. Using members from our X-ray sample as well as F- and G-type members of Sco-Cen, we create an age map of the Sco-Cen complex. We find that the star-formation histories of the UCL and LCC, the older subgroups, are indicative of substructure and suggest the division into three subgroups is overly simplistic and a separation into smaller units may be warranted.

Table 4.4. Photometry and Proper Motion Data for Candidates in Sco-Cen Region

2MASS	μ_α (mas yr^{-1})	μ_δ (mas yr^{-1})	Ref.	V (mag)	Ref.	B–V (mag)	Ref.	J (mag)	H (mag)	K_S (mag)	Note
10004365-6522155	-11.7 ± 1.9	12.4 ± 1.9	PX	10.972 ± 0.046	A7	0.650 ± 0.077	A7	9.614 ± 0.026	9.193 ± 0.026	9.018 ± 0.019	
10065573-6352086	-19.6 ± 1.5	10.3 ± 1.8	U4	10.950 ± 0.012	A7	0.862 ± 0.018	A7	9.262 ± 0.028	8.744 ± 0.061	8.580 ± 0.024	
10092184-6736381	-14.6 ± 1.8	19.6 ± 1.0	U4	11.512 ± 0.017	A7	0.849 ± 0.051	A7	10.027 ± 0.026	9.497 ± 0.024	9.382 ± 0.021	
10111521-6620282	-26.5 ± 1.6	11.3 ± 1.6	U4	12.242 ± 0.028	A7	0.825 ± 0.035	A7	10.680 ± 0.024	10.223 ± 0.026	10.073 ± 0.023	
10293275-6349156	-11.3 ± 1.4	14.7 ± 1.5	U4	11.373 ± 0.014	A7	0.822 ± 0.027	A7	9.818 ± 0.022	9.349 ± 0.022	9.290 ± 0.019	
10313710-6901587	-18.6 ± 1.1	13.3 ± 2.1	U4	11.904 ± 0.010	A7	1.005 ± 0.028	A7	10.104 ± 0.023	9.609 ± 0.023	9.494 ± 0.025	
10334180-6413457	-14.1 ± 1.7	11.8 ± 2.5	U4	11.796 ± 0.010	A7	0.829 ± 0.038	A7	9.926 ± 0.024	9.451 ± 0.024	9.291 ± 0.024	
10342989-6235572	-14.2 ± 1.3	10.5 ± 2.5	U4	10.612 ± 0.060	T2	0.795 ± 0.074	T2	9.059 ± 0.032	8.596 ± 0.044	8.458 ± 0.027	
10412300-6940431	-30.3 ± 1.5	23.3 ± 1.6	PX	10.270 ± 0.010	T06	0.720 ± 0.010	T06	8.916 ± 0.034	8.539 ± 0.067	8.384 ± 0.020	
10441393-6446273	-14.9 ± 2.0	7.7 ± 1.7	U4	11.327 ± 0.032	A7	0.873 ± 0.047	A7	9.450 ± 0.024	8.930 ± 0.025	8.750 ± 0.023	
10463300-6527183	-13.4 ± 2.4	9.3 ± 1.4	U4	10.938 ± 0.035	A7	0.683 ± 0.053	A7	9.684 ± 0.022	9.289 ± 0.023	9.149 ± 0.021	
10474221-5510143	-44.2 ± 2.3	0.2 ± 2.6	U4					9.966 ± 0.021	9.327 ± 0.025	9.131 ± 0.021	
10484283-5442328	-27.5 ± 2.2	25.7 ± 4.3	U4	11.166 ± 0.093	T2	1.247 ± 0.182	T2	9.336 ± 0.022	8.734 ± 0.031	8.595 ± 0.021	
10494839-6446284	-16.3 ± 2.0	5.6 ± 2.2	U4	11.569 ± 0.035	A7	0.802 ± 0.039	A7	10.079 ± 0.024	9.622 ± 0.022	9.480 ± 0.019	
10541737-6440512	-15.8 ± 1.5	3.4 ± 1.8	U4	11.702 ± 0.032	A7	0.874 ± 0.048	A7	10.058 ± 0.023	9.614 ± 0.022	9.542 ± 0.021	
10544998-6526458	-20.4 ± 1.5	9.7 ± 1.9	U4	12.078 ± 0.023	A7	0.980 ± 0.051	A7	10.178 ± 0.024	9.656 ± 0.022	9.544 ± 0.023	
10552886-6629147	-19.2 ± 1.8	8.7 ± 1.8	PX	11.315 ± 0.033	A7	0.827 ± 0.034	A7	9.700 ± 0.024	9.249 ± 0.023	9.109 ± 0.024	
10560422-6152054	-34.1 ± 3.9	4.0 ± 3.9	PX	11.623 ± 0.043	A7	1.233 ± 0.057	A7	9.350 ± 0.024	8.689 ± 0.051	8.504 ± 0.021	
10574936-6913599	-35.2 ± 1.2	6.1 ± 1.9	U4	10.390 ± 0.010	T06	0.970 ± 0.010	T06	8.484 ± 0.034	8.009 ± 0.051	7.792 ± 0.016	
10591218-6438089	-9.9 ± 1.8	22.4 ± 3.8	U4	12.152 ± 0.029	A7	0.824 ± 0.037	A7	10.311 ± 0.015	9.822 ± 0.042	9.676 ± 0.027	a

Table 4.4 (cont'd)

2MASS	μ_α (mas yr^{-1})	μ_δ (mas yr^{-1})	Ref.	V (mag)	Ref.	B–V (mag)	Ref.	J (mag)	H (mag)	K_S (mag)	Note
11001895-6118020	-29.4 ± 2.1	2.7 ± 1.9	U4	10.303 ± 0.042	A7	0.664 ± 0.056	A7	8.828 ± 0.024	8.426 ± 0.053	8.322 ± 0.021	
11033159-6321581	-37.5 ± 1.7	13.9 ± 1.7	U4					9.513 ± 0.026	8.860 ± 0.049	8.656 ± 0.019	
11080791-6341469	-37.1 ± 1.9	8.3 ± 1.9	U4	11.722 ± 0.045	A7	1.241 ± 0.051	A7	9.144 ± 0.023	8.484 ± 0.042	8.291 ± 0.023	
11132622-4523427	-43.9 ± 1.4	-7.4 ± 1.4	U4	12.833 ± 0.010	A7	1.537 ± 0.016	A7	9.415 ± 0.028	8.727 ± 0.040	8.495 ± 0.031	
11143442-4418240	-23.3 ± 1.4	-2.6 ± 1.2	T2	9.730 ± 0.030	T2	1.033 ± 0.044	T2	7.863 ± 0.046	7.360 ± 0.057	7.183 ± 0.018	
11145608-7101430	-18.6 ± 3.4	-3.0 ± 1.6	U4					9.519 ± 0.023	8.881 ± 0.059	8.698 ± 0.021	
11154143-5511082	-51.8 ± 1.5	0.3 ± 1.5	U4	11.949 ± 0.200	T2	0.733 ± 0.264	T2	10.409 ± 0.023	9.939 ± 0.022	9.806 ± 0.019	
11165870-4406222	-15.3 ± 1.5	5.8 ± 1.0	U4	10.979 ± 0.078	T2	1.103 ± 0.142	T2	9.609 ± 0.026	9.215 ± 0.022	9.095 ± 0.021	
11175186-6402056	-23.8 ± 3.8	-5.4 ± 3.1	U4	11.885 ± 0.075	A7	1.112 ± 0.089	A7	9.391 ± 0.024	8.591 ± 0.036	8.177 ± 0.027	
11202645-5834023	1.8 ± 2.1	-22.6 ± 2.1	PX	10.401 ± 0.057	T2	0.558 ± 0.066	T2	9.021 ± 0.024	8.626 ± 0.057	8.486 ± 0.024	
11214451-4954076	-20.6 ± 0.7	-3.2 ± 0.7	PX	8.750 ± 0.010	HP	0.920 ± 0.016	HP	7.125 ± 0.021	6.689 ± 0.018	6.575 ± 0.020	
11265293-5846387	-43.2 ± 2.2	-1.4 ± 2.2	U4	11.537 ± 0.137	T2	0.981 ± 0.219	T2	10.005 ± 0.027	9.523 ± 0.023	9.424 ± 0.021	
11272881-3952572	-30.7 ± 1.0	-8.5 ± 3.0	U4	10.654 ± 0.023	A7	0.934 ± 0.032	A7	8.905 ± 0.024	8.407 ± 0.046	8.262 ± 0.016	
11275535-6626046	-36.6 ± 1.7	6.1 ± 1.7	PX	10.820 ± 0.010	T06	0.940 ± 0.010	T06	9.006 ± 0.026	8.484 ± 0.029	8.358 ± 0.029	
11320835-5803199	-38.6 ± 1.7	-7.9 ± 1.4	U4	9.924 ± 0.032	T2	0.891 ± 0.044	T2	8.080 ± 0.029	7.629 ± 0.040	7.472 ± 0.029	
11370003-6516164	-20.4 ± 1.3	2.9 ± 2.2	U4	11.952 ± 0.100	A7	0.940 ± 0.116	A7	10.160 ± 0.023	9.704 ± 0.024	9.604 ± 0.021	
11402787-6201337	-33.2 ± 4.2	-10.3 ± 1.6	U4	11.936 ± 0.095	A7	1.249 ± 0.129	A7	9.359 ± 0.027	8.683 ± 0.063	8.463 ± 0.024	
11403346-5641458	-14.2 ± 2.7	0.8 ± 1.7	U4	10.502 ± 0.051	T2	1.081 ± 0.076	T2	8.475 ± 0.019	7.900 ± 0.040	7.685 ± 0.036	
11430455-6714211	1.5 ± 1.4	22.4 ± 1.1	U4	11.763 ± 0.171	T2	1.107 ± 0.261	T2	9.428 ± 0.022	8.801 ± 0.038	8.646 ± 0.019	
11434903-6904232	-5.1 ± 1.6	17.6 ± 1.6	U4					9.878 ± 0.023	9.252 ± 0.022	9.081 ± 0.023	

Table 4.4 (cont'd)

2MASS	μ_α (mas yr^{-1})	μ_δ (mas yr^{-1})	Ref.	V (mag)	Ref.	B–V (mag)	Ref.	J (mag)	H (mag)	K_S (mag)	Note
11445217-6438548	-34.1 ± 1.7	-1.0 ± 1.7	U4	11.957 ± 0.105	A7	1.270 ± 0.119	A7	9.430 ± 0.022	8.709 ± 0.034	8.567 ± 0.021	
11452016-5749094	-22.5 ± 1.5	-2.2 ± 1.5	U4	12.341 ± 0.070	A7	0.781 ± 0.094	A7	10.737 ± 0.024	10.280 ± 0.022	10.159 ± 0.021	
11454278-5739285	-29.3 ± 1.4	-9.6 ± 1.4	U4	11.599 ± 0.036	A7	1.127 ± 0.054	A7	9.380 ± 0.024	8.766 ± 0.021	8.591 ± 0.021	
11472064-4953042	-35.5 ± 2.2	-7.7 ± 2.2	PX					9.152 ± 0.029	8.474 ± 0.040	8.278 ± 0.033	
11485263-5657441	-8.1 ± 2.7	-0.5 ± 2.7	U4					10.858 ± 0.024	10.231 ± 0.023	10.092 ± 0.024	
11492309-4801013	-23.0 ± 1.0	8.4 ± 0.7	U4	10.410 ± 0.040	T2	0.744 ± 0.052	T2	8.867 ± 0.026	8.427 ± 0.057	8.311 ± 0.020	
11515049-6407278	-22.5 ± 2.3	3.7 ± 1.6	U4	11.871 ± 0.006	A7	0.858 ± 0.054	A7	10.203 ± 0.023	9.734 ± 0.025	9.628 ± 0.021	
11522157-6444302	-20.8 ± 1.8	1.6 ± 1.7	U4	11.349 ± 0.020	A7	0.799 ± 0.039	A7	9.919 ± 0.024	9.498 ± 0.024	9.388 ± 0.023	
11522242-6156016	-17.2 ± 1.3	5.6 ± 1.5	U4	11.197 ± 0.118	T2	1.398 ± 0.256	T2	8.825 ± 0.021	8.159 ± 0.027	7.893 ± 0.029	
11524466-5514070	-17.3 ± 1.3	12.5 ± 1.6	U4	10.140 ± 0.038	T2	1.129 ± 0.057	T2	8.275 ± 0.021	7.770 ± 0.051	7.632 ± 0.049	
11554295-5637314	-37.5 ± 3.2	-3.3 ± 2.5	U4	11.440 ± 0.042	A7	1.205 ± 0.050	A7	8.851 ± 0.029	8.247 ± 0.029	8.035 ± 0.021	
11560730-6314096	-16.6 ± 2.9	-2.0 ± 2.9	PX	10.270 ± 0.052	T2	1.152 ± 0.080	T2	7.761 ± 0.018	7.118 ± 0.023	6.898 ± 0.016	
11575693-5821291	-42.8 ± 4.8	6.1 ± 2.1	U4	11.647 ± 0.153	T2	0.767 ± 0.206	T2	9.850 ± 0.018	9.415 ± 0.043	9.282 ± 0.038	a
11592560-5407445	-24.7 ± 1.3	0.3 ± 1.9	U4	10.905 ± 0.063	T2	0.835 ± 0.084	T2	9.022 ± 0.023	8.546 ± 0.049	8.389 ± 0.021	
11594608-6101132	-30.7 ± 1.9	-4.5 ± 2.4	U4	11.340 ± 0.036	A7	1.139 ± 0.050	A7	9.305 ± 0.029	8.753 ± 0.030	8.617 ± 0.029	
11594986-6136246	-31.1 ± 2.3	-11.4 ± 2.2	U4	12.130 ± 0.010	A7	1.422 ± 0.014	A7	9.271 ± 0.025	8.613 ± 0.029	8.414 ± 0.023	
12051254-5331233	-33.9 ± 5.8	0.0 ± 5.8	PX	12.801 ± 0.070	A7	0.950 ± 0.081	A7	10.034 ± 0.007	9.390 ± 0.032	9.212 ± 0.029	a
12061352-5702168	-25.3 ± 2.4	-5.8 ± 1.2	U4	10.550 ± 0.010	T06	0.730 ± 0.010	T06	9.230 ± 0.034	8.835 ± 0.026	8.728 ± 0.023	
12063292-4247508	-50.3 ± 1.3	-2.5 ± 1.0	U4	10.660 ± 0.010	T06	0.790 ± 0.010	T06	9.172 ± 0.023	8.689 ± 0.029	8.579 ± 0.023	
12065276-5044463	-41.7 ± 1.4	-15.0 ± 1.4	U4	12.466 ± 0.041	A7	1.283 ± 0.060	A7	10.002 ± 0.024	9.330 ± 0.022	9.162 ± 0.019	

Table 4.4 (cont'd)

2MASS	μ_α (mas yr^{-1})	μ_δ (mas yr^{-1})	Ref.	V (mag)	Ref.	B–V (mag)	Ref.	J (mag)	H (mag)	K_S (mag)	Note
12074236-6227282	-29.4 ± 2.1	-9.1 ± 1.5	U4	10.900 ± 0.010	T06	1.030 ± 0.010	T06	8.621 ± 0.023	8.066 ± 0.020	7.914 ± 0.020	
12090225-5120410	-33.4 ± 0.9	-9.5 ± 1.0	U4	11.118 ± 0.035	A7	1.007 ± 0.041	A7	9.385 ± 0.026	8.778 ± 0.024	8.598 ± 0.019	
12092655-4923487	-38.1 ± 1.7	-9.6 ± 1.0	U4	11.311 ± 0.018	A7	1.201 ± 0.028	A7	8.718 ± 0.021	8.080 ± 0.020	7.918 ± 0.023	
12094184-5854450	-35.2 ± 1.8	-14.9 ± 2.1	U4	10.230 ± 0.010	T06	0.940 ± 0.010	T06	8.322 ± 0.023	7.812 ± 0.024	7.661 ± 0.018	
12101065-4855476	-35.9 ± 2.3	-12.9 ± 0.9	U4	11.082 ± 0.015	A7	1.016 ± 0.022	A7	9.113 ± 0.026	8.595 ± 0.042	8.417 ± 0.023	
12103705-5727208	-22.4 ± 4.1	-4.7 ± 4.1	PX	12.040 ± 0.084	A7	0.982 ± 0.090	A7	10.176 ± 0.036	9.663 ± 0.051	9.535 ± 0.039	
12113142-5816533	-36.8 ± 1.7	-12.8 ± 1.5	U4	10.190 ± 0.010	T06	0.860 ± 0.010	T06	8.553 ± 0.021	8.089 ± 0.042	7.966 ± 0.026	
12120804-6554549	-36.6 ± 1.6	-9.5 ± 1.6	U4	11.250 ± 0.010	T06	1.080 ± 0.010	T06	9.149 ± 0.023	8.550 ± 0.031	8.426 ± 0.022	
12121119-4950081	-29.8 ± 2.0	-10.8 ± 0.9	U4	11.329 ± 0.009	A7	1.040 ± 0.010	T06	9.502 ± 0.023	8.899 ± 0.044	8.803 ± 0.024	
12123577-5520273	-31.4 ± 1.4	-12.5 ± 1.4	U4	10.460 ± 0.010	T06	0.920 ± 0.010	T06	8.731 ± 0.024	8.235 ± 0.034	8.123 ± 0.020	
12124890-6230317	-41.6 ± 1.4	-4.4 ± 1.8	U4	11.470 ± 0.010	T06	1.300 ± 0.010	T06	8.775 ± 0.018	8.103 ± 0.034	7.955 ± 0.023	
12131860-4815588	-20.4 ± 0.8	-9.2 ± 0.8	U4					9.722 ± 0.024	9.153 ± 0.023	8.991 ± 0.019	
12135166-5419527	-13.2 ± 1.7	1.4 ± 1.6	U4					8.525 ± 0.029	7.790 ± 0.029	7.570 ± 0.031	
12135700-6255129	-32.9 ± 2.5	-12.7 ± 2.4	U4	11.580 ± 0.010	T06	1.190 ± 0.010	T06	9.161 ± 0.020	8.531 ± 0.038	8.394 ± 0.021	
12141149-5456022	-16.8 ± 2.9	4.2 ± 2.2	U4	11.661 ± 0.134	T2	0.625 ± 0.169	T2	9.960 ± 0.024	9.346 ± 0.022	9.172 ± 0.021	
12143187-5110156	-38.5 ± 1.4	-54.5 ± 1.4	U4					9.955 ± 0.024	9.335 ± 0.028	9.095 ± 0.021	
12143410-5110124	-35.7 ± 2.1	-12.9 ± 1.9	T2	10.200 ± 0.010	T06	0.850 ± 0.010	T06	8.672 ± 0.023	8.246 ± 0.042	8.141 ± 0.021	
12145229-5547037	-36.8 ± 1.8	-11.1 ± 1.8	U4	9.770 ± 0.010	HP	0.800 ± 0.010	T06	8.063 ± 0.024	7.656 ± 0.047	7.507 ± 0.020	
12160114-5614068	-31.0 ± 3.5	-10.7 ± 1.8	U4	11.220 ± 0.010	T06	1.150 ± 0.010	T06	8.768 ± 0.026	8.164 ± 0.038	7.956 ± 0.020	
12163007-6711477	-35.0 ± 1.1	-7.9 ± 1.0	U4	11.560 ± 0.010	T06	1.400 ± 0.010	T06	8.620 ± 0.020	8.024 ± 0.053	7.851 ± 0.026	

Table 4.4 (cont'd)

2MASS	μ_α (mas yr^{-1})	μ_δ (mas yr^{-1})	Ref.	V (mag)	Ref.	B–V (mag)	Ref.	J (mag)	H (mag)	K_S (mag)	Note
12164023-7007361	-35.6 ± 1.6	-10.4 ± 1.6	PX	10.648 ± 0.025	A7	1.052 ± 0.026	A7	8.800 ± 0.026	8.281 ± 0.034	8.092 ± 0.029	
12172809-5122215	-19.5 ± 0.9	0.1 ± 0.9	U4	10.455 ± 0.041	T2	1.051 ± 0.058	T2	8.544 ± 0.026	8.040 ± 0.034	7.888 ± 0.033	
12174048-5000266	-29.2 ± 1.3	-10.3 ± 1.2	U4	13.501 ± 0.022	A7	1.453 ± 0.042	A7	10.550 ± 0.026	9.913 ± 0.026	9.700 ± 0.021	
12182762-5943128	-42.6 ± 2.3	-11.5 ± 2.3	PX	10.434 ± 0.046	A7	0.963 ± 0.050	A7	8.467 ± 0.019	7.847 ± 0.029	7.726 ± 0.017	
12185802-5737191	-34.3 ± 1.3	-9.4 ± 1.1	U4	9.960 ± 0.010	A7	0.856 ± 0.021	A7	7.964 ± 0.023	7.484 ± 0.034	7.367 ± 0.027	
12192161-6454101	-37.6 ± 2.4	-9.1 ± 2.4	PX	9.870 ± 0.010	T06	0.990 ± 0.010	T06	8.056 ± 0.020	7.554 ± 0.040	7.400 ± 0.024	
12195938-5018404	-22.1 ± 1.1	-20.8 ± 1.2	U4	12.639 ± 0.064	A7	1.238 ± 0.099	A7	10.184 ± 0.014	9.554 ± 0.023	9.341 ± 0.011	a
12202301-5242165	-29.7 ± 3.0	-5.1 ± 3.0	PX	11.511 ± 0.027	A7	1.357 ± 0.045	A7	8.612 ± 0.023	7.878 ± 0.027	7.711 ± 0.021	
12205449-6457242	-41.0 ± 2.4	-11.2 ± 2.4	PX	11.000 ± 0.010	T06	1.100 ± 0.010	T06	8.863 ± 0.021	8.243 ± 0.038	8.081 ± 0.033	
12205588-6534365	-37.8 ± 10.8	-1.1 ± 5.5	U4	12.957 ± 0.063	A7	1.420 ± 0.107	A7	9.941 ± 0.023	9.249 ± 0.025	9.058 ± 0.023	
12210499-7116493	-42.7 ± 1.8	-10.2 ± 1.6	U4	11.730 ± 0.043	A7	1.322 ± 0.052	A7	9.088 ± 0.024	8.419 ± 0.038	8.241 ± 0.026	
12210808-5212226	-32.0 ± 0.9	-9.0 ± 0.9	U4	11.850 ± 0.010	T06	1.210 ± 0.010	T06	9.457 ± 0.025	8.796 ± 0.023	8.655 ± 0.021	
12213087-6403530	-44.9 ± 1.4	-8.2 ± 1.3	U4	10.753 ± 0.028	A7	1.131 ± 0.059	A7	8.243 ± 0.026	7.629 ± 0.023	7.407 ± 0.023	
12215566-4946125	-37.4 ± 1.5	-14.2 ± 1.3	T2	10.015 ± 0.027	T2	0.798 ± 0.037	T2	8.513 ± 0.024	8.053 ± 0.026	8.010 ± 0.031	
12220430-4841248	-28.4 ± 1.0	-11.6 ± 0.9	U4	10.499 ± 0.039	T2	0.840 ± 0.051	T2	8.809 ± 0.024	8.275 ± 0.036	8.163 ± 0.021	
12222200-5114260	-35.9 ± 1.0	-24.0 ± 1.3	U4					10.858 ± 0.024	10.368 ± 0.024	10.294 ± 0.021	
12234012-5616325	-33.9 ± 1.1	-14.3 ± 1.6	U4	10.859 ± 0.060	A7	0.825 ± 0.075	T2	8.953 ± 0.021	8.452 ± 0.057	8.307 ± 0.024	
12234749-6402549	-37.3 ± 1.1	-11.4 ± 1.2	U4	10.854 ± 0.010	A7	1.099 ± 0.014	A7	8.960 ± 0.030	8.392 ± 0.031	8.241 ± 0.040	
12240975-6003416	-32.1 ± 1.6	-15.9 ± 2.9	U4	12.084 ± 0.143	A7	1.163 ± 0.172	A7	9.578 ± 0.023	8.980 ± 0.025	8.747 ± 0.020	
12244195-6437015	-28.6 ± 1.2	-6.4 ± 1.3	U4	11.132 ± 0.112	T2	1.178 ± 0.209	T2	8.708 ± 0.039	8.058 ± 0.031	7.870 ± 0.027	

Table 4.4 (cont'd)

2MASS	μ_α (mas yr^{-1})	μ_δ (mas yr^{-1})	Ref.	V (mag)	Ref.	B–V (mag)	Ref.	J (mag)	H (mag)	K_S (mag)	Note
12245648-4854270	-33.7 ± 1.3	-7.4 ± 1.4	U4	11.937 ± 0.060	A7	1.223 ± 0.081	A7	9.490 ± 0.022	8.851 ± 0.027	8.699 ± 0.026	
12252542-5353568	-46.8 ± 2.3	12.9 ± 2.3	U4					10.694 ± 0.023	10.215 ± 0.022	10.095 ± 0.024	
12253370-7227480	-40.7 ± 1.3	-11.0 ± 1.4	U4	12.524 ± 0.025	A7	1.467 ± 0.038	A7	9.191 ± 0.024	8.439 ± 0.029	8.221 ± 0.020	
12263934-6113406	-34.0 ± 1.5	-6.8 ± 1.5	U4	11.798 ± 0.032	A7	1.203 ± 0.062	A7	9.519 ± 0.023	8.883 ± 0.024	8.741 ± 0.021	
12264842-5215070	-37.6 ± 1.6	-13.2 ± 1.1	U4	11.792 ± 0.045	A7	1.232 ± 0.050	A7	9.063 ± 0.017	8.419 ± 0.033	8.282 ± 0.034	
12271665-6239142	-36.2 ± 1.7	-12.0 ± 1.0	U4	10.723 ± 0.068	A7	1.025 ± 0.097	A7	8.807 ± 0.035	8.266 ± 0.040	8.117 ± 0.027	
12282540-6320589	-38.4 ± 1.5	-13.3 ± 1.4	U4	9.250 ± 0.010	T06	0.770 ± 0.010	T06	7.848 ± 0.032	7.474 ± 0.047	7.333 ± 0.031	
12283577-4948021	-8.3 ± 1.3	-3.7 ± 1.3	U4					10.090 ± 0.026	9.411 ± 0.026	9.183 ± 0.019	
12302957-5222269	-29.8 ± 1.0	-21.8 ± 1.7	U4	11.669 ± 0.031	A7	1.115 ± 0.055	A7	9.559 ± 0.026	8.957 ± 0.026	8.818 ± 0.024	
12313807-4558593	-63.5 ± 1.1	-27.8 ± 1.1	U4	13.184 ± 0.037	A7	1.500 ± 0.055	A7	9.331 ± 0.030	8.693 ± 0.063	8.412 ± 0.029	
12314481-4808482	-31.7 ± 1.8	10.6 ± 0.8	U4	11.713 ± 0.165	T2	0.952 ± 0.233	T2	10.272 ± 0.026	9.729 ± 0.023	9.555 ± 0.019	
12321483-4217502	-12.6 ± 1.6	-0.2 ± 1.0	U4	9.869 ± 0.031	T2	1.300 ± 0.052	T2	7.608 ± 0.020	7.008 ± 0.057	6.833 ± 0.024	
12333381-5714066	-39.2 ± 0.8	-12.7 ± 1.0	U4	10.920 ± 0.010	T06	1.020 ± 0.010	T06	8.947 ± 0.023	8.398 ± 0.036	8.272 ± 0.031	
12351574-4919517	-30.9 ± 2.3	5.1 ± 2.3	PX					10.141 ± 0.026	9.705 ± 0.026	9.607 ± 0.021	
12361767-5042421	-33.3 ± 1.0	-13.6 ± 0.9	U4	11.557 ± 0.054	A7	1.085 ± 0.085	A7	9.429 ± 0.023	8.862 ± 0.051	8.683 ± 0.023	
12363895-6344436	-36.0 ± 1.7	-12.4 ± 1.7	U4	9.940 ± 0.010	T06	0.960 ± 0.010	T06	8.058 ± 0.027	7.523 ± 0.046	7.369 ± 0.024	
12365895-5412178	-27.3 ± 1.6	-12.0 ± 1.4	U4	10.350 ± 0.023	A7	0.860 ± 0.030	A7	8.764 ± 0.041	8.292 ± 0.036	8.180 ± 0.027	
12373737-5143113	-38.0 ± 1.2	-16.9 ± 1.2	U4	12.268 ± 0.010	A7	1.311 ± 0.054	A7	9.366 ± 0.026	8.679 ± 0.034	8.474 ± 0.024	
12374883-5209463	-33.0 ± 0.9	-12.9 ± 1.0	U4	12.039 ± 0.042	A7	1.167 ± 0.082	A7	9.658 ± 0.023	9.000 ± 0.022	8.876 ± 0.023	
12383556-5916438	-40.6 ± 2.7	-20.3 ± 2.7	PX	11.537 ± 0.111	A7	1.038 ± 0.179	A7	9.539 ± 0.022	8.902 ± 0.021	8.791 ± 0.019	

Table 4.4 (cont'd)

2MASS	μ_α (mas yr^{-1})	μ_δ (mas yr^{-1})	Ref.	V (mag)	Ref.	B–V (mag)	Ref.	J (mag)	H (mag)	K_S (mag)	Note
12390790-5811593	-15.5 ± 1.0	-4.0 ± 0.9	U4	11.511 ± 0.121	T2	0.997 ± 0.199	T2	8.634 ± 0.043	8.011 ± 0.053	7.827 ± 0.024	
12391307-5429052	-9.5 ± 2.9	0.3 ± 2.0	U4					10.084 ± 0.024	9.511 ± 0.026	9.340 ± 0.021	
12391404-5454469	-28.6 ± 2.6	-13.0 ± 1.3	U4	11.935 ± 0.028	A7	1.157 ± 0.045	A7	9.398 ± 0.020	8.778 ± 0.037	8.625 ± 0.011	a
12392312-7244039	-16.8 ± 1.8	-11.4 ± 1.3	U4	12.104 ± 0.211	T2	1.357 ± 0.344	T2	9.322 ± 0.039	8.518 ± 0.059	8.329 ± 0.033	
12393796-5731406	-34.2 ± 0.9	-18.2 ± 1.7	U4	10.212 ± 0.010	A7	0.745 ± 0.014	A7	8.711 ± 0.021	8.239 ± 0.046	8.133 ± 0.029	
12404664-5211046	-22.6 ± 1.4	-12.4 ± 1.1	U4	11.910 ± 0.010	T06	1.020 ± 0.010	T06	9.936 ± 0.029	9.441 ± 0.028	9.280 ± 0.024	
12404975-5048077	-57.2 ± 1.3	-28.0 ± 0.9	U4	11.960 ± 0.174	T2	0.880 ± 0.236	T2	9.526 ± 0.026	8.923 ± 0.027	8.789 ± 0.026	
12405458-5031550	-43.1 ± 1.0	-18.3 ± 1.3	U4	11.984 ± 0.014	A7	1.235 ± 0.054	A7	9.481 ± 0.021	8.844 ± 0.055	8.724 ± 0.023	
12411820-5825558	-37.4 ± 2.1	-16.5 ± 2.1	PX	9.970 ± 0.010	T06	0.770 ± 0.010	T06	8.416 ± 0.023	8.014 ± 0.031	7.890 ± 0.023	
12420050-5759486	-29.3 ± 1.5	-15.0 ± 1.4	U4	13.425 ± 0.044	A7	1.469 ± 0.054	A7	9.884 ± 0.036	9.190 ± 0.037	8.840 ± 0.029	
12434124-4204055	-25.5 ± 1.5	-10.7 ± 1.1	U4					10.190 ± 0.023	9.567 ± 0.023	9.382 ± 0.019	
12443482-6331463	-35.7 ± 2.4	-16.0 ± 1.8	U4	10.800 ± 0.010	T06	1.010 ± 0.010	T06	8.585 ± 0.029	8.024 ± 0.044	7.880 ± 0.020	
12444949-4918474	-36.2 ± 1.2	-9.5 ± 1.2	U4	12.808 ± 0.065	A7	1.368 ± 0.109	A7	9.974 ± 0.024	9.291 ± 0.023	9.120 ± 0.023	
12450674-4742580	-29.1 ± 0.7	-8.7 ± 1.6	U4	10.397 ± 0.040	T2	0.762 ± 0.052	T2	8.665 ± 0.037	8.202 ± 0.029	8.134 ± 0.034	
12454884-5410583	-33.0 ± 1.7	-11.8 ± 1.8	U4	11.400 ± 0.010	T06	1.020 ± 0.010	T06	9.477 ± 0.024	8.893 ± 0.022	8.735 ± 0.019	
12472196-6808397	-35.5 ± 1.1	-15.4 ± 1.1	U4	11.090 ± 0.004	A7	1.164 ± 0.038	A7	8.796 ± 0.041	8.179 ± 0.036	8.034 ± 0.040	
12472609-5445156	-20.8 ± 3.5	-8.9 ± 1.7	U4	12.128 ± 0.033	A7	1.198 ± 0.052	A7	9.835 ± 0.023	9.193 ± 0.021	9.000 ± 0.021	
12474824-5431308	-33.1 ± 1.6	-10.8 ± 1.3	U4	11.780 ± 0.010	T06	1.280 ± 0.010	T06	8.858 ± 0.009	8.227 ± 0.031	8.004 ± 0.005	c
12475186-5126382	-30.9 ± 0.9	-9.6 ± 0.9	PX	9.520 ± 0.010	HP	0.796 ± 0.025	HP	7.813 ± 0.024	7.384 ± 0.033	7.262 ± 0.027	
12480778-4439167	-37.3 ± 0.9	-16.9 ± 0.9	U4	9.830 ± 0.010	T06	0.820 ± 0.010	T06	8.131 ± 0.021	7.672 ± 0.055	7.513 ± 0.024	

Table 4.4 (cont'd)

2MASS	μ_α (mas yr^{-1})	μ_δ (mas yr^{-1})	Ref.	V (mag)	Ref.	B–V (mag)	Ref.	J (mag)	H (mag)	K_S (mag)	Note
12483152-5944493	-37.9 ± 2.8	-18.3 ± 2.0	U4	11.061 ± 0.037	A7	1.289 ± 0.071	A7	8.311 ± 0.032	7.684 ± 0.069	7.483 ± 0.029	
12484652-5417333	-36.2 ± 2.3	1.0 ± 1.7	U4	11.335 ± 0.100	T2	0.833 ± 0.151	T2	9.835 ± 0.024	9.417 ± 0.022	9.298 ± 0.021	
12484818-5635378	-27.0 ± 1.3	-10.0 ± 0.9	U4	10.400 ± 0.010	T06	0.770 ± 0.010	T06	8.934 ± 0.026	8.454 ± 0.027	8.367 ± 0.023	
12504491-5654485	-31.1 ± 1.9	-15.1 ± 1.9	U4	12.644 ± 0.028	A7	1.469 ± 0.058	A7	9.118 ± 0.027	8.435 ± 0.031	8.219 ± 0.023	
12505143-5156353	-32.7 ± 1.6	-17.8 ± 2.3	U4	11.704 ± 0.090	A7	1.141 ± 0.123	A7	9.331 ± 0.011	8.704 ± 0.029	8.534 ± 0.008	a
12510413-5253320	-19.1 ± 1.1	1.1 ± 1.1	U4	11.851 ± 0.162	T2	0.868 ± 0.212	T2	9.693 ± 0.029	9.105 ± 0.025	8.960 ± 0.030	
12510556-5253121	-30.6 ± 1.1	-15.3 ± 1.1	U4	12.072 ± 0.035	A7	1.189 ± 0.066	A7	9.652 ± 0.024	8.976 ± 0.023	8.804 ± 0.019	
12543050-5031482	-24.3 ± 1.7	-10.9 ± 1.7	U4	12.932 ± 0.055	A7	1.332 ± 0.104	A7	10.113 ± 0.023	9.449 ± 0.022	9.267 ± 0.021	
12560830-6926539	-37.4 ± 2.7	-9.2 ± 2.7	PX	11.800 ± 0.010	T06	1.320 ± 0.010	T06	8.910 ± 0.024	8.247 ± 0.042	7.989 ± 0.031	
12560940-6127256	-52.5 ± 1.9	-14.7 ± 1.9	T2	9.620 ± 0.010	T06	0.800 ± 0.010	T06	7.816 ± 0.018	7.363 ± 0.038	7.260 ± 0.016	
12582559-7028490	-39.4 ± 1.6	-17.4 ± 1.1	U4	9.950 ± 0.010	T06	0.940 ± 0.010	T06	8.184 ± 0.029	7.702 ± 0.063	7.545 ± 0.027	
13010856-5901533	-34.3 ± 2.1	-12.4 ± 2.1	U4	13.272 ± 0.063	A7	1.478 ± 0.095	A7	9.856 ± 0.022	9.216 ± 0.026	8.956 ± 0.019	
13015069-5304581	-27.5 ± 1.8	-11.4 ± 1.8	U4	11.330 ± 0.010	T06	1.010 ± 0.010	T06	9.460 ± 0.024	8.931 ± 0.024	8.787 ± 0.021	
13015435-4249422	-27.4 ± 0.6	-21.3 ± 0.6	U4	11.340 ± 0.057	A7	0.854 ± 0.102	A7	9.678 ± 0.026	9.206 ± 0.023	9.095 ± 0.021	
13024703-6213589	-34.5 ± 1.8	-22.6 ± 1.6	U4	10.174 ± 0.034	T2	0.858 ± 0.046	T2	8.406 ± 0.023	7.993 ± 0.059	7.846 ± 0.016	
13032904-4723160	-28.3 ± 0.8	-16.7 ± 0.9	U4	11.680 ± 0.074	A7	1.155 ± 0.092	A7	9.193 ± 0.026	8.552 ± 0.046	8.379 ± 0.031	
13055087-5304181	-31.6 ± 1.3	-19.7 ± 1.3	U4	12.575 ± 0.074	A7	1.259 ± 0.117	A7	10.069 ± 0.024	9.448 ± 0.029	9.270 ± 0.026	
13064012-5159386	-33.4 ± 2.1	-14.9 ± 2.1	PX	10.826 ± 0.009	A7	0.900 ± 0.010	T06	8.921 ± 0.024	8.441 ± 0.055	8.274 ± 0.026	
13065439-4541313	-29.9 ± 0.8	-23.1 ± 1.2	U4	11.713 ± 0.054	A7	1.199 ± 0.081	A7	9.290 ± 0.026	8.642 ± 0.057	8.506 ± 0.023	
13071310-5952108	-33.1 ± 2.3	-19.8 ± 2.3	PX	10.320 ± 0.067	A7	0.816 ± 0.122	A7	8.280 ± 0.021	7.786 ± 0.024	7.658 ± 0.016	

Table 4.4 (cont'd)

2MASS	μ_α (mas yr^{-1})	μ_δ (mas yr^{-1})	Ref.	V (mag)	Ref.	B–V (mag)	Ref.	J (mag)	H (mag)	K_S (mag)	Note
13095880-4527388	-27.2 ± 1.0	-14.8 ± 1.2	U4	11.021 ± 0.037	A7	0.946 ± 0.054	A7	9.203 ± 0.024	8.671 ± 0.038	8.537 ± 0.023	
13103245-4817036	-36.2 ± 1.2	-16.3 ± 1.8	U4	11.584 ± 0.081	A7	1.114 ± 0.119	A7	9.341 ± 0.032	8.764 ± 0.047	8.596 ± 0.019	
13112902-4252418	-38.1 ± 1.1	-22.9 ± 1.1	U4	13.597 ± 0.094	A7	1.475 ± 0.137	A7	10.144 ± 0.029	9.421 ± 0.027	9.244 ± 0.027	
13121764-5508258	-29.9 ± 1.9	-17.5 ± 1.2	U4	11.841 ± 0.031	A7	1.227 ± 0.071	A7	9.406 ± 0.022	8.806 ± 0.026	8.655 ± 0.021	
13121859-5439054	-30.6 ± 3.5	-7.2 ± 3.5	PX					9.834 ± 0.023	9.297 ± 0.024	9.189 ± 0.023	
13130714-4537438	-27.4 ± 2.2	-15.4 ± 1.7	U4	11.630 ± 0.010	T06	1.210 ± 0.010	T06	9.170 ± 0.024	8.518 ± 0.038	8.328 ± 0.040	
13132326-5442156	-20.5 ± 2.3	-7.8 ± 1.8	U4	12.282 ± 0.041	A7	1.074 ± 0.069	A7	10.049 ± 0.024	9.488 ± 0.022	9.358 ± 0.024	
13140112-6846384	-13.4 ± 1.1	-8.0 ± 1.3	U4	11.264 ± 0.043	A7	0.978 ± 0.072	A7	9.152 ± 0.021	8.617 ± 0.034	8.459 ± 0.023	
13142382-5054018	-24.6 ± 2.1	-14.5 ± 1.2	U4	10.390 ± 0.010	T06	0.830 ± 0.010	T06	8.682 ± 0.030	8.251 ± 0.036	8.103 ± 0.040	
13151666-5058072	1.6 ± 0.7	-20.4 ± 0.9	PX	9.090 ± 0.010	HP	0.890 ± 0.024	HP	7.451 ± 0.029	7.002 ± 0.049	6.817 ± 0.021	
13173283-7037429	-36.2 ± 1.4	0.2 ± 2.5	U4					9.303 ± 0.024	8.704 ± 0.027	8.554 ± 0.026	
13174687-4456534	-29.9 ± 1.0	-24.6 ± 2.3	U4	12.076 ± 0.011	A7	1.194 ± 0.053	A7	9.598 ± 0.023	8.954 ± 0.022	8.833 ± 0.023	
13175314-5058481	-19.2 ± 1.5	-14.9 ± 1.5	U4	12.551 ± 0.035	A7	1.271 ± 0.051	A7	9.978 ± 0.027	9.326 ± 0.025	9.151 ± 0.021	
13191370-4506326	-25.6 ± 2.3	-15.2 ± 2.3	PX	11.915 ± 0.070	A7	1.088 ± 0.098	A7	9.787 ± 0.026	9.235 ± 0.024	9.071 ± 0.021	
13203307-4927514	-29.1 ± 1.1	-11.5 ± 1.1	U4	12.161 ± 0.022	A7	1.107 ± 0.023	A7	10.068 ± 0.023	9.552 ± 0.027	9.368 ± 0.023	
13204539-4611377	-31.3 ± 1.1	-17.7 ± 1.0	U4	12.396 ± 0.055	A7	1.189 ± 0.078	A7	9.806 ± 0.022	9.187 ± 0.023	9.013 ± 0.019	
13220753-6938121	-39.1 ± 1.2	-19.9 ± 1.6	U4	10.350 ± 0.010	T06	1.010 ± 0.010	T06	8.277 ± 0.032	7.641 ± 0.023	7.293 ± 0.018	
13233587-4718467	-29.9 ± 1.1	-17.4 ± 1.0	U4	11.190 ± 0.010	T06	1.040 ± 0.010	T06	9.032 ± 0.023	8.403 ± 0.034	8.312 ± 0.029	
13251211-6456207	-36.3 ± 2.0	-14.2 ± 1.6	U4	11.056 ± 0.030	A7	0.972 ± 0.034	A7	9.072 ± 0.026	8.562 ± 0.042	8.392 ± 0.027	
13270594-4856180	-35.8 ± 1.3	-22.5 ± 1.0	U4	10.679 ± 0.078	T2	0.980 ± 0.107	T2	8.523 ± 0.021	7.945 ± 0.034	7.808 ± 0.026	

Table 4.4 (cont'd)

2MASS	μ_α (mas yr^{-1})	μ_δ (mas yr^{-1})	Ref.	V (mag)	Ref.	B–V (mag)	Ref.	J (mag)	H (mag)	K_S (mag)	Note
13274874-6622488	-15.3 ± 1.6	-1.6 ± 1.6	PX	10.189 ± 0.038	T2	1.109 ± 0.056	T2	7.609 ± 0.020	6.974 ± 0.024	6.771 ± 0.024	
13281508-4446377	-37.9 ± 0.9	-5.8 ± 0.9	U4	11.879 ± 0.196	T2	0.573 ± 0.248	T2	9.994 ± 0.021	9.597 ± 0.025	9.451 ± 0.021	
13290963-4755545	-30.3 ± 0.9	-28.8 ± 0.9	U4					10.518 ± 0.024	9.878 ± 0.022	9.799 ± 0.021	
13291766-4614230	-24.9 ± 0.9	-18.0 ± 0.9	U4	12.163 ± 0.033	A7	1.112 ± 0.064	A7	9.955 ± 0.023	9.375 ± 0.023	9.226 ± 0.025	
13294575-4844366	-29.2 ± 1.4	6.9 ± 1.4	U4	13.048 ± 0.023	A7	1.084 ± 0.037	A7	10.121 ± 0.024	9.482 ± 0.025	9.266 ± 0.025	
13315360-5113330	-25.3 ± 1.4	-15.0 ± 1.1	U4	9.840 ± 0.010	HP	0.750 ± 0.010	T06	8.391 ± 0.024	8.010 ± 0.047	7.831 ± 0.023	
13334410-6359345	-30.0 ± 4.6	-26.2 ± 4.4	U4	11.380 ± 0.056	A7	1.108 ± 0.074	A7	9.305 ± 0.022	8.708 ± 0.047	8.590 ± 0.019	
13335329-6536473	-28.4 ± 2.0	-20.4 ± 2.0	U4					9.369 ± 0.026	8.647 ± 0.047	8.472 ± 0.021	
13335481-6536414	-31.6 ± 2.3	-18.6 ± 1.7	U4	11.311 ± 0.041	A7	1.176 ± 0.061	A7	8.740 ± 0.024	8.035 ± 0.031	7.809 ± 0.033	
13342461-6517473	-28.2 ± 2.7	-25.7 ± 2.7	U4	13.455 ± 0.067	A7	1.440 ± 0.089	A7	10.205 ± 0.024	9.526 ± 0.024	9.276 ± 0.023	
13343188-4209305	-37.5 ± 0.9	-23.6 ± 1.2	U4	10.695 ± 0.069	T2	0.974 ± 0.094	T2	8.783 ± 0.019	8.280 ± 0.042	8.093 ± 0.018	
13354082-4818124	-38.6 ± 1.1	-24.4 ± 1.0	U4	11.311 ± 0.061	A7	1.125 ± 0.108	A7	9.295 ± 0.028	8.652 ± 0.033	8.505 ± 0.021	
13364090-4043359	-33.3 ± 1.5	-13.5 ± 1.5	U4	12.552 ± 0.019	A7	1.274 ± 0.044	A7	9.827 ± 0.010	9.169 ± 0.036	8.955 ± 0.014	a
13375730-4134419	-35.5 ± 1.2	-24.6 ± 1.1	U4	10.120 ± 0.010	T06	0.870 ± 0.010	T06	8.437 ± 0.023	8.031 ± 0.046	7.880 ± 0.026	
13380596-4344564	-24.9 ± 1.5	-17.8 ± 1.2	U4	11.132 ± 0.106	T2	1.105 ± 0.196	T2	9.160 ± 0.021	8.672 ± 0.023	8.535 ± 0.020	
13381128-5214251	-26.0 ± 1.2	-12.2 ± 0.9	U4	10.735 ± 0.048	A7	0.669 ± 0.080	T2	9.227 ± 0.027	8.797 ± 0.046	8.696 ± 0.019	
13384937-4237234	-28.4 ± 0.8	-19.2 ± 0.8	U4	11.421 ± 0.023	A7	0.999 ± 0.031	A7	9.519 ± 0.024	8.983 ± 0.023	8.894 ± 0.020	
13402554-4633514	-29.9 ± 2.9	-14.1 ± 1.0	U4	11.656 ± 0.052	A7	1.074 ± 0.064	A7	9.207 ± 0.025	8.623 ± 0.022	8.443 ± 0.022	
13405585-4244505	-23.8 ± 1.4	-22.5 ± 1.4	U4	13.241 ± 0.053	A7	1.415 ± 0.076	A7	10.009 ± 0.023	9.337 ± 0.022	9.122 ± 0.023	
13431296-4155366	-11.2 ± 1.0	-8.6 ± 1.0	U4	11.254 ± 0.107	T2	0.734 ± 0.142	T2	9.496 ± 0.024	8.987 ± 0.022	8.857 ± 0.021	

Table 4.4 (cont'd)

2MASS	μ_α (mas yr^{-1})	μ_δ (mas yr^{-1})	Ref.	V (mag)	Ref.	B–V (mag)	Ref.	J (mag)	H (mag)	K_S (mag)	Note
13431682-4233127	-23.6 ± 2.1	6.9 ± 0.9	U4	10.733 ± 0.071	T2	0.916 ± 0.090	T2	8.961 ± 0.024	8.471 ± 0.023	8.388 ± 0.024	
13442441-4706343	-23.9 ± 1.2	-17.7 ± 1.8	U4	10.504 ± 0.008	A7	0.934 ± 0.019	A7	8.668 ± 0.027	8.160 ± 0.027	8.029 ± 0.034	
13444279-6347495	-32.8 ± 1.9	-26.7 ± 1.4	U4	11.040 ± 0.010	T06	1.180 ± 0.010	T06	8.522 ± 0.024	7.888 ± 0.029	7.739 ± 0.029	
13445275-6800331	-37.9 ± 1.5	-3.1 ± 1.5	U4					10.837 ± 0.022	10.443 ± 0.025	10.320 ± 0.023	
13451319-6128149	-26.4 ± 2.5	-9.8 ± 2.0	U4	11.955 ± 0.156	T2	0.525 ± 0.189	T2	9.506 ± 0.023	8.915 ± 0.024	8.744 ± 0.021	
13454424-4904500	-25.4 ± 2.2	-18.5 ± 2.2	PX	10.607 ± 0.047	A7	0.890 ± 0.060	A7	8.749 ± 0.035	8.240 ± 0.055	8.123 ± 0.026	
13455599-5222255	-29.2 ± 1.0	-16.3 ± 1.1	U4	11.148 ± 0.014	A7	1.034 ± 0.045	A7	9.332 ± 0.023	8.725 ± 0.047	8.592 ± 0.023	
13475054-4902056	-25.8 ± 2.1	-16.0 ± 2.1	PX	10.890 ± 0.010	T06	0.850 ± 0.010	T06	9.294 ± 0.023	8.803 ± 0.057	8.694 ± 0.021	
13475144-4901486	-23.9 ± 1.3	-12.2 ± 1.3	U4					10.104 ± 0.023	9.498 ± 0.021	9.367 ± 0.019	
13493502-4452104	-4.9 ± 0.9	-11.0 ± 1.2	U4	11.047 ± 0.099	T2	0.985 ± 0.159	T2	9.265 ± 0.025	8.743 ± 0.022	8.629 ± 0.020	
13503387-4810150	-23.2 ± 1.0	-19.5 ± 1.0	U4	12.953 ± 0.105	A7	1.288 ± 0.140	A7	10.288 ± 0.026	9.587 ± 0.023	9.427 ± 0.021	
13515351-4846505	-28.6 ± 1.4	-17.2 ± 1.4	U4	12.490 ± 0.049	A7	1.192 ± 0.053	A7	9.953 ± 0.022	9.347 ± 0.024	9.163 ± 0.021	
13522045-3825345	-40.0 ± 1.4	-27.5 ± 1.4	U4	13.212 ± 0.028	A7	1.484 ± 0.043	A7	9.859 ± 0.026	9.184 ± 0.025	8.916 ± 0.021	
13540743-6733449	-28.7 ± 1.4	-3.9 ± 0.9	U4	10.930 ± 0.010	T06	0.750 ± 0.010	T06	9.435 ± 0.024	9.046 ± 0.024	8.900 ± 0.023	
13544209-4820578	-32.4 ± 1.7	-22.0 ± 0.8	U4	11.240 ± 0.010	T06	0.920 ± 0.010	T06	9.285 ± 0.024	8.796 ± 0.049	8.700 ± 0.021	
13552552-4706563	-28.2 ± 0.8	-23.7 ± 1.5	U4	11.260 ± 0.029	A7	1.151 ± 0.053	A7	8.859 ± 0.021	8.213 ± 0.024	8.095 ± 0.023	
13562964-3839129	-26.1 ± 1.1	-19.7 ± 1.3	U4					9.213 ± 0.026	8.635 ± 0.029	8.551 ± 0.025	
13563469-4907146	-30.3 ± 2.4	-20.3 ± 1.6	U4	11.528 ± 0.063	A7	0.964 ± 0.104	A7	9.522 ± 0.027	8.946 ± 0.027	8.814 ± 0.026	
13575106-4431482	-26.8 ± 1.2	-19.2 ± 1.2	U4	12.065 ± 0.042	A7	1.153 ± 0.059	A7	9.533 ± 0.024	8.922 ± 0.022	8.797 ± 0.019	
13581812-4504043	-18.1 ± 4.0	-4.1 ± 1.3	U4					10.865 ± 0.024	10.368 ± 0.025	10.269 ± 0.023	

Table 4.4 (cont'd)

2MASS	μ_α (mas yr^{-1})	μ_δ (mas yr^{-1})	Ref.	V (mag)	Ref.	B–V (mag)	Ref.	J (mag)	H (mag)	K_S (mag)	Note
13591330-7136541	-37.7 ± 1.0	-26.2 ± 0.9	U4	10.454 ± 0.044	T2	0.969 ± 0.062	T2	8.078 ± 0.027	7.530 ± 0.034	7.391 ± 0.027	
14001181-4230334	-23.0 ± 2.9	-18.8 ± 1.4	U4	13.285 ± 0.072	A7	1.395 ± 0.119	A7	10.446 ± 0.026	9.763 ± 0.027	9.549 ± 0.023	
14003189-6416245	-16.9 ± 3.6	-14.4 ± 2.3	U4	12.476 ± 0.014	A7	0.852 ± 0.030	A7	10.823 ± 0.024	10.300 ± 0.023	10.162 ± 0.021	
14004970-4236569	-24.8 ± 0.9	-21.7 ± 0.9	U4	11.074 ± 0.072	A7	0.932 ± 0.103	A7	9.396 ± 0.023	8.868 ± 0.025	8.720 ± 0.020	
14014823-4100264	-4.8 ± 2.2	-17.4 ± 2.2	PX					10.416 ± 0.024	9.913 ± 0.026	9.782 ± 0.023	
14015020-4059234	-10.6 ± 1.4	-10.4 ± 1.4	U4					10.828 ± 0.024	10.272 ± 0.026	10.147 ± 0.021	
14022072-4144509	-21.8 ± 1.5	-20.6 ± 1.1	U4	10.624 ± 0.033	A7	0.854 ± 0.055	A7	8.983 ± 0.027	8.537 ± 0.042	8.401 ± 0.031	
14040272-4436503	-12.2 ± 1.0	-17.0 ± 1.0	U4					9.706 ± 0.044	9.247 ± 0.043	9.060 ± 0.023	
14055695-6149126	-63.2 ± 3.3	-30.8 ± 2.0	U4	12.021 ± 0.220	T2	0.761 ± 0.294	T2	10.107 ± 0.015	9.713 ± 0.035	9.584 ± 0.010	a
14060042-4112249	-23.2 ± 1.5	-24.4 ± 1.5	U4	11.566 ± 0.030	A7	0.977 ± 0.049	A7	9.520 ± 0.022	8.970 ± 0.021	8.826 ± 0.019	
14074792-3945427	-24.3 ± 1.7	-19.4 ± 2.0	U4	12.336 ± 0.034	A7	1.202 ± 0.058	A7	9.997 ± 0.022	9.425 ± 0.023	9.257 ± 0.020	
14081015-4123525	-31.3 ± 1.9	-27.5 ± 2.2	U4	12.233 ± 0.123	A7	1.261 ± 0.191	A7	9.553 ± 0.024	8.823 ± 0.040	8.542 ± 0.023	
14085608-4403488	-27.7 ± 1.2	-20.3 ± 1.2	U4	11.456 ± 0.011	A7	1.018 ± 0.019	A7	9.237 ± 0.024	8.708 ± 0.027	8.522 ± 0.019	
14122451-4327149	-31.3 ± 2.1	-32.9 ± 0.8	U4	11.003 ± 0.047	A7	0.873 ± 0.064	A7	9.321 ± 0.026	8.843 ± 0.029	8.725 ± 0.021	
14124691-3831220	-30.3 ± 0.9	-25.7 ± 1.5	U4	11.566 ± 0.073	A7	1.080 ± 0.128	A7	9.438 ± 0.024	8.784 ± 0.027	8.678 ± 0.023	
14144477-4207224	-32.7 ± 0.9	-2.2 ± 1.0	U4	11.689 ± 0.165	T2	0.455 ± 0.190	T2	10.038 ± 0.026	9.580 ± 0.023	9.506 ± 0.021	
14165395-5356098	-49.2 ± 1.4	-19.2 ± 1.6	U4	11.805 ± 0.181	T2	1.261 ± 0.289	T2	10.238 ± 0.022	9.789 ± 0.022	9.692 ± 0.021	
14184440-5850045	-19.8 ± 2.2	-13.0 ± 2.5	U4	11.048 ± 0.118	T2	1.385 ± 0.257	T2	8.655 ± 0.021	8.057 ± 0.047	7.806 ± 0.024	
14185327-4827313	-18.2 ± 1.2	-21.9 ± 1.2	U4	11.575 ± 0.045	A7	1.062 ± 0.069	A7	9.432 ± 0.022	8.813 ± 0.036	8.677 ± 0.021	
14201202-5339537	-23.1 ± 1.8	-16.3 ± 1.6	U4	11.595 ± 0.041	A7	0.819 ± 0.070	A7	9.945 ± 0.024	9.475 ± 0.027	9.328 ± 0.023	

Table 4.4 (cont'd)

2MASS	μ_α (mas yr^{-1})	μ_δ (mas yr^{-1})	Ref.	V (mag)	Ref.	B–V (mag)	Ref.	J (mag)	H (mag)	K_S (mag)	Note
14201211-4917224	-2.9 ± 3.4	-9.8 ± 2.0	U4					9.610 ± 0.024	9.008 ± 0.026	8.851 ± 0.021	
14204893-4748442	-27.0 ± 1.1	-21.4 ± 1.4	U4	11.585 ± 0.046	A7	1.235 ± 0.073	A7	8.979 ± 0.018	8.335 ± 0.034	8.160 ± 0.029	
14213051-3845252	-17.5 ± 2.6	-23.0 ± 1.4	U4	12.434 ± 0.507	A7	0.915 ± 0.508	A7	9.706 ± 0.028	9.003 ± 0.027	8.870 ± 0.026	
14214378-4652082	-25.0 ± 1.1	-20.0 ± 1.0	U4	11.226 ± 0.059	A7	0.964 ± 0.104	A7	9.215 ± 0.037	8.683 ± 0.029	8.611 ± 0.019	
14214499-5429040	-26.6 ± 2.1	-18.9 ± 2.1	U4					9.990 ± 0.022	9.344 ± 0.023	9.184 ± 0.024	
14220732-5417055	-21.0 ± 1.4	-23.4 ± 1.1	U4	11.132 ± 0.057	A7	0.944 ± 0.103	A7	9.226 ± 0.026	8.655 ± 0.038	8.559 ± 0.024	
14223029-3532190	-26.2 ± 1.1	-22.9 ± 1.3	U4	11.329 ± 0.017	A7	1.070 ± 0.040	A7	9.100 ± 0.020	8.582 ± 0.029	8.401 ± 0.023	
14224364-4628054	-18.6 ± 2.5	-17.3 ± 1.1	U4	11.582 ± 0.031	A7	0.961 ± 0.051	A7	9.755 ± 0.024	9.253 ± 0.026	9.095 ± 0.023	
14234748-5935261	-26.4 ± 2.0	-23.4 ± 1.9	U4	11.000 ± 0.010	T06	1.020 ± 0.010	T06	8.884 ± 0.026	8.193 ± 0.018	7.940 ± 0.020	
14241649-5013282	-4.5 ± 2.0	-19.4 ± 2.0	PX	9.616 ± 0.023	T2	0.960 ± 0.033	T2	7.725 ± 0.020	7.251 ± 0.036	7.099 ± 0.016	
14244779-5041333	-20.7 ± 1.4	-19.5 ± 1.4	U4	11.910 ± 0.010	T06	0.890 ± 0.010	T06	10.232 ± 0.024	9.807 ± 0.024	9.693 ± 0.023	
14250165-4822361	-25.1 ± 1.7	-8.5 ± 1.4	T2	9.068 ± 0.018	T2	0.961 ± 0.025	T2	7.195 ± 0.021	6.722 ± 0.023	6.593 ± 0.020	
14262134-3644057	-41.3 ± 1.5	-19.7 ± 1.3	U4	10.563 ± 0.012	A7	0.800 ± 0.018	A7	9.042 ± 0.027	8.585 ± 0.046	8.511 ± 0.021	
14270556-4714217	-24.5 ± 0.9	-21.1 ± 0.9	U4	10.615 ± 0.008	A7	0.797 ± 0.030	A7	9.062 ± 0.030	8.649 ± 0.034	8.542 ± 0.024	
14275425-5944350	-17.1 ± 4.4	-20.2 ± 4.5	PX	12.170 ± 0.058	A7	1.181 ± 0.085	A7	9.762 ± 0.021	9.179 ± 0.022	9.030 ± 0.021	
14280929-4414175	-22.2 ± 1.8	-22.7 ± 0.9	U4	9.782 ± 0.033	T2	0.799 ± 0.043	T2	8.313 ± 0.019	7.931 ± 0.033	7.794 ± 0.034	
14281937-4219341	-17.6 ± 1.8	-21.6 ± 0.9	U4	10.290 ± 0.029	A7	0.703 ± 0.073	T2	8.917 ± 0.020	8.506 ± 0.038	8.389 ± 0.034	
14291483-6752209	4.3 ± 2.8	-4.9 ± 3.1	U4	12.159 ± 0.014	A7	1.842 ± 0.021	A7	8.428 ± 0.019	7.510 ± 0.038	7.205 ± 0.018	
14301461-4520277	-34.2 ± 2.4	-29.4 ± 2.6	U4	12.279 ± 0.052	A7	0.958 ± 0.076	A7	10.417 ± 0.024	9.880 ± 0.022	9.767 ± 0.021	
14301594-5904014	-15.4 ± 2.5	1.2 ± 2.5	PX	10.081 ± 0.041	T2	1.092 ± 0.061	T2	7.909 ± 0.032	7.354 ± 0.038	7.131 ± 0.026	

Table 4.4 (cont'd)

2MASS	μ_α (mas yr^{-1})	μ_δ (mas yr^{-1})	Ref.	V (mag)	Ref.	B–V (mag)	Ref.	J (mag)	H (mag)	K_S (mag)	Note
14321121-5826058	-27.7 ± 2.3	-32.7 ± 1.8	U4	11.454 ± 0.055	A7	1.194 ± 0.066	A7	9.168 ± 0.022	8.524 ± 0.031	8.413 ± 0.023	
14345213-4004459	-19.6 ± 1.4	-19.1 ± 2.3	U4	11.906 ± 0.035	A7	1.097 ± 0.064	A7	9.705 ± 0.023	9.127 ± 0.023	8.959 ± 0.019	
14345603-7030069	4.4 ± 1.6	-40.3 ± 1.6	PX	11.210 ± 0.036	A7	0.833 ± 0.050	A7	9.692 ± 0.026	9.234 ± 0.025	9.103 ± 0.021	
14372053-4410053	-18.9 ± 1.2	-48.1 ± 1.1	U4	10.026 ± 0.033	T2	0.859 ± 0.045	T2	8.463 ± 0.020	7.943 ± 0.061	7.836 ± 0.023	
14374904-4928268	-25.5 ± 1.4	-30.3 ± 1.4	U4	12.038 ± 0.095	A7	1.240 ± 0.119	A7	9.473 ± 0.024	8.811 ± 0.026	8.603 ± 0.021	
14375022-5457411	-25.4 ± 1.8	-27.2 ± 1.4	U4	10.750 ± 0.010	T06	0.920 ± 0.010	T06	8.964 ± 0.020	8.447 ± 0.063	8.299 ± 0.026	
14375134-5456495	-41.5 ± 2.3	-32.9 ± 2.3	U4					9.967 ± 0.026	9.305 ± 0.026	9.061 ± 0.019	
14380350-4932023	-23.5 ± 2.0	-23.5 ± 1.9	U4	11.666 ± 0.058	A7	1.154 ± 0.066	A7	9.355 ± 0.026	8.680 ± 0.031	8.606 ± 0.026	
14380862-4322008	-26.3 ± 1.4	-20.2 ± 5.8	U4	12.736 ± 0.036	A7	1.363 ± 0.046	A7	9.817 ± 0.030	9.094 ± 0.023	8.888 ± 0.024	
14385440-4310223	-20.8 ± 1.1	-22.7 ± 1.4	U4	11.374 ± 0.039	A7	1.084 ± 0.069	A7	8.871 ± 0.035	8.278 ± 0.049	8.108 ± 0.023	
14392060-3905282	-15.1 ± 1.4	-19.0 ± 0.9	U4	10.759 ± 0.039	A7	0.871 ± 0.051	A7	9.147 ± 0.048	8.684 ± 0.038	8.509 ± 0.023	
14405601-7046138	-10.5 ± 1.1	-6.3 ± 2.0	U4	11.214 ± 0.088	T2	1.161 ± 0.171	T2	8.646 ± 0.023	7.973 ± 0.046	7.742 ± 0.023	
14411942-5001199	-26.8 ± 1.3	-23.3 ± 1.2	U4	12.010 ± 0.010	T06	1.210 ± 0.010	T06	9.324 ± 0.022	8.698 ± 0.067	8.500 ± 0.020	
14413499-4700288	-27.0 ± 0.9	-27.5 ± 0.9	U4	10.004 ± 0.027	T2	0.785 ± 0.036	T2	8.465 ± 0.024	8.005 ± 0.040	7.901 ± 0.020	
14421471-5951445	-22.7 ± 1.7	-6.8 ± 1.7	U4					10.978 ± 0.021	10.500 ± 0.024	10.398 ± 0.025	
14421590-4100183	-31.6 ± 2.4	-25.1 ± 2.4	PX	11.052 ± 0.117	A7	1.013 ± 0.119	A7	9.281 ± 0.020	8.710 ± 0.046	8.598 ± 0.014	a
14421965-4432065	0.8 ± 1.0	11.9 ± 1.0	U4	9.722 ± 0.043	T2	1.326 ± 0.073	T2	7.508 ± 0.020	6.841 ± 0.040	6.651 ± 0.024	
14432493-5643393	-15.1 ± 2.3	-12.2 ± 2.2	PX	10.638 ± 0.017	A7	0.723 ± 0.026	A7	9.103 ± 0.018	8.722 ± 0.025	8.552 ± 0.020	
14433325-5241213	-9.7 ± 1.2	-19.7 ± 1.1	U4					10.716 ± 0.023	10.254 ± 0.027	10.139 ± 0.025	
14442536-4329552	-21.3 ± 1.9	-18.3 ± 2.1	U4	14.099 ± 0.012	A7	1.402 ± 0.071	A7	10.983 ± 0.023	10.279 ± 0.021	10.104 ± 0.023	

Table 4.4 (cont'd)

2MASS	μ_α (mas yr^{-1})	μ_δ (mas yr^{-1})	Ref.	V (mag)	Ref.	B–V (mag)	Ref.	J (mag)	H (mag)	K_S (mag)	Note
14472343-3503134	-27.8 ± 0.9	-37.7 ± 1.3	U4	11.552 ± 0.017	A7	1.045 ± 0.043	A7	9.608 ± 0.023	9.057 ± 0.026	8.929 ± 0.023	
14481320-4102590	-20.5 ± 1.2	-22.1 ± 1.8	U4	11.180 ± 0.059	A7	0.922 ± 0.070	A7	9.305 ± 0.026	8.761 ± 0.046	8.620 ± 0.021	
14502581-3506486	-15.4 ± 0.9	-16.4 ± 2.0	U4	10.629 ± 0.039	A7	0.893 ± 0.042	A7	8.751 ± 0.025	8.243 ± 0.023	8.109 ± 0.023	
14503508-3459056	-15.1 ± 0.9	-20.2 ± 1.2	U4	12.055 ± 0.083	A7	1.081 ± 0.122	A7	9.643 ± 0.025	9.038 ± 0.024	8.881 ± 0.023	
14522619-3740088	-17.9 ± 0.8	-19.7 ± 1.1	U4	12.075 ± 0.042	A7	1.116 ± 0.072	A7	9.917 ± 0.024	9.353 ± 0.023	9.227 ± 0.023	
14524198-4141552	-20.4 ± 1.1	-20.9 ± 1.1	U4	11.159 ± 0.024	A7	1.032 ± 0.057	A7	9.045 ± 0.024	8.380 ± 0.026	8.289 ± 0.031	
14541121-3955233	-24.8 ± 1.0	-25.0 ± 1.0	U4	11.631 ± 0.038	A7	1.000 ± 0.064	A7	9.700 ± 0.024	9.126 ± 0.024	8.999 ± 0.021	
14552673-5129013	-18.2 ± 1.3	-18.4 ± 2.1	U4	10.588 ± 0.056	T2	0.641 ± 0.067	T2	9.165 ± 0.018	8.763 ± 0.036	8.663 ± 0.019	
14560001-3124581	-16.6 ± 0.8	-4.2 ± 0.8	U4	11.469 ± 0.161	T2	0.761 ± 0.233	T2	9.491 ± 0.023	9.048 ± 0.026	8.865 ± 0.023	
14571217-3107596	-10.6 ± 1.9	-4.7 ± 1.0	U4					9.166 ± 0.027	8.411 ± 0.040	8.262 ± 0.018	
14574495-4141394	-23.6 ± 1.6	-18.2 ± 3.3	U4	12.913 ± 0.065	A7	1.299 ± 0.086	A7	10.163 ± 0.023	9.477 ± 0.024	9.351 ± 0.021	
14583744-3915033	-28.0 ± 2.1	-27.0 ± 2.0	U4	12.980 ± 0.071	A7	1.461 ± 0.107	A7	9.537 ± 0.026	8.841 ± 0.047	8.648 ± 0.026	
14583769-3540302	-21.6 ± 1.0	-23.3 ± 1.1	U4	10.793 ± 0.034	A7	1.012 ± 0.047	A7	8.639 ± 0.024	8.062 ± 0.055	7.870 ± 0.026	
14584573-3315102	-40.0 ± 4.3	-25.4 ± 3.2	PX	11.367 ± 0.056	A7	0.893 ± 0.069	A7	9.646 ± 0.011	9.172 ± 0.020	9.100 ± 0.019	a
14592275-4013120	-26.5 ± 1.1	-25.5 ± 1.4	U4	9.712 ± 0.045	T2	0.765 ± 0.058	T2	8.324 ± 0.021	7.955 ± 0.046	7.814 ± 0.027	
14594473-3425465	-27.1 ± 1.8	-28.2 ± 1.1	U4	10.939 ± 0.031	A7	1.062 ± 0.059	A7	8.884 ± 0.024	8.299 ± 0.026	8.154 ± 0.024	
15003768-4308339	-17.0 ± 1.0	-21.2 ± 1.0	U4	11.897 ± 0.045	A7	1.053 ± 0.088	A7	9.715 ± 0.023	9.094 ± 0.025	8.950 ± 0.023	
15005189-4331212	-20.1 ± 2.1	-19.1 ± 2.0	T2	11.196 ± 0.059	A7	0.880 ± 0.083	A7	9.316 ± 0.023	8.853 ± 0.025	8.734 ± 0.023	
15022600-3405131	-18.1 ± 1.2	-19.6 ± 2.9	U4	12.151 ± 0.108	A7	1.179 ± 0.134	A7	10.115 ± 0.027	9.510 ± 0.032	9.277 ± 0.025	
15023844-4156105	-8.3 ± 2.7	-3.5 ± 1.3	U4					10.824 ± 0.023	10.164 ± 0.025	10.010 ± 0.023	

Table 4.4 (cont'd)

2MASS	μ_α (mas yr^{-1})	μ_δ (mas yr^{-1})	Ref.	V (mag)	Ref.	B–V (mag)	Ref.	J (mag)	H (mag)	K_S (mag)	Note
15033281-3033435	-32.3 ± 2.0	-8.4 ± 1.3	U4					10.197 ± 0.025	9.632 ± 0.021	9.454 ± 0.017	
15034365-5156318	-9.0 ± 1.5	-18.6 ± 2.7	U4	12.054 ± 0.251	T2	0.524 ± 0.299	T2	10.330 ± 0.024	9.823 ± 0.024	9.697 ± 0.021	
15035213-3906283	-26.4 ± 1.4	-22.5 ± 1.0	U4	11.840 ± 0.035	A7	1.248 ± 0.042	A7	9.393 ± 0.024	8.719 ± 0.049	8.560 ± 0.021	
15044217-3018552	-8.0 ± 1.7	2.1 ± 1.7	U4					10.600 ± 0.022	10.121 ± 0.027	9.977 ± 0.022	
15052586-3857031	-25.0 ± 1.0	-25.4 ± 1.1	U4	12.088 ± 0.010	A7	1.329 ± 0.014	A7	9.869 ± 0.023	9.253 ± 0.022	9.124 ± 0.021	
15054424-3312508	-22.4 ± 1.1	-19.7 ± 1.4	U4	12.283 ± 0.049	A7	1.140 ± 0.056	A7	9.982 ± 0.022	9.404 ± 0.022	9.234 ± 0.021	
15055685-4312031	-25.8 ± 1.1	-27.7 ± 1.1	U4	12.782 ± 0.061	A7	1.356 ± 0.097	A7	9.893 ± 0.022	9.209 ± 0.025	9.039 ± 0.022	
15064258-3047326	-24.3 ± 1.6	-28.3 ± 1.6	U4	13.063 ± 0.114	A7	1.361 ± 0.184	A7	10.225 ± 0.024	9.557 ± 0.026	9.368 ± 0.023	
15071481-3504595	-30.2 ± 1.7	-28.5 ± 1.1	U4	10.494 ± 0.064	T2	0.874 ± 0.084	T2	8.893 ± 0.021	8.416 ± 0.053	8.336 ± 0.023	
15072758-4601073	-19.0 ± 1.3	-18.1 ± 1.2	U4	11.330 ± 0.046	A7	0.844 ± 0.072	A7	9.735 ± 0.024	9.284 ± 0.030	9.131 ± 0.021	
15075415-4730288	-25.2 ± 0.9	-16.9 ± 1.0	U4	11.385 ± 0.045	A7	0.956 ± 0.067	A7	9.536 ± 0.027	8.975 ± 0.022	8.809 ± 0.021	
15080509-3337556	-28.2 ± 1.1	-28.5 ± 1.1	U4	11.949 ± 0.060	A7	1.197 ± 0.074	A7	9.454 ± 0.024	8.822 ± 0.031	8.620 ± 0.023	
15082754-5801220	-13.4 ± 1.0	-17.9 ± 1.2	U4	11.798 ± 0.194	T2	0.958 ± 0.274	T2	10.092 ± 0.015	9.721 ± 0.024	9.491 ± 0.015	a
15083773-4423170	-16.9 ± 1.9	-15.4 ± 1.6	U4	10.579 ± 0.054	A7	0.659 ± 0.057	A7	9.359 ± 0.024	8.925 ± 0.024	8.809 ± 0.021	
15083849-4400519	-23.5 ± 2.1	-24.2 ± 1.9	T2	10.538 ± 0.058	T2	0.637 ± 0.072	T2	8.950 ± 0.024	8.518 ± 0.029	8.446 ± 0.020	
15085379-3715467	-20.3 ± 0.9	-25.4 ± 1.3	U4					9.767 ± 0.024	9.146 ± 0.022	9.002 ± 0.019	
15085472-4303136	-22.2 ± 1.2	-21.4 ± 2.7	U4	11.182 ± 0.047	A7	0.903 ± 0.051	A7	9.531 ± 0.024	9.032 ± 0.022	8.916 ± 0.021	
15092793-4650572	-21.9 ± 1.2	-17.5 ± 1.0	U4	10.495 ± 0.056	T2	0.951 ± 0.074	T2	8.377 ± 0.041	7.816 ± 0.040	7.716 ± 0.024	
15102954-3902566	-18.3 ± 1.1	-19.3 ± 1.3	U4	11.624 ± 0.028	A7	0.977 ± 0.048	A7	9.945 ± 0.026	9.396 ± 0.022	9.274 ± 0.021	
15105821-3926499	-20.2 ± 1.2	-39.7 ± 1.2	U4	11.172 ± 0.098	T2	0.945 ± 0.155	T2	8.878 ± 0.006	8.375 ± 0.013	8.264 ± 0.009	a

Table 4.4 (cont'd)

2MASS	μ_α (mas yr^{-1})	μ_δ (mas yr^{-1})	Ref.	V (mag)	Ref.	B–V (mag)	Ref.	J (mag)	H (mag)	K_S (mag)	Note
15105821-3926499	-20.2 ± 1.2	-39.7 ± 1.2	U4	11.172 ± 0.098	T2	0.945 ± 0.155	T2	8.878 ± 0.006	8.375 ± 0.013	8.264 ± 0.009	a
15110450-3251304	-21.9 ± 2.5	-24.4 ± 0.9	U4	11.786 ± 0.037	A7	1.247 ± 0.061	A7	9.467 ± 0.040	8.770 ± 0.036	8.670 ± 0.035	
15113968-3248560	-14.5 ± 1.9	-19.7 ± 1.2	U4	13.767 ± 0.047	A7	1.529 ± 0.062	A7	10.266 ± 0.026	9.605 ± 0.023	9.376 ± 0.021	
15122700-4453385	-35.9 ± 1.6	7.1 ± 1.7	U4	11.550 ± 0.154	T2	1.029 ± 0.236	T2	9.999 ± 0.024	9.603 ± 0.025	9.490 ± 0.019	
15124447-3116482	-17.2 ± 1.3	-22.9 ± 0.8	U4	11.610 ± 0.056	A7	1.009 ± 0.069	A7	9.601 ± 0.024	9.079 ± 0.024	8.919 ± 0.019	
15130869-4450158	-9.5 ± 2.6	-10.0 ± 1.3	U4	10.763 ± 0.089	T2	1.462 ± 0.217	T2	8.527 ± 0.018	7.969 ± 0.053	7.806 ± 0.033	
15135817-4629145	-14.8 ± 2.2	-20.1 ± 2.2	U4	12.627 ± 0.058	A7	1.283 ± 0.085	A7	10.161 ± 0.023	9.528 ± 0.022	9.359 ± 0.019	
15140754-4103361	-21.8 ± 1.3	-29.8 ± 1.2	U4	10.370 ± 0.010	HP	0.508 ± 0.057	T2	9.142 ± 0.032	8.721 ± 0.044	8.570 ± 0.023	
15144748-4220149	-20.3 ± 2.1	-15.7 ± 1.4	U4	11.289 ± 0.042	A7	0.890 ± 0.057	A7	9.561 ± 0.022	9.126 ± 0.022	9.011 ± 0.021	
15151856-4146354	-25.5 ± 1.7	-23.3 ± 1.7	U4	13.075 ± 0.016	A7	1.405 ± 0.026	A7	10.072 ± 0.026	9.410 ± 0.022	9.235 ± 0.019	
15152295-5441088	-16.5 ± 2.5	-22.1 ± 1.4	U4	11.971 ± 0.039	A7	1.037 ± 0.079	A7	9.927 ± 0.029	9.458 ± 0.037	9.149 ± 0.023	
15153210-3005336	-49.8 ± 0.9	-14.9 ± 1.1	U4	10.586 ± 0.083	T2	0.997 ± 0.113	T2	9.040 ± 0.023	8.513 ± 0.026	8.469 ± 0.024	
15154537-3331597	-25.2 ± 1.3	-25.2 ± 1.3	U4	10.726 ± 0.049	A7	0.925 ± 0.069	A7	8.981 ± 0.022	8.461 ± 0.020	8.384 ± 0.023	
15155274-4418173	-18.9 ± 1.8	-20.5 ± 2.9	U4	12.446 ± 0.088	A7	1.070 ± 0.136	A7	10.181 ± 0.021	9.573 ± 0.022	9.454 ± 0.021	
15161044-3851565	-18.5 ± 1.0	0.6 ± 1.0	U4	10.261 ± 0.051	T2	0.930 ± 0.071	T2	8.495 ± 0.024	7.955 ± 0.040	7.859 ± 0.018	
15163663-4407204	-19.2 ± 1.5	-20.2 ± 2.6	U4	11.968 ± 0.017	A7	1.027 ± 0.022	A7	9.898 ± 0.022	9.316 ± 0.022	9.193 ± 0.019	
15171083-3434194	-24.5 ± 3.2	-23.9 ± 3.2	PX					9.269 ± 0.023	8.805 ± 0.046	8.647 ± 0.023	
15180123-4444269	-25.0 ± 1.4	-29.9 ± 2.1	U4	11.621 ± 0.014	A7	0.953 ± 0.045	A7	9.925 ± 0.024	9.494 ± 0.027	9.343 ± 0.023	
15182692-3738021	-19.4 ± 1.0	-23.2 ± 1.8	U4	10.825 ± 0.018	A7	0.859 ± 0.042	A7	9.081 ± 0.035	8.618 ± 0.046	8.506 ± 0.021	
15185282-4050528	-19.3 ± 1.1	-20.7 ± 1.5	U4	10.929 ± 0.013	A7	0.917 ± 0.032	A7	9.145 ± 0.030	8.659 ± 0.020	8.547 ± 0.027	

Table 4.4 (cont'd)

2MASS	μ_α (mas yr^{-1})	μ_δ (mas yr^{-1})	Ref.	V (mag)	Ref.	B–V (mag)	Ref.	J (mag)	H (mag)	K_S (mag)	Note
15191600-4056075	-23.9 ± 1.3	-27.6 ± 1.9	U4	11.456 ± 0.078	A7	0.985 ± 0.125	A7	9.549 ± 0.026	9.021 ± 0.025	8.830 ± 0.021	
15191807-2943204	-15.0 ± 1.6	-24.1 ± 2.5	U4	12.889 ± 0.111	A7	1.259 ± 0.131	A7	10.124 ± 0.026	9.483 ± 0.024	9.287 ± 0.021	
15193457-2846217	-14.2 ± 1.4	2.5 ± 3.3	U4	10.596 ± 0.082	T2	0.936 ± 0.102	T2	9.137 ± 0.030	8.604 ± 0.029	8.537 ± 0.035	
15200259-4638340	-23.9 ± 1.3	-14.7 ± 1.3	U4	11.227 ± 0.113	T2	0.557 ± 0.126	T2	9.661 ± 0.023	9.286 ± 0.024	9.157 ± 0.023	
15202415-3037317	-26.7 ± 1.4	-31.6 ± 1.1	U4	11.245 ± 0.101	A7	1.175 ± 0.154	A7	8.784 ± 0.030	8.155 ± 0.046	7.957 ± 0.021	
15215241-2842383	-19.1 ± 1.1	-27.4 ± 1.5	U4	11.528 ± 0.047	A7	0.934 ± 0.070	A7	9.534 ± 0.024	9.088 ± 0.029	8.909 ± 0.023	
15220457-5634346	-24.5 ± 1.1	-23.9 ± 1.0	U4	11.273 ± 0.123	T2	0.601 ± 0.147	T2	9.643 ± 0.023	9.207 ± 0.025	9.073 ± 0.026	
15220743-3930140	-27.2 ± 1.8	-28.7 ± 1.8	U4					10.411 ± 0.022	9.822 ± 0.021	9.676 ± 0.019	
15221162-3959509	-20.7 ± 1.3	-25.3 ± 1.9	U4	12.008 ± 0.067	A7	1.039 ± 0.107	A7	9.906 ± 0.023	9.297 ± 0.023	9.100 ± 0.019	
15221627-2652252	-7.8 ± 2.2	-8.3 ± 1.7	U4	11.848 ± 0.236	T2	1.257 ± 0.362	T2	9.520 ± 0.023	8.869 ± 0.024	8.658 ± 0.023	
15222449-3337352	-20.0 ± 1.3	-17.1 ± 2.5	U4					10.286 ± 0.024	9.788 ± 0.022	9.652 ± 0.023	
15230505-3627294	-35.3 ± 1.6	-30.1 ± 1.6	U4					10.402 ± 0.027	9.771 ± 0.023	9.587 ± 0.024	
15232557-4055467	-23.9 ± 1.1	-25.0 ± 2.0	U4	12.069 ± 0.020	A7	1.038 ± 0.041	A7	9.957 ± 0.023	9.389 ± 0.023	9.260 ± 0.023	
15234137-4004455	-2.7 ± 1.2	-12.5 ± 1.2	U4					10.568 ± 0.027	10.013 ± 0.022	9.905 ± 0.021	
15235794-3619585	-19.2 ± 1.3	-20.8 ± 2.4	U4	12.036 ± 0.010	A7	1.135 ± 0.014	A7	9.976 ± 0.023	9.423 ± 0.024	9.296 ± 0.021	
15240305-3209508	-20.7 ± 1.0	-24.0 ± 1.4	U4	12.343 ± 0.031	A7	1.267 ± 0.081	A7	9.502 ± 0.026	8.817 ± 0.040	8.644 ± 0.020	
15240670-3601013	-12.9 ± 0.9	-31.1 ± 0.9	PX	8.730 ± 0.010	HP	0.893 ± 0.026	T2	7.037 ± 0.018	6.596 ± 0.034	6.470 ± 0.021	
15241147-3030582	-20.4 ± 1.8	-28.1 ± 1.0	U4	10.921 ± 0.075	T2	0.832 ± 0.100	T2	9.312 ± 0.027	8.840 ± 0.059	8.682 ± 0.019	
15241303-3030572	-11.3 ± 1.7	-13.0 ± 3.6	U4					10.416 ± 0.009	9.727 ± 0.027	9.507 ± 0.019	a
15243236-3652027	-16.5 ± 2.1	-21.7 ± 1.9	U4	11.159 ± 0.010	A7	0.897 ± 0.014	A7	9.549 ± 0.023	9.049 ± 0.022	8.930 ± 0.019	

Table 4.4 (cont'd)

2MASS	μ_α (mas yr^{-1})	μ_δ (mas yr^{-1})	Ref.	V (mag)	Ref.	B–V (mag)	Ref.	J (mag)	H (mag)	K_S (mag)	Note
15243933-2102040	3.0 ± 0.9	-34.6 ± 1.5	U4	10.674 ± 0.079	T2	0.835 ± 0.096	T2	9.421 ± 0.025	9.022 ± 0.025	8.919 ± 0.023	
15244741-4257591	-11.6 ± 0.9	-26.6 ± 0.9	U4					9.864 ± 0.024	9.354 ± 0.026	9.200 ± 0.025	
15250358-3604455	-14.3 ± 3.4	-16.3 ± 1.4	U4	10.740 ± 0.010	A7	0.869 ± 0.014	A7	8.998 ± 0.030	8.465 ± 0.038	8.320 ± 0.023	
15251724-2729309	-46.1 ± 1.1	-30.4 ± 0.9	U4	10.848 ± 0.097	T2	1.237 ± 0.197	T2	8.815 ± 0.026	8.280 ± 0.047	8.158 ± 0.024	
15253316-3613467	-15.5 ± 1.2	-18.6 ± 2.4	U4	11.679 ± 0.010	A7	1.028 ± 0.014	A7	9.564 ± 0.024	9.004 ± 0.022	8.842 ± 0.021	
15253666-3537319	-17.8 ± 1.4	-23.7 ± 1.4	U4	12.440 ± 0.010	W97	1.240 ± 0.020	W97	9.780 ± 0.021	9.135 ± 0.024	8.963 ± 0.019	
15255964-4501157	-21.1 ± 1.0	-20.1 ± 1.1	U4	10.872 ± 0.042	A7	0.812 ± 0.060	A7	9.443 ± 0.023	8.984 ± 0.059	8.901 ± 0.019	
15262805-5549569	-30.3 ± 2.4	-16.3 ± 1.9	U4	12.228 ± 0.010	A7	0.863 ± 0.014	A7	10.556 ± 0.026	10.040 ± 0.024	9.968 ± 0.027	
15264407-3849588	-7.3 ± 1.0	-6.1 ± 2.0	U4	11.883 ± 0.189	T2	1.347 ± 0.312	T2	10.625 ± 0.024	10.094 ± 0.023	9.989 ± 0.023	
15264611-3849198	0.5 ± 0.9	-11.0 ± 1.8	U4					8.933 ± 0.021	8.140 ± 0.034	7.986 ± 0.024	
15265257-3722062	-27.2 ± 1.1	-31.8 ± 1.1	U4					9.981 ± 0.026	9.319 ± 0.023	9.141 ± 0.023	
15271052-4138334	-0.3 ± 2.0	-41.1 ± 1.6	U4	10.330 ± 0.010	HP	0.681 ± 0.062	T2	8.729 ± 0.026	8.293 ± 0.034	8.166 ± 0.023	
15272286-3604087	-28.5 ± 1.3	-27.0 ± 1.3	U4					9.351 ± 0.029	8.672 ± 0.055	8.436 ± 0.024	
15280113-3751360	-6.4 ± 1.4	-9.4 ± 1.6	U4	12.118 ± 0.245	T2	0.918 ± 0.348	T2	9.946 ± 0.021	9.359 ± 0.022	9.266 ± 0.021	
15280288-3751087	-7.0 ± 0.9	-10.3 ± 1.2	U4					9.655 ± 0.024	9.101 ± 0.025	8.985 ± 0.021	
15280322-2600034	-16.1 ± 2.0	-18.0 ± 1.4	U4	12.246 ± 0.247	T2	0.398 ± 0.319	T2	9.428 ± 0.027	8.734 ± 0.042	8.584 ± 0.021	
15284402-3117387	19.9 ± 2.0	48.0 ± 1.9	T2	9.546 ± 0.029	T2	0.910 ± 0.040	T2	7.434 ± 0.027	7.022 ± 0.036	6.919 ± 0.023	
15284402-3117387	19.9 ± 2.0	48.0 ± 1.9	T2	9.788 ± 0.037	T2	0.743 ± 0.046	T2	7.434 ± 0.027	7.022 ± 0.036	6.919 ± 0.023	
15293858-3546513	-21.7 ± 2.0	-26.1 ± 2.1	T2	10.632 ± 0.010	A7	0.952 ± 0.014	A7	8.788 ± 0.020	8.257 ± 0.033	8.119 ± 0.016	
15294727-3628374	-14.8 ± 1.0	-18.4 ± 1.4	U4	11.875 ± 0.010	A7	1.051 ± 0.014	A7	9.643 ± 0.025	9.106 ± 0.027	8.970 ± 0.025	

Table 4.4 (cont'd)

2MASS	μ_α (mas yr^{-1})	μ_δ (mas yr^{-1})	Ref.	V (mag)	Ref.	B–V (mag)	Ref.	J (mag)	H (mag)	K_S (mag)	Note
15294888-4522457	-16.1 ± 2.7	-24.4 ± 1.2	U4	12.778 ± 0.200	A7	1.173 ± 0.248	A7	10.041 ± 0.026	9.384 ± 0.022	9.251 ± 0.019	
15295661-3135446	-24.6 ± 1.2	-25.6 ± 1.3	U4	12.258 ± 0.023	A7	1.213 ± 0.053	A7	9.864 ± 0.028	9.241 ± 0.031	9.062 ± 0.023	
15304790-3022054	-23.9 ± 0.8	-26.7 ± 0.9	U4					9.381 ± 0.024	8.805 ± 0.034	8.704 ± 0.023	
15311824-4333323	-16.7 ± 1.6	-14.2 ± 1.5	U4					9.979 ± 0.027	9.358 ± 0.022	9.196 ± 0.021	
15312047-3855116	-0.3 ± 0.9	-13.9 ± 0.9	U4	11.023 ± 0.100	T2	1.287 ± 0.201	T2	8.680 ± 0.023	8.075 ± 0.027	7.924 ± 0.023	
15312193-3329394	-21.6 ± 1.3	-28.9 ± 1.0	U4	10.824 ± 0.021	A7	0.818 ± 0.040	A7	9.391 ± 0.022	8.941 ± 0.067	8.801 ± 0.021	
15312961-3021537	-16.1 ± 1.9	-21.6 ± 1.0	U4					9.981 ± 0.026	9.318 ± 0.027	9.102 ± 0.021	
15313413-3602287	-17.5 ± 1.1	-20.6 ± 1.0	U4	11.672 ± 0.010	A7	1.069 ± 0.014	A7	9.681 ± 0.023	9.101 ± 0.026	9.006 ± 0.025	
15313716-2156489	7.0 ± 1.7	16.3 ± 0.8	U4	11.227 ± 0.156	T2	1.447 ± 0.350	T2	9.249 ± 0.022	8.711 ± 0.034	8.587 ± 0.019	
15320739-2427130	-21.2 ± 0.9	-3.3 ± 0.8	U4	10.354 ± 0.065	T2	1.215 ± 0.108	T2	8.470 ± 0.026	8.032 ± 0.049	7.876 ± 0.031	
15333037-2003264	-11.1 ± 1.0	-9.8 ± 1.1	U4	9.594 ± 0.036	T2	0.909 ± 0.050	T2	7.670 ± 0.020	7.215 ± 0.047	7.122 ± 0.029	
15340737-3916171	-24.7 ± 1.1	-26.3 ± 1.1	U4	10.889 ± 0.026	A7	0.869 ± 0.055	A7	9.141 ± 0.024	8.646 ± 0.053	8.553 ± 0.023	
15342292-2514386	-22.5 ± 1.1	-0.4 ± 1.6	U4	10.316 ± 0.055	T2	1.081 ± 0.082	T2	7.862 ± 0.023	7.266 ± 0.033	7.096 ± 0.020	
15342313-3300087	-17.1 ± 0.9	-23.6 ± 2.5	U4					9.967 ± 0.022	9.299 ± 0.023	9.130 ± 0.021	
15343816-4002280	-24.8 ± 1.2	-34.0 ± 1.2	U4	12.085 ± 0.048	A7	1.211 ± 0.048	A7	9.554 ± 0.024	8.908 ± 0.022	8.754 ± 0.019	
15350044-3915143	-11.2 ± 1.1	-44.5 ± 1.5	U4	11.551 ± 0.172	T2	1.483 ± 0.329	T2	9.878 ± 0.024	9.327 ± 0.022	9.173 ± 0.023	
15351524-4156586	-13.4 ± 1.1	-10.3 ± 1.1	U4	11.359 ± 0.116	T2	1.088 ± 0.208	T2	9.831 ± 0.022	9.243 ± 0.023	9.067 ± 0.026	
15355780-2324046	-15.9 ± 1.4	-17.8 ± 0.9	U4	12.373 ± 0.023	A7	1.091 ± 0.033	A7	10.161 ± 0.023	9.605 ± 0.027	9.425 ± 0.025	
15355876-4456355	-23.3 ± 2.1	-27.6 ± 2.0	U4					10.056 ± 0.023	9.335 ± 0.024	9.154 ± 0.020	
15364094-2923574	-28.8 ± 2.0	-14.5 ± 1.8	U4	14.029 ± 0.020	A7	1.131 ± 0.022	A7	10.437 ± 0.026	9.861 ± 0.030	9.574 ± 0.026	

Table 4.4 (cont'd)

2MASS	μ_α (mas yr^{-1})	μ_δ (mas yr^{-1})	Ref.	V (mag)	Ref.	B–V (mag)	Ref.	J (mag)	H (mag)	K_S (mag)	Note
15370214-3136398	-18.2 ± 1.5	-29.3 ± 1.4	PX	9.989 ± 0.044	T2	0.629 ± 0.054	T2	8.266 ± 0.032	7.787 ± 0.042	7.742 ± 0.026	
15370261-2942430	-17.0 ± 1.7	-10.8 ± 1.3	U4					9.984 ± 0.026	9.465 ± 0.025	9.243 ± 0.025	
15371129-4015566	-16.8 ± 1.5	-21.6 ± 1.4	PX	10.570 ± 0.010	HP	0.844 ± 0.021	A7	8.957 ± 0.021	8.437 ± 0.047	8.292 ± 0.033	
15371218-2644516	2.8 ± 2.5	15.0 ± 1.3	U4					10.285 ± 0.024	9.786 ± 0.021	9.657 ± 0.021	
15371991-3041150	4.3 ± 1.0	-15.4 ± 2.2	U4					9.897 ± 0.024	9.250 ± 0.025	9.050 ± 0.019	
15374917-1840449	-12.8 ± 1.3	-10.2 ± 1.7	U4	11.684 ± 0.021	A7	0.936 ± 0.030	A7	9.892 ± 0.023	9.349 ± 0.024	9.254 ± 0.023	
15375134-3045160	-19.8 ± 1.0	-20.7 ± 1.1	U4	11.683 ± 0.068	A7	1.011 ± 0.110	A7	9.300 ± 0.024	8.755 ± 0.036	8.563 ± 0.019	
15380264-3807230	-20.3 ± 1.0	-23.2 ± 1.0	U4	12.317 ± 0.006	A7	1.145 ± 0.012	A7	10.112 ± 0.026	9.572 ± 0.024	9.376 ± 0.024	
15381792-2337306	-9.3 ± 1.4	-24.1 ± 2.0	U4					10.603 ± 0.021	10.107 ± 0.021	9.962 ± 0.019	
15383827-3916553	-19.8 ± 1.2	-26.4 ± 3.3	U4	11.606 ± 0.023	A7	1.039 ± 0.029	A7	9.594 ± 0.027	9.008 ± 0.025	8.854 ± 0.023	
15384306-4411474	-23.2 ± 1.6	-28.4 ± 1.5	T2	10.277 ± 0.052	T2	0.756 ± 0.068	T2	8.805 ± 0.054	8.344 ± 0.042	8.210 ± 0.031	
15392776-3446171	-19.5 ± 1.9	-14.3 ± 1.9	U4					9.189 ± 0.036	8.414 ± 0.067	7.982 ± 0.017	
15394637-3451027	-15.0 ± 3.2	-16.9 ± 1.4	U4					9.631 ± 0.027	8.993 ± 0.025	8.861 ± 0.026	
15400244-4634187	-22.9 ± 1.8	-18.1 ± 1.8	U4					9.861 ± 0.023	9.284 ± 0.023	9.117 ± 0.019	
15404116-3756185	-22.8 ± 1.4	-26.8 ± 1.4	U4	12.366 ± 0.061	A7	1.195 ± 0.089	A7	9.927 ± 0.024	9.324 ± 0.029	9.187 ± 0.026	
15410679-2656263	-17.7 ± 1.2	-26.1 ± 1.9	U4	11.254 ± 0.078	A7	0.889 ± 0.093	A7	9.509 ± 0.024	9.061 ± 0.027	8.920 ± 0.023	
15413114-5330296	-24.5 ± 2.2	-33.2 ± 1.4	U4	11.070 ± 0.010	T06	0.980 ± 0.010	T06	9.060 ± 0.025	8.475 ± 0.021	8.384 ± 0.022	
15413121-2520363	-18.2 ± 1.6	-27.4 ± 1.5	PX	9.939 ± 0.039	T2	0.813 ± 0.054	T2	7.974 ± 0.030	7.367 ± 0.033	7.241 ± 0.024	
15414732-1804591	4.1 ± 0.9	-9.1 ± 1.0	U4	10.560 ± 0.070	T2	0.778 ± 0.088	T2	9.127 ± 0.028	8.614 ± 0.044	8.581 ± 0.024	
15420518-3601317	-23.2 ± 1.4	-24.6 ± 1.4	U4					9.919 ± 0.023	9.250 ± 0.030	9.088 ± 0.023	

Table 4.4 (cont'd)

2MASS	μ_α (mas yr^{-1})	μ_δ (mas yr^{-1})	Ref.	V (mag)	Ref.	B–V (mag)	Ref.	J (mag)	H (mag)	K_S (mag)	Note
15421600-4435440	-5.9 ± 1.2	-11.4 ± 1.0	U4	10.442 ± 0.078	T2	1.391 ± 0.169	T2	8.162 ± 0.027	7.629 ± 0.057	7.370 ± 0.023	
15422385-4625471	-15.1 ± 3.1	-13.4 ± 3.1	PX					10.812 ± 0.024	10.391 ± 0.026	10.275 ± 0.024	
15424991-2536406	-19.0 ± 1.1	-23.5 ± 1.3	U4	10.793 ± 0.088	T2	0.778 ± 0.105	T2	8.843 ± 0.023	8.320 ± 0.031	8.177 ± 0.020	
15430669-4643064	-4.7 ± 2.1	-24.2 ± 2.4	U4					10.336 ± 0.024	9.706 ± 0.023	9.570 ± 0.022	
15433953-2909035	-12.1 ± 1.8	3.9 ± 5.1	U4					10.967 ± 0.022	10.356 ± 0.022	10.235 ± 0.021	
15434883-3927377	-16.2 ± 3.5	-16.6 ± 3.3	U4					10.461 ± 0.030	9.923 ± 0.028	9.775 ± 0.023	
15435905-2622516	-11.9 ± 1.9	-24.5 ± 1.9	U4	14.073 ± 0.034	A7	1.436 ± 0.072	A7	10.717 ± 0.026	10.042 ± 0.022	9.833 ± 0.021	
15440376-3311110	-18.3 ± 1.5	-25.3 ± 1.8	U4	10.959 ± 0.020	A7	0.902 ± 0.021	A7	9.062 ± 0.021	8.546 ± 0.021	8.414 ± 0.026	
15441334-2522590	-17.2 ± 2.0	-23.8 ± 2.0	U4	12.920 ± 0.048	A7	1.423 ± 0.075	A7	9.986 ± 0.023	9.272 ± 0.023	9.082 ± 0.027	
15442874-4745415	-13.8 ± 1.5	-27.7 ± 1.5	U4	12.749 ± 0.013	A7	1.433 ± 0.040	A7	9.785 ± 0.024	9.068 ± 0.022	8.893 ± 0.021	
15444712-3811406	-25.4 ± 1.8	-21.5 ± 1.3	U4	11.807 ± 0.020	A7	1.328 ± 0.022	A7	9.202 ± 0.009	8.571 ± 0.019	8.373 ± 0.013	a
15451286-3417305	-16.2 ± 1.6	-19.9 ± 1.3	PX	10.310 ± 0.010	HP	1.264 ± 0.009	HP	7.573 ± 0.021	6.866 ± 0.029	6.480 ± 0.020	
15455225-4222163	-16.6 ± 1.4	-28.8 ± 0.9	U4	10.565 ± 0.037	A7	0.967 ± 0.049	A7	8.673 ± 0.023	8.081 ± 0.040	7.933 ± 0.024	
15462958-5217239	-20.5 ± 0.9	-22.9 ± 0.9	U4	11.160 ± 0.017	A7	0.757 ± 0.048	A7	9.653 ± 0.024	9.278 ± 0.028	9.150 ± 0.023	
15463111-5216580	-21.5 ± 1.4	-25.9 ± 1.4	U4					10.321 ± 0.023	9.641 ± 0.021	9.425 ± 0.019	
15464121-3618472	-14.4 ± 1.2	-21.8 ± 2.1	U4	11.458 ± 0.025	A7	0.887 ± 0.051	A7	9.490 ± 0.024	8.947 ± 0.025	8.783 ± 0.021	
15471063-1736244	-17.8 ± 1.6	-24.1 ± 1.7	U4	13.918 ± 0.045	A7	1.462 ± 0.082	A7	10.471 ± 0.022	9.765 ± 0.025	9.567 ± 0.025	
15474176-4018267	-18.0 ± 0.9	-28.0 ± 1.0	U4	11.200 ± 0.031	A7	0.929 ± 0.043	A7	9.294 ± 0.024	8.811 ± 0.034	8.662 ± 0.025	
15475575-2300331	-13.3 ± 1.3	-28.1 ± 1.2	U4					10.921 ± 0.023	10.374 ± 0.023	10.135 ± 0.019	
15480291-2908369	-16.5 ± 1.6	-22.4 ± 1.1	U4	10.887 ± 0.019	A7	0.860 ± 0.045	A7	9.212 ± 0.023	8.719 ± 0.026	8.624 ± 0.023	

Table 4.4 (cont'd)

2MASS	μ_α (mas yr^{-1})	μ_δ (mas yr^{-1})	Ref.	V (mag)	Ref.	B–V (mag)	Ref.	J (mag)	H (mag)	K_S (mag)	Note
15481148-4712297	-20.0 ± 1.9	-31.9 ± 1.0	U4	11.473 ± 0.039	A7	0.938 ± 0.080	A7	9.435 ± 0.024	8.889 ± 0.026	8.705 ± 0.021	
15481299-2349523	-25.7 ± 1.9	-24.9 ± 1.9	U4	13.934 ± 0.068	A7	1.466 ± 0.099	A7	10.190 ± 0.024	9.539 ± 0.023	9.268 ± 0.021	
15484204-4335207	-11.9 ± 2.2	-16.5 ± 1.2	U4	11.603 ± 0.050	A7	0.852 ± 0.093	A7	9.951 ± 0.023	9.475 ± 0.023	9.324 ± 0.019	
15490271-3102537	-20.0 ± 0.8	-21.4 ± 0.8	U4	10.947 ± 0.061	A7	0.886 ± 0.111	A7	9.163 ± 0.034	8.726 ± 0.024	8.552 ± 0.021	
15490667-1813113	-15.4 ± 1.9	3.7 ± 2.0	U4	11.990 ± 0.064	A7	0.879 ± 0.085	A7	10.498 ± 0.026	10.061 ± 0.029	9.943 ± 0.026	
15492100-2600062	-16.5 ± 1.1	-26.4 ± 0.9	U4	11.178 ± 0.043	A7	1.155 ± 0.048	A7	8.645 ± 0.020	8.127 ± 0.034	7.912 ± 0.027	
15494499-3925089	-19.0 ± 1.1	-25.5 ± 1.0	U4	10.640 ± 0.010	HP	0.940 ± 0.057	A7	8.833 ± 0.024	8.266 ± 0.027	8.141 ± 0.034	
15495840-4306370	-13.7 ± 1.2	-16.4 ± 1.1	U4	12.074 ± 0.109	A7	1.010 ± 0.158	A7	10.053 ± 0.024	9.473 ± 0.022	9.367 ± 0.021	
15495920-3629574	-13.7 ± 1.0	-22.7 ± 0.9	U4	11.536 ± 0.093	A7	0.962 ± 0.130	A7	9.560 ± 0.026	9.021 ± 0.024	8.884 ± 0.024	
15510142-1548286	-7.7 ± 2.7	-22.4 ± 3.0	U4	14.254 ± 0.033	A7	1.521 ± 0.053	A7	10.262 ± 0.027	9.644 ± 0.023	9.393 ± 0.023	
15510660-2402190	-15.7 ± 1.5	-19.8 ± 1.5	U4					10.665 ± 0.023	9.961 ± 0.025	9.734 ± 0.025	
15514535-2456513	-10.8 ± 1.0	-19.8 ± 1.0	U4	12.371 ± 0.026	A7	1.118 ± 0.127	A7	10.238 ± 0.024	9.726 ± 0.030	9.532 ± 0.025	
15521613-3218449	-18.6 ± 1.0	-16.6 ± 1.5	U4	11.558 ± 0.123	T2	1.172 ± 0.206	T2	10.203 ± 0.009	9.775 ± 0.022	9.655 ± 0.014	a
15522589-3920512	-17.2 ± 1.3	-28.3 ± 1.3	U4	12.314 ± 0.038	A7	1.112 ± 0.047	A7	10.048 ± 0.023	9.468 ± 0.022	9.299 ± 0.026	
15523122-2633529	-23.1 ± 1.0	-33.4 ± 2.1	U4					9.783 ± 0.022	9.166 ± 0.024	8.976 ± 0.023	
15530683-2247174	-14.0 ± 1.0	-24.8 ± 2.4	U4	13.543 ± 0.107	A7	1.541 ± 0.159	A7	9.684 ± 0.022	8.972 ± 0.049	8.677 ± 0.021	
15545141-3154463	-9.7 ± 1.3	-23.5 ± 1.4	U4	12.184 ± 0.192	A7	0.879 ± 0.234	A7	9.599 ± 0.026	8.773 ± 0.034	8.233 ± 0.020	
15550624-2521102	-12.5 ± 1.0	-23.8 ± 1.1	U4					9.411 ± 0.027	8.616 ± 0.031	8.510 ± 0.021	
15551621-1355136	-32.8 ± 1.1	-24.4 ± 1.3	U4					9.956 ± 0.022	9.343 ± 0.023	9.146 ± 0.021	
15552621-3338232	-16.9 ± 1.1	-29.9 ± 1.3	U4	12.376 ± 0.047	A7	1.126 ± 0.060	A7	10.158 ± 0.023	9.540 ± 0.024	9.353 ± 0.022	

Table 4.4 (cont'd)

2MASS	μ_α (mas yr^{-1})	μ_δ (mas yr^{-1})	Ref.	V (mag)	Ref.	B–V (mag)	Ref.	J (mag)	H (mag)	K_S (mag)	Note
15555324-4041435	-1.7 ± 2.4	-30.0 ± 2.4	PX					10.457 ± 0.022	10.071 ± 0.021	9.951 ± 0.020	
15560250-3643472	-25.0 ± 1.0	-39.3 ± 1.0	U4					9.352 ± 0.023	8.759 ± 0.024	8.593 ± 0.025	
15560921-3756057	-2.0 ± 4.0	-21.5 ± 4.0	PX	11.570 ± 0.010	HP			8.783 ± 0.021	8.089 ± 0.040	7.739 ± 0.023	
15561488-2100408	-12.6 ± 0.9	-39.7 ± 0.9	U4					10.442 ± 0.026	9.937 ± 0.022	9.794 ± 0.019	
15564402-4242301	-13.4 ± 1.8	-24.6 ± 2.5	U4	12.190 ± 0.010	T06	1.370 ± 0.010	T06	9.196 ± 0.035	8.481 ± 0.020	8.265 ± 0.029	
15565905-3933430	-15.1 ± 2.0	-21.6 ± 2.0	T2	10.830 ± 0.010	T06	0.790 ± 0.010	T06	9.254 ± 0.024	8.793 ± 0.021	8.694 ± 0.020	
15570234-1950419	-10.8 ± 1.1	-22.3 ± 1.3	U4	11.596 ± 0.020	A7	1.171 ± 0.051	A7	9.177 ± 0.025	8.488 ± 0.024	8.372 ± 0.025	
15573430-2321123	-13.3 ± 1.7	-26.5 ± 1.8	U4	13.833 ± 0.095	A7	1.738 ± 0.378	A7	9.932 ± 0.024	9.235 ± 0.026	8.992 ± 0.021	
15574362-4143377	-14.7 ± 1.5	-21.2 ± 1.7	U4	12.651 ± 0.056	A7	1.351 ± 0.082	A7	9.825 ± 0.023	9.078 ± 0.025	8.743 ± 0.023	
15574440-4049276	-17.1 ± 2.9	-19.4 ± 2.9	PX	12.446 ± 0.205	A7	1.272 ± 0.308	A7	9.193 ± 0.023	8.417 ± 0.029	8.120 ± 0.018	
15575002-2305094	-11.4 ± 4.3	-26.1 ± 1.3	U4					10.175 ± 0.026	9.480 ± 0.026	9.265 ± 0.021	
15581270-2328364	-11.1 ± 1.0	-22.1 ± 0.9	U4	10.310 ± 0.010	T06	0.810 ± 0.010	T06	8.574 ± 0.024	8.124 ± 0.021	8.018 ± 0.024	
15581474-4029175	-7.0 ± 2.9	-29.5 ± 2.9	PX	12.750 ± 0.037	A7	1.357 ± 0.048	A7	9.655 ± 0.023	8.982 ± 0.026	8.797 ± 0.023	
15582054-1837252	-14.7 ± 0.9	-23.6 ± 1.1	U4	10.231 ± 0.039	T2	0.821 ± 0.051	T2	8.279 ± 0.035	7.774 ± 0.063	7.614 ± 0.021	
15582850-1610379	-17.8 ± 2.1	-10.8 ± 2.5	U4	11.915 ± 0.179	T2	0.932 ± 0.253	T2	10.262 ± 0.026	9.792 ± 0.023	9.664 ± 0.024	
15583692-2257153	-9.6 ± 0.8	-19.7 ± 0.8	U4	10.139 ± 0.038	T2	0.778 ± 0.049	T2	8.358 ± 0.024	7.689 ± 0.047	7.053 ± 0.031	
15584772-1757595	-14.1 ± 1.0	-18.4 ± 1.0	U4	12.009 ± 0.054	A7	1.281 ± 0.065	A7	9.261 ± 0.022	8.535 ± 0.042	8.325 ± 0.024	
15590208-1844142	-7.7 ± 2.1	-24.5 ± 1.5	U4	12.022 ± 0.086	A7	1.278 ± 0.112	A7	9.002 ± 0.024	8.340 ± 0.017	8.106 ± 0.014	
15591101-1850442	-8.2 ± 1.6	-22.7 ± 1.6	U4	13.379 ± 0.150	A7	1.492 ± 0.185	A7	10.086 ± 0.024	9.324 ± 0.017	9.130 ± 0.015	
15591452-2606182	-10.1 ± 2.9	-27.7 ± 1.8	U4					9.925 ± 0.010	9.318 ± 0.038	9.116 ± 0.019	a

Table 4.4 (cont'd)

2MASS	μ_α (mas yr^{-1})	μ_δ (mas yr^{-1})	Ref.	V (mag)	Ref.	B–V (mag)	Ref.	J (mag)	H (mag)	K_S (mag)	Note
15591647-4157102	-8.9 ± 2.2	-20.5 ± 2.1	U4	13.158 ± 0.130	A7	1.327 ± 0.289	A7	9.933 ± 0.024	9.083 ± 0.022	8.608 ± 0.023	
15593661-3255340	-2.2 ± 2.7	-13.3 ± 2.7	PX					10.265 ± 0.026	9.734 ± 0.030	9.567 ± 0.025	
15593706-3255414	-10.5 ± 1.2	10.3 ± 1.2	U4					10.748 ± 0.024	10.244 ± 0.030	10.105 ± 0.023	
15594951-3628279	-26.7 ± 1.1	-41.8 ± 1.8	U4	11.000 ± 0.010	HP	1.100 ± 0.010	T06	8.773 ± 0.023	8.150 ± 0.020	8.029 ± 0.026	
16003134-2027050	-10.7 ± 1.7	-22.2 ± 1.9	U4					9.786 ± 0.024	9.054 ± 0.027	8.827 ± 0.027	
16003317-2726185	-7.5 ± 0.8	2.0 ± 2.3	U4	10.780 ± 0.066	T2	1.017 ± 0.101	T2	8.218 ± 0.027	7.545 ± 0.049	7.363 ± 0.024	
16004056-2200322	-12.4 ± 1.0	-20.4 ± 1.5	U4	11.233 ± 0.028	A7	0.980 ± 0.065	A7	9.085 ± 0.027	8.543 ± 0.038	8.443 ± 0.021	
16004277-2127380	-11.5 ± 2.7	-25.8 ± 2.0	U4					9.804 ± 0.026	9.132 ± 0.027	8.922 ± 0.022	
16010801-2113184	-12.0 ± 1.2	-21.3 ± 1.2	U4					9.701 ± 0.026	9.029 ± 0.044	8.803 ± 0.021	
16011070-4804438	-23.4 ± 1.0	-28.8 ± 1.0	U4	11.693 ± 0.008	A7	1.080 ± 0.010	T06	9.651 ± 0.022	9.097 ± 0.023	8.923 ± 0.020	
16012563-2240403	-12.4 ± 0.9	-24.7 ± 1.7	U4	11.709 ± 0.059	A7	1.123 ± 0.078	A7	9.324 ± 0.023	8.706 ± 0.029	8.523 ± 0.021	
16014743-2049457	-10.4 ± 1.4	-22.2 ± 1.4	U4					9.587 ± 0.021	8.851 ± 0.026	8.614 ± 0.020	
16014943-4026192	-16.7 ± 3.0	-20.9 ± 3.0	PX					9.842 ± 0.023	9.230 ± 0.025	9.057 ± 0.023	
16015061-4758342	-13.5 ± 1.0	-19.3 ± 1.8	U4	11.452 ± 0.128	T2	0.771 ± 0.182	T2	9.340 ± 0.023	8.987 ± 0.027	8.764 ± 0.023	
16015149-2445249	-10.9 ± 1.1	-22.4 ± 1.1	U4					9.408 ± 0.024	8.659 ± 0.044	8.485 ± 0.026	
16015568-2412329	-14.2 ± 1.1	-8.7 ± 1.1	U4					10.577 ± 0.026	10.187 ± 0.023	10.069 ± 0.019	
16015822-2008121	-7.5 ± 0.8	-22.6 ± 0.8	U4	10.590 ± 0.010	T06	0.990 ± 0.010	T06	8.350 ± 0.020	7.808 ± 0.026	7.672 ± 0.020	
16015918-3612555	-18.6 ± 1.6	-24.0 ± 3.2	U4	11.862 ± 0.051	A7	1.073 ± 0.059	A7	9.599 ± 0.023	8.972 ± 0.025	8.854 ± 0.025	
16020039-2221237	-16.6 ± 1.1	-31.2 ± 1.2	U4					9.824 ± 0.021	9.101 ± 0.023	8.842 ± 0.022	
16021045-2241280	-22.3 ± 0.8	-31.7 ± 0.9	U4	11.344 ± 0.052	A7	1.134 ± 0.065	A7	8.866 ± 0.023	8.258 ± 0.023	8.058 ± 0.026	

Table 4.4 (cont'd)

2MASS	μ_α (mas yr^{-1})	μ_δ (mas yr^{-1})	Ref.	V (mag)	Ref.	B–V (mag)	Ref.	J (mag)	H (mag)	K_S (mag)	Note
16023814-2541389	-13.3 ± 5.3	-22.2 ± 2.9	U4	13.007 ± 0.100	A7	1.639 ± 0.799	A7	10.170 ± 0.026	9.546 ± 0.026	9.332 ± 0.021	
16023910-2542078	-20.4 ± 1.1	-32.5 ± 1.1	U4	12.119 ± 0.044	A7	1.124 ± 0.051	A7	9.835 ± 0.024	9.234 ± 0.024	9.117 ± 0.023	
16025123-2401574	-11.7 ± 1.3	-22.1 ± 1.3	U4					9.726 ± 0.024	9.083 ± 0.024	8.927 ± 0.021	
16025243-2402226	-13.4 ± 1.0	-8.2 ± 1.3	U4	11.042 ± 0.056	A7	1.351 ± 0.062	A7	8.525 ± 0.027	7.837 ± 0.049	7.645 ± 0.018	
16025396-2022480	-8.5 ± 1.3	-21.7 ± 1.2	U4					9.161 ± 0.022	8.465 ± 0.044	8.190 ± 0.026	
16030269-1806050	-8.1 ± 1.0	-20.8 ± 1.1	U4	12.026 ± 0.058	A7	1.229 ± 0.075	A7	9.557 ± 0.023	8.921 ± 0.024	8.727 ± 0.025	
16032367-1751422	-13.1 ± 1.6	-17.5 ± 1.6	U4	13.381 ± 0.082	A7	1.581 ± 0.102	A7	9.635 ± 0.032	8.914 ± 0.035	8.611 ± 0.026	
16033550-2245560	-10.8 ± 0.8	-25.8 ± 0.9	U4	10.960 ± 0.010	T06	0.990 ± 0.010	T06	9.030 ± 0.023	8.500 ± 0.034	8.360 ± 0.025	
16034536-4355492	-12.5 ± 1.1	-22.6 ± 1.4	T2	9.700 ± 0.010	HP	0.922 ± 0.039	T2	7.927 ± 0.024	7.413 ± 0.034	7.314 ± 0.018	
16035250-3939013	-15.5 ± 1.7	-28.9 ± 1.2	U4	11.114 ± 0.051	A7	1.048 ± 0.067	A7	8.941 ± 0.025	8.355 ± 0.029	8.224 ± 0.027	
16035625-3624496	-19.3 ± 1.2	-3.1 ± 1.5	U4	11.193 ± 0.101	T2	0.918 ± 0.156	T2	9.071 ± 0.023	8.487 ± 0.040	8.326 ± 0.025	
16035836-1751041	0.1 ± 1.7	-14.6 ± 1.7	U4	14.599 ± 0.066	A7	1.587 ± 0.155	A7	10.280 ± 0.022	9.519 ± 0.022	9.239 ± 0.019	
16042165-2130284	-14.2 ± 1.5	-15.4 ± 3.9	U4					9.948 ± 0.023	9.103 ± 0.024	8.506 ± 0.021	
16042291-4448088	-20.7 ± 2.1	-13.6 ± 2.9	U4					10.215 ± 0.023	9.498 ± 0.022	9.332 ± 0.023	
16043056-3207287	-18.9 ± 0.9	-23.2 ± 0.9	U4	10.880 ± 0.010	T06	0.890 ± 0.010	T06	9.168 ± 0.018	8.690 ± 0.049	8.565 ± 0.021	
16044776-1930230	-9.3 ± 1.2	-19.7 ± 0.9	U4	11.290 ± 0.010	T06	1.140 ± 0.010	T06	8.875 ± 0.021	8.269 ± 0.038	8.043 ± 0.017	
16051598-1158039	-10.9 ± 1.8	-32.2 ± 1.8	T2	11.407 ± 0.143	T2	0.679 ± 0.192	T2	9.270 ± 0.021	8.784 ± 0.040	8.647 ± 0.021	
16054266-2004150	-10.8 ± 1.8	-21.2 ± 1.8	U4	14.256 ± 0.047	A7	1.630 ± 0.074	A7	10.181 ± 0.028	9.436 ± 0.026	9.159 ± 0.027	
16054499-3906065	-16.0 ± 1.2	-27.4 ± 1.9	U4	10.550 ± 0.010	T06	0.790 ± 0.010	T06	8.910 ± 0.029	8.523 ± 0.046	8.362 ± 0.027	
16055065-2533136	-21.3 ± 1.1	-33.2 ± 1.0	U4	10.930 ± 0.010	T06	0.930 ± 0.010	T06	9.108 ± 0.030	8.589 ± 0.055	8.461 ± 0.023	

Table 4.4 (cont'd)

2MASS	μ_α (mas yr^{-1})	μ_δ (mas yr^{-1})	Ref.	V (mag)	Ref.	B–V (mag)	Ref.	J (mag)	H (mag)	K_S (mag)	Note
16055207-3439331	-9.2 ± 1.2	-20.6 ± 1.2	U4	11.401 ± 0.029	A7	1.086 ± 0.033	A7	9.243 ± 0.023	8.635 ± 0.033	8.459 ± 0.023	
16061222-4507155	-14.2 ± 1.9	-14.9 ± 1.9	U4	12.431 ± 0.025	A7	1.118 ± 0.038	A7	10.181 ± 0.024	9.599 ± 0.022	9.448 ± 0.021	
16061254-2036472	-9.6 ± 1.4	-25.9 ± 1.4	U4					9.900 ± 0.027	9.137 ± 0.024	8.898 ± 0.019	
16061466-4413135	9.2 ± 2.7	-22.8 ± 1.7	U4	12.152 ± 0.039	A7	0.960 ± 0.059	A7	10.097 ± 0.023	9.550 ± 0.022	9.404 ± 0.021	
16062196-1928445	-9.9 ± 1.6	-20.6 ± 1.6	U4	13.493 ± 0.085	A7	1.502 ± 0.108	A7	9.827 ± 0.026	9.011 ± 0.024	8.621 ± 0.026	
16062334-4447355	-17.6 ± 2.0	-27.1 ± 1.9	U4					10.230 ± 0.026	9.571 ± 0.022	9.426 ± 0.021	
16062354-1814187	-6.2 ± 1.2	-21.1 ± 2.6	U4	11.900 ± 0.041	A7	1.293 ± 0.051	A7	9.276 ± 0.029	8.525 ± 0.036	8.308 ± 0.027	
16063169-2036232	-11.9 ± 1.4	-22.4 ± 1.4	U4	13.063 ± 0.115	A7	1.406 ± 0.165	A7	9.731 ± 0.027	8.952 ± 0.023	8.732 ± 0.023	
16063245-2208245	-4.6 ± 3.6	-29.1 ± 3.4	U4	12.418 ± 0.035	A7	1.310 ± 0.055	A7	9.749 ± 0.024	9.048 ± 0.026	8.880 ± 0.021	
16065436-2416107	-8.9 ± 1.3	-21.5 ± 2.6	U4	12.670 ± 0.066	A7	1.367 ± 0.070	A7	9.816 ± 0.030	9.236 ± 0.040	8.863 ± 0.027	
16065795-2743094	-6.7 ± 1.4	-20.3 ± 0.8	U4	8.190 ± 0.010	HP	0.397 ± 0.015	HP	7.095 ± 0.032	6.538 ± 0.067	5.888 ± 0.018	
16070356-2036264	-13.2 ± 1.1	-21.9 ± 1.1	U4					9.088 ± 0.035	8.324 ± 0.024	8.098 ± 0.024	
16070393-1911338	-9.5 ± 1.8	-26.6 ± 1.8	U4					10.240 ± 0.027	9.521 ± 0.027	9.218 ± 0.026	
16073366-3759242	-14.1 ± 1.1	-31.5 ± 1.1	U4	12.928 ± 0.050	A7	1.288 ± 0.050	A7	10.222 ± 0.039	9.555 ± 0.023	9.348 ± 0.044	b
16073490-2445412	-21.8 ± 1.4	-3.8 ± 1.3	U4	9.247 ± 0.028	T2	1.111 ± 0.045	T2	7.315 ± 0.021	6.816 ± 0.059	6.604 ± 0.023	
16074006-2148426	-10.8 ± 1.7	-17.8 ± 1.7	U4	13.759 ± 0.054	A7	1.470 ± 0.098	A7	10.611 ± 0.026	9.855 ± 0.026	9.674 ± 0.019	
16080019-4116119	-22.1 ± 2.9	-26.7 ± 2.9	PX	11.957 ± 0.020	A7	1.138 ± 0.034	A7	9.509 ± 0.026	8.973 ± 0.025	8.761 ± 0.023	
16080141-2027416	-9.7 ± 1.6	-20.4 ± 1.6	U4	13.913 ± 0.051	A7	1.586 ± 0.093	A7	10.298 ± 0.026	9.501 ± 0.026	9.291 ± 0.023	
16080772-5041556	-18.3 ± 3.4	-41.4 ± 1.4	U4	12.042 ± 0.013	A7	1.280 ± 0.032	A7	9.546 ± 0.025	8.870 ± 0.026	8.640 ± 0.023	
16081081-1904479	-10.3 ± 2.0	-20.2 ± 1.6	U4	11.656 ± 0.070	A7	1.247 ± 0.101	A7	9.245 ± 0.030	8.604 ± 0.029	8.467 ± 0.032	

Table 4.4 (cont'd)

2MASS	μ_α (mas yr^{-1})	μ_δ (mas yr^{-1})	Ref.	V (mag)	Ref.	B–V (mag)	Ref.	J (mag)	H (mag)	K_S (mag)	Note
16081474-1908327	-8.7 ± 1.8	-24.5 ± 0.9	U4	11.403 ± 0.049	A7	1.111 ± 0.076	A7	9.158 ± 0.030	8.603 ± 0.042	8.426 ± 0.020	
16081824-3844052	-22.0 ± 5.2	-33.1 ± 2.1	U4	12.243 ± 0.010	A6	1.275 ± 0.014	A6	9.564 ± 0.024	8.919 ± 0.025	8.714 ± 0.021	
16082061-4109504	-4.6 ± 2.2	-18.7 ± 2.2	PX	11.442 ± 0.141	T2	1.127 ± 0.236	T2	8.767 ± 0.035	8.103 ± 0.057	7.945 ± 0.036	
16083436-1911563	-10.2 ± 1.6	-20.0 ± 1.9	U4	11.668 ± 0.012	A7	1.287 ± 0.054	A7	8.753 ± 0.026	8.009 ± 0.044	7.785 ± 0.029	
16083617-3923024	-8.9 ± 2.9	-25.3 ± 2.8	U4	13.113 ± 0.092	A7	1.476 ± 0.141	A7	9.884 ± 0.026	9.043 ± 0.023	8.658 ± 0.021	
16084340-2602168	-8.6 ± 1.9	-22.5 ± 1.6	U4	10.440 ± 0.010	T06	0.900 ± 0.010	T06	8.550 ± 0.020	8.050 ± 0.034	7.908 ± 0.016	
16085427-3906057	-10.9 ± 2.7	-24.0 ± 2.7	PX	10.752 ± 0.046	A7	1.023 ± 0.054	A7	8.909 ± 0.030	8.375 ± 0.047	8.212 ± 0.029	
16085438-4148364	-32.4 ± 2.3	-33.2 ± 2.3	PX					10.164 ± 0.024	9.726 ± 0.022	9.650 ± 0.019	
16085673-2033460	-9.4 ± 1.3	-22.9 ± 1.3	U4	12.208 ± 0.064	A7	1.318 ± 0.096	A7	9.505 ± 0.024	8.778 ± 0.065	8.619 ± 0.024	
16090075-1908526	-5.5 ± 1.7	-26.9 ± 1.7	U4	13.906 ± 0.053	A7	1.417 ± 0.138	A7	10.220 ± 0.023	9.475 ± 0.026	9.154 ± 0.027	
16092918-1852536	-6.6 ± 2.7	-22.8 ± 1.7	U4	12.736 ± 0.016	A7	1.426 ± 0.038	A7	9.461 ± 0.027	8.624 ± 0.040	8.375 ± 0.038	
16093030-2104589	-9.8 ± 1.2	-21.0 ± 1.3	U4	12.782 ± 0.025	A7	1.386 ± 0.055	A7	9.820 ± 0.027	9.121 ± 0.023	8.916 ± 0.021	
16093969-2200466	-10.1 ± 1.5	-20.3 ± 6.7	U4	13.990 ± 0.086	A7	1.589 ± 0.153	A7	10.300 ± 0.023	9.593 ± 0.023	9.301 ± 0.019	
16094098-2217594	-10.6 ± 1.3	-21.2 ± 1.2	U4	12.529 ± 0.046	A7	1.472 ± 0.109	A7	9.483 ± 0.027	8.677 ± 0.051	8.441 ± 0.027	
16100321-5026121	-15.1 ± 1.1	-11.5 ± 1.2	U4	9.863 ± 0.010	A7	1.152 ± 0.014	A7	7.653 ± 0.021	7.153 ± 0.042	6.940 ± 0.017	
16100478-4016122	-16.2 ± 1.2	-27.9 ± 1.7	U4	11.180 ± 0.010	T06	0.980 ± 0.010	T06	9.339 ± 0.024	8.796 ± 0.057	8.619 ± 0.023	
16100577-2626068	-1.7 ± 2.1	-3.0 ± 0.9	U4					10.839 ± 0.021	10.475 ± 0.022	10.337 ± 0.021	
16101171-3226360	-11.4 ± 0.9	-18.5 ± 0.9	U4	11.707 ± 0.050	A7	1.150 ± 0.074	A7	9.274 ± 0.026	8.637 ± 0.028	8.408 ± 0.025	
16101264-2104446	-7.3 ± 1.3	-20.0 ± 1.4	U4	11.711 ± 0.023	A7	1.142 ± 0.040	A7	9.335 ± 0.026	8.722 ± 0.051	8.546 ± 0.021	
16101729-1910263	-19.3 ± 1.9	-13.6 ± 1.5	U4	12.693 ± 0.057	A7	1.432 ± 0.072	A7	9.533 ± 0.040	8.772 ± 0.044	8.531 ± 0.037	

Table 4.4 (cont'd)

2MASS	μ_α (mas yr^{-1})	μ_δ (mas yr^{-1})	Ref.	V (mag)	Ref.	B–V (mag)	Ref.	J (mag)	H (mag)	K_S (mag)	Note
16101918-2502301	-10.6 ± 1.9	-23.9 ± 1.6	U4	11.960 ± 0.010	T06	1.370 ± 0.010	T06	9.253 ± 0.024	8.538 ± 0.049	8.364 ± 0.021	
16102174-1904067	-12.2 ± 2.1	-23.2 ± 1.6	U4	14.782 ± 0.080	A7	1.530 ± 0.081	A7	10.679 ± 0.030	9.908 ± 0.031	9.624 ± 0.023	
16102653-2756293	-3.9 ± 1.1	-26.5 ± 3.9	U4	13.938 ± 0.016	A7	1.336 ± 0.311	A7	10.411 ± 0.023	9.788 ± 0.022	9.575 ± 0.023	
16102888-2213477	-8.3 ± 1.0	-21.6 ± 0.7	U4	9.620 ± 0.010	HP	0.860 ± 0.010	T06	7.849 ± 0.019	7.335 ± 0.042	7.226 ± 0.016	
16104202-2101319	-5.9 ± 1.0	-21.4 ± 1.3	U4	12.379 ± 0.109	A7	1.325 ± 0.142	A7	9.425 ± 0.013	8.774 ± 0.064	8.488 ± 0.015	a
16110890-1904468	-8.5 ± 2.1	-22.4 ± 1.2	U4	11.921 ± 0.014	A7	1.360 ± 0.040	A7	8.761 ± 0.029	7.983 ± 0.047	7.694 ± 0.020	
16111534-1757214	-9.6 ± 1.3	-23.7 ± 1.4	U4	14.099 ± 0.026	A7	1.566 ± 0.088	A7	10.227 ± 0.027	9.486 ± 0.023	9.204 ± 0.019	
16114387-2526350	-19.5 ± 1.7	-20.7 ± 1.4	U4	11.768 ± 0.093	A7	1.963 ± 1.417	A7	9.483 ± 0.021	8.893 ± 0.034	8.745 ± 0.019	
16115334-3902158	-17.8 ± 2.1	-21.3 ± 2.1	U4					10.287 ± 0.024	9.629 ± 0.022	9.438 ± 0.025	
16120140-3840276	-8.7 ± 2.6	-18.3 ± 2.8	U4					9.057 ± 0.030	8.432 ± 0.049	8.179 ± 0.021	
16123916-1859284	-2.5 ± 4.7	-26.1 ± 1.5	U4	14.045 ± 0.069	A7	1.565 ± 0.144	A7	10.278 ± 0.027	9.468 ± 0.026	9.111 ± 0.028	
16124051-1859282	-3.9 ± 1.1	-19.5 ± 1.1	U4	10.905 ± 0.086	A7	1.207 ± 0.098	A7	8.313 ± 0.020	7.661 ± 0.055	7.494 ± 0.026	
16124682-2213317	-9.0 ± 0.8	-23.7 ± 0.9	U4	11.222 ± 0.008	A7	1.142 ± 0.013	A7	8.881 ± 0.027	8.199 ± 0.029	8.033 ± 0.017	
16125265-2319560	-4.3 ± 1.1	-25.2 ± 1.0	U4	12.207 ± 0.010	A7	1.196 ± 0.014	A7	9.870 ± 0.023	9.218 ± 0.026	9.042 ± 0.023	
16130271-2257446	-6.2 ± 0.8	-21.1 ± 0.8	U4	11.798 ± 0.014	A7	1.210 ± 0.072	A7	9.322 ± 0.023	8.651 ± 0.047	8.455 ± 0.027	
16131267-3803513	-15.5 ± 1.0	-22.9 ± 1.7	U4					9.677 ± 0.042	9.029 ± 0.020	8.880 ± 0.017	
16131738-2922198	-24.7 ± 1.9	-23.1 ± 1.3	U4					9.849 ± 0.024	9.134 ± 0.022	8.909 ± 0.021	
16131858-2212489	-8.8 ± 0.8	-20.0 ± 0.9	U4	10.389 ± 0.069	T2	1.044 ± 0.098	T2	8.180 ± 0.021	7.595 ± 0.036	7.428 ± 0.024	
16132929-2311075	-6.5 ± 1.5	-25.1 ± 1.4	U4	11.741 ± 0.010	A7			9.317 ± 0.027	8.624 ± 0.042	8.494 ± 0.019	
16134366-2214594	-10.0 ± 1.1	-20.8 ± 1.3	U4	13.217 ± 0.040	A7	1.393 ± 0.098	A7	10.074 ± 0.027	9.358 ± 0.023	9.114 ± 0.021	

Table 4.4 (cont'd)

2MASS	μ_α (mas yr^{-1})	μ_δ (mas yr^{-1})	Ref.	V (mag)	Ref.	B–V (mag)	Ref.	J (mag)	H (mag)	K_S (mag)	Note
16135801-3618133	-18.6 ± 1.8	-31.5 ± 1.8	U4	11.000 ± 0.010	T06	0.860 ± 0.010	T06	9.437 ± 0.040	8.981 ± 0.049	8.851 ± 0.039	
16140035-2108439	-11.6 ± 1.9	-20.9 ± 1.5	U4	13.786 ± 0.040	A7	1.433 ± 0.080	A7	10.560 ± 0.024	9.815 ± 0.024	9.603 ± 0.022	
16140211-2301021	-4.9 ± 1.5	-19.4 ± 1.8	U4	11.187 ± 0.010	A7	0.902 ± 0.014	A7	9.375 ± 0.026	8.774 ± 0.053	8.608 ± 0.023	
16141107-2305362	-8.1 ± 1.2	-20.3 ± 0.9	U4	10.660 ± 0.010	T06	1.150 ± 0.010	T06	8.280 ± 0.032	7.708 ± 0.049	7.458 ± 0.027	
16141904-3326041	-24.1 ± 0.9	-26.1 ± 0.9	U4	10.900 ± 0.010	T06	0.730 ± 0.010	T06	9.405 ± 0.023	8.979 ± 0.025	8.864 ± 0.023	
16143884-2525000	-10.6 ± 1.2	-34.3 ± 1.2	U4	13.734 ± 0.107	A7	1.557 ± 0.123	A7	9.897 ± 0.021	9.168 ± 0.022	8.952 ± 0.021	
16145207-5026187	-19.9 ± 2.1	-29.2 ± 2.0	T2	10.240 ± 0.010	T06	0.920 ± 0.010	T06	8.348 ± 0.021	7.863 ± 0.026	7.701 ± 0.033	
16145918-2750230	-13.5 ± 0.9	-21.5 ± 1.6	U4	11.170 ± 0.010	T06	0.970 ± 0.010	T06	9.334 ± 0.021	8.800 ± 0.040	8.686 ± 0.022	
16152831-3402319	-24.1 ± 1.2	0.3 ± 1.2	U4					9.604 ± 0.025	8.956 ± 0.018	8.787 ± 0.022	
16153456-2242421	-6.8 ± 1.0	-29.5 ± 4.5	U4	12.684 ± 0.010	A6	1.178 ± 0.014	A6	9.382 ± 0.038	8.334 ± 0.038	7.909 ± 0.023	
16153587-2529008	-10.1 ± 1.0	-24.0 ± 1.1	U4	12.389 ± 0.032	A7	1.289 ± 0.047	A7	9.646 ± 0.024	8.961 ± 0.024	8.744 ± 0.019	
16154270-2901016	-8.3 ± 1.6	-9.6 ± 2.0	U4					9.215 ± 0.024	8.555 ± 0.044	8.390 ± 0.027	
16155664-3947163	-20.9 ± 1.8	-27.3 ± 1.8	U4					10.049 ± 0.023	9.403 ± 0.022	9.187 ± 0.019	
16161423-2643148	-1.9 ± 1.7	-36.1 ± 1.0	U4	11.909 ± 0.040	A7	1.183 ± 0.068	A7	9.245 ± 0.021	8.635 ± 0.031	8.452 ± 0.007	a
16161795-2339476	-6.4 ± 2.3	-20.4 ± 1.6	U4	10.560 ± 0.010	T06	0.920 ± 0.010	T06	8.727 ± 0.024	8.236 ± 0.029	8.102 ± 0.018	
16165205-2154235	-24.1 ± 1.8	-17.3 ± 2.0	U4					10.594 ± 0.023	10.020 ± 0.023	9.855 ± 0.021	
16172711-5023213	-4.5 ± 0.9	-6.6 ± 2.0	U4	11.175 ± 0.097	T2	0.759 ± 0.128	T2	9.229 ± 0.022	8.785 ± 0.023	8.659 ± 0.021	
16173138-2303360	-10.1 ± 1.2	-16.6 ± 0.9	U4	10.130 ± 0.010	T06	0.810 ± 0.010	T06	8.514 ± 0.034	8.085 ± 0.051	7.967 ± 0.027	
16175569-3828132	-40.5 ± 1.9	-18.4 ± 1.9	U4					10.259 ± 0.024	9.595 ± 0.024	9.406 ± 0.024	
16180479-2224394	0.6 ± 0.8	-18.8 ± 0.8	U4	10.585 ± 0.062	T2	0.972 ± 0.083	T2	8.463 ± 0.032	7.892 ± 0.042	7.673 ± 0.018	

Table 4.4 (cont'd)

2MASS	μ_α (mas yr^{-1})	μ_δ (mas yr^{-1})	Ref.	V (mag)	Ref.	B–V (mag)	Ref.	J (mag)	H (mag)	K_S (mag)	Note
16181107-2911125	-11.4 ± 2.0	-20.6 ± 2.4	U4	10.520 ± 0.010	T06	0.790 ± 0.010	T06	8.906 ± 0.021	8.534 ± 0.053	8.377 ± 0.034	
16183723-2405226	-8.8 ± 1.5	-39.9 ± 1.5	U4	10.879 ± 0.062	A7	0.986 ± 0.088	A7	9.020 ± 0.039	8.370 ± 0.067	7.899 ± 0.061	
16185958-2213283	-8.3 ± 0.8	-6.4 ± 1.0	U4	10.572 ± 0.064	T2	1.094 ± 0.100	T2	8.686 ± 0.024	8.200 ± 0.057	7.977 ± 0.026	
16191035-3851041	-19.7 ± 1.0	-11.6 ± 2.0	U4	10.808 ± 0.090	T2	1.353 ± 0.200	T2	8.091 ± 0.021	7.452 ± 0.016	7.225 ± 0.021	
16191217-2550383	-7.8 ± 1.6	-22.8 ± 1.6	U4	13.289 ± 0.061	A7	1.603 ± 0.065	A7	9.873 ± 0.024	9.129 ± 0.025	8.824 ± 0.026	
16193334-2807397	0.0 ± 2.0	-8.6 ± 2.5	U4	12.783 ± 0.056	A7	1.915 ± 0.099	A7	8.268 ± 0.029	7.333 ± 0.044	6.984 ± 0.016	
16193396-2228294	-11.2 ± 1.2	-21.6 ± 1.2	U4	11.110 ± 0.010	T06	1.020 ± 0.010	T06	9.230 ± 0.019	8.659 ± 0.036	8.509 ± 0.019	
16195068-2154355	-10.7 ± 1.6	-14.8 ± 2.5	U4	12.498 ± 0.010	A6	1.400 ± 0.014	A6	9.140 ± 0.030	8.443 ± 0.029	8.203 ± 0.016	
16200368-4801298	7.3 ± 0.9	10.0 ± 0.9	U4	10.580 ± 0.058	T2	0.859 ± 0.071	T2	8.804 ± 0.026	8.328 ± 0.044	8.184 ± 0.021	
16202930-3254096	-1.9 ± 4.4	-28.0 ± 4.2	PX	11.875 ± 0.020	A7	1.085 ± 0.030	A7	9.721 ± 0.023	9.132 ± 0.023	8.991 ± 0.021	
16202983-2716240	-6.4 ± 1.0	-8.5 ± 1.7	U4	11.256 ± 0.053	A7	0.790 ± 0.057	A7	9.461 ± 0.026	9.109 ± 0.022	8.949 ± 0.019	
16204468-2431384	-6.0 ± 1.7	-17.6 ± 1.2	U4					9.354 ± 0.026	8.733 ± 0.046	8.526 ± 0.021	
16230783-2300596	-22.8 ± 2.3	-7.6 ± 2.1	U4	11.853 ± 0.043	A7	1.263 ± 0.066	A7	9.042 ± 0.032	8.343 ± 0.040	8.184 ± 0.024	
16233234-2523485	-16.1 ± 2.6	-20.8 ± 2.6	PX	11.383 ± 0.028	A7	1.269 ± 0.039	A7	8.600 ± 0.024	7.979 ± 0.046	7.695 ± 0.023	
16234698-2850023	-10.9 ± 1.5	-22.4 ± 2.2	U4	10.860 ± 0.010	T06	0.860 ± 0.010	T06	9.216 ± 0.025	8.785 ± 0.027	8.659 ± 0.026	
16235484-3312370	-17.6 ± 1.7	-28.3 ± 1.3	U4	11.736 ± 0.018	A7	1.090 ± 0.039	A7	9.373 ± 0.024	8.751 ± 0.026	8.601 ± 0.023	
16235844-4706089	-9.2 ± 1.0	-10.4 ± 1.1	U4	9.628 ± 0.026	T2	1.176 ± 0.041	T2	7.408 ± 0.029	6.836 ± 0.055	6.644 ± 0.016	
16240289-2524539	-11.4 ± 1.2	-25.5 ± 1.0	PX	9.410 ± 0.010	HP	0.748 ± 0.032	HP	7.289 ± 0.018	6.942 ± 0.026	6.719 ± 0.024	
16240373-4319261	-12.8 ± 2.1	-25.2 ± 2.0	T2	11.016 ± 0.004	A7	0.759 ± 0.017	A7	9.319 ± 0.026	8.889 ± 0.036	8.816 ± 0.026	
16240632-2456468	-12.3 ± 1.8	-21.6 ± 1.8	U4	12.992 ± 0.014	A7	1.549 ± 0.038	A7	9.445 ± 0.022	8.597 ± 0.044	8.280 ± 0.020	

Table 4.4 (cont'd)

2MASS	μ_α (mas yr^{-1})	μ_δ (mas yr^{-1})	Ref.	V (mag)	Ref.	B–V (mag)	Ref.	J (mag)	H (mag)	K_S (mag)	Note
16241860-2854475	-4.6 ± 1.9	-15.8 ± 1.3	U4	11.380 ± 0.052	A7	1.112 ± 0.066	A7	9.056 ± 0.027	8.489 ± 0.033	8.328 ± 0.023	
16243416-2606367	-4.7 ± 1.3	-0.1 ± 1.2	U4					8.838 ± 0.019	8.093 ± 0.036	7.960 ± 0.033	
16245136-2239325	-10.8 ± 1.8	-20.0 ± 1.1	U4	9.660 ± 0.010	T06	0.950 ± 0.010	T06	7.779 ± 0.027	7.280 ± 0.027	7.084 ± 0.018	
16250991-3047572	-16.7 ± 1.4	-31.7 ± 1.4	T2	9.003 ± 0.020	T2	0.628 ± 0.025	T2	7.774 ± 0.026	7.372 ± 0.021	7.267 ± 0.021	
16251923-2426526	-21.2 ± 1.9	-24.6 ± 1.8	PX	10.049 ± 0.047	T2	0.924 ± 0.067	T2	8.363 ± 0.024	7.982 ± 0.049	7.798 ± 0.026	
16252863-2346265	7.8 ± 2.0	-37.5 ± 2.5	U4	12.002 ± 0.059	A7	1.236 ± 0.074	A7	8.833 ± 0.027	8.081 ± 0.021	7.822 ± 0.027	
16253849-2613540	-9.8 ± 2.2	-21.5 ± 2.7	U4	11.700 ± 0.010	T06	1.300 ± 0.010	T06	8.688 ± 0.019	7.947 ± 0.055	7.517 ± 0.024	
16262736-2756508	-9.8 ± 1.1	-37.1 ± 1.3	U4	11.832 ± 0.042	A7	1.234 ± 0.065	A7	9.021 ± 0.030	8.381 ± 0.069	8.185 ± 0.027	
16263591-3314481	-9.0 ± 1.2	-18.3 ± 1.6	U4	11.110 ± 0.021	A7	0.881 ± 0.032	A7	9.486 ± 0.035	8.958 ± 0.036	8.838 ± 0.035	
16265280-2343127	-14.7 ± 3.3	-37.4 ± 3.3	PX	11.019 ± 0.037	A7	1.305 ± 0.050	A7	7.884 ± 0.018	7.086 ± 0.047	6.702 ± 0.020	
16265700-3032232	-24.1 ± 3.0	-31.0 ± 1.7	U4					9.588 ± 0.025	8.976 ± 0.027	8.785 ± 0.023	
16265763-3032279	4.7 ± 2.4	-28.3 ± 3.4	U4	11.210 ± 0.055	A7	1.157 ± 0.089	A7	9.090 ± 0.020	8.453 ± 0.012	8.228 ± 0.016	a
16270927-2339055	-14.3 ± 5.1	-43.1 ± 4.8	PX	13.119 ± 0.040	A7	1.621 ± 0.052	A7	9.021 ± 0.029	8.146 ± 0.047	7.819 ± 0.027	
16271951-2441403	-10.3 ± 1.6	-24.5 ± 1.9	U4	13.211 ± 0.038	A7	1.544 ± 0.104	A7	9.424 ± 0.023	8.631 ± 0.044	8.408 ± 0.036	
16272373-2855286	-4.3 ± 1.6	-13.1 ± 1.6	U4					10.274 ± 0.024	9.717 ± 0.022	9.575 ± 0.027	
16272794-4542403	-11.3 ± 1.8	-21.3 ± 1.7	T2	11.130 ± 0.010	T06	0.860 ± 0.010	T06	9.279 ± 0.029	8.814 ± 0.025	8.662 ± 0.021	
16273956-2245230	-8.6 ± 2.5	-20.8 ± 1.4	U4	11.590 ± 0.010	T06	1.210 ± 0.010	T06	8.942 ± 0.019	8.306 ± 0.053	8.084 ± 0.026	
16274028-2422040	-12.9 ± 2.6	-30.7 ± 2.7	PX	11.515 ± 0.052	A7	1.299 ± 0.076	A7	8.440 ± 0.027	7.667 ± 0.042	7.207 ± 0.023	
16282453-4740395	-17.8 ± 2.0	-30.0 ± 2.0	U4	13.813 ± 0.058	A7	1.482 ± 0.109	A7	10.391 ± 0.023	9.708 ± 0.025	9.519 ± 0.024	
16282493-2723182	-10.0 ± 1.2	-20.7 ± 0.9	U4	11.139 ± 0.098	T2	0.605 ± 0.112	T2	8.614 ± 0.037	8.149 ± 0.046	7.962 ± 0.027	

Table 4.4 (cont'd)

2MASS	μ_α (mas yr^{-1})	μ_δ (mas yr^{-1})	Ref.	V (mag)	Ref.	B–V (mag)	Ref.	J (mag)	H (mag)	K_S (mag)	Note
16290446-2600389	-1.4 ± 1.8	1.0 ± 1.0	U4	11.326 ± 0.159	T2	1.573 ± 0.339	T2	8.273 ± 0.021	7.584 ± 0.057	7.310 ± 0.020	
16290585-3145250	-18.1 ± 1.4	-33.8 ± 1.5	U4	12.344 ± 0.051	A7	1.189 ± 0.082	A7	9.901 ± 0.024	9.262 ± 0.022	9.093 ± 0.021	
16293397-2455303	-15.2 ± 1.8	-17.2 ± 3.9	U4	12.278 ± 0.043	A7	1.284 ± 0.075	A7	9.425 ± 0.039	8.758 ± 0.038	8.531 ± 0.019	
16294869-2152118	-7.7 ± 2.2	-22.6 ± 1.0	U4	11.380 ± 0.010	T06	1.240 ± 0.010	T06	8.677 ± 0.026	8.003 ± 0.036	7.756 ± 0.024	
16294991-2728498	-12.9 ± 0.8	-26.3 ± 0.7	U4	11.010 ± 0.010	T06	0.930 ± 0.010	T06	9.275 ± 0.024	8.743 ± 0.049	8.648 ± 0.025	
16303162-4718119	-9.6 ± 2.0	-13.8 ± 2.2	PX	10.756 ± 0.061	T2	1.195 ± 0.112	T2	8.473 ± 0.024	7.845 ± 0.044	7.655 ± 0.026	
16303796-2954222	-13.0 ± 1.1	-30.8 ± 1.3	U4	10.940 ± 0.010	T06	1.010 ± 0.010	T06	9.050 ± 0.026	8.534 ± 0.063	8.385 ± 0.026	
16303840-2418312	-10.6 ± 2.1	-34.5 ± 2.1	PX	11.127 ± 0.111	T2	1.345 ± 0.221	T2	8.298 ± 0.027	7.627 ± 0.026	7.414 ± 0.026	
16310436-2404330	-7.9 ± 3.9	-17.9 ± 2.5	U4	12.308 ± 0.065	A7	1.432 ± 0.072	A7	8.861 ± 0.026	8.004 ± 0.046	7.784 ± 0.026	
16310837-2651062	-14.7 ± 1.2	-28.5 ± 2.5	U4					10.123 ± 0.023	9.447 ± 0.022	9.274 ± 0.021	
16315346-2636169	-12.6 ± 1.1	-22.1 ± 1.3	U4	11.634 ± 0.033	A7	1.102 ± 0.059	A7	9.603 ± 0.024	9.064 ± 0.029	8.892 ± 0.024	
16320058-2530287	-7.3 ± 3.0	-21.9 ± 1.6	U4					10.346 ± 0.024	9.626 ± 0.022	9.478 ± 0.024	
16320160-2530253	-12.4 ± 6.6	-15.8 ± 1.6	U4					10.255 ± 0.024	9.554 ± 0.022	9.395 ± 0.024	
16320352-2830179	-7.6 ± 1.8	-22.5 ± 1.7	PX	10.270 ± 0.010	T06	0.790 ± 0.010	T06	8.470 ± 0.021	8.095 ± 0.036	7.939 ± 0.031	
16321179-2440213	-1.4 ± 1.5	-19.2 ± 1.5	U4	13.611 ± 0.095	A7	1.770 ± 0.136	A7	9.245 ± 0.024	8.351 ± 0.031	7.929 ± 0.061	
16322432-1703399	-3.2 ± 3.4	-19.7 ± 2.2	U4	12.508 ± 0.048	A7	1.477 ± 0.126	A7	8.962 ± 0.026	8.143 ± 0.038	7.961 ± 0.024	
16323765-4541547	-0.6 ± 3.0	-50.0 ± 3.0	PX					10.995 ± 0.033	10.447 ± 0.052	10.271 ± 0.038	
16334191-2523342	-4.9 ± 1.1	-26.8 ± 1.0	U4	11.730 ± 0.010	T06	1.290 ± 0.010	T06	8.807 ± 0.019	8.153 ± 0.051	7.949 ± 0.024	
16340585-2658441	-10.9 ± 1.4	-24.2 ± 2.0	U4	12.383 ± 0.043	A7	1.277 ± 0.060	A7	9.648 ± 0.021	8.982 ± 0.022	8.785 ± 0.023	
16344629-2606324	-7.2 ± 1.1	-22.8 ± 1.4	U4	12.525 ± 0.045	A7	1.312 ± 0.085	A7	10.062 ± 0.024	9.391 ± 0.022	9.208 ± 0.019	

Table 4.4 (cont'd)

2MASS	μ_α (mas yr^{-1})	μ_δ (mas yr^{-1})	Ref.	V (mag)	Ref.	B–V (mag)	Ref.	J (mag)	H (mag)	K_S (mag)	Note
16345314-2518167	-16.5 ± 1.3	-25.1 ± 0.8	U4	10.250 ± 0.010	T06	0.840 ± 0.010	T06	8.539 ± 0.026	8.068 ± 0.031	7.980 ± 0.026	
16351188-2845520	-11.2 ± 1.4	-23.6 ± 2.8	U4	12.682 ± 0.043	A7	1.356 ± 0.072	A7	9.851 ± 0.023	9.128 ± 0.022	8.991 ± 0.023	
16353547-2541194	-14.0 ± 1.0	-12.9 ± 1.1	U4	12.156 ± 0.027	A7	0.914 ± 0.040	A7	10.207 ± 0.023	9.720 ± 0.026	9.603 ± 0.024	
16354836-2148396	-3.7 ± 1.7	-18.0 ± 7.2	U4	13.155 ± 0.127	A7	1.500 ± 0.188	A7	9.517 ± 0.023	8.754 ± 0.047	8.479 ± 0.021	
16361809-1828333	-11.5 ± 2.0	4.1 ± 2.4	U4					10.397 ± 0.022	9.836 ± 0.022	9.654 ± 0.019	
16363716-2340011	0.4 ± 3.8	-6.9 ± 1.5	U4	13.188 ± 0.017	A7	1.632 ± 0.063	A7	9.419 ± 0.026	8.659 ± 0.057	8.315 ± 0.021	
16384946-2735294	-1.8 ± 2.4	-21.3 ± 2.6	PX	11.310 ± 0.010	T06	0.950 ± 0.010	T06	9.308 ± 0.028	8.742 ± 0.051	8.636 ± 0.030	
16395498-2328007	-18.2 ± 2.1	-8.2 ± 2.1	U4					10.074 ± 0.023	9.319 ± 0.025	9.122 ± 0.023	
16430140-4405275	-9.3 ± 1.5	-17.7 ± 1.5	U4					10.189 ± 0.021	9.748 ± 0.024	9.675 ± 0.024	
16432519-3022477	-5.3 ± 2.7	-21.5 ± 1.6	U4	11.480 ± 0.010	T06	0.960 ± 0.010	T06	9.636 ± 0.024	9.112 ± 0.023	8.992 ± 0.021	
16452615-2503169	-4.8 ± 1.5	-20.2 ± 2.0	U4	11.060 ± 0.010	T06	1.100 ± 0.010	T06	8.794 ± 0.039	8.069 ± 0.033	7.725 ± 0.026	
16455772-4321044	-8.2 ± 2.2	-15.3 ± 2.2	PX	12.321 ± 0.080	A7	0.825 ± 0.081	A7	10.407 ± 0.007	9.858 ± 0.006	9.647 ± 0.015	a
16473710-2014268	-6.6 ± 1.3	-23.3 ± 1.4	U4	12.263 ± 0.022	A7	0.975 ± 0.042	A7	10.081 ± 0.021	9.544 ± 0.021	9.414 ± 0.019	
16491330-4355279	-17.5 ± 1.9	-42.2 ± 1.9	U4	10.100 ± 0.010	T06	0.770 ± 0.010	T06	8.750 ± 0.037	8.298 ± 0.047	8.242 ± 0.034	
16493599-2728078	-9.2 ± 0.9	-7.7 ± 0.8	U4	10.385 ± 0.019	A7	0.844 ± 0.021	A7	8.815 ± 0.021	8.350 ± 0.042	8.179 ± 0.031	
16520069-2122553	-31.2 ± 3.1	-35.0 ± 1.2	U4					9.793 ± 0.023	9.259 ± 0.025	9.149 ± 0.023	
16542415-2500202	-17.2 ± 1.7	-40.8 ± 2.1	U4					10.095 ± 0.024	9.419 ± 0.023	9.260 ± 0.023	

Note. — Notes – (a) 2MASS JHK_S aperture photometry; (b) 2MASS JHK_S 6x catalog; (c) 2MASS H PSF photometry / JK_S aperture photometry;
References – (PX) PPMX, Röser et al. (2008); (U4) UCAC4, Zacharias et al. (2013); (T2) Tycho-2, Høg et al. (2000); (A6) APASS DR6 (Henden et al., 2012); (A7) APASS DR7 (Henden et al., 2012); (HP) Hipparcos, ESA (1997); (W97) Wichmann et al. (1997); (T06) Torres et al. (2006);

Table 4.5. Membership Properties for Candidate Members.

2MASS	SpT	Ref.	$EW(Li)$ (Å)	Ref.	Membership				
					Li?	PM?	log(g)?	HRD?	Final
10004365-6522155	G3V	PM	0.24	PM	Y	N	Y?	...	N
10065573-6352086	K0Ve	T06	0.35	T06	Y	Y	...	Y	Y
10092184-6736381	K1IV(e)	PM	0.32	PM	Y	Y	Y?	Y	Y
10111521-6620282	K0IV	PM	0.33	PM	Y	Y	Y?	N	N
10293275-6349156	K1IV	PM	0.23	PM	Y?	N	Y?	...	N
10313710-6901587	K2.5IV(e)	PM	0.48	PM	Y	Y	Y?	Y	Y
10334180-6413457	K2.5IV(e)	PM	0.42	PM	Y	Y?	Y?	Y	Y
10342989-6235572	G7Ve	PM	0.27	PM	Y	N	Y?	...	N
10412300-6940431	G8Ve	T06	0.23	T06	Y?	Y	...	Y	Y
10441393-6446273	K1V(e)	PM	0.50	PM	Y	N	Y?	...	N
10463300-6527183	G6V	PM	0.24	PM	Y	N	Y?	...	N
10474221-5510143	K6IVe	PM	0.00	PM	N	N	Y?	...	N
10484283-5442328	G9V	PM	0.00	PM	N	Y	Y?	...	N
10494839-6446284	G9Ve	T06	0.32	T06	Y	Y?	...	Y	Y
10541737-6440512	K2IV	PM	0.30	PM	Y	N	Y?	...	N
10544998-6526458	K2Ve	PM	0.38	PM	Y	Y	Y?	Y	Y
10552886-6629147	K0IV	PM	0.42	PM	Y	Y?	Y?	Y	Y
10560422-6152054	K5V-IVe	PM	0.53	PM	Y	Y	Y?	Y	Y
10574936-6913599	K2IV	PM	0.34	M02	Y	Y	...	Y	Y
10591218-6438089	K0V(e)	PM	0.51	PM	Y	N	Y?	...	N
11001895-6118020	G6V	PM	0.26	PM	Y	Y	Y?	Y	Y
11033159-6321581	K8IV(e)	PM	0.00	PM	N	Y?	Y?	...	N
11080791-6341469	M0Ve	T06	0.26	T06	Y	Y	...	Y	Y
11132622-4523427	K8IVe	PM	0.74	PM	Y	N	Y?	...	N
11143442-4418240	K2IV	PM	0.67	PM	Y	Y	Y?	Y	Y
11145608-7101430	K3IV	PM	0.00	PM	N	N	Y?	...	N
11154143-5511082	K2.5IV	PM	0.00	PM	N	N	Y?	...	N
11165870-4406222	G5V	PM	0.00	PM	N	N	Y?	...	N
11175186-6402056	K3IVe	PM	0.72	PM	Y	Y	Y?	Y	Y
11202645-5834023	K0IV	PM	0.00	PM	N	N	Y?	...	N
11214451-4954076	K0IV	PM	0.00	PM	N	Y?	Y?	...	N

Table 4.5 (cont'd)

2MASS	SpT	Ref.	$EW(Li)$ (Å)	Ref.	Membership				
					Li?	PM?	log(g)?	HRD?	Final
11265293-5846387	K2.5IV	PM	0.02	PM	N	Y?	Y?	...	N
11272881-3952572	K3IV(e)	PM	0.66	PM	Y	Y	Y?	Y	Y
11275535-6626046	K1Ve	T06	0.37	T06	Y	Y	...	Y	Y
11320835-5803199	K1IV	PM	0.45	M02	Y	Y	...	Y	Y
11370003-6516164	K3IV	PM	0.24	PM	Y?	Y?	Y?	Y	Y
11402787-6201337	K5IVe	PM	0.78	PM	Y	Y	Y?	Y	Y
11403346-5641458	K3IV	PM	0.00	PM	N	N	Y?	...	N
11430455-6714211	K5IVe	PM	0.00	PM	N	N	Y?	...	N
11434903-6904232	K2III	PM	0.00	PM	N	N	N	...	N
11445217-6438548	K6IVe	PM	0.72	PM	Y	Y	Y?	Y	Y
11452016-5749094	K2IV	PM	0.36	PM	Y	Y	Y?	Y	Y
11454278-5739285	K4IVe	PM	0.32	PM	Y	Y	Y?	Y	Y
11472064-4953042	K7e	Z01	0.40	Z01	Y	Y	...	Y	Y
11485263-5657441	K4III	PM	0.00	PM	N	N	N	...	N
11492309-4801013	G5V	PM	0.00	PM	N	Y?	Y?	...	N
11515049-6407278	K1V	T06	0.34	T06	Y	Y?	...	Y	Y
11522157-6444302	K1IV	PM	0.34	PM	Y	Y?	Y?	Y	Y
11522242-6156016	K4III	PM	0.00	PM	N	N	N	...	N
11524466-5514070	K3III	PM	0.00	PM	N	N	N	...	N
11554295-5637314	M0Ve	T06	0.42	T06	Y	Y	...	Y	Y
11560730-6314096	K3IV	PM	0.00	PM	N	N	Y?	...	N
11575693-5821291	K2V	PM	0.00	PM	N	Y	Y?	...	N
11592560-5407445	K0IV	PM	0.00	PM	N	Y	Y?	...	N
11594608-6101132	K4V(e)	T06	0.48	T06	Y	Y	...	Y	Y
11594986-6136246	K5IVe	PM	0.67	PM	Y	Y	Y?	Y	Y
12051254-5331233	K4IVe	PM	0.62	PM	Y	Y	Y?	Y	Y
12061352-5702168	G5IV	PM	0.23	M02	Y?	Y	...	Y	Y
12063292-4247508	K0V	T06	0.26	T06	Y?	Y?	...	Y	Y
12065276-5044463	K6IV(e)	PM	0.44	PM	Y	Y?	Y?	Y	Y
12074236-6227282	K3Ve	T06	0.45	T06	Y	Y	...	Y	Y
12090225-5120410	K3IV(e)	PM	0.59	PM	Y	Y	Y?	Y	Y

Table 4.5 (cont'd)

2MASS	SpT	Ref.	$EW(Li)$ (Å)	Ref.	Membership				
					Li?	PM?	log(g)?	HRD?	Final
12092655-4923487	K4IVe	PM	0.69	PM	Y	Y	Y?	Y	Y
12094184-5854450	K2IV	PM	0.33	M02	Y	Y	...	Y	Y
12101065-4855476	K3IV(e)	PM	0.78	PM	Y	Y	Y?	Y	Y
12103705-5727208	K3IVe	PM	0.86	PM	Y	Y?	Y?	Y	Y
12113142-5816533	K1.5IV	PM	0.31	M02	Y	Y	...	Y	Y
12120804-6554549	K3Ve	T06	0.47	T06	Y	Y	...	Y	Y
12121119-4950081	K2Ve	T06	0.43	T06	Y	Y	...	Y	Y
12123577-5520273	K2IV	PM	0.34	M02	Y	Y	...	Y	Y
12124890-6230317	K7Ve	T06	0.55	T06	Y	Y	...	Y	Y
12131860-4815588	K3III(e)	PM	0.00	PM	N	Y?	N	...	N
12135166-5419527	K6IV	PM	0.00	PM	N	N	Y?	...	N
12135700-6255129	K4Ve	T06	0.47	T06	Y	Y	...	Y	Y
12141149-5456022	K3IIIe	PM	0.00	PM	N	N	N	...	N
12143410-5110124	K0IV	PM	0.33	M02	Y	Y	...	Y	Y
12145229-5547037	G6IV	PM	0.27	M02	Y	Y	...	Y	Y
12160114-5614068	K5Ve	T06	0.48	T06	Y	Y	...	Y	Y
12163007-6711477	K4IVe	T06	0.43	T06	Y	Y	...	Y	Y
12164023-7007361	K3IV(e)	PM	0.66	PM	Y	Y	Y?	Y	Y
12172809-5122215	K3III	PM	0.00	PM	N	Y?	N	...	N
12174048-5000266	K9IVe	PM	0.10	PM	Y?	Y	Y?	Y	Y
12182762-5943128	K2.5IV	PM	0.30	M02	Y	Y?	...	Y	Y
12185802-5737191	K1.5IV	PM	0.35	M02	Y	Y	...	Y	Y
12192161-6454101	K2IV	PM	0.32	M02	Y	Y	...	Y	Y
12195938-5018404	K5IVe	PM	0.58	PM	Y	Y	Y?	Y	Y
12202301-5242165	K9IVe	PM	0.68	PM	Y	Y	Y?	Y	Y
12205449-6457242	K4Ve	T06	0.47	T06	Y	Y	...	Y	Y
12205588-6534365	K9IVe	PM	0.41	PM	Y	Y	Y?	Y	Y
12210499-7116493	K6IVe	PM	0.66	PM	Y	Y?	Y?	Y	Y
12210808-5212226	K4Ve	T06	0.48	T06	Y	Y	...	Y	Y
12213087-6403530	K3.5IVe	PM	0.60	PM	Y	Y?	Y?	Y	Y
12215566-4946125	G6V	PM	0.28	M02	Y	Y	...	Y	Y

Table 4.5 (cont'd)

2MASS	SpT	Ref.	$EW(Li)$ (Å)	Ref.	Membership				
					Li?	PM?	log(g)?	HRD?	Final
12220430-4841248	K2IV	PM	0.34	M02	Y	Y	...	Y	Y
12222200-5114260	G2V	PM	0.00	PM	N	Y	Y?	...	N
12234012-5616325	K2V	PM	0.36	M02	Y	Y	...	Y	Y
12234749-6402549	K3IVe	PM	0.60	PM	Y	Y	Y?	Y	Y
12240975-6003416	K5IVe	PM	0.68	PM	Y	Y	Y?	Y	Y
12244195-6437015	K3III(e)	PM	0.07	PM	N	Y	N	...	N
12245648-4854270	K5IVe	PM	0.47	PM	Y	Y	Y?	Y	Y
12252542-5353568	K3V-IV(e)	PM	0.00	PM	N	Y	Y?	...	N
12253370-7227480	M0IV-Ve	PM	0.50	PM	Y	Y	Y?	Y	Y
12263934-6113406	K5IV(e)	PM	0.52	PM	Y	Y	Y?	Y	Y
12264842-5215070	K5Ve	T06	0.42	T06	Y	Y	...	Y	Y
12271665-6239142	K3IV(e)	PM	0.57	PM	Y	Y	Y?	Y	Y
12282540-6320589	G7V	T06	0.29	T06	Y	Y	...	Y	Y
12283577-4948021	K6III	PM	0.00	PM	N	N	N	...	N
12302957-5222269	K3V(e)	T06	0.42	T06	Y	Y	...	Y	Y
12313807-4558593	M3IVe	PM	0.24	PM	Y	N	Y?	...	N
12314481-4808482	K3V(e)	PM	0.00	PM	N	Y	Y?	...	N
12321483-4217502	K3III	PM	0.00	PM	N	N	N	...	N
12333381-5714066	K1V(e)	T06	0.42	T06	Y	Y	...	Y	Y
12351574-4919517	K0V	PM	0.00	PM	N	Y	Y?	...	N
12361767-5042421	K4Ve	T06	0.48	T06	Y	Y	...	Y	Y
12363895-6344436	K1IV	PM	0.37	M02	Y	Y	...	Y	Y
12365895-5412178	K2IV	PM	0.32	M02	Y	Y	...	Y	Y
12373737-5143113	K9IVe	PM	0.55	PM	Y	Y	Y?	Y	Y
12374883-5209463	K5IVe	PM	0.40	PM	Y	Y	Y?	Y	Y
12383556-5916438	K3Ve	T06	0.47	T06	Y	Y?	...	Y	Y
12390790-5811593	K4III	PM	0.00	PM	N	N	N	...	N
12391307-5429052	K0IV	PM	0.00	PM	N	N	Y?	...	N
12391404-5454469	K5IVe	PM	0.58	PM	Y	Y	Y?	Y	Y
12392312-7244039	K2III	T06	0.00	T06	N	N	...	...	N
12393796-5731406	G6V	PM	0.26	M02	Y	Y	...	Y	Y

Table 4.5 (cont'd)

2MASS	SpT	Ref.	$EW(Li)$ (Å)	Ref.	Membership				
					Li?	PM?	log(g)?	HRD?	Final
12404664-5211046	K2V(e)	T06	0.35	T06	Y	Y	...	Y	Y
12404975-5048077	K5IV(e)	PM	0.00	PM	N	N	Y?	...	N
12405458-5031550	K5V-IVe	PM	0.32	PM	Y	Y?	Y?	Y	Y
12411820-5825558	G1V	PM	0.29	M02	Y	Y	...	Y	Y
12420050-5759486	M0Ve	PM	0.46	PM	Y	Y	Y?	Y	Y
12434124-4204055	K5III(e)	PM	0.00	PM	N	Y	N	...	N
12443482-6331463	K2IV	PM	0.38	M02	Y	Y	...	Y	Y
12444949-4918474	K7IVe	PM	0.38	PM	Y	Y	Y?	Y	Y
12450674-4742580	G7IV	PM	0.30	M02	Y	Y	...	Y	Y
12454884-5410583	K2V(e)	T06	0.44	T06	Y	Y	...	Y	Y
12472196-6808397	K4IVe	PM	0.54	PM	Y	Y	Y?	Y	Y
12472609-5445156	K5IVe	PM	0.49	PM	Y	Y?	Y?	Y	Y
12474824-5431308	M0Ve	T06	0.54	T06	Y	Y	...	Y	Y
12475186-5126382	G2IV	PM	0.24	M02	Y	Y	...	Y	Y
12480778-4439167	G7V	PM	0.28	M02	Y	Y	...	Y	Y
12483152-5944493	K7IVe	PM	0.61	PM	Y	Y	Y?	Y	Y
12484652-5417333	G4Vn	PM	0.00	PM	N	Y	Y?	...	N
12484818-5635378	G3V	PM	0.22	M02	Y	Y	...	Y	Y
12504491-5654485	M1IVe	PM	0.54	PM	Y	Y	Y?	Y	Y
12505143-5156353	K5Ve	T06	0.50	T06	Y	Y	...	Y	Y
12510413-5253320	K5III	PM	0.00	PM	N	N	N	...	N
12510556-5253121	K5IVe	PM	0.60	PM	Y	Y	Y?	Y	Y
12543050-5031482	K7IVe	PM	0.38	PM	Y	Y	Y?	Y	Y
12560830-6926539	K7Ve	T06	0.51	T06	Y	Y	...	Y	Y
12560940-6127256	K0Ve	T06	0.35	T06	Y	N	...	...	N
12582559-7028490	K2IV	PM	0.37	M02	Y	Y	...	Y	Y
13010856-5901533	M0IVe	PM	0.20	PM	Y	Y	Y?	Y	Y
13015069-5304581	K3IV	PM	0.33	M02	Y	Y	...	Y	Y
13015435-4249422	K3IV	PM	0.44	PM	Y	Y	Y?	Y	Y
13024703-6213589	K0IV	PM	0.50	PM	Y	Y	Y?	Y	Y
13032904-4723160	K5IVe	PM	0.55	PM	Y	Y	Y?	Y	Y

Table 4.5 (cont'd)

2MASS	SpT	Ref.	$EW(Li)$ (Å)	Ref.	Membership				
					Li?	PM?	log(g)?	HRD?	Final
13055087-5304181	K6IVe	PM	0.50	PM	Y	Y	Y?	Y	Y
13064012-5159386	K1IV	PM	0.34	M02	Y	Y	...	Y	Y
13065439-4541313	K5Ve	T06	0.47	T06	Y	Y	...	Y	Y
13071310-5952108	K3IV	PM	0.47	PM	Y	Y	Y?	Y	Y
13095880-4527388	K2.5IVe	PM	0.56	PM	Y	Y	Y?	Y	Y
13103245-4817036	K4IVe	PM	0.74	PM	Y	Y	Y?	Y	Y
13112902-4252418	M0Ve	PM	0.29	PM	Y	Y	Y?	Y	Y
13121764-5508258	K5Ve	PM	0.48	PM	Y	Y	Y?	Y	Y
13121859-5439054	G7IV-V	PM	0.31	PM	Y	Y	Y?	Y	Y
13130714-4537438	K5Ve	T06	0.42	T06	Y	Y	...	Y	Y
13132326-5442156	K3IVe	PM	0.62	PM	Y	Y?	Y?	Y	Y
13140112-6846384	G9Ve	T06	0.37	T06	Y	N	...	...	N
13142382-5054018	G6IV	PM	0.32	M02	Y	Y	...	Y	Y
13151666-5058072	G6III	T06	0.01	T06	N	N	...	...	N
13173283-7037429	K6IVe	PM	0.00	PM	N	Y	Y?	...	N
13174687-4456534	K5IVe	PM	0.29	PM	Y	Y	Y?	Y	Y
13175314-5058481	K5IVe	PM	0.43	PM	Y	Y?	Y?	Y	Y
13191370-4506326	K5IVe	PM	0.51	PM	Y	Y	Y?	Y	Y
13203307-4927514	K4IV(e)	PM	0.53	PM	Y	Y	Y?	Y	Y
13204539-4611377	K5IVe	PM	0.60	PM	Y	Y	Y?	Y	Y
13220753-6938121	K1.5IV	PM	0.37	M02	Y	Y	...	Y	Y
13233587-4718467	K3Ve	T06	0.41	T06	Y	Y	...	Y	Y
13251211-6456207	K3IV	PM	0.43	PM	Y	Y	Y?	Y	Y
13270594-4856180	K3Ve	T06	0.44	T06	Y	Y	...	Y	Y
13274874-6622488	K3III	PM	0.00	PM	N	N	N	...	N
13281508-4446377	K1V	PM	0.00	PM	N	Y	Y?	...	N
13290963-4755545	K5Ve	PM	0.00	PM	N	Y	Y?	...	N
13291766-4614230	K5IVe	PM	0.45	PM	Y	Y	Y?	Y	Y
13294575-4844366	K9IVe	PM	0.35	PM	Y	Y?	Y?	Y	Y
13315360-5113330	G1V	PM	0.28	M02	Y	Y	...	Y	Y
13334410-6359345	K3.5IV(e)	PM	0.37	PM	Y	Y	Y?	Y	Y

Table 4.5 (cont'd)

2MASS	SpT	Ref.	$EW(Li)$ (Å)	Ref.	Membership				
					Li?	PM?	log(g)?	HRD?	Final
13335329-6536473	K9IVe	PM	0.56	PM	Y	Y	Y?	Y	Y
13335481-6536414	K5IVe	PM	0.52	PM	Y	Y	Y?	Y	Y
13342461-6517473	K9IVe	PM	0.65	PM	Y	Y	Y?	Y	Y
13343188-4209305	K2IVe	T06	0.40	T06	Y	Y	...	Y	Y
13354082-4818124	K3.5IV(e)	PM	0.56	PM	Y	Y	Y?	Y	Y
13364090-4043359	K6IVe	PM	0.76	PM	Y	Y	Y?	Y	Y
13375730-4134419	K1IV	PM	0.30	M02	Y	Y?	...	Y	Y
13380596-4344564	K3IV	PM	0.42	PM	Y	Y	Y?	Y	Y
13381128-5214251	K0IV	PM	0.37	PM	Y	Y	Y?	Y	Y
13384937-4237234	K3.5IV	PM	0.33	PM	Y	Y	Y?	Y	Y
13402554-4633514	K3Ve	T06	0.42	T06	Y	Y	...	Y	Y
13405585-4244505	K8IVe	PM	0.47	PM	Y	Y	Y?	Y	Y
13431296-4155366	G8V	PM	0.00	PM	N	N	Y?	...	N
13431682-4233127	K1III	PM	0.00	PM	N	N	N	...	N
13442441-4706343	K2IVn	PM	0.41	PM	Y	Y	Y?	Y	Y
13444279-6347495	K4Ve	T06	0.46	T06	Y	Y	...	Y	Y
13445275-6800331	G9V	PM	0.10	PM	N	Y	Y?	...	N
13451319-6128149	K2Ve	PM	0.00	PM	N	Y	Y?	...	N
13454424-4904500	K2.5IV	PM	0.43	PM	Y	Y	Y?	Y	Y
13455599-5222255	K3Ve	T06	0.41	T06	Y	Y	...	Y	Y
13475054-4902056	G6V	PM	0.29	M02	Y	Y	...	Y	Y
13493502-4452104	K3III	PM	0.00	PM	N	N	N	...	N
13503387-4810150	K8IVe	PM	0.45	PM	Y	Y	Y?	Y	Y
13515351-4846505	K5IVe	PM	0.56	PM	Y	Y	Y?	Y	Y
13522045-3825345	M1IVe	PM	0.18	PM	Y	N	Y?	...	N
13540743-6733449	G6V	T06	0.22	T06	Y?	Y	...	Y	Y
13544209-4820578	K2Ve	T06	0.33	T06	Y	Y	...	Y	Y
13552552-4706563	K4IVe	PM	0.50	PM	Y	Y	Y?	Y	Y
13562964-3839129	K3IV(e)	PM	0.42	PM	Y	Y	Y?	Y	Y
13563469-4907146	K3IV(e)	PM	0.53	PM	Y	Y	Y?	Y	Y
13575106-4431482	K3.5IVe	PM	0.46	PM	Y	Y	Y?	Y	Y

Table 4.5 (cont'd)

2MASS	SpT	Ref.	$EW(Li)$ (Å)	Ref.	Membership				
					Li?	PM?	log(g)?	HRD?	Final
13581812-4504043	K3III	PM	0.00	PM	N	Y?	N	...	N
13591330-7136541	K3III	PM	0.00	PM	N	Y	N	...	N
14001181-4230334	K8IVe	PM	0.50	PM	Y	Y	Y?	Y	Y
14003189-6416245	K2IV	PM	0.51	PM	Y	Y?	Y?	Y	Y
14004970-4236569	K0IV(e)	T06	0.36	T06	Y	Y	...	Y	Y
14014823-4100264	F5	PM	0.00	PM	N	N	...	...	N
14015020-4059234	K0III	PM	0.00	PM	N	N	N	...	N
14022072-4144509	G9IV	PM	0.23	M02	Y?	Y	...	Y	Y
14040272-4436503	F8	PM	0.00	PM	N	Y?	...	...	N
14055695-6149126	G2V	PM	0.00	PM	N	N	Y?	...	N
14060042-4112249	K3Ve	T06	0.40	T06	Y	Y	...	Y	Y
14074792-3945427	K5IV(e)	PM	0.45	PM	Y	Y	Y?	Y	Y
14081015-4123525	K7IVe	PM	0.80	PM	Y	Y	Y?	Y	Y
14085608-4403488	K3IVe	PM	0.39	PM	Y	Y	Y?	Y	Y
14122451-4327149	K2.5IV(e)	PM	0.35	PM	Y	Y?	Y?	Y	Y
14124691-3831220	K3Ve	T06	0.42	T06	Y	Y	...	Y	Y
14144477-4207224	G6V	PM	0.13	PM	N	Y	Y?	...	N
14165395-5356098	K1V	PM	0.00	PM	N	N	Y?	...	N
14184440-5850045	K3III-IV	PM	0.00	PM	N	Y	Y?	...	N
14185327-4827313	K3IVe	T06	0.61	T06	Y	Y	...	Y	Y
14201202-5339537	K2.5IV(e)	PM	0.43	PM	Y	Y	Y?	Y	Y
14201211-4917224	K0IIIe	PM	0.00	PM	N	N	N	...	N
14204893-4748442	K5Ve	T06	0.51	T06	Y	Y	...	Y	Y
14213051-3845252	K6IVe	PM	0.54	PM	Y	Y	Y?	Y	Y
14214378-4652082	K2V(e)	T06	0.42	T06	Y	Y	...	Y	Y
14214499-5429040	K3III(e)	PM	0.00	PM	N	Y	N	...	N
14220732-5417055	K3IVe	PM	0.41	PM	Y	Y	Y?	Y	Y
14223029-3532190	K3Ve	T06	0.41	T06	Y	Y	...	Y	Y
14224364-4628054	K2.5IV(e)	PM	0.52	PM	Y	Y	Y?	Y	Y
14234748-5935261	K2V(e)	T06	0.40	T06	Y	Y	...	Y	Y
14241649-5013282	K2III	PM	0.00	PM	N	N	N	...	N

Table 4.5 (cont'd)

2MASS	SpT	Ref.	$EW(Li)$ (Å)	Ref.	Membership				
					Li?	PM?	log(g)?	HRD?	Final
14244779-5041333	K1V	T06	0.27	T06	Y?	Y	...	Y	Y
14250165-4822361	G9III	T06	0.00	T06	N	Y	...	...	N
14262134-3644057	K0IV	PM	0.34	PM	Y	Y?	Y?	Y	Y
14270556-4714217	G6V	PM	0.26	M02	Y	Y	...	Y	Y
14275425-5944350	K5IVe	PM	0.48	PM	Y	Y	Y?	Y	Y
14280929-4414175	G5V	PM	0.22	M02	Y?	Y	...	Y	Y
14281937-4219341	G2V	PM	0.21	M02	Y	Y	...	Y	Y
14291483-6752209	A7	PM	0.00	PM	...	N	...	...	N
14301461-4520277	K3IV(e)	PM	0.35	PM	Y	Y?	Y?	N	N
14301594-5904014	K3III	PM	0.00	PM	N	N	N	...	N
14321121-5826058	K5IVe	PM	0.48	PM	Y	Y	Y?	Y	Y
14345213-4004459	K3.5IVe	PM	0.45	PM	Y	Y	Y?	Y	Y
14345603-7030069	K0V	T06	0.18	T06	N	N	...	...	N
14372053-4410053	G8V	PM	0.00	PM	N	Y?	Y?	...	N
14374904-4928268	K8IVe	PM	0.39	PM	Y	Y	Y?	Y	Y
14375022-5457411	G9IV	PM	0.32	M02	Y	Y	...	Y	Y
14380350-4932023	K4Ve	T06	0.45	T06	Y	Y	...	Y	Y
14380862-4322008	K7IVe	PM	0.51	PM	Y	Y	Y?	Y	Y
14385440-4310223	K3Ve	T06	0.45	T06	Y	Y	...	Y	Y
14392060-3905282	K1IV	PM	0.36	PM	Y	Y	Y?	Y	Y
14405601-7046138	G9III(e)	T06	0.00	T06	N	N	...	...	N
14411942-5001199	K4Ve	T06	0.42	T06	Y	Y	...	Y	Y
14413499-4700288	G5V	PM	0.23	M02	Y?	Y	...	Y	Y
14421471-5951445	K1V-IV	PM	0.09	PM	N	Y?	Y?	...	N
14421590-4100183	K3IV(e)	PM	0.37	PM	Y	Y	Y?	Y	Y
14421965-4432065	K5III	PM	0.00	PM	N	N	N	...	N
14432493-5643393	G2V	PM	0.24	PM	Y	Y?	Y?	Y	Y
14433325-5241213	G8V(e)	PM	0.00	PM	N	Y?	Y?	...	N
14442536-4329552	K8IVe	PM	0.87	PM	Y	Y	Y?	Y	Y
14472343-3503134	K3	W97	0.30	W97	Y	Y?	...	Y	Y
14481320-4102590	K2	W97	0.55	W97	Y	Y	...	Y	Y

Table 4.5 (cont'd)

2MASS	SpT	Ref.	$EW(Li)$ (Å)	Ref.	Membership				
					Li?	PM?	log(g)?	HRD?	Final
14502581-3506486	K1IV	PM	0.28	M02	Y	Y	...	Y	Y
14503508-3459056	K4	W97	0.56	W97	Y	Y	...	Y	Y
14522619-3740088	K3	W97	0.64	W97	Y	Y	...	Y	Y
14524198-4141552	K3IV	PM	0.35	M02	Y	Y	...	Y	Y
14541121-3955233	K2	W97	0.55	W97	Y	Y	...	Y	Y
14552673-5129013	G7V	T06	0.22	T06	Y?	Y	...	Y	Y
14560001-3124581	K2IV	PM	0.00	PM	N	N	Y?	...	N
14571217-3107596	K6III	PM	0.00	PM	N	N	N	...	N
14574495-4141394	K7IVe	PM	0.68	PM	Y	Y	Y?	Y	Y
14583744-3915033	M0IVe	PM	0.50	PM	Y	Y	Y?	Y	Y
14583769-3540302	K2.5IV	PM	0.37	M02	Y	Y	...	Y	Y
14584573-3315102	K1	W97	0.53	W97	Y	Y?	...	Y	Y
14592275-4013120	G7V	PM	0.23	M02	Y?	Y	...	Y	Y
14594473-3425465	K3Ve	T06	0.42	T06	Y	Y	...	Y	Y
15003768-4308339	K3	W97	0.56	W97	Y	Y	...	Y	Y
15005189-4331212	K1IV	PM	0.33	M02	Y	Y	...	Y	Y
15022600-3405131	K4	W97	0.45	W97	Y	Y	...	Y	Y
15023844-4156105	K7III	PM	0.00	PM	N	N	N	...	N
15033281-3033435	K3V	PM	0.00	PM	N	Y	Y?	...	N
15034365-5156318	K2.5V(e)	PM	0.00	PM	N	Y?	Y?	...	N
15035213-3906283	K6Ve	PM	0.50	PM	Y	Y	Y?	Y	Y
15044217-3018552	K1V-IV(e)	PM	0.12	PM	N	N	Y?	...	N
15052586-3857031	K6	W97	0.52	W97	Y	Y	...	Y	Y
15054424-3312508	K4IVe	PM	0.52	PM	Y	Y	Y?	Y	Y
15055685-4312031	K7	W97	0.68	W97	Y	Y	...	Y	Y
15064258-3047326	K7	W97	0.68	W97	Y	Y	...	Y	Y
15071481-3504595	K1IV	PM	0.25	M02	Y?	Y	...	Y	Y
15072758-4601073	K1	W97	0.43	W97	Y	Y	...	Y	Y
15075415-4730288	K1IV(e)	T06	0.40	T06	Y	Y	...	Y	Y
15080509-3337556	K6	K97	0.46	W97	Y	Y	...	Y	Y
15082754-5801220	F8	PM	0.00	PM	N	Y?	...	...	N

Table 4.5 (cont'd)

2MASS	SpT	Ref.	$EW(Li)$ (Å)	Ref.	Membership				
					Li?	PM?	log(g)?	HRD?	Final
15083773-4423170	G6IV(e)	PM	0.27	M02	Y	Y	Y?	Y	Y
15083849-4400519	G0V	PM	0.24	M02	Y	Y	...	Y	Y
15085379-3715467	K5	K97	...		Y	Y	...	Y	Y
15085472-4303136	K3IV	PM	0.55	PM	Y	Y	Y?	Y	Y
15092793-4650572	K0IV	M02	0.12	T06	N	Y	...	...	N
15102954-3902566	K3IV(e)	PM	0.49	PM	Y	Y	Y?	Y	Y
15105821-3926499	K1Ve	T06	0.15	T06	N	Y	...	...	N
15105821-3926499	K1Ve	T06	0.15	T06	N	Y	...	...	N
15110450-3251304	K6	W97	0.54	W97	Y	Y	...	Y	Y
15113968-3248560	M1.5	W97	0.34	W97	Y	Y	...	Y	Y
15122700-4453385	G8V	PM	0.03	PM	N	Y?	Y?	...	N
15124447-3116482	K2Ve	T06	0.38	T06	Y	Y	...	Y	Y
15130869-4450158	K4III	PM	0.00	PM	N	N	N	...	N
15135817-4629145	K7	K97	0.48	W99	Y	Y	...	Y	Y
15140754-4103361	G7	W97	0.35	W97	Y	Y	...	Y	Y
15144748-4220149	K1	K97	0.68	W97	Y	Y	...	Y	Y
15151856-4146354	K9V-IVe	PM	0.32	PM	Y	Y	Y?	Y	Y
15152295-5441088	K4IVe	PM	0.40	PM	Y	Y	Y?	Y	Y
15153210-3005336	K3V-IV	PM	0.00	PM	N	Y	Y?	...	N
15154537-3331597	K0	W97	0.66	W97	Y	Y	...	Y	Y
15155274-4418173	K1	W97	0.60	W97	Y	Y	...	Y	Y
15161044-3851565	K0III	T06	0.00	T06	N	N	...	...	N
15163663-4407204	K2	K97	0.57	W99	Y	Y	...	Y	Y
15171083-3434194	K3IVe	PM	0.42	PM	Y	Y	Y?	Y	Y
15180123-4444269	K2	W97	0.33	W97	Y	Y	...	Y	Y
15182692-3738021	G8IV	PM	0.26	M02	Y	Y	...	Y	Y
15185282-4050528	G8	K97	0.48	W99	Y	Y	...	Y	Y
15191600-4056075	K0	K97	0.41	T06	Y	Y	...	Y	Y
15191807-2943204	K7IVe	PM	0.48	PM	Y	Y	Y?	Y	Y
15193457-2846217	K1V	T06	0.04	T06	N	N	...	...	N
15200259-4638340	G9V	PM	0.00	PM	N	Y	Y?	...	N

Table 4.5 (cont'd)

2MASS	SpT	Ref.	$EW(Li)$ (Å)	Ref.	Membership				
					Li?	PM?	log(g)?	HRD?	Final
15202415-3037317	K4IVe	T06	0.57	T06	Y	Y	...	Y	Y
15215241-2842383	K3IV(e)	PM	0.42	PM	Y	Y	Y?	Y	Y
15220457-5634346	G8V	PM	0.05	PM	N	Y	Y?	...	N
15220743-3930140	K5Ve	PM	0.07	PM	N	Y	Y?	...	N
15221162-3959509	K3	K97	0.50	W99	Y	Y	...	Y	Y
15221627-2652252	K4IV(e)	PM	0.00	P98	N	N	Y?	...	N
15222449-3337352	K2V	PM	0.00	PM	N	Y	Y?	...	N
15230505-3627294	K7Ve	PM	0.06	PM	N	Y?	Y?	...	N
15232557-4055467	K2	K97	0.39	W99	Y	Y	...	Y	Y
15234137-4004455	K1IV	PM	0.00	PM	N	N	Y?	...	N
15235794-3619585	K4IV	PM	0.61	PM	Y	Y	Y?	Y	Y
15240305-3209508	K7	K97	0.37	W99	Y	Y	...	Y	Y
15240670-3601013	G4V	PM	0.00	PM	N	Y	Y?	...	N
15241147-3030582	K0	K00	...		Y	Y	...	Y	Y
15241303-3030572	M1	K00	...		Y	Y?	...	Y	Y
15243236-3652027	K1	K97	0.38	T06	Y	Y	...	Y	Y
15243933-2102040	G2V	PM	0.00	PM	N	Y	Y?	...	N
15244741-4257591	K0V(e)	PM	0.00	PM	N	Y	Y?	...	N
15250358-3604455	K1	K97	0.37	T06	Y	Y	...	Y	Y
15251724-2729309	K0V	PM	0.00	P98	N	N	Y?	...	N
15253316-3613467	K2	K97	0.43	W99	Y	Y	...	Y	Y
15253666-3537319	K6	K97	0.46	W99	Y	Y	...	Y	Y
15255964-4501157	K0IV	PM	0.26	M02	Y?	Y	...	Y	Y
15262805-5549569	K3IV(e)	PM	0.42	PM	Y	Y	Y?	Y	Y
15264407-3849588	G8V	PM	0.00	PM	N	N	Y?	...	N
15264611-3849198	K3III	PM	0.00	PM	N	N	N	...	N
15265257-3722062	M0.5	K97	...		Y	Y	...	Y	Y
15271052-4138334	G9IV	T06	0.06	T06	N	Y	...	...	N
15272286-3604087	K7-M0	K97	...		Y	Y	...	Y	Y
15280113-3751360	K4V	PM	0.00	PM	N	N	Y?	...	N
15280288-3751087	K5	K97	...		N	N	...	...	N

Table 4.5 (cont'd)

2MASS	SpT	Ref.	$EW(Li)$ (Å)	Ref.	Membership				
					Li?	PM?	log(g)?	HRD?	Final
15280322-2600034	K3	K00	...		Y	Y	...	Y	Y
15284402-3117387	G9III	T06	0.04	T06	N	N	...	...	N
15284402-3117387	G6IV	T06	0.00	T06	N	N	...	...	N
15293858-3546513	K1IV	PM	0.25	M02	Y?	Y	...	Y	Y
15294727-3628374	K2	K97	0.45	T06	Y	Y	...	Y	Y
15294888-4522457	K6	W97	0.67	W97	Y	Y	...	Y	Y
15295661-3135446	K5IVe	PM	0.66	PM	Y	Y	Y?	Y	Y
15304790-3022054	K2	K00	...		Y	Y	...	Y	Y
15311824-4333323	K0	K97	...		N	Y?	...	...	N
15312047-3855116	K4IV	PM	0.00	PM	N	N	Y?	...	N
15312193-3329394	G9.5V	M02	0.35	W07	Y	Y	...	Y	Y
15312961-3021537	M0	K00	...		Y	Y	...	Y	Y
15313413-3602287	K3V(e)	T06	0.42	T06	Y	Y	...	Y	Y
15313716-2156489	K4V	PM	0.00	PM	N	N	Y?	...	N
15320739-2427130	K1IV	PM	0.00	PM	N	Y?	Y?	...	N
15333037-2003264	K0V	PM	0.00	PM	N	Y?	Y?	...	N
15340737-3916171	K1	K97	0.24	W99	Y?	Y	...	Y	Y
15342292-2514386		P98	0.10	P98	...	N	...	...	N
15342313-3300087	M0	K00	...		Y	Y	...	Y	Y
15343816-4002280	K6	W97	0.66	W97	Y	Y	...	Y	Y
15350044-3915143	K2Ve	T06	0.05	T06	N	Y	...	...	N
15351524-4156586	K0III	T06	0.13	T06	N	N	...	...	N
15355780-2324046	K3:	P98	0.42	P98	Y	Y	...	Y	Y
15355876-4456355	K7IVe	PM	0.33	PM	Y	Y	Y?	Y	Y
15364094-2923574	M1IVe	PM	0.09	PM	Y	Y	Y?	Y	Y
15370214-3136398	G5V	PM	0.23	M02	Y?	Y	...	Y	Y
15370261-2942430	K0V	PM	0.00	PM	N	Y?	Y?	...	N
15371129-4015566	G7V	PM	0.30	M02	Y	Y	...	Y	Y
15371218-2644516	K0V	PM	0.00	PM	N	N	Y?	...	N
15371991-3041150	K5III	PM	0.00	PM	N	N	N	...	N
15374917-1840449	G5:	P98	0.20	P98	Y?	Y?	...	Y	Y

Table 4.5 (cont'd)

2MASS	SpT	Ref.	$EW(Li)$ (Å)	Ref.	Membership				
					Li?	PM?	log(g)?	HRD?	Final
15375134-3045160	K4	K00	0.41	T06	Y	Y	...	Y	Y
15380264-3807230	K5	K97	0.46	W99	Y	Y	...	Y	Y
15381792-2337306		P98	0.05	P98	...	Y	...	...	N
15383827-3916553	K4	K97	0.38	W99	Y	Y	...	Y	Y
15384306-4411474	K0.5IV	PM	0.27	M02	Y?	Y	...	Y	Y
15392776-3446171	K7	K00	0.61	F87	Y	Y	...	Y	Y
15394637-3451027	K4	K97	...		Y	Y	...	Y	Y
15400244-4634187	K4	K97	...		Y	Y	...	Y	Y
15404116-3756185	K6	K97	0.49	W99	Y	Y	...	Y	Y
15410679-2656263	G7	P98	0.25	W07	Y	Y	...	Y	Y
15413114-5330296	K2Ve	T06	0.42	T06	Y	Y	...	Y	Y
15413121-2520363	G9IVe	T06	0.41	T06	Y	Y	...	Y	Y
15414732-1804591	K0V-IV	PM	0.00	PM	N	N	Y?	...	N
15420518-3601317	K7	K97	...		Y	Y	...	Y	Y
15421600-4435440	K6III	PM	0.00	PM	N	N	N	...	N
15422385-4625471	K0IV	PM	0.00	PM	N	Y?	Y?	...	N
15424991-2536406	G5	P98	0.26	P98	Y	Y	...	Y	Y
15430669-4643064	K6V(e)	PM	0.00	PM	N	Y?	Y?	...	N
15433953-2909035	K3III	PM	0.04	PM	N	N	N	...	N
15435905-2622516	K9Ve	PM	0.41	PM	Y	Y	Y?	Y	Y
15440376-3311110	K2V	PM	0.30	M02	Y	Y	...	Y	Y
15441334-2522590	M1e	P98	0.61	P98	Y	Y	...	Y	Y
15442874-4745415	K9IVe	PM	0.31	PM	Y	Y	Y?	Y	Y
15444712-3811406	K7	K97	0.49	T06	Y	Y	...	Y	Y
15451286-3417305	K2e	H94	0.40	T06	Y	Y	...	Y	Y
15455225-4222163	K2.5IV	PM	0.39	M02	Y	Y	...	Y	Y
15462958-5217239	K0IV	PM	0.25	PM	Y?	Y	Y?	Y	Y
15463111-5216580	M0Ve	PM	0.00	PM	Y?	Y	Y?	Y	Y
15464121-3618472	K1	K97	0.38	T06	Y	Y	...	Y	Y
15471063-1736244	M0Ve	PM	0.67	PM	Y	Y	Y?	Y	Y
15474176-4018267	K1	K97	0.38	T06	Y	Y	...	Y	Y

Table 4.5 (cont'd)

2MASS	SpT	Ref.	$EW(Li)$ (Å)	Ref.	Membership				
					Li?	PM?	log(g)?	HRD?	Final
15475575-2300331	K2V	PM	0.00	PM	N	Y	Y?	...	N
15480291-2908369	G9	K00	0.34	T06	Y	Y	...	Y	Y
15481148-4712297	K3IVe	PM	0.37	PM	Y	Y	Y?	Y	Y
15481299-2349523	M0.5Ve	PM	0.14	PM	Y	Y	Y?	Y	Y
15484204-4335207	G8	K97	0.36	T06	Y	Y?	...	Y	Y
15490271-3102537	K0	K00	0.37	T06	Y	Y	...	Y	Y
15490667-1813113	G1V	PM	0.14	PM	Y?	N	Y?	N	N
15492100-2600062	K0	K00	0.40	T06	Y	Y	...	Y	Y
15494499-3925089	K2.5IV	PM	0.32	M02	Y	Y	...	Y	Y
15495840-4306370	K3IV(e)	PM	0.31	PM	Y	Y?	Y?	Y	Y
15495920-3629574	K2	K97	0.37	W99	Y	Y	...	Y	Y
15510142-1548286	M1IVe	PM	0.10	PM	Y	Y	Y?	Y	Y
15510660-2402190	M2	K00	...		Y	Y	...	Y	Y
15514535-2456513	K3IV	PM	0.43	PM	Y	Y	Y?	Y	Y
15521613-3218449	K1V	PM	0.00	PM	N	Y	Y?	...	N
15522589-3920512	K4IVe	PM	0.34	PM	Y	Y	Y?	Y	Y
15523122-2633529	M0	P99	...		Y	Y?	...	Y	Y
15530683-2247174	M0IV-Ve	PM	0.60	PM	Y	Y	Y?	Y	Y
15545141-3154463	K5IVe	PM	0.61	PM	Y	Y	Y?	Y	Y
15550624-2521102	M1	P99	...		Y	Y	...	Y	Y
15551621-1355136	K6IVe	PM	0.09	PM	Y?	Y?	Y?	Y	Y
15552621-3338232	K5	K97	0.46	W99	Y	Y	...	Y	Y
15555324-4041435	F5	PM	0.00	PM	N	Y	...	...	N
15560250-3643472	K6	K97	...		N	Y?	...	...	N
15560921-3756057	M0e	H94	0.55	C	Y	Y?	...	Y	Y
15561488-2100408		P98	0.05	P98	...	N	...	...	N
15564402-4242301	K6IVe	T06	0.53	T06	Y	Y	...	Y	Y
15565905-3933430	G7IV	PM	0.21	M02	Y?	Y	...	Y	Y
15570234-1950419	K7:e	P98	0.55	P98	Y	Y	...	Y	Y
15573430-2321123	M1IVe	PM	0.52	PM	Y	Y	Y?	Y	Y
15574362-4143377	K6IVe	PM	0.56	PM	Y	Y	Y?	Y	Y

Table 4.5 (cont'd)

2MASS	SpT	Ref.	$EW(Li)$ (Å)	Ref.	Membership				
					Li?	PM?	log(g)?	HRD?	Final
15574440-4049276	K9IVe	PM	0.57	PM	Y	Y	Y?	Y	Y
15575002-2305094	M0	K00	...		Y	Y	...	Y	Y
15581270-2328364	G2IV	PM	0.28	T06	Y	Y	Y?	Y	Y
15581474-4029175	K8IVe	PM	0.77	PM	Y	Y	Y?	Y	Y
15582054-1837252	G3e	P98	0.25	P98	Y	Y	...	Y	Y
15582850-1610379	G9V	PM	0.00	PM	N	Y	Y?	...	N
15583692-2257153	G5IVe	PM	0.40	W07	Y	Y	Y?	Y	Y
15584772-1757595	K3e	P98	0.35	W07	Y	Y	...	Y	Y
15590208-1844142	K6e	P98	0.45	P98	Y	Y	...	Y	Y
15591101-1850442	K6IVe	PM	0.67	PM	Y	Y	Y?	Y	Y
15591452-2606182	K2	K00	...		Y	Y	...	Y	Y
15591647-4157102	K7IVe	PM	0.67	PM	Y	Y?	Y?	Y	Y
15593661-3255340	G8	K00	...		Y	N	...	...	N
15593706-3255414	G8	K00	...		Y	N	...	...	N
15594951-3628279	K3	K97	0.48	T06	Y	Y?	...	Y	Y
16003134-2027050	M1	P99	...		Y	Y	...	Y	Y
16003317-2726185	K3IIIe	PM	0.00	PM	N	N	N	...	N
16004056-2200322	G9	P99	0.31	W07	Y	Y	...	Y	Y
16004277-2127380	K7	P99	...		Y	Y	...	Y	Y
16010801-2113184	M0	P99	...		Y	Y	...	Y	Y
16011070-4804438	K3Ve	T06	0.43	T06	Y	Y	...	Y	Y
16012563-2240403	K1IV	W94	0.48	W07	Y	Y	...	Y	Y
16014743-2049457	M0	P99	...		Y	Y	...	Y	Y
16014943-4026192	K7	K97	...		Y	Y	...	Y	Y
16015061-4758342	F8	PM	0.06	PM	N	Y	...	...	N
16015149-2445249	K7	P99	...		Y	Y	...	Y	Y
16015568-2412329	G8V	PM	0.06	PM	N	Y?	Y?	...	N
16015822-2008121	G5	P99	0.25	W07	Y	Y	...	Y	Y
16015918-3612555	K3	K97	0.44	W99	Y	Y	...	Y	Y
16020039-2221237	M1	P99	...		Y	Y	...	Y	Y
16021045-2241280	K5IV	W94	0.36	W94	Y	Y?	...	Y	Y

Table 4.5 (cont'd)

2MASS	SpT	Ref.	$EW(Li)$ (Å)	Ref.	Membership				
					Li?	PM?	log(g)?	HRD?	Final
16023814-2541389	K8IVe	PM	0.56	PM	Y	Y	Y?	Y	Y
16023910-2542078	K7e	P98	0.35	P98	Y	Y?	...	Y	Y
16025123-2401574	K4	P99	...		Y	Y	...	Y	Y
16025243-2402226	K0	K00	...		Y	Y?	...	Y	Y
16025396-2022480	K7	P99	...		Y	Y	...	Y	Y
16030269-1806050	K4e	P98	0.40	W07	Y	Y	...	Y	Y
16032367-1751422	M2e	P98	0.45	P98	Y	Y	...	Y	Y
16033550-2245560	G9	P99	0.43	T06	Y	Y	...	Y	Y
16034536-4355492	K1IV	PM	0.35	M02	Y	Y	...	Y	Y
16035250-3939013	K3IV	PM	0.38	M02	Y	Y	...	Y	Y
16035625-3624496	K3IV	PM	0.00	PM	N	N	Y?	...	N
16035836-1751041	M0IVe	PM	0.57	PM	Y	Y?	Y?	Y	Y
16042165-2130284	K2	P99	...		Y	Y	...	Y	Y
16042291-4448088	K5III(e)	PM	0.00	PM	N	Y	N	...	N
16043056-3207287	K2	K97	0.35	T06	Y	Y	...	Y	Y
16044776-1930230	K2IV	W94	0.40	W07	Y	Y	...	Y	Y
16051598-1158039	G8V	PM	0.00	PM	N	Y?	Y?	...	N
16054266-2004150	M2V	W94	0.52	W94	Y	Y	...	Y	Y
16054499-3906065	G8V	PM	0.32	M02	Y	Y	...	Y	Y
16055065-2533136	G7e	P98	0.47	P98	Y	Y?	...	Y	Y
16055207-3439331	K2Ve	T06	0.40	T06	Y	Y	...	Y	Y
16061222-4507155	K3IV(e)	PM	0.72	PM	Y	Y?	Y?	Y	Y
16061254-2036472	K5	P99	...		Y	Y	...	Y	Y
16061466-4413135	K3V(e)	PM	0.19	PM	Y?	N	Y?	...	N
16062196-1928445	M0.5V	W94	0.47	W94	Y	Y	...	Y	Y
16062334-4447355	K4	K97	...		Y	Y	...	Y	Y
16062354-1814187	K5IVe	PM	0.59	PM	Y	Y	Y?	Y	Y
16063169-2036232	K6e	P98	0.56	P98	Y	Y	...	Y	Y
16063245-2208245	K6IVe	PM	0.57	PM	Y	Y	Y?	Y	Y
16065436-2416107	M3e	P98	0.62	P98	Y	Y	...	Y	Y
16065795-2743094	A9IVe var	PM	0.06	PM	...	Y	...	Y	Y

Table 4.5 (cont'd)

2MASS	SpT	Ref.	$EW(Li)$ (Å)	Ref.	Membership				
					Li?	PM?	log(g)?	HRD?	Final
16070356-2036264	M0	P99	...		Y	Y	...	Y	Y
16070393-1911338	M1	P99	...		Y	Y	...	Y	Y
16073366-3759242	K7IVe	PM	0.54	PM	Y	Y	Y?	Y	Y
16073490-2445412	K1IV-III	PM	0.49	PM	Y	Y?	Y?	N	N
16074006-2148426	K7IVe	PM	0.68	PM	Y	Y	Y?	Y	Y
16080019-4116119	K3.5IVe	PM	0.55	PM	Y	Y	Y?	Y	Y
16080141-2027416	K8e	P02	0.83	P02	Y	Y	...	Y	Y
16080772-5041556	K6IVe	PM	0.36	PM	Y	Y	Y?	Y	Y
16081081-1904479	K3IVe	PM	0.51	PM	Y	Y	Y?	Y	Y
16081474-1908327	K2	P98	0.41	W07	Y	Y	...	Y	Y
16081824-3844052	K7	K97	0.50	W99	Y	Y	...	Y	Y
16082061-4109504	K0III	PM	0.13	PM	N	Y?	N	...	N
16083436-1911563	K5:	P98	0.25	P98	Y	Y	...	Y	Y
16083617-3923024	K6	K97	0.48	W99	Y	Y	...	Y	Y
16084340-2602168	G7	P98	0.45	P98	Y	Y	...	Y	Y
16085427-3906057	K2	K97	0.49	W99	Y	Y	...	Y	Y
16085438-4148364	K3III	PM	0.00	PM	N	Y?	N	...	N
16085673-2033460	K5e	P98	0.45	P98	Y	Y	...	Y	Y
16090075-1908526	K9e	P01	0.53	P02	Y	Y	...	Y	Y
16092918-1852536	K4IVe	PM	0.47	PM	Y	Y	Y?	Y	Y
16093030-2104589	M0e	P98	0.54	P98	Y	Y	...	Y	Y
16093969-2200466	K9IVe	PM	0.66	PM	Y	Y	Y?	Y	Y
16094098-2217594	M0e	P98	0.52	P98	Y	Y	...	Y	Y
16100321-5026121	K0III	T06	0.20	T06	Y?	Y?	...	N	N
16100478-4016122	K2	K97	0.42	T06	Y	Y	...	Y	Y
16100577-2626068		P98	0.08	P98	...	N	...	...	N
16101171-3226360	K5IVe	PM	0.46	PM	Y	Y	Y?	Y	Y
16101264-2104446	K3IV	PM	0.40	PM	Y	Y	Y?	Y	Y
16101729-1910263	K5IVe	PM	0.45	PM	Y	Y	Y?	Y	Y
16101918-2502301	M1e	P98	0.52	P98	Y	Y	...	Y	Y
16102174-1904067	M1V	W94	0.50	PM	Y	Y	...	Y	Y

Table 4.5 (cont'd)

2MASS	SpT	Ref.	$EW(Li)$ (Å)	Ref.	Membership				
					Li?	PM?	log(g)?	HRD?	Final
16102653-2756293	M3Ve	PM	0.00	PM	Y?	Y	Y?	Y	Y
16102888-2213477	G5V	H88	0.24	T06	Y	Y	...	Y	Y
16104202-2101319	K5e	P98	0.52	P98	Y	Y	...	Y	Y
16110890-1904468	K4IVe	PM	0.41	PM	Y	Y	Y?	Y	Y
16111534-1757214	M1e	P02	0.55	P02	Y	Y	...	Y	Y
16114387-2526350	K3IV(e)	PM	0.48	PM	Y	Y	Y?	Y	Y
16115334-3902158	K7/M0e	H94	...		Y	Y	...	Y	Y
16120140-3840276	K5	K97	...		Y	Y?	...	Y	Y
16123916-1859284	K2.5IV	PM	0.44	PM	Y	Y	Y?	Y	Y
16124051-1859282	K0IV	W94	0.41	W07	Y	Y	...	Y	Y
16124682-2213317	K3IV(e)	PM	0.38	PM	Y	Y	Y?	Y	Y
16125265-2319560	K3IV(e)	PM	0.46	PM	Y	Y	Y?	Y	Y
16130271-2257446	K4e	P98	0.46	P98	Y	Y	...	Y	Y
16131267-3803513	K5	K97	...		Y	Y	...	Y	Y
16131738-2922198	M0IVe	PM	0.56	PM	Y	Y	Y?	Y	Y
16131858-2212489	G9	P98	0.47	P98	Y	Y	...	Y	Y
16132929-2311075	K1e	P98	0.49	W07	Y	Y	...	Y	Y
16134366-2214594	K7IVe	PM	0.56	PM	Y	Y	Y?	Y	Y
16135801-3618133	G8V	PM	0.27	M02	Y	Y	...	Y	Y
16140035-2108439	K8IVe	PM	0.53	PM	Y	Y	Y?	Y	Y
16140211-2301021	G4	P98	0.44	P98	Y	Y	...	Y	Y
16141107-2305362	K0	P98	0.49	P98	Y	Y	...	Y	Y
16141904-3326041	G8V	T06	0.18	T06	N	Y	...	...	N
16143884-2525000	M0.5IVe	PM	0.39	PM	Y	Y	Y?	Y	Y
16145207-5026187	K1IV	PM	0.32	M02	Y	Y	...	Y	Y
16145918-2750230	G5	P98	0.26	W07	Y	Y	...	Y	Y
16152831-3402319	K3III	PM	0.06	PM	N	N	N	...	N
16153456-2242421	K5Ve	T06	0.45	P98	Y	Y	...	Y	Y
16153587-2529008	K2.5IVe	PM	0.46	PM	Y	Y	Y?	Y	Y
16154270-2901016	K5III	PM	0.00	PM	N	N	N	...	N
16155664-3947163	M0.5	K97	...		Y	Y	...	Y	Y

Table 4.5 (cont'd)

2MASS	SpT	Ref.	$EW(Li)$ (Å)	Ref.	Membership				
					Li?	PM?	log(g)?	HRD?	Final
16161423-2643148	K5IVe	PM	0.34	PM	Y	Y	Y?	Y	Y
16161795-2339476	G7	P98	0.21	W07	Y?	Y	...	Y	Y
16165205-2154235	K4IV(e)	PM	0.09	PM	N	Y	Y?	...	N
16172711-5023213	G3V	PM	0.00	PM	N	N	Y?	...	N
16173138-2303360	G0IV	W94	0.22	W07	Y	Y	...	Y	Y
16175569-3828132	M0Ve	PM	0.00	PM	Y?	Y	Y?	Y	Y
16180479-2224394	K0III	T06	0.07	P98	N	Y	...	...	N
16181107-2911125	G6	C06	0.30	T06	Y	Y	...	Y	Y
16183723-2405226	G5V	PM	0.26	PM	Y	Y?	Y?	Y	Y
16185958-2213283	K3III	PM	0.00	PM	N	N	N	...	N
16191035-3851041	G9V	PM	0.00	PM	N	Y?	Y?	...	N
16191217-2550383	K3IV	PM	0.39	PM	Y	Y	Y?	Y	Y
16193334-2807397	M2III	PM	0.00	PM	Y?	N	N	N	N
16193396-2228294	K0e	P98	0.55	P98	Y	Y	...	Y	Y
16195068-2154355	K8IVe	PM	0.55	PM	Y	Y	Y?	Y	Y
16200368-4801298	K1V	T06	0.00	T06	N	N	...	...	N
16202930-3254096	K4IV(e)	PM	0.47	PM	Y	Y	Y?	Y	Y
16202983-2716240	F0	PM	0.03	PM	Y	N	...	N	N
16204468-2431384	G0	P98	0.12	P98	Y?	Y	...	Y	Y
16230783-2300596	K2	P98	0.61	P98	Y	Y?	...	Y	Y
16233234-2523485	G1	P98	0.42	P98	Y	Y	...	Y	Y
16234698-2850023	G8IV	T06	0.31	T06	Y	Y	...	Y	Y
16235484-3312370	K6IVe	PM	0.35	PM	Y	Y	Y?	Y	Y
16235844-4706089	G5III	PM	0.00	PM	N	N	N	...	N
16240289-2524539	B8V	G67	0.00	PM	...	Y	...	Y	Y
16240373-4319261	G3V	PM	0.27	PM	Y	Y	Y?	Y	Y
16240632-2456468	K3IVe	PM	0.44	PM	Y	Y	Y?	Y	Y
16241860-2854475	G5Ve	PM	0.30	PM	Y	Y?	Y?	Y	Y
16243416-2606367	K4III	PM	0.00	PM	N	N	N	...	N
16245136-2239325	G6e	P98	0.40	P98	Y	Y	...	Y	Y
16250991-3047572	G1V	PM	0.30	PM	Y	Y	Y?	Y	Y

Table 4.5 (cont'd)

2MASS	SpT	Ref.	$EW(Li)$ (Å)	Ref.	Membership				
					Li?	PM?	log(g)?	HRD?	Final
16251923-2426526	G1IV	W94	0.29	W94	Y	Y	...	Y	Y
16252863-2346265	K2IV	PM	0.27	PM	Y?	Y	Y?	Y	Y
16253849-2613540	K7Ve	T06	0.49	T06	Y	Y	...	Y	Y
16262736-2756508	K4IVe	PM	0.63	PM	Y	Y?	Y?	Y	Y
16263591-3314481	K2IV(e)	PM	0.33	PM	Y	Y	Y?	Y	Y
16265280-2343127	K1IVe	PM	0.45	PM	Y	Y?	Y?	Y	Y
16265700-3032232	K6IVe	PM	0.43	PM	Y	Y	Y?	Y	Y
16265763-3032279	M0IVe	PM	0.27	PM	Y	Y	Y?	Y	Y
16270927-2339055	K4IVe	PM	0.74	PM	Y	N	Y?	...	N
16271951-2441403	M0IVe	PM	0.61	PM	Y	Y	Y?	Y	Y
16272373-2855286	K3IV	PM	0.00	PM	N	Y?	Y?	...	N
16272794-4542403	G8Ve	T06	0.30	T06	Y	Y	...	Y	Y
16273956-2245230	K1e	P98	0.55	P98	Y	Y	...	Y	Y
16274028-2422040	K5e	T06	0.49	T06	Y	Y	...	Y	Y
16282453-4740395	M0IVe	PM	0.35	PM	Y	Y	Y?	Y	Y
16282493-2723182	F8	PM	0.03	PM	N	Y	...	...	N
16290446-2600389	K3III	PM	0.00	PM	N	N	N	...	N
16290585-3145250	K5IVe	PM	0.46	PM	Y	Y	Y?	Y	Y
16293397-2455303	K1IV	PM	0.39	PM	Y	Y	Y?	Y	Y
16294869-2152118	KIV	W94	0.44	W07	Y	Y	...	Y	Y
16294991-2728498	K1V(e)	T06	0.42	T06	Y	Y	...	Y	Y
16303162-4718119	K4III	PM	0.00	PM	N	N	N	...	N
16303796-2954222	K2Ve	T06	0.42	T06	Y	Y	...	Y	Y
16303840-2418312	K1V	PM	0.00	PM	N	Y	Y?	...	N
16310436-2404330	K4IVe	PM	0.41	PM	Y	Y	Y?	Y	Y
16310837-2651062	K8IVe	PM	0.26	PM	Y	Y	Y?	Y	Y
16315346-2636169	K4IV(e)	PM	0.39	PM	Y	Y	Y?	Y	Y
16320058-2530287	K7IVe	PM	0.35	PM	Y	Y	Y?	Y	Y
16320160-2530253	K5IVe	PM	0.66	PM	Y	Y	Y?	Y	Y
16320352-2830179	G7IV	T06	0.25	T06	Y?	Y	...	Y	Y
16321179-2440213	K8IVe	PM	0.56	PM	Y	Y	Y?	Y	Y

Table 4.5 (cont'd)

2MASS	SpT	Ref.	$EW(Li)$ (Å)	Ref.	Membership				
					Li?	PM?	log(g)?	HRD?	Final
16322432-1703399	K9IVe	PM	0.60	PM	Y	Y	Y?	Y	Y
16323765-4541547	K3III(e)	PM	0.06	PM	N	Y	N	...	N
16334191-2523342	K4IVe	T06	0.58	T06	Y	Y	...	Y	Y
16340585-2658441	K3IVe	PM	0.39	PM	Y	Y	Y?	Y	Y
16344629-2606324	K4.5IVe	PM	0.47	PM	Y	Y	Y?	Y	Y
16345314-2518167	G9IV	T06	0.30	T06	Y	Y	...	Y	Y
16351188-2845520	K7IVe	PM	0.49	PM	Y	Y	Y?	Y	Y
16353547-2541194	G8IV	PM	0.29	PM	Y	Y?	Y?	Y	Y
16354836-2148396	M0e	P98	0.67	P98	Y	Y	...	Y	Y
16361809-1828333	K1V	PM	0.00	PM	N	N	Y?	...	N
16363716-2340011	K5IVe	PM	0.27	PM	Y	N	Y?	N	N
16384946-2735294	K0V(e)	T06	0.32	T06	Y	Y	...	Y	Y
16395498-2328007	K1III	PM	0.00	PM	N	Y?	N	...	N
16430140-4405275	G7V	B	0.34	B	Y	Y?	Y?	Y	Y
16432519-3022477	K0V(e)	T06	0.35	T06	Y	Y	...	Y	Y
16452615-2503169	K3Ve	T06	0.50	T06	Y	Y	...	Y	Y
16455772-4321044	G7V	PM	0.36	PM	Y	N	Y?	...	N
16473710-2014268	K4IV(e)	PM	0.30	PM	Y	Y	Y?	Y	Y
16491330-4355279	K0IV	T06	0.29	T06	Y	Y	...	Y	Y
16493599-2728078	K0Ve	T06	0.23	T06	Y?	N	...	...	N
16520069-2122553	K3IV	PM	0.14	PM	N	N	Y?	...	N
16542415-2500202	K9Ve	PM	0.00	PM	N	N	Y?	...	N

Note. — References – (PM) - This work; (G67) - Garrison (1967); (F87) - Finkenzeller & Basri (1987); (H88) - Houk & Smith-Moore (1988); (W94) - Walter et al. (1994); (H94) - Hughes et al. (1994); (W97) - Wichmann et al. (1997); (K97) - Krautter et al. (1997); (P98) - Preibisch et al. (1998); (P99) - Preibisch & Zinnecker (1999); (W99) - Wichmann et al. (1999); (K00) - Köhler et al. (2000); (P01) - Preibisch et al. (2001); (M02) - Mamajek et al. (2002); (P02) - Preibisch et al. (2002); (Z01) - Zuckerman et al. (2001); (T06) - Torres et al. (2006); (R06) - Riaz et al. (2006); (C06) - Carpenter et al. (2006); (W07) - White et al. (2007); (A) - measured from spectrum downloaded from the ESO archive, program 083.A-9003(A); (B) - E. Mamajek, Private Communication, 2012 (C) - measured from spectrum downloaded from the ESO archive, program 081.C-0779(A);

Table 4.6. Stellar Properties for Sco-Cen Members.

ID No.	2MASS	Grp.	SpT	Ref.	EW(Hα) (Å)	Ref.	A_V (mag)	π_{kin} (mas)	log($T_{\rm eff}$) (dex)	log($L/L_\odot$) (dex)	Age (Myr)	Mass ($M_\odot$)	Other Name
1	10065573-6352086	LCC	K0Ve	T06	0.0	T06	0.16±0.04	7.54±0.83	3.702±0.009	-0.061±0.097	15	1.1	
2	10092184-6736381	LCC	K1IV(e)	PM	-0.2	PM	0.00±0.10	7.03±0.76	3.692±0.012	-0.336±0.096	30	0.9	TYC 9210-1484-1
3	10313710-6901587	LCC	K2.5IV(e)	PM	-0.1	PM	0.00±0.13	6.91±0.72	3.668±0.019	-0.382±0.095	22	0.9	
4	10334180-6413457	LCC	K2.5IV(e)	PM	0.0	PM	0.00±0.15	5.29±0.85	3.668±0.019	-0.079±0.143	7	1.2	V542 Car
5	10412300-6940431	LCC	G8Ve	T06	0.0	T06	0.00±0.02	11.05±0.97	3.717±0.007	-0.252±0.078	35	0.9	
6	10494839-6446284	LCC	G9Ve	T06	-0.5	T06	0.00±0.04	5.29±0.75	3.709±0.008	-0.088±0.124	18	1.1	V570 Car
7	10544998-6526458	LCC	K2Ve	PM	-1.7	PM	0.10±0.04	6.66±0.71	3.678±0.017	-0.357±0.095	25	0.9	TYC 8966-1241-1
8	10552886-6629147	LCC	K0IV	PM	1.5	PM	0.01±0.02	6.26±0.73	3.702±0.009	-0.090±0.102	16	1.1	TYC 8970-1170-1
9	10560422-6152054	LCC	K5V-IVe	PM	-0.6	PM	0.00±0.19	10.60±1.44	3.617±0.016	-0.511±0.122	12	0.9	
10	10574936-6913599	LCC	K2IV	PM	0.7	M02	0.11±0.02	10.77±0.87	3.678±0.017	-0.096±0.074	10	1.2	
11	11001895-6118020	LCC	G6V	PM	2.7	PM	0.13±0.16	9.04±0.93	3.732±0.008	-0.006±0.092	21	1.1	HD 305810
12	11080791-6341469	LCC	M0Ve	T06	-0.6	T06	0.00±0.05	11.29±1.00	3.576±0.014	-0.539±0.080	4	0.6	
13	11143442-4418240	LCC	K2IV	PM	1.3	PM	0.06±0.12	6.56±0.60	3.678±0.017	0.577±0.085	2	1.7	CD-43 6891
14	11175186-6402056	LCC	K3IVe	PM	-10.3	PM	0.88±0.18	6.95±1.25	3.658±0.021	-0.016±0.160	5	1.2	
15	11272881-3952572	LCC	K3IV(e)	PM	0.1	PM	0.00±0.06	8.50±0.64	3.658±0.021	-0.091±0.071	6	1.2	CD-39 7118B
16	11275535-6626046	LCC	K1Ve	T06	0.0	T06	0.19±0.04	10.64±0.89	3.692±0.012	-0.267±0.075	24	1.0	TYC 8984-2245-1
17	11320835-5803199	LCC	K1IV	PM	0.4	M02	0.16±0.03	11.18±0.91	3.692±0.012	0.057±0.073	8	1.3	HD 304428
18	11370003-6516164	LCC	K3IV	PM	1.1	PM	0.00±0.05	5.79±0.55	3.658±0.021	-0.260±0.087	12	1.1	
19	11402787-6201337	LCC	K5IVe	PM	-2.8	PM	0.14±0.02	9.57±1.33	3.617±0.016	-0.410±0.123	8	0.9	
20	11445217-6438548	LCC	K6IVe	PM	-1.7	PM	0.00±0.04	9.57±0.80	3.604±0.009	-0.469±0.074	7	0.8	

Table 4.6 (cont'd)

ID No.	2MASS	Grp.	SpT	Ref.	EW(Hα) (Å)	Ref.	A_V (mag)	π_{kin} (mas)	log($T_{\rm eff}$) (dex)	log($L/L_\odot$) (dex)	Age (Myr)	Mass ($M_\odot$)	Other Name
21	11452016-5749094	LCC	K2IV	PM	1.2	PM	0.00±0.02	6.24±0.59	3.678±0.017	-0.535±0.085	45	0.8	
22	11454278-5739285	LCC	K4IVe	PM	-0.3	PM	0.00±0.05	8.44±0.68	3.636±0.021	-0.303±0.075	8	1.0	
23	11472064-4953042	LCC	K7e	Z01	-2.8	Z01	0.11±0.28	9.72±0.86	3.599±0.004	-0.365±0.083	4	0.7	TWA 19B
24	11515049-6407278	LCC	K1V	T06	...	T06	0.00±0.03	6.11±0.77	3.692±0.012	-0.284±0.111	25	1.0	
25	11522157-6444302	LCC	K1IV	PM	2.1	PM	0.00±0.09	5.70±0.63	3.692±0.012	-0.111±0.098	14	1.1	TYC 8981-1580-1
26	11554295-5637314	LCC	M0Ve	T06	-1.5	T06	0.00±0.02	10.08±1.09	3.576±0.014	-0.323±0.097	2	0.5	
27	11594608-6101132	LCC	K4V(e)	T06	0.0	T06	0.00±0.19	8.42±0.76	3.636±0.021	-0.271±0.086	7	1.0	
28	11594986-6136246	LCC	K5IVe	PM	-3.1	PM	0.48±0.13	8.85±0.86	3.617±0.016	-0.271±0.088	4	0.9	
29	12051254-5331233	LCC	K4IVe	PM	-1.2	PM	0.67±0.04	8.50±1.68	3.636±0.021	-0.499±0.174	18	0.9	
30	12061352-5702168	LCC	G5IV	PM	0.6	M02	0.06±0.04	6.88±0.76	3.740±0.009	0.078±0.098	19	1.1	
31	12063292-4247508	LCC	K0V	T06	...	T06	0.00±0.04	11.70±0.78	3.702±0.009	-0.424±0.060	46	0.8	
32	12065276-5044463	LCC	K6IV(e)	PM	0.3	PM	0.00±0.18	11.45±0.80	3.604±0.009	-0.853±0.065	34	0.7	
33	12074236-6227282	LCC	K3Ve	T06	-0.3	T06	0.30±0.12	8.21±0.77	3.658±0.021	0.084±0.086	3	1.2	
34	12090225-5120410	LCC	K3IV(e)	PM	-0.1	PM	0.00±0.13	8.95±0.60	3.658±0.021	-0.328±0.066	15	1.0	TYC 8241-2652-1
35	12092655-4923487	LCC	K4IVe	PM	-2.4	PM	0.41±0.06	9.99±0.75	3.636±0.021	-0.140±0.071	4	1.0	TYC 8237-1980-1
36	12094184-5854450	LCC	K2IV	PM	-0.1	M02	0.09±0.03	10.00±0.81	3.678±0.017	0.031±0.074	7	1.3	
37	12101065-4855476	LCC	K3IV(e)	PM	-0.1	PM	0.00±0.04	9.72±0.82	3.658±0.021	-0.291±0.078	13	1.0	
38	12103705-5727208	LCC	K3IVe	PM	-0.7	PM	0.00±0.02	6.02±1.15	3.658±0.021	-0.300±0.168	13	1.0	
39	12113142-5816533	LCC	K1.5IV	PM	0.3	M02	0.00±0.04	10.24±0.79	3.686±0.014	-0.080±0.070	11	1.2	
40	12120804-6554549	LCC	K3Ve	T06	-0.7	T06	0.13±0.05	10.12±0.79	3.658±0.021	-0.326±0.073	15	1.0	

Table 4.6 (cont'd)

ID No.	2MASS	Grp.	SpT	Ref.	EW(Hα) (Å)	Ref.	A_V (mag)	π_{kin} (mas)	log($T_{\rm eff}$) (dex)	log($L/L_\odot$) (dex)	Age (Myr)	Mass ($M_\odot$)	Other Name
41	12121119-4950081	LCC	K2Ve	T06	-0.1	T06	0.08±0.14	8.08±0.69	3.678±0.017	-0.257±0.079	17	1.0	
42	12123577-5520273	LCC	K2IV	PM	0.2	M02	0.00±0.06	8.77±0.66	3.678±0.017	-0.028±0.069	8	1.2	
43	12124890-6230317	LCC	K7Ve	T06	-0.9	T06	0.00±0.07	11.11±0.81	3.599±0.004	-0.342±0.065	4	0.7	
44	12135700-6255129	LCC	K4Ve	T06	-0.5	T06	0.22±0.04	9.25±0.90	3.636±0.021	-0.271±0.089	7	1.0	
45	12143410-5110124	LCC	K0IV	PM	0.2	M02	0.00±0.10	9.69±0.80	3.702±0.009	-0.060±0.074	14	1.1	
46	12145229-5547037	LCC	G6IV	PM	0.6	M02	0.44±0.10	9.99±0.78	3.732±0.008	0.247±0.071	10	1.3	
47	12160114-5614068	LCC	K5Ve	T06	-1.3	T06	0.00±0.01	8.51±1.02	3.617±0.016	-0.087±0.106	2	0.8	
48	12163007-6711477	LCC	K4IVe	T06	-0.6	T06	0.87±0.08	9.59±0.69	3.636±0.021	-0.017±0.068	3	1.0	
49	12164023-7007361	LCC	K3IV(e)	PM	0.0	PM	0.00±0.15	9.84±0.77	3.658±0.021	-0.176±0.075	8	1.1	TYC 9231-1185-1
50	12174048-5000266	LCC	K9IVe	PM	-2.4	PM	0.07±0.09	7.81±0.58	3.589±0.010	-0.755±0.068	15	0.7	
51	12182762-5943128	LCC	K2.5IV	PM	-0.3	M02	0.08±0.08	11.56±0.95	3.668±0.019	-0.165±0.076	10	1.1	
52	12185802-5737191	LCC	K1.5IV	PM	0.1	M02	0.26±0.17	9.24±0.67	3.686±0.014	0.273±0.069	3	1.5	
53	12192161-6454101	LCC	K2IV	PM	0.3	M02	0.00±0.09	10.26±0.92	3.678±0.017	0.105±0.081	5	1.4	
54	12195938-5018404	LCC	K5IVe	PM	-1.2	PM	0.00±0.00	7.09±0.53	3.617±0.016	-0.495±0.068	11	0.9	
55	12202301-5242165	LCC	K9IVe	PM	-3.6	PM	0.03±0.05	7.54±0.90	3.589±0.010	0.046±0.105	1	0.5	
56	12205449-6457242	LCC	K4Ve	T06	-1.1	T06	0.00±0.06	11.23±0.96	3.636±0.021	-0.344±0.079	10	1.0	
57	12205588-6534365	LCC	K9IVe	PM	-3.2	PM	0.18±0.02	9.93±2.97	3.589±0.010	-0.708±0.260	12	0.7	
58	12210499-7116493	LCC	K6IVe	PM	-1.1	PM	0.00±0.13	11.69±0.90	3.604±0.009	-0.506±0.070	9	0.8	GSC 09235-01702
59	12210808-5212226	LCC	K4Ve	T06	-0.8	T06	0.21±0.07	8.39±0.56	3.636±0.021	-0.307±0.064	8	1.0	
60	12213087-6403530	LCC	K3.5IVe	PM	-0.7	PM	0.50±0.12	12.06±0.85	3.647±0.021	-0.091±0.068	5	1.1	TYC 8983-564-1

Table 4.6 (cont'd)

ID No.	2MASS	Grp.	SpT	Ref.	EW(Hα) (Å)	Ref.	A_V (mag)	π_{kin} (mas)	log($T_{\rm eff}$) (dex)	log($L/L_\odot$) (dex)	Age (Myr)	Mass ($M_\odot$)	Other Name
61	12215566-4946125	LCC	G6V	PM	1.5	M02	0.18±0.04	10.01±0.71	3.732±0.008	0.037±0.064	19	1.1	
62	12220430-4841248	LCC	K2IV	PM	-0.1	M02	0.00±0.06	7.64±0.52	3.678±0.017	0.060±0.063	6	1.3	
63	12234012-5616325	LCC	K2V	PM	1.1	M02	0.08±0.18	9.40±0.66	3.678±0.017	-0.169±0.067	13	1.1	
64	12234749-6402549	LCC	K3IVe	PM	-0.7	PM	0.00±0.18	10.24±0.71	3.658±0.021	-0.275±0.069	12	1.0	TYC 8983-854-1
65	12240975-6003416	LCC	K5IVe	PM	-1.8	PM	0.00±0.02	9.14±0.77	3.617±0.016	-0.473±0.076	10	0.9	TYC 8975-871-1
66	12245648-4854270	LCC	K5IVe	PM	-1.3	PM	0.00±0.03	8.41±0.60	3.617±0.016	-0.366±0.065	7	0.9	ASAS J122456-4854.4
67	12253370-7227480	LCC	M0IV-Ve	PM	-4.9	PM	0.37±0.09	11.14±0.80	3.576±0.014	-0.506±0.067	4	0.5	[SWB2008] NGC 4372 1
68	12263934-6113406	LCC	K5IV(e)	PM	-0.2	PM	0.00±0.16	8.99±0.68	3.617±0.016	-0.435±0.071	9	0.9	
69	12264842-5215070	LCC	K5Ve	T06	-1.5	T06	0.24±0.07	9.99±0.72	3.617±0.016	-0.319±0.066	5	0.9	
70	12271665-6239142	LCC	K3IV(e)	PM	-0.2	PM	0.00±0.01	9.92±0.76	3.658±0.021	-0.186±0.072	9	1.1	
71	12282540-6320589	LCC	G7V	T06	0.2	A	0.00±0.03	10.56±0.77	3.723±0.007	0.226±0.066	9	1.4	
72	12302957-5222269	LCC	K3V(e)	T06	0.0	T06	0.15±0.08	8.91±0.63	3.658±0.021	-0.378±0.067	18	1.0	
73	12333381-5714066	LCC	K1V(e)	T06	0.0	T06	0.40±0.06	10.44±0.67	3.692±0.012	-0.204±0.059	19	1.0	
74	12361767-5042421	LCC	K4Ve	T06	-0.4	T06	0.00±0.01	8.82±0.57	3.636±0.021	-0.361±0.062	10	1.0	
75	12363895-6344436	LCC	K1IV	PM	0.6	M02	0.30±0.03	9.81±0.75	3.692±0.012	0.194±0.069	5	1.4	
76	12365895-5412178	LCC	K2IV	PM	0.7	M02	0.00±0.06	7.41±0.59	3.678±0.017	0.105±0.074	5	1.4	
77	12373737-5143113	LCC	K9IVe	PM	-3.5	PM	0.03±0.09	10.22±0.67	3.589±0.010	-0.520±0.060	6	0.7	
78	12374883-5209463	LCC	K5IVe	PM	-0.6	PM	0.00±0.04	8.72±0.56	3.617±0.016	-0.464±0.060	10	0.9	TYC 8244-298-1
79	12383556-5916438	LCC	K3Ve	T06	-0.6	T06	0.00±0.05	11.39±0.98	3.658±0.021	-0.599±0.079	40	0.8	
80	12391404-5454469	LCC	K5IVe	PM	-0.6	PM	0.00±0.05	7.80±0.76	3.617±0.016	-0.263±0.087	4	0.9	

Table 4.6 (cont'd)

ID No.	2MASS	Grp.	SpT	Ref.	EW(Hα) (Å)	Ref.	A_V (mag)	π_{kin} (mas)	log($T_{\rm eff}$) (dex)	log($L/L_\odot$) (dex)	Age (Myr)	Mass ($M_\odot$)	Other Name
81	12393796-5731406	LCC	G6V	PM	0.1	M02	0.20±0.09	9.63±0.65	3.732±0.008	-0.006±0.062	21	1.1	
82	12404664-5211046	LCC	K2V(e)	T06	0.0	T06	0.18±0.05	6.29±0.50	3.678±0.017	-0.202±0.073	14	1.1	CD-51 6900
83	12405458-5031550	LCC	K5V-IVe	PM	-0.7	PM	0.01±0.10	11.39±0.71	3.617±0.016	-0.625±0.059	19	0.8	TYC 8240-182-1
84	12411820-5825558	LCC	G1V	PM	-0.6	M02	0.67±0.07	10.26±0.82	3.776±0.007	0.171±0.071	25	1.1	HD 110244
85	12420050-5759486	LCC	M0Ve	PM	-8.5	PM	0.61±0.21	8.19±0.62	3.576±0.014	-0.490±0.074	4	0.5	
86	12443482-6331463	LCC	K2IV	PM	-0.7	M02	0.50±0.12	9.91±0.85	3.678±0.017	-0.022±0.079	8	1.2	FI Cru
87	12444949-4918474	LCC	K7IVe	PM	-1.2	PM	0.13±0.03	8.84±0.59	3.599±0.004	-0.610±0.059	11	0.8	
88	12450674-4742580	LCC	G7IV	PM	0.0	M02	0.37±0.18	7.14±0.45	3.723±0.007	0.279±0.061	8	1.4	HD 110817
89	12454884-5410583	LCC	K2V(e)	T06	0.0	T06	0.21±0.06	8.58±0.66	3.678±0.017	-0.285±0.071	19	1.0	
90	12472196-6808397	LCC	K4IVe	PM	-1.4	PM	0.05±0.07	9.87±0.68	3.636±0.021	-0.200±0.067	5	1.0	TYC 9228-1355-1
91	12472609-5445156	LCC	K5IVe	PM	-1.1	PM	0.00±0.14	5.55±0.87	3.617±0.016	-0.143±0.138	3	0.8	
92	12474824-5431308	LCC	M0Ve	T06	-1.8	T06	0.00±0.09	8.50±0.63	3.576±0.014	-0.178±0.068	2	0.5	
93	12475186-5126382	LCC	G2IV	PM	-1.8	M02	0.82±0.11	7.75±0.50	3.769±0.009	0.666±0.059	8	1.6	V940 Cen
94	12480778-4439167	LCC	G7V	PM	-0.1	M02	0.37±0.10	9.57±0.58	3.723±0.007	0.238±0.056	9	1.4	HD 111227
95	12483152-5944493	LCC	K7IVe	PM	-1.7	PM	0.00±0.03	10.48±0.92	3.599±0.004	-0.106±0.078	2	0.6	GSC 08659-01804
96	12484818-5635378	LCC	G3V	PM	1.2	M02	0.48±0.07	7.10±0.52	3.759±0.009	0.244±0.066	18	1.2	
97	12504491-5654485	LCC	M1IVe	PM	-7.4	PM	0.23±0.08	8.50±0.69	3.560±0.017	-0.280±0.076	2	0.5	
98	12505143-5156353	LCC	K5Ve	T06	-0.8	T06	0.00±0.02	8.96±0.68	3.617±0.016	-0.357±0.069	6	0.9	V1257 Cen
99	12510556-5253121	LCC	K5IVe	PM	-2.3	PM	0.00±0.05	8.28±0.55	3.617±0.016	-0.417±0.062	8	0.9	
100	12543050-5031482	LCC	K7IVe	PM	-1.2	PM	0.09±0.03	6.34±0.54	3.599±0.004	-0.380±0.075	4	0.7	

Table 4.6 (cont'd)

ID No.	2MASS	Grp.	SpT	Ref.	EW(Hα) (Å)	Ref.	A_V (mag)	π_{kin} (mas)	log($T_{\rm eff}$) (dex)	log($L/L_\odot$) (dex)	Age (Myr)	Mass ($M_\odot$)	Other Name
101	12560830-6926539	LCC	K7Ve	T06	-1.2	T06	0.19±0.03	9.90±0.93	3.599±0.004	-0.276±0.083	3	0.7	
102	12582559-7028490	LCC	K2IV	PM	0.0	M02	0.00±0.06	10.94±0.79	3.678±0.017	-0.002±0.067	7	1.3	
103	13010856-5901533	LCC	M0IVe	PM	-3.4	PM	0.39±0.05	8.93±0.74	3.576±0.014	-0.578±0.076	5	0.6	
104	13015069-5304581	LCC	K3IV	PM	0.2	M02	0.00±0.09	7.09±0.59	3.658±0.021	-0.156±0.077	8	1.1	
105	13015435-4249422	LCC	K3IV	PM	0.2	PM	0.00±0.03	7.86±0.45	3.658±0.021	-0.332±0.056	15	1.0	
106	13024703-6213589	LCC	K0IV	PM	1.5	PM	0.15±0.03	10.01±0.74	3.702±0.009	0.035±0.066	11	1.2	HD 312273
107	13032904-4723160	LCC	K5IVe	PM	-1.4	PM	0.00±0.02	7.63±0.47	3.617±0.016	-0.162±0.057	3	0.8	
108	13055087-5304181	LCC	K6IVe	PM	-1.1	PM	0.00±0.02	8.81±0.59	3.604±0.009	-0.652±0.060	16	0.8	
109	13064012-5159386	LCC	K1IV	PM	-0.3	M02	0.27±0.06	8.62±0.70	3.692±0.012	-0.042±0.073	11	1.2	
110	13065439-4541313	LCC	K5Ve	T06	-0.5	T06	0.00±0.03	8.60±0.53	3.617±0.016	-0.305±0.058	5	0.9	
111	13071310-5952108	LCC	K3IV	PM	0.6	PM	0.00±0.05	9.35±0.79	3.658±0.021	0.076±0.078	3	1.2	
112	13095880-4527388	LCC	K2.5IVe	PM	-0.4	PM	0.00±0.03	7.07±0.46	3.668±0.019	-0.041±0.062	7	1.2	
113	13103245-4817036	LCC	K4IVe	PM	-1.9	PM	0.00±0.02	9.13±0.59	3.636±0.021	-0.356±0.063	10	1.0	
114	13112902-4252418	LCC	M0Ve	PM	-4.3	PM	0.51±0.04	10.03±0.60	3.576±0.014	-0.781±0.057	10	0.6	
115	13121764-5508258	LCC	K5Ve	PM	-0.7	PM	0.00±0.12	8.22±0.63	3.617±0.016	-0.312±0.071	5	0.9	
116	13121859-5439054	LCC	G7IV-V	PM	2.4	PM	0.97±0.20	7.24±0.95	3.723±0.007	-0.136±0.117	27	1.0	
117	13130714-4537438	LCC	K5Ve	T06	-0.5	T06	0.00±0.06	7.15±0.62	3.617±0.016	-0.097±0.078	2	0.8	CD-45 8499
118	13132326-5442156	LCC	K3IVe	PM	-3.0	PM	0.24±0.05	5.16±0.61	3.658±0.021	-0.090±0.106	6	1.2	
119	13142382-5054018	LCC	G6IV	PM	1.1	M02	0.45±0.07	6.64±0.58	3.732±0.008	0.356±0.078	8	1.5	
120	13174687-4456534	LCC	K5IVe	PM	-2.0	PM	0.00±0.06	8.67±0.60	3.617±0.016	-0.435±0.064	9	0.9	

Table 4.6 (cont'd)

ID No.	2MASS	Grp.	SpT	Ref.	EW(Hα) (Å)	Ref.	A_V (mag)	π_{kin} (mas)	log($T_{\rm eff}$) (dex)	log($L/L_\odot$) (dex)	Age (Myr)	Mass ($M_\odot$)	Other Name
121	13175314-5058481	LCC	K5IVe	PM	-0.7	PM	0.11±0.09	5.57±0.47	3.617±0.016	-0.192±0.077	3	0.8	
122	13191370-4506326	LCC	K5IVe	PM	-0.5	PM	0.00±0.02	6.72±0.63	3.617±0.016	-0.290±0.084	5	0.9	
123	13203307-4927514	LCC	K4IV(e)	PM	-0.1	PM	0.00±0.13	7.08±0.47	3.636±0.021	-0.426±0.065	13	1.0	
124	13204539-4611377	LCC	K5IVe	PM	-3.4	PM	0.07±0.04	8.13±0.50	3.617±0.016	-0.455±0.057	10	0.9	V1267 Cen
125	13220753-6938121	LCC	K1.5IV	PM	-39.9	M02	0.50±0.14	10.92±0.73	3.686±0.014	0.028±0.064	8	1.3	MP Mus
126	13233587-4718467	LCC	K3Ve	T06	-0.4	T06	0.16±0.07	7.83±0.49	3.658±0.021	-0.053±0.061	5	1.2	
127	13251211-6456207	LCC	K3IV	PM	0.5	PM	0.00±0.03	9.52±0.74	3.658±0.021	-0.256±0.073	11	1.1	TYC 8998-760-1
128	13270594-4856180	LCC	K3Ve	T06	-0.6	T06	0.18±0.03	9.61±0.59	3.658±0.021	-0.026±0.059	5	1.2	
129	13291766-4614230	LCC	K5IVe	PM	-0.6	PM	0.00±0.10	6.88±0.42	3.617±0.016	-0.377±0.058	7	0.9	
130	13294575-4844366	LCC	K9IVe	PM	-2.4	PM	0.01±0.40	4.73±0.52	3.589±0.010	-0.154±0.106	2	0.6	
131	13315360-5113330	LCC	G1V	PM	1.2	M02	0.54±0.07	6.71±0.48	3.776±0.007	0.536±0.064	12	1.4	HD 117524
132	13334410-6359345	LCC	K3.5IV(e)	PM	-0.1	PM	0.00±0.10	9.29±1.25	3.647±0.021	-0.343±0.120	12	1.0	TYC 8999-844-1
133	13335329-6536473	LCC	K9IVe	PM	-6.0	PM	0.16±0.21	8.36±0.70	3.589±0.010	-0.332±0.078	3	0.6	
134	13335481-6536414	LCC	K5IVe	PM	-8.2	PM	0.13±0.08	8.88±0.74	3.617±0.016	-0.098±0.076	2	0.8	
135	13342461-6517473	LCC	K9IVe	PM	-28.1	PM	0.46±0.02	8.87±0.86	3.589±0.010	-0.686±0.086	11	0.7	IRAS 13309-6502
136	13343188-4209305	LCC	K2IVe	T06	-1.0	T06	0.11±0.01	9.71±0.56	3.678±0.017	-0.126±0.054	11	1.1	
137	13354082-4818124	LCC	K3.5IV(e)	PM	-0.1	PM	0.00±0.05	10.25±0.60	3.647±0.021	-0.425±0.058	17	0.9	TYC 8265-229-1
138	13364090-4043359	UCL	K6IVe	PM	-2.9	PM	0.08±0.02	8.69±0.69	3.604±0.009	-0.535±0.070	10	0.8	
139	13375730-4134419	UCL	K1IV	PM	0.7	M02	0.00±0.05	10.83±0.77	3.692±0.012	-0.075±0.065	12	1.2	
140	13380596-4344564	LCC	K3IV	PM	0.5	PM	0.00±0.04	6.74±0.47	3.658±0.021	0.008±0.066	4	1.2	TYC 7800-858-1

Table 4.6 (cont'd)

ID No.	2MASS	Grp.	SpT	Ref.	EW(Hα) (Å)	Ref.	A_V (mag)	π_{kin} (mas)	log($T_{\rm eff}$) (dex)	log($L/L_\odot$) (dex)	Age (Myr)	Mass ($M_\odot$)	Other Name
141	13381128-5214251	LCC	K0IV	PM	1.9	PM	0.00±0.13	6.49±0.44	3.702±0.009	0.066±0.063	10	1.3	TYC 8273-917-1
142	13384937-4237234	UCL	K3.5IV	PM	0.2	PM	0.00±0.08	8.63±0.61	3.647±0.021	-0.365±0.068	14	1.0	TYC 7796-286-1
143	13402554-4633514	LCC	K3Ve	T06	-1.2	T06	0.54±0.16	7.23±0.71	3.658±0.021	-0.013±0.091	5	1.2	
144	13405585-4244505	UCL	K8IVe	PM	-4.3	PM	0.52±0.12	8.18±0.65	3.595±0.005	-0.522±0.071	7	0.7	
145	13442441-4706343	UCL	K2IVn	PM	0.3	PM	0.01±0.02	7.61±0.63	3.678±0.017	0.121±0.075	5	1.4	TYC 8266-2914-1
146	13444279-6347495	LCC	K4Ve	T06	-0.3	T06	0.31±0.05	9.91±0.70	3.636±0.021	-0.066±0.067	3	1.0	
147	13454424-4904500	UCL	K2.5IV	PM	0.4	PM	0.00±0.07	8.13±0.79	3.668±0.019	0.019±0.089	5	1.3	TYC 8270-2021-1
148	13455599-5222255	LCC	K3Ve	T06	-0.8	T06	0.00±0.13	7.54±0.47	3.658±0.021	-0.158±0.062	8	1.1	
149	13475054-4902056	UCL	G6V	PM	-0.5	M02	0.37±0.05	7.82±0.76	3.732±0.008	-0.040±0.086	24	1.0	
150	13503387-4810150	UCL	K8IVe	PM	-1.8	PM	0.00±0.03	7.72±0.58	3.595±0.005	-0.639±0.067	11	0.8	
151	13515351-4846505	UCL	K5IVe	PM	-1.7	PM	0.02±0.03	8.51±0.68	3.617±0.016	-0.558±0.072	15	0.9	
152	13540743-6733449	LCC	G6V	T06	...	T06	0.16±0.05	6.52±0.52	3.732±0.008	0.039±0.071	19	1.1	
153	13544209-4820578	UCL	K2Ve	T06	-0.2	T06	0.10±0.08	9.96±0.77	3.678±0.017	-0.350±0.071	24	0.9	
154	13552552-4706563	UCL	K4IVe	PM	-0.9	PM	0.16±0.04	9.29±0.68	3.636±0.021	-0.160±0.069	5	1.0	
155	13562964-3839129	UCL	K3IV(e)	PM	2.2	PM	0.00±0.23	7.93±0.58	3.658±0.021	-0.154±0.073	8	1.1	
156	13563469-4907146	UCL	K3IV(e)	PM	-0.1	PM	0.00±0.03	9.29±0.84	3.658±0.021	-0.415±0.083	21	0.9	TYC 8271-864-1
157	13575106-4431482	UCL	K3.5IVe	PM	-1.9	PM	0.47±0.10	8.20±0.62	3.647±0.021	-0.276±0.072	10	1.1	
158	14001181-4230334	UCL	K8IVe	PM	-2.6	PM	0.07±0.00	7.30±0.76	3.595±0.005	-0.646±0.091	12	0.8	
159	14003189-6416245	LCC	K2IV	PM	0.4	PM	0.00±0.03	5.16±0.80	3.678±0.017	-0.404±0.136	29	0.9	
160	14004970-4236569	UCL	K0IV(e)	T06	0.0	T06	0.18±0.05	8.10±0.57	3.702±0.009	-0.174±0.063	21	1.0	

Table 4.6 (cont'd)

ID No.	2MASS	Grp.	SpT	Ref.	EW(Hα) (Å)	Ref.	A_V (mag)	π_{kin} (mas)	log($T_{\rm eff}$) (dex)	log($L/L_\odot$) (dex)	Age (Myr)	Mass ($M_\odot$)	Other Name
161	14022072-4144509	UCL	G9IV	PM	0.2	M02	0.13±0.02	7.32±0.57	3.709±0.008	0.083±0.069	11	1.3	
162	14060042-4112249	UCL	K3Ve	T06	-0.3	T06	0.01±0.06	8.13±0.64	3.658±0.021	-0.298±0.073	13	1.0	
163	14074792-3945427	UCL	K5IV(e)	PM	-0.3	PM	0.00±0.15	7.49±0.65	3.617±0.016	-0.468±0.080	10	0.9	
164	14081015-4123525	UCL	K7IVe	PM	-2.2	PM	0.01±0.07	10.11±0.81	3.599±0.004	-0.571±0.071	10	0.8	V1032 Cen
165	14085608-4403488	UCL	K3IVe	PM	-1.1	PM	0.22±0.10	8.41±0.62	3.658±0.021	-0.192±0.070	9	1.1	TYC 7815-1041-1
166	14122451-4327149	UCL	K2.5IV(e)	PM	0.0	PM	0.00±0.03	11.02±0.81	3.668±0.019	-0.474±0.069	31	0.9	TYC 7816-859-1
167	14124691-3831220	UCL	K3Ve	T06	-0.4	T06	0.16±0.06	9.49±0.66	3.658±0.021	-0.383±0.066	18	1.0	
168	14185327-4827313	UCL	K3IVe	T06	-1.2	T06	0.16±0.04	6.94±0.55	3.658±0.021	-0.108±0.074	7	1.2	
169	14201202-5339537	UCL	K2.5IV(e)	PM	0.5	PM	0.00±0.04	7.19±0.65	3.668±0.019	-0.353±0.083	20	1.0	
170	14204893-4748442	UCL	K5Ve	T06	-1.0	T06	0.14±0.03	8.50±0.63	3.617±0.016	-0.155±0.067	3	0.8	
171	14213051-3845252	UCL	K6IVe	PM	-1.2	PM	0.08±0.04	6.76±0.63	3.604±0.009	-0.268±0.083	3	0.7	
172	14214378-4652082	UCL	K2V(e)	T06	0.0	T06	0.24±0.06	7.86±0.57	3.678±0.017	-0.101±0.068	10	1.2	
173	14220732-5417055	UCL	K3IVe	PM	-0.5	PM	0.00±0.04	7.89±0.62	3.658±0.021	-0.155±0.073	8	1.1	
174	14223029-3532190	UCL	K3Ve	T06	-0.3	T06	0.21±0.04	8.16±0.58	3.658±0.021	-0.111±0.067	7	1.2	
175	14224364-4628054	UCL	K2.5IV(e)	PM	0.0	PM	0.00±0.05	6.22±0.63	3.668±0.019	-0.151±0.092	10	1.1	
176	14234748-5935261	UCL	K2V(e)	T06	0.0	T06	0.48±0.14	9.21±0.82	3.678±0.017	-0.080±0.082	9	1.2	
177	14244779-5041333	UCL	K1V	T06	...	T06	0.00±0.08	7.08±0.58	3.692±0.012	-0.424±0.074	40	0.8	
178	14262134-3644057	UCL	K0IV	PM	1.9	PM	0.00±0.04	10.22±0.73	3.702±0.009	-0.254±0.064	27	0.9	CD-36 9353
179	14270556-4714217	UCL	G6V	PM	1.1	M02	0.23±0.03	7.92±0.56	3.732±0.008	0.027±0.064	19	1.1	
180	14275425-5944350	UCL	K5IVe	PM	-1.0	PM	0.00±0.04	6.72±1.28	3.617±0.016	-0.280±0.167	5	0.9	GSC 08691-01183

Table 4.6 (cont'd)

ID No.	2MASS	Grp.	SpT	Ref.	EW(Hα) (Å)	Ref.	A_V (mag)	π_{kin} (mas)	log($T_{\rm eff}$) (dex)	log($L/L_\odot$) (dex)	Age (Myr)	Mass ($M_\odot$)	Other Name
181	14280929-4414175	UCL	G5V	PM	1.4	M02	0.24±0.04	7.65±0.59	3.740±0.009	0.372±0.069	9	1.5	HD 126670
182	14281937-4219341	UCL	G2V	PM	1.0	M02	0.39±0.07	6.60±0.53	3.769±0.009	0.318±0.071	17	1.2	
183	14321121-5826058	UCL	K5IVe	PM	-0.8	PM	0.00±0.15	10.83±0.91	3.617±0.016	-0.456±0.077	10	0.9	
184	14345213-4004459	UCL	K3.5IVe	PM	-1.0	PM	0.08±0.02	6.47±0.60	3.647±0.021	-0.180±0.085	7	1.1	
185	14374904-4928268	UCL	K8IVe	PM	-1.2	PM	0.00±0.02	9.61±0.71	3.595±0.005	-0.503±0.065	6	0.7	
186	14375022-5457411	UCL	G9IV	PM	0.1	M02	0.38±0.04	9.31±0.74	3.709±0.008	-0.092±0.070	18	1.1	
187	14380350-4932023	UCL	K4Ve	T06	-0.4	T06	0.11±0.06	8.13±0.71	3.636±0.021	-0.249±0.081	7	1.0	
188	14380862-4322008	UCL	K7IVe	PM	-1.9	PM	0.25±0.02	7.87±1.02	3.599±0.004	-0.432±0.113	5	0.7	
189	14385440-4310223	UCL	K3Ve	T06	-1.2	T06	0.61±0.18	7.32±0.55	3.658±0.021	0.118±0.074	3	1.2	
190	14392060-3905282	UCL	K1IV	PM	1.4	PM	0.00±0.07	5.66±0.44	3.692±0.012	0.204±0.072	5	1.5	TYC 7806-1040-1
191	14411942-5001199	UCL	K4Ve	T06	-1.0	T06	0.53±0.10	8.70±0.64	3.636±0.021	-0.250±0.070	7	1.0	
192	14413499-4700288	UCL	G5V	PM	1.2	M02	0.33±0.05	9.30±0.63	3.740±0.009	0.152±0.062	16	1.2	
193	14421590-4100183	UCL	K3IV(e)	PM	0.2	PM	0.00±0.04	9.47±0.82	3.658±0.021	-0.335±0.080	15	1.0	
194	14432493-5643393	UCL	G2V	PM	2.9	PM	0.58±0.11	4.91±0.66	3.769±0.009	0.521±0.118	12	1.4	TYC 8688-2450-1
195	14442536-4329552	UCL	K8IVe	PM	-2.3	PM	0.40±0.08	6.66±0.63	3.595±0.005	-0.746±0.084	17	0.7	
196	14472343-3503134	UCL	K3	W97	...		0.00±0.09	10.74±0.71	3.658±0.021	-0.576±0.064	37	0.8	
197	14481320-4102590	UCL	K2	W97	...		0.07±0.05	7.08±0.57	3.678±0.017	-0.065±0.074	9	1.2	
198	14502581-3506486	UCL	K1IV	PM	0.0	M02	0.23±0.06	5.20±0.48	3.692±0.012	0.461±0.083	2	1.7	
199	14503508-3459056	UCL	K4	W97	...		0.19±0.03	5.78±0.44	3.636±0.021	-0.059±0.071	3	1.0	
200	14522619-3740088	UCL	K3	W97	...		0.19±0.07	6.18±0.44	3.658±0.021	-0.199±0.068	9	1.1	

Table 4.6 (cont'd)

ID No.	2MASS	Grp.	SpT	Ref.	EW(Hα) (Å)	Ref.	A_V (mag)	π_{kin} (mas)	log($T_{\rm eff}$) (dex)	log($L/L_\odot$) (dex)	Age (Myr)	Mass ($M_\odot$)	Other Name
201	14524198-4141552	UCL	K3IV	PM	-0.6	M02	0.13±0.08	6.86±0.50	3.658±0.021	0.053±0.069	4	1.2	CD-41 9236
202	14541121-3955233	UCL	K2	W97	...		0.19±0.04	8.22±0.56	3.678±0.017	-0.339±0.063	23	0.9	
203	14552673-5129013	UCL	G7V	T06	...	T06	0.00±0.16	6.31±0.59	3.723±0.007	0.146±0.084	12	1.3	
204	14574495-4141394	UCL	K7IVe	PM	-1.1	PM	0.01±0.05	6.90±0.71	3.599±0.004	-0.483±0.090	6	0.8	
205	14583744-3915033	UCL	M0IVe	PM	-5.9	PM	0.46±0.04	9.03±0.73	3.576±0.014	-0.452±0.074	3	0.5	
206	14583769-3540302	UCL	K2.5IV	PM	-0.3	M02	0.33±0.09	7.32±0.51	3.668±0.019	0.190±0.066	3	1.3	
207	14584573-3315102	UCL	K1	W97	...		0.03±0.06	10.48±1.15	3.692±0.012	-0.527±0.097	54	0.8	CD-32 10508
208	14592275-4013120	UCL	G7V	PM	1.5	M02	0.00±0.03	8.56±0.60	3.723±0.007	0.218±0.063	9	1.4	HD 132264
209	14594473-3425465	UCL	K3Ve	T06	-0.3	T06	0.07±0.04	8.98±0.64	3.658±0.021	-0.123±0.067	7	1.2	
210	15003768-4308339	UCL	K3	W97	-0.4	T06	0.22±0.03	6.37±0.46	3.658±0.021	-0.141±0.068	7	1.1	
211	15005189-4331212	UCL	K1IV	PM	0.1	M02	0.22±0.03	6.51±0.63	3.692±0.012	0.039±0.086	8	1.3	
212	15022600-3405131	UCL	K4	W97	...		0.00±0.05	6.12±0.64	3.636±0.021	-0.318±0.095	9	1.0	
213	15035213-3906283	UCL	K6Ve	PM	-0.9	PM	0.00±0.14	7.97±0.57	3.604±0.009	-0.295±0.065	4	0.7	
214	15052586-3857031	UCL	K6	W97	...		0.00±0.39	8.24±0.56	3.604±0.009	-0.514±0.074	9	0.8	
215	15054424-3312508	UCL	K4IVe	PM	-1.0	PM	0.04±0.04	6.77±0.50	3.636±0.021	-0.348±0.069	10	1.0	
216	15055685-4312031	UCL	K7	W97	0.6	K97	0.20±0.03	8.87±0.61	3.599±0.004	-0.572±0.061	10	0.8	
217	15064258-3047326	UCL	K7	W97	...		0.12±0.02	8.51±0.63	3.599±0.004	-0.678±0.065	15	0.8	RX J1506.7-3047
218	15071481-3504595	UCL	K1IV	PM	1.2	M02	0.00±0.03	9.49±0.66	3.692±0.012	-0.143±0.063	15	1.1	
219	15072758-4601073	UCL	K1	W97	0.5	K97	0.00±0.04	6.19±0.49	3.692±0.012	-0.109±0.071	14	1.1	
220	15075415-4730288	UCL	K1IV(e)	T06	0.0	T06	0.30±0.05	7.03±0.50	3.692±0.012	-0.108±0.065	14	1.1	

Table 4.6 (cont'd)

ID No.	2MASS	Grp.	SpT	Ref.	EW(Hα) (Å)	Ref.	A_V (mag)	π_{kin} (mas)	log(T_{eff}) (dex)	log($L/L_\odot$) (dex)	Age (Myr)	Mass ($M_\odot$)	Other Name
221	15080509-3337556	UCL	K6	K97	-0.2	K97	0.00±0.05	9.16±0.61	3.604±0.009	-0.440±0.060	6	0.8	
222	15083773-4423170	UCL	G6IV(e)	PM	-0.8	M02	0.00±0.06	5.35±0.53	3.732±0.008	0.224±0.088	20	1.2	LQ Lup
223	15083849-4400519	UCL	G0V	PM	1.2	M02	0.76±0.26	7.91±0.68	3.782±0.004	0.199±0.081	25	1.1	HD 133938
224	15085379-3715467	UCL	K5	K97	-1.0	K97	0.00±0.19	7.48±0.53	3.617±0.016	-0.375±0.068	7	0.9	
225	15085472-4303136	UCL	K3IV	PM	1.1	PM	0.00±0.07	7.19±0.66	3.658±0.021	-0.196±0.084	9	1.1	TYC 7829-2168-1
226	15102954-3902566	UCL	K3IV(e)	PM	0.1	PM	0.00±0.14	6.14±0.47	3.658±0.021	-0.225±0.073	10	1.1	TYC 7822-2509-1
227	15110450-3251304	UCL	K6	W97	0.6	K97	0.00±0.21	7.49±0.61	3.604±0.009	-0.271±0.077	3	0.7	
228	15113968-3248560	UCL	M1.5	W97	...		0.04±0.08	5.57±0.48	3.551±0.016	-0.404±0.080	2	0.4	
229	15124447-3116482	UCL	K2Ve	T06	-0.1	T06	0.24±0.01	6.51±0.45	3.678±0.017	-0.091±0.064	10	1.2	
230	15135817-4629145	UCL	K7	K97	-0.2	W99	0.00±0.01	5.86±0.64	3.599±0.004	-0.341±0.096	4	0.7	
231	15140754-4103361	UCL	G7	W97	3.1	K97	0.00±0.25	8.53±0.60	3.723±0.007	-0.106±0.069	25	1.0	HD 134974
232	15144748-4220149	UCL	K1	K97	2.5	K97	0.01±0.05	5.86±0.57	3.692±0.012	0.010±0.087	9	1.2	
233	15151856-4146354	UCL	K9V-IVe	PM	-2.3	PM	0.12±0.03	7.97±0.63	3.589±0.010	-0.576±0.071	7	0.7	
234	15152295-5441088	UCL	K4IVe	PM	-0.5	PM	0.00±0.07	6.69±0.63	3.636±0.021	-0.320±0.087	9	1.0	
235	15154537-3331597	UCL	K0	W97	1.7	K97	0.21±0.07	8.11±0.57	3.702±0.009	-0.006±0.063	12	1.2	LT Lup
236	15155274-4418173	UCL	K1	W97	0.1	K97	0.76±0.04	6.52±0.70	3.692±0.012	-0.250±0.095	22	1.0	LS Lup
237	15163663-4407204	UCL	K2	K97	-0.1	K97	0.32±0.04	6.51±0.64	3.678±0.017	-0.202±0.088	14	1.1	
238	15171083-3434194	UCL	K3IVe	PM	-0.5	PM	0.00±0.20	7.79±0.87	3.658±0.021	-0.161±0.103	8	1.1	CD-34 10292B
239	15180123-4444269	UCL	K2	W97	...		0.00±0.13	9.12±0.71	3.678±0.017	-0.540±0.072	46	0.8	
240	15182692-3738021	UCL	G8IV	PM	0.4	M02	0.33±0.06	6.95±0.55	3.717±0.007	0.120±0.071	11	1.3	LW Lup

Table 4.6 (cont'd)

ID No.	2MASS	Grp.	SpT	Ref.	EW(Hα) (Å)	Ref.	A_V (mag)	π_{kin} (mas)	log($T_{\rm eff}$) (dex)	log($L/L_\odot$) (dex)	Age (Myr)	Mass ($M_\odot$)	Other Name
241	15185282-4050528	UCL	G8	K97	1.9	K97	0.40±0.02	6.54±0.50	3.717±0.007	0.155±0.068	10	1.3	LX Lup
242	15191600-4056075	UCL	K0	K97	0.4	K97	0.46±0.04	8.45±0.64	3.702±0.009	-0.243±0.068	26	1.0	LY Lup
243	15191807-2943204	UCL	K7IVe	PM	-1.3	PM	0.00±0.02	6.40±0.65	3.599±0.004	-0.403±0.089	5	0.7	
244	15202415-3037317	UCL	K4IVe	T06	-1.0	T06	0.27±0.01	9.41±0.63	3.636±0.021	-0.130±0.064	4	1.0	
245	15215241-2842383	UCL	K3IV(e)	PM	0.2	PM	0.00±0.07	7.57±0.55	3.658±0.021	-0.242±0.069	11	1.1	TYC 6775-1218-1
246	15221162-3959509	UCL	K3	K97	0.1	K97	0.18±0.04	7.54±0.60	3.658±0.021	-0.368±0.074	17	1.0	LZ Lup
247	15232557-4055467	UCL	K2	K97	1.1	K97	0.37±0.03	7.97±0.62	3.678±0.017	-0.396±0.071	28	0.9	MM Lup
248	15235794-3619585	UCL	K4IV	PM	0.1	PM	0.00±0.18	6.47±0.60	3.636±0.021	-0.311±0.087	8	1.0	
249	15240305-3209508	UCL	K7	K97	-0.2	K97	0.14±0.03	7.21±0.52	3.599±0.004	-0.243±0.064	3	0.7	MO Lup
250	15241147-3030582	UCL	K0	K00	...		0.03±0.03	7.89±0.56	3.702±0.009	-0.134±0.064	18	1.1	
251	15241303-3030572	UCL	M1	K00	...		0.06±0.13	3.91±0.71	3.560±0.017	-0.144±0.160	41	0.7	
252	15243236-3652027	UCL	K1	K97	1.4	K97	0.00±0.10	6.24±0.59	3.692±0.012	-0.041±0.085	11	1.2	MP Lup
253	15250358-3604455	UCL	K1	K97	0.9	K97	0.08±0.04	4.95±0.64	3.692±0.012	0.389±0.114	3	1.6	
254	15253316-3613467	UCL	K2	K97	0.6	K97	0.39±0.04	5.54±0.57	3.678±0.017	0.079±0.092	5	1.3	MQ Lup
255	15253666-3537319	UCL	K6	K97	-0.1	K97	0.00±0.03	6.77±0.52	3.604±0.009	-0.308±0.068	4	0.7	MR Lup
256	15255964-4501157	UCL	K0IV	PM	1.1	M02	0.00±0.10	6.76±0.48	3.702±0.009	-0.055±0.064	14	1.1	MS Lup
257	15262805-5549569	UCL	K3IV(e)	PM	0.4	PM	0.00±0.04	7.90±0.78	3.658±0.021	-0.688±0.090	54	0.7	
258	15265257-3722062	UCL	M0.5	K97	-1.5	K97	0.00±0.22	9.58±0.63	3.568±0.016	-0.740±0.066	7	0.5	
259	15272286-3604087	UCL	K7-M0	K97	0.1	K97	0.31±0.24	8.89±0.61	3.593±0.007	-0.356±0.067	4	0.6	
260	15280322-2600034	UCL	K3	K00	...		1.09±0.05	5.48±0.51	3.658±0.021	0.198±0.085	2	1.2	RX J1528.0-2600

Table 4.6 (cont'd)

ID No.	2MASS	Grp.	SpT	Ref.	EW(Hα) (Å)	Ref.	A_V (mag)	π_{kin} (mas)	log($T_{\rm eff}$) (dex)	log($L/L_\odot$) (dex)	Age (Myr)	Mass ($M_\odot$)	Other Name
261	15293858-3546513	UCL	K1IV	PM	0.1	M02	0.24±0.04	7.75±0.66	3.692±0.012	0.101±0.076	7	1.3	
262	15294727-3628374	UCL	K2	K97	0.9	K97	0.50±0.07	5.40±0.43	3.678±0.017	0.082±0.073	5	1.3	
263	15294888-4522457	UCL	K6	W97	-0.2	K97	0.09±0.05	6.78±0.59	3.604±0.009	-0.404±0.077	5	0.8	
264	15295661-3135446	UCL	K5IVe	PM	-1.3	PM	0.00±0.11	8.04±0.56	3.617±0.016	-0.476±0.065	10	0.9	
265	15304790-3022054	UCL	K2	K00	...		0.24±0.21	8.13±0.52	3.678±0.017	-0.196±0.064	14	1.1	
266	15312193-3329394	UCL	G9.5V	M02	0.9	W07	0.00±0.09	8.21±0.55	3.706±0.008	-0.198±0.060	24	1.0	
267	15312961-3021537	UCL	M0	K00	...		0.00±0.21	6.12±0.48	3.576±0.014	-0.342±0.075	2	0.5	
268	15313413-3602287	UCL	K3V(e)	T06	0.0	T06	0.00±0.10	6.17±0.44	3.658±0.021	-0.123±0.068	7	1.2	
269	15340737-3916171	UCL	K1	K97	1.2	K97	0.04±0.03	8.24±0.56	3.692±0.012	-0.115±0.062	14	1.1	
270	15342313-3300087	UCL	M0	K00	-0.4	K97	0.00±0.19	6.63±0.62	3.576±0.014	-0.406±0.087	3	0.5	
271	15343816-4002280	UCL	K6	W97	0.8	K97	0.00±0.06	9.66±0.65	3.604±0.009	-0.526±0.060	9	0.8	
272	15355780-2324046	US	K3:	P98	0.0	P98	0.24±0.01	6.18±0.55	3.658±0.021	-0.291±0.082	13	1.0	
273	15355876-4456355	UCL	K7IVe	PM	-1.6	PM	0.29±0.19	8.39±0.70	3.599±0.004	-0.580±0.076	10	0.8	
274	15364094-2923574	UCL	M1IVe	PM	-6.4	PM	0.23±0.54	6.60±0.63	3.560±0.017	-0.588±0.105	3	0.5	
275	15370214-3136398	UCL	G5V	PM	0.4	M02	0.54±0.34	7.80±0.57	3.740±0.009	0.407±0.076	9	1.4	CPD-31 4161
276	15371129-4015566	UCL	G7V	PM	-0.9	M02	0.31±0.07	6.28±0.50	3.723±0.007	0.267±0.071	8	1.4	
277	15374917-1840449	US	G5:	P98	1.5	P98	0.74±0.06	4.15±0.53	3.740±0.009	0.326±0.112	10	1.4	TYC 6189-101-1
278	15375134-3045160	UCL	K4	K00	-0.4	T06	0.09±0.04	6.47±0.46	3.636±0.021	-0.031±0.067	3	1.0	
279	15380264-3807230	UCL	K5	K97	0.9	K97	0.00±0.15	7.03±0.48	3.617±0.016	-0.459±0.065	10	0.9	MT Lup
280	15383827-3916553	UCL	K4	K97	1.1	K97	0.00±0.06	7.56±0.78	3.636±0.021	-0.293±0.094	8	1.0	

Table 4.6 (cont'd)

ID No.	2MASS	Grp.	SpT	Ref.	EW(Hα) (Å)	Ref.	A_V (mag)	π_{kin} (mas)	log($T_{\rm eff}$) (dex)	log($L/L_\odot$) (dex)	Age (Myr)	Mass ($M_\odot$)	Other Name
281	15384306-4411474	UCL	K0.5IV	PM	0.5	M02	0.00±0.03	8.49±0.63	3.697±0.010	-0.005±0.069	11	1.2	
282	15392776-3446171	UCL	K7	K00	-3.3	F87	2.19±0.25	5.28±0.55	3.599±0.004	0.375±0.096	86	1.4	IK Lup
283	15394637-3451027	UCL	K4	K97	-0.2	K97	0.02±0.23	5.13±0.62	3.636±0.021	0.031±0.111	2	1.0	
284	15400244-4634187	UCL	K4	K97	0.5	K97	0.00±0.19	6.61±0.59	3.636±0.021	-0.283±0.084	8	1.0	
285	15404116-3756185	UCL	K6	K97	0.9	K97	0.00±0.04	8.03±0.58	3.604±0.009	-0.515±0.064	9	0.8	MU Lup
286	15410679-2656263	US	G7	P98	1.0	W07	0.44±0.02	8.20±0.75	3.723±0.007	-0.172±0.081	30	1.0	
287	15413114-5330296	UCL	K2Ve	T06	-0.4	T06	0.23±0.06	9.85±0.75	3.678±0.017	-0.236±0.070	16	1.0	
288	15413121-2520363	US	G9IVe	T06	-2.2	T06	0.61±0.27	8.62±0.75	3.709±0.008	0.395±0.082	4	1.7	
289	15420518-3601317	UCL	K7	K97	0.3	K97	0.00±0.20	7.66±0.56	3.599±0.004	-0.477±0.068	6	0.8	
290	15424991-2536406	US	G5	P98	1.4	P98	0.95±0.05	7.82±0.66	3.740±0.009	0.217±0.076	14	1.3	TYC 6781-1046-1
291	15435905-2622516	US	K9Ve	PM	-4.1	PM	0.55±0.17	7.12±0.72	3.589±0.010	-0.690±0.091	11	0.7	
292	15440376-3311110	UCL	K2V	PM	-1.1	M02	0.07±0.07	7.10±0.58	3.678±0.017	0.030±0.075	7	1.3	
293	15441334-2522590	US	M1e	P98	-3.2	P98	0.00±0.18	7.67±0.77	3.560±0.017	-0.563±0.093	3	0.5	
294	15442874-4745415	UCL	K9IVe	PM	-3.1	PM	0.13±0.04	7.09±0.56	3.589±0.010	-0.358±0.071	3	0.6	
295	15444712-3811406	UCL	K7	K97	-0.6	K97	0.00±0.15	7.40±0.58	3.599±0.004	-0.160±0.070	2	0.7	
296	15451286-3417305	UCL	K2e	H94	-8.0	T06	1.29±0.17	5.83±0.48	3.678±0.017	0.929±0.077	2	1.0	HT Lup
297	15455225-4222163	UCL	K2.5IV	PM	-0.8	M02	0.01±0.04	7.59±0.52	3.668±0.019	0.110±0.065	4	1.3	
298	15462958-5217239	UCL	K0IV	PM	2.4	PM	0.00±0.02	7.27±0.50	3.702±0.009	-0.203±0.061	23	1.0	
299	15463111-5216580	UCL	M0Ve	PM	-2.9	PM	0.06±0.19	7.98±0.60	3.576±0.014	-0.702±0.072	7	0.6	
300	15464121-3618472	UCL	K1	K97	-0.7	K97	0.38±0.13	5.94±0.56	3.692±0.012	0.066±0.085	8	1.3	

Table 4.6 (cont'd)

ID No.	2MASS	Grp.	SpT	Ref.	EW(Hα) (Å)	Ref.	A_V (mag)	π_{kin} (mas)	log(T_{eff}) (dex)	log($L/L_\odot$) (dex)	Age (Myr)	Mass ($M_\odot$)	Other Name
301	15471063-1736244	US	M0Ve	PM	-6.8	PM	0.48±0.03	8.16±0.78	3.576±0.014	-0.736±0.086	9	0.6	
302	15474176-4018267	UCL	K1	K97	1.6	K97	0.26±0.02	7.60±0.51	3.692±0.012	-0.082±0.061	13	1.2	
303	15480291-2908369	US	G9	K00	...	T06	0.18±0.03	7.15±0.62	3.709±0.008	0.017±0.077	13	1.2	
304	15481148-4712297	UCL	K3IVe	PM	-1.1	PM	0.02±0.11	8.73±0.62	3.658±0.021	-0.324±0.068	15	1.0	
305	15481299-2349523	US	M0.5Ve	PM	-6.3	PM	0.65±0.06	9.07±0.86	3.568±0.016	-0.707±0.086	6	0.5	
306	15484204-4335207	UCL	G8	K97	1.1	K97	0.27±0.04	4.69±0.47	3.717±0.007	0.108±0.088	12	1.3	
307	15490271-3102537	UCL	K0	K00	-0.4	T06	0.22±0.01	6.61±0.44	3.702±0.009	0.099±0.060	9	1.3	
308	15492100-2600062	US	K0	K00	-0.1	T06	1.20±0.08	8.17±0.65	3.702±0.009	0.228±0.071	6	1.5	
309	15494499-3925089	UCL	K2.5IV	PM	-0.2	M02	0.00±0.03	7.27±0.50	3.668±0.019	0.083±0.065	4	1.3	HD 141277
310	15495840-4306370	UCL	K3IV(e)	PM	-0.2	PM	0.00±0.04	4.91±0.40	3.658±0.021	-0.074±0.076	6	1.2	TYC 7845-55-1
311	15495920-3629574	UCL	K2	K97	1.1	K97	0.19±0.02	6.02±0.42	3.678±0.017	-0.012±0.065	7	1.3	MV Lup
312	15510142-1548286	US	M1IVe	PM	-5.5	PM	0.72±0.25	6.47±0.98	3.560±0.017	-0.448±0.137	2	0.4	
313	15510660-2402190	US	M2	K00	...		0.16±0.21	6.60±0.64	3.543±0.017	-0.710±0.091	3	0.4	
314	15514535-2456513	US	K3IV	PM	-0.5	PM	0.10±0.02	5.96±0.52	3.658±0.021	-0.305±0.080	14	1.0	
315	15522589-3920512	UCL	K4IVe	PM	-0.5	PM	0.00±0.03	7.54±0.54	3.636±0.021	-0.472±0.068	16	0.9	
316	15523122-2633529	US	M0	P99	...		0.00±0.20	10.59±0.92	3.576±0.014	-0.739±0.082	9	0.6	
317	15530683-2247174	US	M0IV-Ve	PM	-7.9	PM	1.01±0.04	7.61±0.81	3.576±0.014	-0.303±0.095	2	0.5	
318	15545141-3154463	UCL	K5IVe	PM	-15.9	PM	0.33±0.23	5.64±0.47	3.617±0.016	-0.026±0.079	2	0.8	IRAS 15517-3145
319	15550624-2521102	US	M1	P99	...		0.01±0.21	7.11±0.60	3.560±0.017	-0.266±0.081	2	0.5	
320	15551621-1355136	US	K6IVe	PM	-1.1	PM	0.00±0.19	10.59±0.92	3.604±0.009	-0.767±0.079	<1	...	

Table 4.6 (cont'd)

ID No.	2MASS	Grp.	SpT	Ref.	EW(Hα) (Å)	Ref.	A_V (mag)	π_{kin} (mas)	log($T_{\rm eff}$) (dex)	log($L/L_\odot$) (dex)	Age (Myr)	Mass ($M_\odot$)	Other Name
321	15552621-3338232	UCL	K5	K97	0.0	K97	0.00±0.09	7.77±0.55	3.617±0.016	-0.564±0.065	15	0.9	
322	15560921-3756057	UCL	M0e	H94	-4.9	C	0.00±0.10	4.28±1.08	3.576±0.014	0.448±0.221	75	1.2	IM Lup
323	15564402-4242301	UCL	K6IVe	T06	-2.3	T06	0.44±0.02	6.38±0.67	3.604±0.009	0.025±0.093	2	0.7	
324	15565905-3933430	UCL	G7IV	PM	1.2	M02	0.19±0.07	6.01±0.58	3.723±0.007	0.174±0.085	11	1.3	
325	15570234-1950419	US	K7:e	P98	-0.8	P98	0.00±0.05	6.75±0.62	3.599±0.004	-0.070±0.081	2	0.7	
326	15573430-2321123	US	M1IVe	PM	-9.0	PM	0.71±0.04	7.93±0.76	3.560±0.017	-0.494±0.087	3	0.4	V1148 Sco
327	15574362-4143377	UCL	K6IVe	PM	-5.5	PM	0.30±0.08	5.91±0.52	3.604±0.009	-0.176±0.078	2	0.7	
328	15574440-4049276	UCL	K9IVe	PM	-22.9	PM	0.57±0.05	5.88±0.76	3.589±0.010	0.088±0.114	1	0.5	Hen 3-1122
329	15575002-2305094	US	M0	K00	...		0.14±0.21	7.61±0.80	3.576±0.014	-0.593±0.097	5	0.6	
330	15581270-2328364	US	G2IV	PM	1.5	B	0.86±0.11	6.61±0.55	3.769±0.009	0.504±0.075	12	1.4	
331	15581474-4029175	UCL	K8IVe	PM	-3.4	PM	0.34±0.12	6.44±0.81	3.595±0.005	-0.191±0.111	2	0.6	
332	15582054-1837252	US	G3e	P98	-0.9	P98	1.10±0.23	7.62±0.65	3.759±0.009	0.512±0.081	9	1.5	HD 142987
333	15583692-2257153	US	G5IVe	PM	-10.7	W07	0.79±0.45	5.87±0.49	3.740±0.009	0.643±0.089	6	1.7	HD 143006
334	15584772-1757595	US	K3e	P98	-0.4	W07	1.02±0.10	6.31±0.56	3.658±0.021	0.135±0.082	3	1.2	
335	15590208-1844142	US	K6e	P98	-1.5	P98	0.43±0.03	6.94±0.69	3.604±0.009	0.028±0.088	5	0.8	
336	15591101-1850442	US	K6IVe	PM	-0.8	PM	0.86±0.04	6.57±0.67	3.604±0.009	-0.312±0.090	4	0.7	
337	15591452-2606182	US	K2	K00	...		1.07±0.13	7.73±0.77	3.678±0.017	-0.281±0.090	19	1.0	
338	15591647-4157102	UCL	K7IVe	PM	-22.8	PM	0.80±0.16	5.02±0.58	3.599±0.004	-0.029±0.102	2	0.7	
339	15594951-3628279	UCL	K3	K97	0.7	K97	0.27±0.04	11.28±0.77	3.658±0.021	-0.255±0.065	11	1.1	
340	16003134-2027050	US	M1	P99	5.7	R06	0.37±0.23	6.71±0.72	3.560±0.017	-0.327±0.100	2	0.4	

Table 4.6 (cont'd)

ID No.	2MASS	Grp.	SpT	Ref.	EW(Hα) (Å)	Ref.	A_V (mag)	π_{kin} (mas)	log($T_{\rm eff}$) (dex)	log($L/L_\odot$) (dex)	Age (Myr)	Mass ($M_\odot$)	Other Name
341	16004056-2200322	US	G9	P99	0.7	W07	0.78±0.11	6.42±0.61	3.709±0.008	0.226±0.085	7	1.4	
342	16004277-2127380	US	K7	P99	3.5	R06	0.16±0.21	7.63±0.82	3.599±0.004	-0.410±0.097	5	0.7	
343	16010801-2113184	US	M0	P99	2.4	R06	0.07±0.21	6.62±0.60	3.576±0.014	-0.291±0.085	2	0.5	
344	16011070-4804438	UCL	K3Ve	T06	-0.5	T06	0.03±0.07	8.60±0.58	3.658±0.021	-0.396±0.064	19	1.0	
345	16012563-2240403	US	K1IV	W94	-0.5	W07	0.95±0.07	7.43±0.70	3.692±0.012	0.000±0.084	10	1.2	V1152 Sco
346	16014743-2049457	US	M0	P99	...		0.54±0.18	6.66±0.63	3.576±0.014	-0.200±0.087	2	0.6	
347	16014943-4026192	UCL	K7	K97	0.0	K97	0.00±0.20	6.09±0.78	3.599±0.004	-0.247±0.114	3	0.7	
348	16015149-2445249	US	K7	P99	...		0.42±0.22	6.63±0.58	3.599±0.004	-0.102±0.081	2	0.6	
349	16015822-2008121	US	G5	P99	0.9	W07	1.27±0.17	6.43±0.54	3.740±0.009	0.620±0.077	5	1.8	
350	16015918-3612555	UCL	K3	K97	-0.5	K97	0.31±0.08	6.89±0.74	3.658±0.021	-0.153±0.097	8	1.1	NN Lup
351	16020039-2221237	US	M1	P99	...		0.51±0.19	9.52±0.79	3.560±0.017	-0.630±0.079	4	0.5	
352	16021045-2241280	US	K5IV	W94	-0.7	W94	0.00±0.04	10.31±0.81	3.617±0.016	-0.293±0.071	5	0.9	V1154 Sco
353	16023814-2541389	US	K8IVe	PM	-2.8	PM	0.00±0.03	6.83±1.10	3.595±0.005	-0.485±0.141	6	0.7	
354	16023910-2542078	US	K7e	P98	-0.6	P98	0.00±0.08	10.11±0.81	3.599±0.004	-0.684±0.071	15	0.8	
355	16025123-2401574	US	K4	P99	-1.2	D12	0.20±0.20	6.68±0.61	3.636±0.021	-0.217±0.086	6	1.0	
356	16025243-2402226	US	K0	K00	...		1.36±0.16	3.55±0.44	3.702±0.009	1.018±0.110	2	2.7	RX J1602.8-2401
357	16025396-2022480	US	K7	P99	0.6	R06	0.72±0.21	6.33±0.59	3.599±0.004	0.070±0.085	11	0.8	
358	16030269-1806050	US	K4e	P98	-0.2	W07	0.29±0.05	6.15±0.57	3.636±0.021	-0.068±0.085	3	1.0	
359	16032367-1751422	US	M2e	P98	-4.9	P98	0.23±0.05	5.98±0.65	3.543±0.017	-0.206±0.098	8	0.5	
360	16033550-2245560	US	G9	P99	0.0	T06	0.57±0.03	7.51±0.62	3.709±0.008	0.088±0.073	10	1.3	

Table 4.6 (cont'd)

ID No.	2MASS	Grp.	SpT	Ref.	EW(Hα) (Å)	Ref.	A_V (mag)	π_{kin} (mas)	log($T_{\rm eff}$) (dex)	log($L/L_\odot$) (dex)	Age (Myr)	Mass ($M_\odot$)	Other Name
361	16034536-4355492	UCL	K1IV	PM	0.7	M02	0.12±0.05	5.90±0.47	3.692±0.012	0.669±0.072	2	1.9	HD 143677
362	16035250-3939013	UCL	K3IV	PM	-0.4	M02	0.18±0.05	7.44±0.54	3.658±0.021	0.029±0.068	4	1.2	
363	16035836-1751041	US	M0IVe	PM	-8.7	PM	1.59±0.06	3.59±0.60	3.576±0.014	0.174±0.147	>100	4.0	
364	16042165-2130284	US	K2	P99	-2.7	D12	5.03±0.20	5.45±0.95	3.678±0.017	0.441±0.154	2	1.5	RX J1604.3-2130
365	16043056-3207287	US	K2	K97	1.6	K97	0.00±0.03	7.51±0.60	3.678±0.017	-0.068±0.073	9	1.2	
366	16044776-1930230	US	K2IV	W94	-0.1	W07	0.82±0.08	5.98±0.53	3.678±0.017	0.335±0.080	2	1.4	V1156 Sco
367	16054266-2004150	US	M2V	W94	-4.0	W94	0.65±0.06	6.52±0.70	3.543±0.017	-0.454±0.097	2	0.4	
368	16054499-3906065	UCL	G8V	PM	0.3	M02	0.17±0.07	7.21±0.59	3.717±0.007	0.139±0.073	10	1.3	
369	16055065-2533136	US	G7e	P98	-0.2	P98	0.55±0.05	10.40±0.82	3.723±0.007	-0.206±0.071	33	0.9	
370	16055207-3439331	UCL	K2Ve	T06	-0.3	T06	0.50±0.03	5.06±0.41	3.678±0.017	0.298±0.074	3	1.4	
371	16061222-4507155	UCL	K3IV(e)	PM	-0.1	PM	0.31±0.02	4.67±0.53	3.658±0.021	-0.048±0.102	5	1.2	
372	16061254-2036472	US	K5	P99	...		1.14±0.21	7.50±0.69	3.617±0.016	-0.307±0.086	5	0.9	
373	16062196-1928445	US	M0.5V	W94	-19.3	W94	0.73±0.10	6.29±0.65	3.568±0.016	-0.235±0.094	2	0.5	
374	16062334-4447355	UCL	K4	K97	0.3	K97	0.23±0.21	7.43±0.63	3.636±0.021	-0.507±0.082	19	0.9	
375	16062354-1814187	US	K5IVe	PM	-0.8	PM	0.28±0.07	6.00±0.85	3.617±0.016	0.044±0.125	2	0.8	
376	16063169-2036232	US	K6e	P98	-1.6	P98	0.91±0.02	6.92±0.65	3.604±0.009	-0.209±0.083	3	0.7	GSC 06208-00834
377	16063245-2208245	US	K6IVe	PM	-0.8	PM	0.03±0.09	7.63±1.12	3.604±0.009	-0.396±0.129	5	0.8	
378	16065436-2416107	US	M3e	P98	-3.6	P98	0.00±0.43	6.22±0.81	3.526±0.022	-0.358±0.125	63	0.6	
380	16070356-2036264	US	M0	P99	...		0.64±0.27	6.96±0.61	3.576±0.014	-0.027±0.085	1	0.5	
381	16070393-1911338	US	M1	P99	...		0.76±0.23	7.73±0.78	3.560±0.017	-0.589±0.095	3	0.5	

Table 4.6 (cont'd)

ID No.	2MASS	Grp.	SpT	Ref.	EW(Hα) (Å)	Ref.	A_V (mag)	π_{kin} (mas)	log(T_{eff}) (dex)	log($L/L_\odot$) (dex)	Age (Myr)	Mass ($M_\odot$)	Other Name
382	16073366-3759242	UCL	K7IVe	PM	-1.9	PM	0.00±0.03	7.75±0.53	3.599±0.004	-0.608±0.062	11	0.8	
383	16074006-2148426	US	K7IVe	PM	-2.7	PM	0.56±0.03	5.62±0.63	3.599±0.004	-0.425±0.098	5	0.7	
384	16080019-4116119	UCL	K3.5IVe	PM	-1.6	PM	0.33±0.06	7.86±0.82	3.647±0.021	-0.244±0.095	8	1.1	
385	16080141-2027416	US	K8e	P02	-2.3	P02	1.13±0.04	6.18±0.65	3.595±0.005	-0.328±0.092	3	0.7	
386	16080772-5041556	UCL	K6IVe	PM	-1.2	PM	0.00±0.14	10.40±0.78	3.604±0.009	-0.587±0.069	12	0.8	
387	16081081-1904479	US	K3IVe	PM	-0.8	PM	0.53±0.04	6.26±0.67	3.658±0.021	0.095±0.097	3	1.2	
388	16081474-1908327	US	K2	P98	1.2	W07	0.57±0.01	7.13±0.62	3.678±0.017	0.042±0.079	6	1.3	
389	16081824-3844052	UCL	K7	K97	0.1	K97	0.00±0.04	9.05±0.94	3.599±0.004	-0.480±0.091	6	0.8	NQ Lup
390	16083436-1911563	US	K5:	P98	0.0	P98	0.59±0.12	6.20±0.70	3.617±0.016	0.257±0.101	1	0.7	GSC 06209-01215
391	16083617-3923024	UCL	K6	K97	-7.4	K97	0.90±0.11	5.93±0.75	3.604±0.009	-0.138±0.111	2	0.7	V1094 Sco
392	16084340-2602168	US	G7	P98	0.3	P98	0.63±0.10	6.38±0.65	3.723±0.007	0.451±0.090	5	1.7	
393	16085427-3906057	UCL	K2	K97	0.8	K97	0.06±0.11	5.94±0.72	3.678±0.017	0.245±0.108	4	1.4	
394	16085673-2033460	US	K5e	P98	-0.5	P98	0.28±0.04	6.76±0.63	3.617±0.016	-0.152±0.084	3	0.8	
395	16090075-1908526	US	K9e	P01	-12.7	P02	1.10±0.02	7.34±0.75	3.589±0.010	-0.458±0.090	4	0.6	
396	16092918-1852536	US	K4IVe	PM	-1.5	PM	1.42±0.20	6.47±0.71	3.636±0.021	0.049±0.101	2	1.0	
397	16093030-2104589	US	M0e	P98	-1.1	P98	0.00±0.02	6.32±0.60	3.576±0.014	-0.305±0.086	2	0.5	GSC 06213-01358
398	16093969-2200466	US	K9IVe	PM	-6.7	PM	1.03±0.04	6.15±1.70	3.589±0.010	-0.344±0.241	3	0.6	
399	16094098-2217594	US	M0e	P98	-4.6	P98	0.12±0.08	6.42±0.59	3.576±0.014	-0.171±0.084	2	0.5	
400	16100478-4016122	UCL	K2	K97	0.9	K97	0.08±0.05	7.34±0.57	3.678±0.017	-0.109±0.071	10	1.2	V1096 Sco
401	16101171-3226360	US	K5IVe	PM	-1.7	PM	0.00±0.02	5.58±0.47	3.617±0.016	0.077±0.076	2	0.8	

Table 4.6 (cont'd)

ID No.	2MASS	Grp.	SpT	Ref.	EW(Hα) (Å)	Ref.	A_V (mag)	π_{kin} (mas)	log($T_{\rm eff}$) (dex)	log($L/L_\odot$) (dex)	Age (Myr)	Mass ($M_\odot$)	Other Name
402	16101264-2104446	US	K3IV	PM	0.3	PM	0.47±0.04	5.79±0.58	3.658±0.021	0.121±0.091	3	1.2	
403	16101729-1910263	US	K5IVe	PM	-2.7	PM	0.91±0.06	5.71±0.72	3.617±0.016	0.052±0.112	2	0.8	
404	16101918-2502301	US	M1e	P98	-0.8	P98	0.00±0.23	6.98±0.68	3.560±0.017	-0.188±0.092	1	0.5	
405	16102174-1904067	US	M1V	W94	-7.3	PM	1.05±0.01	7.25±0.74	3.560±0.017	-0.678±0.092	4	0.5	
406	16102653-2756293	US	M3Ve	PM	-5.5	PM	0.00±0.02	6.78±1.17	3.526±0.022	-0.671±0.152	2	0.3	
407	16102888-2213477	US	G5V	H88	0.0	T06	0.66±0.09	6.26±0.52	3.740±0.009	0.777±0.075	3	2.1	HD 145208
408	16104202-2101319	US	K5e	P98	-2.1	P98	0.61±0.03	5.97±0.58	3.617±0.016	0.024±0.087	2	0.8	
409	16110890-1904468	US	K4IVe	PM	-3.0	PM	1.26±0.21	6.61±0.64	3.636±0.021	0.293±0.091	13	1.1	V1000 Sco
410	16111534-1757214	US	M1e	P02	-2.4	P02	0.75±0.01	7.12±0.68	3.560±0.017	-0.514±0.087	3	0.4	
411	16114387-2526350	US	K3IV(e)	PM	-0.2	PM	0.36±0.03	7.18±0.69	3.658±0.021	-0.138±0.087	7	1.2	
412	16115334-3902158	UCL	K7/M0e	H94	-1.6	H94	0.00±0.22	6.27±0.61	3.593±0.007	-0.460±0.089	5	0.7	HBC 631
413	16120140-3840276	UCL	K5	K97	-0.7	K97	0.37±0.23	4.57±0.69	3.617±0.016	0.377±0.135	21	1.0	
414	16123916-1859284	US	K2.5IV	PM	0.2	PM	2.57±0.03	6.83±0.70	3.668±0.019	-0.163±0.093	10	1.1	GSC 06209-01312
415	16124051-1859282	US	K0IV	W94	-0.3	W07	1.36±0.04	5.35±0.52	3.702±0.009	0.747±0.086	1	2.0	V1002 Sco
416	16124682-2213317	US	K3IV(e)	PM	-0.2	PM	0.46±0.06	6.87±0.58	3.658±0.021	0.153±0.078	3	1.2	TYC 6213-85-1
417	16125265-2319560	US	K3IV(e)	PM	-0.2	PM	0.49±0.05	6.66±0.58	3.658±0.021	-0.213±0.080	10	1.1	
418	16130271-2257446	US	K4e	P98	-0.4	P98	0.32±0.02	5.88±0.50	3.636±0.021	0.069±0.078	2	1.0	
419	16131267-3803513	UCL	K5	K97	-0.5	K97	0.00±0.28	6.29±0.51	3.617±0.016	-0.188±0.081	3	0.8	
420	16131738-2922198	US	M0IVe	PM	-9.2	PM	0.33±0.20	8.15±0.76	3.576±0.014	-0.502±0.087	4	0.5	
421	16131858-2212489	US	G9	P98	0.0	P98	0.96±0.04	5.94±0.51	3.709±0.008	0.675±0.076	2	2.0	

Table 4.6 (cont'd)

ID No.	2MASS	Grp.	SpT	Ref.	EW(Hα) (Å)	Ref.	A_V (mag)	π_{kin} (mas)	log($T_{\rm eff}$) (dex)	log($L/L_\odot$) (dex)	Age (Myr)	Mass ($M_\odot$)	Other Name
422	16132929-2311075	US	K1e	P98	-0.4	W07	1.04±0.07	6.90±0.65	3.692±0.012	0.077±0.084	8	1.3	
423	16134366-2214594	US	K7IVe	PM	-3.2	PM	0.54±0.01	6.27±0.59	3.599±0.004	-0.306±0.083	3	0.7	
424	16135801-3618133	UCL	G8V	PM	-0.5	M02	0.14±0.05	8.31±0.64	3.717±0.007	-0.198±0.070	29	1.0	
425	16140035-2108439	US	K8IVe	PM	-2.9	PM	0.58±0.11	6.52±0.67	3.595±0.005	-0.538±0.091	7	0.7	
426	16140211-2301021	US	G4	P98	0.0	P98	0.89±0.13	5.32±0.64	3.750±0.009	0.348±0.107	12	1.4	
427	16141107-2305362	US	K0	P98	1.0	P98	1.05±0.04	5.90±0.52	3.702±0.009	0.642±0.078	3	1.9	
428	16143884-2525000	US	M0.5IVe	PM	-8.1	PM	0.83±0.04	9.52±0.78	3.568±0.016	-0.612±0.075	4	0.5	
429	16145207-5026187	UCL	K1IV	PM	0.6	M02	0.25±0.03	8.23±0.69	3.692±0.012	0.226±0.075	6	1.5	
430	16145918-2750230	US	G5	P98	0.6	W07	0.82±0.06	6.63±0.62	3.740±0.009	0.151±0.083	16	1.2	
431	16153456-2242421	US	K5Ve	T06	-20.4	P98	1.28±0.63	8.05±1.36	3.617±0.016	-0.146±0.163	3	0.8	VV Sco
432	16153587-2529008	US	K2.5IVe	PM	-0.6	PM	1.14±0.08	6.95±0.60	3.668±0.019	-0.080±0.080	8	1.2	
433	16155664-3947163	UCL	M0.5	K97	-0.2	K97	0.00±0.19	7.80±0.62	3.568±0.016	-0.589±0.076	4	0.5	
434	16161423-2643148	US	K5IVe	PM	-2.1	PM	0.15±0.08	8.98±0.73	3.617±0.016	-0.309±0.074	5	0.9	
435	16161795-2339476	US	G7	P98	0.7	W07	0.55±0.05	5.73±0.63	3.723±0.007	0.465±0.097	5	1.7	
436	16173138-2303360	US	G0IV	W94	1.8	W07	0.80±0.07	5.22±0.48	3.782±0.004	0.739±0.082	9	1.6	HD 146516
437	16175569-3828132	UCL	M0Ve	PM	-3.5	PM	0.00±0.21	8.42±0.72	3.576±0.014	-0.730±0.081	8	0.6	
438	16181107-2911125	US	G6	C06	0.0	T06	0.30±0.06	6.15±0.76	3.732±0.008	0.316±0.109	8	1.4	
439	16183723-2405226	US	G5V	PM	2.1	PM	1.02±0.25	10.81±0.92	3.740±0.009	-0.127±0.082	33	1.0	CD-23 12840
440	16191217-2550383	US	K3IV	PM	0.8	PM	1.91±0.04	6.42±0.64	3.658±0.021	-0.028±0.091	5	1.2	
441	16193396-2228294	US	K0e	P98	-0.8	P98	0.47±0.10	6.61±0.60	3.702±0.009	0.099±0.081	9	1.3	

Table 4.6 (cont'd)

ID No.	2MASS	Grp.	SpT	Ref.	EW(Hα) (Å)	Ref.	A_V (mag)	π_{kin} (mas)	log($T_{\rm eff}$) (dex)	log($L/L_\odot$) (dex)	Age (Myr)	Mass ($M_\odot$)	Other Name
442	16195068-2154355	US	K8IVe	PM	-5.2	PM	0.71±0.21	4.88±0.73	3.595±0.005	0.295±0.133	>100	2.2	
443	16202930-3254096	US	K4IV(e)	PM	-0.6	PM	0.00±0.05	6.92±1.25	3.636±0.021	-0.267±0.159	7	1.0	TYC 7347-2197-1
444	16204468-2431384	US	G0	P98	3.0	P98	3.12±0.21	4.99±0.51	3.782±0.004	0.693±0.092	10	1.5	GSC 06798-00091
445	16230783-2300596	US	K2	P98	1.5	P98	1.33±0.15	4.32±1.00	3.678±0.017	0.606±0.203	2	1.7	
446	16233234-2523485	US	G1	P98	0.4	P98	2.38±0.16	6.80±0.89	3.776±0.007	0.639±0.116	10	1.5	
447	16234698-2850023	US	G8IV	T06	...	T06	0.20±0.01	6.56±0.73	3.717±0.007	0.103±0.098	12	1.3	
448	16235484-3312370	US	K6IVe	PM	-3.1	PM	0.00±0.02	8.50±0.72	3.604±0.009	-0.343±0.075	4	0.8	
450	16240373-4319261	UCL	G3V	PM	2.3	PM	0.70±0.14	6.44±0.60	3.759±0.009	0.198±0.084	20	1.2	HD 325602
451	16240632-2456468	US	K3IVe	PM	-1.2	PM	2.14±0.23	6.64±0.70	3.658±0.021	0.138±0.098	3	1.2	
452	16241860-2854475	US	G5Ve	PM	-0.4	PM	1.40±0.07	4.32±0.48	3.740±0.009	0.697±0.099	4	1.9	TYC 6806-638-1
453	16245136-2239325	US	G6e	P98	-0.6	P98	0.72±0.06	6.17±0.59	3.732±0.008	0.810±0.085	3	2.2	HD 147808
454	16250991-3047572	US	G1V	PM	2.6	PM	0.25±0.10	9.32±0.78	3.776±0.007	0.466±0.074	14	1.3	HD 147810
455	16251923-2426526	US	G1IV	W94	0.7	W94	0.89±0.10	8.31±0.82	3.776±0.007	0.399±0.087	16	1.3	
456	16252863-2346265	US	K2IV	PM	0.7	PM	1.86±0.40	8.60±1.04	3.678±0.017	0.149±0.116	5	1.4	
457	16253849-2613540	US	K7Ve	T06	-4.9	T06	0.39±0.20	6.31±0.85	3.599±0.004	0.226±0.119	>100	1.6	V896 Sco
458	16262736-2756508	US	K4IVe	PM	-4.4	PM	0.69±0.14	10.10±0.83	3.636±0.021	-0.241±0.078	6	1.0	
459	16263591-3314481	US	K2IV(e)	PM	0.4	PM	0.00±0.05	5.27±0.55	3.678±0.017	0.112±0.094	5	1.4	TYC 7348-952-1
460	16265280-2343127	US	K1IVe	PM	-2.6	PM	2.04±0.33	10.91±1.22	3.692±0.012	0.360±0.105	3	1.6	VSS II-28
461	16265700-3032232	US	K6IVe	PM	-1.7	PM	0.00±0.21	9.87±0.96	3.604±0.009	-0.559±0.089	11	0.8	
462	16265763-3032279	US	M0IVe	PM	-3.4	PM	0.00±0.08	6.46±1.13	3.576±0.014	-0.032±0.154	1	0.5	

Table 4.6 (cont'd)

ID No.	2MASS	Grp.	SpT	Ref.	EW(Hα) (Å)	Ref.	A_V (mag)	π_{kin} (mas)	log($T_{\rm eff}$) (dex)	log($L/L_\odot$) (dex)	Age (Myr)	Mass ($M_\odot$)	Other Name
463	16271951-2441403	US	M0IVe	PM	-10.8	PM	0.98±0.02	7.17±0.74	3.576±0.014	-0.151±0.093	1	0.5	V2247 Oph
464	16272794-4542403	UCL	G8Ve	T06	-0.1	T06	0.48±0.12	5.52±0.52	3.717±0.007	0.258±0.084	7	1.4	HD 328252
465	16273956-2245230	US	K1e	P98	-0.6	P98	1.31±0.10	6.15±0.64	3.692±0.012	0.356±0.093	4	1.6	
466	16274028-2422040	US	K5e	T06	-12.0	T06	0.82±0.26	9.00±1.00	3.617±0.016	0.084±0.103	2	0.8	V2129 Oph
467	16282453-4740395	UCL	M0IVe	PM	-6.6	PM	0.42±0.05	8.03±0.67	3.576±0.014	-0.696±0.076	7	0.6	
468	16290585-3145250	US	K5IVe	PM	-1.9	PM	0.00±0.02	9.93±0.82	3.617±0.016	-0.674±0.075	23	0.8	
469	16293397-2455303	US	K1IV	PM	1.3	PM	1.59±0.12	5.82±1.01	3.692±0.012	0.240±0.153	4	1.5	
470	16294869-2152118	US	KIV	W94	0.1	W07	1.53±0.12	6.56±0.60	3.702±0.009	0.442±0.082	4	1.7	V2505 Oph
471	16294991-2728498	US	K1V(e)	T06	0.0	T06	0.09±0.07	7.77±0.61	3.692±0.012	-0.112±0.071	14	1.1	
472	16303796-2954222	US	K2Ve	T06	0.0	T06	0.09±0.08	8.79±0.73	3.678±0.017	-0.149±0.076	12	1.1	CD-29 12588
473	16310436-2404330	US	K4IVe	PM	-2.0	PM	1.63±0.29	5.31±0.86	3.636±0.021	0.483±0.147	<1	...	VSS II-46, HBC 644
474	16310837-2651062	US	K8IVe	PM	-1.8	PM	0.00±0.20	8.52±0.89	3.595±0.005	-0.658±0.094	12	0.8	
475	16315346-2636169	US	K4IV(e)	PM	-0.5	PM	0.00±0.14	6.73±0.61	3.636±0.021	-0.196±0.085	5	1.0	TYC 6803-994-1
476	16320058-2530287	US	K7IVe	PM	-0.8	PM	0.08±0.21	6.21±0.67	3.599±0.004	-0.457±0.097	6	0.7	V939 Sco
477	16320160-2530253	US	K5IVe	PM	-2.1	PM	0.26±0.21	5.17±1.26	3.617±0.016	-0.221±0.214	4	0.9	V940 Sco
478	16320352-2830179	US	G7IV	T06	...	T06	0.43±0.16	6.30±0.65	3.723±0.007	0.472±0.092	5	1.7	HD 148862
479	16321179-2440213	US	K8IVe	PM	-18.3	PM	2.16±0.04	4.99±0.57	3.595±0.005	0.391±0.100	83	1.5	V2248 Oph
480	16322432-1703399	US	K9IVe	PM	-3.2	PM	0.91±0.04	5.56±0.79	3.589±0.010	0.266±0.125	>100	0.8	
481	16334191-2523342	US	K4IVe	T06	-4.6	T06	0.84±0.13	7.23±0.61	3.636±0.021	0.151±0.079	2	0.9	V877 Sco
482	16340585-2658441	US	K3IVe	PM	-2.9	PM	0.96±0.08	7.08±0.74	3.658±0.021	-0.126±0.095	7	1.2	

Table 4.6 (cont'd)

ID No.	2MASS	Grp.	SpT	Ref.	EW(Hα) (Å)	Ref.	A_V (mag)	π_{kin} (mas)	log($T_{\rm eff}$) (dex)	log($L/L_\odot$) (dex)	Age (Myr)	Mass ($M_\odot$)	Other Name
483	16344629-2606324	US	K4.5IVe	PM	-1.1	PM	0.12±0.02	6.42±0.61	3.626±0.019	-0.338±0.086	7	1.0	V878 Sco
484	16345314-2518167	US	G9IV	T06	...	T06	0.19±0.04	7.91±0.66	3.709±0.008	0.199±0.074	7	1.4	HD 149309
485	16351188-2845520	US	K7IVe	PM	-4.3	PM	0.15±0.06	6.89±0.86	3.599±0.004	-0.341±0.109	4	0.7	
486	16353547-2541194	US	G8IV	PM	2.4	PM	0.60±0.10	4.57±0.47	3.717±0.007	0.063±0.091	13	1.2	
487	16354836-2148396	US	M0e	P98	-4.0	P98	0.78±0.01	5.01±2.01	3.576±0.014	0.102±0.349	>100	1.3	GSC 06228-01359
488	16384946-2735294	US	K0V(e)	T06	0.0	T06	0.53±0.08	5.51±0.83	3.702±0.009	0.233±0.132	7	1.4	
489	16430140-4405275	UCL	G7V	B	...		0.15±0.20	4.56±0.44	3.723±0.007	0.035±0.088	<1	...	HD 328585
490	16432519-3022477	US	K0V(e)	T06	0.0	T06	0.35±0.05	5.82±0.62	3.702±0.009	0.035±0.094	11	1.2	
491	16452615-2503169	US	K3Ve	T06	-7.2	T06	0.42±0.16	5.62±0.69	3.658±0.021	0.358±0.112	2	1.3	
492	16473710-2014268	US	K4IV(e)	PM	-0.3	PM	0.00±0.11	6.81±0.67	3.636±0.021	-0.397±0.090	12	1.0	
493	16491330-4355279	UCL	K0IV	T06	...	T06	0.00±0.09	10.37±0.76	3.702±0.009	-0.150±0.067	19	1.0	HD 326277

Note. — EW(Hα)< 0 denotes emission, EW(Hα)> 0 denotes absorption.
References – (PM) - This work; (G67) - Garrison (1967); (F87) - Finkenzeller & Basri (1987); (H88) - Houk & Smith-Moore (1988); (W94) - Walter et al. (1994); (H94) - Hughes et al. (1994); (W97) - Wichmann et al. (1997); (K97) - Krautter et al. (1997); (P98) - Preibisch et al. (1998); (P99) - Preibisch & Zinnecker (1999); (W99) - Wichmann et al. (1999); (K00) - Köhler et al. (2000); (P01) - Preibisch et al. (2001); (M02) - Mamajek et al. (2002); (P02) - Preibisch et al. (2002); (Z01) - Zuckerman et al. (2001); (T06) - Torres et al. (2006); (R06) - Riaz et al. (2006); (C06) - Carpenter et al. (2006); (W07) - White et al. (2007); (D12) - Dahm et al. (2012); (A) - measured from spectrum downloaded from the ESO archive, program 083.A-9003(A); (B) - E. Mamajek, Private Communication, 2012 (C) - measured from spectrum downloaded from the ESO archive, program 081.C-0779(A);

Table 4.7. Objects Rejected as Sco-Cen Members

2MASS	SpT	Ref.	Rejection Reason	Other Names
10004365-6522155	G3V	PM	μ	
10111521-6620282	K0IV	PM	HRD position	
10293275-6349156	K1IV	PM	μ	TYC 8964-165-1
10342989-6235572	G7Ve	PM	μ	HD 307772
10441393-6446273	K1V(e)	PM	μ	HD 307960
10463300-6527183	G6V	PM	μ	HD 31013
10474221-5510143	K6IVe	PM	Li, μ	
10484283-5442328	G9V	PM	Li	TYC 8618-427-1
10541737-6440512	K2IV	PM	μ	TYC 8966-142-1
10591218-6438089	K0V(e)	PM	μ	
11033159-6321581	K8IV(e)	PM	Li	TYC 8962-1373-1
11132622-4523427	K8IVe	PM	μ	V1215 Cen, TWA 14
11145608-7101430	K3IV	PM	Li, μ	
11154143-5511082	K2.5IV	PM	Li, μ	TYC 8620-489-1
11165870-4406222	G5V	PM	Li, μ	TYC 7738-1638-1
11202645-5834023	K0IV	PM	Li, μ	HD 304169
11214451-4954076	K0IV	PM	Li	HD 98803
11265293-5846387	K2.5IV	PM	Li	TYC 8629-386-1
11403346-5641458	K3IV	PM	Li, μ	TYC 8638-2548-1
11430455-6714211	K5IVe	PM	Li, μ	TYC 8985-607-1
11434903-6904232	K2III	PM	Li, μ, log(g)	
11485263-5657441	K4III	PM	Li, μ, log(g)	
11492309-4801013	G5V	PM	Li	TYC 8220-950-1
11522242-6156016	K4III	PM	Li, μ, log(g)	TYC 8977-9124-1
11524466-5514070	K3III	PM	Li, μ, log(g)	TYC 8635-1764-1
11560730-6314096	K3IV	PM	Li, μ	HD 309346
11575693-5821291	K2V	PM	Li	TYC 8643-152-1
11592560-5407445	K0IV	PM	Li	TYC 8631-489-1
12131860-4815588	K3III(e)	PM	Li, log(g)	
12135166-5419527	K6IV	PM	Li, μ	TYC 8633-2476-1
12141149-5456022	K3IIIe	PM	Li, μ, log(g)	TYC 8637-2220-1
12172809-5122215	K3III	PM	Li, log(g)	TYC 8242-1079-1

Table 4.7 (cont'd)

2MASS	SpT	Ref.	Rejection Reason	Other Names
12222200-5114260	G2V	PM	Li	
12244195-6437015	K3III(e)	PM	Li, log(g)	TYC 8983-2153-1
12252542-5353568	K3V-IV(e)	PM	Li	
12283577-4948021	K6III	PM	Li, μ, log(g)	
12313807-4558593	M3IVe	PM	μ	GSC 08231-02642, TWA 20
12314481-4808482	K3V(e)	PM	Li	TYC 8235-2143-1
12321483-4217502	K3III	PM	Li, μ, log(g)	HD 109075
12351574-4919517	K0V	PM	Li	
12390790-5811593	K4III	PM	Li, μ, log(g)	TYC 8658-174-1
12391307-5429052	K0IV	PM	Li, μ	
12392312-7244039	K2III	T06	Li, μ	TYC 9236-254-1
12404975-5048077	K5IV(e)	PM	Li, μ	TYC 8244-550-1
12434124-4204055	K5III(e)	PM	Li, log(g)	
12484652-5417333	G4Vn	PM	Li	TYC 8647-403-1
12510413-5253320	K5III	PM	Li, μ, log(g)	TYC 8647-2425-1
12560940-6127256	K0Ve	T06	μ	HD 112245
13140112-6846384	G9Ve	T06	μ	
13151666-5058072	G6III	T06	Li, μ	HD 115029
13173283-7037429	K6IVe	PM	Li	
13274874-6622488	K3III	PM	Li, μ, log(g)	TYC 9003-1880-1
13281508-4446377	K1V	PM	Li	
13290963-4755545	K5Ve	PM	Li	
13431296-4155366	G8V	PM	Li, μ	TYC 7797-615-1
13431682-4233127	K1III	PM	Li, μ, log(g)	TYC 7797-1361-1
13445275-6800331	G9V	PM	Li	
13451319-6128149	K2Ve	PM	Li	
13493502-4452104	K3III	PM	Li, μ, log(g)	TYC 7801-1053-1
13522045-3825345	M1IVe	PM	μ	
13581812-4504043	K3III	PM	Li, log(g)	
13591330-7136541	K3III	PM	Li, log(g)	TYC 9251-1662-1
14014823-4100264	F5	PM	Li, μ	
14015020-4059234	K0III	PM	Li, μ, log(g)	

Table 4.7 (cont'd)

2MASS	SpT	Ref.	Rejection Reason	Other Names
14040272-4436503	F8	PM	Li	
14055695-6149126	G2V	PM	Li, μ	TYC 9005-3316-1
14144477-4207224	G6V	PM	Li	TYC 7812-465-1
14165395-5356098	K1V	PM	Li, μ	TYC 8678-1562-1
14184440-5850045	K3III-IV	PM	Li	TYC 8690-2876-1
14201211-4917224	K0IIIe	PM	Li, μ, log(g)	
14214499-5429040	K3III(e)	PM	Li, log(g)	
14241649-5013282	K2III	PM	Li, μ, log(g)	CD-49 8711
14250165-4822361	G9III	T06	Li	HD 126113
14291483-6752209	A7	PM		TYC 9257-162-1
14301461-4520277	K3IV(e)	PM	HRD position	
14301594-5904014	K3III	PM	Li, μ, log(g)	TYC 8691-2027-1
14345603-7030069	K0V	T06	Li, μ	
14372053-4410053	G8V	PM	Li	CD-43 9198
14405601-7046138	G9III(e)	T06	Li, μ	TYC 9261-1334-1
14421471-5951445	K1V-IV	PM	Li	
14421965-4432065	K5III	PM	Li, μ, log(g)	CPD-44 6913
14433325-5241213	G8V(e)	PM	Li	
14560001-3124581	K2IV	PM	Li, μ	TYC 7298-1077-1
14571217-3107596	K6III	PM	Li, μ, log(g)	
15023844-4156105	K7III	PM	Li, μ, log(g)	
15033281-3033435	K3V	PM	Li	
15034365-5156318	K2.5V(e)	PM	Li	TYC 8305-1737-1
15044217-3018552	K1V-IV(e)	PM	Li, μ	
15082754-5801220	F8	PM	Li	TYC 8702-17-1
15092793-4650572	K0IV	M02	Li	CD-46 9829
15105821-3926499	K1Ve	T06	Li	CD-38 10027A
15105821-3926499	K1Ve	T06	Li	CD-38 10027B
15122700-4453385	G8V	PM	Li	TYC 7834-255-1
15130869-4450158	K4III	PM	Li, μ, log(g)	TYC 7834-783-1
15153210-3005336	K3V-IV	PM	Li	CD-29 11614
15161044-3851565	K0III	T06	Li, μ	CD-38 10127

Table 4.7 (cont'd)

2MASS	SpT	Ref.	Rejection Reason	Other Names
15193457-2846217	K1V	T06	Li, μ	
15200259-4638340	G9V	PM	Li	TYC 8294-327-1
15220457-5634346	G8V	PM	Li	TYC 8703-1058-1
15220743-3930140	K5Ve	PM	Li	
15221627-2652252	K4IV(e)	PM	Li, μ	PX Lib
15222449-3337352	K2V	PM	Li	
15230505-3627294	K7Ve	PM	Li	
15234137-4004455	K1IV	PM	Li, μ	
15240670-3601013	G4V	PM	Li	HD 136853
15243933-2102040	G2V	PM	Li	BD-20 4227
15244741-4257591	K0V(e)	PM	Li	
15251724-2729309	K0V	PM	Li, μ	TYC 6771-369-1
15264407-3849588	G8V	PM	Li, μ	TYC 7835-2042-1
15264611-3849198	K3III	PM	Li, μ, log(g)	TYC 7835-1429-1
15271052-4138334	G9IV	T06	Li	
15280113-3751360	K4V	PM	Li, μ	TYC 7835-4-1
15280288-3751087	K5	K97	Li, μ	RX J1528.0-3751
15284402-3117387	G9III	T06	Li, μ	CCDM J15287-3118A
15284402-3117387	G6IV	T06	Li, μ	CCDM J15287-3118B
15311824-4333323	K0	K97	Li	RX J1531.2-4333
15312047-3855116	K4IV	PM	Li, μ	TYC 7836-1623-1
15313716-2156489	K4V	PM	Li, μ	TYC 6196-1611-1
15320739-2427130	K1IV	PM	Li	CD-24 12146
15333037-2003264	K0V	PM	Li	HD 138563
15342292-2514386		P98	Li, μ	TYC 6768-1212-1
15350044-3915143	K2Ve	T06	Li	
15351524-4156586	K0III	T06	Li, μ	TYC 7844-2273-1
15370261-2942430	K0V	PM	Li	
15371218-2644516	K0V	PM	Li, μ	
15371991-3041150	K5III	PM	Li, μ, log(g)	
15381792-2337306		P98	Li	GSC 06777-00831
15414732-1804591	K0V-IV	PM	Li, μ	TYC 6189-262-1

Table 4.7 (cont'd)

2MASS	SpT	Ref.	Rejection Reason	Other Names
15421600-4435440	K6III	PM	Li, μ, log(g)	CD-44 10327
15422385-4625471	K0IV	PM	Li	
15430669-4643064	K6V(e)	PM	Li	
15433953-2909035	K3III	PM	Li, μ, log(g)	
15475575-2300331	K2V	PM	Li	
15490667-1813113	G1V	PM	μ	
15521613-3218449	K1V	PM	Li	TYC 7332-167-1
15555324-4041435	F5	PM	Li	PQ Lup
15560250-3643472	K6	K97	Li	RX J1556.0-3643
15561488-2100408		P98	Li, μ	GSC 06199-01511
15582850-1610379	G9V	PM	Li	TYC 6187-1442-1
15593661-3255340	G8	K00	μ	RX J1559.6-3255
15593706-3255414	G8	K00	μ	
16003317-2726185	K3IIIe	PM	Li, μ, log(g)	TYC 6787-1267-1
16015061-4758342	F8	PM	Li	HD 330220
16015568-2412329	G8V	PM	Li	
16035625-3624496	K3IV	PM	Li, μ	TYC 7342-865-1
16042291-4448088	K5III(e)	PM	Li, log(g)	
16051598-1158039	G8V	PM	Li	TYC 5620-723-1
16061466-4413135	K3V(e)	PM	μ	
16073490-2445412	K1IV-III	PM	HRD position	HD 144610
16082061-4109504	K0III	PM	Li, log(g)	TYC 7855-67-1
16085438-4148364	K3III	PM	Li, log(g)	[HHC93] F407
16100321-5026121	K0III	T06	HRD position	CD-50 10181
16100577-2626068		P98	Li, μ	GSC 06788-00326
16141904-3326041	G8V	T06	Li	
16152831-3402319	K3III	PM	Li, μ, log(g)	
16154270-2901016	K5III	PM	Li, μ, log(g)	
16165205-2154235	K4IV(e)	PM	Li	
16172711-5023213	G3V	PM	Li, μ	TYC 8319-1530-1
16180479-2224394	K0III	T06	Li	CD-22 11485
16185958-2213283	K3III	PM	Li, μ, log(g)	BD-21 4333

Table 4.7 (cont'd)

2MASS	SpT	Ref.	Rejection Reason	Other Names
16191035-3851041	G9V	PM	Li	CD-38 10948
16193334-2807397	M2III	PM		GSC 06806-00016
16200368-4801298	K1V	T06	Li, μ	HD 330514
16202983-2716240	F0	PM	μ	TYC 6802-810-1
16235844-4706089	G5III	PM	Li, μ, log(g)	HD 330587
16243416-2606367	K4III	PM	Li, μ, log(g)	
16270927-2339055	K4IVe	PM	μ	
16272373-2855286	K3IV	PM	Li	
16282493-2723182	F8	PM	Li	TYC 6803-1071-1
16290446-2600389	K3III	PM	Li, μ, log(g)	
16303162-4718119	K4III	PM	Li, μ, log(g)	TYC 8329-2103-1
16303840-2418312	K1V	PM	Li	TYC 6795-600-1
16323765-4541547	K3III(e)	PM	Li, log(g)	
16361809-1828333	K1V	PM	Li, μ	
16363716-2340011	K5IVe	PM	μ	RAVE J163637.2-234001
16395498-2328007	K1III	PM	Li, log(g)	
16455772-4321044	G7V	PM	μ	
16493599-2728078	K0Ve	T06	μ	
16520069-2122553	K3IV	PM	Li, μ	
16542415-2500202	K9Ve	PM	Li, μ	

Note. — References– (PM) - This work; (K97) - Krautter et al. (1997); (P98) - Preibisch et al. (1998); (K00) - Köhler et al. (2000); (M02) - Mamajek et al. (2002); (T06) - Torres et al. (2006);

Table 4.8. Infrared Data and Excesses For Members of Sco-Cen

2MASS	Grp.	$W1$	$W2$	$W3$	$W4$	$E(K_S - W1)$	$E(K_S - W2)$	$E(K_S - W3)$	$E(K_S - W4)$	Disk Type
10065573-6352086	LCC	8.513 ± 0.023	8.531 ± 0.021	8.446 ± 0.018	8.301 ± 0.131	-0.025 ± 0.033	-0.006 ± 0.032	0.041 ± 0.030	0.115 ± 0.133	...
10092184-6736381	LCC	9.056 ± 0.019	9.177 ± 0.018	9.201 ± 0.020	8.916 ± 0.190	0.233 ± 0.028	0.142 ± 0.028	0.078 ± 0.029	0.291 ± 0.191	...
10313710-6901587	LCC	9.414 ± 0.023	9.431 ± 0.021	9.360 ± 0.025	9.622 ± 0.435	-0.013 ± 0.034	-0.011 ± 0.033	0.013 ± 0.035	-0.325 ± 0.436	...
10334180-6413457	LCC	9.236 ± 0.025	9.218 ± 0.021	9.167 ± 0.030	...	-0.038 ± 0.035	-0.001 ± 0.032	0.003 ± 0.038	...	...
10412300-6940431	LCC	8.304 ± 0.022	8.330 ± 0.020	8.216 ± 0.015	7.858 ± 0.082	-0.008 ± 0.030	0.012 ± 0.028	0.093 ± 0.025	0.382 ± 0.084	...
10494839-6446284	LCC	9.159 ± 0.018	9.361 ± 0.018	9.350 ± 0.022	9.200 ± 0.247	0.230 ± 0.026	0.071 ± 0.026	0.046 ± 0.029	0.127 ± 0.248	...
10544998-6526458	LCC	9.405 ± 0.022	9.415 ± 0.020	9.380 ± 0.030	...	0.046 ± 0.032	0.058 ± 0.030	0.049 ± 0.038	...	...
10552886-6629147	LCC	9.031 ± 0.023	9.033 ± 0.019	8.936 ± 0.020	8.792 ± 0.205	-0.014 ± 0.033	0.021 ± 0.031	0.080 ± 0.031	0.153 ± 0.206	...
10560422-6152054	LCC	8.394 ± 0.022	8.441 ± 0.018	8.348 ± 0.030	...	0.016 ± 0.030	-0.032 ± 0.028	0.000 ± 0.037	...	...
10574936-6913599	LCC	7.716 ± 0.024	7.744 ± 0.020	7.685 ± 0.017	7.594 ± 0.077	-0.017 ± 0.029	-0.023 ± 0.026	-0.008 ± 0.023	0.009 ± 0.079	...
11001895-6118020	LCC	8.211 ± 0.023	8.174 ± 0.020	7.422 ± 0.038	...	0.029 ± 0.031	0.116 ± 0.029	0.839 ± 0.043	...	Evolved
11080791-6341469	LCC	8.173 ± 0.023	8.176 ± 0.021	8.110 ± 0.019	8.174 ± 0.148	0.006 ± 0.033	-0.052 ± 0.031	-0.065 ± 0.030	-0.267 ± 0.150	...
11143442-4418240	LCC	7.114 ± 0.030	7.176 ± 0.020	7.106 ± 0.016	7.078 ± 0.074	-0.024 ± 0.035	-0.064 ± 0.027	-0.038 ± 0.024	-0.084 ± 0.076	...
11175186-6402056	LCC	7.747 ± 0.023	7.494 ± 0.020	6.419 ± 0.015	3.875 ± 0.017	0.337 ± 0.035	0.605 ± 0.034	1.630 ± 0.031	4.097 ± 0.032	Full
11272881-3952572	LCC	8.255 ± 0.023	8.276 ± 0.020	8.192 ± 0.019	8.067 ± 0.185	-0.086 ± 0.028	-0.092 ± 0.026	-0.058 ± 0.025	-0.010 ± 0.186	...
11275535-6626046	LCC	8.286 ± 0.022	8.315 ± 0.020	8.266 ± 0.019	8.119 ± 0.128	-0.021 ± 0.036	-0.020 ± 0.035	-0.011 ± 0.035	0.064 ± 0.131	...
11320835-5803199	LCC	7.401 ± 0.029	7.431 ± 0.021	7.386 ± 0.017	7.310 ± 0.083	-0.022 ± 0.041	-0.022 ± 0.036	-0.017 ± 0.034	-0.013 ± 0.088	...
11370003-6516164	LCC	9.461 ± 0.022	9.519 ± 0.020	9.612 ± 0.048	...	0.050 ± 0.030	0.007 ± 0.029	-0.136 ± 0.052	...	...
11402787-6201337	LCC	8.371 ± 0.023	8.335 ± 0.020	8.309 ± 0.035	8.763 ± 0.321	-0.002 ± 0.033	0.033 ± 0.031	-0.002 ± 0.042	-0.542 ± 0.322	...
11445217-6438548	LCC	8.392 ± 0.021	8.386 ± 0.019	8.325 ± 0.030	8.342 ± 0.217	0.080 ± 0.030	0.077 ± 0.028	0.070 ± 0.037	-0.040 ± 0.218	...
11452016-5749094	LCC	10.038 ± 0.022	10.067 ± 0.019	10.233 ± 0.061	...	0.028 ± 0.030	0.021 ± 0.028	-0.189 ± 0.065	...	...

Table 4.8 (cont'd)

2MASS	Grp.	$W1$	$W2$	$W3$	$W4$	$E(K_S - W1)$	$E(K_S - W2)$	$E(K_S - W3)$	$E(K_S - W4)$	Disk Type
11454278-5739285	LCC	8.434 ± 0.023	8.471 ± 0.020	8.441 ± 0.024	9.183 ± 0.499	0.063 ± 0.031	0.034 ± 0.029	0.009 ± 0.032	-0.814 ± 0.499	...
11472064-4953042	LCC	8.178 ± 0.023	8.141 ± 0.020	8.060 ± 0.017	8.003 ± 0.128	0.003 ± 0.040	0.022 ± 0.039	0.030 ± 0.037	-0.015 ± 0.132	...
11515049-6407278	LCC	9.468 ± 0.023	9.484 ± 0.019	9.736 ± 0.061	...	0.067 ± 0.031	0.081 ± 0.028	-0.211 ± 0.065	...	...
11522157-6444302	LCC	9.293 ± 0.023	9.332 ± 0.020	9.153 ± 0.032	...	0.002 ± 0.033	-0.007 ± 0.030	0.132 ± 0.039	...	...
11554295-5637314	LCC	7.898 ± 0.024	7.841 ± 0.020	7.734 ± 0.016	7.646 ± 0.075	0.025 ± 0.032	0.027 ± 0.029	0.055 ± 0.026	0.005 ± 0.078	...
11594608-6101132	LCC	8.360 ± 0.022	8.402 ± 0.019	8.315 ± 0.028	6.445 ± 0.045	0.163 ± 0.036	0.129 ± 0.035	0.161 ± 0.040	1.950 ± 0.054	Debris
11594986-6136246	LCC	8.300 ± 0.022	8.216 ± 0.019	8.181 ± 0.027	...	0.020 ± 0.032	0.103 ± 0.030	0.077 ± 0.035	...	...
12051254-5331233	LCC	8.974 ± 0.021	8.929 ± 0.019	8.932 ± 0.022	8.549 ± 0.215	0.144 ± 0.036	0.197 ± 0.035	0.139 ± 0.036	0.441 ± 0.217	...
12061352-5702168	LCC	8.643 ± 0.023	8.668 ± 0.020	8.649 ± 0.022	...	0.007 ± 0.033	0.031 ± 0.030	0.024 ± 0.032	...	...
12063292-4247508	LCC	8.511 ± 0.023	8.525 ± 0.021	8.393 ± 0.018	7.923 ± 0.111	-0.024 ± 0.033	-0.001 ± 0.031	0.093 ± 0.029	0.492 ± 0.113	...
12065276-5044463	LCC	9.059 ± 0.022	9.073 ± 0.020	8.989 ± 0.024	...	0.008 ± 0.029	-0.015 ± 0.028	0.001 ± 0.031	...	...
12074236-6227282	LCC	7.867 ± 0.023	7.851 ± 0.019	7.695 ± 0.022	7.364 ± 0.113	-0.046 ± 0.030	-0.015 ± 0.028	0.091 ± 0.030	0.345 ± 0.115	...
12090225-5120410	LCC	8.532 ± 0.023	8.554 ± 0.020	8.411 ± 0.019	7.424 ± 0.083	-0.027 ± 0.030	-0.034 ± 0.028	0.059 ± 0.027	0.969 ± 0.085	Debris
12092655-4923487	LCC	7.818 ± 0.024	7.797 ± 0.021	7.693 ± 0.016	7.692 ± 0.088	0.006 ± 0.033	0.035 ± 0.031	0.084 ± 0.028	0.004 ± 0.091	...
12094184-5854450	LCC	7.531 ± 0.024	7.542 ± 0.019	7.502 ± 0.017	7.652 ± 0.115	0.037 ± 0.030	0.048 ± 0.026	0.044 ± 0.025	-0.180 ± 0.116	...
12101065-4855476	LCC	8.228 ± 0.021	8.235 ± 0.019	8.240 ± 0.018	8.001 ± 0.118	0.096 ± 0.031	0.104 ± 0.030	0.049 ± 0.029	0.211 ± 0.120	...
12103705-5727208	LCC	9.436 ± 0.025	9.404 ± 0.021	9.471 ± 0.052	...	0.006 ± 0.046	0.053 ± 0.044	-0.064 ± 0.065	...	...
12113142-5816533	LCC	7.867 ± 0.023	7.910 ± 0.018	7.865 ± 0.022	7.395 ± 0.101	0.006 ± 0.035	-0.011 ± 0.032	-0.008 ± 0.034	0.389 ± 0.104	...
12120804-6554549	LCC	8.382 ± 0.022	8.391 ± 0.020	8.282 ± 0.018	7.962 ± 0.103	-0.049 ± 0.031	-0.043 ± 0.030	0.016 ± 0.028	0.259 ± 0.105	...
12121119-4950081	LCC	8.586 ± 0.022	8.611 ± 0.020	8.545 ± 0.020	8.581 ± 0.215	0.124 ± 0.033	0.121 ± 0.031	0.143 ± 0.031	0.033 ± 0.216	...
12123577-5520273	LCC	8.054 ± 0.022	8.080 ± 0.020	8.024 ± 0.020	7.540 ± 0.090	-0.024 ± 0.030	-0.028 ± 0.028	-0.016 ± 0.028	0.394 ± 0.092	...

Table 4.8 (cont'd)

2MASS	Grp.	$W1$	$W2$	$W3$	$W4$	$E(K_S - W1)$	$E(K_S - W2)$	$E(K_S - W3)$	$E(K_S - W4)$	Disk Type
12124890-6230317	LCC	7.663 ± 0.020	7.665 ± 0.017	7.485 ± 0.031	...	0.195 ± 0.030	0.175 ± 0.029	0.282 ± 0.039	...	...
12135700-6255129	LCC	8.278 ± 0.023	8.317 ± 0.021	...	...	0.022 ± 0.031	-0.009 ± 0.030	...	...	...
12143410-5110124	LCC	8.078 ± 0.024	8.086 ± 0.020	8.016 ± 0.017	8.083 ± 0.155	-0.029 ± 0.032	0.000 ± 0.029	0.032 ± 0.027	-0.106 ± 0.156	...
12145229-5547037	LCC	7.504 ± 0.025	7.539 ± 0.019	7.455 ± 0.016	7.385 ± 0.083	-0.079 ± 0.032	-0.064 ± 0.028	-0.009 ± 0.026	-0.008 ± 0.085	...
12160114-5614068	LCC	7.874 ± 0.023	7.854 ± 0.019	7.738 ± 0.016	7.656 ± 0.099	-0.012 ± 0.030	0.007 ± 0.028	0.062 ± 0.026	0.058 ± 0.101	...
12163007-6711477	LCC	7.733 ± 0.022	7.760 ± 0.020	7.690 ± 0.016	7.830 ± 0.100	0.024 ± 0.034	0.005 ± 0.033	0.020 ± 0.031	-0.201 ± 0.103	...
12164023-7007361	LCC	7.863 ± 0.023	7.865 ± 0.020	7.833 ± 0.020	7.947 ± 0.150	0.136 ± 0.037	0.149 ± 0.035	0.131 ± 0.035	-0.060 ± 0.153	...
12174048-5000266	LCC	9.561 ± 0.024	9.516 ± 0.021	9.483 ± 0.028	...	0.034 ± 0.032	0.039 ± 0.030	-0.008 ± 0.035	...	...
12182762-5943128	LCC	7.610 ± 0.025	7.627 ± 0.020	7.542 ± 0.019	7.221 ± 0.064	0.023 ± 0.030	0.025 ± 0.026	0.063 ± 0.025	0.308 ± 0.066	...
12185802-5737191	LCC	7.214 ± 0.030	7.241 ± 0.019	7.099 ± 0.016	6.872 ± 0.057	0.060 ± 0.040	0.059 ± 0.033	0.159 ± 0.031	0.313 ± 0.063	...
12192161-6454101	LCC	7.308 ± 0.027	7.338 ± 0.020	7.283 ± 0.017	7.238 ± 0.086	-0.001 ± 0.036	-0.009 ± 0.031	0.002 ± 0.029	-0.027 ± 0.089	...
12195938-5018404	LCC	9.145 ± 0.023	9.118 ± 0.021	9.144 ± 0.031	8.971 ± 0.331	0.102 ± 0.025	0.128 ± 0.024	0.041 ± 0.033	0.128 ± 0.331	...
12202301-5242165	LCC	7.587 ± 0.023	7.559 ± 0.019	7.490 ± 0.015	7.332 ± 0.064	0.019 ± 0.031	0.007 ± 0.028	-0.004 ± 0.026	0.030 ± 0.067	...
12205449-6457242	LCC	7.904 ± 0.022	7.912 ± 0.020	7.838 ± 0.019	7.996 ± 0.143	0.083 ± 0.040	0.083 ± 0.039	0.102 ± 0.038	-0.137 ± 0.147	...
12205588-6534365	LCC	8.871 ± 0.023	8.817 ± 0.020	8.878 ± 0.027	...	0.082 ± 0.033	0.096 ± 0.030	-0.045 ± 0.035	...	...
12210499-7116493	LCC	8.164 ± 0.023	8.161 ± 0.021	8.079 ± 0.020	7.989 ± 0.143	-0.018 ± 0.035	-0.024 ± 0.033	-0.010 ± 0.033	-0.013 ± 0.145	...
12210808-5212226	LCC	8.606 ± 0.022	8.595 ± 0.020	8.504 ± 0.020	8.464 ± 0.186	-0.045 ± 0.030	-0.026 ± 0.029	0.010 ± 0.029	-0.031 ± 0.187	...
12213087-6403530	LCC	7.225 ± 0.027	7.192 ± 0.020	7.107 ± 0.021	6.844 ± 0.056	0.089 ± 0.035	0.133 ± 0.030	0.166 ± 0.031	0.350 ± 0.061	...
12215566-4946125	LCC	7.916 ± 0.023	7.951 ± 0.021	7.916 ± 0.017	7.786 ± 0.110	0.012 ± 0.039	0.027 ± 0.037	0.033 ± 0.035	0.094 ± 0.114	...
12220430-4841248	LCC	8.089 ± 0.021	8.107 ± 0.018	8.041 ± 0.015	7.717 ± 0.124	-0.019 ± 0.030	-0.015 ± 0.028	0.007 ± 0.026	0.257 ± 0.126	...
12234012-5616325	LCC	8.207 ± 0.023	8.224 ± 0.021	8.194 ± 0.020	8.319 ± 0.178	0.007 ± 0.033	0.012 ± 0.032	-0.002 ± 0.031	-0.201 ± 0.180	...

Table 4.8 (cont'd)

2MASS	Grp.	$W1$	$W2$	$W3$	$W4$	$E(K_S-W1)$	$E(K_S-W2)$	$E(K_S-W3)$	$E(K_S-W4)$	Disk Type
12234749-6402549	LCC	8.116 ± 0.024	8.131 ± 0.021	8.080 ± 0.022	8.064 ± 0.138	0.032 ± 0.047	0.032 ± 0.045	0.033 ± 0.046	-0.028 ± 0.144	...
12240975-6003416	LCC	8.712 ± 0.023	8.709 ± 0.021	8.567 ± 0.025	...	-0.059 ± 0.030	-0.057 ± 0.029	0.024 ± 0.032	...	...
12245648-4854270	LCC	8.578 ± 0.021	8.581 ± 0.017	8.471 ± 0.016	8.405 ± 0.191	0.027 ± 0.033	0.023 ± 0.031	0.072 ± 0.031	0.052 ± 0.193	...
12253370-7227480	LCC	8.144 ± 0.022	8.086 ± 0.020	7.957 ± 0.017	7.961 ± 0.152	-0.035 ± 0.030	-0.032 ± 0.028	0.018 ± 0.026	-0.124 ± 0.153	...
12263934-6113406	LCC	8.642 ± 0.022	8.676 ± 0.020	8.557 ± 0.028	7.786 ± 0.119	0.005 ± 0.030	-0.030 ± 0.029	0.028 ± 0.035	0.713 ± 0.121	...
12264842-5215070	LCC	8.203 ± 0.022	8.187 ± 0.020	8.087 ± 0.018	8.118 ± 0.149	-0.015 ± 0.040	0.000 ± 0.039	0.039 ± 0.038	-0.078 ± 0.153	...
12271665-6239142	LCC	8.033 ± 0.023	8.083 ± 0.021	8.140 ± 0.037	7.712 ± 0.139	-0.009 ± 0.035	-0.044 ± 0.034	-0.151 ± 0.046	0.200 ± 0.142	...
12282540-6320589	LCC	7.217 ± 0.027	7.250 ± 0.020	6.698 ± 0.020	5.324 ± 0.044	0.031 ± 0.041	0.046 ± 0.037	0.567 ± 0.037	1.872 ± 0.054	Evolved
12302957-5222269	LCC	8.724 ± 0.024	8.752 ± 0.021	8.645 ± 0.020	8.390 ± 0.188	0.001 ± 0.034	-0.012 ± 0.032	0.045 ± 0.031	0.223 ± 0.190	...
12333381-5714066	LCC	8.154 ± 0.022	8.200 ± 0.020	7.997 ± 0.020	7.326 ± 0.096	0.025 ± 0.038	0.009 ± 0.037	0.172 ± 0.037	0.771 ± 0.101	...
12361767-5042421	LCC	8.596 ± 0.023	8.631 ± 0.020	8.563 ± 0.021	8.401 ± 0.203	-0.007 ± 0.033	-0.034 ± 0.030	-0.021 ± 0.031	0.060 ± 0.204	...
12363895-6344436	LCC	7.293 ± 0.027	7.293 ± 0.020	7.147 ± 0.019	6.983 ± 0.103	-0.017 ± 0.036	0.013 ± 0.031	0.119 ± 0.031	0.211 ± 0.106	...
12365895-5412178	LCC	8.097 ± 0.022	8.124 ± 0.019	8.041 ± 0.016	8.054 ± 0.118	-0.010 ± 0.035	-0.015 ± 0.033	0.024 ± 0.031	-0.063 ± 0.121	...
12373737-5143113	LCC	8.348 ± 0.023	8.303 ± 0.020	8.162 ± 0.017	7.959 ± 0.112	0.021 ± 0.033	0.026 ± 0.031	0.087 ± 0.029	0.166 ± 0.115	...
12374883-5209463	LCC	8.811 ± 0.024	8.839 ± 0.021	8.724 ± 0.020	8.023 ± 0.116	-0.029 ± 0.033	-0.058 ± 0.031	-0.004 ± 0.030	0.611 ± 0.118	...
12383556-5916438	LCC	8.626 ± 0.021	8.643 ± 0.019	8.556 ± 0.023	7.836 ± 0.104	0.072 ± 0.028	0.070 ± 0.027	0.107 ± 0.030	0.750 ± 0.106	...
12391404-5454469	LCC	8.499 ± 0.022	8.502 ± 0.019	8.479 ± 0.023	8.221 ± 0.169	0.032 ± 0.025	0.028 ± 0.022	-0.010 ± 0.025	0.162 ± 0.169	...
12393796-5731406	LCC	8.032 ± 0.022	8.059 ± 0.020	8.001 ± 0.021	7.865 ± 0.130	0.019 ± 0.036	0.042 ± 0.035	0.071 ± 0.036	0.138 ± 0.133	...
12404664-5211046	LCC	9.047 ± 0.022	9.018 ± 0.020	8.980 ± 0.023	8.543 ± 0.193	0.140 ± 0.033	0.191 ± 0.031	0.185 ± 0.033	0.548 ± 0.194	...
12405458-5031550	LCC	8.605 ± 0.020	8.632 ± 0.018	8.566 ± 0.018	8.456 ± 0.211	0.025 ± 0.030	-0.003 ± 0.029	0.002 ± 0.029	0.026 ± 0.212	...
12411820-5825558	LCC	7.801 ± 0.024	7.821 ± 0.021	7.764 ± 0.017	7.367 ± 0.067	0.028 ± 0.033	0.037 ± 0.031	0.089 ± 0.029	0.414 ± 0.071	...

Table 4.8 (cont'd)

2MASS	Grp.	$W1$	$W2$	$W3$	$W4$	$E(K_S-W1)$	$E(K_S-W2)$	$E(K_S-W3)$	$E(K_S-W4)$	Disk Type
12420050-5759486	LCC	8.655 ± 0.023	8.523 ± 0.020	8.396 ± 0.023	7.897 ± 0.102	0.073 ± 0.037	0.150 ± 0.035	0.198 ± 0.037	0.559 ± 0.106	...
12443482-6331463	LCC	7.700 ± 0.022	7.662 ± 0.019	7.621 ± 0.022	7.502 ± 0.120	0.087 ± 0.030	0.147 ± 0.028	0.144 ± 0.030	0.189 ± 0.122	...
12444949-4918474	LCC	9.031 ± 0.023	9.043 ± 0.020	8.927 ± 0.023	8.434 ± 0.185	-0.008 ± 0.033	-0.038 ± 0.030	0.005 ± 0.033	0.396 ± 0.186	...
12450674-4742580	LCC	8.016 ± 0.023	8.045 ± 0.020	7.972 ± 0.017	7.479 ± 0.093	0.033 ± 0.041	0.052 ± 0.039	0.094 ± 0.038	0.518 ± 0.099	...
12454884-5410583	LCC	8.625 ± 0.022	8.644 ± 0.019	8.634 ± 0.023	8.668 ± 0.259	0.017 ± 0.029	0.020 ± 0.027	-0.014 ± 0.030	-0.122 ± 0.260	...
12472196-6808397	LCC	7.996 ± 0.023	8.000 ± 0.020	7.892 ± 0.020	7.723 ± 0.122	-0.056 ± 0.046	-0.052 ± 0.045	0.001 ± 0.045	0.089 ± 0.128	...
12472609-5445156	LCC	8.889 ± 0.023	8.880 ± 0.019	8.827 ± 0.022	...	0.017 ± 0.031	0.025 ± 0.028	0.017 ± 0.030	...	...
12474824-5431308	LCC	7.845 ± 0.023	7.768 ± 0.020	7.689 ± 0.016	7.562 ± 0.091	0.047 ± 0.024	0.069 ± 0.021	0.069 ± 0.017	0.058 ± 0.091	...
12475186-5126382	LCC	7.193 ± 0.029	7.203 ± 0.020	7.148 ± 0.015	7.040 ± 0.060	0.004 ± 0.040	0.029 ± 0.034	0.073 ± 0.031	0.110 ± 0.066	...
12480778-4439167	LCC	7.438 ± 0.028	7.436 ± 0.020	7.369 ± 0.016	7.166 ± 0.089	-0.010 ± 0.037	0.040 ± 0.031	0.076 ± 0.029	0.210 ± 0.092	...
12483152-5944493	LCC	7.371 ± 0.027	7.349 ± 0.020	7.278 ± 0.019	7.062 ± 0.127	0.015 ± 0.040	0.019 ± 0.035	0.017 ± 0.035	0.131 ± 0.130	...
12484818-5635378	LCC	8.244 ± 0.023	8.268 ± 0.020	8.236 ± 0.020	8.325 ± 0.173	0.053 ± 0.033	0.071 ± 0.030	0.086 ± 0.030	-0.074 ± 0.175	...
12504491-5654485	LCC	8.016 ± 0.022	7.919 ± 0.019	7.791 ± 0.016	7.747 ± 0.100	0.081 ± 0.032	0.104 ± 0.030	0.154 ± 0.028	0.049 ± 0.103	...
12505143-5156353	LCC	8.370 ± 0.021	8.333 ± 0.019	8.261 ± 0.018	7.936 ± 0.123	0.070 ± 0.022	0.106 ± 0.021	0.117 ± 0.020	0.356 ± 0.123	...
12510556-5253121	LCC	8.696 ± 0.022	8.694 ± 0.018	8.655 ± 0.023	9.118 ± 0.388	0.014 ± 0.029	0.015 ± 0.026	-0.007 ± 0.030	-0.556 ± 0.388	...
12543050-5031482	LCC	9.211 ± 0.023	9.219 ± 0.020	9.039 ± 0.023	8.754 ± 0.248	-0.041 ± 0.031	-0.067 ± 0.029	0.040 ± 0.031	0.223 ± 0.249	...
12560830-6926539	LCC	7.861 ± 0.022	7.776 ± 0.020	7.591 ± 0.018	7.018 ± 0.077	0.031 ± 0.038	0.098 ± 0.037	0.210 ± 0.036	0.681 ± 0.083	...
12582559-7028490	LCC	7.433 ± 0.027	7.471 ± 0.021	7.415 ± 0.018	7.444 ± 0.126	0.019 ± 0.038	0.003 ± 0.034	0.015 ± 0.032	-0.088 ± 0.129	...
13010856-5901533	LCC	8.826 ± 0.023	8.746 ± 0.019	8.658 ± 0.022	...	0.018 ± 0.030	0.043 ± 0.027	0.052 ± 0.029	...	...
13015069-5304581	LCC	8.662 ± 0.023	8.709 ± 0.020	8.601 ± 0.021	8.526 ± 0.221	0.032 ± 0.031	0.000 ± 0.029	0.058 ± 0.030	0.056 ± 0.222	...
13015435-4249422	LCC	9.002 ± 0.024	8.968 ± 0.021	8.967 ± 0.026	9.138 ± 0.404	0.000 ± 0.032	0.049 ± 0.030	0.000 ± 0.033	-0.248 ± 0.405	...

Table 4.8 (cont'd)

2MASS	Grp.	$W1$	$W2$	$W3$	$W4$	$E(K_S - W1)$	$E(K_S - W2)$	$E(K_S - W3)$	$E(K_S - W4)$	Disk Type
13024703-6213589	LCC	7.609 ± 0.022	7.616 ± 0.018	7.722 ± 0.070	7.123 ± 0.179	0.145 ± 0.027	0.175 ± 0.024	0.031 ± 0.072	0.559 ± 0.180	...
13032904-4723160	LCC	8.308 ± 0.022	8.309 ± 0.018	8.255 ± 0.016	8.578 ± 0.251	-0.023 ± 0.038	-0.025 ± 0.036	-0.032 ± 0.035	-0.441 ± 0.253	...
13055087-5304181	LCC	9.150 ± 0.023	9.144 ± 0.020	9.041 ± 0.022	8.907 ± 0.265	0.025 ± 0.035	0.022 ± 0.033	0.057 ± 0.034	0.098 ± 0.266	...
13064012-5159386	LCC	8.271 ± 0.022	8.290 ± 0.020	8.096 ± 0.017	7.969 ± 0.155	-0.090 ± 0.034	-0.079 ± 0.033	0.075 ± 0.031	0.130 ± 0.157	...
13065439-4541313	LCC	8.445 ± 0.022	8.444 ± 0.020	8.314 ± 0.018	8.402 ± 0.174	-0.033 ± 0.032	-0.033 ± 0.030	0.036 ± 0.029	-0.138 ± 0.176	...
13071310-5952108	LCC	7.510 ± 0.023	7.519 ± 0.018	7.505 ± 0.015	7.409 ± 0.087	0.055 ± 0.028	0.061 ± 0.024	0.025 ± 0.022	0.044 ± 0.088	...
13095880-4527388	LCC	8.421 ± 0.023	8.437 ± 0.020	8.369 ± 0.019	7.952 ± 0.131	0.023 ± 0.033	0.026 ± 0.030	0.047 ± 0.030	0.388 ± 0.133	...
13103245-4817036	LCC	8.504 ± 0.022	8.534 ± 0.019	8.449 ± 0.019	8.187 ± 0.162	-0.002 ± 0.029	-0.024 ± 0.027	0.006 ± 0.027	0.187 ± 0.163	...
13112902-4252418	LCC	9.150 ± 0.022	9.079 ± 0.020	9.020 ± 0.027	9.184 ± 0.402	-0.018 ± 0.035	-0.002 ± 0.034	-0.022 ± 0.038	-0.324 ± 0.403	...
13121764-5508258	LCC	8.379 ± 0.020	8.448 ± 0.019	8.311 ± 0.017	7.983 ± 0.119	0.182 ± 0.029	0.112 ± 0.028	0.188 ± 0.027	0.430 ± 0.121	...
13121859-5439054	LCC	9.074 ± 0.022	9.095 ± 0.020	8.835 ± 0.022	8.514 ± 0.209	0.030 ± 0.032	0.057 ± 0.030	0.286 ± 0.032	0.538 ± 0.210	...
13130714-4537438	LCC	8.232 ± 0.023	8.213 ± 0.020	8.133 ± 0.018	8.408 ± 0.196	0.002 ± 0.046	0.020 ± 0.045	0.039 ± 0.044	-0.322 ± 0.200	...
13132326-5442156	LCC	9.316 ± 0.022	9.308 ± 0.019	9.128 ± 0.023	8.458 ± 0.181	-0.051 ± 0.033	-0.028 ± 0.031	0.102 ± 0.033	0.695 ± 0.183	...
13142382-5054018	LCC	7.988 ± 0.022	7.981 ± 0.018	7.960 ± 0.014	7.837 ± 0.120	0.033 ± 0.046	0.090 ± 0.044	0.082 ± 0.042	0.136 ± 0.126	...
13174687-4456534	LCC	8.705 ± 0.023	8.706 ± 0.020	8.595 ± 0.021	9.220 ± 0.472	0.034 ± 0.033	0.032 ± 0.030	0.082 ± 0.031	-0.629 ± 0.473	...
13175314-5058481	LCC	9.041 ± 0.022	9.040 ± 0.020	8.990 ± 0.027	9.255 ± 0.447	0.016 ± 0.030	0.016 ± 0.029	0.005 ± 0.034	-0.346 ± 0.447	...
13191370-4506326	LCC	9.026 ± 0.023	9.038 ± 0.021	9.002 ± 0.025	9.224 ± 0.366	-0.049 ± 0.031	-0.062 ± 0.030	-0.087 ± 0.033	-0.395 ± 0.367	...
13203307-4927514	LCC	9.230 ± 0.024	9.265 ± 0.020	9.205 ± 0.024	8.682 ± 0.213	0.044 ± 0.033	0.017 ± 0.030	0.022 ± 0.033	0.464 ± 0.214	...
13204539-4611377	LCC	8.909 ± 0.023	8.874 ± 0.019	8.724 ± 0.020	8.703 ± 0.235	0.010 ± 0.030	0.044 ± 0.027	0.133 ± 0.028	0.068 ± 0.236	...
13220753-6938121	LCC	6.577 ± 0.039	6.183 ± 0.022	4.063 ± 0.015	1.587 ± 0.016	0.623 ± 0.043	1.043 ± 0.028	3.121 ± 0.023	5.524 ± 0.024	Full
13233587-4718467	LCC	8.165 ± 0.023	8.134 ± 0.020	7.942 ± 0.017	7.103 ± 0.066	0.054 ± 0.037	0.100 ± 0.035	0.242 ± 0.034	1.004 ± 0.072	Debris

Table 4.8 (cont'd)

2MASS	Grp.	$W1$	$W2$	$W3$	$W4$	$E(K_S-W1)$	$E(K_S-W2)$	$E(K_S-W3)$	$E(K_S-W4)$	Disk Type
13251211-6456207	LCC	8.366 ± 0.024	8.375 ± 0.020	8.319 ± 0.028	...	-0.067 ± 0.036	-0.061 ± 0.034	-0.055 ± 0.039	...	...
13270594-4856180	LCC	7.714 ± 0.026	7.682 ± 0.021	7.605 ± 0.017	7.488 ± 0.125	0.001 ± 0.037	0.048 ± 0.033	0.075 ± 0.031	0.115 ± 0.128	...
13291766-4614230	LCC	9.194 ± 0.022	9.213 ± 0.020	9.145 ± 0.026	8.846 ± 0.286	-0.062 ± 0.033	-0.082 ± 0.032	-0.075 ± 0.036	0.138 ± 0.287	...
13294575-4844366	LCC	9.086 ± 0.021	9.048 ± 0.018	8.992 ± 0.022	8.985 ± 0.311	0.075 ± 0.033	0.073 ± 0.031	0.049 ± 0.033	-0.068 ± 0.312	...
13315360-5113330	LCC	7.744 ± 0.024	7.771 ± 0.019	7.740 ± 0.019	7.796 ± 0.120	0.026 ± 0.033	0.028 ± 0.030	0.054 ± 0.030	-0.074 ± 0.122	...
13334410-6359345	LCC	8.502 ± 0.024	8.550 ± 0.022	8.479 ± 0.028	8.643 ± 0.381	-0.005 ± 0.031	-0.042 ± 0.029	-0.023 ± 0.034	-0.266 ± 0.381	...
13335329-6536473	LCC	8.331 ± 0.023	8.273 ± 0.020	8.008 ± 0.022	7.560 ± 0.197	0.036 ± 0.031	0.054 ± 0.029	0.239 ± 0.030	0.563 ± 0.198	...
13335481-6536414	LCC	7.462 ± 0.027	7.082 ± 0.020	5.095 ± 0.014	3.179 ± 0.023	0.253 ± 0.043	0.632 ± 0.039	2.558 ± 0.036	4.388 ± 0.040	Full
13342461-6517473	LCC	8.921 ± 0.024	8.750 ± 0.020	7.332 ± 0.020	3.582 ± 0.023	0.250 ± 0.033	0.381 ± 0.030	1.719 ± 0.030	5.345 ± 0.033	Full
13343188-4209305	LCC	7.941 ± 0.023	7.959 ± 0.018	7.909 ± 0.016	7.931 ± 0.122	0.059 ± 0.029	0.063 ± 0.025	0.069 ± 0.024	-0.027 ± 0.123	...
13354082-4818124	LCC	8.403 ± 0.023	8.433 ± 0.019	8.351 ± 0.019	8.133 ± 0.148	0.009 ± 0.031	-0.010 ± 0.028	0.020 ± 0.028	0.159 ± 0.149	...
13364090-4043359	UCL	8.918 ± 0.029	8.908 ± 0.029	8.817 ± 0.030	...	-0.058 ± 0.032	-0.057 ± 0.032	-0.034 ± 0.033	...	...
13375730-4134419	UCL	7.793 ± 0.023	7.840 ± 0.020	7.774 ± 0.017	7.216 ± 0.073	-0.006 ± 0.035	-0.023 ± 0.033	0.003 ± 0.031	0.489 ± 0.077	...
13380596-4344564	LCC	8.466 ± 0.023	8.498 ± 0.020	8.427 ± 0.019	8.186 ± 0.152	-0.024 ± 0.030	-0.041 ± 0.028	-0.020 ± 0.028	0.144 ± 0.153	...
13381128-5214251	LCC	8.626 ± 0.022	8.665 ± 0.020	8.555 ± 0.018	7.960 ± 0.110	-0.022 ± 0.029	-0.024 ± 0.028	0.048 ± 0.026	0.572 ± 0.112	...
13384937-4237234	UCL	8.808 ± 0.023	8.843 ± 0.020	8.765 ± 0.022	9.029 ± 0.361	-0.007 ± 0.030	-0.031 ± 0.028	-0.005 ± 0.030	-0.348 ± 0.362	...
13402554-4633514	LCC	8.308 ± 0.023	8.251 ± 0.020	8.154 ± 0.017	8.321 ± 0.169	0.042 ± 0.032	0.114 ± 0.030	0.161 ± 0.028	-0.083 ± 0.170	...
13405585-4244505	UCL	9.015 ± 0.022	8.947 ± 0.020	8.852 ± 0.021	8.645 ± 0.239	0.007 ± 0.032	0.047 ± 0.030	0.064 ± 0.031	0.159 ± 0.240	...
13442441-4706343	UCL	7.937 ± 0.023	7.961 ± 0.019	7.864 ± 0.015	7.690 ± 0.113	-0.001 ± 0.041	-0.003 ± 0.039	0.050 ± 0.037	0.150 ± 0.118	...
13444279-6347495	LCC	7.635 ± 0.026	7.614 ± 0.020	7.491 ± 0.032	6.853 ± 0.096	0.010 ± 0.039	0.039 ± 0.035	0.107 ± 0.043	0.664 ± 0.100	...
13454424-4904500	UCL	8.037 ± 0.023	8.070 ± 0.021	7.971 ± 0.017	7.663 ± 0.090	-0.007 ± 0.035	-0.021 ± 0.033	0.031 ± 0.031	0.263 ± 0.094	...

Table 4.8 (cont'd)

2MASS	Grp.	$W1$	$W2$	$W3$	$W4$	$E(K_S - W1)$	$E(K_S - W2)$	$E(K_S - W3)$	$E(K_S - W4)$	Disk Type
13455599-5222255	LCC	8.443 ± 0.023	8.485 ± 0.020	8.399 ± 0.020	8.406 ± 0.187	0.056 ± 0.033	0.029 ± 0.030	0.065 ± 0.030	-0.019 ± 0.188	...
13475054-4902056	UCL	8.501 ± 0.023	8.491 ± 0.019	8.391 ± 0.018	8.048 ± 0.130	0.111 ± 0.031	0.171 ± 0.028	0.242 ± 0.028	0.516 ± 0.132	...
13503387-4810150	UCL	9.340 ± 0.022	9.343 ± 0.020	9.152 ± 0.023	8.489 ± 0.183	-0.013 ± 0.030	-0.044 ± 0.029	0.069 ± 0.031	0.620 ± 0.184	...
13515351-4846505	UCL	9.016 ± 0.022	9.001 ± 0.019	8.945 ± 0.025	8.727 ± 0.286	0.053 ± 0.030	0.067 ± 0.028	0.062 ± 0.033	0.194 ± 0.287	...
13540743-6733449	LCC	8.772 ± 0.023	8.773 ± 0.020	8.768 ± 0.021	8.530 ± 0.288	0.046 ± 0.033	0.095 ± 0.030	0.071 ± 0.031	0.240 ± 0.289	...
13544209-4820578	UCL	8.624 ± 0.023	8.656 ± 0.020	8.606 ± 0.021	8.693 ± 0.257	-0.017 ± 0.031	-0.027 ± 0.029	-0.021 ± 0.030	-0.182 ± 0.258	...
13552552-4706563	UCL	8.003 ± 0.024	7.996 ± 0.019	7.925 ± 0.017	7.569 ± 0.091	-0.002 ± 0.033	0.013 ± 0.030	0.029 ± 0.029	0.304 ± 0.094	...
13562964-3839129	UCL	8.391 ± 0.022	8.412 ± 0.020	8.362 ± 0.018	8.308 ± 0.187	0.067 ± 0.033	0.061 ± 0.032	0.061 ± 0.031	0.038 ± 0.189	...
13563469-4907146	UCL	8.642 ± 0.022	8.630 ± 0.020	8.573 ± 0.021	8.894 ± 0.287	0.079 ± 0.034	0.106 ± 0.033	0.113 ± 0.033	-0.285 ± 0.288	...
13575106-4431482	UCL	8.681 ± 0.023	8.636 ± 0.019	8.532 ± 0.020	8.434 ± 0.174	0.023 ± 0.030	0.079 ± 0.027	0.131 ± 0.028	0.150 ± 0.175	...
14001181-4230334	UCL	9.491 ± 0.023	9.485 ± 0.020	9.384 ± 0.027	...	-0.042 ± 0.033	-0.064 ± 0.030	-0.041 ± 0.035	...	...
14003189-6416245	LCC	9.974 ± 0.024	10.003 ± 0.021	10.732 ± 0.157	...	0.095 ± 0.032	0.088 ± 0.030	-0.685 ± 0.158	...	...
14004970-4236569	UCL	8.591 ± 0.023	8.614 ± 0.020	8.539 ± 0.020	8.610 ± 0.256	0.037 ± 0.030	0.051 ± 0.028	0.088 ± 0.028	-0.054 ± 0.257	...
14022072-4144509	UCL	8.363 ± 0.023	8.402 ± 0.020	8.343 ± 0.019	8.352 ± 0.195	-0.053 ± 0.039	-0.049 ± 0.037	-0.026 ± 0.036	-0.104 ± 0.197	...
14060042-4112249	UCL	8.772 ± 0.022	8.800 ± 0.019	8.743 ± 0.020	8.489 ± 0.200	-0.039 ± 0.029	-0.052 ± 0.027	-0.045 ± 0.028	0.132 ± 0.201	...
14074792-3945427	UCL	9.237 ± 0.022	9.262 ± 0.020	9.178 ± 0.026	8.765 ± 0.276	-0.074 ± 0.030	-0.100 ± 0.028	-0.077 ± 0.033	0.250 ± 0.277	...
14081015-4123525	UCL	8.026 ± 0.023	7.714 ± 0.020	5.716 ± 0.016	3.357 ± 0.019	0.419 ± 0.033	0.713 ± 0.030	2.638 ± 0.028	4.895 ± 0.030	Full
14085608-4403488	UCL	8.430 ± 0.022	8.409 ± 0.019	8.306 ± 0.018	8.547 ± 0.241	-0.001 ± 0.029	0.035 ± 0.027	0.088 ± 0.026	-0.230 ± 0.242	...
14122451-4327149	UCL	8.696 ± 0.023	8.727 ± 0.020	8.666 ± 0.021	9.084 ± 0.325	-0.064 ± 0.031	-0.076 ± 0.029	-0.062 ± 0.030	-0.556 ± 0.326	...
14124691-3831220	UCL	8.563 ± 0.023	8.571 ± 0.020	8.479 ± 0.020	8.466 ± 0.211	0.022 ± 0.033	0.029 ± 0.030	0.071 ± 0.030	0.007 ± 0.212	...
14185327-4827313	UCL	8.605 ± 0.022	8.616 ± 0.019	8.531 ± 0.022	...	-0.021 ± 0.030	-0.017 ± 0.028	0.018 ± 0.030	...	...

Table 4.8 (cont'd)

2MASS	Grp.	$W1$	$W2$	$W3$	$W4$	$E(K_S-W1)$	$E(K_S-W2)$	$E(K_S-W3)$	$E(K_S-W4)$	Disk Type
14201202-5339537	UCL	9.294 ± 0.022	9.301 ± 0.019	9.139 ± 0.027	8.769 ± 0.334	-0.059 ± 0.032	-0.047 ± 0.030	0.068 ± 0.035	0.362 ± 0.335	...
14204893-4748442	UCL	8.068 ± 0.023	8.078 ± 0.018	7.958 ± 0.018	7.571 ± 0.116	-0.002 ± 0.037	-0.013 ± 0.034	0.046 ± 0.034	0.347 ± 0.120	...
14213051-3845252	UCL	8.713 ± 0.023	8.713 ± 0.019	8.616 ± 0.021	8.472 ± 0.208	0.062 ± 0.035	0.053 ± 0.032	0.082 ± 0.033	0.133 ± 0.210	...
14214378-4652082	UCL	8.594 ± 0.023	8.620 ± 0.021	8.557 ± 0.023	8.235 ± 0.204	-0.076 ± 0.030	-0.080 ± 0.028	-0.061 ± 0.030	0.187 ± 0.205	...
14220732-5417055	UCL	8.456 ± 0.023	8.464 ± 0.020	8.302 ± 0.020	8.496 ± 0.270	0.010 ± 0.033	0.017 ± 0.031	0.129 ± 0.031	-0.142 ± 0.271	...
14223029-3532190	UCL	8.314 ± 0.023	8.299 ± 0.020	8.223 ± 0.019	8.051 ± 0.146	-0.006 ± 0.033	0.024 ± 0.030	0.050 ± 0.030	0.145 ± 0.148	...
14224364-4628054	UCL	8.984 ± 0.024	9.003 ± 0.022	8.937 ± 0.027	8.940 ± 0.441	0.018 ± 0.033	0.018 ± 0.032	0.037 ± 0.035	-0.042 ± 0.442	...
14234748-5935261	UCL	7.802 ± 0.024	7.822 ± 0.021	7.743 ± 0.023	7.337 ± 0.113	0.045 ± 0.031	0.047 ± 0.029	0.082 ± 0.030	0.414 ± 0.115	...
14244779-5041333	UCL	9.574 ± 0.022	9.624 ± 0.020	9.414 ± 0.031	8.216 ± 0.189	0.026 ± 0.032	0.006 ± 0.030	0.176 ± 0.039	1.302 ± 0.190	Debris
14262134-3644057	UCL	8.434 ± 0.023	8.469 ± 0.019	8.402 ± 0.019	8.023 ± 0.164	-0.015 ± 0.031	-0.013 ± 0.028	0.016 ± 0.028	0.324 ± 0.165	...
14270556-4714217	UCL	8.464 ± 0.023	8.497 ± 0.021	8.410 ± 0.021	7.884 ± 0.177	-0.004 ± 0.033	0.013 ± 0.032	0.071 ± 0.032	0.528 ± 0.179	...
14275425-5944350	UCL	8.951 ± 0.024	8.953 ± 0.022	8.886 ± 0.053	8.039 ± 0.203	-0.015 ± 0.032	-0.018 ± 0.030	-0.012 ± 0.057	0.749 ± 0.204	...
14280929-4414175	UCL	7.798 ± 0.024	7.835 ± 0.020	7.753 ± 0.018	7.728 ± 0.142	-0.082 ± 0.042	-0.070 ± 0.039	-0.014 ± 0.038	-0.059 ± 0.146	...
14281937-4219341	UCL	8.315 ± 0.023	8.340 ± 0.020	8.292 ± 0.020	8.519 ± 0.273	0.009 ± 0.041	0.019 ± 0.039	0.056 ± 0.039	-0.242 ± 0.275	...
14321121-5826058	UCL	8.098 ± 0.020	8.179 ± 0.018	8.086 ± 0.025	7.439 ± 0.125	0.221 ± 0.030	0.139 ± 0.029	0.171 ± 0.034	0.732 ± 0.127	...
14345213-4004459	UCL	8.861 ± 0.024	8.838 ± 0.021	8.769 ± 0.023	9.054 ± 0.434	0.005 ± 0.031	0.039 ± 0.028	0.056 ± 0.030	-0.308 ± 0.434	...
14374904-4928268	UCL	8.484 ± 0.022	8.489 ± 0.019	8.459 ± 0.027	...	0.019 ± 0.030	-0.014 ± 0.028	-0.062 ± 0.034	...	...
14375022-5457411	UCL	8.234 ± 0.023	8.256 ± 0.020	7.875 ± 0.018	6.696 ± 0.056	-0.026 ± 0.035	-0.005 ± 0.033	0.340 ± 0.032	1.450 ± 0.062	Debris
14380350-4932023	UCL	8.476 ± 0.023	8.474 ± 0.020	8.411 ± 0.024	8.562 ± 0.319	0.036 ± 0.035	0.046 ± 0.033	0.054 ± 0.035	-0.178 ± 0.320	...
14380862-4322008	UCL	8.790 ± 0.023	8.738 ± 0.021	8.642 ± 0.023	...	0.001 ± 0.033	0.035 ± 0.032	0.058 ± 0.033	...	...
14385440-4310223	UCL	8.062 ± 0.023	8.049 ± 0.021	7.946 ± 0.017	7.863 ± 0.150	-0.047 ± 0.033	-0.019 ± 0.031	0.034 ± 0.029	0.040 ± 0.152	...

Table 4.8 (cont'd)

2MASS	Grp.	$W1$	$W2$	$W3$	$W4$	$E(K_S-W1)$	$E(K_S-W2)$	$E(K_S-W3)$	$E(K_S-W4)$	Disk Type
14392060-3905282	UCL	8.399 ± 0.023	8.419 ± 0.020	8.330 ± 0.021	8.198 ± 0.230	0.017 ± 0.033	0.027 ± 0.030	0.076 ± 0.031	0.136 ± 0.231	...
14411942-5001199	UCL	8.400 ± 0.023	8.366 ± 0.021	8.247 ± 0.019	7.711 ± 0.133	0.006 ± 0.030	0.048 ± 0.029	0.112 ± 0.028	0.567 ± 0.134	...
14413499-4700288	UCL	7.814 ± 0.026	7.833 ± 0.022	7.792 ± 0.022	7.982 ± 0.228	0.009 ± 0.033	0.039 ± 0.030	0.054 ± 0.030	-0.206 ± 0.229	...
14421590-4100183	UCL	8.086 ± 0.023	8.107 ± 0.020	8.136 ± 0.018	7.864 ± 0.149	0.419 ± 0.027	0.413 ± 0.024	0.334 ± 0.023	0.529 ± 0.150	...
14432493-5643393	UCL	8.465 ± 0.024	8.488 ± 0.021	8.511 ± 0.032	...	0.022 ± 0.031	0.034 ± 0.029	0.000 ± 0.038	...	...
14442536-4329552	UCL	9.985 ± 0.025	9.935 ± 0.020	9.788 ± 0.041	...	0.019 ± 0.034	0.041 ± 0.030	0.110 ± 0.047	...	...
14472343-3503134	UCL	8.844 ± 0.025	8.894 ± 0.020	8.802 ± 0.025	8.247 ± 0.256	-0.008 ± 0.034	-0.043 ± 0.030	-0.001 ± 0.034	0.477 ± 0.257	...
14481320-4102590	UCL	8.527 ± 0.023	8.557 ± 0.021	8.480 ± 0.022	8.585 ± 0.315	0.000 ± 0.031	-0.008 ± 0.030	0.025 ± 0.030	-0.154 ± 0.316	...
14502581-3506486	UCL	8.016 ± 0.022	8.016 ± 0.020	7.971 ± 0.019	8.496 ± 0.306	0.000 ± 0.032	0.030 ± 0.030	0.035 ± 0.030	-0.562 ± 0.307	...
14503508-3459056	UCL	8.797 ± 0.024	8.775 ± 0.021	8.680 ± 0.025	8.209 ± 0.215	-0.010 ± 0.033	0.020 ± 0.031	0.060 ± 0.034	0.450 ± 0.216	...
14522619-3740088	UCL	9.059 ± 0.022	9.092 ± 0.018	9.039 ± 0.027	8.841 ± 0.409	0.075 ± 0.032	0.057 ± 0.029	0.060 ± 0.035	0.181 ± 0.410	...
14524198-4141552	UCL	8.246 ± 0.023	8.257 ± 0.021	8.159 ± 0.020	8.014 ± 0.189	-0.050 ± 0.039	-0.046 ± 0.037	0.002 ± 0.037	0.070 ± 0.192	...
14541121-3955233	UCL	8.872 ± 0.023	8.892 ± 0.023	8.807 ± 0.025	...	0.034 ± 0.031	0.036 ± 0.031	0.077 ± 0.033	...	...
14552673-5129013	UCL	8.558 ± 0.022	8.555 ± 0.019	8.509 ± 0.021	8.598 ± 0.303	0.020 ± 0.029	0.071 ± 0.027	0.086 ± 0.028	-0.072 ± 0.304	...
14574495-4141394	UCL	9.226 ± 0.023	9.234 ± 0.022	9.097 ± 0.029	8.945 ± 0.446	0.028 ± 0.031	0.002 ± 0.030	0.066 ± 0.036	0.116 ± 0.446	...
14583744-3915033	UCL	8.493 ± 0.024	8.387 ± 0.020	8.287 ± 0.022	8.829 ± 0.474	0.043 ± 0.035	0.094 ± 0.033	0.115 ± 0.034	-0.565 ± 0.475	...
14583769-3540302	UCL	7.822 ± 0.024	7.837 ± 0.021	7.765 ± 0.019	7.721 ± 0.169	-0.045 ± 0.035	-0.041 ± 0.033	-0.016 ± 0.032	-0.048 ± 0.171	...
14584573-3315102	UCL	8.944 ± 0.023	8.943 ± 0.020	8.948 ± 0.027	8.810 ± 0.422	0.063 ± 0.030	0.094 ± 0.028	0.049 ± 0.033	0.115 ± 0.422	...
14592275-4013120	UCL	7.812 ± 0.024	7.837 ± 0.021	7.784 ± 0.018	7.581 ± 0.142	-0.083 ± 0.036	-0.060 ± 0.034	-0.038 ± 0.032	0.096 ± 0.145	...
14594473-3425465	UCL	8.048 ± 0.023	8.068 ± 0.021	7.999 ± 0.020	7.955 ± 0.207	0.013 ± 0.033	0.008 ± 0.032	0.027 ± 0.031	-0.006 ± 0.208	...
15003768-4308339	UCL	8.882 ± 0.022	8.877 ± 0.019	8.793 ± 0.025	...	-0.025 ± 0.032	-0.005 ± 0.030	0.029 ± 0.034	...	...

Table 4.8 (cont'd)

2MASS	Grp.	$W1$	$W2$	$W3$	$W4$	$E(K_S-W1)$	$E(K_S-W2)$	$E(K_S-W3)$	$E(K_S-W4)$	Disk Type
15005189-4331212	UCL	8.702 ± 0.022	8.689 ± 0.020	8.576 ± 0.021	8.184 ± 0.199	-0.061 ± 0.032	-0.018 ± 0.030	0.055 ± 0.031	0.375 ± 0.200	...
15022600-3405131	UCL	9.062 ± 0.023	9.064 ± 0.021	8.958 ± 0.028	8.717 ± 0.415	0.121 ± 0.034	0.127 ± 0.033	0.178 ± 0.038	0.338 ± 0.416	...
15035213-3906283	UCL	8.412 ± 0.024	8.431 ± 0.020	8.345 ± 0.021	8.463 ± 0.287	0.053 ± 0.032	0.025 ± 0.029	0.043 ± 0.030	-0.168 ± 0.288	...
15052586-3857031	UCL	9.039 ± 0.023	9.021 ± 0.020	8.935 ± 0.026	8.592 ± 0.323	-0.010 ± 0.031	-0.001 ± 0.029	0.017 ± 0.033	0.267 ± 0.324	...
15054424-3312508	UCL	9.090 ± 0.023	9.099 ± 0.020	8.915 ± 0.026	8.133 ± 0.215	0.050 ± 0.031	0.049 ± 0.029	0.178 ± 0.033	0.879 ± 0.216	Debris
15055685-4312031	UCL	9.022 ± 0.024	9.024 ± 0.020	8.913 ± 0.027	...	-0.080 ± 0.033	-0.100 ± 0.030	-0.062 ± 0.035	...	...
15064258-3047326	UCL	9.332 ± 0.024	9.319 ± 0.022	9.191 ± 0.032	...	-0.061 ± 0.033	-0.066 ± 0.032	-0.011 ± 0.039	...	...
15071481-3504595	UCL	8.274 ± 0.023	8.299 ± 0.021	8.206 ± 0.020	7.841 ± 0.166	-0.031 ± 0.033	-0.026 ± 0.031	0.027 ± 0.030	0.320 ± 0.168	...
15072758-4601073	UCL	9.018 ± 0.023	9.031 ± 0.021	8.932 ± 0.025	8.555 ± 0.296	0.020 ± 0.031	0.037 ± 0.030	0.096 ± 0.033	0.401 ± 0.297	...
15075415-4730288	UCL	8.719 ± 0.021	8.690 ± 0.019	8.678 ± 0.027	8.804 ± 0.432	-0.003 ± 0.030	0.056 ± 0.028	0.028 ± 0.034	-0.170 ± 0.433	...
15080509-3337556	UCL	8.514 ± 0.023	8.506 ± 0.019	8.436 ± 0.022	8.051 ± 0.198	0.011 ± 0.033	0.010 ± 0.030	0.012 ± 0.032	0.304 ± 0.199	...
15083773-4423170	UCL	8.696 ± 0.023	8.737 ± 0.019	8.653 ± 0.023	8.472 ± 0.283	0.031 ± 0.031	0.040 ± 0.028	0.095 ± 0.031	0.207 ± 0.284	...
15083849-4400519	UCL	8.373 ± 0.023	8.388 ± 0.022	8.345 ± 0.021	8.667 ± 0.357	0.016 ± 0.030	0.022 ± 0.030	0.068 ± 0.029	-0.327 ± 0.358	...
15085379-3715467	UCL	8.866 ± 0.023	8.873 ± 0.020	8.751 ± 0.025	8.756 ± 0.361	0.042 ± 0.030	0.034 ± 0.028	0.095 ± 0.031	0.004 ± 0.361	...
15085472-4303136	UCL	8.810 ± 0.024	8.845 ± 0.021	8.779 ± 0.025	8.832 ± 0.387	0.013 ± 0.032	-0.007 ± 0.030	0.009 ± 0.033	-0.121 ± 0.388	...
15102954-3902566	UCL	9.150 ± 0.024	9.162 ± 0.022	9.049 ± 0.028	8.580 ± 0.296	0.031 ± 0.032	0.034 ± 0.030	0.097 ± 0.035	0.489 ± 0.297	...
15110450-3251304	UCL	8.248 ± 0.022	8.253 ± 0.021	8.267 ± 0.021	8.465 ± 0.321	0.327 ± 0.041	0.313 ± 0.041	0.231 ± 0.041	-0.060 ± 0.323	...
15113968-3248560	UCL	9.260 ± 0.024	9.175 ± 0.021	9.189 ± 0.033	...	-0.013 ± 0.032	-0.012 ± 0.030	-0.104 ± 0.039	...	...
15124447-3116482	UCL	8.863 ± 0.023	8.871 ± 0.021	8.773 ± 0.028	...	-0.037 ± 0.030	-0.023 ± 0.028	0.031 ± 0.034	...	...
15135817-4629145	UCL	9.248 ± 0.024	9.291 ± 0.021	9.097 ± 0.029	...	0.014 ± 0.031	-0.047 ± 0.028	0.074 ± 0.035	...	...
15140754-4103361	UCL	8.519 ± 0.022	8.512 ± 0.019	8.477 ± 0.022	8.556 ± 0.335	-0.034 ± 0.032	0.021 ± 0.030	0.025 ± 0.032	-0.123 ± 0.336	...

Table 4.8 (cont'd)

2MASS	Grp.	$W1$	$W2$	$W3$	$W4$	$E(K_S - W1)$	$E(K_S - W2)$	$E(K_S - W3)$	$E(K_S - W4)$	Disk Type
15144748-4220149	UCL	8.965 ± 0.024	9.010 ± 0.022	8.948 ± 0.026	8.899 ± 0.384	-0.047 ± 0.032	-0.062 ± 0.030	-0.040 ± 0.033	-0.063 ± 0.385	...
15151856-4146354	UCL	9.097 ± 0.023	9.077 ± 0.022	8.960 ± 0.025	8.469 ± 0.256	0.033 ± 0.030	0.013 ± 0.029	0.050 ± 0.031	0.417 ± 0.257	...
15152295-5441088	UCL	8.970 ± 0.022	8.962 ± 0.019	8.778 ± 0.030	7.952 ± 0.179	0.085 ± 0.032	0.101 ± 0.030	0.230 ± 0.038	0.975 ± 0.180	Debris
15154537-3331597	UCL	8.314 ± 0.023	8.341 ± 0.021	8.224 ± 0.021	7.783 ± 0.173	-0.022 ± 0.033	-0.012 ± 0.031	0.067 ± 0.031	0.437 ± 0.175	...
15155274-4418173	UCL	9.425 ± 0.023	9.414 ± 0.022	9.315 ± 0.036	...	-0.064 ± 0.031	-0.023 ± 0.030	0.036 ± 0.042	...	...
15163663-4407204	UCL	9.143 ± 0.024	9.166 ± 0.021	9.064 ± 0.028	8.339 ± 0.233	-0.043 ± 0.031	-0.044 ± 0.028	0.014 ± 0.034	0.665 ± 0.234	...
15171083-3434194	UCL	8.612 ± 0.022	8.627 ± 0.020	8.619 ± 0.026	8.499 ± 0.341	-0.058 ± 0.032	-0.058 ± 0.030	-0.100 ± 0.035	-0.057 ± 0.342	...
15180123-4444269	UCL	9.204 ± 0.024	9.224 ± 0.021	9.125 ± 0.028	8.122 ± 0.184	0.046 ± 0.033	0.048 ± 0.031	0.103 ± 0.036	1.032 ± 0.185	Debris
15182692-3738021	UCL	8.402 ± 0.023	8.381 ± 0.020	8.349 ± 0.021	8.151 ± 0.205	0.016 ± 0.031	0.083 ± 0.029	0.082 ± 0.030	0.211 ± 0.206	...
15185282-4050528	UCL	8.413 ± 0.023	8.418 ± 0.021	8.358 ± 0.022	8.779 ± 0.440	0.046 ± 0.035	0.087 ± 0.034	0.114 ± 0.035	-0.376 ± 0.441	...
15191600-4056075	UCL	8.639 ± 0.023	8.638 ± 0.019	8.632 ± 0.024	8.592 ± 0.318	0.099 ± 0.031	0.137 ± 0.028	0.105 ± 0.032	0.074 ± 0.319	...
15191807-2943204	UCL	9.179 ± 0.024	9.172 ± 0.021	9.065 ± 0.029	8.122 ± 0.210	0.011 ± 0.032	0.000 ± 0.030	0.034 ± 0.036	0.875 ± 0.211	Debris
15202415-3037317	UCL	7.824 ± 0.023	7.807 ± 0.023	7.731 ± 0.020	7.282 ± 0.149	0.039 ± 0.031	0.064 ± 0.031	0.085 ± 0.029	0.453 ± 0.150	...
15215241-2842383	UCL	8.769 ± 0.023	8.764 ± 0.021	8.728 ± 0.030	...	0.047 ± 0.033	0.067 ± 0.031	0.053 ± 0.038	...	...
15221162-3959509	UCL	9.023 ± 0.022	9.012 ± 0.019	8.935 ± 0.027	...	-0.016 ± 0.029	0.010 ± 0.027	0.037 ± 0.033	...	...
15232557-4055467	UCL	9.210 ± 0.023	9.223 ± 0.021	9.071 ± 0.029	8.060 ± 0.192	-0.043 ± 0.033	-0.034 ± 0.031	0.074 ± 0.037	1.011 ± 0.193	Debris
15235794-3619585	UCL	9.255 ± 0.023	9.298 ± 0.021	9.317 ± 0.041	...	-0.053 ± 0.031	-0.088 ± 0.030	-0.162 ± 0.046	...	...
15240305-3209508	UCL	8.527 ± 0.024	8.490 ± 0.019	8.393 ± 0.023	8.461 ± 0.301	0.020 ± 0.031	0.039 ± 0.028	0.063 ± 0.030	-0.107 ± 0.302	...
15241147-3030582	UCL	8.550 ± 0.023	8.552 ± 0.019	8.574 ± 0.026	7.984 ± 0.242	0.040 ± 0.030	0.075 ± 0.027	0.015 ± 0.032	0.534 ± 0.243	...
15241303-3030572	UCL	9.317 ± 0.024	9.247 ± 0.020	9.230 ± 0.034	8.519 ± 0.330	0.068 ± 0.031	0.064 ± 0.028	0.003 ± 0.039	0.565 ± 0.331	...
15243236-3652027	UCL	8.837 ± 0.024	8.874 ± 0.020	8.849 ± 0.036	...	0.000 ± 0.031	-0.007 ± 0.028	-0.022 ± 0.041	...	...

Table 4.8 (cont'd)

2MASS	Grp.	$W1$	$W2$	$W3$	$W4$	$E(K_S-W1)$	$E(K_S-W2)$	$E(K_S-W3)$	$E(K_S-W4)$	Disk Type
15250358-3604455	UCL	8.217 ± 0.025	8.208 ± 0.021	8.101 ± 0.022	7.821 ± 0.166	0.010 ± 0.034	0.049 ± 0.031	0.116 ± 0.032	0.324 ± 0.168	...
15253316-3613467	UCL	8.728 ± 0.023	8.684 ± 0.022	8.091 ± 0.026	6.767 ± 0.082	0.021 ± 0.031	0.087 ± 0.030	0.636 ± 0.033	1.886 ± 0.085	Evolved
15253666-3537319	UCL	8.811 ± 0.024	8.851 ± 0.021	8.778 ± 0.035	...	0.057 ± 0.031	0.008 ± 0.028	0.013 ± 0.040	...	...
15255964-4501157	UCL	8.815 ± 0.024	8.852 ± 0.021	8.834 ± 0.026	8.557 ± 0.302	-0.006 ± 0.031	-0.006 ± 0.028	-0.026 ± 0.032	0.180 ± 0.303	...
15262805-5549569	UCL	9.781 ± 0.022	9.841 ± 0.021	9.874 ± 0.171	8.257 ± 0.271	0.094 ± 0.035	0.049 ± 0.034	-0.034 ± 0.173	1.506 ± 0.272	...
15265257-3722062	UCL	8.977 ± 0.023	8.956 ± 0.019	8.747 ± 0.025	8.006 ± 0.184	0.047 ± 0.033	0.005 ± 0.030	0.135 ± 0.034	0.732 ± 0.185	...
15272286-3604087	UCL	8.367 ± 0.023	8.340 ± 0.019	8.231 ± 0.022	8.039 ± 0.286	-0.034 ± 0.033	-0.040 ± 0.031	-0.010 ± 0.033	0.064 ± 0.287	...
15280322-2600034	UCL	8.574 ± 0.023	8.568 ± 0.019	8.440 ± 0.023	...	-0.083 ± 0.031	-0.062 ± 0.028	0.016 ± 0.031	...	...
15293858-3546513	UCL	8.001 ± 0.022	8.008 ± 0.021	7.959 ± 0.020	8.109 ± 0.248	0.025 ± 0.027	0.048 ± 0.026	0.057 ± 0.026	-0.165 ± 0.249	...
15294727-3628374	UCL	8.931 ± 0.024	8.883 ± 0.019	8.538 ± 0.025	7.951 ± 0.187	-0.054 ± 0.035	0.016 ± 0.031	0.317 ± 0.035	0.830 ± 0.189	...
15294888-4522457	UCL	9.219 ± 0.023	9.212 ± 0.021	8.970 ± 0.027	8.229 ± 0.206	-0.063 ± 0.030	-0.065 ± 0.028	0.109 ± 0.033	0.757 ± 0.207	...
15295661-3135446	UCL	8.864 ± 0.023	8.850 ± 0.020	8.778 ± 0.031	...	0.104 ± 0.033	0.117 ± 0.030	0.128 ± 0.039	...	...
15304790-3022054	UCL	8.614 ± 0.023	8.665 ± 0.022	8.635 ± 0.027	...	-0.003 ± 0.033	-0.032 ± 0.032	-0.046 ± 0.035	...	...
15312193-3329394	UCL	8.681 ± 0.023	8.713 ± 0.020	8.714 ± 0.032	...	0.028 ± 0.031	0.036 ± 0.029	-0.001 ± 0.038	...	...
15312961-3021537	UCL	8.910 ± 0.023	8.860 ± 0.022	8.811 ± 0.035	...	0.080 ± 0.031	0.075 ± 0.030	0.045 ± 0.041	...	...
15313413-3602287	UCL	8.850 ± 0.023	8.899 ± 0.020	8.685 ± 0.025	7.464 ± 0.111	0.063 ± 0.034	0.029 ± 0.032	0.193 ± 0.035	1.337 ± 0.114	Debris
15340737-3916171	UCL	8.526 ± 0.023	8.612 ± 0.021	8.528 ± 0.026	8.633 ± 0.366	-0.066 ± 0.033	-0.122 ± 0.031	-0.078 ± 0.035	-0.255 ± 0.367	...
15342313-3300087	UCL	9.052 ± 0.022	9.054 ± 0.020	8.910 ± 0.029	8.476 ± 0.304	-0.034 ± 0.030	-0.091 ± 0.029	-0.026 ± 0.036	0.270 ± 0.305	...
15343816-4002280	UCL	8.693 ± 0.024	8.705 ± 0.020	8.604 ± 0.025	8.906 ± 0.481	-0.034 ± 0.031	-0.055 ± 0.028	-0.022 ± 0.031	-0.417 ± 0.481	...
15355780-2324046	US	9.318 ± 0.023	9.293 ± 0.021	9.283 ± 0.041	...	0.014 ± 0.034	0.054 ± 0.033	0.014 ± 0.048	...	...
15355876-4456355	UCL	9.066 ± 0.024	9.060 ± 0.021	8.852 ± 0.025	7.934 ± 0.168	-0.009 ± 0.031	-0.021 ± 0.029	0.114 ± 0.032	0.930 ± 0.169	Debris

Table 4.8 (cont'd)

2MASS	Grp.	$W1$	$W2$	$W3$	$W4$	$E(K_S - W1)$	$E(K_S - W2)$	$E(K_S - W3)$	$E(K_S - W4)$	Disk Type
15364094-2923574	UCL	9.369 ± 0.023	9.218 ± 0.021	9.132 ± 0.035	8.388 ± 0.262	0.083 ± 0.035	0.160 ± 0.033	0.168 ± 0.044	0.763 ± 0.263	...
15370214-3136398	UCL	7.870 ± 0.041	7.875 ± 0.031	7.855 ± 0.030	7.694 ± 0.254	-0.206 ± 0.049	-0.162 ± 0.040	-0.168 ± 0.040	-0.077 ± 0.255	...
15371129-4015566	UCL	8.172 ± 0.024	8.177 ± 0.021	8.156 ± 0.027	8.047 ± 0.236	0.035 ± 0.041	0.078 ± 0.039	0.068 ± 0.043	0.108 ± 0.238	...
15374917-1840449	US	9.181 ± 0.023	9.213 ± 0.019	9.169 ± 0.031	8.571 ± 0.325	-0.005 ± 0.033	0.012 ± 0.030	0.030 ± 0.039	0.558 ± 0.326	...
15375134-3045160	UCL	8.532 ± 0.021	8.515 ± 0.019	8.375 ± 0.023	8.145 ± 0.252	-0.063 ± 0.028	-0.038 ± 0.027	0.047 ± 0.030	0.196 ± 0.253	...
15380264-3807230	UCL	9.252 ± 0.023	9.282 ± 0.020	9.149 ± 0.033	8.325 ± 0.243	0.030 ± 0.033	-0.001 ± 0.031	0.071 ± 0.041	0.809 ± 0.244	...
15383827-3916553	UCL	8.798 ± 0.023	8.801 ± 0.020	8.733 ± 0.026	9.012 ± 0.494	-0.038 ± 0.033	-0.033 ± 0.030	-0.020 ± 0.035	-0.380 ± 0.495	...
15384306-4411474	UCL	8.194 ± 0.021	8.229 ± 0.019	8.100 ± 0.019	7.694 ± 0.141	-0.077 ± 0.037	-0.078 ± 0.036	0.012 ± 0.036	0.347 ± 0.144	...
15392776-3446171	UCL	7.626 ± 0.028	7.178 ± 0.022	5.146 ± 0.015	3.193 ± 0.024	0.259 ± 0.033	0.689 ± 0.028	2.648 ± 0.023	4.499 ± 0.029	Full
15394637-3451027	UCL	8.647 ± 0.024	8.615 ± 0.020	8.407 ± 0.022	7.764 ± 0.165	0.120 ± 0.035	0.160 ± 0.033	0.313 ± 0.034	0.875 ± 0.167	Debris
15400244-4634187	UCL	9.021 ± 0.023	9.039 ± 0.021	8.964 ± 0.026	8.331 ± 0.261	0.002 ± 0.030	-0.008 ± 0.028	0.012 ± 0.032	0.564 ± 0.262	...
15404116-3756185	UCL	9.083 ± 0.022	9.104 ± 0.020	8.932 ± 0.028	9.044 ± 0.483	0.009 ± 0.034	-0.021 ± 0.033	0.083 ± 0.038	-0.122 ± 0.484	...
15410679-2656263	US	8.815 ± 0.021	8.836 ± 0.019	8.790 ± 0.029	...	0.020 ± 0.031	0.047 ± 0.030	0.062 ± 0.037	...	...
15413114-5330296	UCL	8.296 ± 0.023	8.309 ± 0.019	8.290 ± 0.028	7.817 ± 0.196	-0.005 ± 0.032	0.004 ± 0.029	-0.021 ± 0.036	0.378 ± 0.197	...
15413121-2520363	US	7.154 ± 0.033	7.151 ± 0.022	7.125 ± 0.018	6.977 ± 0.089	-0.004 ± 0.041	0.042 ± 0.033	0.032 ± 0.030	0.111 ± 0.092	...
15420518-3601317	UCL	9.023 ± 0.023	9.017 ± 0.019	8.785 ± 0.026	7.817 ± 0.161	-0.032 ± 0.033	-0.044 ± 0.030	0.115 ± 0.035	0.981 ± 0.163	Debris
15424991-2536406	US	8.096 ± 0.023	8.128 ± 0.020	8.110 ± 0.022	8.186 ± 0.260	0.003 ± 0.030	0.020 ± 0.028	0.012 ± 0.030	-0.134 ± 0.261	...
15435905-2622516	US	9.787 ± 0.023	9.747 ± 0.020	9.723 ± 0.056	...	-0.059 ± 0.031	-0.059 ± 0.029	-0.115 ± 0.060	...	...
15440376-3311110	UCL	8.281 ± 0.024	8.261 ± 0.021	8.138 ± 0.020	7.744 ± 0.157	0.040 ± 0.035	0.082 ± 0.033	0.161 ± 0.033	0.481 ± 0.159	...
15441334-2522590	US	8.902 ± 0.023	8.894 ± 0.019	8.849 ± 0.035	...	0.058 ± 0.035	-0.008 ± 0.033	-0.041 ± 0.044	...	...
15442874-4745415	UCL	8.750 ± 0.023	8.718 ± 0.020	8.636 ± 0.024	8.730 ± 0.367	0.038 ± 0.031	0.030 ± 0.029	0.032 ± 0.032	-0.186 ± 0.368	...

Table 4.8 (cont'd)

2MASS	Grp.	$W1$	$W2$	$W3$	$W4$	$E(K_S-W1)$	$E(K_S-W2)$	$E(K_S-W3)$	$E(K_S-W4)$	Disk Type
15444712-3811406	UCL	8.256 ± 0.023	8.219 ± 0.021	8.210 ± 0.022	8.130 ± 0.224	0.020 ± 0.026	0.039 ± 0.025	-0.025 ± 0.026	-0.047 ± 0.224	...
15451286-3417305	UCL	5.723 ± 0.054	4.973 ± 0.032	2.891 ± 0.010	0.856 ± 0.016	0.664 ± 0.058	1.436 ± 0.038	3.474 ± 0.022	5.435 ± 0.026	Full
15455225-4222163	UCL	7.828 ± 0.023	7.821 ± 0.018	7.766 ± 0.019	7.825 ± 0.185	0.012 ± 0.033	0.038 ± 0.030	0.046 ± 0.031	-0.089 ± 0.187	...
15462958-5217239	UCL	8.882 ± 0.023	8.923 ± 0.021	8.755 ± 0.046	...	0.176 ± 0.033	0.172 ± 0.031	0.302 ± 0.051	...	...
15463111-5216580	UCL	9.321 ± 0.024	9.327 ± 0.021	9.137 ± 0.053	7.973 ± 0.257	-0.008 ± 0.031	-0.069 ± 0.028	0.042 ± 0.056	1.068 ± 0.258	...
15464121-3618472	UCL	8.690 ± 0.023	8.666 ± 0.020	8.560 ± 0.024	8.881 ± 0.477	0.000 ± 0.031	0.054 ± 0.029	0.120 ± 0.032	-0.273 ± 0.477	...
15471063-1736244	US	9.482 ± 0.024	9.393 ± 0.022	9.222 ± 0.032	...	-0.027 ± 0.035	0.007 ± 0.033	0.099 ± 0.041	...	...
15474176-4018267	UCL	8.622 ± 0.022	8.669 ± 0.020	8.491 ± 0.022	7.800 ± 0.159	-0.053 ± 0.033	-0.070 ± 0.032	0.068 ± 0.033	0.687 ± 0.161	...
15480291-2908369	US	8.566 ± 0.023	8.587 ± 0.021	8.507 ± 0.022	8.364 ± 0.273	-0.033 ± 0.033	-0.011 ± 0.031	0.033 ± 0.032	0.107 ± 0.274	...
15481148-4712297	UCL	8.589 ± 0.022	8.582 ± 0.018	8.431 ± 0.022	8.134 ± 0.221	0.023 ± 0.030	0.045 ± 0.028	0.146 ± 0.030	0.366 ± 0.222	...
15481299-2349523	US	9.144 ± 0.023	9.032 ± 0.022	8.894 ± 0.033	...	0.007 ± 0.031	0.056 ± 0.030	0.115 ± 0.039	...	...
15484204-4335207	UCL	9.288 ± 0.024	9.311 ± 0.021	9.231 ± 0.030	9.146 ± 0.465	-0.052 ± 0.031	-0.029 ± 0.028	0.018 ± 0.036	0.034 ± 0.465	...
15490271-3102537	UCL	8.484 ± 0.023	8.493 ± 0.020	8.480 ± 0.023	8.235 ± 0.242	-0.024 ± 0.031	0.004 ± 0.029	-0.021 ± 0.031	0.153 ± 0.243	...
15492100-2600062	US	7.855 ± 0.024	7.862 ± 0.022	7.833 ± 0.025	...	-0.035 ± 0.036	-0.005 ± 0.035	-0.014 ± 0.037	...	...
15494499-3925089	UCL	8.057 ± 0.022	8.100 ± 0.019	7.999 ± 0.019	7.677 ± 0.140	-0.009 ± 0.040	-0.033 ± 0.039	0.021 ± 0.039	0.267 ± 0.144	...
15495840-4306370	UCL	9.195 ± 0.023	9.188 ± 0.020	9.177 ± 0.039	8.786 ± 0.447	0.079 ± 0.031	0.101 ± 0.029	0.062 ± 0.044	0.376 ± 0.447	...
15495920-3629574	UCL	8.833 ± 0.023	8.870 ± 0.022	8.756 ± 0.026	...	-0.042 ± 0.033	-0.057 ± 0.033	0.013 ± 0.035	...	...
15510142-1548286	US	9.255 ± 0.024	9.104 ± 0.021	9.051 ± 0.035	8.678 ± 0.397	0.016 ± 0.033	0.093 ± 0.031	0.068 ± 0.042	0.292 ± 0.398	...
15510660-2402190	US	9.638 ± 0.023	9.563 ± 0.021	9.573 ± 0.050	...	-0.041 ± 0.034	-0.063 ± 0.033	-0.150 ± 0.056	...	...
15514535-2456513	US	9.373 ± 0.024	9.356 ± 0.022	9.233 ± 0.039	...	0.066 ± 0.035	0.098 ± 0.033	0.171 ± 0.046	...	...
15522589-3920512	UCL	9.233 ± 0.023	9.226 ± 0.020	9.120 ± 0.031	8.938 ± 0.444	-0.028 ± 0.035	-0.013 ± 0.033	0.038 ± 0.040	0.139 ± 0.445	...

Table 4.8 (cont'd)

2MASS	Grp.	$W1$	$W2$	$W3$	$W4$	$E(K_S - W1)$	$E(K_S - W2)$	$E(K_S - W3)$	$E(K_S - W4)$	Disk Type
15523122-2633529	US	8.831 ± 0.022	8.842 ± 0.021	8.767 ± 0.029	...	0.033 ± 0.032	-0.033 ± 0.031	-0.037 ± 0.037	...	...
15530683-2247174	US	8.467 ± 0.022	8.375 ± 0.018	8.298 ± 0.023	8.663 ± 0.435	0.098 ± 0.030	0.135 ± 0.028	0.133 ± 0.031	-0.370 ± 0.436	...
15545141-3154463	UCL	7.394 ± 0.024	6.987 ± 0.018	5.429 ± 0.015	3.298 ± 0.020	0.745 ± 0.031	1.151 ± 0.027	2.648 ± 0.025	4.693 ± 0.028	Full
15550624-2521102	US	8.375 ± 0.023	8.383 ± 0.019	8.277 ± 0.029	8.742 ± 0.520	0.013 ± 0.031	-0.069 ± 0.028	-0.041 ± 0.036	-0.655 ± 0.520	...
15551621-1355136	US	9.069 ± 0.023	9.067 ± 0.021	8.988 ± 0.030	8.923 ± 0.485	-0.018 ± 0.031	-0.025 ± 0.030	-0.014 ± 0.037	-0.042 ± 0.485	...
15552621-3338232	UCL	9.233 ± 0.023	9.244 ± 0.020	9.329 ± 0.068	...	0.026 ± 0.032	0.014 ± 0.030	-0.132 ± 0.071	...	...
15560921-3756057	UCL	6.938 ± 0.035	6.423 ± 0.022	4.474 ± 0.015	2.622 ± 0.022	0.689 ± 0.042	1.149 ± 0.032	3.019 ± 0.027	4.733 ± 0.032	Full
15564402-4242301	UCL	8.100 ± 0.023	8.066 ± 0.023	7.997 ± 0.033	...	0.070 ± 0.037	0.095 ± 0.037	0.096 ± 0.044	...	...
15565905-3933430	UCL	8.562 ± 0.023	8.600 ± 0.021	8.598 ± 0.029	...	0.047 ± 0.030	0.057 ± 0.029	0.028 ± 0.035	...	...
15570234-1950419	US	8.214 ± 0.022	8.219 ± 0.019	8.222 ± 0.029	...	0.061 ± 0.033	0.038 ± 0.031	-0.038 ± 0.038	...	...
15573430-2321123	US	8.796 ± 0.024	8.687 ± 0.020	8.360 ± 0.030	5.626 ± 0.041	0.074 ± 0.032	0.109 ± 0.029	0.358 ± 0.037	2.943 ± 0.046	Debris
15574362-4143377	UCL	8.234 ± 0.024	7.777 ± 0.021	6.174 ± 0.016	4.725 ± 0.026	0.414 ± 0.033	0.862 ± 0.031	2.397 ± 0.028	3.753 ± 0.035	Full
15574440-4049276	UCL	7.714 ± 0.023	7.315 ± 0.019	5.520 ± 0.014	3.372 ± 0.024	0.301 ± 0.029	0.660 ± 0.026	2.375 ± 0.023	4.399 ± 0.030	Full
15575002-2305094	US	9.134 ± 0.021	9.101 ± 0.019	9.041 ± 0.034	...	0.019 ± 0.030	-0.003 ± 0.028	-0.022 ± 0.040	...	...
15581270-2328364	US	7.926 ± 0.024	7.968 ± 0.021	7.805 ± 0.019	...	0.027 ± 0.034	0.020 ± 0.032	0.172 ± 0.031	...	...
15581474-4029175	UCL	8.702 ± 0.024	8.664 ± 0.020	8.616 ± 0.026	...	-0.005 ± 0.033	0.005 ± 0.030	-0.025 ± 0.035	...	...
15582054-1837252	US	7.432 ± 0.025	7.442 ± 0.021	7.387 ± 0.017	7.357 ± 0.116	0.112 ± 0.033	0.144 ± 0.030	0.182 ± 0.027	0.141 ± 0.118	...
15583692-2257153	US	5.823 ± 0.051	5.125 ± 0.029	4.079 ± 0.014	1.283 ± 0.022	1.152 ± 0.060	1.899 ± 0.042	2.919 ± 0.034	5.645 ± 0.038	Full
15584772-1757595	US	8.286 ± 0.024	8.259 ± 0.021	8.079 ± 0.021	7.474 ± 0.129	-0.054 ± 0.034	-0.012 ± 0.032	0.118 ± 0.032	0.646 ± 0.131	...
15590208-1844142	US	7.932 ± 0.022	7.875 ± 0.020	7.745 ± 0.018	7.190 ± 0.110	0.079 ± 0.026	0.127 ± 0.024	0.189 ± 0.023	0.651 ± 0.111	...
15591101-1850442	US	8.988 ± 0.022	8.979 ± 0.020	8.725 ± 0.025	8.376 ± 0.292	0.047 ± 0.027	0.047 ± 0.025	0.233 ± 0.029	0.489 ± 0.292	...

Table 4.8 (cont'd)

2MASS	Grp.	$W1$	$W2$	$W3$	$W4$	$E(K_S-W1)$	$E(K_S-W2)$	$E(K_S-W3)$	$E(K_S-W4)$	Disk Type
15591452-2606182	US	8.916 ± 0.022	8.874 ± 0.020	8.752 ± 0.027	...	0.107 ± 0.029	0.171 ± 0.028	0.249 ± 0.033	...	...
15591647-4157102	UCL	7.820 ± 0.023	7.366 ± 0.019	5.721 ± 0.016	3.598 ± 0.017	0.691 ± 0.033	1.127 ± 0.030	2.699 ± 0.028	4.720 ± 0.029	Full
15594951-3628279	UCL	7.949 ± 0.023	7.966 ± 0.019	7.884 ± 0.022	7.977 ± 0.240	-0.013 ± 0.035	-0.015 ± 0.032	0.017 ± 0.034	-0.153 ± 0.241	...
16003134-2027050	US	8.705 ± 0.023	8.622 ± 0.020	8.510 ± 0.023	8.959 ± 0.481	0.000 ± 0.035	0.009 ± 0.034	0.043 ± 0.035	-0.555 ± 0.482	...
16004056-2200322	US	8.340 ± 0.023	8.359 ± 0.020	8.315 ± 0.025	8.591 ± 0.394	0.012 ± 0.031	0.036 ± 0.029	0.044 ± 0.033	-0.301 ± 0.395	...
16004277-2127380	US	8.869 ± 0.023	8.808 ± 0.021	8.773 ± 0.030	8.209 ± 0.253	-0.044 ± 0.032	-0.001 ± 0.030	-0.039 ± 0.037	0.423 ± 0.254	...
16010801-2113184	US	8.638 ± 0.023	8.595 ± 0.021	8.487 ± 0.029	...	0.053 ± 0.031	0.041 ± 0.030	0.070 ± 0.036	...	...
16011070-4804438	UCL	8.866 ± 0.022	8.905 ± 0.019	8.787 ± 0.029	9.032 ± 0.452	-0.036 ± 0.030	-0.060 ± 0.028	0.008 ± 0.035	-0.314 ± 0.452	...
16012563-2240403	US	8.415 ± 0.022	8.412 ± 0.019	8.342 ± 0.028	7.567 ± 0.170	0.015 ± 0.030	0.048 ± 0.028	0.078 ± 0.035	0.781 ± 0.171	...
16014743-2049457	US	8.448 ± 0.023	8.373 ± 0.018	8.288 ± 0.023	7.940 ± 0.210	0.054 ± 0.030	0.074 ± 0.027	0.080 ± 0.030	0.290 ± 0.211	...
16014943-4026192	UCL	8.952 ± 0.023	8.912 ± 0.019	8.811 ± 0.025	8.727 ± 0.370	0.008 ± 0.033	0.030 ± 0.030	0.058 ± 0.034	0.040 ± 0.371	...
16015149-2445249	US	8.371 ± 0.023	8.374 ± 0.021	8.315 ± 0.023	8.032 ± 0.230	0.017 ± 0.035	-0.004 ± 0.033	-0.018 ± 0.035	0.163 ± 0.231	...
16015822-2008121	US	7.582 ± 0.024	7.567 ± 0.019	7.524 ± 0.018	7.402 ± 0.133	0.012 ± 0.031	0.076 ± 0.028	0.093 ± 0.027	0.145 ± 0.134	...
16015918-3612555	UCL	8.641 ± 0.020	8.596 ± 0.017	8.719 ± 0.040	8.772 ± 0.487	0.120 ± 0.032	0.180 ± 0.030	0.007 ± 0.047	-0.123 ± 0.488	...
16020039-2221237	US	8.754 ± 0.023	8.650 ± 0.021	8.505 ± 0.026	8.000 ± 0.241	-0.034 ± 0.032	-0.004 ± 0.030	0.063 ± 0.034	0.419 ± 0.242	...
16021045-2241280	US	7.957 ± 0.023	7.965 ± 0.019	7.899 ± 0.022	...	0.007 ± 0.035	-0.002 ± 0.032	0.003 ± 0.034	...	...
16023814-2541389	US	9.222 ± 0.024	9.198 ± 0.021	9.162 ± 0.032	...	0.010 ± 0.032	0.006 ± 0.030	-0.036 ± 0.038	...	...
16023910-2542078	US	8.923 ± 0.024	8.968 ± 0.021	8.816 ± 0.029	...	0.097 ± 0.033	0.034 ± 0.031	0.113 ± 0.037	...	...
16025123-2401574	US	8.921 ± 0.024	8.935 ± 0.020	8.841 ± 0.033	...	-0.088 ± 0.032	-0.094 ± 0.029	-0.055 ± 0.039	...	...
16025243-2402226	US	7.545 ± 0.025	7.669 ± 0.020	7.556 ± 0.019	7.648 ± 0.186	0.008 ± 0.031	-0.079 ± 0.027	-0.004 ± 0.026	-0.167 ± 0.187	...
16025396-2022480	US	8.021 ± 0.023	7.957 ± 0.021	7.833 ± 0.018	7.966 ± 0.200	0.072 ± 0.035	0.118 ± 0.033	0.169 ± 0.032	-0.066 ± 0.202	...

Table 4.8 (cont'd)

2MASS	Grp.	$W1$	$W2$	$W3$	$W4$	$E(K_S - W1)$	$E(K_S - W2)$	$E(K_S - W3)$	$E(K_S - W4)$	Disk Type
16030269-1806050	US	8.558 ± 0.024	8.576 ± 0.021	8.466 ± 0.025	8.050 ± 0.278	0.075 ± 0.035	0.065 ± 0.033	0.120 ± 0.035	0.455 ± 0.279	...
16032367-1751422	US	8.372 ± 0.023	8.282 ± 0.021	8.178 ± 0.021	7.723 ± 0.175	0.102 ± 0.035	0.095 ± 0.033	0.122 ± 0.033	0.423 ± 0.177	...
16033550-2245560	US	8.234 ± 0.023	8.265 ± 0.021	8.220 ± 0.023	7.790 ± 0.203	0.035 ± 0.034	0.047 ± 0.033	0.056 ± 0.034	0.417 ± 0.205	...
16034536-4355492	UCL	7.222 ± 0.031	7.227 ± 0.022	7.180 ± 0.018	7.129 ± 0.108	-0.001 ± 0.036	0.024 ± 0.028	0.031 ± 0.025	0.010 ± 0.109	...
16035250-3939013	UCL	8.142 ± 0.024	8.156 ± 0.019	8.042 ± 0.020	7.464 ± 0.108	-0.011 ± 0.036	-0.010 ± 0.033	0.054 ± 0.034	0.555 ± 0.111	...
16035836-1751041	US	9.128 ± 0.024	8.991 ± 0.021	8.878 ± 0.030	8.023 ± 0.202	-0.001 ± 0.031	0.081 ± 0.028	0.115 ± 0.036	0.832 ± 0.203	...
16042165-2130284	US	7.548 ± 0.022	7.081 ± 0.018	6.686 ± 0.015	4.340 ± 0.024	0.865 ± 0.030	1.354 ± 0.028	1.705 ± 0.026	3.977 ± 0.032	Full
16043056-3207287	US	8.411 ± 0.023	8.413 ± 0.021	8.362 ± 0.024	8.524 ± 0.371	0.061 ± 0.031	0.081 ± 0.030	0.088 ± 0.032	-0.148 ± 0.372	...
16044776-1930230	US	7.923 ± 0.023	7.932 ± 0.021	7.897 ± 0.019	7.971 ± 0.200	0.027 ± 0.029	0.040 ± 0.027	0.031 ± 0.025	-0.117 ± 0.201	...
16054266-2004150	US	8.998 ± 0.023	8.879 ± 0.022	8.787 ± 0.030	8.804 ± 0.470	0.024 ± 0.035	0.046 ± 0.035	0.061 ± 0.040	-0.110 ± 0.471	...
16054499-3906065	UCL	8.279 ± 0.023	8.282 ± 0.021	8.302 ± 0.027	...	-0.005 ± 0.035	0.038 ± 0.034	-0.015 ± 0.038	...	...
16055065-2533136	US	8.402 ± 0.023	8.419 ± 0.020	8.402 ± 0.024	8.343 ± 0.293	-0.026 ± 0.033	0.005 ± 0.030	-0.009 ± 0.033	-0.019 ± 0.294	...
16055207-3439331	UCL	8.308 ± 0.024	8.337 ± 0.020	8.329 ± 0.027	...	0.058 ± 0.033	0.051 ± 0.030	0.015 ± 0.035	...	...
16061222-4507155	UCL	9.300 ± 0.023	9.321 ± 0.020	9.117 ± 0.030	...	0.055 ± 0.031	0.049 ± 0.029	0.203 ± 0.037	...	...
16061254-2036472	US	8.680 ± 0.020	8.665 ± 0.020	8.529 ± 0.023	7.722 ± 0.160	0.124 ± 0.028	0.138 ± 0.028	0.213 ± 0.030	0.934 ± 0.161	Debris
16062196-1928445	US	8.213 ± 0.023	7.896 ± 0.021	6.620 ± 0.017	3.528 ± 0.018	0.291 ± 0.035	0.545 ± 0.033	1.742 ± 0.031	4.690 ± 0.032	Full
16062334-4447355	UCL	9.360 ± 0.024	9.348 ± 0.023	9.141 ± 0.034	8.425 ± 0.245	-0.028 ± 0.032	-0.008 ± 0.031	0.144 ± 0.040	0.779 ± 0.246	...
16062354-1814187	US	8.176 ± 0.021	8.182 ± 0.019	8.105 ± 0.024	7.931 ± 0.207	0.038 ± 0.034	0.031 ± 0.033	0.047 ± 0.036	0.135 ± 0.209	...
16063169-2036232	US	8.659 ± 0.023	8.608 ± 0.021	8.407 ± 0.022	...	-0.022 ± 0.033	0.020 ± 0.031	0.153 ± 0.032	...	...
16063245-2208245	US	8.741 ± 0.024	8.744 ± 0.022	8.654 ± 0.027	8.618 ± 0.410	0.044 ± 0.032	0.032 ± 0.030	0.054 ± 0.034	-0.003 ± 0.411	...
16065436-2416107	US	8.690 ± 0.023	8.652 ± 0.019	8.598 ± 0.026	...	0.016 ± 0.035	-0.073 ± 0.033	-0.097 ± 0.037	...	...

Table 4.8 (cont'd)

2MASS	Grp.	$W1$	$W2$	$W3$	$W4$	$E(K_S - W1)$	$E(K_S - W2)$	$E(K_S - W3)$	$E(K_S - W4)$	Disk Type
16070356-2036264	US	7.921 ± 0.023	7.870 ± 0.019	7.752 ± 0.018	7.174 ± 0.103	0.065 ± 0.033	0.061 ± 0.031	0.100 ± 0.030	0.540 ± 0.106	...
16070393-1911338	US	9.067 ± 0.023	8.957 ± 0.022	8.867 ± 0.031	...	0.029 ± 0.035	0.065 ± 0.034	0.077 ± 0.040	...	...
16073366-3759242	UCL	9.206 ± 0.026	9.214 ± 0.024	9.147 ± 0.046	...	0.045 ± 0.051	0.019 ± 0.050	0.013 ± 0.064	...	...
16074006-2148426	US	9.599 ± 0.023	9.556 ± 0.019	9.452 ± 0.053	8.757 ± 0.463	-0.022 ± 0.030	0.003 ± 0.027	0.034 ± 0.056	0.627 ± 0.463	...
16080019-4116119	UCL	8.643 ± 0.024	8.600 ± 0.020	8.448 ± 0.021	...	0.025 ± 0.033	0.079 ± 0.030	0.179 ± 0.031	...	...
16080141-2027416	US	9.180 ± 0.021	9.160 ± 0.019	8.979 ± 0.030	8.522 ± 0.341	0.011 ± 0.031	0.003 ± 0.030	0.106 ± 0.038	0.451 ± 0.342	...
16080772-5041556	UCL	8.519 ± 0.026	8.516 ± 0.025	8.636 ± 0.091	...	0.026 ± 0.035	0.020 ± 0.034	-0.168 ± 0.094	...	...
16081081-1904479	US	8.326 ± 0.025	8.357 ± 0.022	8.237 ± 0.023	8.093 ± 0.322	0.048 ± 0.041	0.032 ± 0.039	0.102 ± 0.039	0.169 ± 0.324	...
16081474-1908327	US	8.292 ± 0.023	8.304 ± 0.020	8.218 ± 0.023	8.512 ± 0.368	0.041 ± 0.030	0.051 ± 0.028	0.093 ± 0.030	-0.275 ± 0.369	...
16081824-3844052	UCL	8.582 ± 0.023	8.567 ± 0.022	8.577 ± 0.029	...	0.035 ± 0.031	0.032 ± 0.030	-0.051 ± 0.036	...	...
16083436-1911563	US	7.638 ± 0.024	7.579 ± 0.018	7.482 ± 0.019	7.552 ± 0.161	0.053 ± 0.038	0.111 ± 0.034	0.147 ± 0.035	-0.009 ± 0.164	...
16083617-3923024	UCL	7.823 ± 0.023	7.447 ± 0.020	6.295 ± 0.016	4.678 ± 0.031	0.740 ± 0.031	1.107 ± 0.029	2.191 ± 0.026	3.715 ± 0.037	Full
16084340-2602168	US	7.810 ± 0.023	7.812 ± 0.022	7.756 ± 0.020	7.687 ± 0.167	0.013 ± 0.028	0.059 ± 0.027	0.084 ± 0.026	0.084 ± 0.168	...
16085427-3906057	UCL	8.070 ± 0.023	8.093 ± 0.020	7.736 ± 0.026	6.333 ± 0.085	0.049 ± 0.037	0.048 ± 0.035	0.361 ± 0.039	1.690 ± 0.090	Debris
16085673-2033460	US	8.450 ± 0.025	8.462 ± 0.022	8.380 ± 0.022	8.488 ± 0.352	0.075 ± 0.035	0.062 ± 0.033	0.083 ± 0.033	-0.111 ± 0.353	...
16090075-1908526	US	8.705 ± 0.022	8.442 ± 0.019	6.166 ± 0.014	3.630 ± 0.020	0.344 ± 0.035	0.567 ± 0.033	2.763 ± 0.030	5.175 ± 0.034	Full
16092918-1852536	US	8.178 ± 0.023	8.142 ± 0.021	8.078 ± 0.026	...	0.103 ± 0.044	0.147 ± 0.043	0.156 ± 0.046	...	...
16093030-2104589	US	8.767 ± 0.023	8.779 ± 0.021	8.715 ± 0.027	8.804 ± 0.479	0.037 ± 0.031	-0.030 ± 0.030	-0.045 ± 0.034	-0.272 ± 0.479	...
16093969-2200466	US	9.231 ± 0.023	9.137 ± 0.020	9.023 ± 0.032	8.375 ± 0.305	-0.035 ± 0.030	0.019 ± 0.028	0.053 ± 0.037	0.577 ± 0.306	...
16094098-2217594	US	8.353 ± 0.024	8.342 ± 0.023	8.167 ± 0.022	6.503 ± 0.066	-0.024 ± 0.036	-0.068 ± 0.035	0.028 ± 0.035	1.554 ± 0.071	Debris
16100478-4016122	UCL	8.503 ± 0.023	8.498 ± 0.021	8.522 ± 0.033	...	0.023 ± 0.033	0.050 ± 0.031	-0.018 ± 0.040	...	...

Table 4.8 (cont'd)

2MASS	Grp.	$W1$	$W2$	$W3$	$W4$	$E(K_S - W1)$	$E(K_S - W2)$	$E(K_S - W3)$	$E(K_S - W4)$	Disk Type
16101171-3226360	US	8.335 ± 0.025	8.319 ± 0.021	8.239 ± 0.024	8.122 ± 0.274	-0.021 ± 0.035	-0.006 ± 0.033	0.013 ± 0.035	0.044 ± 0.275	...
16101264-2104446	US	8.503 ± 0.023	8.509 ± 0.021	7.537 ± 0.019	3.008 ± 0.028	-0.050 ± 0.031	-0.041 ± 0.030	0.881 ± 0.028	5.333 ± 0.035	Transitional
16101729-1910263	US	8.104 ± 0.023	8.037 ± 0.022	8.022 ± 0.022	...	0.333 ± 0.044	0.399 ± 0.043	0.353 ± 0.043	...	Evolved
16101918-2502301	US	8.288 ± 0.023	8.318 ± 0.021	8.261 ± 0.035	...	-0.046 ± 0.031	-0.150 ± 0.030	-0.171 ± 0.041	...	...
16102174-1904067	US	9.313 ± 0.022	9.171 ± 0.020	9.094 ± 0.036	...	0.189 ± 0.032	0.257 ± 0.030	0.256 ± 0.043	...	...
16102653-2756293	US	9.415 ± 0.022	9.303 ± 0.019	9.151 ± 0.034	8.521 ± 0.383	0.003 ± 0.032	-0.012 ± 0.030	0.062 ± 0.041	0.542 ± 0.384	...
16102888-2213477	US	7.107 ± 0.031	7.103 ± 0.021	7.108 ± 0.020	7.091 ± 0.122	0.041 ± 0.035	0.094 ± 0.026	0.063 ± 0.026	0.010 ± 0.123	...
16104202-2101319	US	8.253 ± 0.023	8.191 ± 0.021	8.027 ± 0.021	7.041 ± 0.095	0.141 ± 0.027	0.202 ± 0.026	0.305 ± 0.026	1.205 ± 0.096	Debris
16110890-1904468	US	7.572 ± 0.025	7.512 ± 0.022	7.389 ± 0.018	7.236 ± 0.127	0.028 ± 0.032	0.096 ± 0.030	0.164 ± 0.027	0.236 ± 0.129	...
16111534-1757214	US	8.754 ± 0.023	8.267 ± 0.021	6.289 ± 0.016	4.706 ± 0.027	0.328 ± 0.030	0.741 ± 0.028	2.641 ± 0.025	4.075 ± 0.033	Full
16114387-2526350	US	8.579 ± 0.023	8.579 ± 0.019	8.494 ± 0.028	...	0.073 ± 0.030	0.088 ± 0.027	0.123 ± 0.034	...	...
16115334-3902158	UCL	9.337 ± 0.023	9.314 ± 0.020	9.260 ± 0.037	8.765 ± 0.388	-0.002 ± 0.034	-0.012 ± 0.032	-0.037 ± 0.045	0.340 ± 0.389	...
16120140-3840276	UCL	8.082 ± 0.022	8.039 ± 0.019	7.997 ± 0.026	8.131 ± 0.256	0.003 ± 0.030	0.045 ± 0.028	0.026 ± 0.033	-0.194 ± 0.257	...
16123916-1859284	US	8.658 ± 0.023	8.244 ± 0.020	6.422 ± 0.016	4.483 ± 0.030	0.360 ± 0.036	0.793 ± 0.034	2.568 ± 0.032	4.431 ± 0.041	Full
16124051-1859282	US	7.378 ± 0.030	7.381 ± 0.020	7.251 ± 0.018	6.200 ± 0.064	0.024 ± 0.040	0.058 ± 0.033	0.150 ± 0.032	1.130 ± 0.069	Debris
16124682-2213317	US	7.869 ± 0.023	7.864 ± 0.019	7.771 ± 0.020	7.462 ± 0.148	0.071 ± 0.029	0.091 ± 0.025	0.134 ± 0.026	0.366 ± 0.149	...
16125265-2319560	US	8.949 ± 0.023	8.948 ± 0.020	8.869 ± 0.031	8.616 ± 0.412	0.000 ± 0.033	0.016 ± 0.030	0.045 ± 0.039	0.221 ± 0.413	...
16130271-2257446	US	8.292 ± 0.023	8.310 ± 0.022	8.200 ± 0.022	7.911 ± 0.230	0.069 ± 0.035	0.059 ± 0.035	0.114 ± 0.035	0.322 ± 0.232	...
16131267-3803513	UCL	8.723 ± 0.021	8.732 ± 0.019	8.695 ± 0.030	...	0.063 ± 0.027	0.053 ± 0.025	0.029 ± 0.034	...	...
16131738-2922198	US	8.508 ± 0.019	8.462 ± 0.018	8.564 ± 0.031	...	0.289 ± 0.028	0.280 ± 0.028	0.099 ± 0.037	...	...
16131858-2212489	US	7.323 ± 0.026	7.342 ± 0.019	7.311 ± 0.018	7.028 ± 0.099	0.014 ± 0.035	0.038 ± 0.031	0.033 ± 0.030	0.247 ± 0.102	...

Table 4.8 (cont'd)

2MASS	Grp.	$W1$	$W2$	$W3$	$W4$	$E(K_S-W1)$	$E(K_S-W2)$	$E(K_S-W3)$	$E(K_S-W4)$	Disk Type
16132929-2311075	US	8.298 ± 0.023	8.282 ± 0.020	8.195 ± 0.025	7.679 ± 0.173	0.103 ± 0.030	0.149 ± 0.028	0.196 ± 0.031	0.640 ± 0.174	...
16134366-2214594	US	9.029 ± 0.023	8.991 ± 0.021	8.852 ± 0.029	8.165 ± 0.243	-0.012 ± 0.031	0.008 ± 0.030	0.074 ± 0.036	0.659 ± 0.244	...
16135801-3618133	UCL	8.705 ± 0.027	8.727 ± 0.028	8.639 ± 0.030	...	0.058 ± 0.047	0.082 ± 0.048	0.137 ± 0.049	...	...
16140035-2108439	US	9.474 ± 0.024	9.449 ± 0.020	9.507 ± 0.052	...	0.029 ± 0.033	0.026 ± 0.030	-0.110 ± 0.056	...	...
16140211-2301021	US	8.409 ± 0.024	8.417 ± 0.021	8.352 ± 0.025	7.784 ± 0.193	0.125 ± 0.033	0.163 ± 0.031	0.206 ± 0.034	0.704 ± 0.194	...
16141107-2305362	US	7.317 ± 0.027	7.052 ± 0.019	5.015 ± 0.016	3.531 ± 0.022	0.049 ± 0.038	0.351 ± 0.033	2.350 ± 0.031	3.763 ± 0.035	Full
16143884-2525000	US	8.819 ± 0.022	8.705 ± 0.019	8.665 ± 0.034	8.073 ± 0.262	0.016 ± 0.030	0.067 ± 0.028	0.028 ± 0.040	0.476 ± 0.263	...
16145207-5026187	UCL	7.548 ± 0.023	7.542 ± 0.020	7.763 ± 0.141	6.110 ± 0.288	0.060 ± 0.040	0.096 ± 0.039	-0.165 ± 0.145	1.416 ± 0.290	...
16145918-2750230	US	8.584 ± 0.023	8.643 ± 0.019	8.538 ± 0.028	7.666 ± 0.177	0.024 ± 0.032	0.014 ± 0.029	0.093 ± 0.036	0.895 ± 0.178	Debris
16153456-2242421	US	7.488 ± 0.026	7.159 ± 0.022	5.136 ± 0.014	2.919 ± 0.022	0.327 ± 0.035	0.655 ± 0.032	2.617 ± 0.027	4.748 ± 0.032	Full
16153587-2529008	US	8.629 ± 0.023	8.610 ± 0.019	8.376 ± 0.030	...	0.022 ± 0.030	0.060 ± 0.027	0.247 ± 0.036	...	...
16155664-3947163	UCL	9.064 ± 0.023	8.978 ± 0.020	8.706 ± 0.024	7.536 ± 0.119	0.006 ± 0.030	0.029 ± 0.028	0.222 ± 0.031	1.248 ± 0.121	Debris
16161423-2643148	US	8.427 ± 0.024	8.398 ± 0.021	8.297 ± 0.029	8.023 ± 0.254	-0.069 ± 0.025	-0.041 ± 0.022	-0.001 ± 0.030	0.187 ± 0.254	...
16161795-2339476	US	8.033 ± 0.023	8.046 ± 0.022	7.996 ± 0.024	7.414 ± 0.122	-0.016 ± 0.029	0.019 ± 0.028	0.038 ± 0.030	0.551 ± 0.123	...
16173138-2303360	US	7.860 ± 0.024	7.894 ± 0.021	7.864 ± 0.021	8.296 ± 0.417	0.050 ± 0.036	0.037 ± 0.034	0.070 ± 0.034	-0.435 ± 0.418	...
16175569-3828132	UCL	9.237 ± 0.024	9.208 ± 0.019	9.076 ± 0.029	8.424 ± 0.308	0.057 ± 0.034	0.031 ± 0.031	0.084 ± 0.038	0.598 ± 0.309	...
16181107-2911125	US	8.321 ± 0.022	8.337 ± 0.020	8.311 ± 0.024	8.273 ± 0.329	-0.026 ± 0.040	0.008 ± 0.039	0.005 ± 0.042	-0.026 ± 0.331	...
16183723-2405226	US	...	...	...	...	...	...	...	...	...
16191217-2550383	US	8.580 ± 0.024	8.555 ± 0.021	8.346 ± 0.035	...	0.151 ± 0.035	0.191 ± 0.033	0.350 ± 0.044	...	Debris
16193396-2228294	US	8.428 ± 0.023	8.451 ± 0.020	8.358 ± 0.026	7.999 ± 0.261	-0.011 ± 0.030	0.003 ± 0.028	0.058 ± 0.032	0.346 ± 0.262	...
16195068-2154355	US	8.065 ± 0.025	8.003 ± 0.021	7.933 ± 0.022	8.185 ± 0.288	0.038 ± 0.030	0.072 ± 0.026	0.064 ± 0.027	-0.300 ± 0.288	...

Table 4.8 (cont'd)

2MASS	Grp.	$W1$	$W2$	$W3$	$W4$	$E(K_S - W1)$	$E(K_S - W2)$	$E(K_S - W3)$	$E(K_S - W4)$	Disk Type
16202930-3254096	US	8.960 ± 0.023	8.989 ± 0.022	8.929 ± 0.029	8.926 ± 0.457	-0.063 ± 0.031	-0.084 ± 0.030	-0.079 ± 0.036	-0.157 ± 0.457	...
16204468-2431384	US	8.292 ± 0.022	8.225 ± 0.020	8.159 ± 0.033	7.975 ± 0.360	0.177 ± 0.030	0.265 ± 0.029	0.334 ± 0.039	0.445 ± 0.361	...
16230783-2300596	US	8.045 ± 0.023	8.033 ± 0.020	7.182 ± 0.085	...	0.046 ± 0.033	0.080 ± 0.031	0.887 ± 0.088	...	Evolved
16233234-2523485	US	7.538 ± 0.025	7.519 ± 0.019	7.398 ± 0.024	6.840 ± 0.134	0.096 ± 0.034	0.144 ± 0.030	0.260 ± 0.033	0.746 ± 0.136	...
16234698-2850023	US	8.537 ± 0.024	8.571 ± 0.021	8.532 ± 0.030	8.752 ± 0.502	0.034 ± 0.035	0.046 ± 0.033	0.052 ± 0.040	-0.237 ± 0.503	...
16235484-3312370	US	8.513 ± 0.022	8.494 ± 0.020	8.479 ± 0.026	8.138 ± 0.269	-0.007 ± 0.032	0.003 ± 0.030	-0.050 ± 0.035	0.198 ± 0.270	...
16240373-4319261	UCL	8.687 ± 0.024	8.678 ± 0.020	8.609 ± 0.027	...	0.059 ± 0.035	0.110 ± 0.033	0.162 ± 0.037	...	...
16240632-2456468	US	8.062 ± 0.025	8.016 ± 0.021	7.955 ± 0.023	7.525 ± 0.228	0.125 ± 0.032	0.186 ± 0.029	0.197 ± 0.030	0.550 ± 0.229	...
16241860-2854475	US	8.207 ± 0.024	8.216 ± 0.020	8.156 ± 0.022	8.027 ± 0.255	0.043 ± 0.033	0.083 ± 0.030	0.117 ± 0.032	0.176 ± 0.256	...
16245136-2239325	US	6.987 ± 0.034	7.003 ± 0.021	6.998 ± 0.020	6.752 ± 0.083	0.015 ± 0.038	0.049 ± 0.028	0.025 ± 0.027	0.202 ± 0.085	...
16250991-3047572	US	7.226 ± 0.029	7.165 ± 0.019	7.227 ± 0.018	7.185 ± 0.112	-0.020 ± 0.036	0.070 ± 0.028	0.003 ± 0.028	-0.027 ± 0.114	...
16251923-2426526	US	7.715 ± 0.024	7.705 ± 0.020	...	...	0.022 ± 0.035	0.061 ± 0.033	...	...	...
16252863-2346265	US	7.699 ± 0.023	7.653 ± 0.019	7.665 ± 0.023	7.689 ± 0.198	0.030 ± 0.035	0.098 ± 0.033	0.042 ± 0.035	-0.056 ± 0.200	...
16253849-2613540	US	6.778 ± 0.041	6.469 ± 0.019	4.844 ± 0.015	2.658 ± 0.025	0.642 ± 0.048	0.933 ± 0.031	2.485 ± 0.028	4.569 ± 0.035	Full
16262736-2756508	US	8.042 ± 0.022	7.967 ± 0.019	7.817 ± 0.021	...	0.049 ± 0.035	0.132 ± 0.033	0.227 ± 0.034	...	...
16263591-3314481	US	8.451 ± 0.021	8.433 ± 0.020	8.483 ± 0.025	...	0.294 ± 0.041	0.334 ± 0.040	0.240 ± 0.043	...	...
16265280-2343127	US	6.317 ± 0.044	6.083 ± 0.020	5.162 ± 0.015	3.202 ± 0.020	0.292 ± 0.048	0.556 ± 0.028	1.437 ± 0.025	3.325 ± 0.028	Transitional
16265700-3032232	US	8.765 ± 0.023	8.771 ± 0.020	8.696 ± 0.032	...	-0.075 ± 0.033	-0.090 ± 0.030	-0.083 ± 0.039	...	...
16265763-3032279	US	7.948 ± 0.024	7.932 ± 0.020	7.994 ± 0.024	7.896 ± 0.232	0.168 ± 0.029	0.129 ± 0.026	-0.012 ± 0.029	-0.052 ± 0.233	...
16271951-2441403	US	8.247 ± 0.022	8.129 ± 0.020	...	...	0.049 ± 0.042	0.112 ± 0.041	...	...	...
16272794-4542403	UCL	8.565 ± 0.025	8.592 ± 0.021	8.478 ± 0.047	7.702 ± 0.179	0.009 ± 0.033	0.028 ± 0.030	0.109 ± 0.051	0.816 ± 0.180	...

Table 4.8 (cont'd)

2MASS	Grp.	$W1$	$W2$	$W3$	$W4$	$E(K_S - W1)$	$E(K_S - W2)$	$E(K_S - W3)$	$E(K_S - W4)$	Disk Type
16273956-2245230	US	8.004 ± 0.024	8.018 ± 0.021	7.884 ± 0.024	7.267 ± 0.134	-0.013 ± 0.035	0.003 ± 0.033	0.097 ± 0.035	0.642 ± 0.136	...
16274028-2422040	US	6.565 ± 0.033	6.101 ± 0.023	4.204 ± 0.015	2.054 ± 0.026	0.548 ± 0.040	1.011 ± 0.033	2.847 ± 0.027	4.911 ± 0.035	Full
16282453-4740395	UCL	9.336 ± 0.024	9.311 ± 0.024	...	...	0.071 ± 0.034	0.041 ± 0.034	...	...	...
16290585-3145250	US	8.951 ± 0.022	8.960 ± 0.020	8.915 ± 0.035	...	0.048 ± 0.030	0.038 ± 0.029	0.022 ± 0.041	...	...
16293397-2455303	US	8.349 ± 0.023	8.351 ± 0.021	8.201 ± 0.037	...	0.089 ± 0.030	0.117 ± 0.028	0.227 ± 0.042	...	...
16294869-2152118	US	7.614 ± 0.024	7.617 ± 0.020	7.523 ± 0.018	6.945 ± 0.094	0.050 ± 0.034	0.084 ± 0.031	0.140 ± 0.030	0.647 ± 0.097	...
16294991-2728498	US	8.503 ± 0.024	8.551 ± 0.020	8.475 ± 0.032	...	0.052 ± 0.035	0.034 ± 0.032	0.070 ± 0.041	...	...
16303796-2954222	US	8.293 ± 0.024	8.299 ± 0.023	8.260 ± 0.038	...	-0.001 ± 0.035	0.015 ± 0.035	0.010 ± 0.046	...	...
16310436-2404330	US	7.575 ± 0.025	7.503 ± 0.021	6.959 ± 0.017	5.242 ± 0.045	0.115 ± 0.036	0.195 ± 0.033	0.684 ± 0.031	2.320 ± 0.052	Evolved
16310837-2651062	US	9.010 ± 0.022	8.976 ± 0.019	9.021 ± 0.039	...	0.164 ± 0.030	0.170 ± 0.028	0.047 ± 0.044	...	...
16315346-2636169	US	8.776 ± 0.023	8.819 ± 0.019	8.786 ± 0.035	...	0.022 ± 0.033	-0.013 ± 0.031	-0.035 ± 0.042	...	...
16320058-2530287	US	9.336 ± 0.024	9.362 ± 0.021	9.409 ± 0.069	...	0.045 ± 0.034	0.001 ± 0.032	-0.119 ± 0.073	...	...
16320160-2530253	US	8.967 ± 0.018	9.046 ± 0.018	9.028 ± 0.050	7.744 ± 0.268	0.334 ± 0.030	0.254 ± 0.030	0.211 ± 0.055	1.409 ± 0.269	...
16320352-2830179	US	7.869 ± 0.023	7.887 ± 0.022	7.860 ± 0.023	...	-0.015 ± 0.039	0.015 ± 0.038	0.011 ± 0.039	...	...
16321179-2440213	US	7.488 ± 0.024	7.302 ± 0.019	6.506 ± 0.016	4.755 ± 0.034	0.341 ± 0.066	0.499 ± 0.064	1.217 ± 0.063	2.856 ± 0.070	Evolved
16322432-1703399	US	7.843 ± 0.023	7.789 ± 0.021	7.811 ± 0.029	8.163 ± 0.463	0.013 ± 0.033	0.027 ± 0.032	-0.075 ± 0.038	-0.551 ± 0.464	...
16334191-2523342	US	7.927 ± 0.024	7.849 ± 0.021	7.739 ± 0.021	7.829 ± 0.185	-0.072 ± 0.034	0.014 ± 0.032	0.069 ± 0.032	-0.102 ± 0.187	...
16340585-2658441	US	8.696 ± 0.023	8.671 ± 0.020	8.630 ± 0.031	8.452 ± 0.331	-0.004 ± 0.033	0.036 ± 0.030	0.027 ± 0.039	0.128 ± 0.332	...
16344629-2606324	US	9.076 ± 0.024	9.090 ± 0.020	8.995 ± 0.032	8.060 ± 0.224	0.038 ± 0.031	0.027 ± 0.028	0.065 ± 0.037	0.916 ± 0.225	Debris
16345314-2518167	US	7.869 ± 0.022	7.878 ± 0.019	7.871 ± 0.020	7.777 ± 0.246	0.020 ± 0.034	0.054 ± 0.032	0.025 ± 0.033	0.050 ± 0.247	...
16351188-2845520	US	8.892 ± 0.023	8.791 ± 0.022	8.628 ± 0.036	7.812 ± 0.222	0.002 ± 0.033	0.085 ± 0.032	0.175 ± 0.043	0.889 ± 0.223	Debris

Table 4.8 (cont'd)

2MASS	Grp.	$W1$	$W2$	$W3$	$W4$	$E(K_S - W1)$	$E(K_S - W2)$	$E(K_S - W3)$	$E(K_S - W4)$	Disk Type
16353547-2541194	US	9.467 ± 0.023	9.477 ± 0.022	9.418 ± 0.057	7.900 ± 0.230	0.048 ± 0.033	0.084 ± 0.033	0.110 ± 0.062	1.559 ± 0.231	Debris
16354836-2148396	US	8.342 ± 0.025	8.230 ± 0.020	8.168 ± 0.028	...	0.025 ± 0.033	0.082 ± 0.029	0.065 ± 0.035	...	...
16384946-2735294	US	8.510 ± 0.023	8.515 ± 0.022	8.493 ± 0.026	...	0.034 ± 0.038	0.066 ± 0.037	0.050 ± 0.040	...	...
16430140-4405275	UCL	9.366 ± 0.021	9.447 ± 0.019	10.062 ± 0.111	...	0.224 ± 0.032	0.191 ± 0.031	-0.455 ± 0.114	...	...
16432519-3022477	US	8.850 ± 0.023	8.885 ± 0.020	8.844 ± 0.031	...	0.050 ± 0.031	0.052 ± 0.029	0.055 ± 0.037	...	...
16452615-2503169	US	6.983 ± 0.034	6.616 ± 0.019	5.388 ± 0.014	3.713 ± 0.021	0.649 ± 0.043	1.031 ± 0.032	2.209 ± 0.030	3.807 ± 0.033	Full
16473710-2014268	US	9.382 ± 0.022	9.369 ± 0.020	9.339 ± 0.042	...	-0.062 ± 0.029	-0.041 ± 0.028	-0.066 ± 0.046	...	...
16491330-4355279	UCL	...	...	...	...	...	...	...	...	...

Table 4.9. Stellar Parameters for Sco-Cen Main Sequence Turnoff Stars

Object Name	Spectral Type	Ref.	Region	A_V (mag)	$\log(T_{\rm eff})$ (dex)	$\log(L/L_\odot)$ (dex)	Age Myr
τ Sco	B0V	1	US	0.109±0.029	4.505±0.004	4.351±0.125	1
δ Sco	B0.5IV	1	US	0.432±0.025	4.479±0.030	4.664±0.133	7
σ Sco	B1III	1	US	1.203±0.009	4.466±0.028	5.019±0.126	8
β^1 Sco	B0.5V	1	US	0.547±0.031	4.464±0.021	4.394±0.096	7
β Cru	B0.5III	2	LCC	0.077±0.006	4.458±0.014	4.414±0.079	8
μ Cen	B2IV-Ve	2	UCL	0.257±0.030	4.456±0.040	4.163±0.092	4
ω Sco	B1V	1	US	0.647±0.013	4.454±0.016	4.013±0.048	1
π Sco	B1V+B2:V:	1	US	0.204±0.005	4.437±0.030	4.411±0.119	10
α^1 Cru	B0.5IV	2	LCC	0.018±0.041	4.436±0.038	4.664±0.094	11
β Cen	B1III	2	LCC	0.075±0.031	4.428±0.022	4.905±0.072	11
δ Cru	B2IV	2	LCC	0.000±0.007	4.403±0.025	3.838±0.056	6
ν Cen	B2IV	2	UCL	0.025±0.003	4.386±0.031	3.772±0.070	8
δ Lup	B1.5IV	2	UCL	0.030±0.017	4.384±0.033	4.455±0.145	15
μ^1 Sco	B1.5IV	2	UCL	0.060±0.010	4.363±0.030	4.011±0.142	19
α Lup	B1.5III	2	UCL	0.094±0.009	4.360±0.014	4.237±0.037	19
μ^2 Sco	B2IV	2	UCL	0.051±0.014	4.356±0.033	3.724±0.072	17
1 Sco	B1.5Vn	1	US	0.462±0.008	4.355±0.016	3.490±0.049	5
β Lup	B2III	2	UCL	0.045±0.008	4.354±0.018	3.891±0.043	20
η Lup	B2.5IV	2	UCL	0.003±0.003	4.352±0.031	3.685±0.070	17
α Mus	B2IV-V	2	LCC	0.015±0.015	4.351±0.024	3.696±0.054	18
η Cen	B1.5Vn	2	UCL	0.021±0.021	4.349±0.021	3.796±0.024	21
ϕ Cen	B2IV	2	UCL	0.000±0.019	4.345±0.030	3.666±0.069	19
ν Sco	B2IV	1	US	0.756±0.021	4.341±0.012	3.800±0.100	23
β^2 Sco	B2IV-V	1	US	0.538±0.025	4.340±0.018	3.190±0.130	<1
γ Lup	B2IV	2	UCL	0.018±0.003	4.337±0.030	3.880±0.085	24
ρ Sco	B2IV-V	1	US	0.081±0.033	4.335±0.032	3.561±0.074	18
HR 6143	B2III	2	UCL	0.161±0.016	4.326±0.019	3.580±0.050	23
υ^1 Cen	B2IV-V	2	UCL	0.009±0.020	4.318±0.027	3.410±0.062	18
ξ^2 Cen	B1.5V	2	LCC	0.061±0.005	4.308±0.029	3.329±0.069	18
κ Cen	B2IV	2	UCL	0.015±0.008	4.306±0.029	3.591±0.082	30
σ Cen	B2V	2	LCC	0.060±0.022	4.303±0.032	3.358±0.073	23

Table 4.9 (cont'd)

Object Name	Spectral Type	Ref.	Region	A_V (mag)	$\log(T_{\rm eff})$ (dex)	$\log(L/L_\odot)$ (dex)	Age Myr
χ Cen	B2V	2	UCL	0.018±0.012	4.302±0.025	3.342±0.061	23
13 Sco	B2V	1	US	0.112±0.005	4.300±0.022	3.234±0.052	15
μ^1 Cru	B2IV-V	2	LCC	0.067±0.009	4.297±0.025	3.309±0.057	24
ϵ Lup	B2IV-V	2	UCL	0.035±0.022	4.277±0.029	3.692±0.114	>30
HR 5378	B7IIIp	2	UCL	0.038±0.012	4.273±0.019	3.152±0.049	28
HR 5471	B3V	2	UCL	0.045±0.002	4.251±0.029	3.034±0.064	>30
θ Lup	B2.5Vn	2	UCL	0.031±0.020	4.248±0.035	3.106±0.092	>30
HR 4618	B2IIIne	2	LCC	0.043±0.009	4.247±0.010	3.058±0.075	>30
ζ Cru	B2.5V	2	LCC	0.021±0.021	4.246±0.025	3.048±0.070	>30
τ Lib	B2.5V	2	UCL	0.028±0.006	4.242±0.031	3.218±0.071	>30

Note. — Ages were estimated using the Ekström et al. (2012) rotating evolutionary models with solar abundances. Spectral Type references: (1) Hiltner et al. (1969); (2) Garrison (1967);

Table 4.10. Stellar Parameters for Sco-Cen G-Type Stars

Object Name	2MASS	Spectral Type	Ref.	Region	A_V (mag)	$\log(T_{\rm eff})$ (dex)	$\log(L/L_\odot)$ (dex)	Age Myr	Mass $M_\odot$
TYC 9216-0524-1	10495605-6951216	G8V	T06	LCC	0.00±0.05	3.717±0.007	-0.384±0.069	49	0.9
TYC 9212-1782-1	10594094-6917037	G6V	T06	LCC	0.00±0.02	3.732±0.008	0.426±0.085	6	1.6
CD-48 6632	11350376-4850219	G7V	T06	LCC	0.00±0.15	3.709±0.008	0.046±0.075	12	1.2
HIP 57524	11472454-4953029	G0V	PM	LCC	0.18±0.04	3.782±0.004	0.411±0.061	17	1.3
CPD-63 2126	12041439-6418516	G8V	T06	LCC	0.00±0.04	3.717±0.007	0.010±0.071	16	1.1
MML 3	12044888-6409555	G1V	PM	LCC	0.38±0.06	3.776±0.007	0.482±0.084	13	1.3
HIP 58996	12054748-5100121	G1V	PM	LCC	0.15±0.04	3.776±0.007	0.405±0.057	16	1.3
MML 7	12113815-7110360	G5V	PM	LCC	0.23±0.02	3.740±0.009	0.336±0.067	10	1.4
HIP 59854	12162783-5008356	G1V	PM	LCC	0.31±0.05	3.776±0.007	0.529±0.061	13	1.4
MML 14	12211648-5317450	G1V	PM	LCC	0.39±0.05	3.776±0.007	0.431±0.067	15	1.3
MML 17	12223322-5333489	G0V	PM	LCC	0.24±0.03	3.782±0.004	0.446±0.066	16	1.3
CD-54 4763	12242065-5443540	G5V	T06	LCC	1.00±0.39	3.740±0.009	0.596±0.085	7	1.7
HIP 60885	12284005-5527193	G0V	PM	LCC	0.20±0.04	3.782±0.004	0.480±0.057	15	1.3
HIP 60913	12290224-6455006	G2V	PM	LCC	0.44±0.04	3.769±0.009	0.496±0.060	11	1.4
MML 29	13023752-5459370	G0V	PM	LCC	0.44±0.10	3.782±0.004	0.255±0.072	23	1.2
HIP 63847	13050530-6413552	G4V	PM	LCC	0.19±0.03	3.750±0.009	0.318±0.058	13	1.3
CD-59 4629	13132810-6000445	G3V	T06	LCC	0.10±0.04	3.759±0.009	0.287±0.068	16	1.2
MML 32	13175694-5317562	G0V	PM	LCC	0.75±0.14	3.782±0.004	0.614±0.102	11	1.4
MML 33	13220446-4503231	G0V	PM	LCC	0.16±0.05	3.782±0.004	0.218±0.057	24	1.1
HIP 65423	13243512-5557242	G3V	T06	LCC	0.00±0.02	3.759±0.009	0.330±0.057	14	1.3

Table 4.10 (cont'd)

Object Name	2MASS	Spectral Type	Ref.	Region	A_V (mag)	$\log(T_{\rm eff})$ (dex)	$\log(L/L_\odot)$ (dex)	Age Myr	Mass $M_\odot$
HIP 65517	13254783-4814577	G1V	PM	LCC	0.23±0.05	3.776±0.007	0.102±0.053	28	1.1
MML 35	13342026-5240360	G0V	PM	LCC	0.38±0.07	3.782±0.004	0.476±0.058	15	1.3
MML 37	13432853-5436434	G0V	PM	LCC	0.33±0.04	3.782±0.004	0.211±0.053	25	1.1
HIP 67522	13500627-4050090	G0V	PM	UCL	0.23±0.04	3.782±0.004	0.231±0.063	24	1.1
MML 42	14160567-6917359	G1V	PM	LCC	0.17±0.02	3.776±0.007	0.260±0.059	22	1.2
HIP 71178	14332578-3432376	G9IV	PM	UCL	0.12±0.02	3.709±0.008	0.029±0.057	13	1.2
MML 49	14473176-4800056	G7IV	PM	UCL	0.00±0.04	3.723±0.007	-0.111±0.067	25	1.0
MML 52	14571962-3612274	G3V	PM	UCL	0.43±0.03	3.759±0.009	0.303±0.062	15	1.2
MML 56	15011155-4120406	G0V	PM	UCL	0.32±0.04	3.782±0.004	0.611±0.068	11	1.4
MML 57	15015882-4755464	G0V	PM	UCL	0.24±0.04	3.782±0.004	0.331±0.071	20	1.2
MML 61	15125018-4508044	G2V	PM	UCL	0.31±0.04	3.769±0.009	0.163±0.082	24	1.1
MML 62	15180174-5317287	G6V	PM	UCL	0.31±0.01	3.732±0.008	0.039±0.063	19	1.1
TYC 8298-1675-1	15193702-4759341	G9IV	T06	UCL	0.00±0.02	3.709±0.008	-0.338±0.069	39	0.9
HIP 75483	15251169-4659132	G9V	T06	UCL	0.00±0.16	3.709±0.008	-0.222±0.067	28	1.0
HIP 75924	15302626-3218122	G3V	PM	UCL	0.33±0.11	3.759±0.009	0.570±0.063	8	1.6
HIP 76472	15370466-4009221	G0V	PM	UCL	0.52±0.03	3.782±0.004	0.558±0.060	13	1.4
MML 69	15392440-2710218	G5V	PM	UCL	0.34±0.11	3.740±0.009	0.449±0.070	7	1.6
HIP 77135	15445769-3411535	G3V	PM	UCL	0.43±0.04	3.759±0.009	0.064±0.064	26	1.1
HIP 77144	15450184-4050310	G0V	PM	UCL	0.19±0.10	3.782±0.004	0.405±0.060	17	1.3
HIP 77190	15454266-4632334	G5IV	T06	UCL	0.00±0.03	3.740±0.009	-0.202±0.059	39	0.9

Table 4.10 (cont'd)

Object Name	2MASS	Spectral Type	Ref.	Region	A_V (mag)	$\log(T_{eff})$ (dex)	$\log(L/L_\odot)$ (dex)	Age Myr	Mass $M_\odot$
MML 72	15465179-4919048	G7V	PM	UCL	0.13±0.04	3.723±0.007	0.134±0.064	12	1.3
HIP 77656	15511373-4218513	G7V	PM	UCL	0.00±0.01	3.723±0.007	0.337±0.062	7	1.5
TYC 7846-1538-1	15532729-4216007	G2	T06	UCL	0.88±0.35	3.769±0.009	0.380±0.067	15	1.3
J155459.9-234718	15545986-2347181	G2IV	W94	US	0.46±0.12	3.769±0.009	0.312±0.070	18	1.2
J155548.7-251223	15554883-2512240	G3	P99	US	0.40±0.03	3.759±0.009	0.430±0.076	12	1.4
HIP 78133	15571468-4130205	G3V	T06	UCL	0.00±0.07	3.759±0.009	0.061±0.066	27	1.1
HD 143099	15595826-3824317	G0V	T66	UCL	0.00±0.05	3.782±0.004	0.447±0.066	16	1.3
J160000.7-250941	16000078-2509423	G0	P99	US	0.37±0.17	3.782±0.004	0.254±0.074	23	1.2
TYC 7333-1260-1	16010792-3254526	G1V	T06	UCL	0.21±0.06	3.776±0.007	0.369±0.061	17	1.2
MML 75	16010896-3320141	G5IV	PM	UCL	0.81±0.05	3.740±0.009	0.478±0.066	7	1.6
HIP 78483	16011842-2652212	G2IV	T06	US	0.33±0.07	3.769±0.009	0.708±0.077	8	1.6
HIP 78581	16024415-3040013	G1V	H82	US	0.08±0.05	3.776±0.007	0.351±0.069	18	1.2
HIP 79462	16125533-2319456	G2V	H88	US	0.53±0.13	3.769±0.009	0.885±0.077	5	1.9
MML 82	16211219-4030204	G8V	PM	UCL	0.00±0.07	3.717±0.007	0.202±0.063	9	1.4
MML 83	16232955-3958008	G1V	PM	UCL	0.48±0.12	3.776±0.007	0.210±0.084	24	1.1
HIP 80320	16235385-2946401	G3IV	T06	US	0.05±0.02	3.759±0.009	0.457±0.071	11	1.4
HIP 80535	16262991-2741203	G0V	H82	US	0.00±0.03	3.782±0.004	0.725±0.071	9	1.6
HIP 80636	16275233-3547003	G0V	PM	UCL	0.36±0.05	3.782±0.004	0.561±0.060	13	1.4
HIP 81380	16371286-3900381	G2V	PM	UCL	0.34±0.08	3.769±0.009	0.796±0.069	6	1.8
HIP 81447	16380553-3401106	G0V	PM	UCL	0.12±0.16	3.782±0.004	0.812±0.065	8	1.7

Table 4.10 (cont'd)

Object Name	2MASS	Spectral Type	Ref.	Region	A_V (mag)	$\log(T_{\rm eff})$ (dex)	$\log(L/L_\odot)$ (dex)	Age Myr	Mass $M_\odot$

Note. — G-type stars not included in Table 4.6. Ages and masses were estimated using the median of Tognelli et al. (2011), Dotter et al. (2008), Siess et al. (2000), and Baraffe et al. (1998) evolutionary models. Spectral Type references: (PM) This work; (T06) Torres et al. (2006); (W94) Walter et al. (1994); (P99) Preibisch & Zinnecker (1999); (T66) Thackeray (1966); (H82) Houk (1982); (H88) Houk & Smith-Moore (1988)
Adopted median subgroup ages (Table 4.1) are preferable to uncertain individual ages listed above.

5 Conclusions

This thesis research was aimed at studying the star-formation history of the three subgroups of the nearest OB association, Scorpius-Centaurus. Before this thesis work began it was thought that Upper Sco was ∼1/3 the age of the two older subgroups. However, a careful analysis of the US mean age gave consistent results, the main sequence turn-off, the massive supergiant Antares, the A-type stars, the F-type stars, and the G-type stars all had age estimates which were significantly older than 5 Myr and consistent with ∼10 Myr. An estimate of the expansion age for Upper Sco gave a 99% confidence lower limit of ∼10.5 Myr. This evidence led me to revise the age upwards by a factor of two. The revision of the age of Upper Sco implies that the substellar companions discovered around US members are significantly more massive than previously thought. The mass is roughly proportional to the square root of the age, so our revised mass estimates for US substellar companions represents an increase of 20-70% over previous estimates using a 5 Myr age, which makes a qualitative difference in the nature of these low-mass objects.

In order to increase the number of known, low-mass members of the two older subgroups of Sco-Cen, I performed a low-resolution spectroscopic survey for new K/M-type members of Sco-Cen. However, motivated by systematic problems with the colors of pre-MS stars, I used known members of nearby, young moving groups –

the TW Hydrae Association (TWA), the β Pic moving group, the Tucana-Horologium Association and the η Cha cluster – to construct a spectral type – intrinsic color – T_{eff}– bolometric correction (BC) sequence for pre-MS stars. This sequence should reduce systematic errors when dereddening pre-MS stars in nearby star-forming regions and placing them on the H-R diagram. This, in turn, should improve accuracy in placing F0 through M5 pre-MS stars on the H-R diagram and provide better tests of stellar evolutionary models. Our T_{eff} scale is systematically $\sim$250 K cooler than dwarf temperatures at a given type for spectral types G5 through K6, while those for F0-G4 and K7-M5 are within $\sim$100 K of their main sequence counterparts. For M0-M5 stars, our T_{eff} scale is much closer to dwarf scales than the widely-used T_{eff} scale constructed for very young ($\sim$3 Myr) pre-MS stars from Luhman (1999); Luhman et al. (2003). Independent observational tests of these T_{eff} scales are currently difficult to implement, but pre-MS eclipsing binaries with high-precision stellar mass and radius measurements would help place the T_{eff} scale on a more model-independent footing.

We use proven X-ray and proper motion selection techniques to improve the census for K and M-type members of all three subgroups of Sco-Cen. We use our newly constructed intrinsic color, T_{eff}, and BC scale for 5-30 Myr old pre-MS stars to place our sample on the H-R diagram. Consistent with previous findings (e.g., Hillenbrand et al., 2008), we see a mass-dependent age trend. To assess the mean ages of the subgroups, we use the ages from the high-mass main sequence turn-off stars, the F-type stars and the G-type stars. We estimate mean ages of 10$\pm$3 Myr for Upper Scorpius, 16$\pm$2 Myr for Upper Centaurus-Lupus, and 16$\pm$3 Myr for Lower Centaurus-Crux. We place constraints on the age spreads in the three subgroups from H-R diagram scatter, which indicates that the 1σ Gaussian age spreads in the three subgroups is $\pm$6 Myr for US, $\pm$5 Myr for UCL and $\pm$6 Myr for LCC. These small age spreads indicate

that star formation proceeded rapidly in Sco-Cen. Using more than 600 members, we create an age map of Sco-Cen, which shows regions which are systematically younger or older than the mean age. This shows an age gradient from UCL into US, and indicates that the older subgroups, UCL and LCC, have a star-formation history which is more complex than US. This map is a first step towards testing models of star formation and evaluating triggered star-formation hypotheses.

Finally, we use Hα as a spectroscopic accretion diagnostic, along with WISE IR photometry to perform a census for primordial gas-rich disks in our sample in order to constrain the protoplanetary disk dispersal timescale and thus constrain planet formation timescales. If we assume all stars are born with a disk (a disk fraction of 100% at t=0 Myr), and only consider our three populations, we find that fitting an exponential decay model to the data gives an e-folding timescale of 4.8 Myr for solar analog ($\sim$0.7-1.2 $M_\odot$) stars, much longer than that estimated by Mamajek (2009) using data from the literature. If the suggestion of Naylor (2009) is correct and most pre-MS cluster ages are underestimated, then disk dispersal timescales are actually $\sim$50% longer than current estimates. This should ease constraints on core-accretion planet simulations, which have difficulty forming planets in $\lesssim$10 Myr (Pollack et al. 1996; though see also Hubickyj et al. 2005).

A Membership of TWA 9 to the TW Hya Association

The membership of TWA 9 to the TW Hya Association merits some discussion. Weinberger et al. (2012) showed that the space motion of TWA 9A is more than 3σ from the mean of the association, and concluded that it was either not a member or the *Hipparcos* distance is underestimated. However, when considering the TWA centroid space motion (Weinberger et al., 2012), the Tycho-2 proper motion (μ_α*=-55.4±2.3 mas yr^{-1}, μ_δ=-17.7±2.3 mas yr^{-1}; Høg et al. 2000) of TWA 9A seems consistent with membership in TWA. Assuming it is a member and adopting the TWA mean group space motions from Weinberger et al. (2012) of (U, V, W) = (-10.9±0.2, -18.2±0.2, -5.3±0.2) km s^{-1}, the kinematic parallax places it at 70.0±3.8 pc. If we adopt this kinematic distance with the Bailey et al. 2012 mean radial velocity for component A and B of 11.964±0.024 km s^{-1}, the 3-D space motion of TWA 9A is then (U, V, W) = (-10.2±1.2, -19.7±0.8, -4.8±0.6) km s^{-1}. This is consistent with the mean TWA space motions in the Weinberger et al. (2012) study. Furthermore, the kinematic distance would decrease the absolute magnitude M_H by ≈0.83 mag over the *Hipparcos* distance (using d=π^{-1}, where π is the trigonometric *Hipparcos* parallax), and thus the isochronal age of TWA 9A would be ∼16 Myr, closer to the isochronal ages obtained by Weinberger et al. (2012) for other TWA members.

TWA 9A exhibits very high Li (EW(Li 6708Å)=470 mÅ; Torres et al. 2006), lies in the direction of other TWA members, has proper motion consistent with membership in TWA, and, adopting the kinematic distance of 70.0±3.8 pc, has a space motion and isochronal age consistent with membership in TWA. Thus, we retain TWA 9A and TWA 9B as members of TWA and suggest that the *Hipparcos* parallax is most likely $\sim 3\sigma$ in error.

B Spectral Transition from K7 to M0

Some spectral surveys implicitly or explicitly do not recognize or use spectral types K8 and K9. While spectral types K8 and K9 are not considered full subtypes of the spectral classification system (Keenan, 1984), it should be pointed out that neither are G1, G3, G4, G6, G7 or G9, yet these classifications are consistently recognized and used (e.g., Gray et al., 2003). Keenan (1984) noted that subdivisions such as G3 simply means the object is closer to G2 than G5, and that they should be used when it is possible to classify the objects accurately enough to justify their use. Keenan (1984) considered K5 and M0 one subtype apart even though the difference in their B–V color is 0.3 mag, larger than the difference between M0 and M4 (see Table C.1). From the standpoint of spectral classification, there is nothing different about the K7 to M0 transition that merits such a gap in spectral types. Therefore we find no compelling reason to omit spectral types K8 and K9 from use and we include them here in all of our analysis.

With low-resolution red optical spectra we can distinguish between subtypes K7, K8, K9 and M0. Unfortunately, K8V and K9V spectral standards do not appear in the literature (e.g., Gray & Corbally 2009). For these subtypes, we adopted stars as standards which were assigned this classification by an expert classifier. For K8V we adopted HIP 111288 (V–K_S=3.519±0.020 mag; Perryman & ESA 1997; Skrutskie

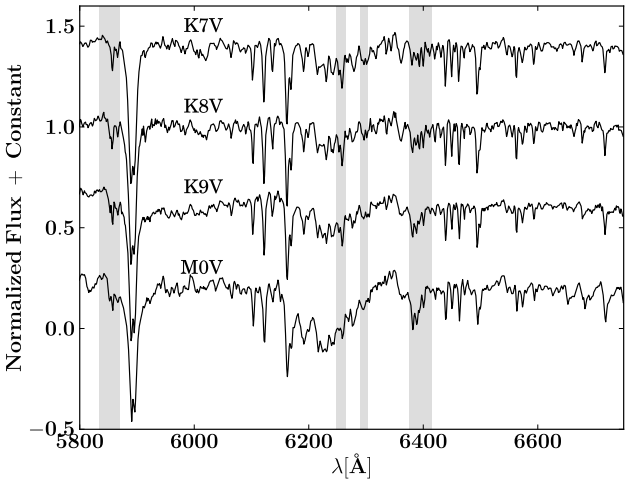

Figure B.1 The spectral transition from K7 to M0, with regions most useful for discriminating among the different spectral types highlighted in grey. GJ 673 (K7V), HIP 111288 (K8Vk), HIP 3261 (K9V) and GJ 701 (M0.0V) are shown.

et al. 2006), classified as K7V by Stephenson (1986) but later classified as K8Vk by Gray et al. (2006). For K9V we adopted HIP 3261 (V–K_S=3.696±0.019 mag; Perryman & ESA 1997; Skrutskie et al. 2006), classified as K7.0 by Hawley et al. (1996) but later classified as K9V by Gray et al. (2006). These were chosen because they were classified as intermediate between K7 and M0 but also because they have V–K_S colors intermediate between K7 and M0. We visually inspected the spectra of both adopted standards and verified that they were morphologically intermediate between the K7V and M0V standards.

Shown in Figure B.1 is the spectral sequence from K7 to M0. The spectra show a distinct progression in the CaH band at $\lambda\lambda$ 6382-6389 (Kirkpatrick et al., 1991; Torres-Dodgen & Weaver, 1993; Allen & Strom, 1995) which gradually becomes stronger than the Fe I lines at 6400Å and 6393Å. Another very useful discriminant is the relative strength of the V, Ti, and Fe blend at 6297Å to the Fe I blend at 6302Å. As the TiO band ∼6080-6390Å increases in strength going from the late K-types to M0,

the relative strength of these two lines gradually changes, with the blend at 6297Å becoming stronger at K8.

Lastly, we mention that skipping from K7 to M0 may hide important discrepancies between models and observations. Casagrande et al. (2008) has noted that, among main sequence dwarf stars, there appears to be a plateau in luminosity in the transition region between K and M where the stars appear to be decreasing in temperature with very little decrease in luminosity. Theoretical models do not appear to reproduce the plateau. Using subtypes K8 and K9, when possible, presents an opportunity for observational work to make contact with theoretical models in this transition region.

C Dwarf Colors

In order to accurately compare the empirical intrinsic colors and $T_{\rm eff}$ scale of pre-MS stars to dwarfs and identify differences, the empirical intrinsic colors of dwarf stars must be accurately tabulated. Here we describe the construction of a modern dwarf color, $T_{\rm eff}$, and bolometric correction sequence, which has been an ongoing process carried out by EM over the course of several years. A preliminary version of this sequence (A0V-G9V) was previously published in Pecaut et al. (2012). The primary motivations for constructing this sequence were that (1) consistent color sequences had not been constructed explicitly including the 2MASS and WISE bands, (2) the methodology of the construction of previous sequences was not always made clear, (3) systematic differences exist between some of the widely cited past sequences, (4) there have been sizable shifts in effective temperatures reported for stars (especially at the hotter and cooler ends) over the past few decades, and (5) there have been subtle changes to the dwarf spectral sequence over the decades, especially among the M dwarfs. In light of the subtle shifts of the MK system over the past decades, improvements in the modeling of stellar atmospheres, and given the large volume of optical-IR photometry and derived stellar parameters in the literature now, a reevaluation of the temperature and colors scales is overdue.

We present our modern intrinsic color-$T_{\rm eff}$-spectral type tabulation for dwarfs in

Table C.1. This color tabulation was independently and empirically derived, and is *not* dependent on previous compendia of dwarf photometric properties. There were several stages that went into assembling Table C.1. When discussing samples of "nearby stars", we assumed that stars with trigonometric parallax distances within 75 pc had negligible reddening (e.g. Reis et al., 2011), and so could be used to estimate intrinsic colors without correction. Medians were used throughout in preference to means to avoid swaying by interloper data (Gott et al., 2001), although stronger weighting was often given to values for individual well-studied standards stars in preference to median values estimated for large numbers of non-standard stars classified as a given subtype. While many of the intrinsic colors are quoted to 0.001 mag precision, the typical uncertainty in the mean colors is $\sim$0.01 mag, but can be upwards of a few hundredths of a magnitude for the M-type dwarfs (where the uncertainties in the mean reflect differences among the colors of the standard stars themselves, and mean colors for stars of a given subtype). The first step was to estimate the mean intrinsic colors for each dwarf spectral subtype among one or more colors sensitive to spectral type, using both standard stars and samples of field stars with subtypes measured by expert classifiers. To anchor spectral type to these colors sensitive to spectral type, we used dereddened U-B colors for OB dwarf stars, B-V colors for AFGK dwarfs, and V-K_s colors for M dwarfs.

Table C.1. Intrinsic Colors of O9-M9 Dwarfs and Adopted T_{eff}, BC Values

Spectral Type	T_{eff} (K)	BC_V (mag)	$U–B$ (mag)	$B–V$ (mag)	$V–I_C$ (mag)	$V–J$ (mag)	$V–H$ (mag)	$V–K_S$ (mag)	$K–W1$ (mag)	$K–W2$ (mag)	$K–W3$ (mag)	$K–W4$ (mag)
O9V	34000	-3.160	-1.114	-0.311	-0.369	-0.765	-0.929	-1.000	...	...	...	...
O9.5V	32000	-3.020	-1.087	-0.305	-0.361	-0.747	-0.908	-0.977	...	...	...	...
B0V	31500	-2.990	-1.070	-0.300	-0.355	-0.734	-0.893	-0.961	...	...	...	...
B0.5V	28000	-2.790	-1.026	-0.295	-0.338	-0.697	-0.850	-0.913	...	...	...	...
B1V	26000	-2.570	-0.995	-0.278	-0.325	-0.669	-0.816	-0.874	...	...	...	...
B1.5V	24800	-2.390	-0.910	-0.250	-0.281	-0.572	-0.704	-0.751	...	...	...	...
B2V	20600	-2.020	-0.790	-0.210	-0.230	-0.459	-0.572	-0.604	...	...	...	...
B2.5V	18500	-1.750	-0.732	-0.193	-0.210	-0.416	-0.521	-0.547	...	...	...	...
B3V	17000	-1.540	-0.673	-0.178	-0.192	-0.374	-0.473	-0.494	...	...	...	...
B4V	16700	-1.490	-0.619	-0.165	-0.176	-0.339	-0.432	-0.449	...	...	...	...
B5V	15700	-1.330	-0.581	-0.156	-0.165	-0.316	-0.405	-0.419	...	...	...	...
B6V	14500	-1.120	-0.504	-0.140	-0.145	-0.271	-0.352	-0.360	...	...	...	...
B7V	14000	-1.030	-0.459	-0.128	-0.133	-0.245	-0.322	-0.326	...	...	...	...
B8V	12500	-0.750	-0.364	-0.109	-0.108	-0.190	-0.258	-0.255	...	...	...	...
B9V	10700	-0.400	-0.200	-0.070	-0.061	-0.087	-0.137	-0.121	...	...	...	...
B9.5V	10400	-0.340	-0.130	-0.050	-0.035	-0.025	-0.069	-0.048	...	...	...	...
A0V	9700	-0.200	-0.005	0.000	0.004	0.046	0.014	0.042	...	...	...	...
A1V	9200	-0.110	0.033	0.043	0.044	0.094	0.070	0.101	...	...	...	...
A2V	8840	-0.060	0.063	0.074	0.092	0.167	0.158	0.192	...	...	...	...
A3V	8550	-0.020	0.077	0.090	0.110	0.197	0.196	0.231	...	...	...	...

Table C.1 (cont'd)

Spectral Type	T_{eff} (K)	BC_V (mag)	$U–B$ (mag)	$B–V$ (mag)	$V–I_C$ (mag)	$V–J$ (mag)	$V–H$ (mag)	$V–K_S$ (mag)	$K–W1$ (mag)	$K–W2$ (mag)	$K–W3$ (mag)	$K–W4$ (mag)
A4V	8270	0.000	0.097	0.140	0.165	0.296	0.318	0.355	...	...	...	...
A5V	8080	0.010	0.100	0.160	0.187	0.334	0.366	0.404	...	...	...	...
A6V	8000	0.020	0.098	0.170	0.198	0.355	0.391	0.429	...	...	...	...
A7V	7800	0.040	0.091	0.210	0.242	0.433	0.488	0.528	...	...	...	...
A8V	7500	0.040	0.082	0.253	0.291	0.512	0.589	0.632	...	...	...	...
A9V	7440	0.040	0.080	0.255	0.294	0.517	0.595	0.638	...	...	...	...
F0V	7200	0.030	0.053	0.294	0.339	0.589	0.687	0.732	0.023	0.037	-0.021	0.054
F1V	7030	0.030	0.021	0.334	0.385	0.662	0.781	0.828	0.027	0.036	-0.019	0.052
F2V	6810	0.020	-0.008	0.374	0.432	0.735	0.875	0.925	0.031	0.034	-0.017	0.050
F3V	6720	0.010	-0.016	0.389	0.449	0.763	0.910	0.961	0.032	0.034	-0.016	0.049
F4V	6640	0.000	-0.026	0.412	0.476	0.806	0.965	1.017	0.035	0.033	-0.014	0.048
F5V	6510	0.000	-0.029	0.438	0.506	0.852	1.025	1.079	0.037	0.032	-0.012	0.047
F6V	6340	-0.010	-0.021	0.484	0.553	0.929	1.128	1.185	0.041	0.030	-0.007	0.045
F7V	6240	-0.020	-0.012	0.510	0.579	0.971	1.184	1.244	0.043	0.028	-0.005	0.045
F8V	6150	-0.030	0.000	0.530	0.599	1.004	1.229	1.290	0.045	0.027	-0.003	0.044
F9V	6040	-0.040	0.014	0.552	0.620	1.040	1.277	1.340	0.046	0.026	-0.001	0.044
G0V	5940	-0.050	0.049	0.588	0.656	1.097	1.355	1.421	0.049	0.024	0.003	0.045
G1V	5880	-0.060	0.067	0.604	0.672	1.123	1.390	1.458	0.050	0.023	0.005	0.045
G2V	5770	-0.070	0.133	0.650	0.713	1.198	1.491	1.564	0.053	0.020	0.009	0.046
G3V	5700	-0.080	0.152	0.661	0.722	1.217	1.516	1.590	0.053	0.019	0.010	0.047

Table C.1 (cont'd)

Spectral Type	T_{eff} (K)	BC_V (mag)	U–B (mag)	B–V (mag)	V–I_C (mag)	V–J (mag)	V–H (mag)	V–K_S (mag)	K–$W1$ (mag)	K–$W2$ (mag)	K–$W3$ (mag)	K–$W4$ (mag)
G4V	5640	-0.100	0.175	0.674	0.733	1.239	1.546	1.621	0.054	0.018	0.011	0.048
G5V	5620	-0.100	0.185	0.680	0.738	1.249	1.559	1.635	0.055	0.017	0.012	0.048
G6V	5580	-0.110	0.229	0.704	0.759	1.290	1.614	1.693	0.056	0.016	0.014	0.050
G7V	5520	-0.120	0.243	0.713	0.766	1.303	1.632	1.712	0.056	0.015	0.015	0.050
G8V	5490	-0.130	0.284	0.737	0.786	1.344	1.686	1.768	0.058	0.013	0.017	0.052
G9V	5340	-0.170	0.358	0.777	0.820	1.409	1.774	1.861	0.059	0.010	0.020	0.056
K0V	5260	-0.200	0.436	0.816	0.853	1.475	1.862	1.953	0.061	0.007	0.023	0.060
K1V	5170	-0.230	0.502	0.847	0.883	1.535	1.940	2.034	0.063	0.005	0.025	0.064
K2V	5040	-0.280	0.600	0.893	0.929	1.624	2.056	2.155	0.065	0.003	0.029	0.070
K3V	4810	-0.390	0.801	0.990	1.025	1.810	2.300	2.410	0.070	0.001	0.039	0.086
K4V	4600	-0.520	1.004	1.100	1.190	2.064	2.608	2.733	0.078	0.008	0.059	0.112
K5V	4500	-0.590	1.056	1.134	1.246	2.145	2.705	2.835	0.082	0.014	0.067	0.121
K6V	4300	-0.730	1.199	1.257	1.448	2.434	3.039	3.190	0.096	0.044	0.110	0.165
K7V	4000	-0.950	1.222	1.336	1.574	2.616	3.239	3.407	0.106	0.072	0.144	0.200
K8V	3960	-1.010	1.213	1.382	1.671	2.743	3.373	3.554	0.113	0.094	0.171	0.228
K9V	3860	-1.100	1.198	1.418	1.802	2.907	3.531	3.728	0.122	0.123	0.204	0.265
M0V	3820	-1.150	1.190	1.431	1.848	2.965	3.587	3.790	0.125	0.134	0.217	0.280
M1V	3700	-1.470	1.171	1.484	2.075	3.265	3.873	4.100	0.140	0.191	0.280	0.357
M2V	3550	-1.610	1.170	1.508	2.173	3.406	4.006	4.240	0.146	0.217	0.308	0.393
M3V	3400	-2.100	1.181	1.544	2.420	3.769	4.348	4.600	0.160	0.277	0.374	0.481

Table C.1 (cont'd)

Spectral Type	T_{eff} (K)	BC_V (mag)	$U–B$ (mag)	$B–V$ (mag)	$V–I_C$ (mag)	$V–J$ (mag)	$V–H$ (mag)	$V–K_S$ (mag)	$K–W1$ (mag)	$K–W2$ (mag)	$K–W3$ (mag)	$K–W4$ (mag)
M4V	3200	-2.550	1.215	1.658	2.825	4.411	4.968	5.250	0.182	0.348	0.465	0.586
M5V	3000	-3.240	1.433	1.874	3.277	5.051	5.631	5.942	0.212	0.380	0.544	0.669
M6V	2750	-4.340	...	2.031	4.114	6.343	6.948	7.300	...	...	...	...
M7V	2550	-5.020	...	2.119	4.544	7.054	7.667	8.053	...	...	...	...
M8V	2450	-5.610	...	2.197	4.571	7.593	8.268	8.714	...	...	...	...
M9V	2350	-5.690	...	2.2	4.577	7.617	8.366	8 .847	...	...	...	...

Extensive notes were taken on the colors and published classifications for *all* O- through M-type dwarf spectral type standard stars found in the literature (see http://www.pas.rochester.edu/~emamajek/spt/). Spectral standard stars for stars of F-type and earlier were mostly drawn from Johnson & Morgan (1953); Morgan & Hiltner (1965); Garrison (1967); Lesh (1968); Abt et al. (1968); Hiltner et al. (1969); Cowley et al. (1969); Garrison (1972); Cowley (1972); Morgan & Keenan (1973); Cowley & Fraquelli (1974); Houk & Cowley (1975); Garrison et al. (1977); Morgan et al. (1978); Garrison & Schild (1979); Gray & Garrison (1987); Walborn & Fitzpatrick (1990); Garrison & Gray (1994); Gray & Corbally (2009). For M-type stars, the primary sources of standard stars were Kirkpatrick et al. (1991, 1997); Henry et al. (2002). Some M-type standards from Keenan's papers (e.g. Keenan & McNeil, 1976; Keenan & Pitts, 1980; Keenan, 1983; Keenan & Yorka, 1988; Keenan & McNeil, 1989) that have conflicting types compared to the newer classifications by Kirkpatrick, Henry, and collaborators, have been deprecated (e.g. GJ 15A, 172, 250B, 526) and were not considered in assessing median colors and $T_{\rm eff}$. Given the immense volume of recent M-star classifications that have been done on the Kirkpatrick & Henry grid (e.g. Reid et al., 1995; Hawley et al., 1996; Henry et al., 2002), these should be preferred to the Keenan types where there is disagreement. Classifications by AFGK field stars by Gray et al. (2003, 2006) were generally preferred over those of the Michigan Atlas (Houk & Cowley, 1975), as it appears that the Gray et al. classifications more closely follow the Morgan-Keenan standards. Differences between Gray et al. and Houk et al. classifications are especially pronounced amongst the early G-type stars. Part of this may stem from disagreement between Morgan and Keenan on the F/G boundary (e.g. η Cas A was considered G0V by Morgan, but later F9V by Keenan). More problematically, Houk & Cowley (1975) considered β Com to be their main G2V standard, but it was considered to be a G0V standard by Johnson & Morgan

(1953); Morgan et al. (1971); Morgan & Keenan (1973); Keenan & McNeil (1976). This appears to explain why the median B-V color for nearby G2V stars in the Hipparcos catalog (dominated by Michigan atlas classifications) is B-V = 0.617, whereas for stars classified G2V by Gray et al. (2001b, 2003, 2006) on Keenan's standard star grid, B-V = 0.647 (remarkably similar to the recent precise estimate of the solar B-V color of 0.653 ± 0.003 by Ramírez et al., 2012). As Keenan's G/K-type standard stars are in common usage, I weight the median colors for field dwarfs classified using the Keenan standards (e.g. Gray's papers) over those from the Michigan Atlas.

The intrinsic $(B–V)_o$ and $(U–B)_o$ colors can be derived for OB dwarfs via the Q-method (e.g., Johnson & Morgan, 1953; Johnson, 1958; Hiltner & Johnson, 1956), where the reddening-free index Q is calculated using the observed colors as Q=(U–B)-0.72(B–V). Functions of $(B–V)_o$ and $(U–B)_o$ as linear functions of Q, especially those that are forced through the origin ($(B–V)_o$, $(U–B)_o$), produce poor fits to the colors of real unreddened OB stars. We calibrated new Q versus intrinsic color relations using UBV photometry from Mermilliod & Mermilliod (1994) of nearby negligibly reddened B-type dwarfs within 75 pc (*Hipparcos* catalog; ESA 1997), and lightly reddened hotter O and early-B luminosity class V and IV stars in nearby associations, dereddened them using published H I column densities (e.g., Fruscione et al., 1994) and the strong correlation between N(H I) and $E(B–V)$; Diplas & Savage (1994). The improved fits are:

$$\begin{aligned}(B-V)_o &= -4.776008156728\times10^{-3} + \\ &\quad 0.5522012574154\,Q + \\ &\quad 1.151583004497\,Q^2 + \\ &\quad 1.829921229667\,Q^3 + \\ &\quad 0.8933113140506\,Q^4\end{aligned}$$

for $-0.32 < (B-V)_o < 0.02$, and

$$\begin{aligned}(U-B)_o &= 6.230566666312\times10^{-3} + \\ &\quad 1.533217755592\,Q + \\ &\quad 1.385407188924\,Q^2 + \\ &\quad 2.167355580182\,Q^3 + \\ &\quad 1.075207514655\,Q^4\end{aligned}$$

for -1.13 < $(U$–$B)_o$ < 0.02. We find that the intrinsic $(B$–$V)_o$ colors of O9/B0 dwarfs are -0.32 to -0.31 (among the calibrator stars 10 Lac, σ Sco, τ Sco, and υ Ori), in agreement with Johnson's classic work (e.g. Johnson & Morgan 1953; Johnson 1966, but at odds with the recent work of Martins & Plez (2006) who claim that $(B$–$V)_o$ colors of Galactic O stars go no bluer than -0.28.

Deriving the main sequence color sequence was fairly straightforward. Photometry for nearby stars came from the following sources: UBV Mermilliod (1991), BVI_C

(ESA, 1997), JHK_S (Skrutskie et al., 2006), $W1$, $W2$, $W3$, and $W4$ (Cutri & et al., 2012). While we did derive median color estimates for each type (some are listed in the individual spectral type files), we decided to fit polynomials to the color-color data for nearby field dwarfs. For some color-color sequences polynomials give inadequate fits. For these instances we found it more reliable to simply construct a well-sampled color-color table based on median colors within a given color bin, and interpolate (e.g. V–K_S vs. B–V, V–I_C, J–H, H–K_S, B–V vs V–I_C and U–B). We fit polynomial relations to V–K_S versus K_S–$W1$, K_S–$W2$, K_S–$W3$, and K_S–$W4$ for objects within 75 pc from the *Hipparcos* catalog and the catalog of bright M dwarfs from Lépine & Gaidos (2011). We adopted V magnitudes from the APASS Data Release 6 catalog (Henden et al., 2012) for objects not present in the *Hipparcos* catalog, and only fit objects with high quality photometry in the relevant band (for 2MASS bands, quality flag 'A'; for WISE bands, contamination and confusion flag '0'). We restricted the data to WISE magnitudes $W1 > 5.0$, $W2 > 6.0$, $W3 > 5.0$ and $W4 > 0.0$ to avoid biases due to saturation. The data is not well-populated for V–$K_S < 0.5$ mag or V–$K_S > 6.0$ mag, so Table C.1 only contains WISE colors for spectral types F0 through M5.

Subtype $T_{\rm eff}$s were estimated by considering published $T_{\rm eff}$s for stars of a given subtype, though greater weighting was given to $T_{\rm eff}$ values for spectral standards which were vetted for consistent classifications in the literature. Our search for published $T_{\rm eff}$s was extensive, but not exhaustive, and given time constraints we are admittedly limited by what values were published in electronic tables that could be easily queried with e.g. Vizier[1]. Many $T_{\rm eff}$s came from large catalogs by e.g. Philip & Egret (1980); Sokolov (1995); Cayrel de Strobel et al. (1997); Blackwell & Lynas-Gray (1998); Gray et al. (2001a, 2003); Taylor (2005); Valenti & Fischer (2005); Paunzen

[1]http://vizier.u-strasbg.fr/viz-bin/VizieR

et al. (2006); Gerbaldi et al. (2007); Fitzpatrick & Massa (2007); Prugniel et al. (2007); Zorec et al. (2009); Soubiran et al. (2010); Casagrande et al. (2011), and the authors calculated photometric T_{eff}s for OB dwarf standards using photometry from Hauck & Mermilliod (1998), dereddening relations from Castelli (1991), and color-temperature relations from Balona & Shobbrook (1984); Napiwotzki et al. (1993); Balona (1994). T_{eff}s were also estimated for OB dwarf standards using U–B vs. T_{eff} data in Bessell et al. (1998).

Here is an example of our evaluation of the median T_{eff} for A0V stars. We find very consistent effective temperatures among A0V standards within a few hundred K of each other. The A0V standard Vega has had a very precise apparent T_{eff} measured by Monnier et al. (2012) of 9660K (in good agreement with many previous estimates), and we find the literature median T_{eff} for the other widely used MK standards γ UMa and HR 3314 to be 9361K and 9760K. While there are other A0V standards, two of these (γ UMa, Vega) are considered "anchor" standards by Garrison & Gray (1994) (i.e. their classifications have not moved in over 7 decades of use), and HR 3314 has retained its A0V standard status throughout (Morgan et al., 1953; Johnson & Morgan, 1953; Garrison & Schild, 1979; Gray & Garrison, 1987; Houk & Swift, 1999; Gray et al., 2003). An exhaustive search for T_{eff}s for A0V stars in the literature (265 estimates) yields a median T_{eff} of 9707K. Based on these values, we adopt a median T_{eff} of 9700K for A0V stars. We find it unlikely that the median A0V T_{eff} could be as high as 10000K (Bessell, 1979; Crowther, 1997), nor as low as 9394 K (Boyajian et al., 2012a), 9520 K (Schmidt-Kaler, 1982), or 9530 K (Theodossiou & Danezis, 1991). We note in particular that the recently published T_{eff} scale by Boyajian et al. (2012a) appears to be most deviant among the A0V T_{eff} values, and while that study relies on new interferometric observations, their survey contained only a single non-standard A0V star (HD 177724). Similarly sized deviations at the hundreds of K level were

seen between our T_{eff} scale and the Boyajian et al. (2012a) T_{eff} scale. So while there are other modern color/T_{eff} scales in the literature, we believe that ours is based on a very broad (but vetted) amount of photometric/T_{eff} literature and classifications.

The bolometric corrections (BC) listed in Table C.1 are derived for each spectral type by adopting the median BC among several T_{eff}-BC scales, including Balona (1994); Bertone et al. (2004); Flower (1996); Bessell et al. (1998); Masana et al. (2006); Schmidt-Kaler (1982); Code et al. (1976); Casagrande et al. (2006, 2008, 2010); Lanz & Hubeny (2007); Vacca et al. (1996); Lanz & Hubeny (2003)[2].

[2]Extensive notes and discussion can be found for each spectral type at http://www.pas.rochester.edu/~emamajek/spt/

References

Abt, H. A. 1981, ApJS, 45, 437

—. 1986, PASP, 98, 307

Abt, H. A., Meinel, A. B., Morgan W. W., & Tapscott I. W. 1968, An Atlas of low-dispersion grating stellar spectra

Abt, H. A., & Morrell, N. I. 1995, ApJS, 99, 135

Alencar, S. H. P., Melo, C. H. F., Dullemond, C. P., Andersen, J., Batalha, C., Vaz, L. P. R., & Mathieu, R. D. 2003, A&A, 409, 1037

Alexander, R. D., Clarke, C. J., & Pringle, J. E. 2006, MNRAS, 369, 216

Allard, F., Homeier, D., & Freytag, B. 2011, in Astronomical Society of the Pacific Conference Series, Vol. 448, 16th Cambridge Workshop on Cool Stars, Stellar Systems, and the Sun, ed. C. Johns-Krull, M. K. Browning, & A. A. West, 91

Allard, F., Homeier, D., & Freytag, B. 2012, Royal Society of London Philosophical Transactions Series A, 370, 2765

Allen, L. E., & Strom, K. M. 1995, AJ, 109, 1379

Allers, K. N., et al. 2007, ApJ, 657, 511

Alonso, A., Arribas, S., & Martínez-Roger, C. 1999, A&AS, 140, 261

Andersen, J., Lindgren, H., Hazen, M. L., & Mayor, M. 1989, A&A, 219, 142

Ardila, D., Martín, E., & Basri, G. 2000, AJ, 120, 479

Artymowicz, P., & Lubow, S. H. 1994, ApJ, 421, 651

Asplund, M., Grevesse, N., & Sauval, A. J. 2005, in Astronomical Society of the Pacific Conference Series, Vol. 336, Cosmic Abundances as Records of Stellar Evolution and Nucleosynthesis, ed. T. G. Barnes, III & F. N. Bash, 25

Asplund, M., Grevesse, N., Sauval, A. J., & Scott, P. 2009, ARA&A, 47, 481

Bailey, III, J. I., White, R. J., Blake, C. H., Charbonneau, D., Barman, T. S., Tanner, A. M., & Torres, G. 2012, ApJ, 749, 16

Balachandran, S. 1991, Mem. Soc. Astron. Italiana, 62, 33

Balona, L. A. 1994, MNRAS, 268, 119

Balona, L. A., & Shobbrook, R. R. 1984, MNRAS, 211, 375

Baraffe, I., Chabrier, G., Allard, F., & Hauschildt, P. H. 1998, A&A, 337, 403

—. 2002, A&A, 382, 563

Barbier-Brossat, M., & Figon, P. 2000, A&AS, 142, 217

Barnes, T. G., & Evans, D. S. 1976, MNRAS, 174, 489

Barrado Y Navascués, D. 2006, A&A, 459, 511

Barrado y Navascués, D., & Martín, E. L. 2003, AJ, 126, 2997

Barrado y Navascués, D., et al. 2007, ApJ, 664, 481

Béjar, V. J. S., Zapatero Osorio, M. R., Pérez-Garrido, A., Álvarez, C., Martín, E. L., Rebolo, R., Villó-Pérez, I., & Díaz-Sánchez, A. 2008, ApJ, 673, L185

Bertelli, G., Bressan, A., Chiosi, C., Fagotto, F., & Nasi, E. 1994, A&AS, 106, 275

Bertone, E., Buzzoni, A., Chávez, M., & Rodríguez-Merino, L. H. 2004, AJ, 128, 829

Bessell, M., & Murphy, S. 2012, PASP, 124, 140

Bessell, M. S. 1979, PASP, 91, 589

Bessell, M. S., & Brett, J. M. 1988, PASP, 100, 1134

Bessell, M. S., Castelli, F., & Plez, B. 1998, A&A, 333, 231

Bevington, P. R., & Robinson, D. K. 2003, Data reduction and error analysis for the physical sciences, ed. Bevington, P. R. & Robinson, D. K.

Bidelman, W. P. 1956, PASP, 68, 318

Bitner, M. A., Chen, C. H., Muzerolle, J., Weinberger, A. J., Pecaut, M., Mamajek, E. E., & Mclure, M. K. 2010, ApJ, 714, 1542

Blaauw, A. 1946, Publications of the Kapteyn Astronomical Laboratory Groningen, 52, 1

—. 1956, ApJ, 123, 408

—. 1964a, ARA&A, 2, 213

Blaauw, A. 1964b, in IAU Symposium, Vol. 20, The Galaxy and the Magellanic Clouds, ed. F. J. Kerr, 50–+

—. 1978, Internal Motions and Age of the Sub-Association Upper Scorpio, ed. L. V. Mirzoyan, 101

Blackwell, D. E., & Lynas-Gray, A. E. 1998, A&AS, 129, 505

Blackwell, D. E., & Shallis, M. J. 1977, MNRAS, 180, 177

Boss, A. P., et al. 2007, Transactions of the International Astronomical Union, Series A, 26, 183

Bouvier, J., Alencar, S. H. P., Harries, T. J., Johns-Krull, C. M., & Romanova, M. M. 2007, Protostars and Planets V, 479

Bouvier, J., Forestini, M., & Allain, S. 1997, A&A, 326, 1023

Boyajian, T. S., et al. 2012a, ApJ, 746, 101

—. 2012b, ApJ, 757, 112

Briceño, C., Preibisch, T., Sherry, W. H., Mamajek, E. A., Mathieu, R. D., Walter, F. M., & Zinnecker, H. 2007, Protostars and Planets V, 345

Brown, A. G. A., Dekker, G., & de Zeeuw, P. T. 1997, MNRAS, 285, 479

Brown, A. G. A., & Verschueren, W. 1997, A&A, 319, 811

Cannon, A. J., & Pickering, E. C. 1918, Annals of Harvard College Observatory, 91, 1

Cargile, P. A., James, D. J., & Jeffries, R. D. 2010, ApJ, 725, L111

Carpenter, J. M. 2001, AJ, 121, 2851

Carpenter, J. M., Mamajek, E. E., Hillenbrand, L. A., & Meyer, M. R. 2006, ApJ, 651, L49

Casagrande, L., Flynn, C., & Bessell, M. 2008, MNRAS, 389, 585

Casagrande, L., Portinari, L., & Flynn, C. 2006, MNRAS, 373, 13

Casagrande, L., Ramírez, I., Meléndez, J., & Asplund, M. 2012, ApJ, 761, 16

Casagrande, L., Ramírez, I., Meléndez, J., Bessell, M., & Asplund, M. 2010, A&A, 512, A54+

Casagrande, L., Schönrich, R., Asplund, M., Cassisi, S., Ramírez, I., Meléndez, J., Bensby, T., & Feltzing, S. 2011, A&A, 530, A138

Castelli, F. 1991, A&A, 251, 106

Castelli, F., & Kurucz, R. L. 2004, ArXiv Astrophysics e-prints

Cayrel de Strobel, G., Soubiran, C., Friel, E. D., Ralite, N., & Francois, P. 1997, A&AS, 124, 299

Chabrier, G., Baraffe, I., Allard, F., & Hauschildt, P. 2000, ApJ, 542, 464

Chen, C. H., Mamajek, E. E., Bitner, M. A., Pecaut, M., Su, K. Y. L., & Weinberger, A. J. 2011, ApJ, 738, 122

Churchwell, E., et al. 2009, PASP, 121, 213

Claret, A. 2004, A&A, 424, 919

Clark, P. C., Bonnell, I. A., Zinnecker, H., & Bate, M. R. 2005, MNRAS, 359, 809

Close, L. M., et al. 2007, ApJ, 660, 1492

Code, A. D., Bless, R. C., Davis, J., & Brown, R. H. 1976, ApJ, 203, 417

Conti, P. S., Leep, E. M., & Lorre, J. J. 1977, ApJ, 214, 759

Cowley, A. 1972, AJ, 77, 750

Cowley, A., Cowley, C., Jaschek, M., & Jaschek, C. 1969, AJ, 74, 375

Cowley, A., & Fraquelli, D. 1974, PASP, 86, 70

Cox, D. P., & Reynolds, R. J. 1987, ARA&A, 25, 303

Crowther, P. A. 1997, in IAU Symposium, Vol. 189, IAU Symposium, ed. T. R. Bedding, A. J. Booth, & J. Davis, 137–146

Cutri, R. M., & et al. 2012, VizieR Online Data Catalog, 2311, 0

Cutri, R. M., et al. 2003, VizieR Online Data Catalog, 2246, 0

Da Rio, N., Robberto, M., Soderblom, D. R., Panagia, N., Hillenbrand, L. A., Palla, F., & Stassun, K. G. 2010, ApJ, 722, 1092

Dahm, S. E., Slesnick, C. L., & White, R. J. 2012, ApJ, 745, 56

Dale, J. E., Bonnell, I. A., & Whitworth, A. P. 2007, MNRAS, 375, 1291

D'Antona, F., & Mazzitelli, I. 1997, Mem. Soc. Astron. Italiana, 68, 807

de Bruijne, J. H. J. 1999a, MNRAS, 306, 381

—. 1999b, MNRAS, 310, 585

de Bruijne, J. H. J., Hoogerwerf, R., & de Zeeuw, P. T. 2001, A&A, 367, 111

de Geus, E. J. 1992, A&A, 262, 258

de Geus, E. J., de Zeeuw, P. T., & Lub, J. 1989, A&A, 216, 44

de la Reza, R., Jilinski, E., & Ortega, V. G. 2006, AJ, 131, 2609

de la Reza, R., Torres, C. A. O., Quast, G., Castilho, B. V., & Vieira, G. L. 1989, ApJ, 343, L61

de Zeeuw, P. T., Hoogerwerf, R., de Bruijne, J. H. J., Brown, A. G. A., & Blaauw, A. 1999, AJ, 117, 354

de Zeeuw, T., & Brand, J. 1985, in Astrophysics and Space Science Library, Vol. 120, Birth and Evolution of Massive Stars and Stellar Groups, ed. W. Boland & H. van Woerden, 95–101

Demarque, P., Woo, J.-H., Kim, Y.-C., & Yi, S. K. 2004, ApJS, 155, 667

Diplas, A., & Savage, B. D. 1994, ApJ, 427, 274

Dirienzo, W. J., Indebetouw, R., Brogan, C., Cyganowski, C. J., Churchwell, E., & Friesen, R. K. 2012, AJ, 144, 173

Dobbie, P. D., Lodieu, N., & Sharp, R. G. 2010, MNRAS, 409, 1002

Dotter, A., Chaboyer, B., Jevremović, D., Kostov, V., Baron, E., & Ferguson, J. W. 2008, ApJS, 178, 89

Duchêne, G., & Kraus, A. 2013, ArXiv e-prints

Duflot, M., Figon, P., & Meyssonnier, N. 1995, A&AS, 114, 269

Ekström, S., et al. 2012, A&A, 537, A146

Elliot, J. L., Rages, K., & Veverka, J. 1976, ApJ, 207, 994

Elmegreen, B. G. 1998, in Astronomical Society of the Pacific Conference Series, Vol. 148, Origins, ed. C. E. Woodward, J. M. Shull, & H. A. Thronson, Jr., 150

Elmegreen, B. G. 2011, in EAS Publications Series, Vol. 51, EAS Publications Series, ed. C. Charbonnel & T. Montmerle, 45–58

Elmegreen, B. G., & Lada, C. J. 1977, ApJ, 214, 725

Epchtein, N., et al. 1997, The Messenger, 87, 27

Erickson, K. L., Wilking, B. A., Meyer, M. R., Robinson, J. G., & Stephenson, L. N. 2011, AJ, 142, 140

ESA. 1997, VizieR Online Data Catalog, 1239, 0

Espaillat, C., et al. 2012, ApJ, 747, 103

Feiden, G. A., & Chaboyer, B. 2012, ApJ, 761, 30

Feigelson, E. D., & Montmerle, T. 1999, ARA&A, 37, 363

Finkenzeller, U., & Basri, G. 1987, ApJ, 318, 823

Fiorucci, M., & Munari, U. 2003, A&A, 401, 781

Fitzpatrick, E. L., & Massa, D. 2007, ApJ, 663, 320

Flower, P. J. 1996, ApJ, 469, 355

Fruscione, A., Hawkins, I., Jelinsky, P., & Wiercigroch, A. 1994, ApJS, 94, 127

Garmany, C. D., Conti, P. S., & Massey, P. 1980, ApJ, 242, 1063

Garrison, R. F. 1967, ApJ, 147, 1003

—. 1972, ApJ, 177, 653

Garrison, R. F., & Gray, R. O. 1994, AJ, 107, 1556

Garrison, R. F., Hiltner, W. A., & Schild, R. E. 1977, ApJS, 35, 111

Garrison, R. F., & Schild, R. E. 1979, AJ, 84, 1020

Gáspár, A., Rieke, G. H., Su, K. Y. L., Balog, Z., Trilling, D., Muzzerole, J., Apai, D., & Kelly, B. C. 2009, ApJ, 697, 1578

Gautier, III, T. N., Rebull, L. M., Stapelfeldt, K. R., & Mainzer, A. 2008, ApJ, 683, 813

Gerbaldi, M., Faraggiana, R., & Caffau, E. 2007, A&A, 472, 241

Getman, K. V., Feigelson, E. D., Garmire, G., Broos, P., & Wang, J. 2007, ApJ, 654, 316

Glaspey, J. W. 1971, PhD thesis, The University of Arizona.

—. 1972, AJ, 77, 474

Gontcharov, G. A. 2006, Astronomy Letters, 32, 759

Gott, III, J. R., Vogeley, M. S., Podariu, S., & Ratra, B. 2001, ApJ, 549, 1

Gray, R. O. 1989, AJ, 98, 1049

Gray, R. O., & Corbally, J., C. 2009, Stellar Spectral Classification, ed. Gray, R. O. & Corbally, C., J.

Gray, R. O., & Corbally, C. J. 1998, AJ, 116, 2530

—. 2002, AJ, 124, 989

Gray, R. O., Corbally, C. J., Garrison, R. F., McFadden, M. T., Bubar, E. J., McGahee, C. E., O'Donoghue, A. A., & Knox, E. R. 2006, AJ, 132, 161

Gray, R. O., Corbally, C. J., Garrison, R. F., McFadden, M. T., & Robinson, P. E. 2003, AJ, 126, 2048

Gray, R. O., & Garrison, R. F. 1987, ApJS, 65, 581

—. 1989, ApJS, 69, 301

Gray, R. O., Graham, P. W., & Hoyt, S. R. 2001a, AJ, 121, 2159

Gray, R. O., Napier, M. G., & Winkler, L. I. 2001b, AJ, 121, 2148

Grevesse, N., & Noels, A. 1993, in Origin and Evolution of the Elements, ed. N. Prantzos, E. Vangioni-Flam, & M. Casse, 15–25

Grevesse, N., & Sauval, A. J. 1998, Space Sci. Rev., 85, 161

Gullbring, E., Hartmann, L., Briceno, C., & Calvet, N. 1998, ApJ, 492, 323

Haberreiter, M., Schmutz, W., & Kosovichev, A. G. 2008, ApJ, 675, L53

Harlan, E. A. 1969, AJ, 74, 916

Harnden, Jr., F. R., Fabricant, D. G., Harris, D. E., & Schwarz, J. 1984, SAO Special Report, 393

Hauck, B., & Mermilliod, M. 1998, A&AS, 129, 431

Hauschildt, P. H., Allard, F., & Baron, E. 1999, ApJ, 512, 377

Hauschildt, P. H., Baron, E., & Allard, F. 1997, ApJ, 483, 390

Hawley, S. L., Gizis, J. E., & Reid, I. N. 1996, AJ, 112, 2799

Henden, A. A., Levine, S. E., Terrell, D., Smith, T. C., & Welch, D. 2012, Journal of the American Association of Variable Star Observers (JAAVSO), 40, 430

Henry, T. J., Walkowicz, L. M., Barto, T. C., & Golimowski, D. A. 2002, AJ, 123, 2002

Herbst, W., Bailer-Jones, C. A. L., Mundt, R., Meisenheimer, K., & Wackermann, R. 2002, A&A, 396, 513

Hernández, J., Calvet, N., Hartmann, L., Briceño, C., Sicilia-Aguilar, A., & Berlind, P. 2005, AJ, 129, 856

Herrero, A., Kudritzki, R. P., Vilchez, J. M., Kunze, D., Butler, K., & Haser, S. 1992, A&A, 261, 209

Hillenbrand, L. A. 1997, AJ, 113, 1733

Hillenbrand, L. A. 2009, in IAU Symposium, Vol. 258, IAU Symposium, ed. E. E. Mamajek, D. R. Soderblom, & R. F. G. Wyse, 81–94

Hillenbrand, L. A., Bauermeister, A., & White, R. J. 2008, in Astronomical Society of the Pacific Conference Series, Vol. 384, 14th Cambridge Workshop on Cool Stars, Stellar Systems, and the Sun, ed. G. van Belle, 200

Hillenbrand, L. A., & White, R. J. 2004, ApJ, 604, 741

Hiltner, W. A., Garrison, R. F., & Schild, R. E. 1969, ApJ, 157, 313

Hiltner, W. A., & Johnson, H. L. 1956, ApJ, 124, 367

Hoff, W., Henning, T., & Pfau, W. 1998, A&A, 336, 242

Høg, E., et al. 2000, A&A, 355, L27

Hoogerwerf, R., & Aguilar, L. A. 1999, MNRAS, 306, 394

Hoogerwerf, R., de Bruijne, J. H. J., & de Zeeuw, P. T. 2000, ApJ, 544, L133

Houk, N. 1978, Michigan catalogue of two-dimensional spectral types for the HD stars, ed. Houk, N.

—. 1982, Michigan Catalogue of Two-dimensional Spectral Types for the HD stars. Volume_3., ed. Houk, N.

Houk, N., & Cowley, A. P. 1975, University of Michigan Catalogue of two-dimensional spectral types for the HD stars. Volume I., ed. Houk, N. & Cowley, A. P.

Houk, N., & Smith-Moore, M. 1988, Michigan Catalogue of Two-dimensional Spectral Types for the HD Stars. Volume 4, ed. Houk, N. & Smith-Moore, M.

Houk, N., & Swift, C. 1999, Michigan catalogue of two-dimensional spectral types for the HD Stars ; vol. 5, ed. Houk, N. & Swift, C.

Hubickyj, O., Bodenheimer, P., & Lissauer, J. J. 2005, Icarus, 179, 415

Hughes, J., Hartigan, P., Krautter, J., & Kelemen, J. 1994, AJ, 108, 1071

Hutchinson, M. G., Evans, A., Winkler, H., & Spencer Jones, J. 1990, A&A, 234, 230

Iben, Jr., I. 1965, ApJ, 141, 993

Ireland, M. J., Kraus, A., Martinache, F., Law, N., & Hillenbrand, L. A. 2011, ApJ, 726, 113

Ishihara, D., et al. 2010, A&A, 514, A1

Jarrett, T. H., et al. 2011, ApJ, 735, 112

Jayawardhana, R., & Ivanov, V. D. 2006, Science, 313, 1279

Jeffries, R. D. 1995, MNRAS, 273, 559

Jeffries, R. D., Littlefair, S. P., Naylor, T., & Mayne, N. J. 2011, MNRAS, 418, 1948

Johnson, H. L. 1958, Lowell Observatory Bulletin, 4, 37

—. 1966, ARA&A, 4, 193

Johnson, H. L., & Morgan, W. W. 1953, ApJ, 117, 313

Jones, B. F., Fischer, D. A., & Stauffer, J. R. 1996, AJ, 112, 1562

Jorgensen, U. G. 1996, in IAU Symposium, Vol. 178, Molecules in Astrophysics: Probes & Processes, ed. E. F. van Dishoeck, 441

Kapteyn, J. C. 1914, ApJ, 40, 43

Kastner, J. H., Zuckerman, B., & Bessell, M. 2008, A&A, 491, 829

Keenan, P. C. 1983, Bulletin d'Information du Centre de Donnees Stellaires, 24, 19

Keenan, P. C. 1984, in The MK Process and Stellar Classification, ed. R. F. Garrison, 29

Keenan, P. C., & McNeil, R. C. 1976, An atlas of spectra of the cooler stars: Types G,K,M,S, and C. Part 1: Introduction and tables

—. 1989, ApJS, 71, 245

Keenan, P. C., & Pitts, R. E. 1980, ApJS, 42, 541

Keenan, P. C., & Yorka, S. B. 1988, Bulletin d'Information du Centre de Donnees Stellaires, 35, 37

Kenyon, S. J., & Hartmann, L. 1995, ApJS, 101, 117

Kessel-Deynet, O., & Burkert, A. 2003, MNRAS, 338, 545

Kirkpatrick, J. D., Beichman, C. A., & Skrutskie, M. F. 1997, ApJ, 476, 311

Kirkpatrick, J. D., Henry, T. J., & McCarthy, Jr., D. W. 1991, ApJS, 77, 417

Kiss, L. L., et al. 2011, MNRAS, 411, 117

Koen, C., Kilkenny, D., van Wyk, F., & Marang, F. 2010, MNRAS, 403, 1949

Koenigl, A. 1991, ApJ, 370, L39

Köhler, R., Kunkel, M., Leinert, C., & Zinnecker, H. 2000, A&A, 356, 541

Kraus, A. L., & Hillenbrand, L. A. 2009, ApJ, 704, 531

Kraus, A. L., & Ireland, M. J. 2012, ApJ, 745, 5

Kraus, A. L., Tucker, R. A., Thompson, M. I., Craine, E. R., & Hillenbrand, L. A. 2011, ApJ, 728, 48

Krautter, J., Wichmann, R., Schmitt, J. H. M. M., Alcala, J. M., Neuhauser, R., & Terranegra, L. 1997, A&AS, 123, 329

Kroupa, P. 2001, MNRAS, 322, 231

Kroupa, P., Aarseth, S., & Hurley, J. 2001, MNRAS, 321, 699

Kupka, F., Piskunov, N., Ryabchikova, T. A., Stempels, H. C., & Weiss, W. W. 1999, A&AS, 138, 119

Lada, C. J., & Lada, E. A. 2003, ARA&A, 41, 57

Lafrasse, S., Mella, G., Bonneau, D., Duvert, G., Delfosse, X., Chesneau, O., & Chelli, A. 2010, in Society of Photo-Optical Instrumentation Engineers (SPIE) Conference Series, Vol. 7734

Lafrenière, D., Jayawardhana, R., Janson, M., Helling, C., Witte, S., & Hauschildt, P. 2011, ApJ, 730, 42

Lafrenière, D., Jayawardhana, R., & van Kerkwijk, M. H. 2008, ApJ, 689, L153

—. 2010, ApJ, 719, 497

Lanz, T., & Hubeny, I. 2003, ApJS, 146, 417

—. 2007, ApJS, 169, 83

Larson, R. B. 1986, MNRAS, 218, 409

Lawson, W. A., Crause, L. A., Mamajek, E. E., & Feigelson, E. D. 2001, MNRAS, 321, 57

—. 2002, MNRAS, 329, L29

Lépine, S., & Gaidos, E. 2011, AJ, 142, 138

Lépine, S., & Simon, M. 2009, AJ, 137, 3632

Lesh, J. R. 1968, ApJS, 17, 371

Levesque, E. M., Massey, P., Olsen, K. A. G., Plez, B., Josselin, E., Maeder, A., & Meynet, G. 2005, ApJ, 628, 973

Littlefair, S. P., Naylor, T., Mayne, N. J., Saunders, E. S., & Jeffries, R. D. 2010, MNRAS, 403, 545

Looper, D. L., Bochanski, J. J., Burgasser, A. J., Mohanty, S., Mamajek, E. E., Faherty, J. K., West, A. A., & Pitts, M. A. 2010a, AJ, 140, 1486

Looper, D. L., Burgasser, A. J., Kirkpatrick, J. D., & Swift, B. J. 2007, ApJ, 669, L97

Looper, D. L., et al. 2010b, ApJ, 714, 45

Luhman, K. L. 1999, ApJ, 525, 466

Luhman, K. L., Allen, P. R., Espaillat, C., Hartmann, L., & Calvet, N. 2010a, ApJS, 189, 353

—. 2010b, ApJS, 186, 111

Luhman, K. L., Allers, K. N., Jaffe, D. T., Cushing, M. C., Williams, K. A., Slesnick, C. L., & Vacca, W. D. 2007, ApJ, 659, 1629

Luhman, K. L., & Mamajek, E. E. 2012, ApJ, 758, 31

Luhman, K. L., Stauffer, J. R., Muench, A. A., Rieke, G. H., Lada, E. A., Bouvier, J., & Lada, C. J. 2003, ApJ, 593, 1093

Luhman, K. L., & Steeghs, D. 2004, ApJ, 609, 917

Lyo, A.-R., Lawson, W. A., Feigelson, E. D., & Crause, L. A. 2004, MNRAS, 347, 246

MacDonald, J., & Mullan, D. J. 2009, ApJ, 700, 387

Macdonald, J., & Mullan, D. J. 2010, ApJ, 723, 1599

Maeder, A. 1981, A&A, 102, 401

Maeder, A., & Meynet, G. 2000, ARA&A, 38, 143

Mamajek, E. E. 2005, ApJ, 634, 1385

Mamajek, E. E. 2009, in American Institute of Physics Conference Series, Vol. 1158, American Institute of Physics Conference Series, ed. T. Usuda, M. Tamura, & M. Ishii, 3–10

—. 2012, ApJ, 754, L20

Mamajek, E. E., Lawson, W. A., & Feigelson, E. D. 1999, ApJ, 516, L77

Mamajek, E. E., Meyer, M. R., & Liebert, J. 2002, AJ, 124, 1670

—. 2006, AJ, 131, 2360

Martins, F., & Plez, B. 2006, A&A, 457, 637

Masana, E., Jordi, C., & Ribas, I. 2006, A&A, 450, 735

McCarthy, K. A., & White, R. J. 2012, ArXiv e-prints

Megeath, S. T., Hartmann, L., Luhman, K. L., & Fazio, G. G. 2005, ApJ, 634, L113

Mentuch, E., Brandeker, A., van Kerkwijk, M. H., Jayawardhana, R., & Hauschildt, P. H. 2008, ApJ, 689, 1127

Mermilliod, J. C. 1991, Homogeneous Means in the UBV System

—. 2006, VizieR Online Data Catalog, 2168, 0

Mermilliod, J.-C., & Mermilliod, M. 1994, Catalogue of Mean UBV Data on Stars, ed. Mermilliod, J.-C. & Mermilliod, M.

Meyer, M. R., Calvet, N., & Hillenbrand, L. A. 1997, AJ, 114, 288

Meynet, G., & Maeder, A. 2000, A&A, 361, 101

Monnier, J. D., et al. 2012, ApJ, 761, L3

Mora, A., et al. 2001, A&A, 378, 116

Morgan, W. W., & Abt, H. A. 1973, AJ, 78, 386

Morgan, W. W., Abt, H. A., & Tapscott, J. W. 1978, Revised MK Spectral Atlas for stars earlier than the sun, ed. Morgan, W. W., Abt, H. A., & Tapscott, J. W.

Morgan, W. W., Harris, D. L., & Johnson, H. L. 1953, ApJ, 118, 92

Morgan, W. W., & Hiltner, W. A. 1965, ApJ, 141, 177

Morgan, W. W., Hiltner, W. A., & Garrison, R. F. 1971, AJ, 76, 242

Morgan, W. W., & Keenan, P. C. 1973, ARA&A, 11, 29

Muzerolle, J., et al. 2006, ApJ, 643, 1003

Napiwotzki, R., Schoenberner, D., & Wenske, V. 1993, A&A, 268, 653

Naylor, T. 2009, MNRAS, 399, 432

Neckel, T., & Klare, G. 1980, A&AS, 42, 251

Nguyen, D. C., Jayawardhana, R., van Kerkwijk, M. H., Brandeker, A., Scholz, A., & Damjanov, I. 2009, ApJ, 695, 1648

Nieva, M.-F. 2013, A&A, 550, A26

North, J. R., Davis, J., Tuthill, P. G., Tango, W. J., & Robertson, J. G. 2007, MNRAS, 380, 1276

Paunzen, E., Duffee, B., Heiter, U., Kuschnig, R., & Weiss, W. W. 2001, A&A, 373, 625

Paunzen, E., Schnell, A., & Maitzen, H. M. 2006, A&A, 458, 293

Pecaut, M. J., & Mamajek, E. E. 2013, ApJ, submitted

Pecaut, M. J., Mamajek, E. E., & Bubar, E. J. 2012, ApJ, 746, 154

Perryman, M. A. C., & ESA, eds. 1997, ESA Special Publication, Vol. 1200, The HIPPARCOS and TYCHO catalogues. Astrometric and photometric star catalogues derived from the ESA HIPPARCOS Space Astrometry Mission

Philip, A. D., & Egret, D. 1980, A&AS, 40, 199

Pollack, J. B., Hubickyj, O., Bodenheimer, P., Lissauer, J. J., Podolak, M., & Greenzweig, Y. 1996, Icarus, 124, 62

Preibisch, T., Brown, A. G. A., Bridges, T., Guenther, E., & Zinnecker, H. 2002, AJ, 124, 404

Preibisch, T., Guenther, E., & Zinnecker, H. 2001, AJ, 121, 1040

Preibisch, T., Guenther, E., Zinnecker, H., Sterzik, M., Frink, S., & Roeser, S. 1998, A&A, 333, 619

Preibisch, T., & Mamajek, E. 2008, The Nearest OB Association: Scorpius-Centaurus (Sco OB2), ed. Reipurth, B., 235–+

Preibisch, T., & Zinnecker, H. 1999, AJ, 117, 2381

Preibisch, T., & Zinnecker, H. 2007, in IAU Symposium, Vol. 237, IAU Symposium, ed. B. G. Elmegreen & J. Palous, 270–277

Prugniel, P., Soubiran, C., Koleva, M., & Le Borgne, D. 2007, ArXiv Astrophysics e-prints

Quanz, S. P., Amara, A., Meyer, M. R., Kenworthy, M. A., Kasper, M., & Girard, J. H. 2013, ApJ, 766, L1

Raghavan, D., et al. 2010, ApJS, 190, 1

Ramírez, I., et al. 2012, ApJ, 752, 5

Randich, S., Aharpour, N., Pallavicini, R., Prosser, C. F., & Stauffer, J. R. 1997, A&A, 323, 86

Rebull, L. M. 2001, AJ, 121, 1676

Rebull, L. M., Stauffer, J. R., Megeath, S. T., Hora, J. L., & Hartmann, L. 2006, ApJ, 646, 297

Rebull, L. M., et al. 2008, ApJ, 681, 1484

Reid, A. H. N., et al. 1993, ApJ, 417, 320

Reid, I. N., Hawley, S. L., & Gizis, J. E. 1995, AJ, 110, 1838

Reid, N. 2003, MNRAS, 342, 837

Reis, W., Corradi, W., de Avillez, M. A., & Santos, F. P. 2011, ApJ, 734, 8

Riaz, B., Gizis, J. E., & Harvin, J. 2006, AJ, 132, 866

Rice, E. L., Barman, T., Mclean, I. S., Prato, L., & Kirkpatrick, J. D. 2010a, ApJS, 186, 63

Rice, E. L., Faherty, J. K., & Cruz, K. L. 2010b, ApJ, 715, L165

Richichi, A., & Lisi, F. 1990, A&A, 230, 355

Rieke, G. H., et al. 2008, AJ, 135, 2245

Rizzuto, A. C., Ireland, M. J., & Robertson, J. G. 2011, MNRAS, 416, 3108

Robertson, T. H., & Hamilton, J. E. 1987, AJ, 93, 959

Rodriguez, D. R., Bessell, M. S., Zuckerman, B., & Kastner, J. H. 2011, ApJ, 727, 62

Röser, S., Schilbach, E., Schwan, H., Kharchenko, N. V., Piskunov, A. E., & Scholz, R.-D. 2008, A&A, 488, 401

Savage, B. D., & Mathis, J. S. 1979, ARA&A, 17, 73

Scandariato, G., Da Rio, N., Robberto, M., Pagano, I., & Stassun, K. 2012, ArXiv e-prints

Schlieder, J. E., Lépine, S., Rice, E., Simon, M., Fielding, D., & Tomasino, R. 2012a, AJ, 143, 114

Schlieder, J. E., Lépine, S., & Simon, M. 2010, AJ, 140, 119

—. 2012b, AJ, 143, 80

Schmidt-Kaler, T. 1982, in Landolt-Börnstein - Group VI Astronomy and Astrophysics, Vol. 2b, Stars and Star Clusters, ed. K. Schaifers & H. Voigt (Springer Berlin Heidelberg), 451–456

Schneider, A., Melis, C., & Song, I. 2012a, ApJ, 754, 39

Schneider, A., Song, I., Melis, C., Zuckerman, B., & Bessell, M. 2012b, ApJ, 757, 163

Scholz, R.-D., McCaughrean, M. J., Zinnecker, H., & Lodieu, N. 2005, A&A, 430, L49

Shkolnik, E., Liu, M. C., & Reid, I. N. 2009, ApJ, 699, 649

Shkolnik, E. L., Liu, M. C., Reid, I. N., Dupuy, T., & Weinberger, A. J. 2011, ApJ, 727, 6

Shobbrook, R. R. 1983, MNRAS, 205, 1215

Shu, F. H., Adams, F. C., & Lizano, S. 1987, ARA&A, 25, 23

Sicilia-Aguilar, A., et al. 2006, ApJ, 638, 897

—. 2009, ApJ, 701, 1188

Siess, L., Dufour, E., & Forestini, M. 2000, A&A, 358, 593

Simon, M., & Schaefer, G. H. 2011, ApJ, 743, 158

Skrutskie, M. F., et al. 2006, AJ, 131, 1163

Slesnick, C. L., Carpenter, J. M., & Hillenbrand, L. A. 2006, AJ, 131, 3016

Slesnick, C. L., Hillenbrand, L. A., & Carpenter, J. M. 2008, ApJ, 688, 377

Smartt, S. J. 2009, ARA&A, 47, 63

Soderblom, D. R. 2010, ARA&A, 48, 581

Soderblom, D. R., Jones, B. F., Balachandran, S., Stauffer, J. R., Duncan, D. K., Fedele, S. B., & Hudon, J. D. 1993, AJ, 106, 1059

Sokolov, N. A. 1995, A&AS, 110, 553

Song, I., Bessell, M. S., & Zuckerman, B. 2002, ApJ, 581, L43

Song, I., Zuckerman, B., & Bessell, M. S. 2003, ApJ, 599, 342

—. 2004, ApJ, 600, 1016

—. 2012, AJ, 144, 8

Soubiran, C., Le Campion, J.-F., Cayrel de Strobel, G., & Caillo, A. 2010, A&A, 515, A111

Spiegel, D. S., Burrows, A., & Milsom, J. A. 2011, ApJ, 727, 57

Spinrad, H. 1962, ApJ, 135, 715

Stauffer, J., et al. 2010, PASP, 122, 885

Stauffer, J. R., Jones, B. F., Backman, D., Hartmann, L. W., Barrado y Navascués, D., Pinsonneault, M. H., Terndrup, D. M., & Muench, A. A. 2003, AJ, 126, 833

Stauffer, J. R., Schultz, G., & Kirkpatrick, J. D. 1998, ApJ, 499, L199

Stephenson, C. B. 1986, AJ, 91, 144

Stephenson, C. B., & Sanduleak, N. 1977, Publications of the Warner & Swasey Observatory, 2, 71

Stephenson, C. B., & Sanwal, N. B. 1969, AJ, 74, 689

Sterzik, M. F., Alcalá, J. M., Covino, E., & Petr, M. G. 1999, A&A, 346, L41

Stickland, D. J., Lloyd, C., Koch, R. H., & Pachoulakis, I. 1996, The Observatory, 116, 387

Strassmeier, K. G., & Rice, J. B. 2000, A&A, 360, 1019

Talon, S., Zahn, J.-P., Maeder, A., & Meynet, G. 1997, A&A, 322, 209

Tango, W. J., Davis, J., Jacob, A. P., Mendez, A., North, J. R., O'Byrne, J. W., Seneta, E. B., & Tuthill, P. G. 2009, MNRAS, 396, 842

Taylor, B. J. 2005, ApJS, 161, 444

Teixeira, R., Ducourant, C., Chauvin, G., Krone-Martins, A., Bonnefoy, M., & Song, I. 2009, A&A, 503, 281

Teixeira, R., Ducourant, C., Chauvin, G., Krone-Martins, A., Song, I., & Zuckerman, B. 2008, A&A, 489, 825

Tetzlaff, N., Eisenbeiss, T., Neuhäuser, R., & Hohle, M. M. 2011, MNRAS, 417, 617

Thackeray, A. D. 1966, MmRAS, 70, 33

Theodossiou, E., & Danezis, E. 1991, Ap&SS, 183, 91

Tognelli, E., Prada Moroni, P. G., & Degl'Innocenti, S. 2011, A&A, 533, A109

Torres, C. A. O., Quast, G. R., da Silva, L., de La Reza, R., Melo, C. H. F., & Sterzik, M. 2006, A&A, 460, 695

Torres, C. A. O., Quast, G. R., Melo, C. H. F., & Sterzik, M. F. 2008, Young Nearby Loose Associations, ed. B. Reipurth, 757

Torres, G. 2010, AJ, 140, 1158

Torres, G., & Ribas, I. 2002, ApJ, 567, 1140

Torres-Dodgen, A. V., & Weaver, W. B. 1993, PASP, 105, 693

Vacca, W. D., Garmany, C. D., & Shull, J. M. 1996, ApJ, 460, 914

Vacca, W. D., & Sandell, G. 2011, ApJ, 732, 8

Valdes, F., Gupta, R., Rose, J. A., Singh, H. P., & Bell, D. J. 2004, ApJS, 152, 251

Valenti, J. A., & Fischer, D. A. 2005, ApJS, 159, 141

van Belle, G. T., et al. 1999, AJ, 117, 521

van Leeuwen, F. 2007, A&A, 474, 653

Viana Almeida, P., Santos, N. C., Melo, C., Ammler-von Eiff, M., Torres, C. A. O., Quast, G. R., Gameiro, J. F., & Sterzik, M. 2009, A&A, 501, 965

Vieira, S. L. A., Corradi, W. J. B., Alencar, S. H. P., Mendes, L. T. S., Torres, C. A. O., Quast, G. R., Guimarães, M. M., & da Silva, L. 2003, AJ, 126, 2971

Voges, W., et al. 1999, A&A, 349, 389

—. 2000, IAU Circ., 7432, 3

Vyssotsky, A. N. 1956, AJ, 61, 201

Walborn, N. R., & Fitzpatrick, E. L. 1990, PASP, 102, 379

Walter, F. M., Stringfellow, G. S., Sherry, W. H., & Field-Pollatou, A. 2004, AJ, 128, 1872

Walter, F. M., Vrba, F. J., Mathieu, R. D., Brown, A., & Myers, P. C. 1994, AJ, 107, 692

Weinberger, A. J., Anglada-Escudé, G., & Boss, A. P. 2012, ArXiv e-prints

Weis, E. W. 1993, AJ, 105, 1962

Werner, M. W., et al. 2004, ApJS, 154, 1

White, R. J., & Basri, G. 2003, ApJ, 582, 1109

White, R. J., Gabor, J. M., & Hillenbrand, L. A. 2007, AJ, 133, 2524

White, R. J., & Hillenbrand, L. A. 2004, ApJ, 616, 998

Wichmann, R., Covino, E., Alcalá, J. M., Krautter, J., Allain, S., & Hauschildt, P. H. 1999, MNRAS, 307, 909

Wichmann, R., Sterzik, M., Krautter, J., Metanomski, A., & Voges, W. 1997, A&A, 326, 211

Wright, E. L., et al. 2010, AJ, 140, 1868

Wright, J. T. 2005, AJ, 129, 1776

Yee, J. C., & Jensen, E. L. N. 2010, ApJ, 711, 303

Zacharias, N., Finch, C. T., Girard, T. M., Henden, A., Bartlett, J. L., Monet, D. G., & Zacharias, M. I. 2013, AJ, 145, 44

Zhang, K., Pontoppidan, K. M., Salyk, C., & Blake, G. A. 2013, ApJ, 766, 82

Zorec, J., Cidale, L., Arias, M. L., Frémat, Y., Muratore, M. F., Torres, A. F., & Martayan, C. 2009, A&A, 501, 297

Zuckerman, B., Rhee, J. H., Song, I., & Bessell, M. S. 2011, ApJ, 732, 61

Zuckerman, B., & Song, I. 2004, ARA&A, 42, 685

Zuckerman, B., Song, I., Bessell, M. S., & Webb, R. A. 2001, ApJ, 562, L87